



N°d'ordre  
2017LYSEI022

**THESE de DOCTORAT DE L'UNIVERSITE DE LYON**  
opérée au sein de  
**L'INSTITUT NATIONAL DES SCIENCES APPLIQUEES DE LYON**

**Ecole Doctorale N° ED206**  
**Ecole Doctorale de Chimie de Lyon**

**Spécialité Chimie**

Soutenue publiquement le 31/03/2016, par  
**Sizhe LI**

---

**Signalisation chimique du Quorum Sensing  
bactérien: Conception, synthèse et évaluation  
biologique de mimes d'autoinducteurs et  
d'analogues d'agrocinopines.**

**Chemical Signalling in Bacterial Quorum Sensing:  
Design, Synthesis and Biological Investigations of  
Autoinducers Mimics and Analogues of  
Agrocinopines.**

---

**Directeur et co-directeur de thèse: Dr. Yves Queneau, Dr. Laurent Soulière**

Devant le jury composé de:

<b>Mme. Catherine Guillou, Directeur de Recherche CNRS à l'ICSN</b>	<b>Rapporteure</b>
<b>M. David Bonnaffé, Professeur à l'Université Paris Sud</b>	<b>Rapporteur</b>
<b>M. Olivier Martin, Professeur à l'Université d'Orléans</b>	<b>Examineur</b>
<b>M. Yves Queneau, Directeur de Recherche CNRS à l'INSA de Lyon</b>	<b>Directeur</b>
<b>M. Laurent Soulière, Maître de conférence à l'INSA de Lyon</b>	<b>Co-directeur</b>



## Département FEDORA – INSA Lyon - Ecoles Doctorales – Quinquennal 2016-2020

SIGLE	ECOLE DOCTORALE	NOM ET COORDONNEES DU RESPONSABLE
<b>CHIMIE</b>	<b>CHIMIE DE LYON</b> <a href="http://www.edchimie-lyon.fr">http://www.edchimie-lyon.fr</a> Sec : Renée EL MELHEM Bat Blaise Pascal 3 <sup>e</sup> etage <a href="mailto:secretariat@edchimie-lyon.fr">secretariat@edchimie-lyon.fr</a> Insa : R. GOURDON	M. Stéphane Daniele IRCELYON, Institut de recherches sur la catalyse et l'environnement de Lyon, UMR5256 2 avenue Albert Einstein 69626 VILLEURBANNE Cedex Tél : 04.72.44 53 60 <a href="mailto:Stephane.daniele@ircelyon.univ-lyon1.fr">Stephane.daniele@ircelyon.univ-lyon1.fr</a>
<b>E.E.A.</b>	<b>ELECTRONIQUE, ELECTROTECHNIQUE, AUTOMATIQUE</b> <a href="http://edeea.ec-lyon.fr">http://edeea.ec-lyon.fr</a> Sec : M.C. HAVGOUDOUKIAN <a href="mailto:Ecole-Doctorale.eea@ec-lyon.fr">Ecole-Doctorale.eea@ec-lyon.fr</a>	<b>M. Gérard SCORLETTI</b> Ecole Centrale de Lyon 36 avenue Guy de Collongue 69134 ECULLY Tél : 04.72.18 60 97 Fax : 04 78 43 37 17 <a href="mailto:Gerard.scorletti@ec-lyon.fr">Gerard.scorletti@ec-lyon.fr</a>
<b>E2M2</b>	<b>EVOLUTION, ECOSYSTEME, MICROBIOLOGIE, MODELISATION</b> <a href="http://e2m2.universite-lyon.fr">http://e2m2.universite-lyon.fr</a> Sec : Sylvie ROBERJOT Bat Atrium - UCB Lyon 1 04.72.44.83.62 Insa : H. CHARLES <a href="mailto:secretariat.e2m2@univ-lyon1.fr">secretariat.e2m2@univ-lyon1.fr</a>	<b>M. Fabrice CORDEY</b> CNRS UMR 5276 Lab. de géologie de Lyon Université Claude Bernard Lyon 1 Bat Géode 2 rue Raphael Dubois 69622 VILLEURBANNE Cédex Tél : 06.07.53.89.13 <a href="mailto:cordey@univ-lyon1.fr">cordey@univ-lyon1.fr</a>
<b>EDISS</b>	<b>INTERDISCIPLINAIRE SCIENCES- SANTÉ</b> <a href="http://ww2.ibcp.fr/ediss">http://ww2.ibcp.fr/ediss</a> Sec : Sylvie ROBERJOT Bat Atrium - UCB Lyon 1 04.72.44.83.62 Insa : M. LAGARDE <a href="mailto:secretariat.ediss@univ-lyon1.fr">secretariat.ediss@univ-lyon1.fr</a>	<b>Mme Emmanuelle CANET-SOULAS</b> INSERM U1060, CarMeN lab, Univ. Lyon 1 Batiment IMBL 11 avenue Jean Capelle INSA de Lyon 696621 Villeurbanne Tél : 04.72.68.49.09 Fax :04 72 68 49 16 <a href="mailto:Emmanuelle.canet@univ-lyon1.fr">Emmanuelle.canet@univ-lyon1.fr</a>
<b>INFOMATHS</b>	<b>INFORMATIQUE ET MATHEMATIQUES</b> <a href="http://infomaths.univ-lyon1.fr">http://infomaths.univ-lyon1.fr</a> Sec :Renée EL MELHEM Bat Blaise Pascal 3 <sup>e</sup> etage <a href="mailto:infomaths@univ-lyon1.fr">infomaths@univ-lyon1.fr</a>	<b>Mme Sylvie CALABRETTO</b> LIRIS – INSA de Lyon Bat Blaise Pascal 7 avenue Jean Capelle 69622 VILLEURBANNE Cedex Tél : 04.72. 43. 80. 46 Fax 04 72 43 16 87 <a href="mailto:Sylvie.calabretto@insa-lyon.fr">Sylvie.calabretto@insa-lyon.fr</a>
<b>Matériaux</b>	<b>MATERIAUX DE LYON</b> <a href="http://ed34.universite-lyon.fr">http://ed34.universite-lyon.fr</a> Sec : M. LABOUNE PM : 71.70 –Fax : 87.12 Bat. Direction <a href="mailto:Ed.materiaux@insa-lyon.fr">Ed.materiaux@insa-lyon.fr</a>	<b>M. Jean-Yves BUFFIERE</b> INSA de Lyon MATEIS Bâtiment Saint Exupéry 7 avenue Jean Capelle 69621 VILLEURBANNE Cédex Tél : 04.72.43 83 18 Fax 04 72 43 85 28 <a href="mailto:Jean-yves.buffiere@insa-lyon.fr">Jean-yves.buffiere@insa-lyon.fr</a>
<b>MEGA</b>	<b>MECANIQUE, ENERGETIQUE, GENIE CIVIL, ACOUSTIQUE</b> <a href="http://mega.universite-lyon.fr">http://mega.universite-lyon.fr</a> Sec : M. LABOUNE PM : 71.70 –Fax : 87.12 Bat. Direction <a href="mailto:mega@insa-lyon.fr">mega@insa-lyon.fr</a>	<b>M. Philippe BOISSE</b> INSA de Lyon Laboratoire LAMCOS Bâtiment Jacquard 25 bis avenue Jean Capelle 69621 VILLEURBANNE Cedex Tél :04.72.18.71.70 Fax : 04 72 43 72 37 <a href="mailto:Philippe.boisse@insa-lyon.fr">Philippe.boisse@insa-lyon.fr</a>
<b>ScSo</b>	<b>ScSo*</b> <a href="http://recherche.univ-lyon2.fr/scso/">http://recherche.univ-lyon2.fr/scso/</a> Sec : Viviane POLSINELLI Brigitte DUBOIS Insa : J.Y. TOUSSAINT Tél : 04 78 69 72 76 <a href="mailto:viviane.polsinelli@univ-lyon2.fr">viviane.polsinelli@univ-lyon2.fr</a>	<b>M. OBADIA Lionel</b> Université Lyon 2 86 rue Pasteur 69365 LYON Cedex 07 Tél : 04.78.69.72.76 Fax : 04.37.28.04.48 <a href="mailto:Lionel.Obadia@univ-lyon2.fr">Lionel.Obadia@univ-lyon2.fr</a>

\*ScSo : Histoire, Géographie, Aménagement, Urbanisme, Archéologie, Science politique, Sociologie, Anthropologie



# Acknowledgement

In 2013, I was recommended by Prof. Qian Wan, who is a professor in Huazhong University of Science and Technology (HUST), to join the UT-INSA program to start my PhD in Laboratory of Organic and Bioorganic Chemistry (COB) of INSA Lyon under the supervision of Prof. Dr. Yves Queneau. Without his recommendation, I might have no chance, I greatly appreciated his help. In 2017, it is time for my PhD defense. How time flies!

First and foremost, I would like to express my special appreciation to my supervisor, Dr. Yves Queneau, Directeur de Recherche CNRS à l'INSA de Lyon, for giving me the valuable opportunity to be part of the excellent research group. During the past 42 months, my professional knowledge, skills and personality were extremely improved. When I started my PhD, I was too shy to share my ideas with others fluently, even in the informal meeting. It is you who gave me lots of chances and encouragements to practice my oral English and presentation and writing skills, which will undoubtedly change my life. Moreover, you inspired me to develop my ideas for the research, provided innovative and professional guidance to sharpen the ideas and conclusions drawn from the experimental work. Furthermore, I have appreciated the trust you gave me in establishing collaborations and make steps forward in the project. Finally, this thesis would not complete soon without your patience and effective guidance. THANK YOU.

I also would like to express my gratitude to my co-supervisor, Dr. Laurent Soulère, who gave me millions of helps in my bench work, collaboration contact, consistent and useful instruction on the writing of this thesis and scientific papers. The most important thing I learned is patience and seriousness. Without his patient instruction and expert guidance, the completion of this thesis would not have been possible.

I also greatly appreciated for the kind assistance of Dr. Ahmar Mohammed in my research and life. Thank you for helping me to solve difficulties in my research. I will never forget your help in translating Franch into English in several letters, making some appointments with doctors and your practical suggestions in life. You are more than a colleague at work, but also a very good friend. Many thanks!

I would like to acknowledge all persons who are in collaboration with my PhD projects. My sincere thanks are given to Dr. Abbas El Sahili, Dr. Solange Moréra at Institute for Integrative Biology of the Cell (I2BC) in Gif-sur-Yvette for their contribution on the binding properties investigation of agropinopines, and Dr. Julien Wawrzyniak at Microbiologie, Adaptation, Pathogénie (MAP) of INSA Lyon for his contribution on the bacterial strains, as well as Dr.

Maha Hachicha, Mr. Vincent Denavit, Fouad Haroun for their contribution on the synthesis of oxadiazoles, and Dr. Yves Dessaux at Gif sur Yvette for his collaboration with us in long chain AHLs analogues. And many thanks to LI Geng at COB-INSA who contributed to the synthesis of agrocinipine A.

I also appreciated all my colleagues in the COB-INSA for the friendly working atmosphere and effective cooperation in both research and life. Thanks to Prof. Florence Popowycz, Dr. Stephane Chambert, Dr. Sylvie Moebs and Mrs. Elyane Chassignol. Many thanks to Mrs. Lucie Grand for her careful maintenance of experimental equipment and technical assistance in the laboratory. My acknowledgements are also given to the colleagues working in the NMR and MS platforms.

Many thanks to all PhD students from the lab: Jia-neng Tan, you are an eloquent and serious man; Xiubin Li, you are a humorous guy and I hope everything will be better and better; Zonglong Yang, you are very friendly and funny, always willing to help others; Weigang Fan, you are a scientific guy, and keep up the good work; Lianjie Wang, enjoying the wonderful life in France; and Manon Boulven, Maiwenn Jacolot. I wish all of you everything goes well in the future.

Thanks to the China Scholarship Council (CSC) for providing the scholarship for my PhD study. Without CSC, it would not have been possible for me to study abroad.

My parents and my wife Heyang Zhang, who sacrificed so much for my education and university studies, deserve my sincere acknowledgements. Without your continuous love, support, confidence and encouragement, this thesis would not exist. I'm very grateful to all of you.

Last but not least, I would like to express my sincere gratitude to the members of examination committee: Prof. David Bonnaffé (from Université Paris Sud), Prof. Olivier Martin (from Université d'Orléans), Dr. Catherine Guillou (from ICSN-CNRS), for having graciously agreed to serve on my committee.

## Abbreviations

Ac	Acetyl
A2P	L-arabinose-2-phosphate
ABC	ATP-binding cassette
acc	Agrocinopine catabolism operon
ACP	acyl carrier protein
AccR	Agrocinopine catabolic regulator
AHL	Acyl homoserine lactone
AI	Autoinducer
AIPS	Autoinducing peptides
ATP	Adenosine triphosphate
BBA	Butane 2,3-bisacetal
BHL	( <i>S</i> )- <i>N</i> - Butanoyl-L-homoserine lactone
Bn	Benzyl
Boc	<i>tert</i> -Butyloxycarbonyl
BocSerOMe	Boc-L-serine methyl ester
BocTyrOMe	Boc-L-Tyrosine methyl ester
Bz	Benzoyl
CAN	Ammonium cerium nitrate
Chv	Chromosomal virulence gene
CK	Cytokinin
COSY	Correlation spectroscopy
DBVS	Docking based virtual screening
DCC	<i>N,N'</i> -Dicyclohexylcarbodiimide
DCE	1,2-Dichloroethane
DCM	Dichloromethane
DEAE	Diethylaminoethanol

DEHD	1-deoxy-D- <i>erythro</i> -hexo-2,3-diulose
DIBAH	Diisobutylaluminium hydride
DIPEA (DIEA)	Diisopropylethylamine
DIPA	Diisopropylamine
DKPs	2,5-Diketopiperazines
DMAP	4-Dimethylaminopyridine
DMF	Dimethylformamide
DMP	Dimethoxypropane
DMSO	Dimethyl sulfoxide
DPD	Dihydroxypentanedione
EC <sub>50</sub>	The half maximal effective concentration
EDC	1-Ethyl-3-(3-dimethylaminopropyl)carbodiimide
EDGs	Electron-donating groups
EWGs	Withdrawing groups
ET	Ethylene
G1P	D-glucose-1-phosphate
G2P	D-glucose-2-phosphate
G2PL	D-glucose-2-phosphate L-lactate
G6P	D-glucose-6-phosphate
GABA	Gamma-aminobutyric acid
GFP	Green fluorescent protein
HAM	Hamamelitannin
HHQ	2-heptyl-4(1H)-quinolone
HMBC	Heteronuclear multiple-bond correlation
HPLC	High Performance Liquid Chromatography
HQNO	4-hydroxy-2-heptylquin-oline-N-oxide
HSL (HL)	Homoserine lactone
HTL	Homoserine thiolactone
HSQC	Heteronuclear single-quantum correlation spectroscopy

IAA	Indole-2-acetic acid
IC <sub>50</sub>	The half maximal inhibitory concentration
LDA	Lithium diisopropylamide
LiHMDS	Lithium bis(trimethylsilyl)amide
<i>m</i> -CPBA	3-Chloroperoxybenzoic acid
MHF	Methyhydroxy furanone
MSNT	1-methylenesulfonic acid (3-nitro-1,2,4-triazolide)
NMR	Nuclear magnetic resonance
NHS	N-Hydroxysuccinimide
OdDHL	( <i>S</i> )- <i>N</i> -(3-oxo-decanoyl)- <i>L</i> -homoserine lactone
OHHL	3-oxo-hexanoyl homoserine lactone
PQS	<i>Pseudomonas</i> quinolone signal
PBP	Periplasmic binding protein
PMB	<i>para</i> -methoxybenzyl
PNP	<i>para</i> -nitrophenyl
QS	Quorum sensing
QSM	Quorum sensing molecule
QSI	Quorum sensing inhibitor
SA	Salicylic acid
SAM	<i>S</i> -adenosyl- <i>L</i> -methionine
<i>S</i> -THMF	(2 <i>S</i> ,4 <i>S</i> )-2-methyl-2,3,3,4-tetrahydroxytetrahydrofuran
<i>S</i> -DHMF	(2 <i>S</i> ,4 <i>S</i> )-2-methyl-2,4-dihydroxydihydrofuran-3-one
TBS	<i>Tert</i> -butyldimethylsilyl
TBAF	<i>Tetra-n</i> -butylammonium fluoride
TBAI	<i>Tetra-n</i> -butylammonium iodide
TFA	Trifluoroacetic acid
THF	Tetrahydrofuran
Ti	Tumor inducing
TIBAL	Triisobutylaluminium

TMAH	<i>Tetra</i> -methylammonium hydroxide
TMS	Trimethylsilyl
TLC	Thin layer chromatography
<i>p</i> -TsOH	<i>p</i> -Toluenesulfonic acid
<i>R</i> -THMF	(2 <i>R</i> ,4 <i>S</i> )-2-methyl-2,3,3,4-tetrahydroxytetrahydrofuran
<i>R</i> -DHMF	(2 <i>R</i> ,4 <i>S</i> )-2-methyl-2,4-dihydroxydihydrofuran-3-one
SAR	Structure-activity relationship
UDP	Uridine-5'-diphosphate disodium salt
UTP	Uridine 5'-triphosphate dihydrate trisodium salt
Vir	Virulene gene
2-AA	2-Aminoacetophenone
2-NA	2-Nitroaniline

# Contents

<b>Acknowledgement</b> .....	- 1 -
<b>Abbreviations</b> .....	- 3 -
<b>General Introduction</b> .....	- 11 -
<b>Part I. Design, Synthesis and Biological Evaluation of Novel Quorum Sensing Inhibitors</b> .....	- 13 -
<b>Chapter I. Bibliography</b> .....	- 13 -
1.1 Introduction .....	- 15 -
1.1.1 What is Quorum Sensing?.....	- 15 -
1.1.2 A brief history of QS.....	- 16 -
1.1.3 QS mechanism and systems .....	- 20 -
1.2 Strategies for designing QS inhibitors and modification of AHLs.....	- 25 -
1.2.1 Application interests .....	- 25 -
1.2.2 Modulation of QS .....	- 25 -
1.3 AHL Heterocyclic analogues .....	- 28 -
1.3.1 Five-membered rings heterocyclic analogues .....	- 30 -
1.3.2 Six-membered rings heterocyclic analogues .....	- 51 -
1.4 Conclusion.....	- 62 -
1.5 Perspectives .....	- 63 -
<b>Chapter II. Results and Discussion</b> .....	- 65 -
2.1 Introduction .....	- 67 -
2.2 Synthesis and biological evaluation of optically pure AHLs and analogues.....	- 69 -
2.2.1 Introduction .....	- 69 -
2.2.2 Preparation of L- and D- homoserine lactone hydrobromide .....	- 70 -
2.2.3 Synthesis of optically pure AHLs analogues.....	- 71 -
2.2.4 Determination of enantiomeric purity .....	- 75 -
2.2.5 Biological evaluation.....	- 83 -
2.2.6 Molecular docking studies.....	- 89 -
2.2.7 Conclusions .....	- 90 -

2.3	Synthesis of AHLs analogues with long chain.....	- 92 -
2.3.1	Introduction .....	- 92 -
2.3.2	Synthesis of HSL-C16.....	- 93 -
2.3.3	Synthesis of HSL-C16-NHS.....	- 93 -
2.3.4	Synthesis of HSL-3-oxo-C18-NHS .....	- 94 -
2.3.5	Conclusion.....	- 98 -
2.4	Design, synthesis and biological evaluation of oxadiazoles as QS modulators .....	- 99 -
2.4.1	Introduction .....	- 99 -
2.4.2	Synthesis of 2,5-disubstituted 1,3,4-oxadiazoles with the carboxymethyl ester .-	99 -
	-	
2.4.3	Synthesis of 2,5-disubstituted 1,3,4-oxadiazoles with the $\gamma$ -lactone .....	- 102 -
2.4.4	Synthesis of 3,5-disubstituted 1,2,4-oxadiazoles with the carboxymethyl ester in 3-position.....	- 104 -
2.4.5	Synthesis of 3,5-disubstituted 1,2,4-oxadiazoles with the $\gamma$ -lactone in 3-position ...-	105 -
2.4.6	Synthesis of 3,5-disubstituted 1,2,4-oxadiazoles with the carboxymethyl ester in 5-position.....	- 107 -
2.4.7	Synthesis of 3,5-disubstituted 1,2,4-oxadiazoles with the $\gamma$ -lactone in 5-position ...-	109 -
2.4.8	Biological evaluation.....	- 111 -
2.4.9	Results and conclusion .....	- 111 -
2.5	An alternative cyclization approach towards the core motif lactone of AHL analogues	- 115 -
2.5.1	Introduction .....	- 115 -
2.5.2	Optimization of the reaction .....	- 115 -
2.5.3	Investigation of the scope of the reaction .....	- 117 -
2.5.4	Biological assays and results .....	- 118 -
2.5.5	Conclusion.....	- 119 -
2.6	Computer aided design of readily available acylated 2-nitroaniline derivatives as LuxR-regulated QS inhibitors .....	- 120 -
2.6.1	Introduction .....	- 120 -
2.6.2	Synthesis of 2-nitroaniline derivatives .....	- 122 -

2.6.3	Biological evaluation.....	- 122 -
2.6.4	Discussion .....	- 123 -
2.7	Conclusion.....	- 128 -
<b>Part II. Investigation of the role of carbohydrate phosphodiester and phosphates in QS Regulation in <i>Agrobacterium tumefaciens</i> .....</b>		<b>- 131 -</b>
<b>Chapter III. Bibliography .....</b>		<b>- 131 -</b>
3.1	Introduction .....	- 133 -
3.2	QS in <i>Agrobacterium tumefaciens</i> .....	- 133 -
3.2.1	<i>Agrobacterium tumefaciens</i> .....	- 133 -
3.2.2	The infection process of <i>A. tumefaciens</i> .....	- 134 -
3.2.3	A brief overview of <i>A. tumefaciens</i> QS .....	- 135 -
3.2.4	<i>A. tumefaciens</i> responses to plant-derived signaling molecules.....	- 136 -
3.2.5	Plant-derived opines as a source of nutrients and activator for <i>Agrobacterium</i> QS ..	- 140 -
3.3	Agrocinopine .....	- 143 -
3.3.1	Agrocin 84 .....	- 144 -
3.3.2	Discovery and chemistry of the agrocinopine opines .....	- 145 -
3.3.3	Agrocinopine A and B .....	- 147 -
3.3.4	Agrocinopine C and D .....	- 160 -
3.3.5	Biological aspects of agrocinopines.....	- 168 -
3.3.6	Other carbohydrate phosphodiester and phosphates.....	- 170 -
3.4	Conclusion.....	- 172 -
<b>Chapter IV. Results and Discussion .....</b>		<b>- 175 -</b>
4.1	Introduction .....	- 177 -
4.2	Synthesis and binding properties of agrocinopine A.....	- 179 -
4.2.1	Preparation of the phosphoramidite .....	- 180 -
4.2.2	Synthesis of the arabinose fragment .....	- 180 -
4.2.3	Synthesis of the sucrose fragment.....	- 181 -
4.2.4	Condensation and deprotection.....	- 182 -
4.2.5	Biological results .....	- 185 -

4.3	Synthesis and binding properties of L-arabinose-2-phosphate (A2P), D-glucose-phosphate (G2P) and their derivatives .....	- 186 -
4.3.1	Synthesis of A2P and its derivatives .....	- 186 -
4.3.2	Synthesis of G2P and its derivatives .....	- 188 -
4.3.3	Synthesis of arabinose-2- <i>p</i> -nitrophenyl phosphate and glucose-2- <i>p</i> -nitrophenyl phosphate .....	- 202 -
4.3.4	Binding mode and biological properties of A2P, G2P and derivatives.....	- 206 -
4.4	Synthesis and binding properties of agrocinopine C and D .....	- 214 -
4.4.1	Synthesis of agrocinopine C .....	- 214 -
4.4.2	Synthesis of agrocinopine D .....	- 221 -
4.4.3	Biological Results for agrocinopine C and D.....	- 224 -
4.5	A convenient phosphorylation method using triallyl phosphite .....	- 225 -
4.5.1	Introduction.....	- 225 -
4.5.2	Optimization of phosphorylation conditions.....	- 225 -
4.5.3	Scope of the reaction.....	- 227 -
4.6	Conclusion.....	- 230 -
	<b>General conclusion .....</b>	<b>- 233 -</b>
	<b>Experimental section.....</b>	<b>- 235 -</b>
	Part I. Supplementary information.....	- 238 -
	Part II. Supplementary information.....	- 267 -
	Annex 1 .....	- 294 -
	<b>References .....</b>	<b>- 301 -</b>
	<b>Abstract.....</b>	<b>- 311 -</b>
	<b>Résumé .....</b>	<b>- 313 -</b>

# General Introduction

Bacteria have been thought to behave as unicellular organisms for a long time. However, it has been discovered that they behave as multicellular systems in which separate cells communicate with each other by using chemical signal molecules called “autoinducers”. This process, called Quorum Sensing (QS), is able to regulate the expression of some important biological functions, according to the bacterial population density. For example, bacterial virulence or biofilm formation, both connected with pathogenicity in human or in plant health, are regulated by QS. This is why QS has been, and still is, the object of many studies both from the biological and chemical points of view. As QS is modulated by several types of molecules, either the autoinducers themselves or other co-inducers, it is therefore an interesting point for synthetic organic chemistry investigations. Two different aspects of the chemistry of QS are studied in this thesis.

The first part contributes to the design, synthesis and biological evaluation of novel QS inhibitors. After giving an overview on QS in its biological and chemical issues, we report our work on various structure-properties relationships of Acyl Homoserine Lactones (AHLs), a kind of chemical molecular autoinducers used by Gram-negative bacteria. The work relates to the chirality of the homoserine moiety, the replacement of the central amide group by heterocyclic scaffolds and the search for AHL structurally unrelated compounds such as nitroaniline systems.

The second part focuses on a specific bacterial species, *Agrobacterium tumefaciens* (AT), which induces crown gall disease in a wide variety of plants, consequently causing the decline of production in agriculture. The infection by AT involves the transfer of a plasmid from the bacteria to the plant cells which triggers the production of molecules called “opines”, which are low molecular weight amino acids and sugar phosphate derivatives. However, all biological functions of opines, including QS co-inducers, are still not completely understood. After some bibliographic information on AT and opines, we report in this second part our studies relating to agrocinopine A, a carbohydrate phosphodiester found in plant tumors after infection by AT.

We notably focused on understanding how agrocinopine A was able to intervene in the QS process, produce AHL signals and activate bacterial virulence.

Overall, this thesis is the combination of two synthetic organic chemistry studies relating to QS, both aimed at improving basic knowledge on this exciting biological process, and possibly contributing to develop new strategies able to control pathogenicity in the future.

# **Part I. Design, Synthesis and Biological Evaluation of Novel Quorum Sensing Inhibitors**

## **Chapter I. Bibliography**



# Bibliography

## 1.1 Introduction

### 1.1.1 What is Quorum Sensing?

In 1970s, Nealson with his research team studied the cellular control of the synthesis and activity of the bacterial luminescent system. They found that bacteria *Vibrio fischeri* did not express their genotype *in vitro* (through the observation of its luminescence), and that this process was determined by a certain population density of bacteria.<sup>[1]</sup> Their discovery opened a new beginning for studying the bacterial communication system. In the following years, biochemical processes (molecular and genetic) involved in this mechanism were characterized, and several research teams discovered that many Gram negative and positive bacteria actually possess a similar system.<sup>[2][3]</sup> The term "quorum-sensing (QS)" was employed to describe the mode of communication used by bacteria to synchronize the expression (or repression) of particular genes, according to their population density.

QS is a type of decision-making process used by decentralized groups to coordinate behavior. In the process of QS, the cell density is controlled by molecular chemical signals called autoinducers which are produced by bacteria. The detection of a minimal threshold stimulatory concentration of an autoinducer leads to an alteration in gene expression.<sup>[4]</sup> Both Gram-positive and Gram-negative bacteria use QS to coordinate their genes to express various phenotypes which are essential for the successful establishment of symbiotic, pathogenic relationships with eukaryotic hosts, and also bioluminescence, motility, antibiotic production, biofilm formation, and virulence factor. But as the basic language of bacteria for communication and expression, the autoinducers varying in different kinds of bacteria: for example, Gram-negative bacteria use acylated homoserine lactones (AHLs) as autoinducers, and Gram-positive bacteria use processed cyclic oligopeptides to communicate, among several types of molecules.

As the study on QS became more widely, it was gradually recognized as an efficient mechanism to regulate expression of specific genes responsible for common behavior of

bacteria.<sup>[3]</sup> Bacteria living in diverse domains have broadly adapted QS systems to optimize their regulation of a variety of activities. In any case bacteria with QS are able to communicate and to adjust behavior in response to the presence of other bacteria. QS acting as a multi-step adjustment mechanism allows bacteria to coordinate global behavior. With the progress of investigations on QS, we are now clearer about the elaborated mechanism of QS, for example how QS facilitate species-specific and interspecies cell-cell communication, how QS controls populations to act synergistically and how QS can be used for different purposes.<sup>[5]</sup> Furthermore, the study related to the bacteria signals including the synthesis of autoinducer mimics and the encoding scheme of these chemical signals for controlling gene expression could offer new potential practical applications. Therefore, further investigations on the mechanism of QS systems could provide powerful tools against pathogenic bacteria.

### 1.1.2 A brief history of QS

Research into AHL based QS started in the late 1960s. The marine bioluminescent bacteria *Vibrio fischeri* was grown in liquid cultures and it was observed that the cultures produced light only when large numbers of bacteria were present.<sup>[6]</sup> The initial explanation for this phenomena was that the culture media contained an inhibitor of luminescence, which was removed by the bacteria when large numbers were present.<sup>[7]</sup> This was suggested because, when grown in media "conditioned" by preliminary exposure to the bacteria, luminescence could be induced even at low cell density. It was later shown that the luminescence was initiated not by the removal of an inhibitor but by the accumulation of an activator molecule or "autoinducer",<sup>[1][8]</sup> which is made by the bacteria and activates luminescence when it has accumulated to a high enough concentration. The bacteria are able to sense their cell density by monitoring the autoinducer concentration. The molecule produced by *V. fischeri* was first isolated and characterized in 1981 by Eberhard et al.<sup>[9]</sup> and identified as *N*-(3-oxohexanoyl)-homoserine lactone (3-oxo-C6-HSL, OHHL). Analysis of the genes involved in QS in *V. fischeri* was first carried out by Engebrecht et al.<sup>[10]</sup> This led to the basic model for QS in *V. fischeri* which is now a paradigm for other similar QS systems. For many years following this, it was thought that AHL-based QS was limited to marine bacteria such as *V. fischeri* and *V. harveyi*. Over the last 20 years, research

into QS carried out worldwide led to the discovery that QS was far more widespread than previously thought.

In General, QS is mediated by several major class<sup>[11-13]</sup> of autoinducers. The first discovered class of autoinducer is acyl homoserine lactone (AHL) which varies in the length and oxidation state of the acyl side chain, and employed by over 70 species of Gram-negative bacteria. The second class of autoinducer is oligopeptides, consisting of 2-10 amino acids, which are generally employed by Gram-positive bacteria that participate in QS, for example, autoinducing peptides (AIPs) in *Staphylococcus aureus*, unlike AHLs, most oligopeptides do not act as transcription factors themselves. The third class of autoinducer is derivatives of the sugar-like molecule dihydroxypentanedione (DPD), for example, AI-2<sup>[14]</sup> in *vibrio harveri*, which is a furanosyl borate diester, has been identified in both Gram-positive and Gram-negative bacteria and would be an evolutionary link between the two major types of QS circuits. There are some other small molecules such as *Pseudomonas* quinolone signal (PQS),<sup>[15]</sup> 3-hydroxypalmitic acid methyl ester,<sup>[16]</sup> bradyoxetin,<sup>[17]</sup> a small molecule autoinducer with unknown structure, used by enterohemorrhagic *E. coli* called AI-3,<sup>[18]</sup> and so on. The following are some examples of QS in different type of bacteria (**Fig 1**).

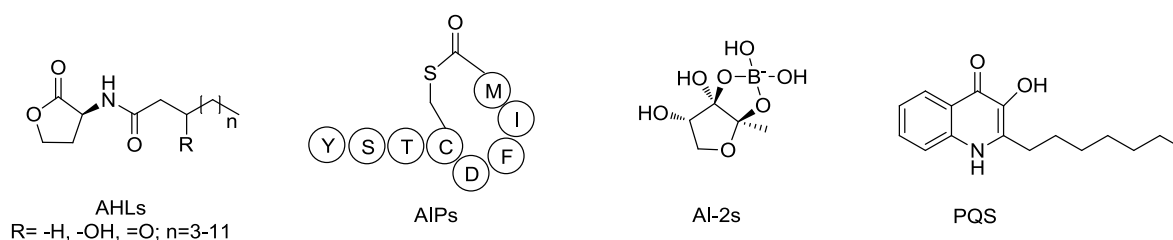


**Fig 1. Examples of QS molecules**

### 1.1.2.1 *Escherichia coli*

In the Gram-negative bacteria *Escherichia coli*, cell division may be partially regulated by AI-2-mediated QS. This species uses AI-2, which is produced and processed by the *lsr* operon.<sup>[19]</sup> *E. coli* and *Salmonella enterica* do not produce AHL signals commonly found in other Gram-negative bacteria. However, they have a receptor called SdiA that detects AHLs from other

bacteria and changes their gene expression in accordance with the presence of other ‘quorate’ populations of Gram-negative bacteria.

### **1.1.2.2 Antibiotic production in *Erwinia carotovora***

In the early 1990s, B. Bycroft, P. Williams and G. Salmond<sup>[20]</sup> studied mutants of *Erwinia carotovora* that were unable to make carbapenem antibiotics. The idea was to find out which genes were defective in different mutants and so build up a picture of all the genes involved in the biosynthetic pathway. One class of mutants could not make antibiotics on their own but could do so when cross-fed by a second group of mutants. Investigations showed that the second group of mutants supplied a signaling molecule which triggered antibiotic synthesis in the first group. The discovery was that the signaling molecule was the same as one used by a completely unrelated bacterium (*V. fischeri*) to trigger the emission of light.<sup>[21][22]</sup> From then on, the researcher began to consider the application of signaling molecule in bioluminescent bacteria. The QS signals significantly attracted the attention of more researchers.

### **1.1.2.3 QS in *Pseudomonas aeruginosa***

In 1991, Gambello et al.<sup>[23]</sup> discovered that the human pathogen *Pseudomonas aeruginosa* also possesses a *V. fischeri*-like QS system. This was shown to regulate the production of elastase, an important virulence factor. The AHL responsible for the induction of elastase was identified as 3-oxo-C12-HSL.<sup>[24]</sup> The second QS system regulating rhamnolipid, haemolysin and other important virulence factors was discovered by Latifi et al.<sup>[25]</sup> Winson et al.<sup>[26]</sup> showed that this system was responsible for the production of C4-HSL.

### **1.1.2.4 AHL-based QS in other bacterial species**

The discovery that bacteria other than marine *Vibrios* use AHL QS systems led to the development of biosensors that can detect AHLs from other bacteria.<sup>[27]</sup> These sensors were used to detect QS systems in *Enterobacter*, *Hafnia*, *Rahnella* and *Serratia*. Since then, this and other methods have been used to identify a large number of other QS species.

### 1.1.2.5 *Vibrio harveyi*

*Vibrio harveyi* like *Vibrio fischeri* is a bioluminescent marine bacterium in which the luminescence genes are regulated by QS. As in all QS systems, a signal molecule is produced and subsequently sensed by the bacteria. *V. harveyi* has two QS systems, one employs *N*-acyl-homoserine lactone (AHL), 3-hydroxy-C4-HSL as the signal. This system is however distinct from that of *V. fischeri* as the genes involved are not homologous to luxR and luxI from *V. fischeri*. The second system in *V. harveyi* relies on the accumulation of a molecule with unknown structure designated AI-2. Both the AHL and AI-2 systems regulate the luminescence genes via two-component regulatory systems.<sup>[28]</sup> The AHL signal 3-hydroxy-C4-HSL,<sup>[29]</sup> which is generated by the protein LuxM, is received by the LuxN protein. AI-2, which is generated via LuxS is received by the LuxP and LuxQ proteins. LuxN and LuxQ contain both sensor kinase and response regulator domains of two component systems. The two receptor systems converge on a protein LuxO, which is homologous to the response regulator domains of two-component signal transduction systems.<sup>[30]</sup> At low cell density, LuxO is phosphorylated by LuxQ and LuxN (via a phosphorelay protein, LuxU). In its phosphorylated state, LuxO activates the transcription of a repressor protein which blocks transcription of the luxCDABE genes. At high cell density, when the two signal molecules are present, LuxN and LuxQ dephosphorylate LuxO preventing from activating transcription of the repressor. This allows a transcriptional activator LuxR which is not homologous to LuxR from *V. fischeri*<sup>[31]</sup> to activate lux gene expression (Fig 2).<sup>[32,33]</sup>

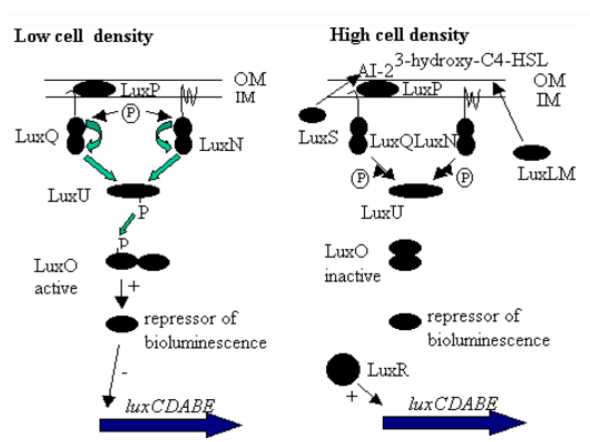


Fig 2. Diagram of the *V. harveyi* system

### 1.1.3 QS mechanism and systems

The QS mechanism is based on the coordinated interaction of the following three key elements:<sup>[34,35]</sup>

- a molecular messenger, called Auto-Inducer (AI),
- an enzyme synthases (eg, LuxI/LuxR families), responsible for the synthesis of the AI,
- a protein, called transcription factor, specifically recognizing the AI and regulating the expression of genes which are controlled by QS.

AIs are able to cross the cell membrane by passive diffusion (or via carriers) in a concentration gradient. In a closed environment, for example, within a biofilm or in a host device, bacterial growth leads to the accumulation of AI. Then it strikes a balance between the intracellular and extracellular concentrations proportional to the bacterial density. When the internal concentration reaches a threshold value, the messenger interacts with regulatory protein. Thus, the formed complex AI or transcription factor recognizes a specific DNA sequence of the genotype and active (or repress) gene expression. Finally, the gene expression encodes the synthase to result in the overproduction of AI, thus lead to a positive feedback loop that allows the bacteria to self-assess the density of their microbial population.

In the case of many Gram-negative bacteria, AI belongs to the family of acyl-homoserine lactones (AHLs) (**Fig 3**). The  $\beta$ -position of the amide function could be a ketone or OH, and the length of the acyl chain may vary from 4 to 18 carbons. These differences induce specific natural AI, for example, in *Vibrio fischeri* AI is 3-oxo-C6-HSL, the AI of *Pseudomonas aeruginosa* is 3-oxo-C12-HSL, and *Agrobacterium tumefaciens* employ 3-oxo-C8-HSL as their communication signals (**Fig 3**).

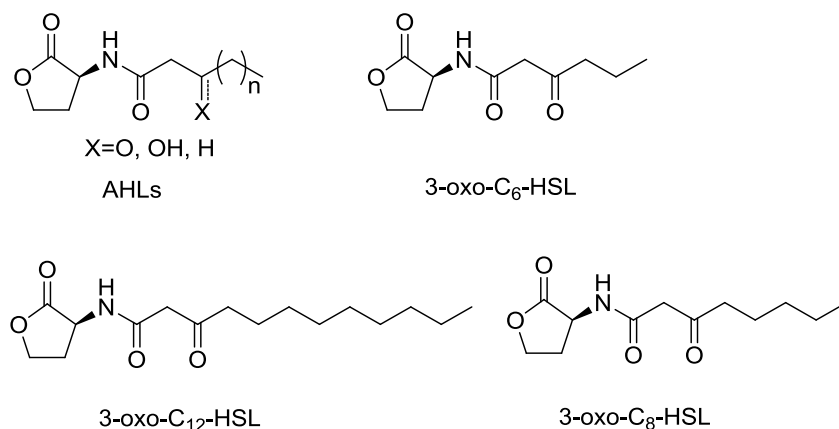
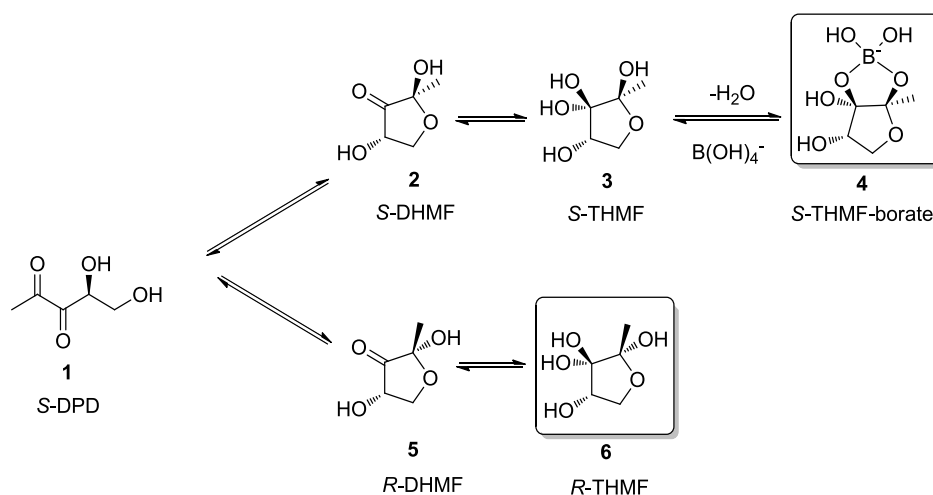


**Fig 3. Structure of AHL type of autoinducers of QS in Gram-negative bacteria**

Apart from AHLs, a number of other signals could also be used for sensing bacteria cell density. The most widely studied are the oligopeptides used by many Gram-positive bacteria. Recently, a family of molecules generically termed autoinducer-2 (AI-2) has been found (**Scheme 1**).<sup>[36]</sup> It has been proposed that AI-2 is a non-species-specific autoinducer that mediates intra- and interspecies communication among Gram-negative and Gram-positive bacteria.<sup>[36,37]</sup>

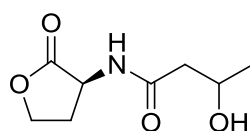


**Scheme 1. The AI-2 pool**

Complex equilibria involving (*S*)-DPD (1) and its derivatives are possible in water and in the presence of borate.

The boxed compounds have been described as known AI-2 signaling molecules.

AI-2 based QS was first identified in 1994 in the Gram-negative Bacterium *V. harveyi*.<sup>[38]</sup> It was observed that an AHL-lacking strain of the bacterium remained ability to produce bioluminescence even without the natural AHL autoinducer 3-hydroxy-C<sub>4</sub>-HSL (**Fig 4**).<sup>[39]</sup> It was presumed that there was a second QS pathway, a different signaling molecule was possible used for the effective action. This novel autoinducer has been elucidated since early 1990s, and was termed AI-2. Subsequently Bassler et al. studied cross-species induction of luminescence in the QS bacterium *Vibrio harveyi*, the result indicated that several species of bacteria, including the pathogens *Vibrio cholerae* and *Vibrio parahaemolyticus* could produce extracellular autoinducer-like activities which stimulate the expression of the luminescence genes in a *V. harveyi* AI-2 reporter strain.<sup>[14]</sup> This suggested that the AI-2 signal may be produced by numerous bacterial species. In 1999, B. L. Bassler and her coworkers found that AI-2 biosynthesis in *V. harveyi*, *E. coli*, and *S. typhimurium* were owed to the same gene.<sup>[40]</sup> This gene was primarily found in over 70 bacterial species and designated luxS.<sup>[39]</sup> From the reported studies, the LuxS gene, produced by the enzyme LuxS, is likely to be responsible for the production of AI-2.<sup>[41]</sup> The above studies combined with the current research proposed AI-2 is a universal signaling molecule language for interspecies communication.<sup>[42]</sup>



3-hydroxy-C<sub>4</sub>-HSL

**Fig 4. Autoinducer of *V. harveyi***

Based on the study of AI-2, several approaches have been proposed targeting the modulation by AI-2 QS system. Such as targeting AI-2 synthesis, AI-2 receptors and modulating LuxR activity. The following are some compounds designed for modulation of AI-2 QS system. Zhou et al.<sup>[43]</sup> reported four naturally occurring brominated furanones **7-10** which were initially isolated from marine red algae, could covalently modify and inactivate LuxS (S-ribosylhomocysteine lyase) and inhibit the production of AI-2, consequently inhibit bacterial biofilm formation, swarming and QS (**Fig 5**).

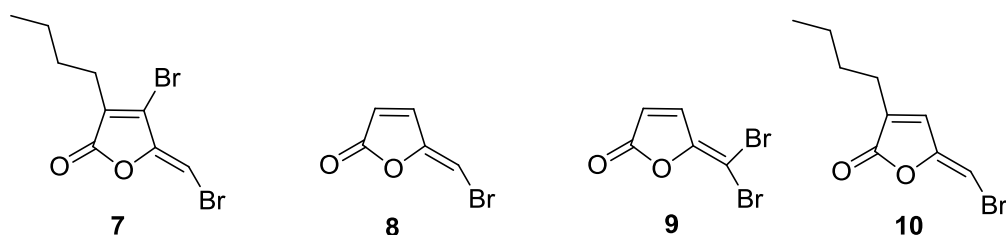


**Fig 5. Structures of brominated furanones**

Two compounds identified by library screening by Li et al. exhibit the highest inhibitory activities against AI-2-mediated luminescence without displaying cytotoxic effects in *V. harveyi* strain MM32.<sup>[44]</sup> The most active compound was **11** (approximately 1.5 times more active than **12**) (**Fig 6**).

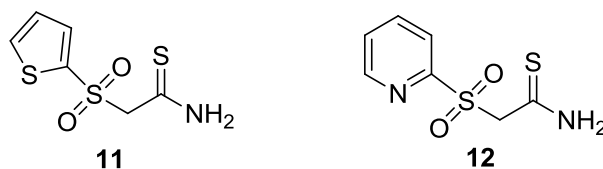


**Fig 6. Novel AI-2 QS inhibitors against *Vibrio harveyi***

Among all bacteria strains, *Pseudomonas aeruginosa* is the mostly reported and studied. *Pseudomonas aeruginosa* is an opportunistic human pathogen that usually appears near the top of public health threat lists worldwide. It causes infections by secreting a wealth of exceptionally active exo-products, leading to tissue damage.<sup>[45]</sup> There exists a hierarchy of QS regulation in *Pseudomonas* by which LasR activation triggers the successive activation of the RhlR and PQS systems (2-heptyl-3-hydroxy-4(1H)-quinolone (termed the *Pseudomonas* quinolone signal or PQS).

Regarding its discovery, in 1999, Pesci et al.<sup>[46]</sup> found unexpectedly that the addition of spent culture supernatant from wild-type cells of the type strain PAO1 was able to greatly stimulate the expression of a lasB'-lacZ reporter constructing in a lasR mutant. Normally, in the absence of lasR, the las and rhl signaling pathways should be inactive and minimally active, respectively. Furthermore, addition of purified OdDHL ((*S*)-N-(3-oxo-decanoyl)-L-homoserine lactone) or BHL ((*S*)-N- Butanoyl-L-homoserine lactone) did not induce the same degree of stimulation as the wild-type culture supernatant did. These findings indicated that a third QS

signaling molecule might be present, which has high potency but has not been characterized yet. The same wild-type culture supernatant did not stimulate lasB expression in a lasI rhlI double mutant, suggesting that LasR might be required for the bioactivity of the new signals. However, additional experiments indicated that LasR was unlikely to be the receptor for the new signaling molecule, indicating that, regardless of the nature of the signal, it probably interfaces with the AHL-dependent QS system at some point between the las and rhl pathways. Subsequent fractionation of the wild-type spent culture supernatant and detailed chemical analyses of the bioactive fractions revealed that the new signaling molecule was an alkyl quinolone, 2-heptyl-3-hydroxy-4-quinolone, or *Pseudomonas* quinolone signal (PQS: **Fig 7**).

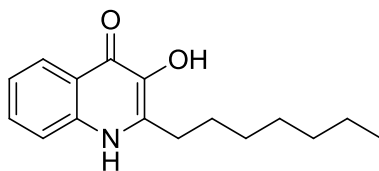


**Fig 7. Structure of PQS**

PQS affects virulence in several ways.<sup>[45]</sup> Initially, PQS directly induces expression of its own biosynthetic gene cluster (pqsA-E) in a PqsR-dependent fashion. Then the expression of many virulence genes was influenced by PQS-dependent PqsE expression indirectly, through modulation of RhIR activity. Subsequently, as a potent post-transcriptional regulator, the expression of RsmA was conducted by PqsR/PQS. And next, PQS controls the formation of extracellular trafficking vesicles. Finally, PQS rapidly depletes the culture of iron by trapping it in an insoluble form due to its iron chelating capability. This iron trapping may have secondary effects, since iron depletion affects rhl signaling by enhancing rhIR transcription.

*P. aeruginosa* produces two primary 4-quinolone/quinolones QS molecules, 2-heptyl-4(1H)-quinolone (HHQ) and PQS,<sup>[46]</sup> as well as other 4-quinolone/quinolones,<sup>[47,48]</sup> many of which remain to be functionally characterized. Coincidentally, some commercially synthesized quinolone antibiotics **15**, **16** share the same basic 4-quinolone backbone with 4-quinolone/quinolones QS molecules produced by *P. aeruginosa*. Interestingly, *P. aeruginosa* produces 4-hydroxy-2-heptylquin-oline-N-oxide (HQNO), bearing 4-quinolone backbone and

possessing antibiotic activity,<sup>[49]</sup> though its mechanism of action differs from that of synthetic quinolone antibiotics (**Fig 8**).<sup>[50]</sup>

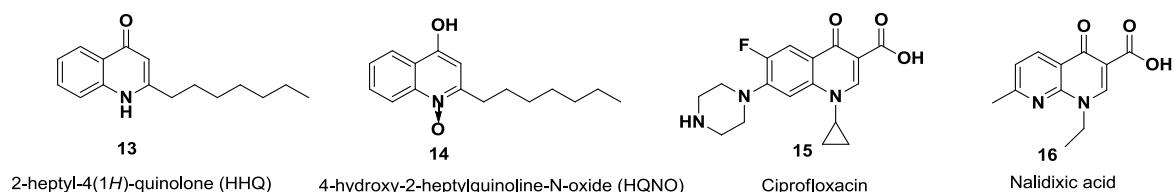


**Fig 8. Structures of common QS signals and synthetic quinolone antibiotics**

## 1.2 Strategies for designing QS inhibitors and modification of AHLs

### 1.2.1 Application interests

The phenotypes regulated by QS in bacteria are full of varieties. For example, the expression of virulence factors, antibiotic production, mobility, bioluminescence or control of biofilm formation are all regulated by QS.<sup>[51]</sup>

In this context, the QS inhibition appears as a new possible strategy for fighting against pathogenic bacteria, by decreasing the production of virulence factors without destructing the bacterial strain. In other words, this would be a bacteriostatic strategy rather than a bactericidal one. This mechanism may be less likely to cause multi-resistant as it would be harmless to bacteria. It could also make them more vulnerable by undermining biofilm, in which bacteria are much more resistant to the immune system and to the traditional antibiotics.

### 1.2.2 Modulation of QS

There are four general strategies which can be devised to inhibit QS and have led to considerable research in the past two decades<sup>[52][53]</sup>. The first and second ones are destruction or sequestration of AI in the extracellular medium before it can be recognized by the transcriptional factor. The third one is inhibition of the biosynthesis of AI by controlling the synthases. The fourth one is the most developed approach inhibiting complex formation (transcription factor/AI) by the use of antagonist analogues which do not induce the biological effect that caused by the natural ligand: the complex formed is then allowed to express the genotype more.

In the latter strategy, there are three possible approaches:<sup>[53]</sup>

- the synthesis of compounds with structures close to that of the autoinducers,
- the synthesis of analogues of natural antagonists,
- the screening (real or virtual) of biological or virtual chemical libraries.

The synthesis of AI analogs based on the changes made on three elements of the structures of AHLs:<sup>[53]</sup> the lactone ring (1), the amide connective function (2) and the side chain including the characteristic carbonyl or hydroxyl substitution or lack thereof at the C-3 position (3) (**Fig 9**). Overall, the three areas endow the AHL amphiphilic. The lipophilic acyl chain varying in long chain is favorable for the diffusion through the membranes and contributes to ligand binding within the receptor pocket. The amide function provides a strongly polar moiety to AHLs, with a high potential to serve as a H-bond donor or acceptor. The lactone ring is subject to degradation by lactonases released into the environment by neighboring bacteria. Apart from screening of libraries of synthetic compounds or natural extracts, some structural analogues could also be designed and synthesized, which is very useful for discovering ligand agonists or antagonists.

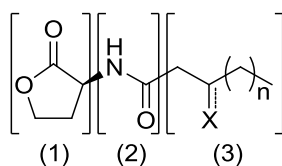


**Fig 9. The three parts in the structure of AHLs**

For the modification of the lactone (1), it could be replaced by either carbocyclic or heterocyclic rings, since the lactone headgroup is a common motif in all AHLs and these two types of groups could not be degraded by AHL degrading enzymes, which would exhibit a broader application range. Thus, there are lot of alterations for the lactone rings, such as thiolactones **18**, lactams **17**,<sup>[54]</sup> halogenated furanones **7-10**,<sup>[55,56]</sup> cycloalkanols **22**,<sup>[57]</sup> cycloalkanones **23**,<sup>[58]</sup> aromatic rings **24** and **25**,<sup>[59]</sup> cyclopentanes **19**,<sup>[60]</sup> enamino-lactones<sup>[61]</sup> **27** and **28** and so on (**Fig 10**). In some cases, the substitution of the lactone (1) with an ethyl ester preserved the activity.<sup>[62]</sup>

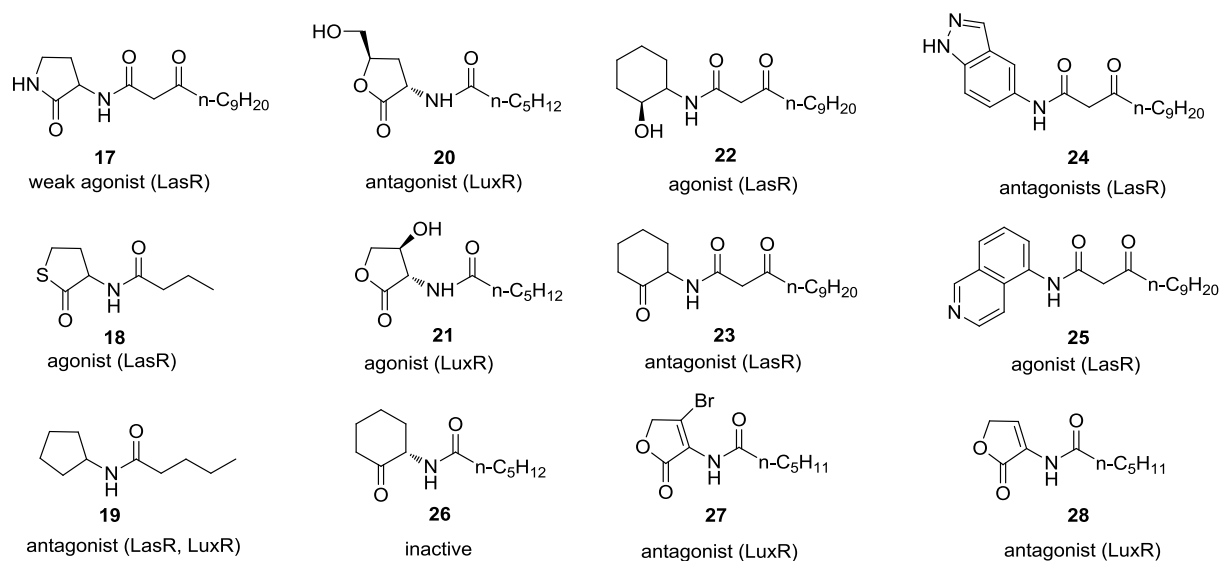


**Fig 10. Examples of alterations for the lactone ring**

A number of changes have been studied in our laboratory. The influence of the side chain, region (3) has been investigated. Some AHLs analogs bearing a modified alkyl chain **29** and **30** seem to show agonistic activities of QS, but when this chain is substituted by an aryl chain, compound **31** and **32** shows antagonistic activities (**Fig 11**).<sup>[63]</sup> Furthermore, depending on the side chain, an AI may show significantly different activities from one bacterial species to another.<sup>[64]</sup>

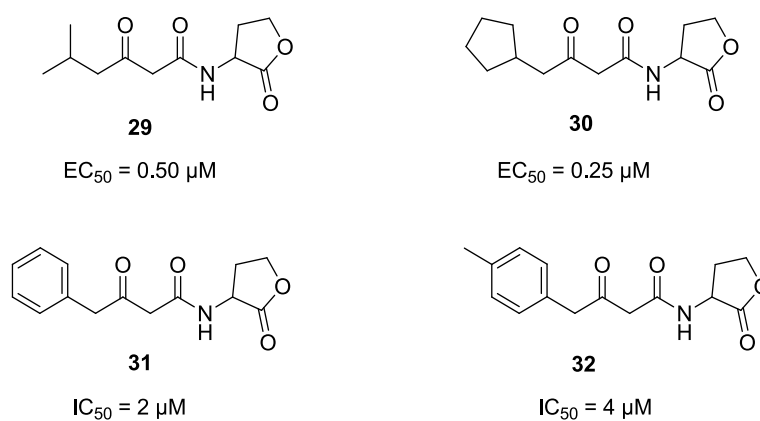


**Fig 11. Changes in the side chain of AHLs**

For the region (2), certain compounds in which the amide function was replaced by a bisosteric function, such as sulfonamides **33** and **36**,<sup>[65]</sup> urea **34** and **37**,<sup>[66]</sup> sulfonylurea **35**

and **38**,<sup>[67]</sup> were synthesized in the laboratory. Each change was evaluated by measuring its efficiency (antagonist or agonist) in bioassays (**Fig 12**).

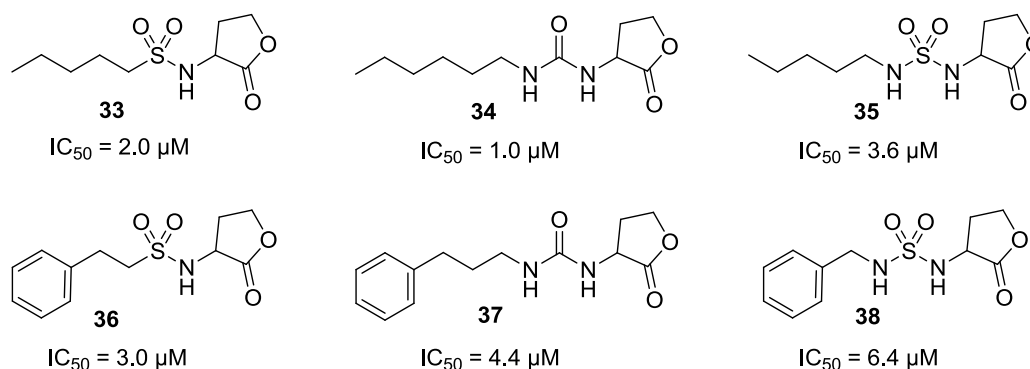


**Fig 12. Main antagonists QS synthesized in the Lyon laboratory in recent years**

Apart from AHLs, some bacteria strains use a large number of other signals to sense cell density. Many Gram-negative bacteria such as *V. harveyi* use the AI-2 molecules (e.g. brominated furanones) for intra-species communication. In addition, there are other seemingly less widely distributed QS signals such as HHQ,<sup>[68]</sup> and PQS which involves QS regulation in *Pseudomonas*,<sup>[46]</sup> diketopiperazines (DKPs)<sup>[69]</sup> belongs to AHL-family signals that could activate LuxR-type receptors, and 3-hydroxypalmitic acid methyl ester (3-OH PAME),<sup>[70]</sup> bradyoxetin,<sup>[71]</sup> autoinducer in *Escherichia coli* (AI-3).<sup>[72]</sup> Thus, based on this many types of autoinducers and QS systems, more strategies would be proposed to stimulate or inhibit QS regulation.

### 1.3 AHL Heterocyclic analogues

It has been widely reported that AHLs analogues varying in lactone, amide function and side chain exhibited agonist or antagonist activities as shown in previous section. For example, the replacement of the amide by bioisostere functions sulfonamide,<sup>[65]</sup> urea,<sup>[66]</sup> sulfonylurea,<sup>[67]</sup> triazole and tetrazole<sup>[62]</sup> was investigated. In the area of medicinal chemistry, heterocycles are frequently used as a scaffold for designing bioactive compounds. However, to our best knowledge, although millions of heterocyclic compounds are widely applied in drug design, within the field of QS modulation, only a rather modest number of AHL analogues built on a central heterocycle have been reported. One example is a tetrazolic compound described by

Greenberg's group<sup>[73]</sup> in 2006, who screened approximately 200,000 compounds and tested as inhibitors of QS in *Pseudomonas aeruginosa* that uses 3-oxo-C12-HSL as AI.<sup>[73]</sup> This screening led to identification of a compound having a strong antagonist activity: tetrazole PD12 (IC<sub>50</sub> = 30 nM (**Fig 13**)).

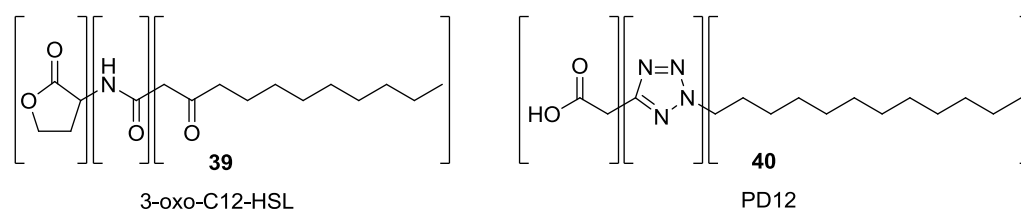


**Fig 13. Structure of an antagonist QS in *Pseudomonas aeruginosa*-discovered by screening libraries, compared with the natural AI**

Due to the great diversity of studied structures in this screening, it was difficult to make conclusive structure-properties relationships, but it is highlighted that the only positive outcome of this screening was obtained from compounds with similarities to natural AI. In fact, when the PD12 is compared with 3-oxo-C12-HSL, it mimics the natural AHLs three zones: the lactone is replaced by the carboxylic acid, the tetrazole imitates the amide function, and the side chain keto alkylated is replaced by the alkyl chain. Our group also contributed to search for new heterocyclic systems with one family of imidazolium compounds, as well as series of new AHL analogues, based on the 1,2,3-triazole or 1,2,3,4- tetrazole scaffolds (**Fig 14**, compounds **41-44**), which were found to be LuxR-dependent QS agonists or antagonists.<sup>[74]</sup>

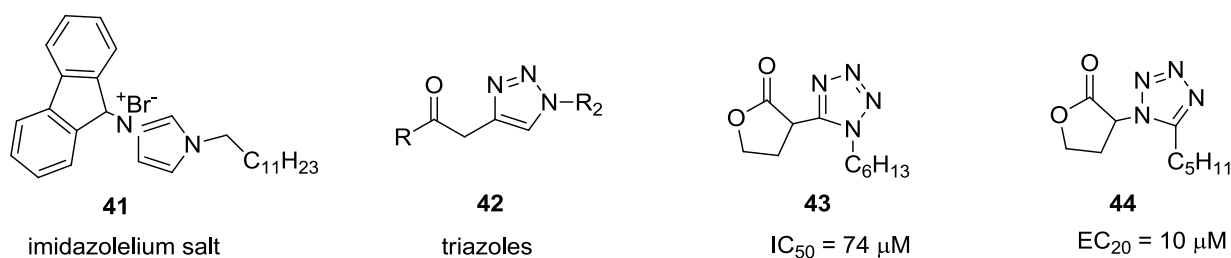


**Fig 14. LuxR-dependent heterocycle QS agonists or antagonists**

Those series of compounds shown in **Fig 14**, as well as other analogues of QS autoinducers (AHL or other types) comprising a heterocyclic moiety in their design reported in literature, are reviewed in the next section. There are classified with respect to the size (five or six) of the

heterocycle, and the nature of heteroatom(s), nitrogen, oxygen, sulfur, or combinations of more than one heteroatom.

Below are described heterocyclic compounds designed with analogy to QS autoinducers. Some heterocycles can contribute to the essential hydrogen bonding normally found between the AHL amide group and ligand such as triazoles, tetrazoles and etc. With respect to AI-2 analogues, there is a wide range of heterocyclic compounds, such as natural brominated furanones, carbohydrate nucleoside, fatty acid-derived heterocyclic systems, and so on. Regarding PQS system, a large family of 4-quinolones provides us a useful toolkit for designing diverse QS signaling molecules. All those compounds are discussed below.

### 1.3.1 Five-membered rings heterocyclic analogues

#### 1.3.1.1 Structure variation

In general, there are many isomeric types of heterocyclic compounds containing nitrogen and oxygen. For example, triazole **45**, tetrazoles **43-46** which exhibited either an agonist or an antagonist as shown in **figure 15**, and oxadiazoles (which are discussed in chapter II). Although so many possible changes occurred theoretically in the modification of five-membered-ring heterocyclic, most of them have different purpose in different fields. For example, triazoles and tetrazoles heterocycles in substitution of the amide function show encouraging results on the use of heterocycles as bioisosteres the peptide bond.<sup>[74]</sup> The highlighted structures in **figure 15** which are aromatic compounds would be considered as the potential scaffold for designing AI mimics. Below thesis we only introduce analogues bearing nitrogen, oxygen, sulfur and other rare heteroatoms boron.

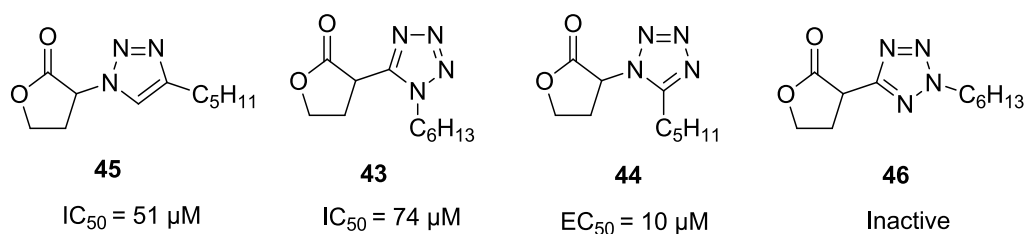
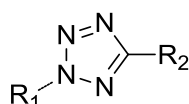


**Fig 15. Bioactivities of triazoles and tetrazoles derivatives**

### 1.3.1.2 Analogues bearing nitrogen

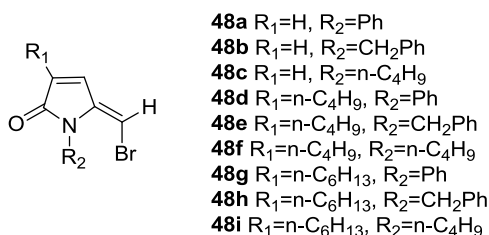
In 2006, a series of tetrazolic compounds were firstly described by Greenberg's group.<sup>[73]</sup> A microarray analysis showed that a tetrazole with a 12-carbon alkyl tail designated PD12, had a 50% inhibitory concentration (IC<sub>50</sub>) of 30 μM. Other compounds also inhibited the production of two QS dependent i.e. virulence factors, elastase and pyocyanin (**Table 1**). These compounds should be useful for studying LasR-dependent gene regulation and might serve as scaffolds for the identification of new QS modulators.

**Table 1. The structure-function relationship of selected tetrazole analogs**



Compounds	R <sub>1</sub>	R <sub>2</sub>	Inhibition (%)
<b>47a</b>	C <sub>6</sub> H <sub>13</sub> (N-2)		-17
<b>47b</b>	C <sub>8</sub> H <sub>17</sub> (N-2)		45
<b>PD12</b>	C <sub>12</sub> H <sub>25</sub> (N-2)		76
<b>47c</b>	C <sub>14</sub> H <sub>29</sub> (N-2)	CH <sub>2</sub> COOH	77
<b>47d</b>	C <sub>6</sub> H <sub>13</sub> (N-1)		10
<b>47e</b>	C <sub>8</sub> H <sub>17</sub> (N-1)		-18
<b>47f</b>	C <sub>12</sub> H <sub>25</sub> (N-1)		-4
<b>47g</b>	C <sub>14</sub> H <sub>29</sub> (N-1)		20

In 2007, N. Kumar<sup>[75]</sup> synthesized a series of novel dihydropyrrolones **48a-48i** using a lactone-lactam conversion reaction of fimbrolide. All compounds were considered to be able to inhibit the bioluminescence of *Serratia liquefaciens*. Thus, these pyrrolones have been proven to be effective QS inhibitors (**Fig 16**).

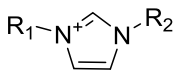
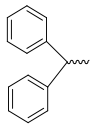
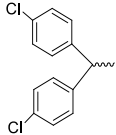
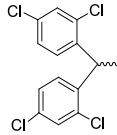
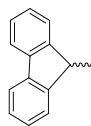


**Fig 16. A series of novel dihydropyrrolones**

In 2011, A. Doutheau and co-workers investigated LuxR dependent QS inhibition of *N,N'*-di-substituted imidazolium salts.<sup>[74]</sup> In this work, they synthesized and evaluated as LuxR modulators thirty *N,N'*-di-substituted imidazolium salts with various lengths of N-alkyl chain including benzhydryl, fluorenyl or cyclopentyl substituent (**Table 2**). The results showed that most of these compounds displayed antagonist activity. Among all of tested compounds, compound **49f1** was the most potent inhibitor, whereas the other alkyl substituted benzhydryl imidazolium salts with C6 to C16 chains exhibited activities with IC<sub>50</sub> ranging from 153 to 5.2 μM. The *N*-benzhydryl derivatives bearing an alkyl chain ending with a phenyl group or a benzyl ether substituent were inactive, as well as the short chain compounds with C4. This sensitivity to chain length is consistent with the known importance of hydrophobic interactions within the binding site for several other families of QS modulators.<sup>[53]</sup> In the case of dichloro- or tetrachloro-benzhydryl compounds having C6 to C18 alkyl chains, IC<sub>50</sub> ranged in the same order of magnitude from 75 to 4.9 μM. However, the optimal chain length of the alkyl substituent was different when compared with non-halogenated compounds, compound **49d3** being the most active in comparison with compound **49f1**. In this series of tetrachloro-benzhydryl, compounds with longer chains, were significantly less active or inactive. The differences between these two series suggested that the variation of the occupied volume in the ligand binding site by the benzhydryl moiety due to the presence of several bulky halogen atoms must be compensated by a smaller size of the alkyl side chain. As for fluorenyl derivatives, the capability of inhibition was enhanced with the increasing chain length up to C14, the longer C16 analogue **49f3** was less active. Cyclopentyl derivatives containing C8-C18 have also been evaluated. As the results indicated that a longer chain is necessary for achieving sufficient binding. Even the longer *N*-cyclopentyl-*N*- C18 remained moderately active. Molecular modelling showed that the fluorenyl moiety replaces the lactone group of the natural ligand 3-oxo-C6-AHL and binds the same space with Trp66 and Trp94. The imidazolium ring mimicking the amid function is located between aromatic residues of Tyr62 and Tyr70 at distances compatible with cation-*π* interactions.<sup>[76]</sup> And the alkyl chain occupies the same space where the alkyl chain of the natural ligand normally sits, interacting with hydrophobic residues, in particular Ile46, Ile56, Ile58, Ile76 and Pro48. Similar docking of the other most active

compounds in each series showed same overall interactions and binding modes. In conclusion, the di-substituted imidazolium scaffold was identified as a new potential pharmacophore in the field of AHL dependent QS inhibition.

**Table 2. Inhibition of bioluminescence with compounds containing various groups**

No.		R <sub>1</sub>				
						
	R <sub>2</sub>	1	2	3	4	5
<b>49a</b>	C <sub>4</sub> H <sub>9</sub>	inactive				
<b>49b</b>	C <sub>6</sub> H <sub>13</sub>	153	63	52		
<b>49c</b>	C <sub>8</sub> H <sub>17</sub>	76	9.8	8.9	35	68
<b>49d</b>	C <sub>10</sub> H <sub>21</sub>	18	5.8	4.9	4.0	33
<b>49e</b>	C <sub>12</sub> H <sub>25</sub>	6.1	6.2	6.5	1.4	11
<b>49f</b>	C <sub>14</sub> H <sub>29</sub>	5.2	75	inactive	2.7	3.4
<b>49g</b>	C <sub>16</sub> H <sub>33</sub>	7.3			14.7	5.3
<b>49h</b>	C <sub>18</sub> H <sub>37</sub>		inactive	inactive		86
<b>49i</b>	CH <sub>2</sub> Ph	inactive				
<b>49j</b>	(CH <sub>2</sub> ) <sub>2</sub> Ph	inactive				
<b>49k</b>	(CH <sub>2</sub> ) <sub>2</sub> OCH <sub>2</sub> Ph	inactive				

In 2012, A. Doutheau, L. Soulere and Y. Queneau designed a new series of compounds based on triazole and tetrazole scaffolds which replaced the function amide, and evaluated their activities as LuxR-dependent QS modulators.<sup>[62]</sup> Among all synthesized 1,4- and 1,5-disubstituted tetrazoles, only compounds substituted with a short alkyl chain (C<sub>6</sub> and C<sub>5</sub>) displayed significantly either antagonistic (**Fig 17**: compounds **43** and **53**) or agonistic activities (compounds **44** and **51**). Interestingly, the position of the nitrogen atoms in the tetrazole ring was able to convert the antagonist tetrazoles **43** and **53** into the agonist isomeric tetrazoles **44** and **51**, namely in 1,5-disubstituted tetrazoles with a short alkyl chain, the C–N connected compounds were agonists whereas the C–C connected ones were antagonists. However, the 2,5-tetrazolic compounds were inactive. Molecular modeling of compound **43** and **44** showed both compounds occupy the same area within the active site as the 3-oxo-C<sub>6</sub>-HSL. For antagonist **43**, the similar interactions as the natural ligand could be observed, and there are

obvious hydrogen bonds between the heterocycle and Tyr70, and possible also with Tyr66. For agonist **44**, two hydrogen bonds with Trp 66 and Tyr 62 could explain its activity, and the differences of interaction between the heterocycle with Tyr62 or Tyr7 may demonstrate why one is agonist and another is antagonist. This study demonstrated that the multi-nitrogen heterocycles could serve as scaffolds for designing new QS modulators.

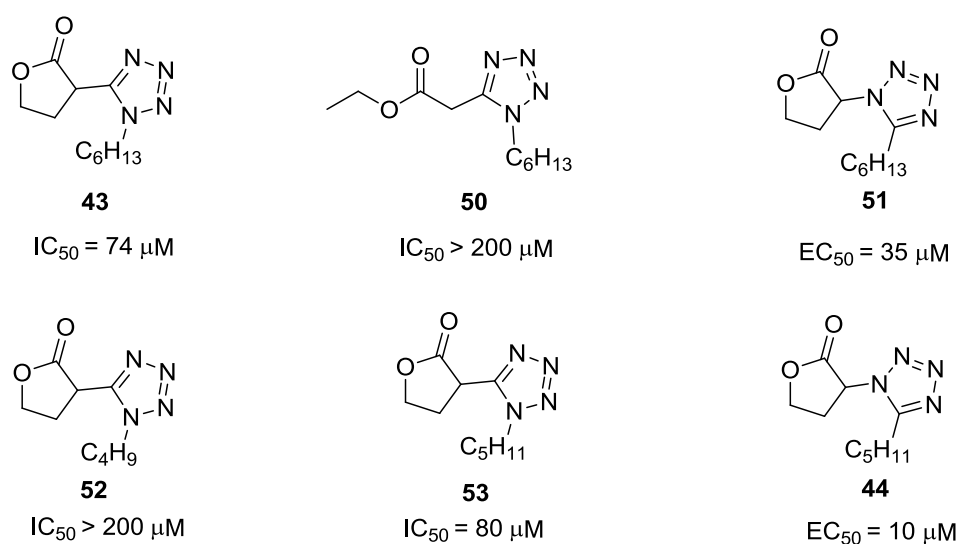


**Fig 17. Inhibition or induction of bioluminescence obtained with compounds**

G. Brackman and his co-workers<sup>[77]</sup> synthesized a series of substituted triazolylidihydrofuranones based on the imitation of amide function by triazole rings in 2012 (**Fig 18**). The compounds were tested for their ability to decrease fluorescence production in an *Escherichia coli* JB523 biosensor strain. All compounds displayed a concentration dependent antagonistic activity, but a loss of activity was observed when replacing the amide with a triazole. Their ability of inhibiting LasR-dependent QS in *P. aeruginosa* QSI2 assay varied in different substituents. Compounds **54a–e** and **54h** were inactive. In contrast, **54f**, **54g**, **54i** and **54j** were moderately potent inhibitors. The results indicated that all compounds can interfere with the LuxR QS system, while only compounds having a C10 or C12 chain length inhibit the LasR QS system. Although the phenyl-substituted triazole compounds acted as active antagonists in both biosensors, compounds best resembling the native signal molecule were the most active. For the inducing evaluation, compounds **54a–e** and **54h** displayed agonistic activities to LuxR QS system, compounds **54e–54j** exhibited moderate agonistic activity to

LasR QS system. These results indicated that compounds with a relatively short acyl chain (4–8 carbons) act as agonists in a short-acyl chain sensitive biosensor, while compounds with relatively longer acyl chains (**54f–g**) or bulky substituents (**54i–j**) are incapable of activating QS in this biosensor. In addition, the most active QSI **54e**, **54g** and **54j** exhibited strong inhibitory and eradicating activities against *B. cenocepacia* and *P. aeruginosa* biofilms.<sup>[77]</sup>

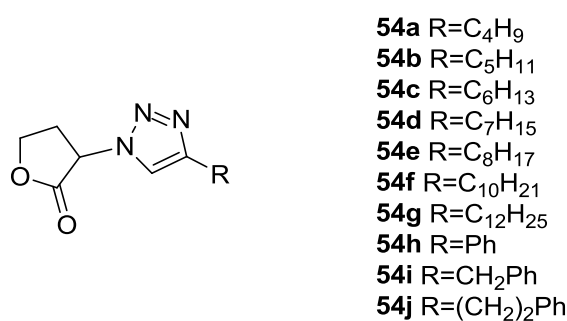


**Fig 18. A series of substituted triazolodihydrofuranones as QSI**

In 2013, Helen E. Blackwell et al<sup>[78]</sup> synthesized five types of triazole derivatives using efficient Cu(I)-catalyzed azide–alkyne couplings (**Fig 19**). These compounds were evaluated for their abilities of agonizing or antagonizing two QS receptors LasR and AbaR – in the clinically relevant pathogens *P. aeruginosa* and *A. baumannii*, respectively. As for LasR antagonism by triazole HLs, among of five types of compounds, the type **55** and **56** triazole HL analogs demonstrated enhanced potency in comparison with the reported AHL analogs with triazole and tetrazole units in place of the native amide bond.<sup>[78]</sup> In the case of compounds **55**, triazole HLs with short alkyl chains were LasR antagonists, while with longer chains were LasR agonists. And acyl chain lengths that mimic native AHL ligands can lend agonistic activity to triazole HLs. For the cycloalkyl triazole derivatives in the type **55** triazole library, with larger ring structures were stronger LasR antagonists than those with smaller rings, and with aryl acyl groups were found to antagonize LasR. The LasR antagonism activity trends for the type **56** triazole HLs were consistent with those observed for type **55** ligands with similar structural scaffold. And for type **56** compounds, inclusion of triazole functionality into the phenylacetanoyl-HL scaffold can augment their inhibitory activity against LasR. Within the type **57** triazole HL library, the phenylthioether derivatives **57c** and **57d** were the most potent LasR antagonists, other members of this library were only weak LasR antagonists, but the *para*-

triazole HL isomers were still typically the most potent. In the case of type **58** triazole HLs, the *para*-substituted were generally stronger LasR antagonists than their *meta*-substituted analogs. LasR antagonism likewise increased with alkyl substituent length, and the size of cycles. However, the *meta*-substituted ligands were more active than the *para*-substituted ligands in the case of type **58** triazole HLs contained relatively bulky aryl substituents. The type **58** triazole HLs contained heterocyclic moieties or related heteroatom substituents were less active than their corresponding type **55** analogs, while the aryl thioether **58ae** was a strongest LasR antagonist ( $IC_{50} = 2.64 \mu M$ ) among all tested compounds, and it was also proved to be a most potent AbaR antagonist ( $IC_{50} = 2.64 \mu M$ ). Interestingly, the structurally related type **55** ligand (**i-n**) was a strong LasR agonist instead, and it was also a the most potent AbaR agonist identified.

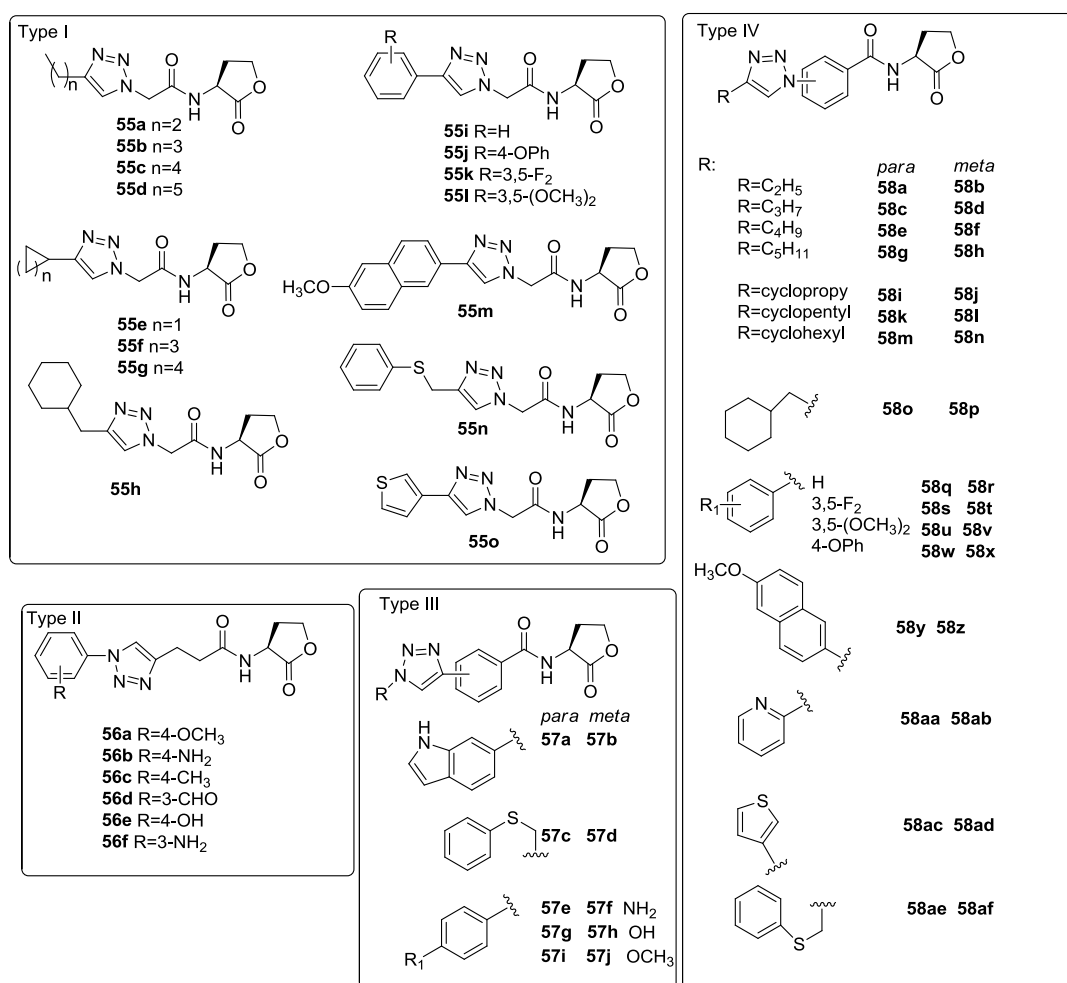
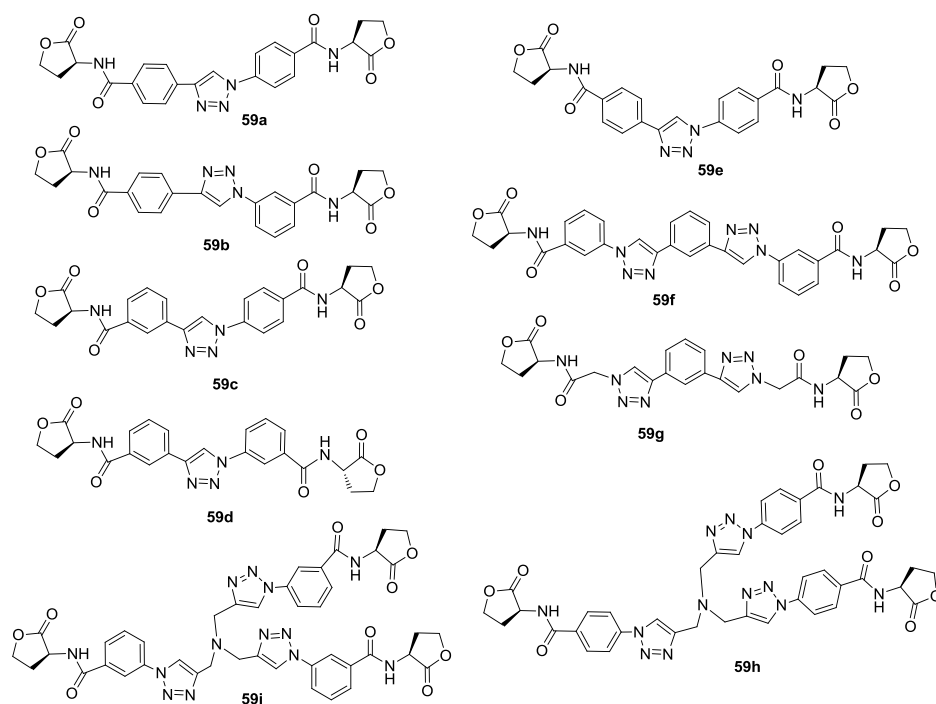


Fig 19. Four types of triazole derivatives

In addition, a type **59** triazole HL library contained derivatives with multiple HL rings linked together by a triazole ring, a phenyl ring or a tertiary amine were also synthesized and bio-evaluated (**Fig 20**). These multivalent scaffolds were only modestly active as LasR antagonists, and the dimeric compounds (**59a-59f**) were more potent than the two trimeric compounds. The ability of all triazole HLs agonizing LasR were evaluated using the *E. coli* strain, only compound **55c**, **55d**, **55h**, **55n**, **56d**, **56f**, **59h** were capable of more than 10% LasR agonism relative OddDHL at 100  $\mu$ M. The rest of derivatives exhibited moderate or no agonistic activity. They also made a SAR trends for LasR and AbaR modulators. The agonistic or antagonistic activity depended on the side chain i.e. long alkyl chain was favorable for LasR agonistic activity, and phenyl thioether was probably favorable for both LasR and AbaR agonistic activity, and for the other substituents such as short alkyl chain, cycloalkyl, phenyl was likely to be responsible for antagonistic activity in both bases. Moreover, the multiple substituents and saturated linear or cycloalkyl were more likely to be LasR antagonist. This study revealed that triazole HLs present a unique scaffold for the modulation of LuxR-type receptor activity and probably find utility as chemical tools to study QS and their role in bacterial virulence.<sup>[78]</sup>



**Fig 20. Structures of the triazole homoserine lactone library**

In 2015, based on the previous studies of triazoles HL as QS modulators,<sup>[78]</sup> Thomas E. Nielsen et al.<sup>[79]</sup> synthesized a range of new 1,2,3-triazole-containing AHL analogues through a combination of solution- and solid-phase synthesis methods (**Fig 21**). All analogues and some 1,2,3-triazole-HLs reported in the previous section, were evaluated for agonistic and antagonistic activities in both *P. aeruginosa* (lasB- gfp; rhlA-gfp) and *E. coli* (luxI-gfp). Among all tested compounds, only compound **56d** exhibited high potency for antagonizing luxI-gfp ( $IC_{50} = 5 \mu M$ ) and agonizing lasB-gfp ( $EC_{50} = 1 \mu M$ ), while none of the novel compounds **60**, **61** and **62** reported showed any noteworthy activities in any of the QSI screens.

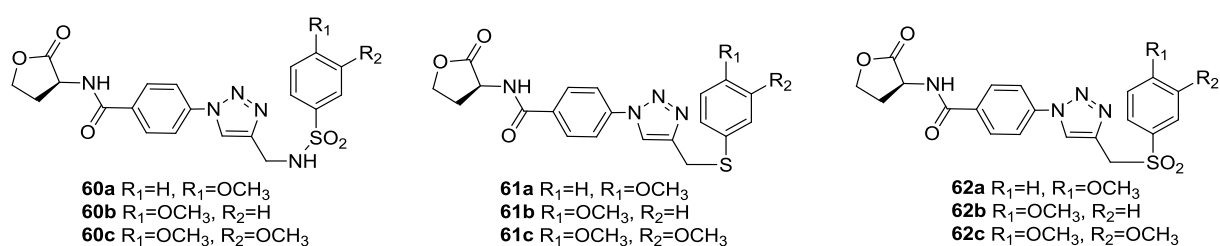


**Fig 21.** 1,2,3-triazole-containing AHL analogues

Previously, in a rather different approach dealing with the known QSI activity of some lipids, a family of synthetic QS molecules for *C. albicans* possess *in vitro* potency comparable to the natural signal of *E,E*-farnesol. Thus, some heterocyclic and oxime-containing farnesol analogs will be reported for their influence on QS and pathogenicity in *Candida albicans* in the following parts.

In 2007, Patrick H. Dussault et al.<sup>[80]</sup> synthesized a series of synthetic molecules combining a geranyl backbone with a heterocyclic or oxime head group, these QS molecules can block the yeast to mycelium transition in the dimorphic fungus *Candida albicans* (**Fig 22**). This design was based on the farnesol which could induce the population dependence of *C. albicans* morphology, and it was the first QS molecule to be discovered in a eukaryotic system. They developed a series of fluorescent farnesol analogs. Pentaene oxime **63** was found with excellent activity ( $IC_{50} = 10 \mu M$ ) and the oxime of farnesaldehyde **64a** was also a potent ( $IC_{50} = 5 \mu M$ ) but with higher toxicity in healthy mice when compared with **63**. However, the corresponding *O*-methyl ether, i.e. farnesaldehyde methoxyoxime **64b**, was inactive ( $IC_{50} > 100 \mu M$ ) which is

consistent with the results of earlier studies pointing to a requirement for an acidic head group.<sup>[81]</sup>

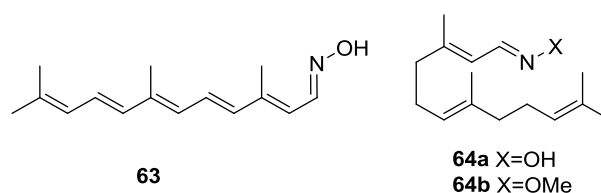


**Fig 22. Structure of farnesol analogues**

Based on the previous discoveries, they studied the replacement of the primary alcohol of farnesol with other acidic functional groups which has been identified as a weakly active QSM (**Fig 23**). Several analogs incorporating a tetrazole in place of C1–C3 of farnesol were chosen for the study object since 5-substituted-1*H*-tetrazoles are weak acids and often used as lipophilic isosteres for carboxylic acids.<sup>[82]</sup> Analogues **65a-65d** were prepared by cycloaddition of the appropriate nitrile with Et<sub>3</sub>NHN<sub>3</sub> and were active as QSM. Among those compounds, compound **65c** was the most active one with non-toxic properties, but it was only marginally soluble in water. Compound **65a** was proved to be a more potent QSM compared the previous research in their group and compound **65b**, and it also revealed that the chain length was crucial for its activity. The results implied a functional equivalency between styrene and 4,8-dimethyl-3,7-nonadiene side chains, suggesting that 3-methyl-5-phenyl-2,4-pentadienol or similar structures might represent productive future targets as synthetic QSMs.

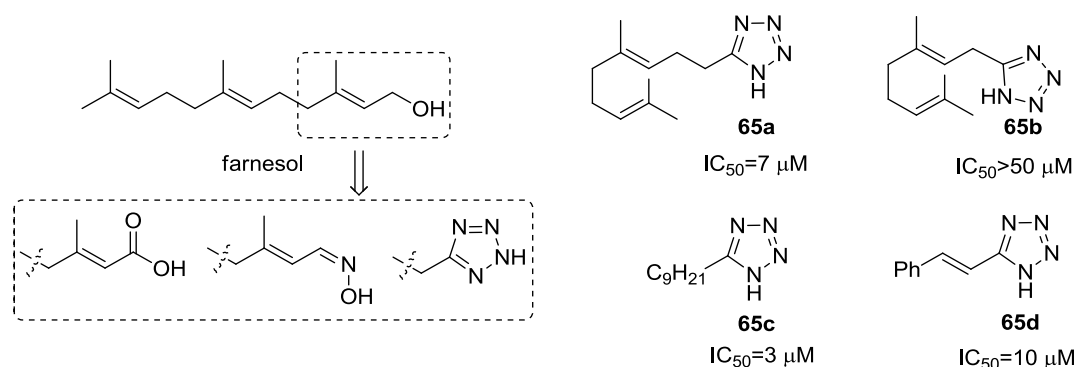


**Fig 23. Design concept of farnesol analogues and tetrazole analogues as QS molecules for *Candida*.**

*albicans*

Subsequently, the same team investigated some additional examples of five-membered heterocyclic analogs possessing the same approximate shape, cross-sections, lipophilicity, and molecular length.<sup>[80]</sup> They focused on sulfur-linked heterocycles, which are readily available via nucleophilic displacement and well-tolerated structural modification by the replacement of a methylene with a sulfur atom (thioether).<sup>[81]</sup> The results indicated that thiotetrazole **66a** and thioimidazole **66d** were only minimally active ( $IC_{50} > 50 \mu M$ ), triazoles **66b**, **66c**, and **66e** were potent QSMs (**Fig 24**). It is notable that two of the analogs (**66b** and **66e**) exhibit QSM activity equal to *E,E*-farnesol, with three other analogs (**65a**, **65c**, and **66c**) displaying surprising activities. And more importantly, none of the compounds shown in **Fig 23** and **Fig 24** are toxicity for the cell growth, even at the highest concentrations tested (100  $\mu M$ ).

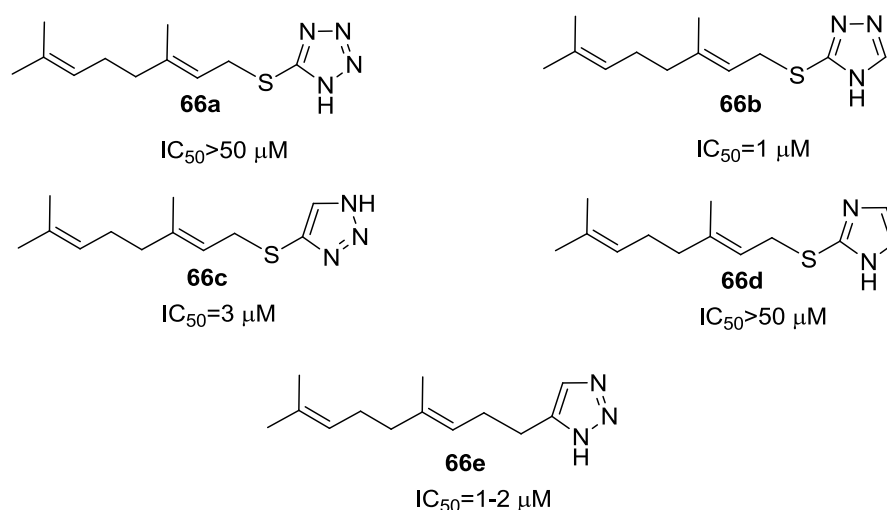


**Fig 24. Heterocyclic analogs as QSMs on candidiasis**

### 1.3.1.3 Analogues bearing oxygen and sulfur

Since the lactone headgroup is a key motif in AHLs, there are several reported analogues based on a modified lactone moiety, such as thiolactones, lactams, aromatic rings, enamino-lactones and so on. In this section, we firstly briefly review heterocyclic lactone analogues bearing oxygen or other heteroatoms.

Eberhardt and co-workers<sup>[83]</sup> firstly synthesized and evaluated the bioluminescence activities of acyl-homoserine-thiolactone (3-oxo-C6-HTL) **67a** and the seven-membered lactam **68** in *V. fischeri*. It was found that compound **67a** was a strong antagonist of 3-oxo-C6-

HSL induction with weak agonist activity whereas compounds **68** was a weak inhibitor for *V. fischeri*. For the SdiA dependent QS, compound **67a** is a strong agonist and compound **68** is inactive. Then Schaeffer et al. tested the longer C12 thiolactone **67b** which was proved to be an inhibitor at higher concentration for LuxR dependent QS such as *V. fischeri*. However, **67b** was an agonist when evaluated with LasR,<sup>[84]</sup> probably due to the structure similarity with the native 3-oxo-C12-HSL, while its lactam counterpart **69** was considerably less active (**Fig 25**).

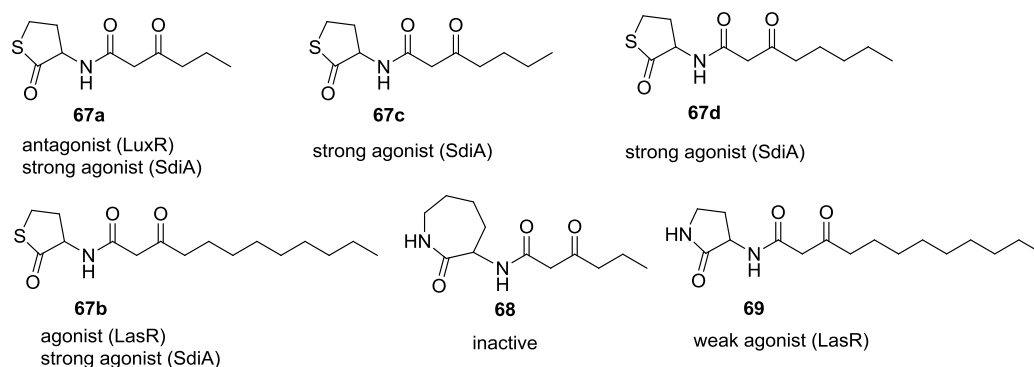


**Fig 25. Some thiolactones and lactams AHL analogues**

In 2002, Ikeda investigated the bioassay of enantiomeric *N*-acyl-homoserine thiolactone (HTL) **70** in *P. aeruginosa*. The L-isomer is likely to be responsible for the QS modulation while the D-isomer was inactive.<sup>[85]</sup> Then a series of AHL analogues and its acylated derivatives including the homocysteine lactone **71** were synthesized and tested on LuxR of *V. fischeri* and SdiA of *S. entericaserovar Typhimurium* by Janssens et al.<sup>[86]</sup> Compound **71** was a weak agonist, surprisingly its acylated derivatives with side chain from C6 to C12 were strong agonist for SdiA but inactive for LuxR (**Fig 25, Fig 26**). Compounds **67a-d, 68, 69, 70, 71** are thiolactones and lactams AHL analogues, playing an important role in the follow-up work and also giving researcher more ideas to design active heterocyclic analogues bearing oxygen and sulfur.

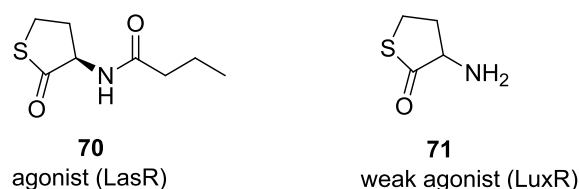


**Fig 26. Thiolactones AHL analogues**

In 2006, Riedel et al. made some attempts to look for QS inhibitors for the opportunistic pathogen *Burkholderia cenocepacia* by virtual screening (**Fig 27**).<sup>[87]</sup> They designed some molecules structurally unrelated to AHLs based on the computer-aided by using the 4Scan software to screen an in-house database containing 1.1 million commercially available compounds and using molecular alignment scores for molecules with structural similarity to 3-oxo-C12-HSL. Hundreds of compounds with the highest alignment scores were tested as QS antagonists with the aid of two GFP-based AHL biosensors: *Pseudomonas putida* F117(pKr-C12) and *P. putida* F177 (pAS-C8).<sup>[88]</sup> It was found that these compounds are inhibitors of the *cep* QS system of *Burkholderia cenocepacia*. Then they carried out virtual screening of a compound database to identify those compounds that were most similar to the autoinducer OdDHL in terms of shape and possible molecular interactions. Compounds from this preliminary screen were tested in various bioassays, and resulting in more focused virtual combinatorial libraries. Iterative cycles of virtual screening and testing were used to improve the biological activities of the compounds. After several rounds proceeding via compounds **72a** and **72b**, compound **72c** was identified as a novel specific inhibitor of the *cep* QS system in *B. cenocepacia*, interfering with a variety of QS regulated functions\without affecting bacterial growth. Exogenous addition of OHHL reversed the inhibitory effect of **72c**, indicating a competitive inhibition mechanism. **Fig 27** showed the evolution of QS inhibitor compound **72c**, compound **72a** was an initial hit. The activity of this compound was improved by iterative rounds of virtual screening and activity testing, yielding compound **72b** and finally compound **72c**, which represented the end point of the optimization procedure.

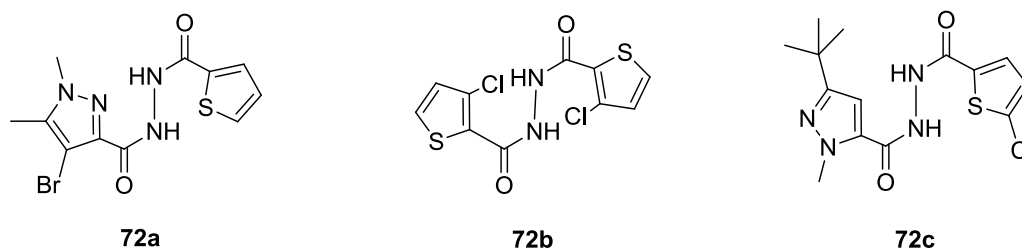


**Fig 27. Heteroaromatic hydrazide QSI (antagonist LasR)**

Olsen et al. designed some *cis* or *trans*  $\gamma$ -lactone AHL analogues **74a-74d** based on halogenated furanones **7** and **73** which have some structural consistency with AHLs. The compounds were screened with the *V. fischeri* LuxI/LuxR-derived QS reporter system.<sup>[89]</sup> The hydroxyl substituted compounds at position 4 of the lactone ring (**74a** and **74b**) were weak antagonists at higher concentration while the 3-substituted analogues **74c** and **74d** (**Fig 28**) were effective agonists, even compound **74c** have almost the same EC<sub>50</sub> as C6-HSL.

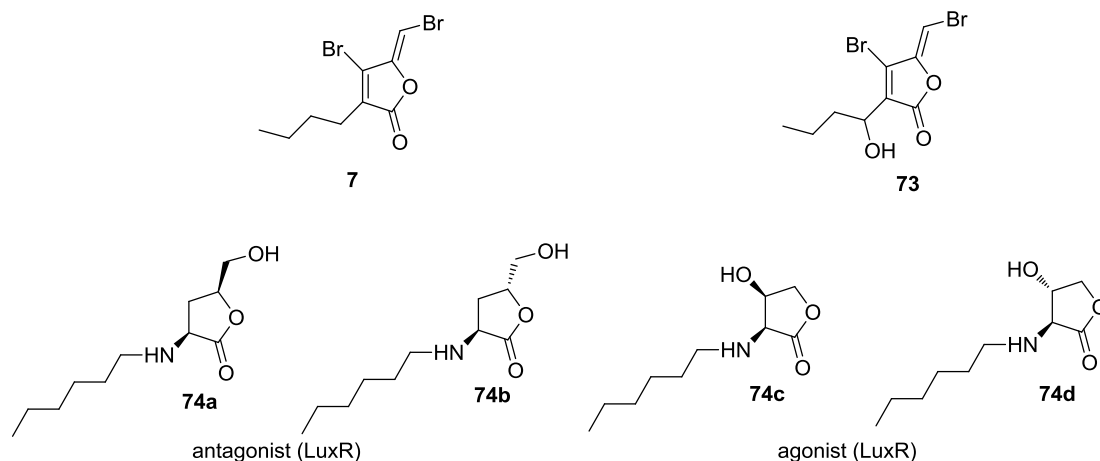


**Fig 28. Synthetized  $\gamma$ -lactone AHL analogues based on halogenated furanones **7** and **73****

In 2006, Tahaet al.<sup>[90]</sup> used the HipHop6refine module of CATALYST158 software as the structure-based virtual screening (SBVS) for QSI. They synthesized the brominated furanones **75a-75c** (**Fig 29**), and employed compound **7** as a control. All compounds were chosen as a training set for pharmacophore modeling (**Fig 31**), and showed antagonistic activity. And based on the previous screening results from the furanones, another 19 compounds were screened and evaluated by measuring the production of pyocyanin for QS inhibitory activity.<sup>[91]</sup> The results showed compound **76** could be a potent QS inhibitor (IC<sub>50</sub> = 800  $\mu$ M) as there was possible interaction of the Pb atom with thiol functions. The same biological evaluation results were observed for other heavy metal-containing compounds **77** and **78** (**Fig 29**).<sup>[90]</sup> Nevertheless, the potential use of heavy metal-containing compounds as future drugs were limited as the heavy metal was toxic for organism.

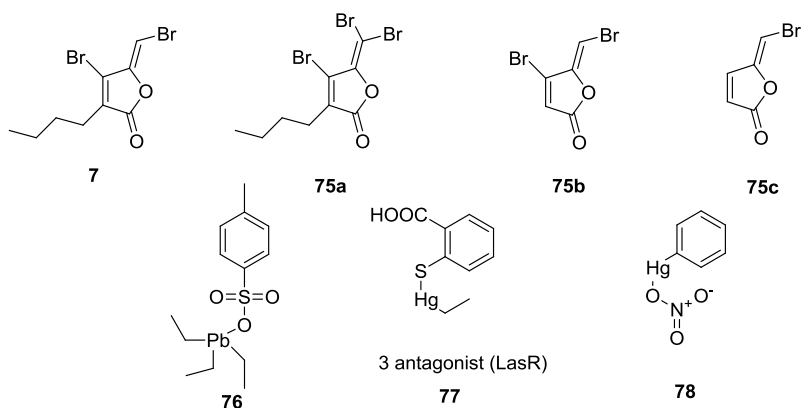


**Fig 29. Heavy metal containing active compounds compared with known furanones QSI**

In 2008, Doutheau and co-workers synthesized three N-acyl-3-amino-5*H*-furanone derivatives **79a-c** and three halogen derivatives **79d-f** (**Fig 30**) and studied its biological evaluation in *V. fischeri*.<sup>[61]</sup> Compounds **79a-f** were analogues of the natural brominated furanone **7** (depicted in **Fig 29**). Those compounds were designed based on the imitation of amide by an enamide function. The *V. fischeri* QS system<sup>[63]</sup> with 3-oxo-C6-HSL as a native inducer was used for the evaluation of bioluminescence. The result showed strong inhibition of brominated analogues **79** whereas compound **79a** was inactive. For the other analogues bearing C<sub>5</sub>H<sub>11</sub> and -CH<sub>2</sub>COC<sub>3</sub>H<sub>7</sub>, compounds **79b** and **79c** were antagonist, undoubtedly as their structure were most close to the natural AHL. Those results were assigned to significant conformational change induced by the enamide function as confirmed by molecular modeling compared with the saturated lactone.<sup>[61]</sup> The modification of the orientation of the side chain is significant enough for preventing the aromatic ring from hampering key residues in the receptor binding site. The other brominated analogues **79e** and **79f** appeared to be stronger inhibitors compared with the inactive unsubstituted counterparts **79a** and **79c**. The results were explained by molecular modeling showing the conjugated enamide group induces two preferential conformations leading to specific binding modes. In addition, the presence of the halogen atom could enhance the fit of the lactone ring through specific interactions with strictly conserved or conservatively replaceable residues in the LuxR protein family, specially the D79, W94, and I81 residues in LuxR.<sup>[61]</sup>

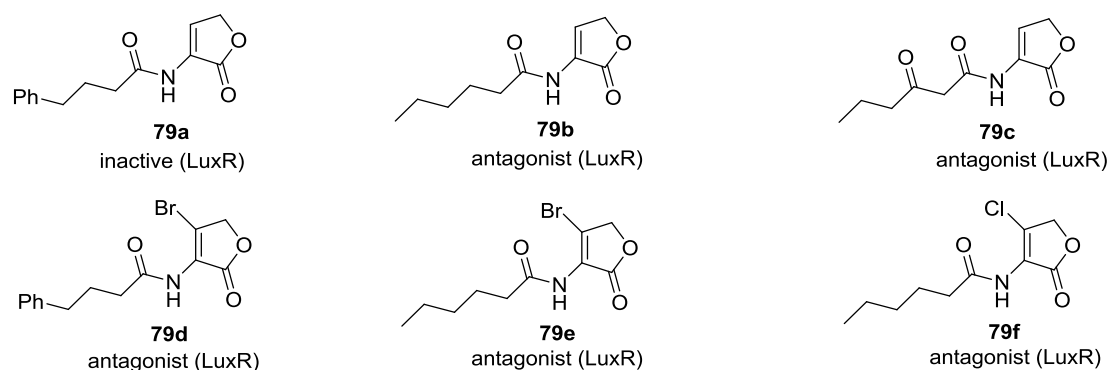


**Fig 30.** *N*-acyl-3-amino-5*H*-furanone derivatives and 3-halogeno derivatives in *V. fischeri*

In 2010, Liu et al. evaluated the QscR inhibitory ability of modified natural QS inhibitor furanone **7** based on the screening of about 100 analogues.<sup>[92]</sup> It was found that compounds bearing an aromatic appendage at the furanone backbone (**80a-d**) (**Fig 31**) were inhibitors of QscR. The furanone **80a** was proved to be the most active one compared with the native 3-oxo-C12-HSL, its activity is at a concentration of 50-fold molar excess over the native 3-oxo-C12-HSL. It revealed the importance of the amino group, since its nitrated analogue **80b** showed much weaker activity, and **80c** also exhibited weak activity. Thus, a strongly electron withdrawing function was favorable for inhibition activity.

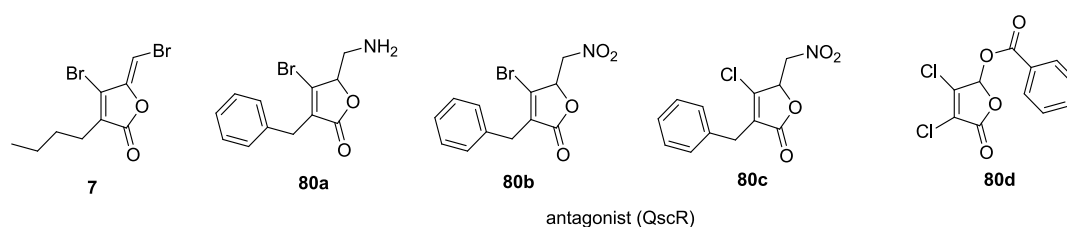


**Fig 31.** Furanones as QscR inhibitors

In 2011, T. Benneche<sup>[93]</sup> synthesized a series of thiophenones from readily available 2-acyl-5-methoxythiophenes **81a-81q** in one step. (**Fig 32**) These compounds could also be alternatively synthesized by using cleavage of the corresponding 2-acyl-5-methoxy heterocycles using oxalyl bromide.<sup>[94]</sup> Only the *Z*-isomers of the *E/Z*-isomers were tested for capacity to reduce biofilm formation by the marine bacterium *V. harveyi* BB120. Apart from compounds **81h**, **81m** and **81p**, all compounds had inhibitory effects on both biofilm formation and planktonic growth. The compounds **81b**, **81d**, **81h**, **81j**, **81k** and **81q** were highly effective,

inhibiting biofilm formation more than 50% at 20  $\mu\text{M}$  or less. Compound **81h** was most effective, reducing biofilm formation by 67% at 5  $\mu\text{M}$ . Moreover, compound **81b** was more effective in inhibiting biofilm formation than the corresponding furanone **75c**. The results demonstrated that thiophenones could act as QS inhibitors.

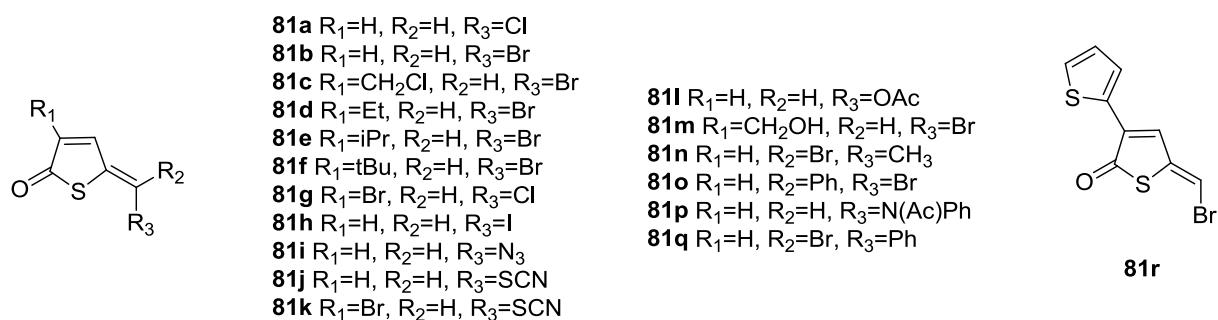


**Fig 32. Thiophenones QSI**

More recently, G. Brackman and S. V. Calenbergh<sup>[95]</sup> synthesized a library of analogues of hamamelitannin (HAM), and evaluated their ability to augment biofilm susceptibility to vancomycin both under pretreatment and under combination treatment regimens. After the screening, compound **82** (**Fig 33**) was found to be the most potent HAM analogue in *S. aureus* Mu50. It displayed no cytotoxicity in MRC-5 lung fibroblast cells at 128  $\mu\text{M}$ , which suggesting an acceptable therapeutic window. Compound **82** alters biofilm susceptibility to antibiotic treatment by affecting both peptidoglycan structure and eDNA release through interfering with the TraP receptor.<sup>[95]</sup> The study revealed that compound **82** has the potency of increasing susceptibility of *Staphylococcus aureus* towards antibiotics *in vitro*, in *Caenorhabditis elegans*, and in a mouse mammary gland infection model, without showing cytotoxicity, and that the effect is superior to that of HAM.<sup>[95]</sup>

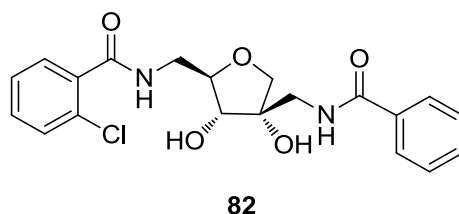


**Fig 33. Analogue of hamamelitannin**

With respect to mimicking AI-2, as early as in 2004, the natural product Laurencione **83** and cyclic compound MHF **84** were found to be capable of inducing bioluminescence in *V. harveyi* by Semmelhack et al.<sup>[96]</sup> Even so its agonistic activity was only 100-fold less than that of enzymatically prepared *S*-DPD (**Fig 34**). Ribose and other prepared compounds **85a-85c** were proved to be inactive in the *V. harveyi* assay.

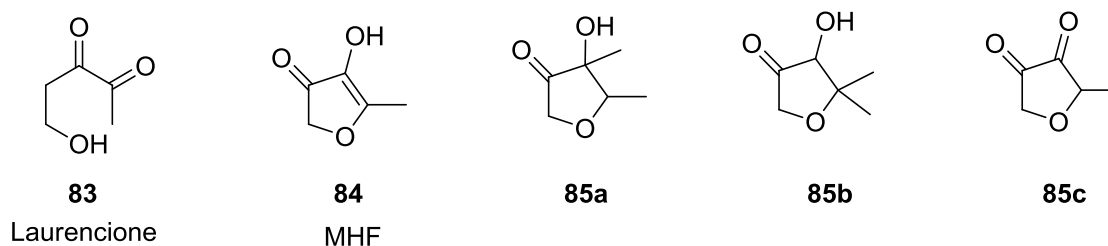


**Fig 34. Compounds investigated by Semmelhack et al. for their ability of modulation AI-2 mediated bioluminescence in *V. harveyi*.**

In 2005, McKenzie et al. have synthesized a variety of metal salts as non-native modulator to study the role of metals other than boron on AI-2 signaling in *V. harveyi*.<sup>[97]</sup> These compounds were evaluated for their ability of inducing light production in *V. harveyi* strain BB170 in boron-free media. They found that the addition of metal carbonates gave surprising positive results, and in return inspired them to evolve another compound *S*-THMF carbonate **86b**, obtained from the reaction of a furanosyl form of *S*-DPD with carbonate, is capable of modulating AI-2 (*S*-THMD-borate) QS in *V. harveyi*, presumably through interaction with the binding pocket of LuxP (**Fig 35**).<sup>[97]</sup>

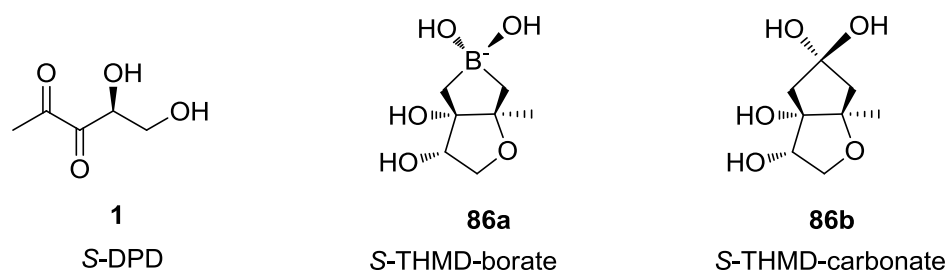


**Fig 35. *S*-THMF-borate and *S*-THMF-carbonate**

In the same year, Lowery et al. synthesized and evaluated a series of natural and non-natural analogues of DPD or DPD derived compounds (*R*-DPD **87**, Laurencione **83**, MHF **84**, and **88-**

**91, Fig 36).**<sup>[98]</sup> The objective of this study was to investigate the specificity of the LuxP binding site. For the investigation, stereo structure, carbon chain length, and OH additions/deletion of DPD were taken into consideration. In addition, several compounds with close structure to DPD or DPD-derived agents were included. These compounds were tested for their ability of inducing bioluminescence production in *V. harveyi* strain MM30. Among all compounds, *S*-DPD **1** was the most potent one and its activity decreased with either OH deletion, or enantiomeric variants, or even cyclization. It was concluded that the LuxP binding cleft can fit a large number of various structural variants of DPD-derived active signaling compounds, although the derivatives had considerably lower activities compared with the native DPD.

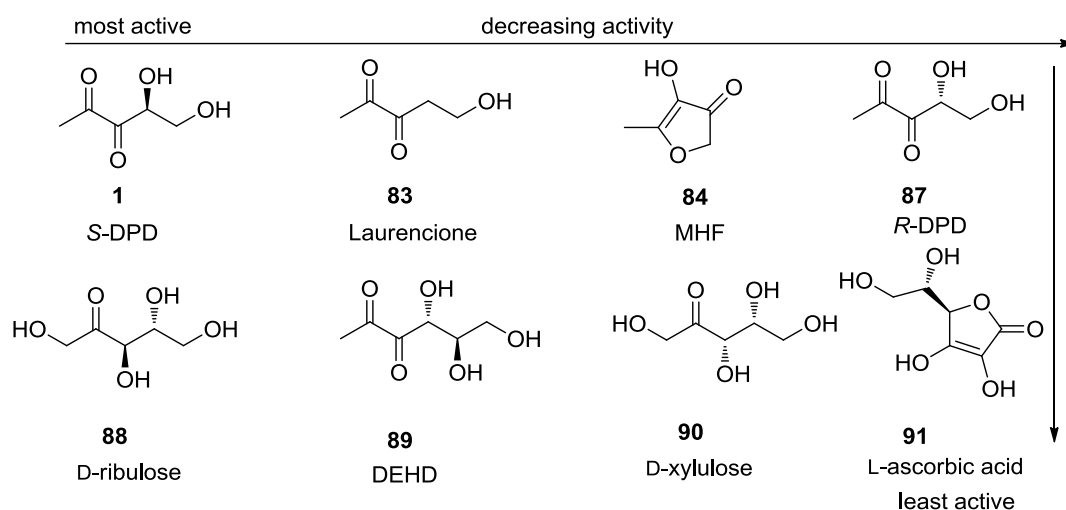


**Fig 36. Structures and order of agonist activities of DPD analogues synthesized by Lowery et al.**

#### 1.3.1.4 Analogues bearing nitrogen and oxygen

The simplest heterocyclic systems bearing both nitrogen and oxygen are oxadiazoles, and many compounds are reported for different purposes such as in medicinal chemistry,<sup>[99]</sup> pesticide chemistry and also polymer and material science.<sup>[100]</sup> Although, none were found in the field of QSI. With respect to more complex N-O-systems, some compounds including boron have been reported. In 2008, Aharoni et al. have reported a series of oxazaborolidine derivatives (**92a-92e**). These compounds contained a negatively charged tetra-coordinated boron atom that have the ability of forming hydrogen bonds (**Fig 37**), and presumptively to be capable to enhance bioluminescence induction in *V. harveyi* synergistically by selectively bind to LuxP.

Among the five compounds, **92a** and **92e** were the most active compounds agitating the production of bioluminescence of the reporter strain *V. harveyi* BB170, the other compounds **92b-92d** were inactive. However, when the bacterial strain was changed to *V. harveyi* mutant (BB886) which was able to synthesize native AHL but lacking AI-2, it could still induce bioluminescence, that was to say no effect on bioluminescence was detected. The results indicated that synthetic DPD or medium containing *S*-THMF-borate **4** was crucial for the activity of **92a** and **92e**. Thus, the action mechanism of these compounds could probably be elaborated by the interaction with the LuxP receptor and the action mode on bioluminescence in *V. harveyi* has co-agonist category property. Some possible SAR trends for this compound series were discussed.<sup>[101]</sup> There were slightly structural similarity between compounds **92a** and **92e** and *S*-THMF-borate **4** except a five-membered heterocyclic ring containing tetrahedral boron bearing a hydroxyl group. The biological results and structural analysis proved the five-membered heterocyclic ring is sufficient for specific interaction with LuxP. Compounds **92b-92c** were inactive probably due to the methyl on the nitrogen which is possible a key factor in modulation of QS in *V. harveyi*. In addition, compound **92a** was more active than **92e**, which may show that the aromatic group attached to the boron in **92a** interacts favorably at the active site of the receptor.<sup>[101]</sup>

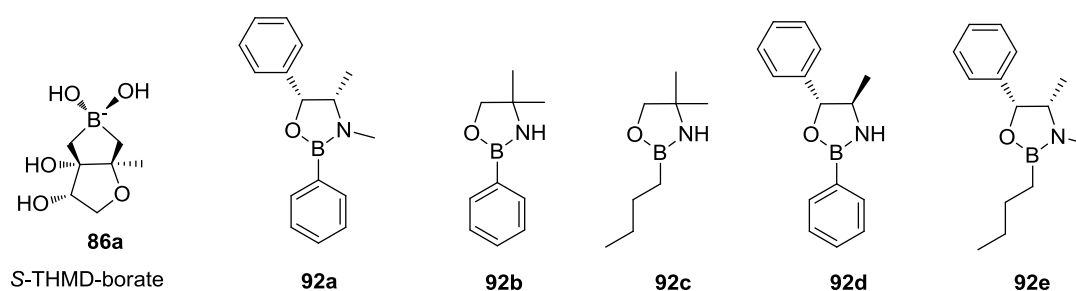


**Fig 37. Structure of oxazaborolidine derivatives**

In 2009, Yang et al.<sup>[102]</sup> screened a library of hundred compounds from the SuperNatural and SuperDrug databases<sup>[103,104]</sup> based on structural similarity with native AHL 3-oxo-C12-HSL, and some medicines such as patulin (compound **93**). Using a Molegro Virtual docker, chlorzoxazone compound **94** and nifuroxazide compound **95** were selected as excellent QS modulator candidate by docking with LasR,<sup>[105]</sup> and they exhibited better docking scores than

the known QS-inhibitor 4-nitropyridine-*N*-oxide.<sup>[106]</sup> Both compound **94** and **95** are antagonists of the LasR system in *P. aeruginosa*, although they have significantly structural disparity. In addition, they also inhibited the production of virulence factors and biofilm development in *P. aeruginosa*. The known nitrofurantoin antiseptic nifuroxazide **95** that inhibit *P. aeruginosa* QS are believed to act via interaction with the LasR protein (**Fig 38**).<sup>[102]</sup>

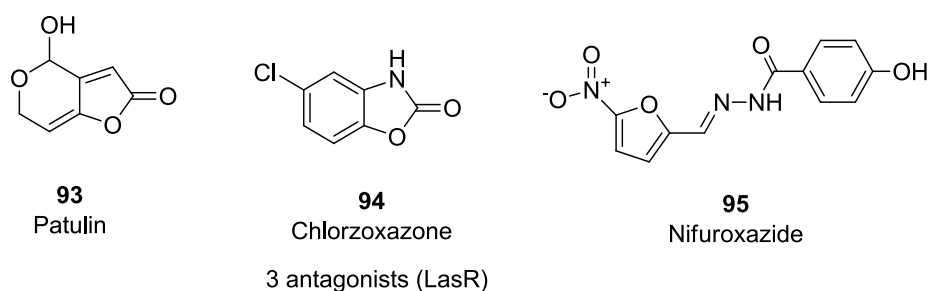


**Fig 38. QS antagonists identified by virtual screening of known drugs**

In 2013, G. Brackman and his co-workers<sup>[107]</sup> synthesized a library of thiazolidinedione and dioxazaborocane analogues (**Fig 39**), and evaluated their effect on AI-2 QS in *vibrio harveyi* BB170 and MM32. All thiazolidinediones (**96a-96e**) and dioxazaborocanes (**97a-97i**) interfered with AI-2 QS. Compound **96b** with a 10 carbon-alkylidene chain without *N*-substitution yields the highest QS-inhibitory activity ( $EC_{50}$  2.1  $\mu$ M and 9.8  $\mu$ M for *vibrio harveyi* BB170 and MM32 respectively), alterations in the alkylidene chain, saturation of the double bond and replacement of the thiazolidine ring by a pyrrolidine ring led to a decrease in QS-inhibitory activity. An increase in activity was observed when the phenyl moiety of the 2-phenyl-1,3,6,2-dioxazaborocanes was substituted with a hydroxy, amino or a carboxyl group ( $EC_{50}$  of 12.2  $\mu$ M, 29.2 and 46.9  $\mu$ M for compounds **97g**, **97b** and **97a** respectively in *V. harveyi* BB170). Compound **97e** resulted in a decrease of bioluminescence signal. In addition, a decrease in activity was observed when the carboxyl function was moved from *para* to *meta* position ( $EC_{50}$  38.8  $\mu$ M and 46.9  $\mu$ M for compounds **97c** and **97a**, respectively in *V. harveyi* BB170) and when the amino group was substituted with hydroxyalkyl moieties ( $EC_{50}$  of 35.7 and 41.3  $\mu$ M for compounds **97h** and **97i**, respectively in *V. harveyi* BB170). Strong AI-2 QS inhibitory activity was observed for compound **97d** (decrease of  $95.8 \pm 0.2\%$  and  $84.2 \pm 7.3\%$  in bioluminescence signal of *V. harveyi* BB170 and MM32, respectively). Among of all tested

compounds, the thiazolidinediones were the most active AI-2 QS inhibitors. Their mechanism of inhibition was elucidated by measuring the effect on bioluminescence in a series of *V. harveyi* QS mutants and by DNA-binding assays with purified LuxR protein. The active compounds neither affected bioluminescence as such nor the production of AI-2. Instead, the thiazolidinediones blocked AI-2 QS in *V. harveyi* by decreasing the DNA-binding ability of LuxR. Additionally, several dioxazaborocanes were found to block AI-2 QS by targeting LuxPQ.<sup>[107][108]</sup>

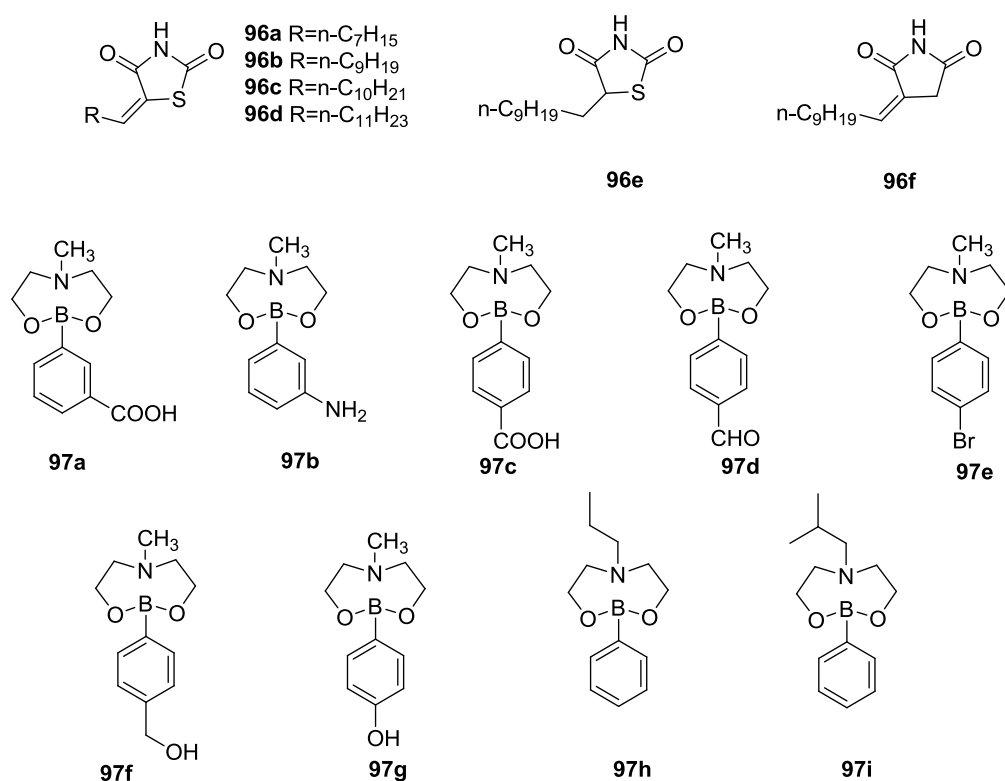


**Fig 39. Thiazolidinedione and dioxazaborocane analogues**

## 1.3.2 Six-membered rings heterocyclic analogues

### 1.3.2.1 Structure variation

Six-membered rings heterocyclic are widely distributed in nature and in the worlds of synthetic chemistry and medicinal chemistry. Many possible structural variations exist in saturated or unsaturated six-membered heterocycles, including aromatic systems isoelectronic with benzene. Below, we will briefly present analogues bearing nitrogen and oxygen, many of them relating to the PQS systems.

### 1.3.2.2 Six-membered analogues bearing nitrogen

In the past two decades, a group of cyclic dipeptides (2,5-diketopiperazines, or DKPs) have been isolated, either individually or as mixtures from culture supernatants of a range of bacterial species. Eight natural DKPs (**98a-98h**) have been reported to modulate LuxR-type receptor activity in sensitive AHL biosensor strains previously considered specific for AHLs.<sup>[109-111]</sup> For example, **98e** and **98g** (**Fig 40**) were reported to be able to inhibit the OHHL-mediated activation of LuxR in *E. coli*.<sup>[111]</sup> After that an accepted hypothesis that DKPs modulate Gram-negative QS through interaction with the LuxR-type proteins was emerged.<sup>[112]</sup>

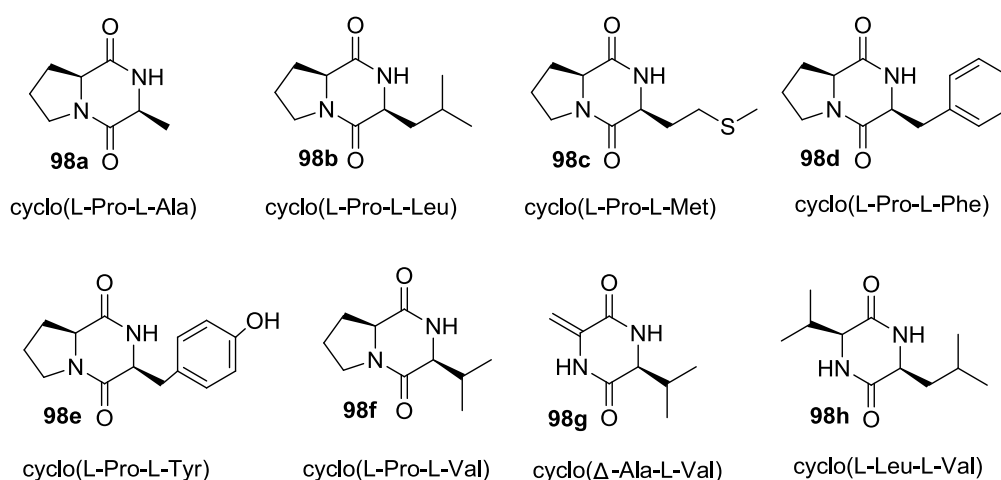


**Fig 40. DKPs reported to modulate LuxR-type protein activity**

From then on, Blackwell and her colleagues designed and synthesized a set of non-natural DKPs (**99-102**) to determine the structural basis of LuxR-type protein activation and inhibition and to find out their mechanism of action (**Fig 41**).<sup>[112]</sup> These DKPs, together with previously reported natural DKPs **98a-98f**, were tested for their abilities to agonize and antagonize LuxR-type proteins such as TraR, LasR, and LuxR itself using both sensitive biosensor strains and reporter strains with native protein levels. It has been previously reported that some non-natural DKPs **98a-98f**, and all of the synthetic DKPs derived from natural D-amino acids, did not display any activities in the native protein level reporter strains examined. But interestingly, another two synthetic DKPs (**100b** and **100c**) were able to antagonize the production of luminescence in *V. fischeri*, further investigation was carried out to elaborate the mechanism. These DKPs do not completely interact with the natural ligand OHHL for LuxR although they

are capable of modulating the LuxR QS system, so the particular mode of action of DKPs in bacterial systems is not clear yet.

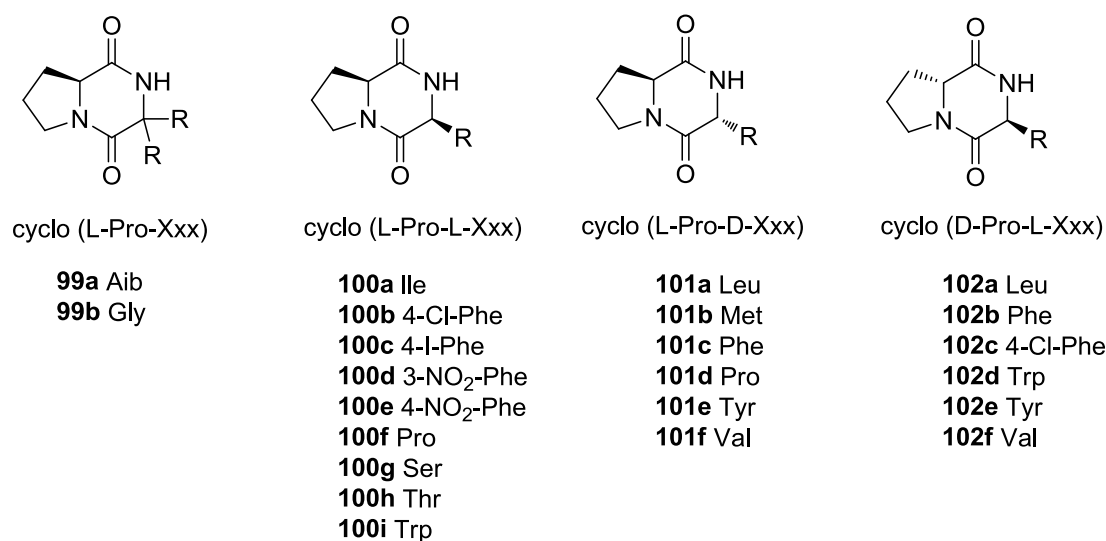


**Fig 41. Structures of DKP sublibraries synthesized and evaluated by Blackwell and co-workers**

After that, in 2009, Campbell and Blackwell<sup>[113]</sup> synthesized a library of over 400 structurally more complex DKPs. with the auxiliary of a macro-array format. In a solution-based cell-based assay, six DKPs **103a-103f** were identified to have the ability to inhibit the QS-modulated luminescence phenotype of *V. fischeri* (**Fig 42**).

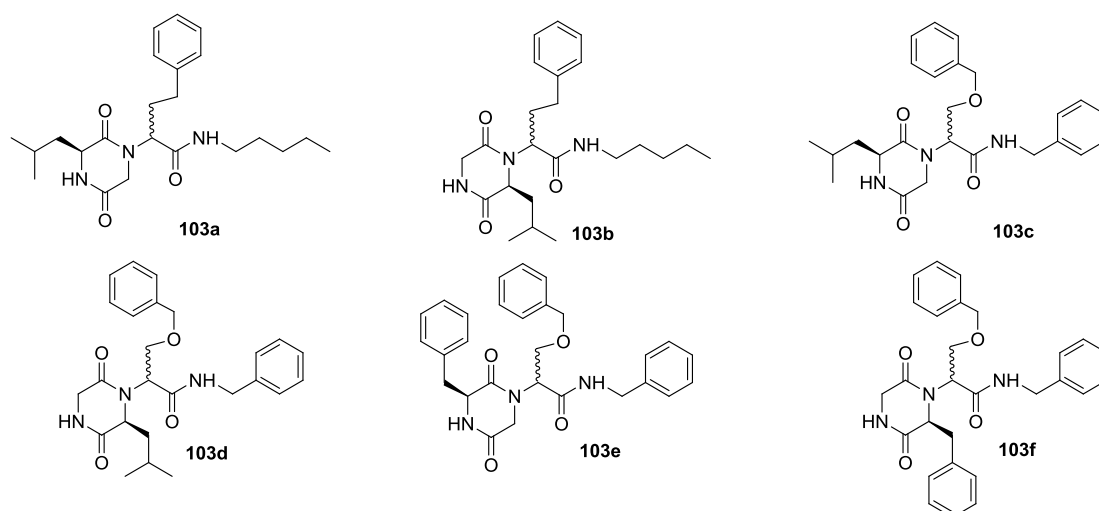


**Fig 42. Structures of the six most active DKPs identified in the study of Campbell and Blackwell**

In 2016, V. Scoffone, L. Chiarelli, V. Makarov and G. Brackman<sup>[114]</sup> reported the discovery of new diketopiperazine inhibitors of the *B. cenocepacia* acyl homoserine lactone synthase CepI and their anti-virulence properties (**Fig 43**). Ten novel diketopiperazines were synthesized based on the structure of diketopiperazines. Out of ten different compounds assayed against recombinant CepI, four of these compounds (**106a**, **106b**, **106c**, and to a lesser extent **104a**), were effective inhibitors of the CepI enzymatic activity, with IC<sub>50</sub> values ranging from 5 to 30 μM. None of compounds altered the susceptibility of *B. cenocepacia* toward the antibiotics tested. Compound **104a** and **106b** interfered with protease and siderophore production, as well as with biofilm formation, and showed good *in vivo* activity in a *Caenorhabditis elegans* infection model. These four molecules were also tested in human cervical carcinoma-derived HeLa cells and showed very low toxicity. Therefore, they could be considered as *in vivo* combined treatments with established or innovative antimicrobials, to improve the current therapeutic strategies against *B. cenocepacia*.

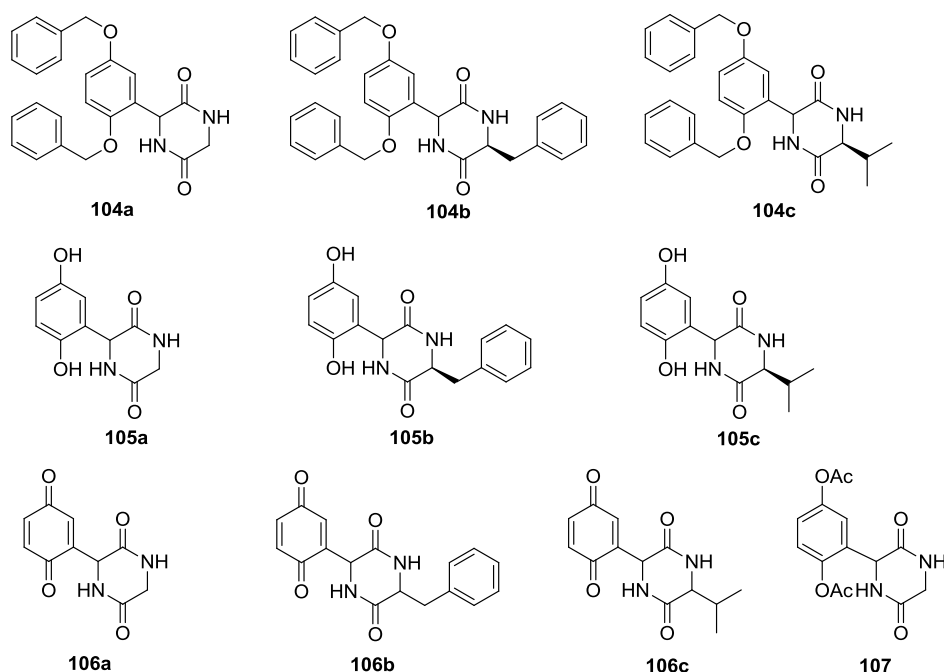


**Fig 43. Diketopiperazine inhibitors of the *B. cenocepacia***

Among some known and recognized drugs exhibiting a six-membered nitrogen heterocyclic backbone, some of them have been reported having QS activities. For example, some macrolide antibiotics have been shown to repress the *P. aeruginosa* AHL synthesis when applied at

subminimal growth-inhibitory concentrations,<sup>[115–117]</sup> possibly at the level of the ribosome rather than via direct interaction with the synthase protein itself.<sup>[117]</sup> And non-macrolide antibiotics were confirmed have effects upon QS systems in Gram-negative bacteria, for example the antibiotics iprofloxacin **108** and ceftazidime **109** are capable of decreasing the expression of a range of QS-regulated virulence factors in *P. aeruginosa* at sub inhibitory concentrations.<sup>[118]</sup> But for the interaction mechanism has not been determined yet as these compounds have a low affinity for the LasR receptor site in silico docking experiments, suggesting a possible alternative mode of action (**Fig 44**).

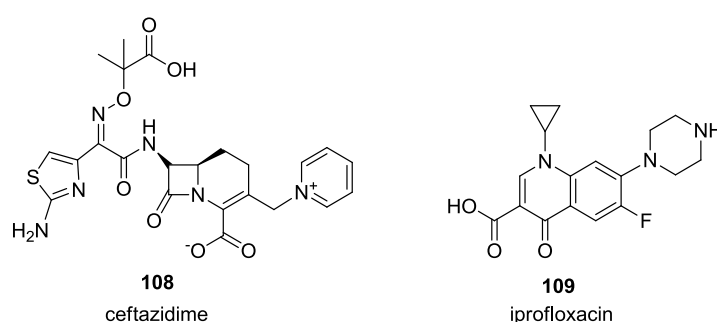


**Fig 44. Structures of some known drug molecules being able to modulate AHL-mediated QS**

In 2012, Rolf W. Hartmann and his co-workers synthesized a series of compounds **125 -132** targeting PqsR (the receptor of PQS system) by following a ligand-based drug design approach.<sup>[119]</sup> They modified the stereo-electronic configuration of HHQ by changing the length of the alkyl side chain and by the introduction of electron-donating groups (EDGs) and withdrawing groups (EWGs) into the benzene moiety of the quinolone structure. Besides, several corresponding PQS analogs were prepared for comparison. Then all compounds were evaluated for the PqsR-mediated transcriptional effect in a HTS  $\beta$ -galactosidase reporter gene assay in *E. coli* containing the plasmid pEAL08-2.<sup>[120]</sup> The biological evaluation indicated that compound **110d** and **110e** which is HHQ with *n*-heptyl and *n*-octyl are the two most potent agonists among all analogues with varying side chains, the agonistic activity decreased along with shortening, elongation or substitution by phenyl group of the chain length. These results indicated that the ability of HHQs activating PqsR is dependent on the side chain with *n*-heptyl being the optimal, which is in agree with the previous study.<sup>[121][122]</sup> However, for the antagonist test, none of the HHQ side-chain analogs at 10  $\mu$ M was able to strongly inhibit the PqsR

stimulation. They also investigated the effect of the introduction of EDGs and EWGs into the different position of benzene part of HHQ. The results showed that introduction of an EDG into 7-position resulted only in agonists (compounds **112a** and **112b**), the introduction of a withdrawing group in 8-position such as Fluorine was favorable for agonistic activity, and the strong EWGs in 6-position was advantageous for antagonistic activity, but this case did not apply for compounds with substituents in 6-position by OH, -OCH<sub>3</sub> and F. Among all of compounds, CF<sub>3</sub> in 6-position was the most potent antagonist. Interestingly, the antagonistic potency of two position isomers of **111g**, compounds **115** and **116** with trifluoromethyl in 7- or 8-position, was strongly reduced compared with the 6-position analog. This research opens a new insights into the ligand-receptor interaction of PqsR and provides a promising starting point for further drug design (**Fig 45**).<sup>[119]</sup>

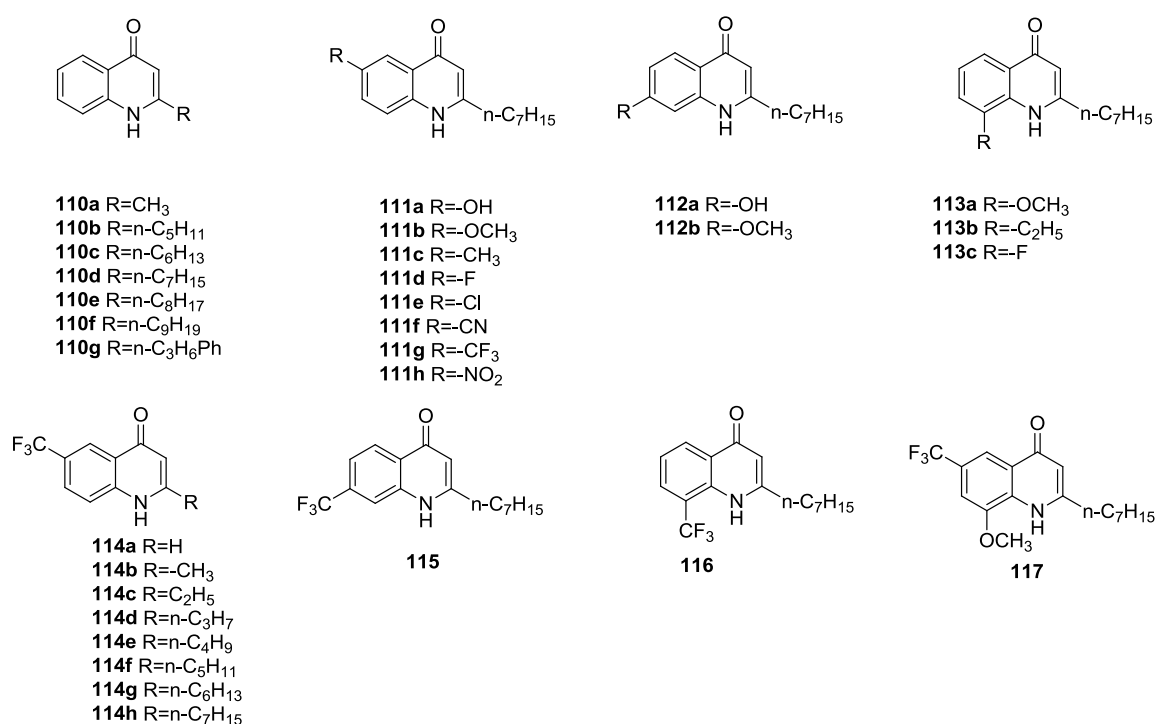
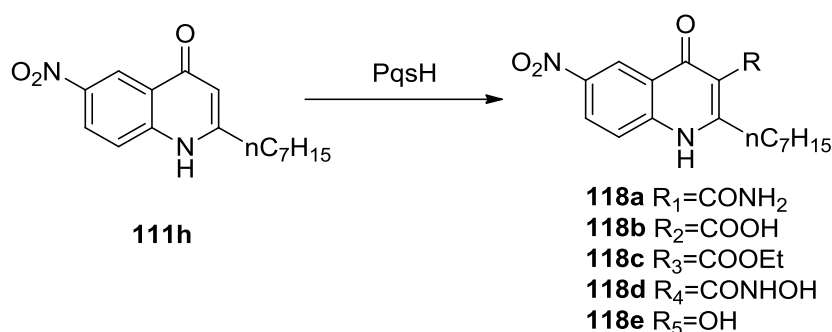


**Fig 45. HHQ and PQS analogues synthesized by Rolf W. Hartmann**

Through this study, Rolf W. Hartmann and co-workers<sup>[119]</sup> found compound **111h** (**Scheme 2**) as the only PqsR antagonist described to date. It showed an IC<sub>50</sub> of 51 μM in an *E. coli* reporter gene assay, and many PQS analogues show agonistic activity. Surprisingly, the antagonistic activity of compound **111h** was transformed to agonistic activity after the

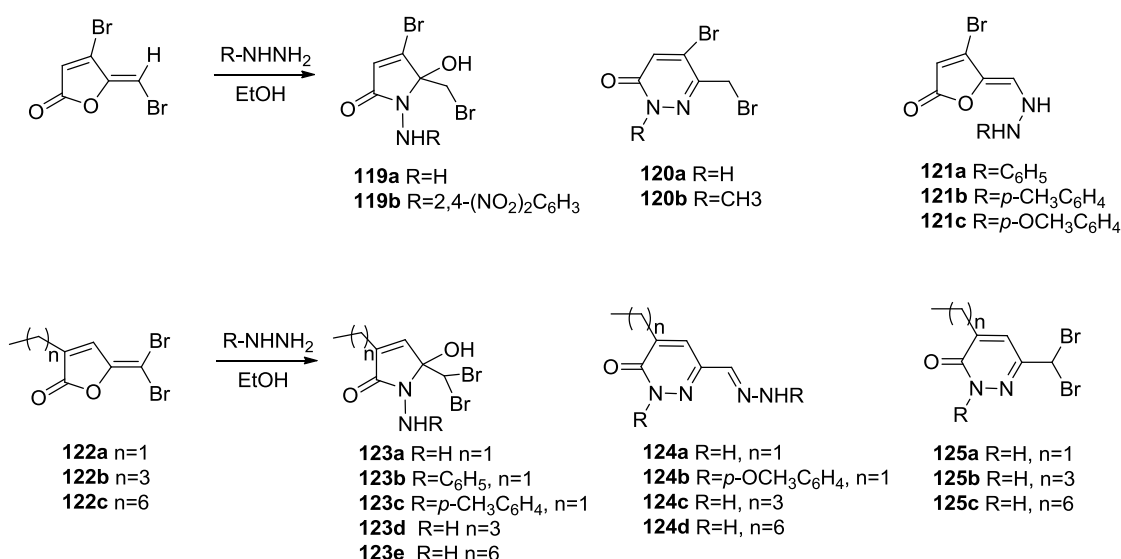
biotransformation to compound **118e** via enzyme PqsH, which was not consistent with the former results that both HHQ and PQS were agonist,<sup>[47][123]</sup> although its biotransformation was also based on the enzyme PqsH. Then they suspected that the changes probably due to the blockade of 3-position by substitution of the hydrogen atom with an appropriate functional group, and synthesized a small library of 3-substituted compounds to explore the potency and stable PqsR antagonists. Among all synthesized compounds, the carboxamide compound **118a** was the most promising analogues which showed high potency in the *E. coli* reporter gene assay, but retained its antagonistic activity in *P. aeruginosa* without displaying any agonistic activity up to 15  $\mu\text{M}$ .<sup>[124]</sup> In addition, compound **118a** could also strongly reduce the levels of HHQ and PQS, and efficiently decreased the pyocyanin levels with an  $\text{IC}_{50}$  of 2  $\mu\text{M}$ . Moreover, compound **118a** were proved to be a strong anti-virulence agent *in vivo* by two animal experiments in *Caenorhabditis elegans* and *Galleria mellonella*.<sup>[124]</sup> This finding provides a promising concept and toolkit for further *in vivo* investigations using mammalian organisms and may open new directions for the development of anti-infective that are less prone to resistance. Furthermore, species-selective targeting of specific regulatory pathways might help minimizing adverse effects that are observed with broad-spectrum antibiotics.



**Scheme 2. Biotransformation of compound 111h**

In 2016, N. Kumar reported a number of novel brominated heterocycles based on aminobromopyrrolone, bromopyridazinone and hydrazinyl furanone scaffolds. These hydrazines based fimbrolides analogues were synthesized from 4-bromo-5-(bromomethylene)-2-(5H)-furanone and 2-alkyl-5-(dibromomethylene) furanones with several different substituted or unsubstituted hydrazines (**Scheme 3**). Five and six membered rings products were

obtained from the reactions of brominated furanones with bi-nucleophiles by ring-opening and ring closure, or Michael-type addition reaction. The *P. aeruginosa* MH602 lasB reporter strain was used to perform the biological assays. The production of AHL signals by this reporter strain led to an increase in green fluorescent protein (GFP) as a result of an active QS system. The result showed that all synthesized compounds displayed good QS inhibitory activity, among them, compounds **121a** and **123c** were the most potent and less toxic agent to reduce GFP fluorescence, with an QS inhibitory activity were 34% and 33% respectively, compared with the control. Three major structure activity relationships (SARs) were concluded. First, five-membered brominated hydrazinyl furanones and brominated hydroxypyrrolones are favored over six-membered pyridazinone heterocycles for QS inhibitory activity. Second, the dibromomethylene group was found to be important for the QSI activity of pyridazinone compounds. This observation is consistent with the findings of Hentzer et al. and Steenackers.<sup>[125,126]</sup> Third, amino-pyrrolone and pyridazinone compounds with shorter alkyl chains showed superior QS inhibitory activity than compounds with longer alkyl chains. This result is also consistent with earlier studies which found that fimbrolides containing shorter alkyl chains are better QS inhibitors,<sup>[125,127–129]</sup> and may offer potential ideas for further development of antimicrobials with less resistance.<sup>[130]</sup>



**Scheme 3. Five and six-membered brominated hydrazinyl furanones and brominated hydroxypyrrolones**

More recently, J. Nielsen and his co-workers<sup>[131]</sup> found that fusaric acid and analogues were able to inhibit the las and rhl QS system in *Pseudomonas aeruginosa* and the lux QS system in *Vibrio fischeri*. In fact, these compounds **126a-126g** (**Fig 46**) were designed based on the possible bioequivalent of fusaric acid and native AHL (C6-HSL), in which an overlap of the ester carbonyl, and C-3 of HSL with C-2 of fusaric acid, and the methylene groups in the side chains of the two molecules were observed. All analogues were prepared from methyl 5-bromopicolinate or ethyl 5-bromopicolinate using microwave-assisted synthesis method. The *lasB*-gfp and *rhlA*-gfp genes in *P. aeruginosa*, the *luxI*-gfp gene and *luxR* gene in *Escherichia coli* were employed for biological assays. After the screening, six compounds **126a-126g** were found to be potent inhibitors for lux QS system without bacterial growth inhibition. No QSI activity was found against two QS reporter strains *lasB*-gfp and *rhlA*-gfp in concentrations up to 100  $\mu\text{M}$ . The structure-activity relationships were concluded:<sup>[131]</sup> (a) the ester group might simulate the intermolecular interaction solicited by the lactone moiety in structures of current QSIs; (b) the zwitterionic character of the free acids prevents penetration over the cell wall of plasma membrane; (c) a lipophilic alkyl group in the 5 position as in the case for FA as well as AHL is not necessary; (d) the ester moiety at C-2 position seems to be favorable for QS inhibition. Thus, a natural product scaffold with homologous structure could serve as a potential framework for design of bio-active QS molecules.

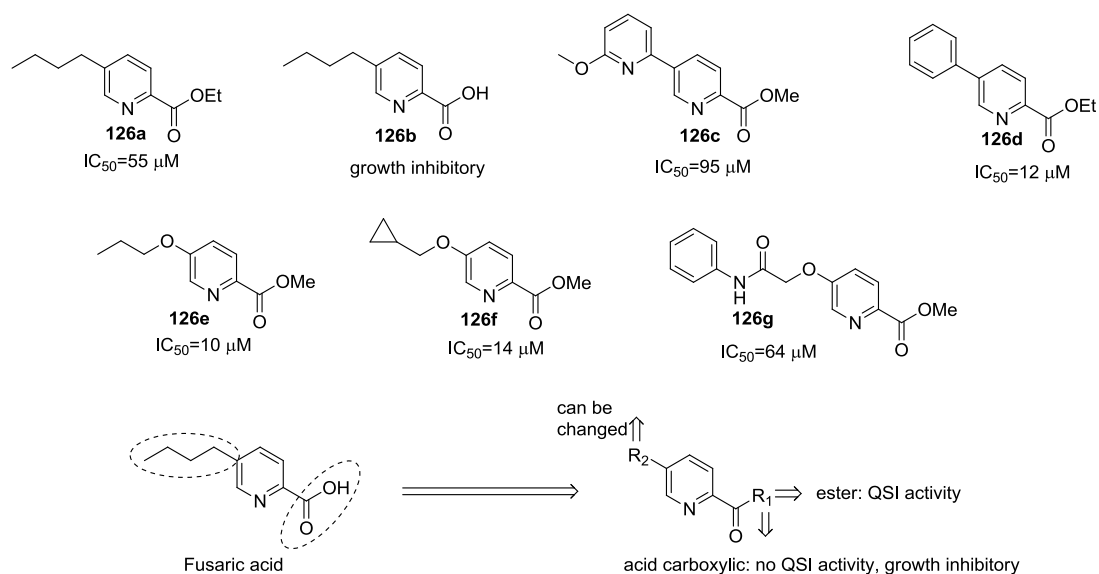


**Fig 46. Fusaric acid and analogues as QSI of *P. aeruginosa* and *V. fischeri***

### 1.3.2.3 Analogues bearing oxygen

A docking based virtual screening (DBVS) for QS inhibitors was reported by Zeng et al.<sup>[87]</sup> They evaluated a library of 51 active components of Traditional Chinese Medicines with antibacterial activities using the DOCK structure based drug design software package which employs flexible ligand minimization to evaluate proposed binding modes.<sup>[132]</sup> These compounds as well as the brominated furanone **75a** were docked as rigid ligands with a maximum of 30,000 orientations in the TraR binding site. The selected benzopyranic and coumarinic compounds **127-129** inhibited biofilm formation of *P. aeruginosa*, and compound **127b** induced TraR degradation *in vitro* (**Fig 47**).

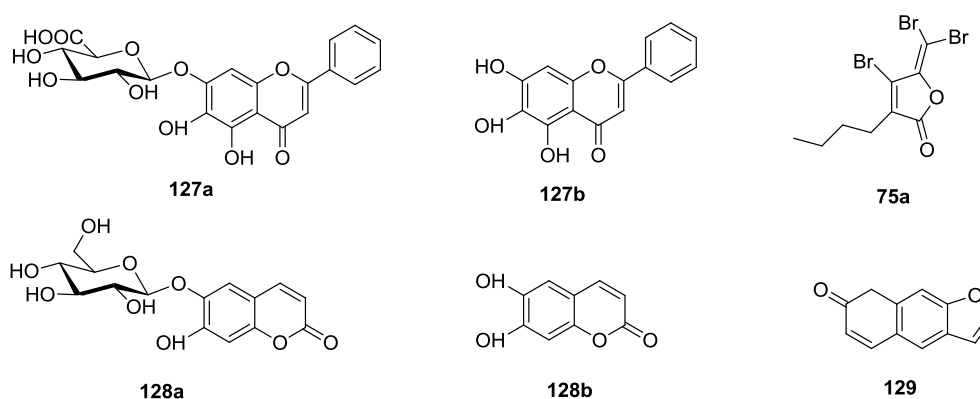


**Fig 47. Benzopyranic and coumarinic QS inhibitors**

### 1.3.2.4 Analogues bearing nitrogen and oxygen

In the series of six membered heterocyclic analogues bearing nitrogen and oxygen, we did not find any that were related to QS in a strict sense.

### 1.3.2.5 Anti-biofilm 6-membered ring heterocyclic systems with hypothetical anti-QS mode of action

As the formation of biofilms is regulated by QS, it can be anticipated that some antibiofilm compounds might act via an anti-QS property. The involvement of QS in biofilm formation and conflicting conclusions have been drawn regarding the importance of QS in bacterial biofilm formation.<sup>[133]</sup> Below are mentioned a few heterocyclic compounds related to anti-biofilm formation, for which we think that their structural similarity with some known PQS active compounds, might allow hypothetic anti-QS mode of action.

In 2014, K. Atmakur and his co-workers<sup>[134]</sup> synthesized a series of 3-benzyl functionalized pyrimidino chromen-2-ones and evaluated anti-microbial and anti-biofilm activities of these compounds in both Gram-positive and Gram-negative bacteria including *Micrococcus luteus* MTCC 2470, *Staphylococcus aureus* MTCC 96, MLS-16 MTCC 2940, *Bacillus subtilis* MTCC 121 and *Pseudomonas aeruginosa* MTCC 2453. All compounds (**Fig 48**) were prepared from the reaction of 6-amino-1,3-di-methyl uracil with a wide range of aldehydes in acetic acid at 120 °C. The results of the anti-microbial activity screening showed that the compounds **130h-130q** with pyrazolo-phenyl substitution on the carbon attached to coumarin and pyrimidine ring made a significant impact against various Gram-positive and Gram-negative bacterial strains. Compounds **130o** and **130p** showed very promising activity against *Micrococcus luteus* MTCC 2470 and exhibited promising activity against *Staphylococcus aureus* MTCC 96 and *Bacillus subtilis* MTCC 121. Compounds **130m** and **130v** showed activity against all the tested Gram-positive strains. Further, compounds **130j**, **130k**, **130r** and **130u** showed good activity against Gram-positive strains like *Micrococcus luteus* MTCC 2470, *Staphylococcus aureus* MTCC 96 and *Bacillus subtilis* MTCC 121. While, compounds **130f** and **130g** showed good activity against *Pseudomonas aeruginosa* MTCC 2453 along with *Micrococcus luteus* MTCC 2470, *Staphylococcus aureus* MLS-16 MTCC 2940 and *Bacillus subtilis* MTCC 121.<sup>[134]</sup>

For the anti-biofilm screening studies, the results showed that the compounds with pyrazolo-phenyl substitution on the carbon attached to coumarin and pyrimidine ring displayed a very remarkable biofilm inhibition activity. Specifically, compound **130m** exhibited an excellent activity against *Staphylococcus aureus* MLS 16 MTCC 2940, and **130o**, **130p** showed very potent activity against *Staphylococcus aureus* MTCC 96. Furthermore, compounds **130h-i**, **130m-n** and **130q**, **130v** showed promising activity against *Staphylococcus aureus* MTCC 96, and **130g**, **130v** displayed very good activity against *Staphylococcus aureus* MLS 16 MTCC 2940.<sup>[134]</sup>

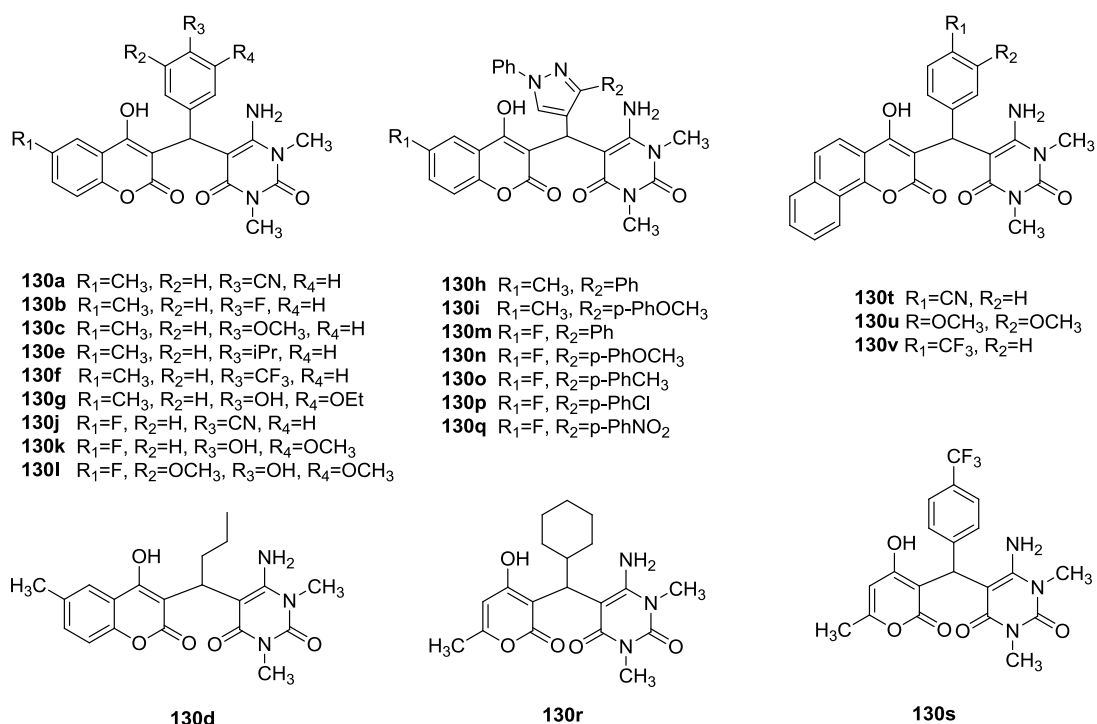


**Fig 48. Structures of 3-benzyl substituted pyrimidino chromen-2-ones**

## 1.4 Conclusion

Heterocyclic compounds are abundant in the field of drug design. In this section, we showed that several families of such compounds were possible QS modulators, especially the five- and six-membered heterocycles containing nitrogen and oxygen atoms. For heterocycles with larger than six-membered rings, also commonly found among bio-active molecules, no example of QS active compound was reported. Five-membered ring heterocycles can serve either as a backbone for mimicking the lactone moiety in AHLs or serve as a bioisostere of the amide function. They also mimic the 5-membered AI-2 skeleton. Six-membered rings heterocycles are more frequently used when PQS and HHQ analogues are designed. Structurally, even tiny modifications of the heterocycle can lead to changes, even a reversal, of bio-activity, as observed for some tetrazoles or some HHQ and PQS derivatives. In general, there are no rules which permit to anticipate the activities of these compounds.

## 1.5 Perspectives

The use of small molecules to modulate bacterial QS systems has attracted significant interest over the course of the last few decades, though it is still in a rather early stage compared with better known and understood other bacterial biological processes. For AHL-related analogues, many of possible structural variations have been performed, limiting the prospect for finding more potent active agonists or antagonists to really innovative structures. For AI-unrelated structural analogues, a large number of structurally diverse derivatives have also been discovered as activators and inhibitors, providing researchers with an extensive set of chemical tools to study this form of intercellular communication. However, AHL heterocyclic analogues found by diverse chemical biology approaches still holds a promising future. Further, it is quite likely that new AHL heterocyclic antagonists will be identified from computer-aided design, analogues of natural products and even from animals, plants, or microorganisms. An increasing number of AHL heterocyclic compounds acting as QS modulator have been reported in the recent literature. In the future, once the relevance of activity and structure of the active heterocyclic compounds is elucidated, new groups of related analogues will be designed and examined for their effectiveness in modulating QS responses, and new strategies will be established based upon the chemical modulation of bacterial QS, which may prove to be of value in a wide range of fields, including medicinal, agricultural, and environmental. Indeed, the field of AHL heterocyclic molecule modulation of QS can be considered to still be in the initial stage in many aspects. Therefore, there is considerable scope for further exciting developments to be made in this area, and the reliance of QS upon a language of small molecules means that AHL heterocyclic compounds might have the chance to be a lead actor in QS.



## **Chapter II. Results and Discussion**



# Design, synthesis and biological evaluation of QS mimics as the modulator of bacterial QS

## 2.1 Introduction

Quorum sensing (QS), as mentioned in the bibliographic section, is based on the synthesis, diffusion and detection of AIs.<sup>[53]</sup> For many Gram-negative bacteria, acyl-homoserine lactones (AHLs, **Fig 49**) of type 1 are the AIs and LuxR type proteins are the transcriptional regulators. AHLs are rather simple molecules for which one can define three areas for chemical modification: (1) the side chain varying in the length, substituents and characteristic presence of carbonyl or hydroxyl substitution at the C-3 position, (2) the central amide connective function, (3) the lactone moiety. On the basis of such modifications of the three areas, many active compounds having close structural analogy with AHLs have been designed, synthesized and found to be active for AHL-dependent QS modulation.<sup>[53,121,135,136]</sup> In this respect, our group has reported the synthesis and the biological evaluation of several families of active analogues in the past several years, with variations in the side chain<sup>[63]</sup> or in the amide mimic (sulfonamides,<sup>[65]</sup> ureas,<sup>[66]</sup> and sulfonylureas<sup>[67]</sup>). All analogues exhibiting a wide range of agonistic and antagonistic activity towards *V. fischeri*, thus being potentially active in the LuxR-regulated QS system.

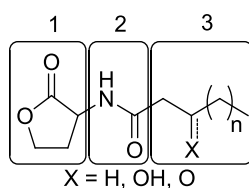


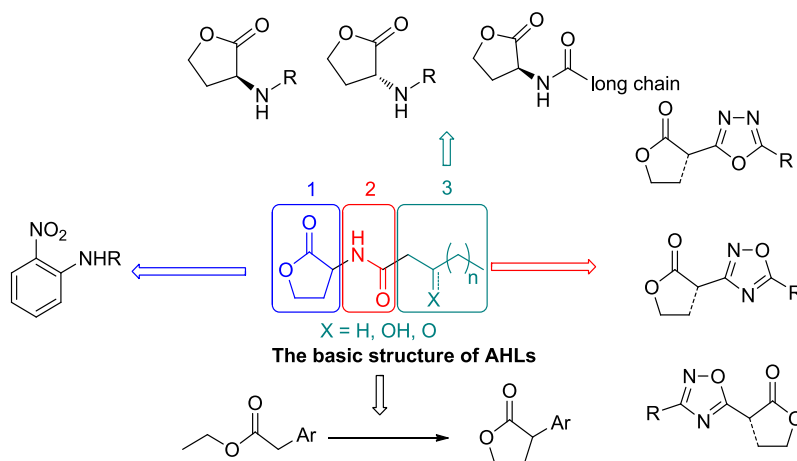
**Fig 49. The basic structure of AHLs**

In this part, my work has been focused on the design, synthesis and biological evaluation of QS mimics as modulators of bacterial QS, and organized in five separate parts (**Scheme 4**).

- Firstly, in keeping with previous work of the team on AHLs analogues, we have investigated the chirality-activity relationship of AHL analogues, necessitating the

synthesis of several types of AHL and analogues in racemic and enantiomerically pure form;

- Secondly, targeting tools aiming at enzyme purification by AHL-structure recognition, AHL derivatives possessing long chains functionalized in the way they can be grafted on a solid support were synthesized;
- Thirdly, as a continuation of the previous studies on the imitation of the amide function of AHLs by heterocyclic rings, we investigated the use of the oxadiazole scaffold, and for this we designed and synthesized six series of oxadiazole derivatives. In the course of this study, we also investigated in a fourth part, an alternative cyclization approach towards the core motif lactone of AHL, which can be applied to oxadiazole-based or other types of AHL analogues;
- Finally, in the fifth part, on the basis of the concept of computer aided design in QS modulation, some readily available acylated 2-nitroaniline derivatives, though structurally unrelated to AHLs, were synthesized and evaluated as LuxR-regulated QS inhibitors.



**Scheme 4. Five parts reported in this chapter**

## 2.2 Synthesis and biological evaluation of optically pure AHLs and analogues

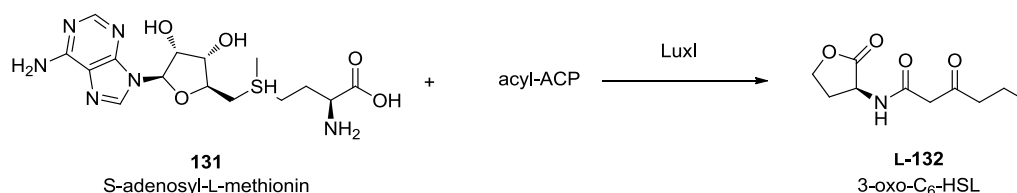
### 2.2.1 Introduction

The first recognition of the importance of chirality in drug design was from the “thalidomide accident” in 1958. From then on, drug discovery as well as asymmetric catalysis were driven by the development of chirality, since the chirality plays an important role in the determination of compound function and activity. It has been widely recognized that compounds with same structure but contrary configurations may exhibit discrepant, sometimes even completely opposite effects. As a potential anti-bacterial strategy, the exploration of QS mimics represents an attractive alternative therapeutic approach for the treatment of human and plant bacterial infections. This is why the synthesis of small molecules which are capable of modulating bacterial QS systems has been widely investigated in the recent years,<sup>[121]</sup> notably those designed around native bacterial auto-inducer, such as AHLs.<sup>[53,121,135]</sup> However, until now, there are few work pertaining to the investigation of enantiomeric character of AHLs. In most investigations of AHL analogues, either only the L-enantiomer (the same configuration as native AHLs) or the racemic mixture was made and studied, and only the L-half of the mixture being thought to be responsible for the QS autoinducing activity and the other half D-isomer being just simply considered as inactive.<sup>[137]</sup> Actually, the capabilities of attenuating or inducing QS modulation of other analogues such as sulfonamides, ureas, sulfonylureas and 3-oxo-AHL derivatives has never been studied in a systematic manner, and this is the purpose of this part of my work.

Herein we report upon our research towards the synthesis and biological evaluation of a variety of optically pure AHLs and analogues, chosen among known QS-active compounds in our library, and representative of several structural variations. All compounds were prepared from L- and D- homoserine lactone hydrobromide *via* the amidation with various acyl chloride. The enantiomeric purity was assessed by polarimetry (allowing comparisons when data were available in literature), with complementary measurements by two methods, namely NMR using an NMR shift reagent and chiral HPLC. The bioassay was conducted in *E. coli* by measuring the value of inducing or inhibiting bioluminescence.

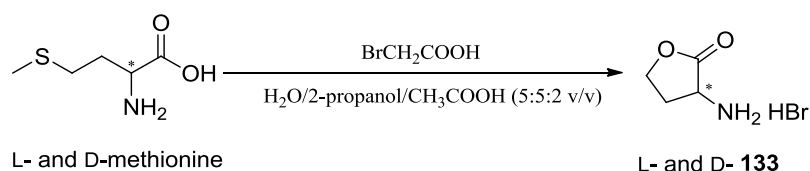
## 2.2.2 Preparation of L- and D- homoserine lactone hydrobromide

As homoserine lactone hydrobromides are very expensive in their pure enantiomeric form, we prepared them from D- or L-methionine following a method reported by B. W. Bycroft.<sup>[138]</sup> Actually, this method mimics the biosynthesis of AHLs (**Scheme 5**): indeed, 3-oxo-C<sub>6</sub>-HSL (OHHL) was bio-synthesized from S-adenosyl-L-methionine (SAM) **131** and an acylated-acyl carrier protein (acyl-ACP).<sup>[139]</sup> LuxI and its homologous proteins bind the substrates SAM and acyl-ACP in sequential order and catalyze the transfer of the acyl group from the acyl-ACP to the amine of SAM. This leads to the release of ACP, followed by homoserine lactone ring formation and dissociation of the AHL from the synthase.<sup>[140]</sup>



**Scheme 5. The biosynthesis pathway of AHL**

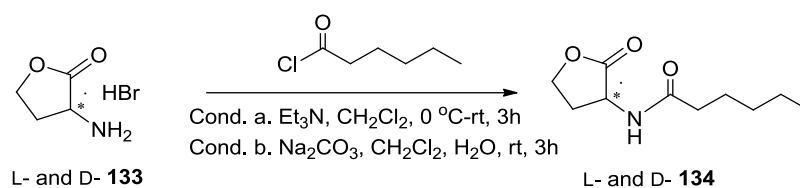
Thus, using methionine instead of SAM as starting material to first prepare homoserine lactone bromide (HSL) **L-133** and **D-133** followed by amidation was proposed for the synthesis of AHLs analogues (**Scheme 6**).



**Scheme 6. Synthesis of L- and D- homoserine lactone hydrobromide**

In this process, bromoacetic acid was used as the halide and the methionine was suspended in acetic acid. The first step was the formation of sulfonium compounds followed by the removal of methylmercapto acetic acid under high temperature and participation of water to afford homoserine hydrobromide, then **L-133** and **D-133** were obtained by the cyclodehydration in 78% and 89% yields respectively. No racemization was observed by





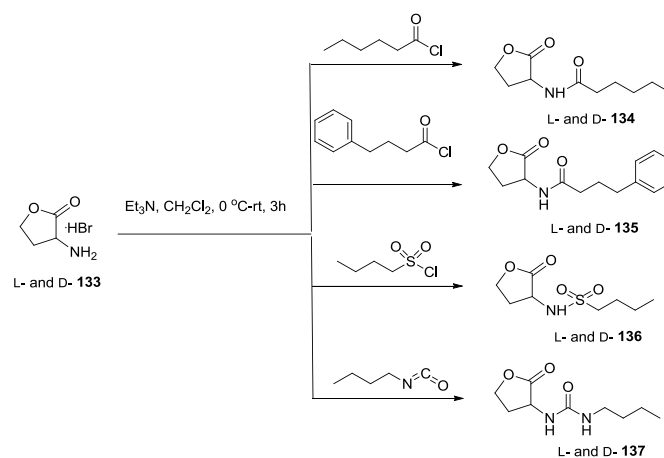
**Scheme 8. Synthesis of enantiomers of compound 134**

Having in hands the two pairs of enantiomers of compound **134** obtained by the two amidation methods, we compared optical rotation with the known literature, and found that although the Schotten–Baumann conditions gave better yields, the  $[\alpha]_D^{22}$  was not consistent with previously reported.<sup>[142]</sup> Therefore, triethylamine was a better base for synthesizing optically pure AHLs analogues with high enantiomeric purity (**Table 3**).

**Table 3. Comparison of optical rotation of two conditions for compounds 134**

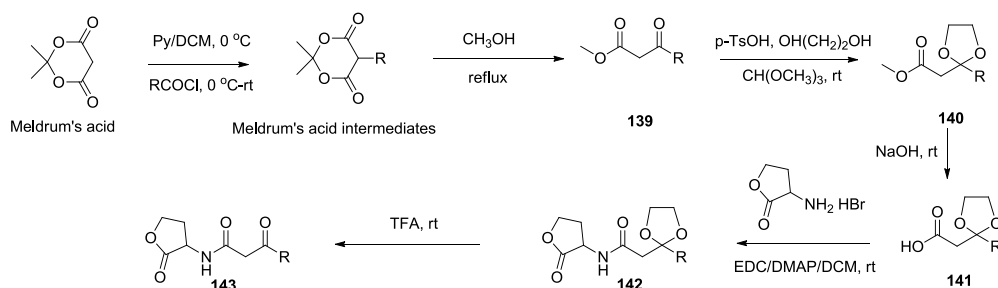
Entry	L-134	D-134	L-134	D-134
Measured $[\alpha]_D^{22}$	+15	-15	+14.6	-14.7
Known $[\alpha]_D^{22}$	+15	-15	+15	-15
Yield	70%	73%	84%	94%

The other compounds with unfunctionalized acyl chains, were then easily prepared from L-**133** and D-**133** by direct acylation with the corresponding acyl chloride (**Scheme 9**) in yields ranging from 46% to 86%. In the case of compound **135**, the acyl chloride was synthesized from 4-phenylbutyric acid by using oxalyl chloride with catalytic dimethylformamide.



**Scheme 9. Synthesis of enantiomers of AHL analogues**

In 2011, David R. Spring et. al<sup>[142]</sup> reported the synthesis of optically pure  $\beta$ -ketoamide AHLs analogues. In the process, some key Meldrum's acid intermediates were firstly prepared, which were subsequently treated in refluxing methanol to give  $\beta$ -ketoesters **139**. The ketone was protected by acetal then the ester was hydrolyzed to afford the acid derivatives **141**. Finally, the optically pure  $\beta$ -ketoamide AHLs analogues **143** were obtained by the EDC-mediated condensation of acid derivatives with L-**133** and D-**133**, followed by an acid-catalyzed acetal deprotection. This synthetic strategy was proved to be an efficient method to obtain optically pure  $\beta$ -ketoamide AHLs analogues with excellent enantiomeric purity, but it took six steps which would be too time-consuming (**Scheme 10**).

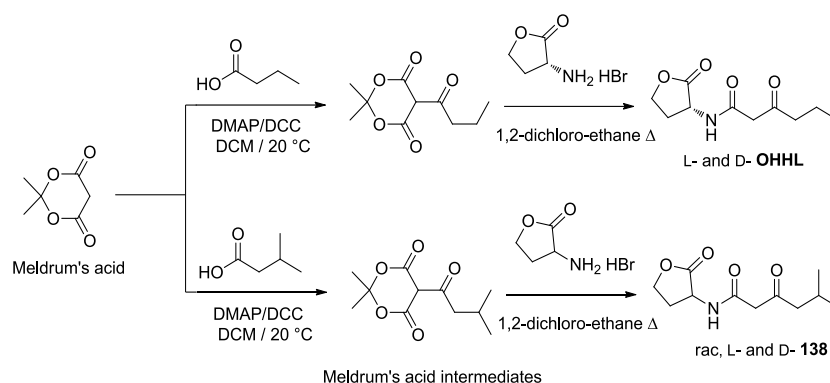


**Scheme 10. Synthesis of optically pure  $\beta$ -ketoamide AHLs analogues reported by David R. Spring**

Our  $\beta$ -ketoamide AHLs **OHHL** and **138** were prepared following a more facile procedure reported by Chhabra,<sup>[138]</sup> using DCC-mediated coupling of carboxylic acid derivatives with Meldrum's acid, as key intermediates (**Scheme 11**). These intermediates were isolated from the reaction mixture by a standard work-up procedure and treated in a separate vessel with compound L- and D-**133** in the presence of a base to afford the corresponding AHL analogues.

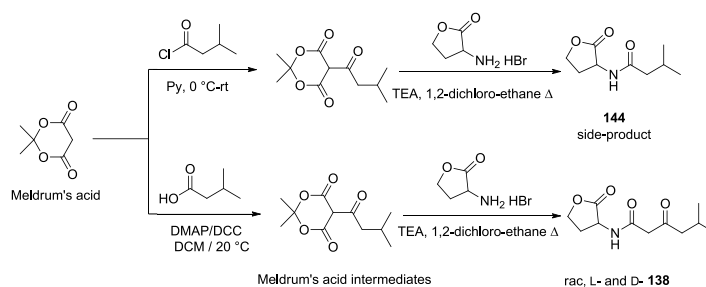
In comparison with the reported method, we made some modification for the formation of Meldrum's acid intermediates. Indeed, after several attempts, acyl chloride and pyridine system gave complicated results which was not favorable for the subsequent steps. When DMAP/DCC was used for the condensation of Meldrum's acid with butyric acid and 3-methylbutanoic acid, the intermediates could be isolated *in situ* by solvent removal upon completion of the reaction, and washing with diluted hydrochloric acid. Then addition of L-**133** and D-**133** to the reaction led directly to the corresponding AHL derivative (**Scheme 11**) under basic conditions in a good

overall yield and with excellent enantiomeric purity. As the racemic and L-**OHHL** are commercially available, only D-**OHHL** was synthesized.



**Scheme 11. Synthesis of  $\beta$ -ketoamide AHLs**

Some unexpected results were also observed in this reaction. If we took the pyridine/acetyl chloride system and the general work-up for the first step, we obtained complicated intermediate mixtures, which would result in the generation of the side product **144** with only trace amount of  $\beta$ -ketoamide AHLs **138**. These two compounds were difficult to be separated by column chromatography. Much better, the DMAP/DCC system could give  $\beta$ -ketoamide AHLs **138** as a pure form (**Scheme 12**). In fact, this significant difference was also observed by David R. Spring et. al.<sup>[142]</sup> In our case, we proposed that the side-product **144** arose in the second stage of the reaction sequence, presumably through amidation of the exocyclic carbonyl group of intermediate, the acidic conditions which were probably introduced from the first stage may have influenced the regio-selectivity of the nucleophilic attack on Meldrum's acid intermediates through some unknown mechanism.<sup>[143]</sup> The base and temperature of the second stage may be also crucial for the regio-selectivity.



**Scheme 12. Two different conditions used for synthesis of  $\beta$ -ketoamide AHLs**

## 2.2.4 Determination of enantiomeric purity

The first step for verification of enantiomeric purity was to measure the optical rotation of these compounds and compared with the known value. Our results are shown in **Table 4**.

**Table 4. Optical rotation of synthesized AHL analogues**

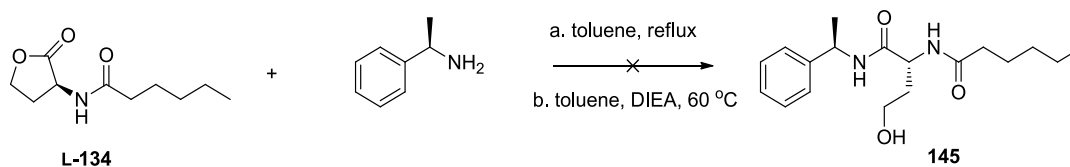
Compounds	Configuration	Yields	$[\alpha]_D^{22}$ (measured)	$[\alpha]_D^{22}$ (known)
<b>133</b>	L	82%	-15.8 (c=1, H <sub>2</sub> O)	-16.14 (c=1, H <sub>2</sub> O)
<b>133</b>	D	88%	+16.2 (c=1, H <sub>2</sub> O)	+16.14 (c=1, H <sub>2</sub> O)
<b>134</b>	L	70%	+15 (c=1, CHCl <sub>3</sub> )	+15 (c=1, CHCl <sub>3</sub> )
<b>134</b>	D	72%	-15 (c=1, CHCl <sub>3</sub> )	New product
<b>135</b>	L	86%	+8.5 (c=0.67, CHCl <sub>3</sub> )	+27.9 (c=0.67, CHCl <sub>3</sub> )
<b>135</b>	D	77%	-8.5 (c=0.67, CHCl <sub>3</sub> )	-24.1 (c=0.67, CHCl <sub>3</sub> )
<b>136</b>	L	65%	-9.3 (c=0.33, CHCl <sub>3</sub> )	+24.6 (c=0.33, CHCl <sub>3</sub> )
<b>136</b>	D	76%	+9.5 (c=0.33, CHCl <sub>3</sub> )	New product
<b>137</b>	L	51%	-9.0 (c=1, CHCl <sub>3</sub> )	New product
<b>137</b>	D	46%	+6.0 (c=1, CHCl <sub>3</sub> )	New product
<b>OHHL</b>	L	c.a	c.a	+7.36 (c=0.95, CHCl <sub>3</sub> )
<b>OHHL</b>	D	73%	-5.7 (c=1, CHCl <sub>3</sub> )	New product
<b>138</b>	L	57%	+6.5 (c=1, CHCl <sub>3</sub> )	New product
<b>138</b>	D	65%	-6.7 (c=1, CHCl <sub>3</sub> )	New product

Compounds L-**133**, D-**133** and L-**134** were consistent with the reported values, D-**OHHL** was close to the opposite of the known value for L-**OHHL**. The enantiomeric purities of other new compounds were uncertain. For compounds L-**135** and D-**135**, distinct differences were observed. With respect to compounds L-**136** and D-**136**, totally opposite value was obtained when compared with the reference. We speculated there were two possibilities: (a) during the sulfonylation step, triethylamine might cause partial or total racemization; (b) the incorrect value of reported references. For verification, we employed Na<sub>2</sub>CO<sub>3</sub> and diisopropylethylamine (DIPEA) to synthesize compounds L-**136** and D-**136** to check whether there was racemization or not, but these three different conditions gave almost the same results (**Table 5**).

**Table 5. Optical rotation of compounds L-136 and D-136 from three different conditions**

Entry	config	conditions	$[\alpha]_D^{22}$ (measured)	$[\alpha]_D^{22}$ (known) <sup>a</sup>
1	L		-9.3 (c=0.33, CHCl <sub>3</sub> )	+24.6 (c=0.33, CHCl <sub>3</sub> )
2	D	TEA, DCM, 0 °C - rt	+9.5 (c=0.33, CHCl <sub>3</sub> )	-
3	L		-10.6 (c=0.33, CHCl <sub>3</sub> )	+24.6 (c=0.33, CHCl <sub>3</sub> )
4	D	Na <sub>2</sub> CO <sub>3</sub> , DCM, H <sub>2</sub> O, rt	+9.5 (c=0.33, CHCl <sub>3</sub> )	-
5	L		-8.5 (c=0.33, CHCl <sub>3</sub> )	+24.6 (c=0.33, CHCl <sub>3</sub> )
6	D	DIPEA, DCM, 0 °C - rt	+8.7 (c=0.33, CHCl <sub>3</sub> )	-

In view of these unexpected results, we began to use other methods to determine the enantiomeric purity. A chemical synthetic method using (*R*)-1-phenylethylamine was proposed. We supposed that our AHLs enantiomers L-134 could react with (*R*)-1-phenylethylamine to furnish a couple of diastereoisomers **145** which have two chiral center and might present differences in <sup>1</sup>H-NMR. Unfortunately, the reaction didn't work (**Scheme 13**).



**Scheme 13. Proposed chemical method for determination of enantiomeric purity**

Then another typical method employing a chemical shift reagent Eu(hfc)<sub>3</sub> (Europium tris[3-(heptafluoropropylhydroxymethylene)-(+)-camphorate]) (**Fig 51**), was considered for the determination of enantiomeric purity. The mechanism is that chiral molecules form a diastereomeric complex with Eu(hfc)<sub>3</sub>, which gives rise to different chemical shifts or integration in proton NMR.

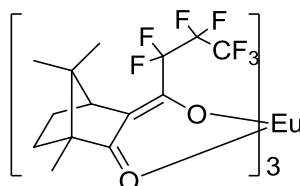


**Fig 51. Eu(hfc)<sub>3</sub>: Europium tris[3-(heptafluoropropylhydroxymethylene)-(+)-camphorate]**

For verification of optical purity of these AHLs enantiomers, firstly, the racemic compounds were treated with different ratio of  $\text{Eu}(\text{hfc})_3$  to compare the full view of  $^1\text{H-NMR}$  and locate the differences of chemical shifts or integration (**Fig 52**); secondly, an appropriate ratio of  $\text{Eu}(\text{hfc})_3$  was confirmed; thirdly, spectra for each sample were recorded with the appropriate ratio of  $\text{Eu}(\text{hfc})_3$ ; finally, we compared the chemical shifts, splitting and integration for each complex and calculated the rough enantiomeric excess. For example, when 30% of  $\text{Eu}(\text{hfc})_3$  was treated with compound **134**, the triplet of  $\text{CH}_3$  was split into a double triplet which were consistent with L-**134** and D-**134** (**Fig 53**).

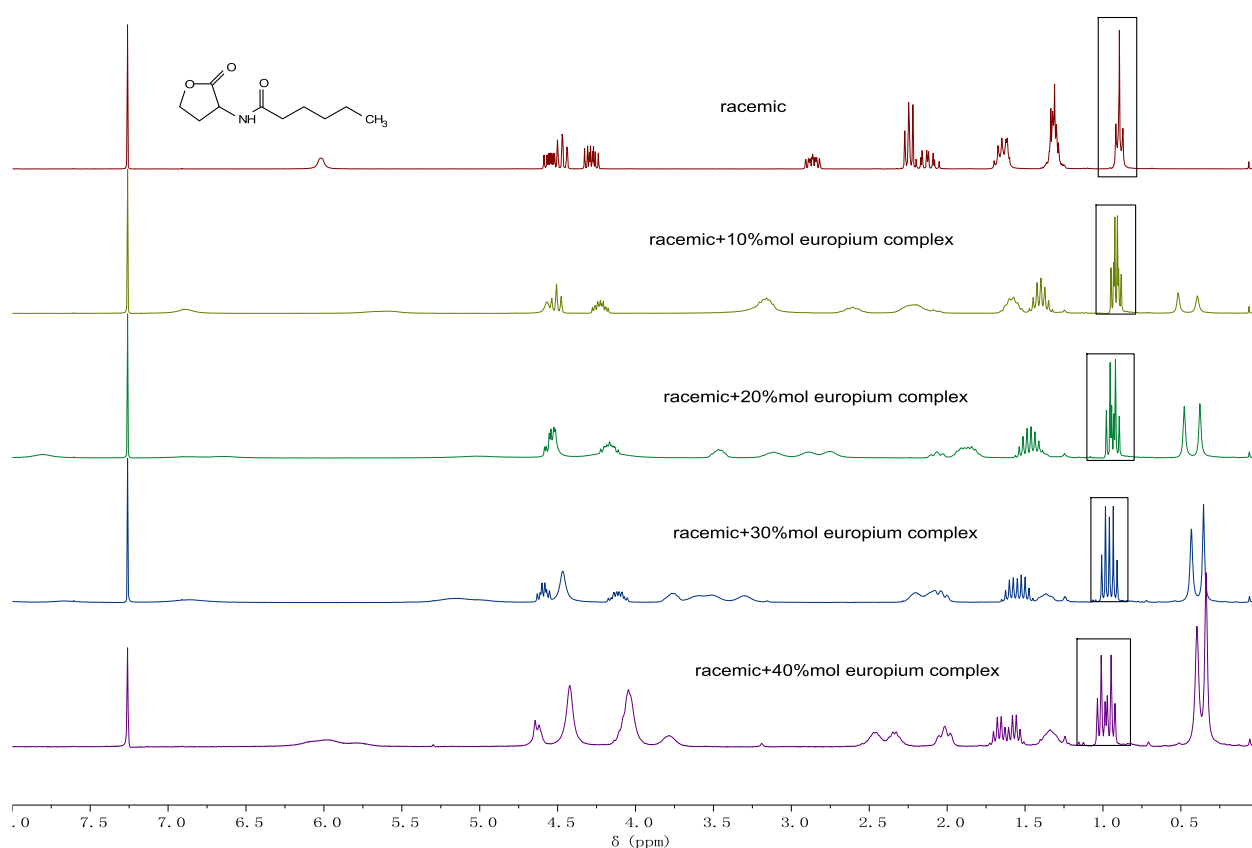


**Fig 52.** Comparison of DL-134 in different ratio of  $\text{Eu}(\text{hfc})_3$  ( $^1\text{H-NMR}$ ,  $\text{CDCl}_3$ , 300 MHz)

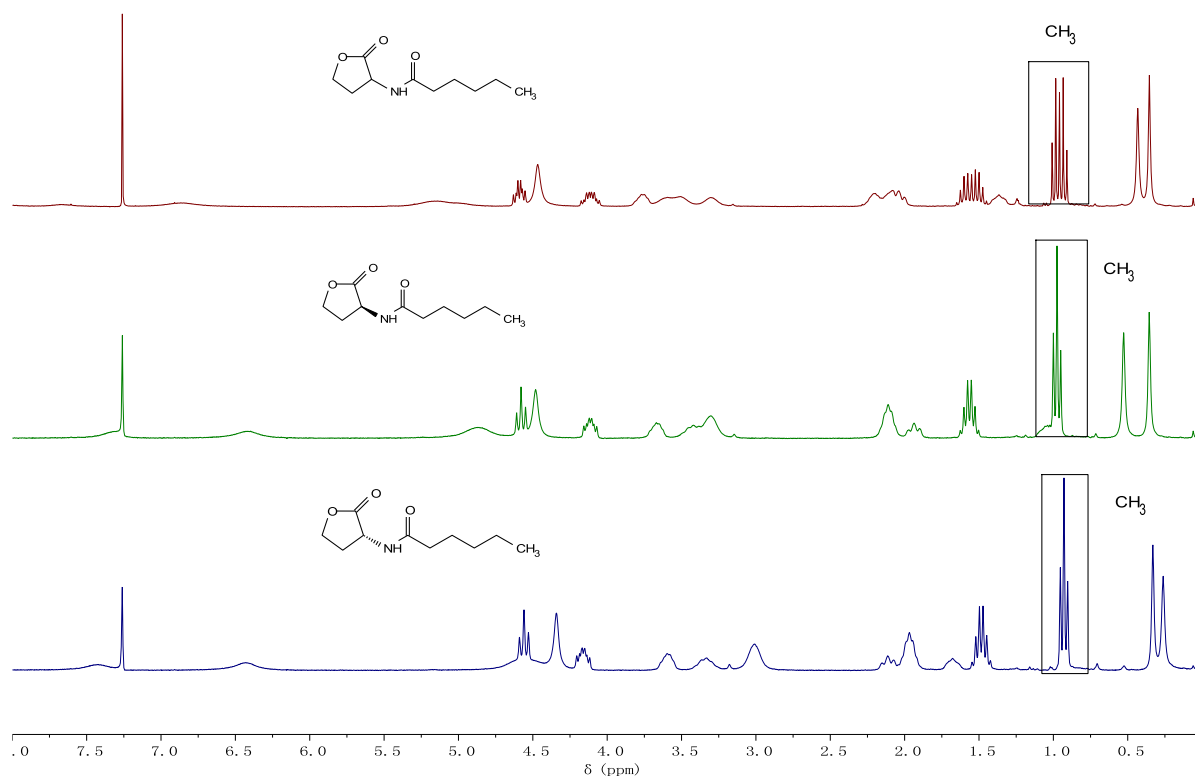


**Fig 53. Comparison of DL-134, L-134, D-134 with 30% mol of Eu(hfc)<sub>3</sub> (<sup>1</sup>H-NMR, CDCl<sub>3</sub>, 300 MHz)**

Compounds L-135 and D-135 were tested with up to 50% mol Eu(hfc)<sub>3</sub>. After comparison of the three spectra, no significant differences in splitting and chemical shift were observed except at aromatic region. The doublet of two phenyl protons in racemic compounds was split up to a double doublet which was consistent with the corresponding doublet in two enantiomers. And the integration of two doublets of AHLs enantiomers indicated the high enantiomeric purity (**Fig 54**).

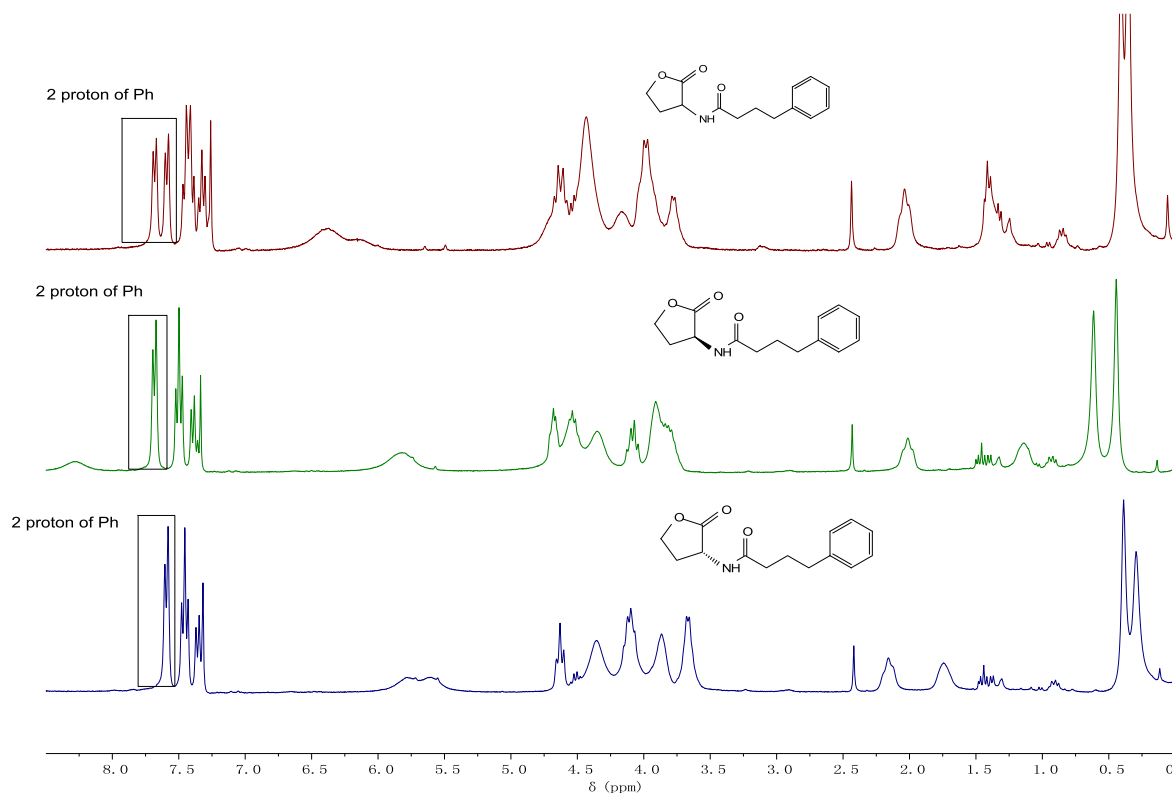


**Fig 54. Comparison of DL-135, L-135, D-135 with 50% mol of  $\text{Eu}(\text{hfc})_3$  ( $^1\text{H-NMR}$ ,  $\text{CDCl}_3$ , 300 MHz)**

Then we determinate the enantiomeric purity of compounds **L-136** and **D-136** using 30% mol  $\text{Eu}(\text{hfc})_3$ . The comparison of three spectra indicated that the triplet of the  $\text{CH}_3$  in the racemic compound were split up to a double triplet which were in agreement with the single triplet in the corresponding AHLs enantiomers. The integration of two doublets of AHLs enantiomers confirmed the high enantiomeric purity (**Fig 55**).

The enantiomeric purity of urea compounds **L-137** and **D-137** were confirmed with 30% mol  $\text{Eu}(\text{hfc})_3$  used for the experiment, which gave the same splitting of  $\text{CH}_3$  signals. High enantiomeric purity was obtained (**Fig 56**).

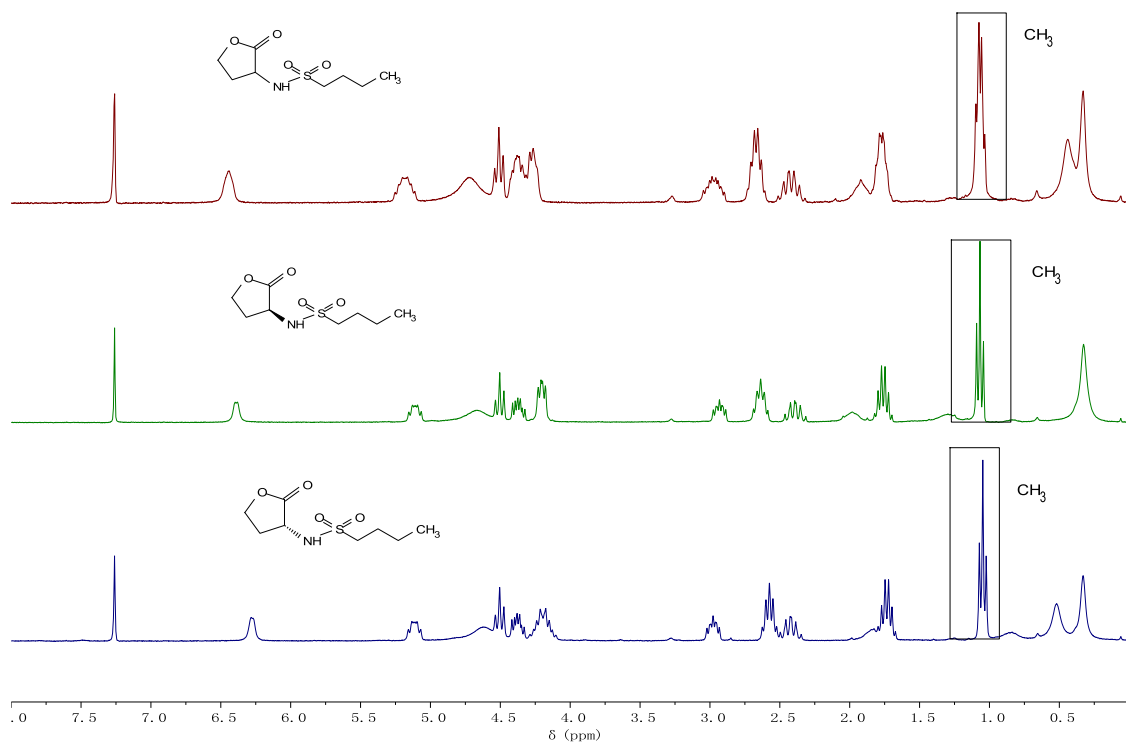


**Fig 55. Comparison of DL-136, L-136, D-136 with 30% mol of  $\text{Eu}(\text{hfc})_3$  ( $^1\text{H-NMR}$ ,  $\text{CDCl}_3$ , 300 MHz)**

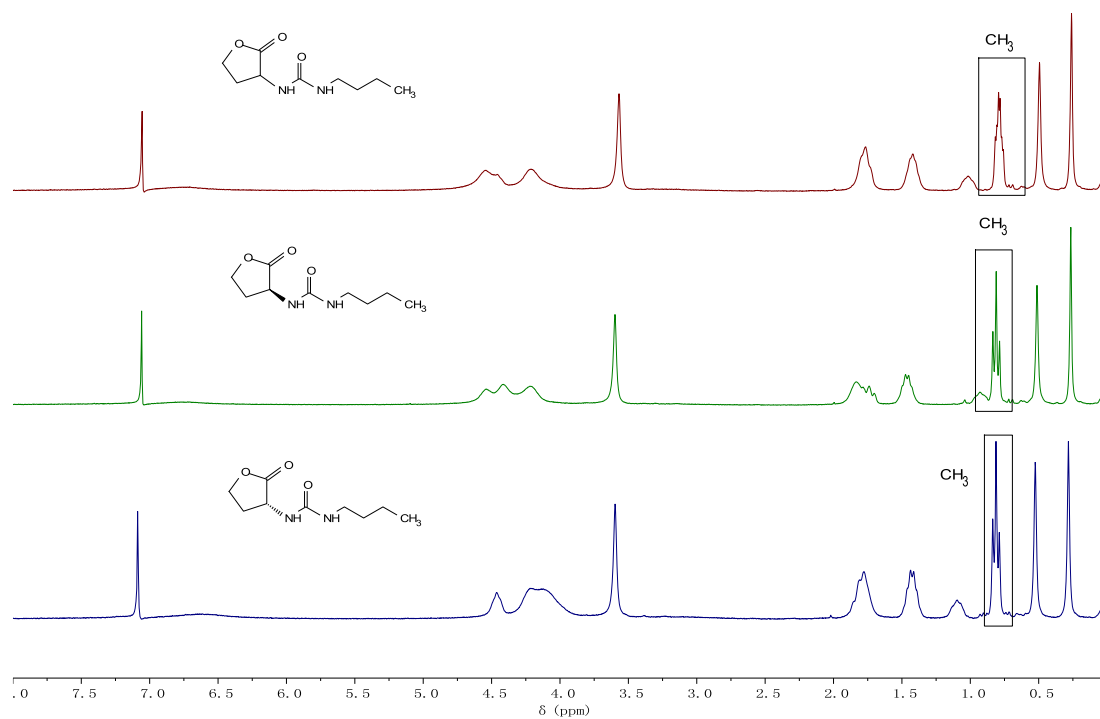


**Fig 56. Comparison of DL-137, L-137, D-137 with 30% mol of  $\text{Eu}(\text{hfc})_3$  ( $^1\text{H-NMR}$ ,  $\text{CDCl}_3$ , 300 MHz)**

The comparison of the spectra of L-OHHL, D-OHHL indicated that OHHL enantiomers have also high enantiomeric purity since dramatic shift changes to low-field region of CH<sub>3</sub>, CH<sub>2</sub>, and lactone were observed after the addition of Eu(hfc)<sub>3</sub>. Interestingly, the chemical shifts of CH<sub>3</sub> and CH<sub>2</sub> in side chain were totally different, although both exhibited triplet or quartet. The same case could also be observed in the CH<sub>2</sub> of the lactone even though it was impaired by the higher concentration of europium complex (Fig 57).

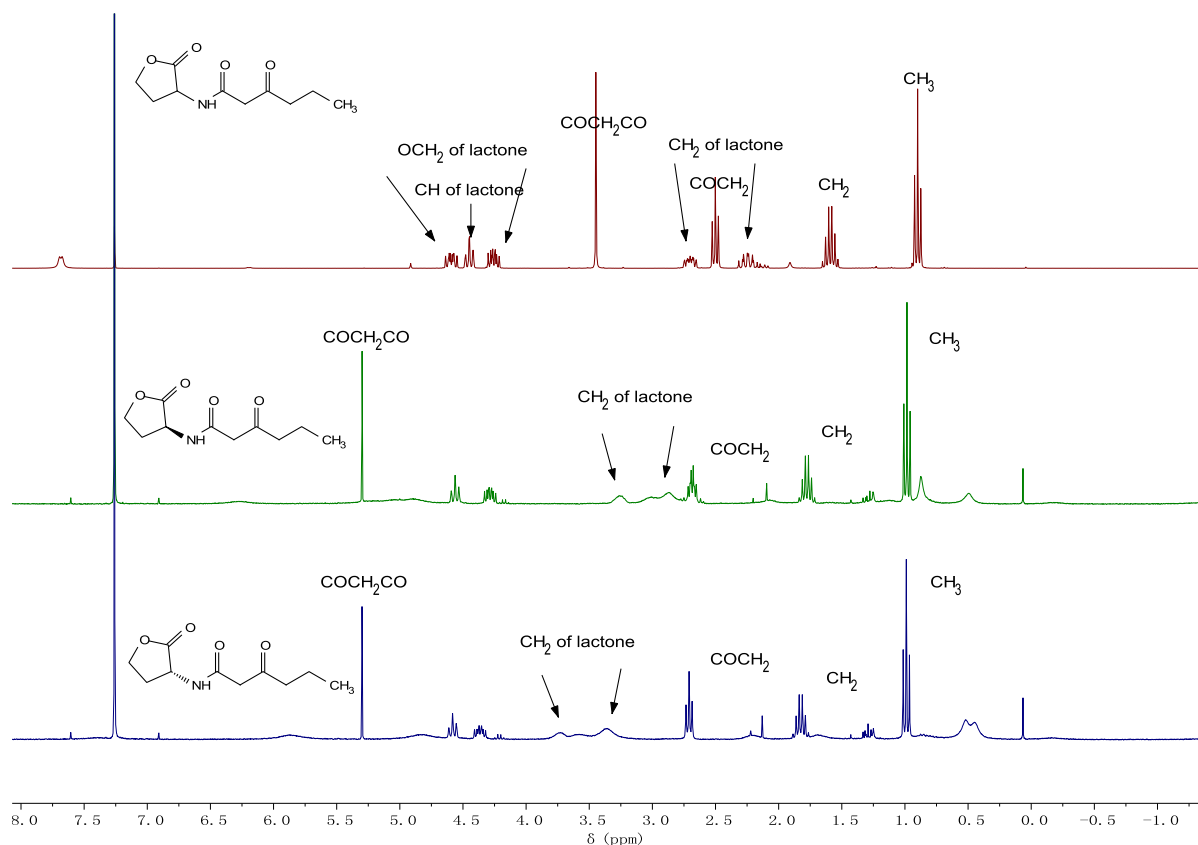
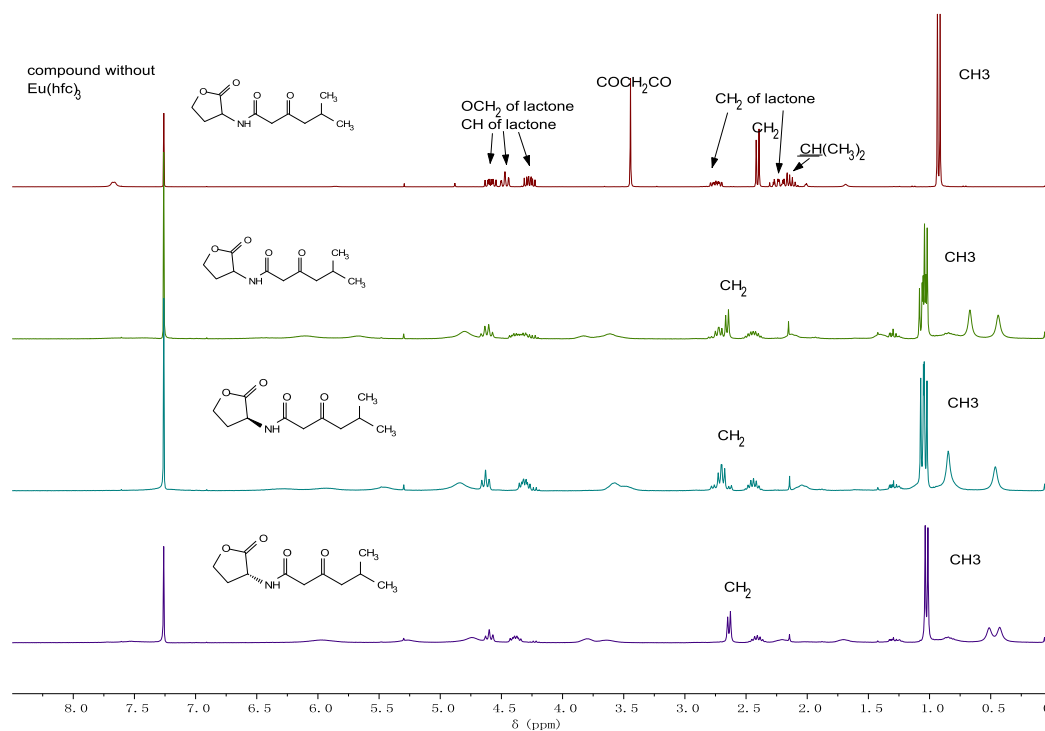


Fig 57. Comparison of DL-OHHL, L-OHHL, D-OHHL with 30% mol of Eu(hfc)<sub>3</sub> (CDCl<sub>3</sub>, 300 MHz)

Compounds **138** series were performed using 30 % mol Eu(hfc)<sub>3</sub>. The chemical shift and integration of compound **138** were completely changed by the introduction of Eu(hfc)<sub>3</sub> especially the side chain (Fig 58). In detail, the doublet of CH<sub>3</sub> was split up to a multiplet including a quartet and a doublet which were from L-**138** and D-**138** respectively. The same case could also be observed in the isopentenyl CH<sub>2</sub>. Surprisingly, the CH<sub>2</sub> between two ketones disappeared, probably because a keto enol tautomerism equilibrium was impacted by Eu(hfc)<sub>3</sub>, and the enol was likely to be a dominant form. There were also some variations in the lactone,

but it was not so obvious compared with the side chain. Therefore, we confirmed the absolute enantiomeric purity simply by the quartet and doublet of CH<sub>3</sub> of the two enantiomers (**Fig 59**).



**Fig 58. Comparison of DL-138, L-138, D-138 with 30% mol of Eu(hfc)<sub>3</sub> (CDCl<sub>3</sub>, 300 MHz)**

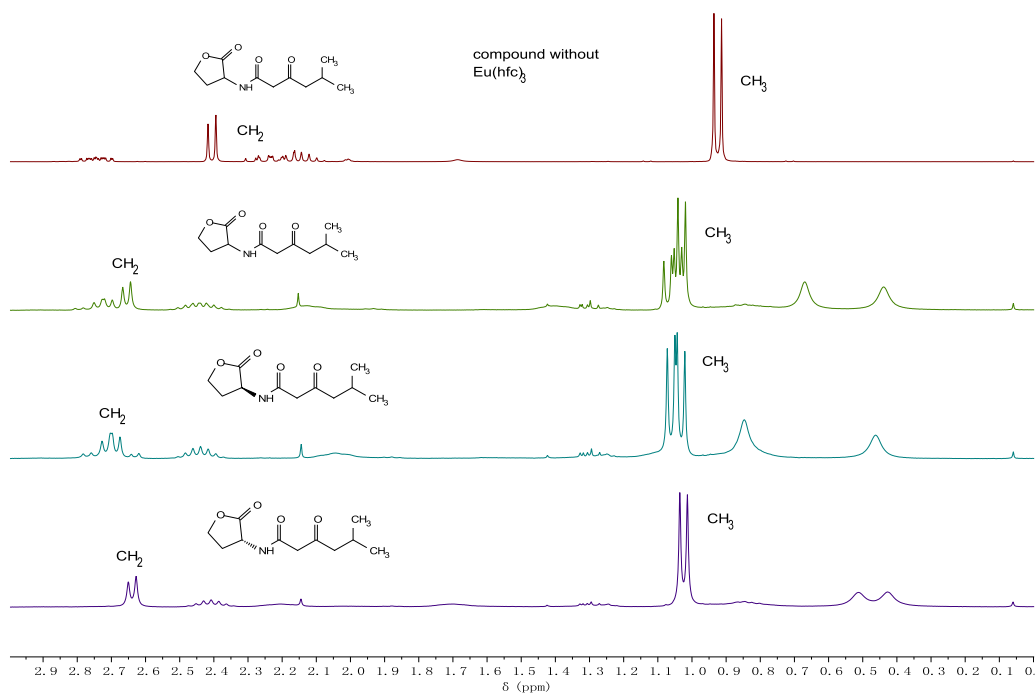


**Fig 59. Enlarged comparison of DL-138, L-138, D-138 with 30% mol of Eu(hfc)<sub>3</sub> (CDCl<sub>3</sub>, 300 MHz)**

NMR experiment using chiral complex was able to confirm the enantiomeric purity, nevertheless, the accuracy of this method was enriched to a far percent. Therefore, the enantiomeric purity was further assessed using chiral HPLC. Referring to the reported conditions,<sup>[142]</sup> all synthesized compounds were conducted in a DAICEL ADH Chiralpak column, eluted with different ratio of heptane/isopropanol. The retention time of racemic compounds were consistent with the corresponding enantiomers indicating that all enantiomers of AHL have excellent level of enantiomeric purities. Further information can be found in experimental sections.

## **2.2.5 Biological evaluation**

### **2.2.5.1 Biological assay conditions**

The biological assays were performed with the help of MAP (Microbiologie, Adaptation, Pathogénie) laboratory of INSA Lyon. We used the recombinant *Escherichia coli* strain NM522 containing the sensor plasmid pSB401 to measure the induction of luminescence by various AHL analogues. In pSB401, the LuxR and the LuxI promoter from *V. fischeri* have been coupled to the entire Lux structural operon (LuxCDABE) from *Photobacterium luminescens*. This construct, present in the biosensor strain (NM522/pSB401), responds to a wide range of AHLs by producing bioluminescence.<sup>[144]</sup> Bacterial cultures were grown in Luria broth, in the presence of tetracycline (20 mg/mL) at 30 °C.

The inducing activity of the various AHL analogues was monitored using the *E. coli* biosensor strain. The AHL activity was measured in a microtiter plate format, with bioluminescence quantified using a Luminoskan luminometer. Concentrations of analogues, ranging from 20 µM to 20 mM, were made up to 0.1 mL volumes with growth medium. The same volume (0.1 mL) of a 1:10 dilution of an overnight culture of the biosensor strain was then added and the plate was incubated at 30 °C. Thus, the final concentration of analogues for agonistic evaluation was 0.1 µM, 0.4 µM, 1 µM, 10 µM, 40 µM, 100 µM, 200 µM. The amount of light produced by the bacteria were detected after 5 h, when the ratio of induced to background light was at its maximum. The amount of light measured was expressed in relative light units.

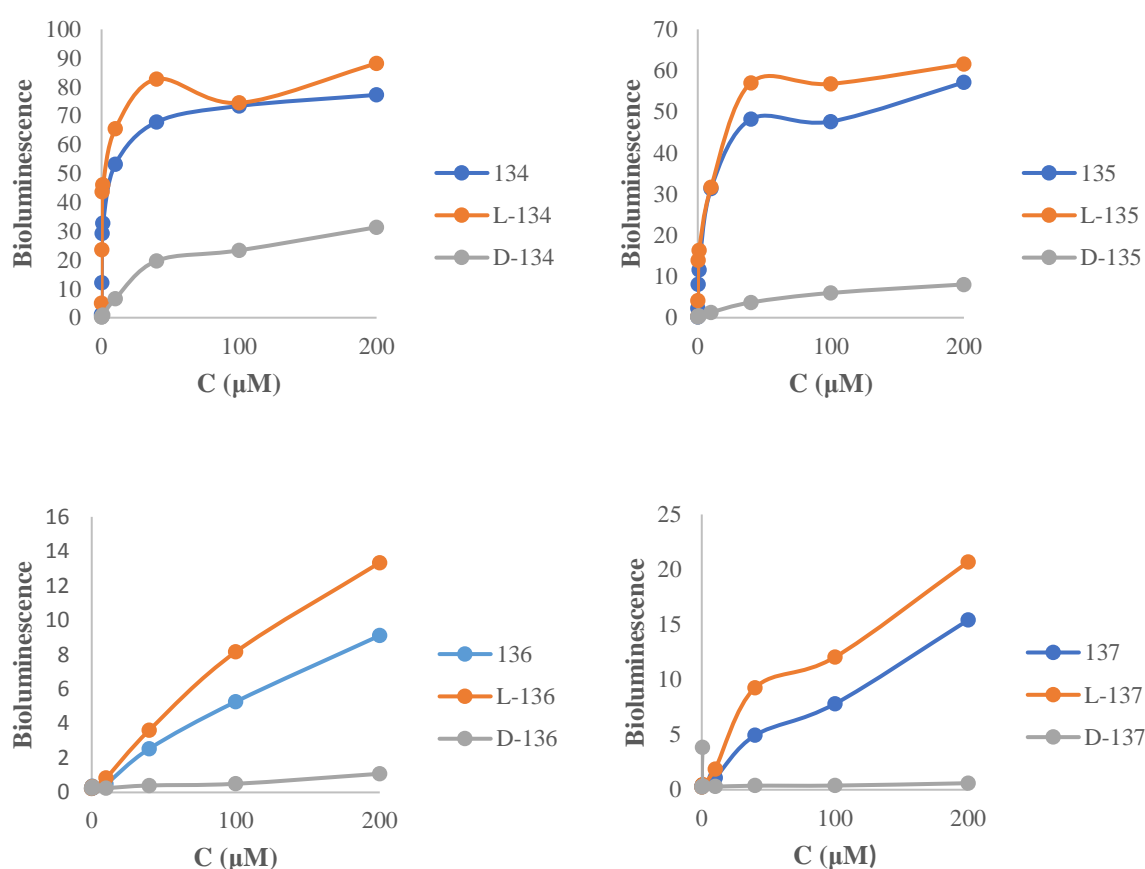
Competition assays were performed in LB growth medium in the presence of 200 nM of 3-oxo-C6-HSL and with simultaneously added analogs, in the following concentrations: 1  $\mu$ M, 4  $\mu$ M, 10  $\mu$ M, 20  $\mu$ M, 40  $\mu$ M, 100  $\mu$ M, 200  $\mu$ M. After inoculation with the biosensor strain, the plate was incubated at 30 °C. The amount of light produced by the bacteria was detected after 5 h and was expressed in relative light units. The experiments were carried out in triplicate. A negative control was performed in the absence of 3-oxo-C6-HSL which gave the basal level of bioluminescence in the absence of an inducer. A positive control was performed in the presence of 3-oxo-C6-HSL only.

### 2.2.5.2 Results and discussion

Firstly, the agonistic activity was evaluated. The results are described in the **figures 60** and **61**. The ability of each analogues to activate the LuxR protein was determined by following the luminescence of the biosensor stain. The natural autoinducer 3-oxo-C6-HSL was used as control. Almost all of racemic compounds exhibited certain level of capability of activating bioluminescence. Based on the inducing level of native autoinducer, compound DL-**134** bearing a hexenyl chain displayed a higher activity than 3-oxo-C6-HSL, and compounds DL-**135** bearing an aryl side chain was as active as 3-oxo-C6-HSL whereas sulfonamide DL-**136** and urea DL-**137** were only active at higher concentration. It revealed that the introduction of aryl group in the terminal of long chain might result a decrease of agonistic activity, and the replacement of carbamide by sulfonamide or urea could devoid of inducing activity. In addition, compound DL-**138** had the same activity with OHHL, which indicated that a tiny change in the function side chain of AHLs analogues didn't impact the activity. This result was consistent with our previous report.<sup>[63]</sup>

To compare each corresponding enantiomer, compounds L-**134**, L-**135**, L-**136**, L-**137** were also tested as agonists. They were found to activate bioluminescence especially compound L-**134**. Compound D-**134** was proved to be inactive compared with the L-one at lower concentration (0.4  $\mu$ M to 1  $\mu$ M), while exerted activity at higher concentration between 10  $\mu$ M to 200  $\mu$ M. Compounds L-**136** and L-**137** were active at high concentrations. In all cases, the L-isomers were the most active ones while the D-isomers were moderately active for compounds

**135** and **136** or inactive for compound **137** at higher concentration (**Fig 60**). At lower concentration, none of D-isomers were found to be active. For  $\beta$ -ketoamide AHLs analogues **OHHL** and **138**, no significant differences were observed between racemic and the corresponding isomers at higher concentration (50  $\mu$ M to 200  $\mu$ M). But at lower concentrations (0.4  $\mu$ M to 1  $\mu$ M), the activity of the D-isomers of  $\beta$ -ketoamide AHLs analogues was not negligible with relative bioluminescence ranging from 10 to 20 compared with the L-isomers which led to the maximum of relative bioluminescence with values from 50 to 60 (**Fig 61**).



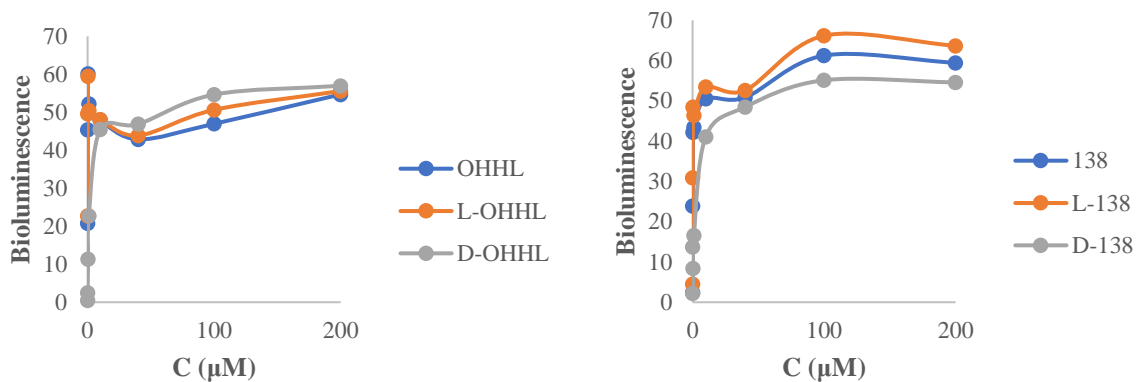


Fig 60. Agonistic activity evaluation at high concentrations

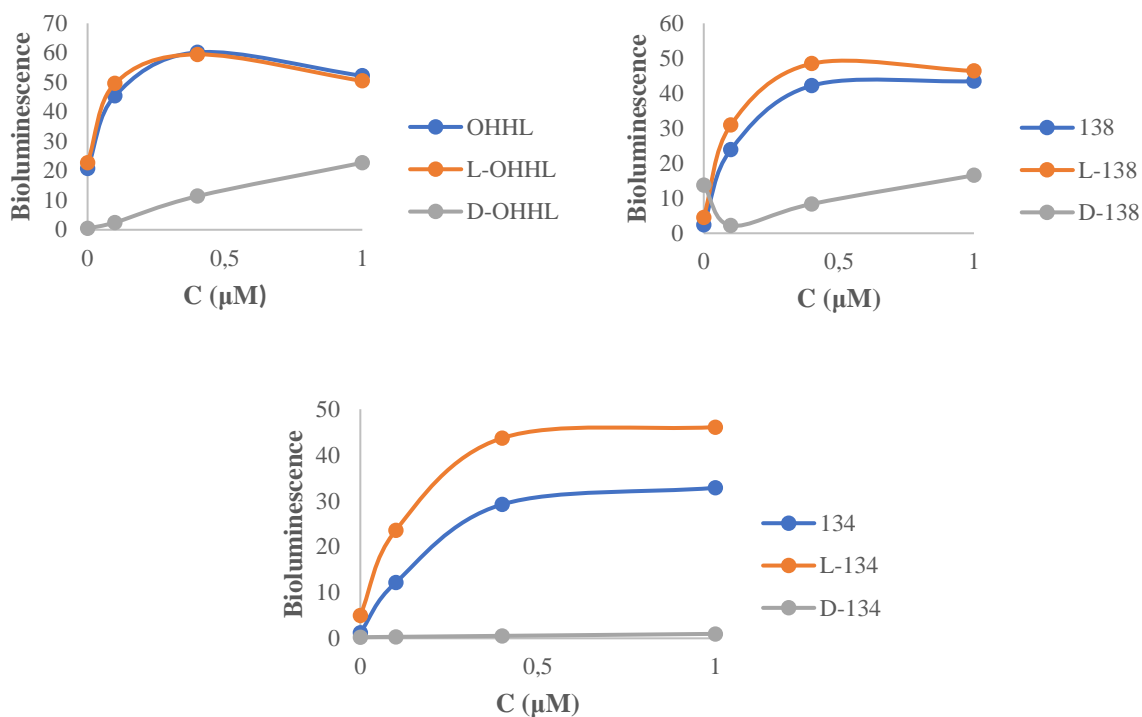
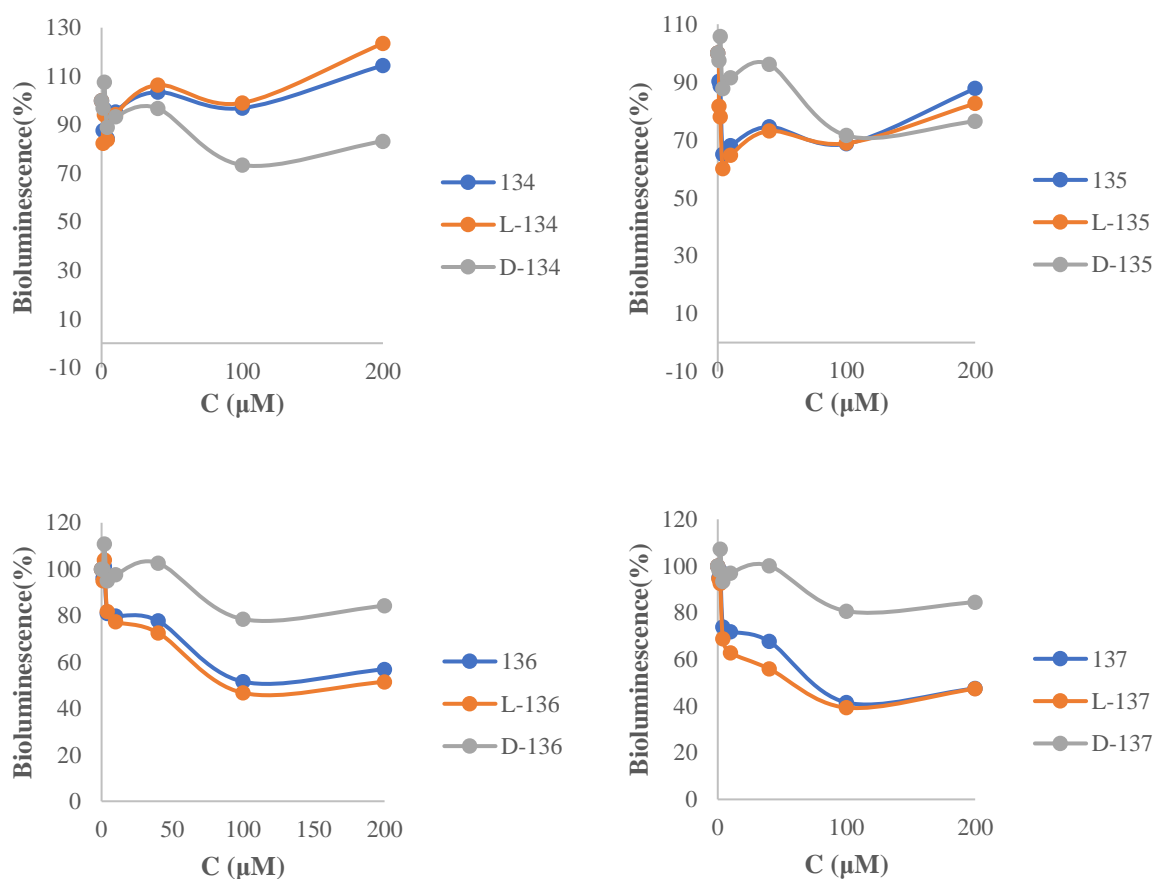
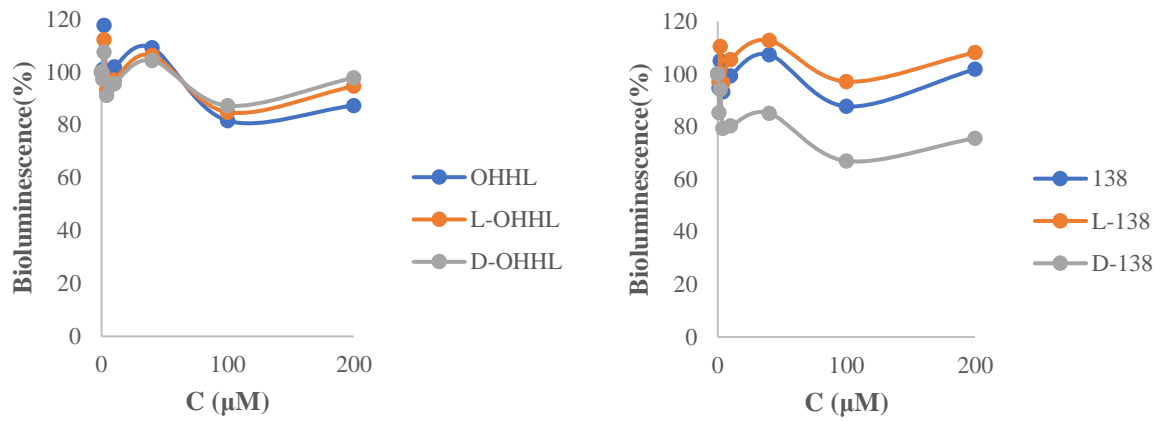


Fig 61. Agonistic activity evaluation at low concentrations

The above synthesized compounds were also evaluated for their antagonistic activity. Compound DL-134 and L-134 were inactive even at higher concentration (200 μM) while the D-isomer exerted an antagonistic activity at high concentrations. Compound DL-135 was an

antagonist, the same result was also found in its L-isomers, the D-isomer was proved to be inactive at lower concentration but a weak antagonist at higher concentration (200  $\mu\text{M}$ ) (**Fig 62**). For compound DL-136 and DL-137 and their enantiomers, it was obvious that both of racemic compounds and L-isomers were strong inhibitors, comparatively the D-isomers were less active. In the case of  $\beta$ -ketoamide AHLs, compound DL-OHHL and DL-138 and their enantiomers were unable to inhibit bioluminescence since they were known as strong agonist.<sup>[63]</sup> There were still no differences of activity observed between racemic compounds and their enantiomers at high concentration, while compound D-138 was found to be weak antagonist even at 1  $\mu\text{M}$  to 10  $\mu\text{M}$  (**Fig 63**).





**Fig 62. Antagonistic activity evaluation at high concentrations**

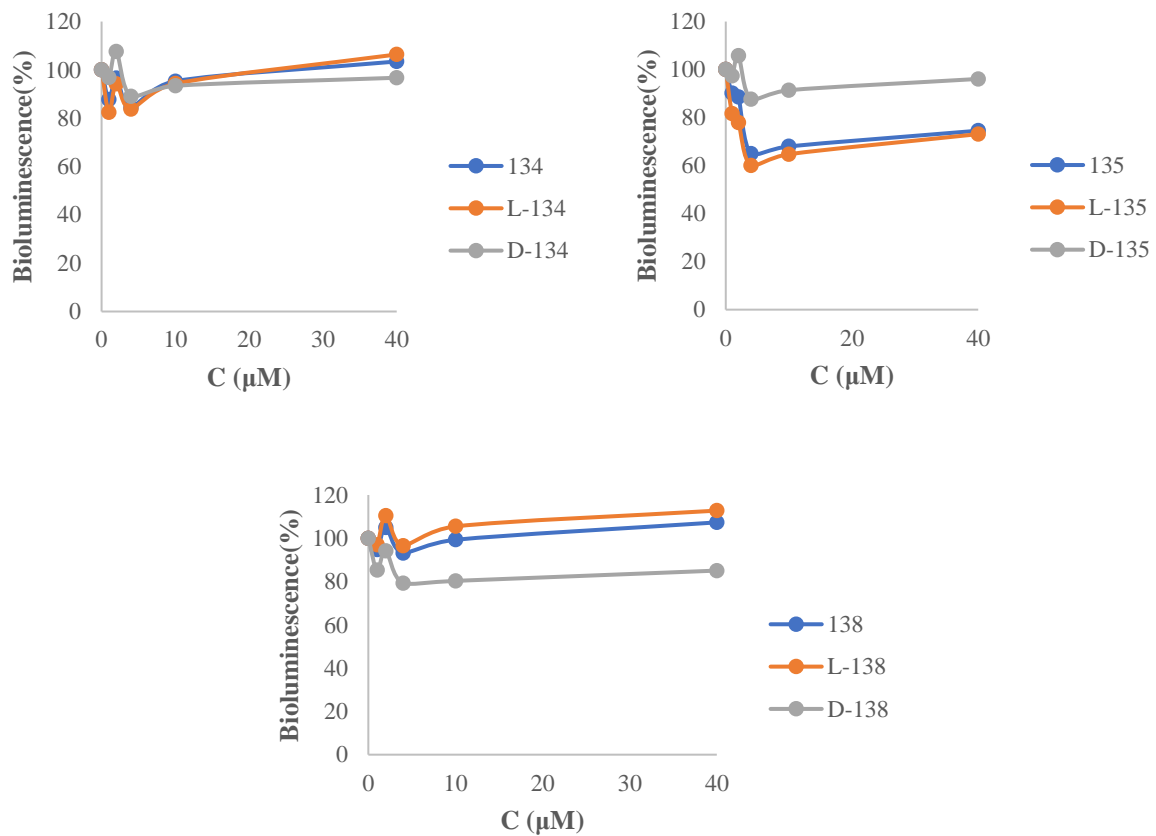
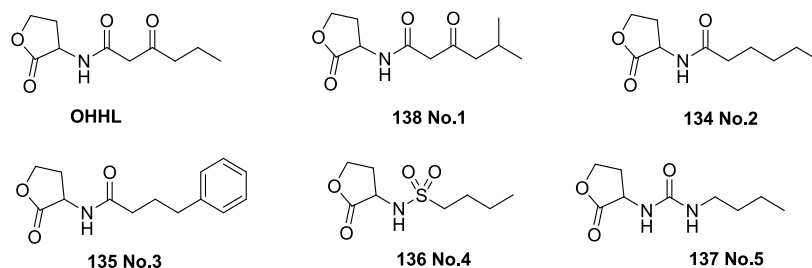


**Fig 63. Antagonistic activity evaluation at low concentrations**

## 2.2.6 Molecular docking studies

To further get insight into structure-activity relationships, we investigated molecular modeling studies on both L and D isomers for each compounds using the LuxR model (**Fig 64**). For compounds **OHHL**, **138** and **134** the binding mode of the D-isomer is very close to the L-one except for the lactone which moves to a different orientation. The hydrogen bonds network is globally identical with a difference with the lactone ring. Indeed, the C=O of the lactone of D-isomer is involved in a hydrogen bond with the Trp66 as for the L-isomer, but the oxygen of the of the lactone is engaged in a hydrogen bond with Tyr62. Overall the global binding mode of all isomer might explain the biological activity of the D-isomer which posses a moderate agonist (OHHL and compound **138** and **134**) or antagonist at high concentration for compound **138** and **134**.

For known antagonists **135**, **136**, **137**, the binding modes obtained as results of molecular docking are very different from the L-ones. Indeed the global orientations are dissimilar with different hydrogens bonds. These differences explain the fact that D-isomers are slightly active at high concentration as antagonists.



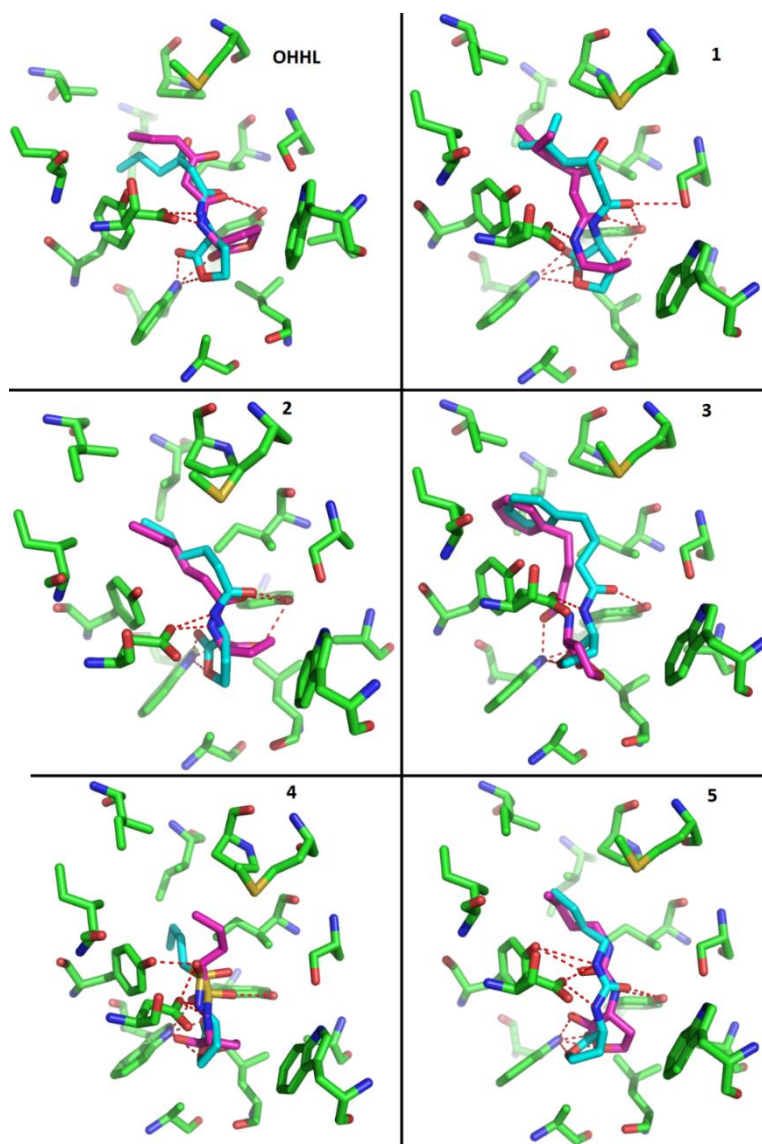


Fig 64. Molecule docking studies of optically pure AHLs

### 2.2.7 Conclusions

We synthesized a range of optically pure AHLs analogues bearing an alkyl, aryl, as well as sulfonamide, urea derivatives in good to excellent yields. The D-enantiomers of natural inducers of the LuxR regulator which were produced by the AHL synthase LuxI of *V. fischeri*: **OHHL** and its analogues compound **138** were also prepared by a reliable and ordinary synthetic route from Meldrum's acid. Chiral NMR shift reagent and chiral HPLC were used to analyze the enantiopurity of the final AHLs, and in all cases, excellent levels were observed. These

results are crucial for the bioluminescence evaluation and provide a basis for the accuracy of chirality-activity relationships.

Considering their biological activity, the racemic AHLs compounds varying in side chain and functional amide have been reported and discussed in previous studies.<sup>[63,145–147]</sup> However, because LuxR-type transcriptional regulators activate gene transcription only after dimerization, which requires the preliminary binding of AHL, definitive understanding of the effect of a racemic mixture remains difficult. Indeed, either homo or heterodimers might be formed.<sup>[148]</sup>

For the enantiomers, L-isomers are confirmed to be the only or the most active enantiomers. However, this work indicates that in several cases, (mostly for very close AHL analogues) the D-isomer should not be considered as totally inactive on QS. Moreover, this activity was found to be either activation or inhibition. Modelling showed that when possible, the lactone moiety of the D-isomer could twist in the way the lactone carbonyl group would still interact with the key residues in the binding site.

## 2.3 Synthesis of AHLs analogues with long chain

### 2.3.1 Introduction

In the last section, several series of chiral AHL analogues have been discussed with a focus on the chirality-bioactivity relationships. In all next sections, racemic molecules are only considered, based on a first approximation that activity relies essentially on the L-isomer, as supported by the above results.

In this section, we discuss another type of AHLs analogues, which could be used for the purification of some specific enzymes being responsible for the AHL lactonase activity in legumes, by the feature of long chain AHL analogs capable of grafting. Such strategies were designed in collaboration with Dr. Yves Dessaux at Gif sur Yvette.

This lactonase is capable of hydrolyzing the long AHLs varying from six to ten carbons. After attempting to purify the lactonase by conventional techniques, some biologists concluded that an affinity column would be a critical element. For this it was important to find a substrate being able to bind the lactonase. We therefore looked for molecules resembling the AHL, for example the known inhibitors of the hydrolysis reaction. One molecule of interest was found to be 3-oxo-C12, which is a non-substrate and effectively acts as an inhibitor of hydrolysis of C6-HSL. After the investigation of biologists, it would be crucial to lengthen the side chain and to add a reactive group allowing the grafting of this side chain on a support magnetic balls or affinity column.

Thus, the AHL analogues are designed to be possibly grafted on a solid support, thanks to a terminal function such as a carboxylic acid. For this purpose, two AHL derivatives with the protected terminal carboxyl group of long chain were prepared, one in the C16 series, and the other in the 3-oxo-C18 series. HSL-C16 was also prepared for the preliminary test of affinity column. The following sections will present the detailed synthetic routes for three target compounds **146**, **147**, **148** (**Fig 65**).

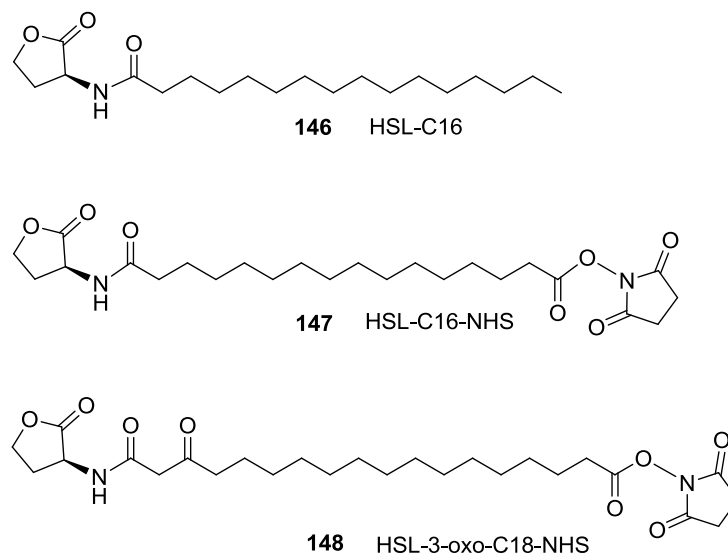
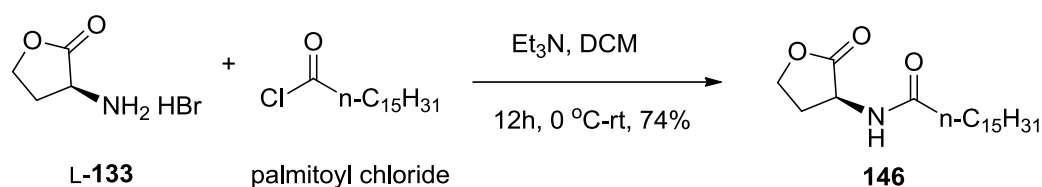


Fig 65. Target long chain AHL analogues

### 2.3.2 Synthesis of HSL-C16

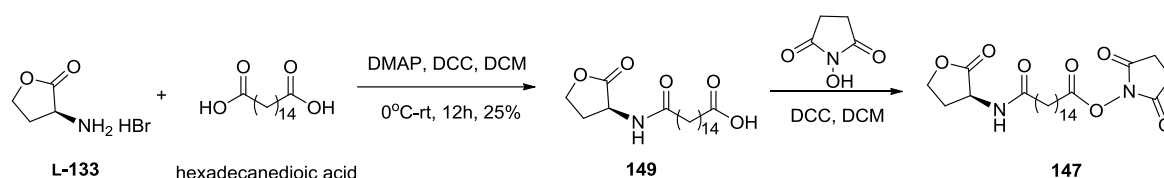
Based on the synthesis of optically pure AHLs analogues in last section, HSL-C16 was synthesized from the acylation of (*S*)-homoserine lactone hydrobromide L-133 with palmitoyl chloride. During the reaction, the desired compound was precipitated from the solution thanks to its poor solubility in dichloromethane, and was obtained as a pure white solid after recrystallization in AcOEt in 74% yield (**Scheme 14**).



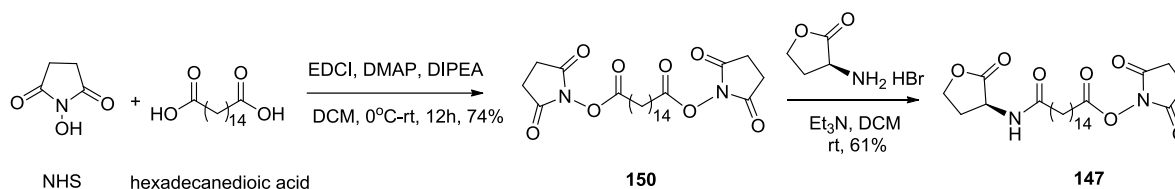
Scheme 14. Synthesis of HSL-C16

### 2.3.3 Synthesis of HSL-C16-NHS

For the synthesis of HSL-C16-NHS, firstly, a reaction sequence of mono-substitution of hexadecanedioic acid **149** and condensation was proposed (**Scheme 15**), but it only gave trace amount of desired product after work-up and purification. Then di-substitution (**Scheme 16**) of hexadecanedioic acid followed by the mono-substitution by (*S*)-homoserine lactone hydrobromide L-133 was proved to be the better sequence,<sup>[149]</sup> which afforded the desired product in good yield.



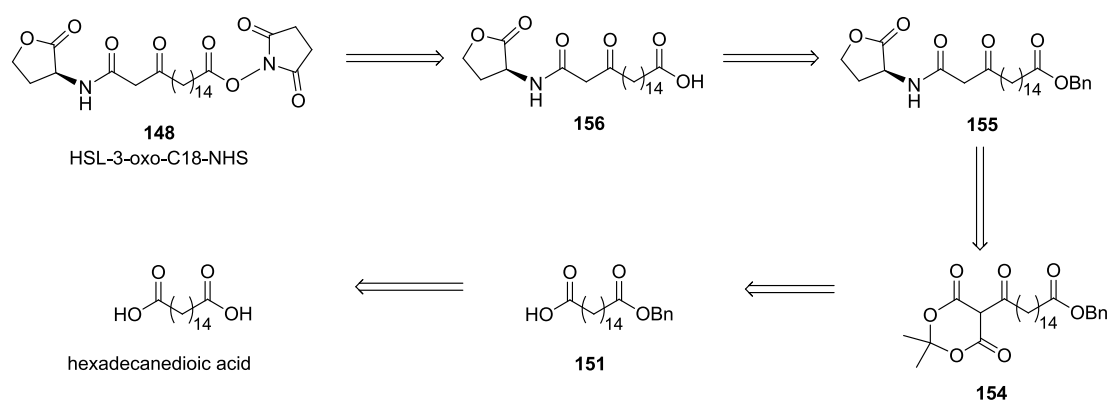
**Scheme 15. Synthesis of HSL-C16-NHS by mono-substitution of hexadecanedioic acid**



**Scheme 16. Synthesis of HSL-C16-NHS by di-substitution of hexadecanedioic acid**

### 2.3.4 Synthesis of HSL-3-oxo-C18-NHS

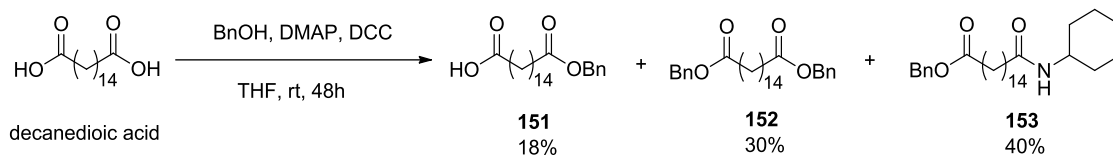
The retrosynthetic analysis of HSL-3-oxo-C18-NHS is shown in **Scheme 17**. The target compound has similar structure as compared with HSL-C16-NHS while bear a 3-keto group. It could be obtained from the condensation of HSL-3-oxo-C18 carboxylic acid **156** with NHS, the 3-keto could be induced by mean of condensation of Meldrum's acid with partially benzylated hexadecanedioic acid **151**. The final point was the preparation of mono-benzylated hexadecanedioic acid **151**.



**Scheme 17. Retrosynthetic analysis of HSL-C16-NHS**

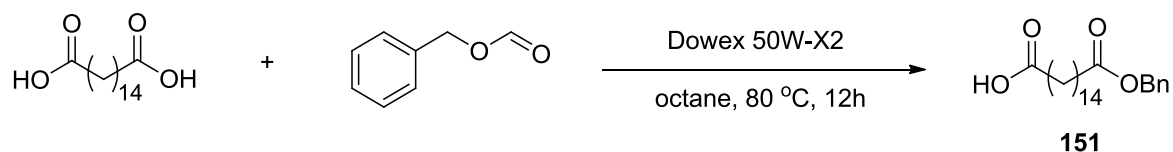
In order to synthesize mono-benzylated hexadecanedioic acid **151**, a typical condensation method using DMAP/DCC was employed.<sup>[150]</sup> We adopted the same condition (1 equivalent of benzyl alcohol, 1.2 equivalent of dehydrant DCC and catalytic amount of DMAP) for the target

product, but the reactivity decreased due to the long chain. The reaction afforded the mono-benzylated product **151** in 18% yield, the di-benzylated compound **152** in 30% yield and an intermediate **153** in 40% yield (**Scheme 18**).



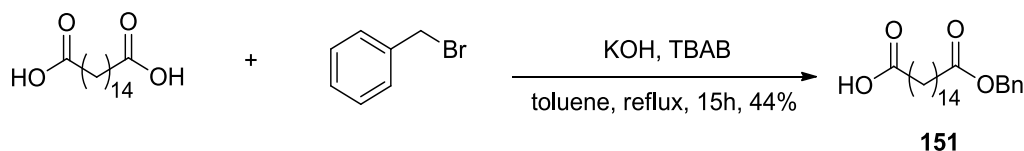
**Scheme 18. Mono-benzylation of decanedioic acid using DMAP/DCC**

Our attention was then turned to other methods. A convenient method using benzyl formate as reagent and Dowex 50W-X8 as catalyst in octane was reported by George W. Gokel.<sup>[151]</sup> After several attempts, the separation of desired product analytically by column chromatography was proved to be extremely difficult as a result of the co-elution with benzyl alcohol (**Scheme 19**). Thus, alternative synthetic route would be considered.



**Scheme 19. Mono-benzylation of decanedioic acid using benzyl formate**

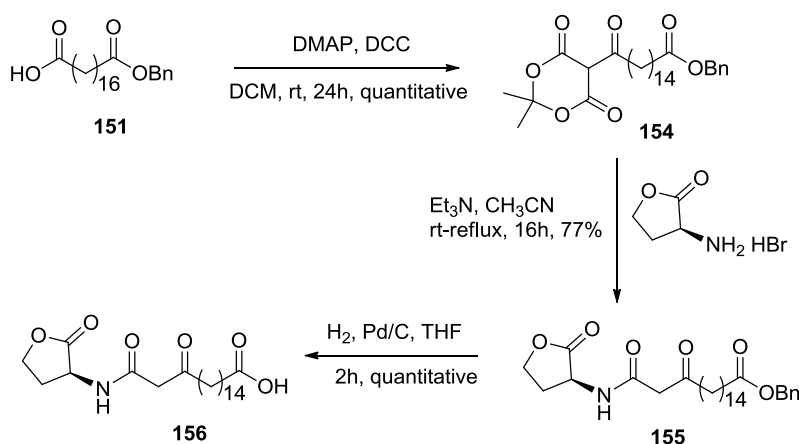
Following the method reported by M. W. Grinstaff<sup>[152]</sup> for the synthesis of mono-benzylated dodecanoic acid using benzyl bromide, KOH and TBAB in the boiling toluene. The desired was obtained in 44% yield with high purity (**Scheme 20**).



**Scheme 20. Mono-benzylation of decanedioic acid using benzyl bromide and TBAB**

For the next step, Meldrum's acid was employed for the combination of 3-oxo protection and alkanolic acid activation.<sup>[138]</sup> The Meldrum's acid derivatives **154** were prepared in nearly quantitative yields by using Meldrum's acid and compound **151** in  $\text{CH}_2\text{Cl}_2$  in the presence of

DCC/DMAP. The isolated product was used without further purification (**Scheme 21**). Its characterization by  $^1\text{H-NMR}$  established not only its identity but also the presence of H-bonded enolic structures **154a** with the enol proton resonating at  $\delta$  15-16 (**Fig 66**). The amidation conditions were screened in two solvents: 1,2-dichloroethane and acetonitrile (**Table 6**). The former was not favorable for the reaction, thus, finally amidation of compound **24** with L-**133** was accomplished in the presence of triethylamine in  $\text{CH}_3\text{CN}$  affording the *N*-(3-oxoalkanyl) compound **155** in 77% yield, followed by a general hydrogenation to furnish carboxylic acid **156** in quantitative yield.



**Scheme 21.** Condensation, amidation and hydrogenation steps for synthesis of compound **156**

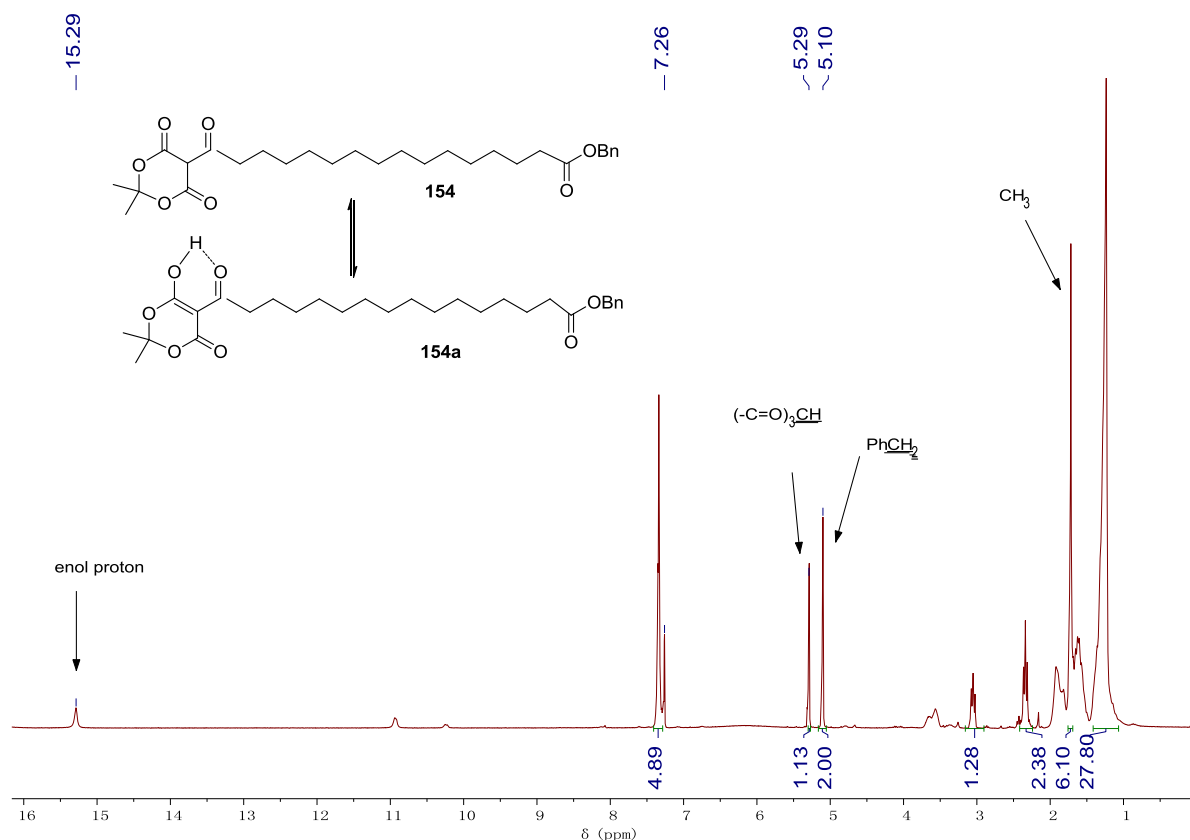


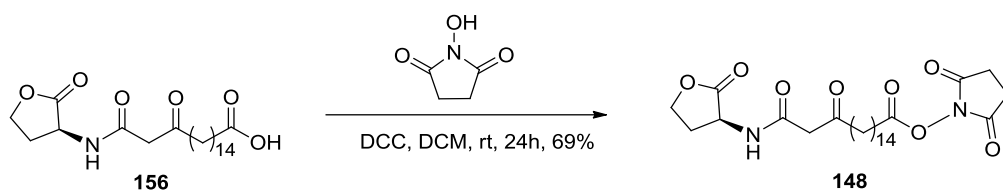
Fig 66. Ketoenol tautomerism of compound 154 (300 MHz,  $\text{CDCl}_3$ )

Table 6. Optimization of amidation step

Entry	solvents	TEA	Conditions	Yields
1	1,2-dichloroethane	1.2 eq	rt-reflux <sup>a</sup> , 16h	26%
2	1,2-dichloroethane	1.8 eq	rt-reflux, 16h	31%
3	acetonitrile	1.2eq	reflux <sup>b</sup> , 12h	50%
4	acetonitrile	1.6eq	rt-reflux, 16h	77%

a. Before the reaction was refluxed, the mixture was stirred at rt for 1 h. b. The reaction was heated up to reflux rapidly.

Finally, the product **148** was obtained by the condensation of carboxylic acid **156** with NHS in the presence of DCC in 66% yield (**Scheme 22**). The product was fully characterized, the methylene group between two ketos locates at  $\delta$  3.5 compared with HSL-C16-NHS (**Fig 67**).



**Scheme 22. Final condensation step for synthesis of compound 148**

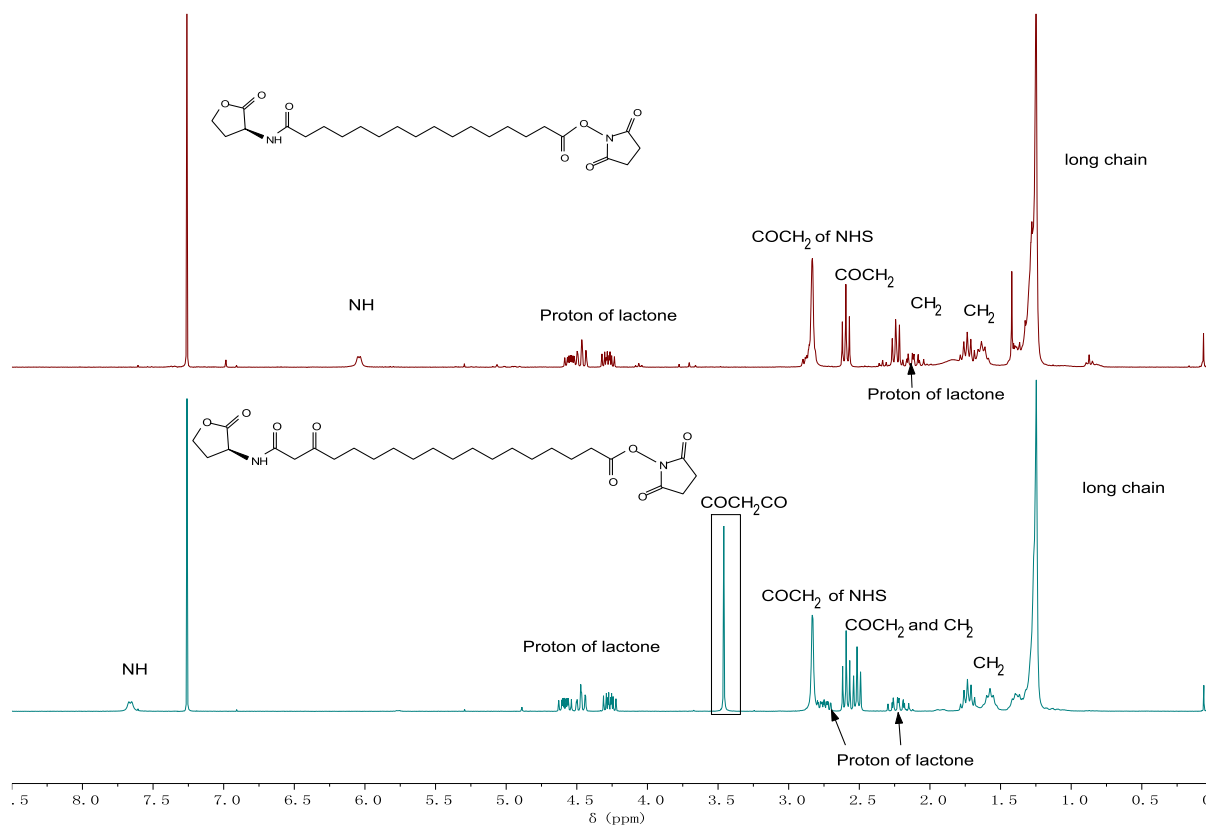


**Fig 67. Comparison of compounds 147 and 148 (300 MHz, CDCl<sub>3</sub>)**

### 2.3.5 Conclusion

These three compounds have been prepared and fully characterized, they have now been provided to our colleagues in Gif sur Yvette and will be used in enzyme purification experiments in a near future.

## 2.4 Design, synthesis and biological evaluation of oxadiazoles as QS modulators

### 2.4.1 Introduction

Pursuing our efforts to identify new QS inhibitors by replacing the amide of AHLs with various functions, our attention was turned to replace the amide by heterocyclic rings in particular oxadiazoles. Oxadiazoles are frequently encountered in bioactive molecules heterocycles. They are good bioisosteres of amide bonds since they are stable in respect of metabolic reactions (oxidation, reduction, acid hydrolysis or basic) and have the ability to form hydrogen bonds or to be involved in interactions of  $\pi$ -stacking with different amino acids of the active sites of enzymes or receptors.<sup>[99,153,154]</sup> Variations in the position of heteroatoms the heterocyclic rings were considered with 1,3,4- and 1,2,4-oxadiazole. For the lactone area, either the native  $\gamma$ -lactone, or the carboxymethyl esters were investigated, and for the side chain, each series were synthesized with a panel of four linear alkyl and aryl side chains of various lengths.

Thus, six families of oxadiazoles were designed and synthesized for the bioluminescence evaluation including two series of 1,3,4-oxadiazoles substituted in position 5 with an alkyl chain and in position 2 with an ester or a lactone function, and two series of 1,2,4-oxadiazole either with carboxymethyl esters or with lactone in position 3, as well as two series of 1,2,4-oxadiazole either with carboxymethyl esters or with lactone in position 5. We will present the detailed synthetic strategies for six series of compounds (**Fig 68**).

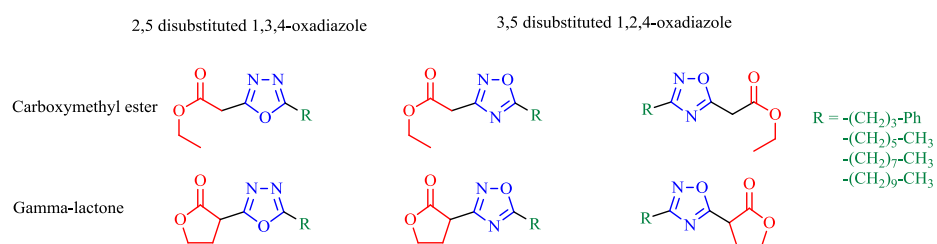
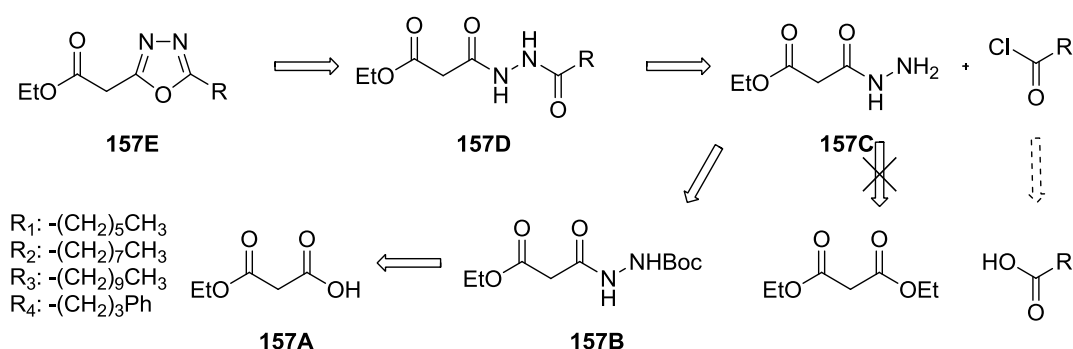


**Fig 68. Target compounds synthesized in this section**

### 2.4.2 Synthesis of 2,5-disubstituted 1,3,4-oxadiazoles with the carboxymethyl ester

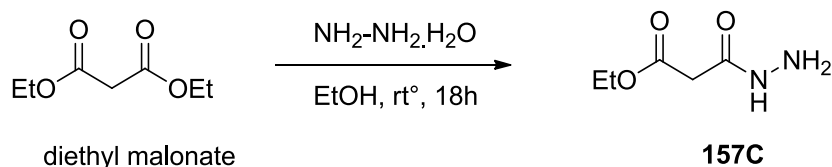
The retrosynthetic analysis is presented in **Scheme 23**. Compounds **157E (1-4)** are prepared by cyclization of diacylhydrazine (bishydrazide) compounds **157D (1-4)** which could be obtained by acylation of hydrazide **157C** with acid chlorides. Non-available acid chlorides are obtained from the corresponding carboxylic acids. Deprotection of the Boc protected hydrazine

**157B** could give compound **157C**, and the hydrazine is available from mono-ethyl malonate **157A**.



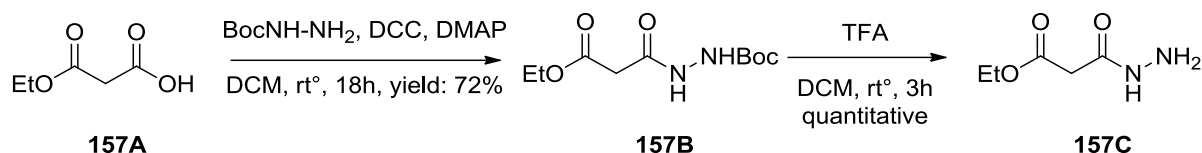
**Scheme 23. Retrosynthetic analysis of 2,5-disubstituted 1,3,4-oxadiazoles with the carboxymethyl ester**

The first issue of the synthetic route was to access the key compound **157C**. It was firstly synthesized directly from diethyl malonate (**Scheme 24**) by substitution of an ester with hydrazine.<sup>[155]</sup> However the compound **157C** was difficult to purify by column chromatography due to its high polarity. Moreover, this method required an excess of diethyl malonate (3 equivalents), which is not commercially available.



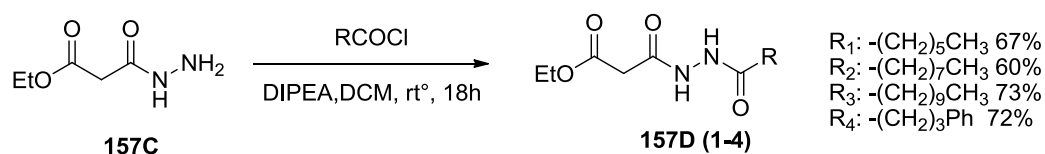
**Scheme 24. Synthesis of compound 157C from diethyl malonate**

Thus, we decided to synthesize compound **157C** from its precursor in which the  $NH_2$  is protected by a Boc group. It was more practical since compound **157C** was obtained quantitatively *via* deprotection in acid medium without purification.<sup>[156]</sup> In detail, compound **157B** was first prepared by coupling of 3-ethoxy-3-oxopropanoic acid **157A** with protected hydrazine in the presence of DCC/DMAP in DCM, in 72% yield after purification. Then, the carbamate was treated with trifluoroacetic acid in dichloromethane gave compound **157C** in quantitative yield after evaporation, which could be used directly for the next steps (**Scheme 25**).



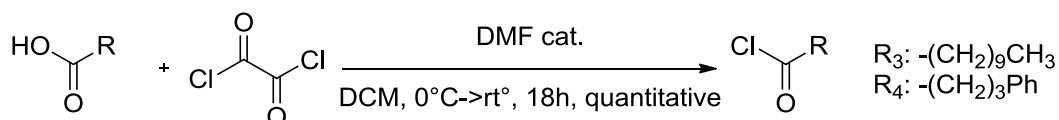
**Scheme 25. Synthesis of compound 157C from ethoxy-3-oxopropanoic acid**

Compounds **157D (1-4)** were then obtained by acylation of **157C** with four acid chlorides in the presence of diisopropylethylamine in dichloromethane. The yields ranged from 60 to 73% after purification. Actually we also optimized the base for acylation, but triethylamine gave poor yields (between 15 and 30%),<sup>[157]</sup> which indicated that a more hindered base might be more appropriate for this case. (**Scheme 26**)



**Scheme 26. Synthesis of compound 157D (1-4)**

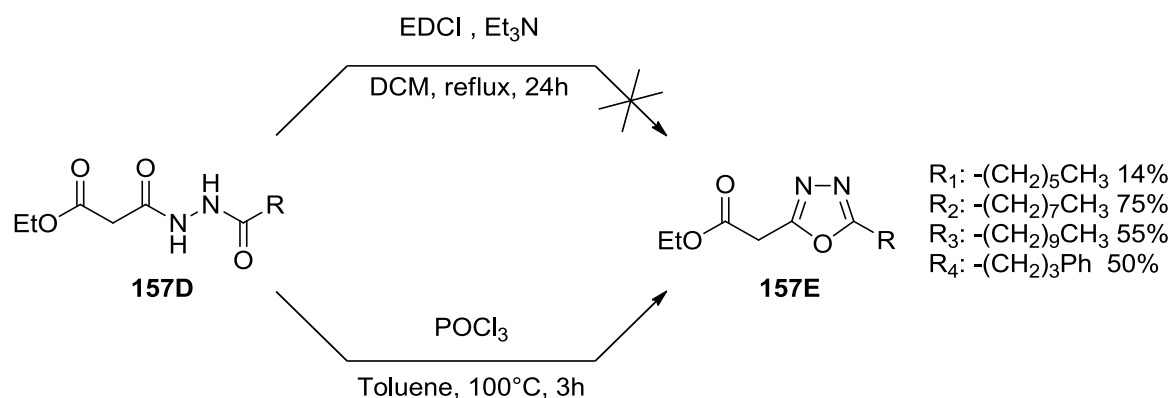
The undecanoyl chloride and 4-phenylbutanoyl chloride are not commercially available, they were quantitatively synthesized from the corresponding carboxylic acids with oxalyl chloride and catalytic DMF without purification (**Scheme 27**). For the other oxadiazole series, the preparation of the acyl chlorides is the same as this case, we will not repeat in the next parts.



**Scheme 27. Preparation of acid chloride**

The final cyclisation step to obtain the compound **157E (1-4)** (**Scheme 28**) was first performed in the presence of EDCI and triethylamine in dichloromethane.<sup>[158]</sup> However, the cyclization was not observed and the starting product was recovered. We assumed that refluxing dichloromethane with low boiling point was not enough for the cyclization and higher temperature might be more favorable. Thus, another condition using POCl<sub>3</sub> in toluene for 3 h

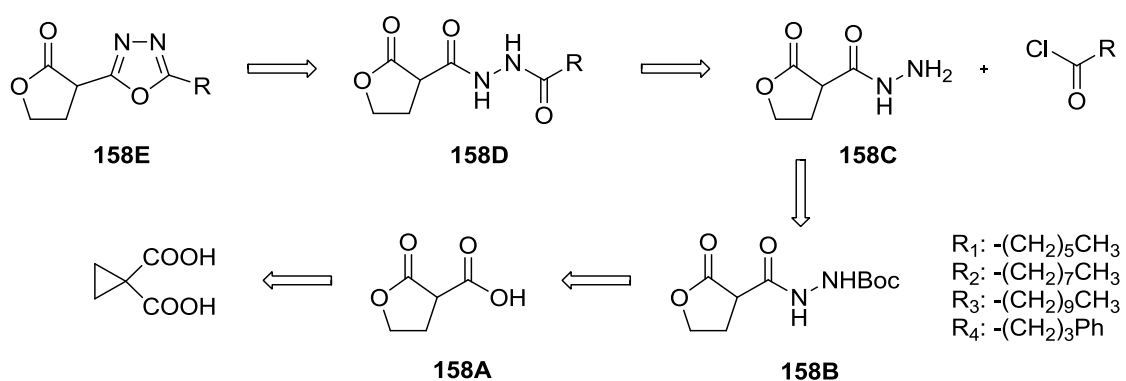
at 100 °C was proved to be efficient for cyclisation step.<sup>[157]</sup> The expected compounds were obtained in yields ranging from 14 to 75% after purification.



**Scheme 28.** Synthesis of 2,5-disubstituted 1,3,4-oxadiazoles with the carboxymethyl ester

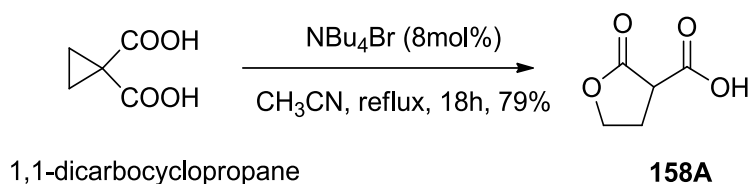
### 2.4.3 Synthesis of 2,5-disubstituted 1,3,4-oxadiazoles with the $\gamma$ -lactone

The retrosynthetic analysis of **158E** (1-4) is shown in **Scheme 29**. The synthetic route is based on the same strategy as the previous series of 2,5-disubstituted 1,3,4-oxadiazoles carboxymethyl ester. But for this series, the carboxymethyl ester was replaced by the  $\gamma$ -lactone, it could be introduced from the 2-oxotetrahydrofuran-3-carboxylic acid **158A**, easily prepared from decarboxylation and rearrangement of cyclopropane-1,1-dicarboxylic acid.



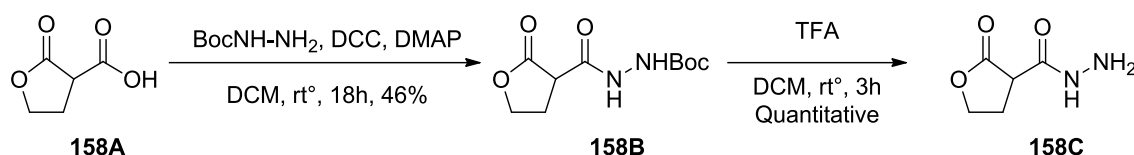
**Scheme 29.** Retrosynthetic analysis of 2,5-disubstituted 1,3,4-oxadiazoles  $\gamma$ -lactone

The synthesis of target products was started with the introduction of the lactone. The key lactone reagent **158A** (**Scheme 30**) was obtained by rearrangement of 1,1-dicarbocyclopropane in the presence of catalytic tetrabutylammonium bromide in refluxing acetonitrile in 79% yield.



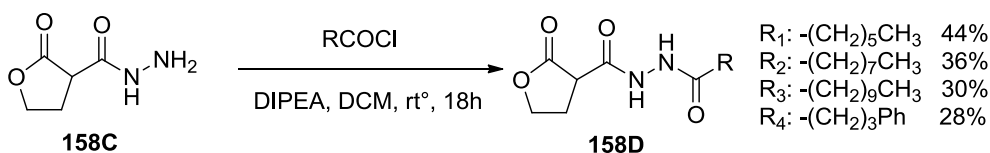
**Scheme 30. Preparation of 2-oxotetrahydrofuran-3-carboxylic acid 158A**

The subsequent steps were performed in the same conditions as for the series of 1,3,4-carboxymethyl ester. The coupling of acid **158A** with the Boc protected hydrazine in the presence of DCC/DMAP afforded compound **158B** (**Scheme 31**) in 46% yield after purification. Deprotection of the Boc group was quantitative.



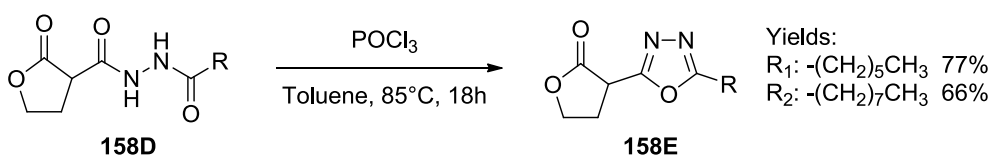
**Scheme 31. Synthesis of compound 28C**

Acylation of compound **158C** (**Scheme 32**) were performed under the same conditions, in yields ranging from 28 to 44%.



**Scheme 32. Synthesis of compound 28D**

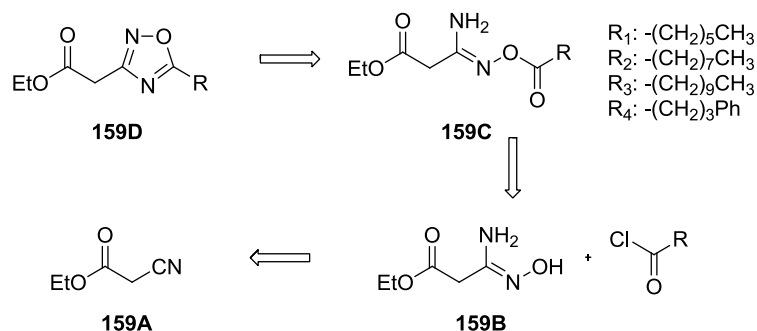
In the last step, considering the sensitivity of the lactone, the cyclization process to access compounds **158E** (**Scheme 33**) was performed at lower temperature than that of the carboxymethyl ester series. Although decreasing temperature lead to a longer reaction time, the conversion was complete. Yields ranged from 66-77% after purification.



**Scheme 33. Cyclization step for accessing to 2,5-disubstituted 1,3,4-oxadiazoles  $\gamma$ -lactone**

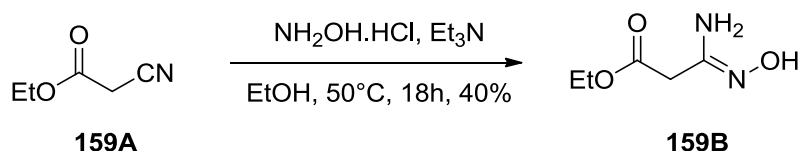
#### 2.4.4 Synthesis of 3,5-disubstituted 1,2,4-oxadiazoles with the carboxymethyl ester in 3-position

The synthesis of 1,2,4-oxadiazoles with the carboxymethyl ester in 3-position **159D** (1-4) is based on a cyclisation of hydroxyimidine acyl **159C** (1-4), which is obtained by acylation of acid chlorides with hydroxyimidine **159B**. Compound **159B** was obtained by addition of hydroxylamine with ethyl cyanoacetate **159A** (Scheme 34).



Scheme 34. Retrosynthesis of 3,5-disubstituted 1,2,4-oxadiazoles with the 3-carboxymethyl ester

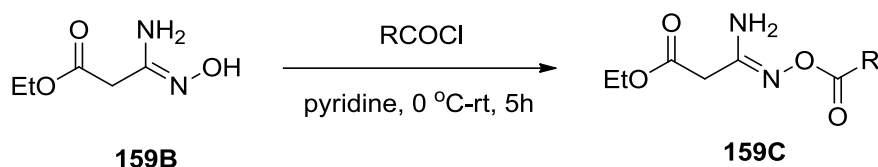
The key step for this series was to prepare the hydroxyimidine **159B** (Scheme 35) by the (*Z*)-stereo-selective addition of hydroxylamine hydrochloride on ethyl 2-cyanoacetate. The desired compound (*Z*)-ethyl 3-amino-3-(hydroxyimino) propanoate **159B** was obtained using an excess amount of ethyl cyanoacetate, hydroxylamine hydrochloride in the presence of triethylamine. Although there were traces of side (*E*)-isomer, mechanistically, the (*Z*)-one was the major product since the hydrogen bond between amino and hydroxyl group was favorable for the syn-addition.<sup>[157]</sup> Compound **159B** was obtained in 40% yield after purification.



Scheme 35. Preparation of compound **159B**

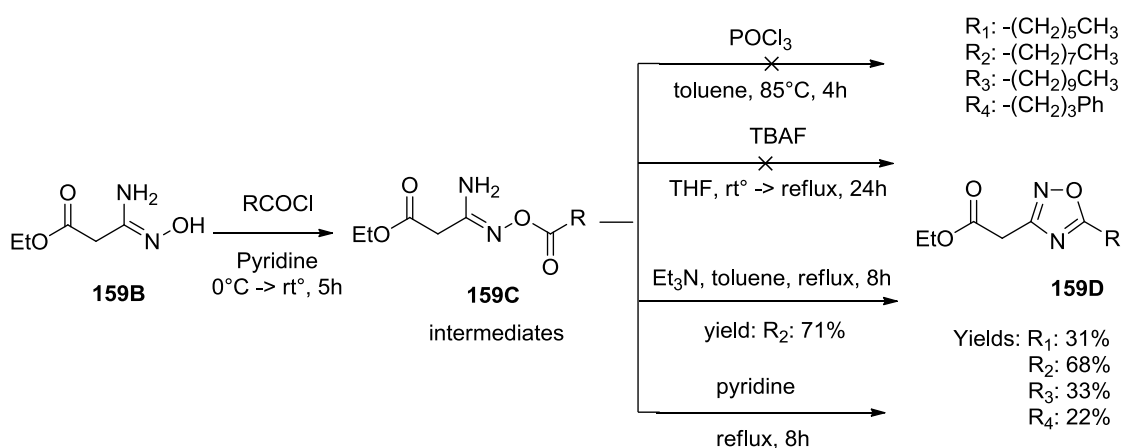
Then intermediates **159C** (1-4) (Scheme 36) were prepared by acylation of **159B** with the corresponding acid chlorides in pyridine. The base DIPEA in dichloromethane could also lead

to compounds **159C** in moderate yield after purification. However, pyridine could be used for the two-steps in one-pot without intermediate purification.



**Scheme 36. Acylation step in pyridine**

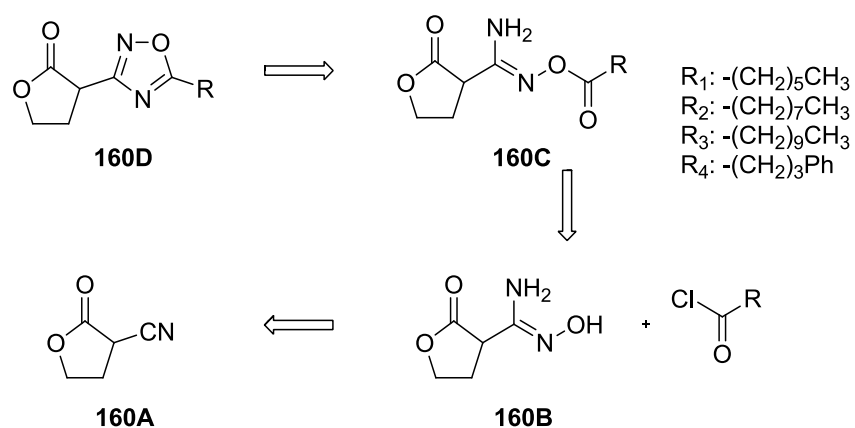
The final products were obtained by cyclization of intermediates **159C** in boiling pyridine, in yields from 22% to 68% over the two steps. The cyclization step was investigated in other set of conditions. (**Scheme 37**) Using  $\text{POCl}_3$ , in analogy to the previous series, resulted in a rapid degradation of the starting material and no desired compound was observed. When using TBAF as a cyclization agent,<sup>[159]</sup> from catalytic amount to one molar equivalent in THF, and from room temperature to reflux, numerous by-products were observed, and no desired product was obtained either. Alternatively, the treatment of compound **159C** (**1-4**) in the presence of triethylamine in boiling toluene gave product **159D** (**1-4**) in various yields, but this method required the purification of intermediate **159C** (**1-4**). Overall, the final products were obtained in good to moderate yields from the acylation/cyclization one-pot reaction in pyridine without isolation of intermediates.



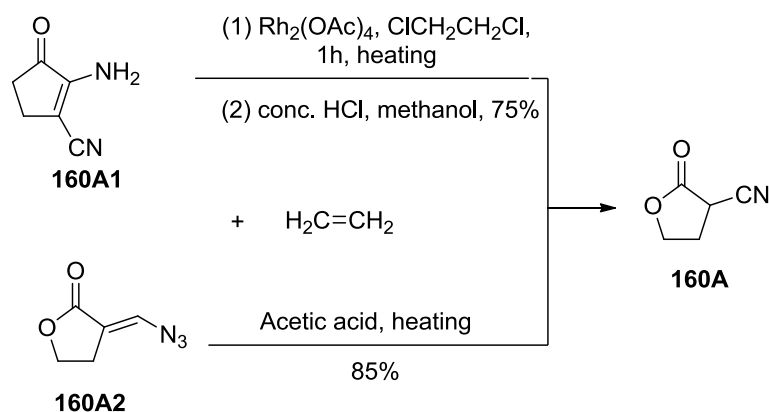
**Scheme 37. Conditions for the synthesis of 3,5-disubstituted 1,2,4-oxadiazoles**

### 2.4.5 Synthesis of 3,5-disubstituted 1,2,4-oxadiazoles with the $\gamma$ -lactone in 3-position

The synthesis of this series is based on the same strategy as for the series of 1,2,4-oxadiazoles (**Scheme 38**). However, compound **160A** is not commercially available, most of reported synthesis require either multiple-steps, or uncommercially available starting materials (**Scheme 39**). Thus, our attention was turned to other alternative methods for synthesis of 1,2,4-oxadiazoles with  $\gamma$ -lactone in 3-position.

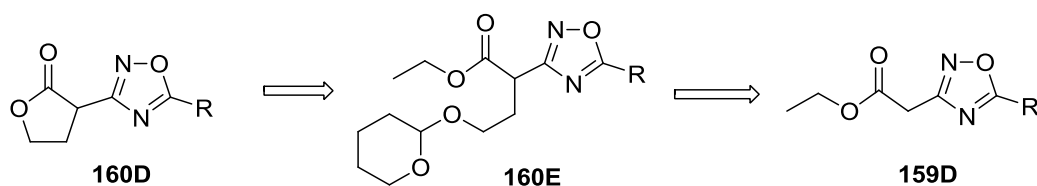


**Scheme 38.** Possible route to **160D** using 2-oxotetrahydrofuran-3-carbonitrile **160A**



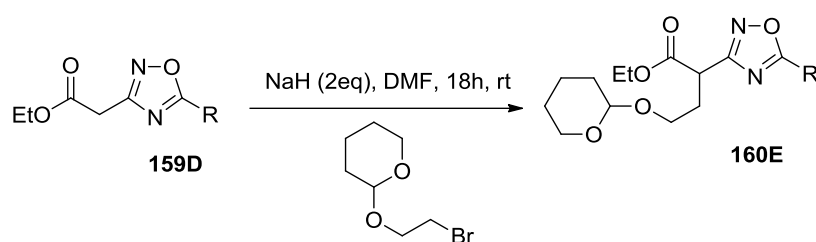
**Scheme 39.** Reported methods for the preparation of 2-oxotetrahydrofuran-3-carbonitrile

Then another synthetic route was proposed in which the lactone was introduced by an intracyclization of alkylated derivatives. These intermediates were prepared from their corresponding carboxymethyl ester, as shown in **Scheme 40**.



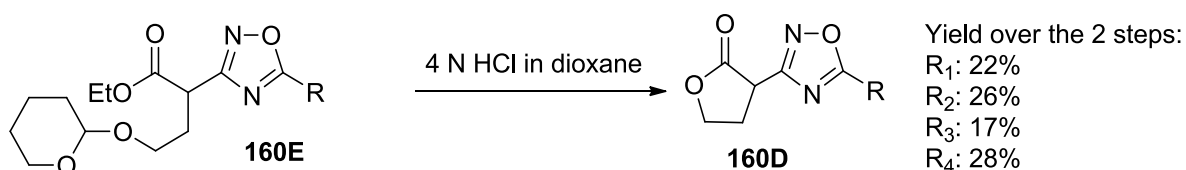
**Scheme 40. Retrosynthesis of  $\gamma$ -lactone series from carboxymethyl ester series**

Two steps are necessary for this strategy: first, an alkylation with 2-(2'-bromoethoxy) tetrahydropyran. However, 1 equivalent of 2-(2'-bromoethoxy) tetrahydropyran and the same amount of NaH in THF resulted in unsuccessful alkylation of compound **159D** (**1-4**), whereas using DMF instead of THF, and increasing the quantity of NaH and 2-(2'-bromoethoxy) tetrahydropyran, afforded the intermediates **160E** (**1-4**) in yields ranging from 17% to 28% (**Scheme 41**).



**Scheme 41. Alkylation step using NaH and 2-(2'-bromoethoxy) tetrahydropyran**

The cyclization was accomplished by treating intermediates **160E** with 4N HCl in dioxane, giving the products **160D** (**1-4**) in quantitative yields (**Scheme 42**).

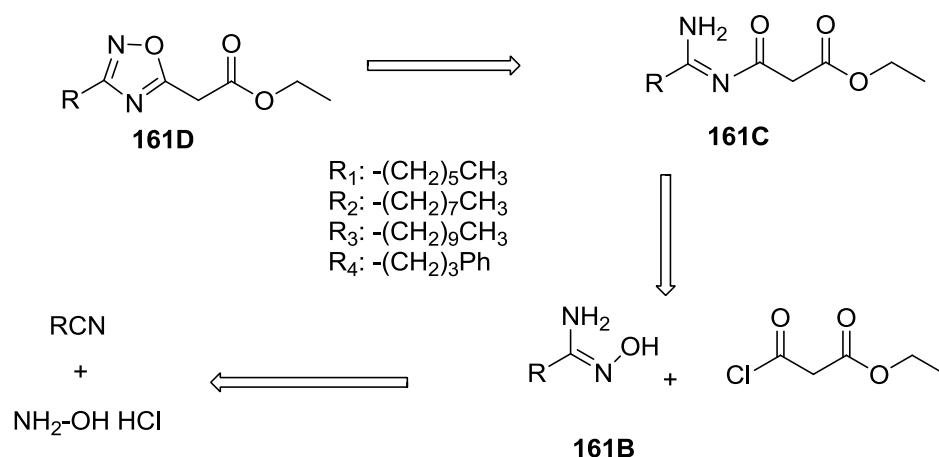


**Scheme 42. Cyclization step of intermediates 160E**

### 2.4.6 Synthesis of 3,5-disubstituted 1,2,4-oxadiazoles with the carboxymethyl ester in 5-position

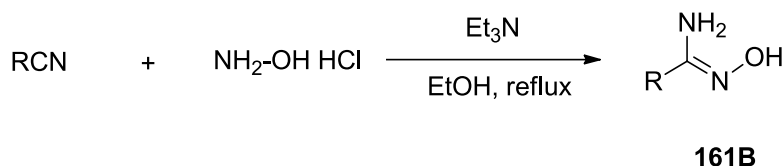
The retrosynthetic analysis of this series is shown in **Scheme 43**. Compounds **161D** (**1-4**) can be prepared by cyclization of compound **161C** (**1-4**) which are obtained by acylation of the amidoxime **161B** (**1-4**) with ethyl 3-chloro-3-oxopropanoate. Compound **161B** (**1-4**)

comes from the nucleophilic addition reaction of different nitrile substrates with hydroxylamine hydrochloride.



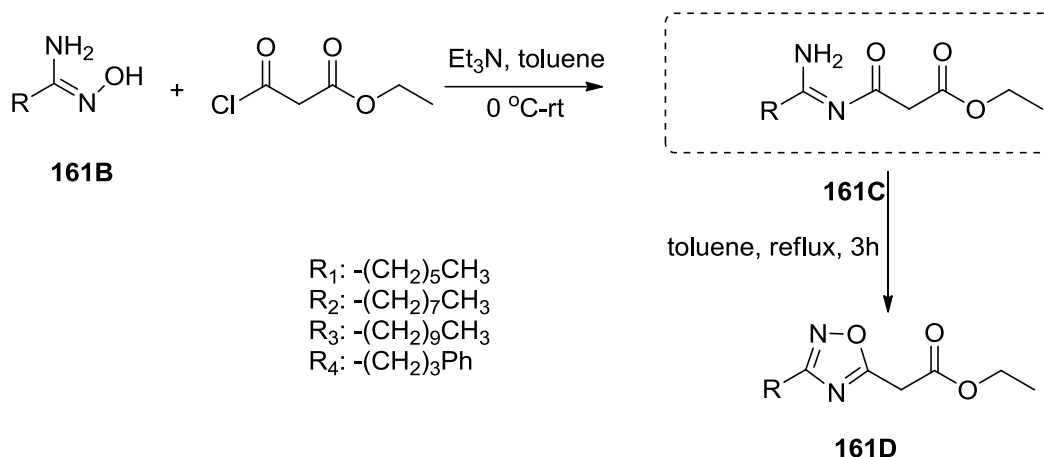
**Scheme 43. Retrosynthesis of 3,5-disubstituted 1,2,4-oxadiazoles with the 5-carboxymethyl ester**

Treatment of nitrile derivatives and hydroxylamine hydrochloride in the presence of triethylamine in ethanol furnished compound **161B (1-4)**. All amidoximes were obtained in a more stable (*Z*)-configuration,<sup>[160]</sup> yields ranging from 39% to 51% (**Scheme 44**).



**Scheme 44. Synthesis of amidoximes**

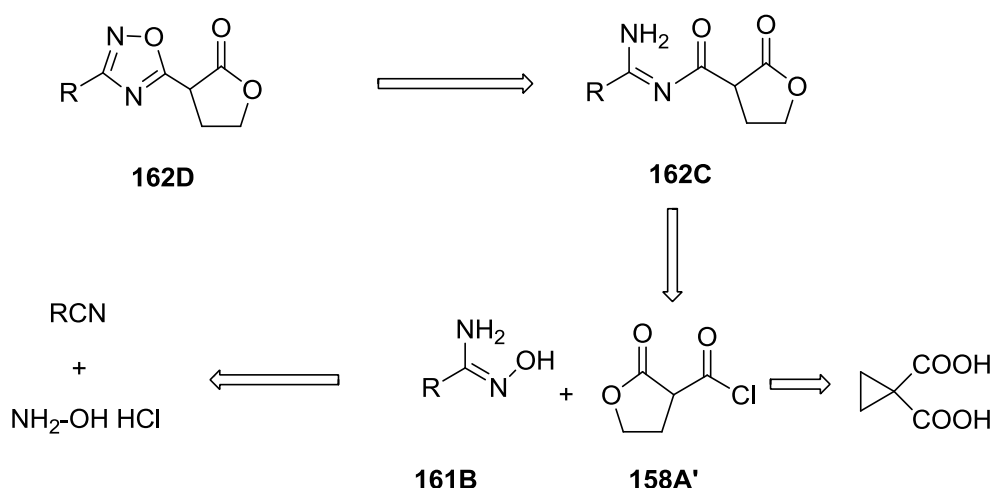
The *O*-acylation of the amidoximes was then obtained by treating compounds **161B (1-4)** and ethyl malonyl chloride in the presence of triethylamine in toluene, and the resulting intermediates **161C (1-4)** were used for the next step without purification. The intramolecular cyclo-dehydrations were accomplished in boiling toluene to afford compounds **161D (1-4)**, in yields from 40% to 65% over the two steps (**Scheme 45**).



Scheme 45. *O*-acylation and intramolecular cyclo-dehydration steps

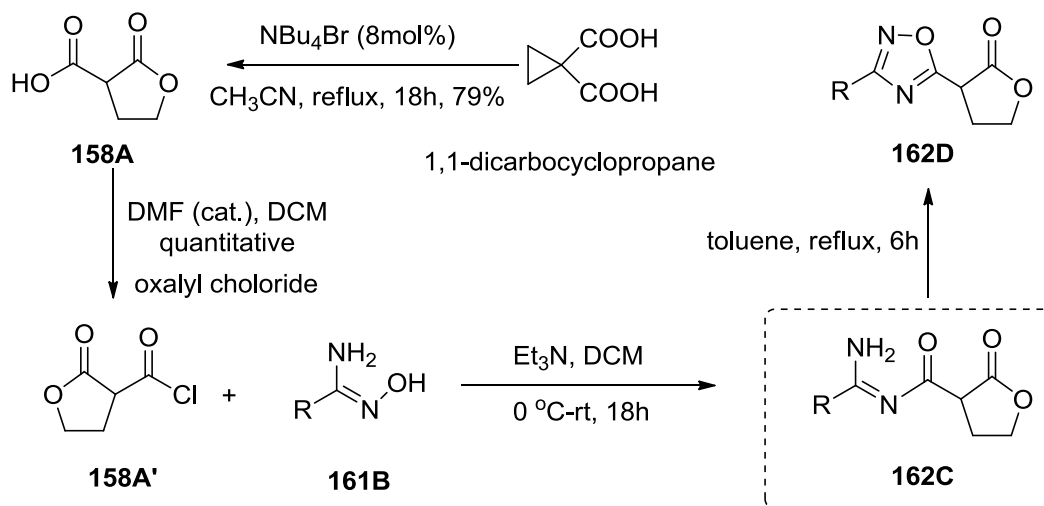
### 2.4.7 Synthesis of 3,5-disubstituted 1,2,4-oxadiazoles with the $\gamma$ -lactone in 5-position

Structurally, this series could be obtained from the alkylation and intra-molecular cyclization of the series of 1,2,4-oxadiazoles with the 5-carboxymethyl ester, based on the same strategy of 1,2,4-oxadiazoles with the 3-carboxymethyl ester for introducing the lactone moiety (section 2.4.5). Alternatively, a more systematic route is based on the previous series of 1,2,4-oxadiazoles with the 5-carboxymethyl ester (section 2.4.6) in which the malonyl chloride is replaced by the 2-oxotetrahydrofuran-3-carbonyl chloride **158A'**, this acyl chloride was synthesized from 2-oxotetrahydrofuran-3-carboxylic acid (section 2.4.3), as shown in **Scheme 46**.



Scheme 46. Synthesis of 3,5-disubstituted 1,2,4-oxadiazoles with the 5- $\gamma$ -lactone

The target products **162D (1-4)** were obtained by treating compound **161B (1-4)** and 2-oxotetrahydrofuran-3-carbonyl chloride **158A'** in the presence of triethylamine in dichloromethane. After evaporation of dichloromethane, the resulting intermediates **162C (1-4)** were used directly in refluxing toluene (**Scheme 47**) to furnish final products in yields ranging from 33% to 56% over the two steps.



**Scheme 47. Acylation and cyclization steps**

Overall, six series of new AHLs analogues with a di-substituted oxadiazoles core varying in two functional group and atoms position were designed and synthesized. We developed several synthetic methods towards di-substituted 1,2,4- and 1,3,4-oxadiazoles. 2,5-disubstituted 1,3,4-oxadiazoles with the carboxymethyl ester and  $\gamma$ -lactone were synthesized from 3-ethoxy-3-oxopropanoic acid and 2-oxotetrahydrofuran-3-carboxylic acid respectively, *via* the transformation of carboxylic acid to hydrazine, acylation with various acyl chloride and cyclization in the presence of phosphorus trioxide in toluene. And 3,5-disubstituted 1,2,4-oxadiazoles with the carboxymethyl ester were obtained from ethyl 2-cyanoacetate, *via* the transformation of nitrile to amidoxime, acylation with the corresponding acyl chloride and cyclization in toluene, and the corresponding  $\gamma$ -lactone series of compounds were obtained from carboxymethyl ester series *via* alkylation with 2-(2'-bromoethoxy) tetrahydropyran and cyclization in acidic condition. Two series of 3,5-disubstituted 1,2,4-oxadiazoles with the carboxymethyl ester and  $\gamma$ -lactone were prepared from different nitrile substrates, *via* a

transformation of nitrile to amidoxime with aid of hydroxylamine hydrochloride, acylation with ethyl malonyl chloride and 2-oxotetrahydrofuran-3-carbonyl chloride respectively, and cyclization in toluene. All oxadiazoles were obtained in moderate to good yield.

#### **2.4.8 Biological evaluation**

The same test as described in section **2.2.5.1** was used. The influence of oxadiazoles on the induction of bioluminescence by 3-oxo-C6-HSL was determined at concentrations ranging from 1 to 200  $\mu\text{M}$  as described previously, and the native autoinducer 3-oxo-C6-HSL was included at a final concentration of 200 nM together with the analogue. The amount of light reduced by the bacteria was measured after 5 h when the ratio of induced to background light was at its maximum, and it was expressed in relative light units. Compound L-**137** was used as a control known as a strong inhibitor for LuxR QS system.

#### **2.4.9 Results and conclusion**

Unfortunately, none of these compounds exhibit any ability of inducing luminescence, and neither of 1,3,4- nor 1,2,4-oxadiazoles displayed any antagonistic activity at concentration up to 200  $\mu\text{M}$ . The results are presented in the **figures 69, 70 and 71**. No matter where the functional groups were located, and which types of functional groups were considered, or which kinds of the side chain was used, both 2,5- and 3,5- di-substituted oxadiazoles were proved to be inactive.

## 1,3,4-oxadiazoles

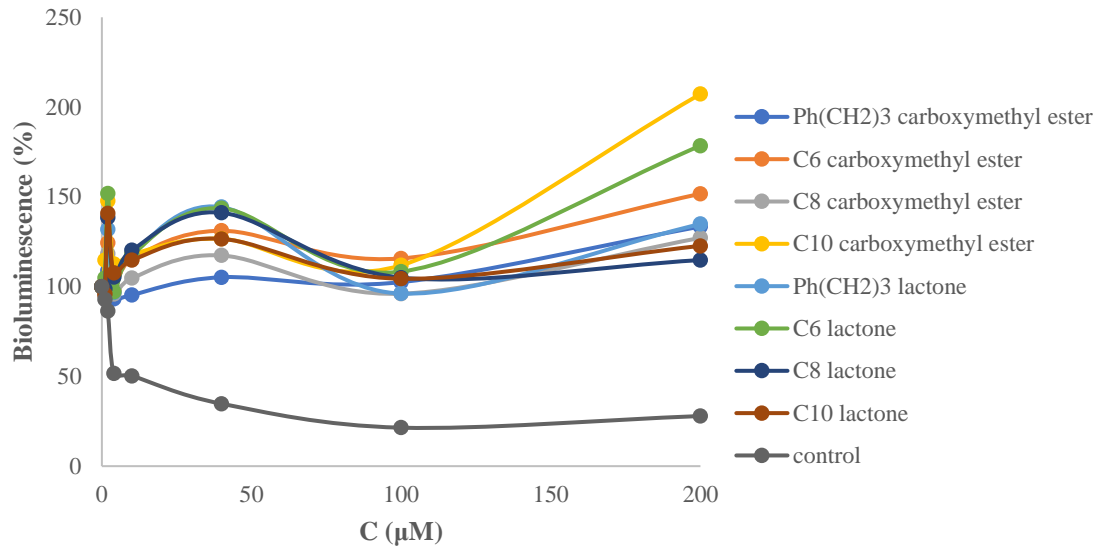


Fig 69. Antagonistic activity of 1,3,4-oxadiazoles

## 1,2,4-oxadiazoles with functional groups in 3-position

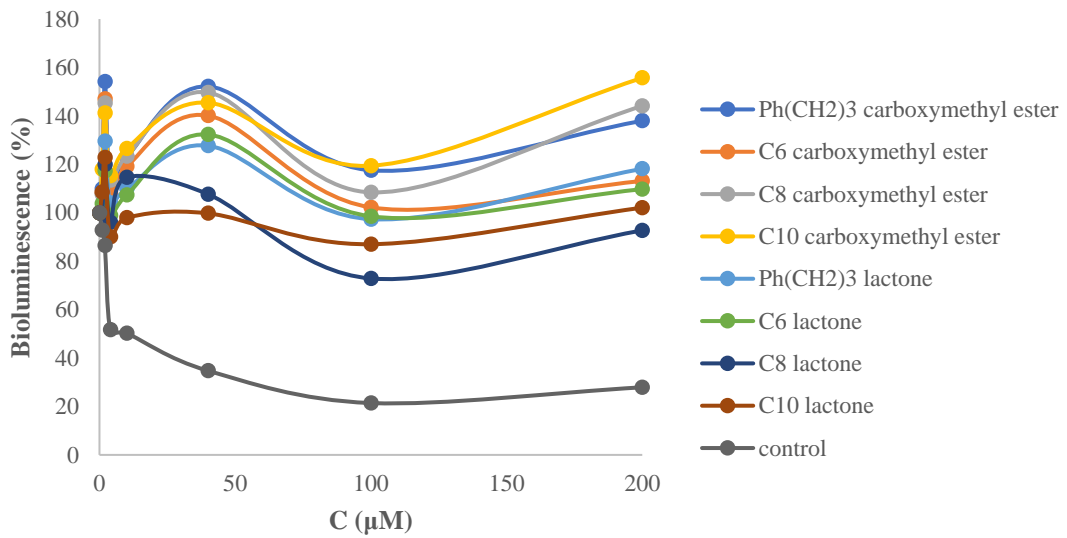
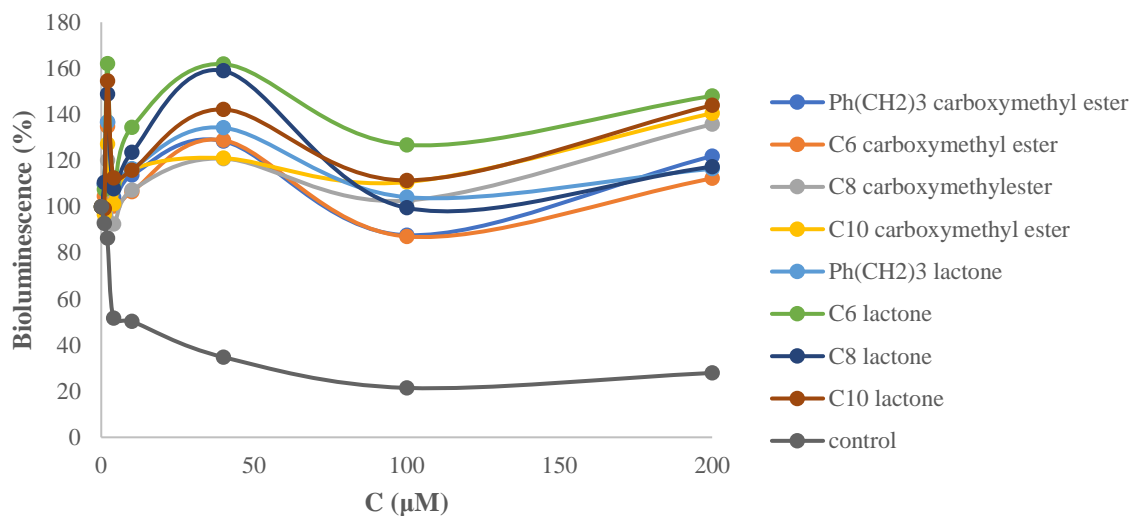


Fig 70. Antagonistic activity of 1,2,4-oxadiazoles with functional groups in 3-position

### 1,2,4-oxadiazoles with functional groups in 5-position



**Fig 71. Antagonistic activity of 1,2,4-oxadiazoles with functional groups in 5-position**

Additionally, we evaluated a different series of 1,2,4-triazoles bearing substituents (**Fig 73**) in position 1, 3 and 5, synthesized by our colleagues in Tunis (Dr. Hachicha). However, the biological evaluation indicated that all those 1,2,4-triazoles were inactive either (**Fig 72**).

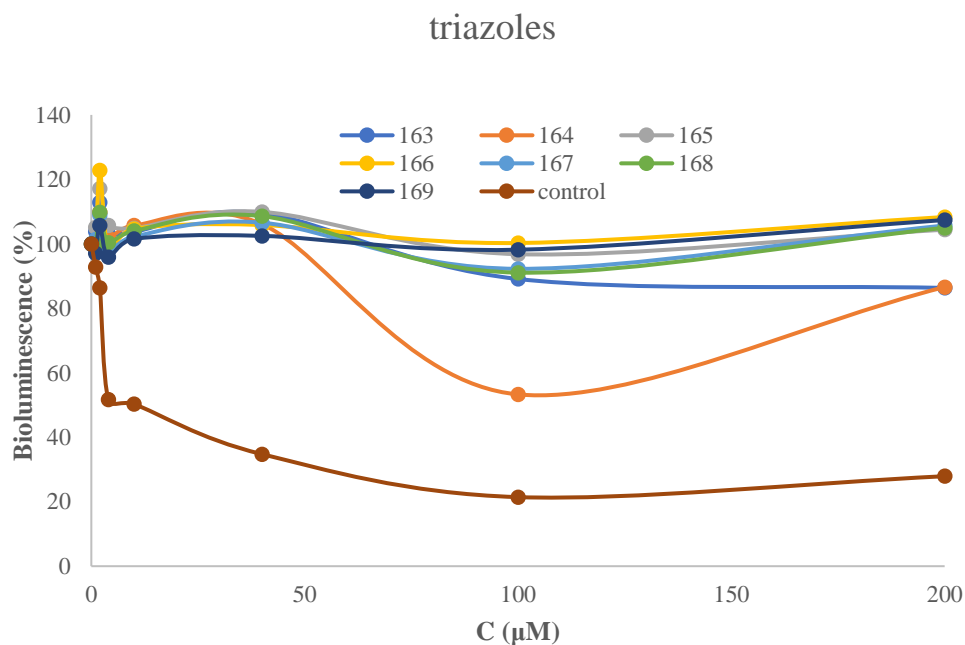


**Fig 72. Antagonistic activity of triazoles synthesized in Tunis**

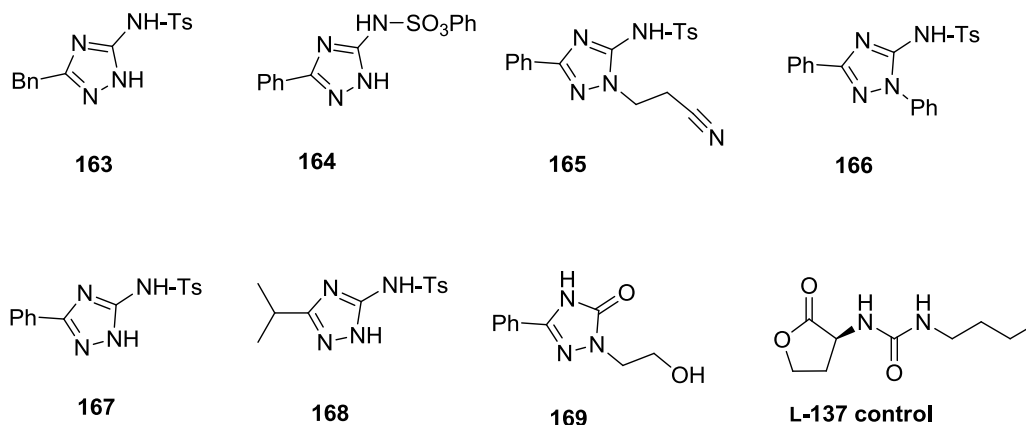


**Fig 73. Structures of triazoles prepared in Tunis**

In conclusion, combined with our previous research on heterocyclic AHLs analogues, we found that among the triazole, tetrazole<sup>[74,161]</sup> and oxadiazole compounds (this work), only the 1,5-tetrazolic systems have shown any activity whereas all 2,5- and 3,5-ones either in tetrazole or oxadiazole series were proved to be inactive (**Fig 74**). These 2,5- and 3,5- di-substituted oxadiazoles might however be active in other LuxR-dependent bacteria strains, and would give a structure-activity relationship with the 1,5- substituted oxadiazoles which are to be designed and evaluated.

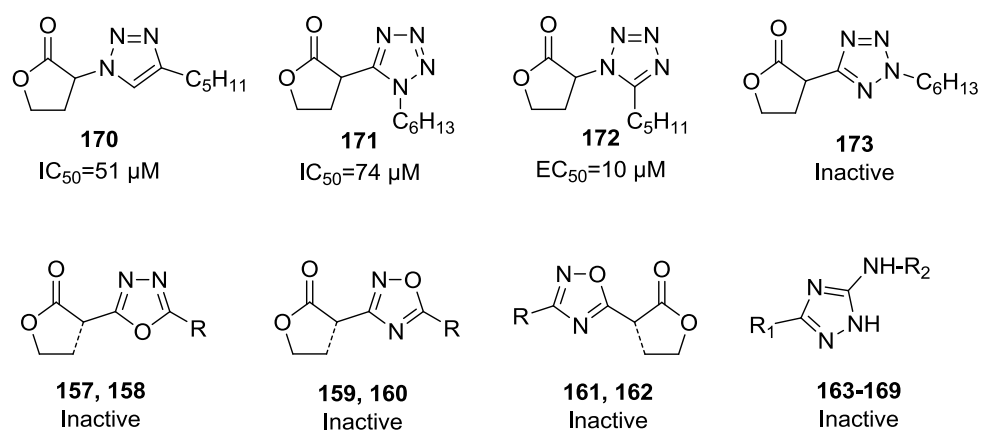


**Fig 74. Comparison of biological activities of some known triazole, tetrazole and oxadiazoles**

Up to now, we have studied only a small fraction of possible structural variations in oxadiazoles, triazoles and tetrazoles. Among possibilities for further studies, based on our hypothesis, the synthesis of four other types of oxadiazoles may be considered, although they are less well described in the literature: 4,5-disubstituted 1,2,3-oxadiazoles, 3,4-disubstituted 1,2,5-oxadiazoles, 2,3-disubstituted 1,2,4- and 1,3,4-oxadiazoles (**Fig 75**). Thus, there is still a long way to go for the investigation of structure-activity relationships of heterocyclic AHLs analogues based on triazole, tetrazole, and including also oxadiazoles scaffolds.

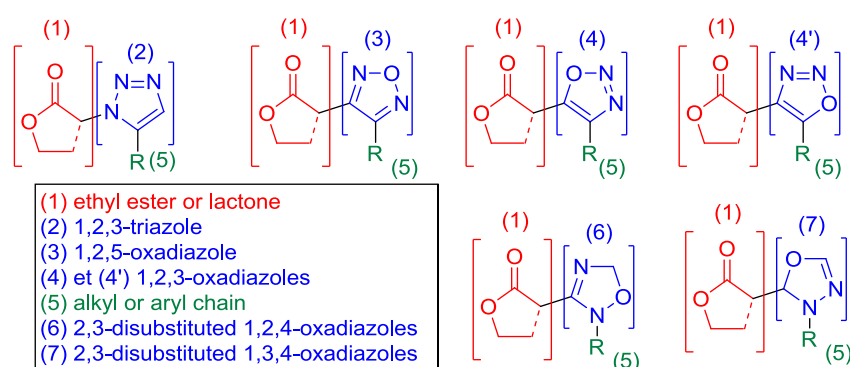


**Fig 75. Possible structures of oxadiazoles for future work**

## 2.5 An alternative cyclization approach towards the core motif lactone of AHL analogues

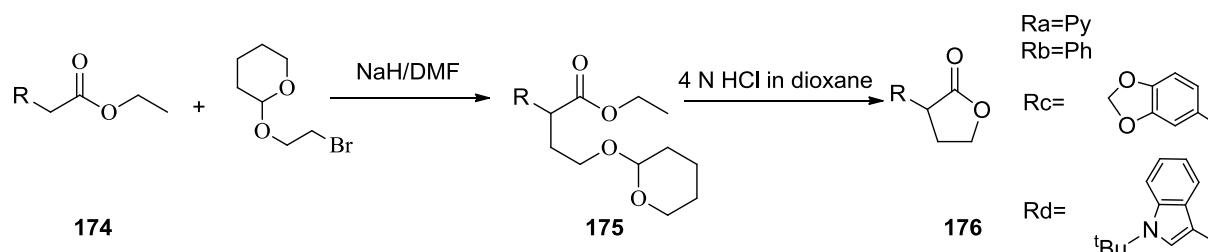
### 2.5.1 Introduction

In the previous oxadiazole section, a straightforward method towards lactone containing oxadiazoles using an alkylation step and subsequent cyclization has been proposed. Owing to the important role of the functional lactone or carboxymethyl ester groups of AHL in designing QS molecules, many new QS-based scaffolds containing this two groups have been prepared, such as fusaric acid analogues, triazoles, tetrazoles, oxadiazoles and some other heterocycles. It was thus important to establish an efficient method being able to converse carboxymethyl ester to lactone. In this section, we present an alternative cyclization approach towards the core motif lactone of AHL using carboxymethyl esters as substrates.

### 2.5.2 Optimization of the reaction

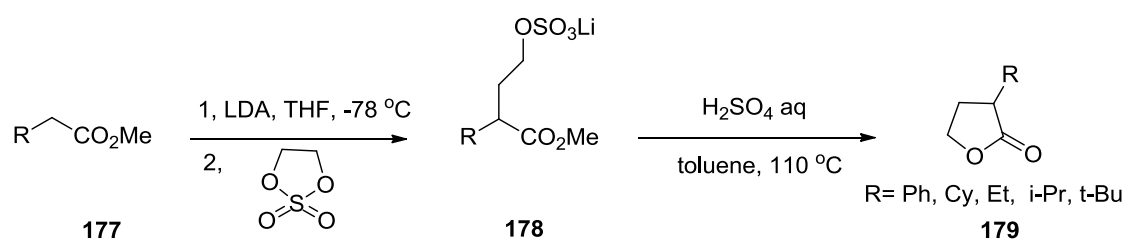
Initially, a two-step method was proposed (**Scheme 48**). The carboxymethyl ester substrates **174** were treated with 2-(2'-bromoethoxy) tetrahydropyran in the presence of NaH in DMF for the alkylation step, followed by an acid catalyzed cyclization. However, the alkylated

intermediates **175** were difficult to separate from the starting material by column chromatography. In addition, the efficiency of the alkylation depended on the substrates, limiting the advantages of this method.



**Scheme 48.** The first proposed cyclization approach using 2-(2'-bromoethoxy) tetrahydropyran

In 2015, A. Togni<sup>[162]</sup> reported a practical method using various methyl esters **177** as substrates, and LDA as alkylation base, then sulfuric acid for the cyclization to prepare compounds containing a lactone (**Scheme 49**).



**Scheme 49.** A cyclization approach reported by A. Togni

Based on this method, we proposed an even mild set of the condition for alkylation. A mild base LiHMDS instead of LDA, and sulfate cyclic was employed at -20 °C, the resulting intermediates could be used for the cyclization step without purification. We optimized the cyclization step using ethyl 2-(pyridin-2-yl)acetate as substrate under several acidic and basic conditions. The results are shown in **Table 7**, using 4 M HCl in dioxane at refluxing temperature gave the desired product in a fair yield.

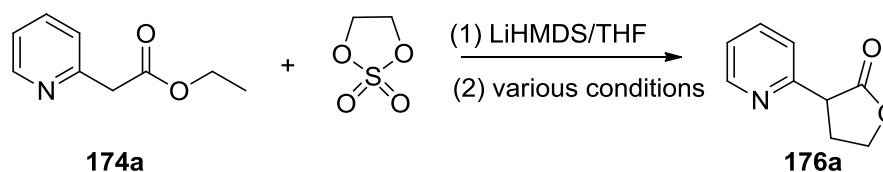


**Table 7. Optimization of alkylation cyclization conditions**

Entry	Sulfate cyclic <sup>a</sup>	LiHMDS	conditions	Reaction time	Yields <sup>b</sup>
1	2.5	1.4	0.2 M H <sub>2</sub> SO <sub>4</sub> /toluene (v/v, 3/2)	Reflux 16 h <sup>d</sup>	- <sup>c</sup>
2	1.1	1.1	2.5 eq CH <sub>3</sub> CH <sub>2</sub> ONa/ethanol	Reflux 16 h	- <sup>c</sup>
3	1.2	1.2	0.2 M H <sub>2</sub> SO <sub>4</sub> /toluene (v/v, 3/2)	Reflux 16 h	5%
4	1.2	1.2	1.34 M HCl in toluene	Reflux 16 h	10%
5	1.1	1.1	4 M HCl in dioxane	rt 16 h	20%
6	1.2	1.2	4 M HCl in dioxane and DCM	40 °C 16 h	33%
7	1.2	1.2	4 M HCl in dioxane	85 °C 16 h	61%

a. The quantity of reagents were indicated in equivalent; b. Isolated yields; c. No product was observed; d. The reaction time and temperature referred to known reported.<sup>[162][163]</sup>

### 2.5.3 Investigation of the scope of the reaction

For the scope of reaction, we targeted first some aromatic compounds, more diversified substrates are on their way. Thus, ethyl 2-phenylacetate **174b**, ethyl 2-(benzo[d][1,3]dioxol-5-yl)acetate **174c** and ethyl 2-(1-(tert-butyl)-1H-indol-3-yl)acetate **174d** were employed for the reaction, and the corresponding lactone product **176 (a-d)** were obtained in yields ranging from 52% to 74% (**Table 8**).

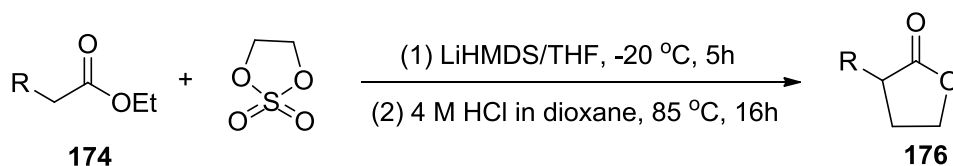
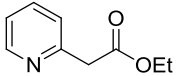
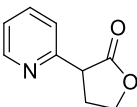
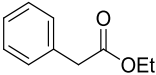
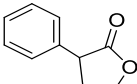
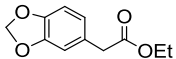
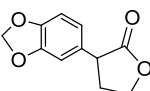
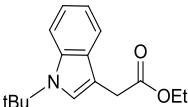
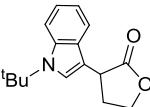
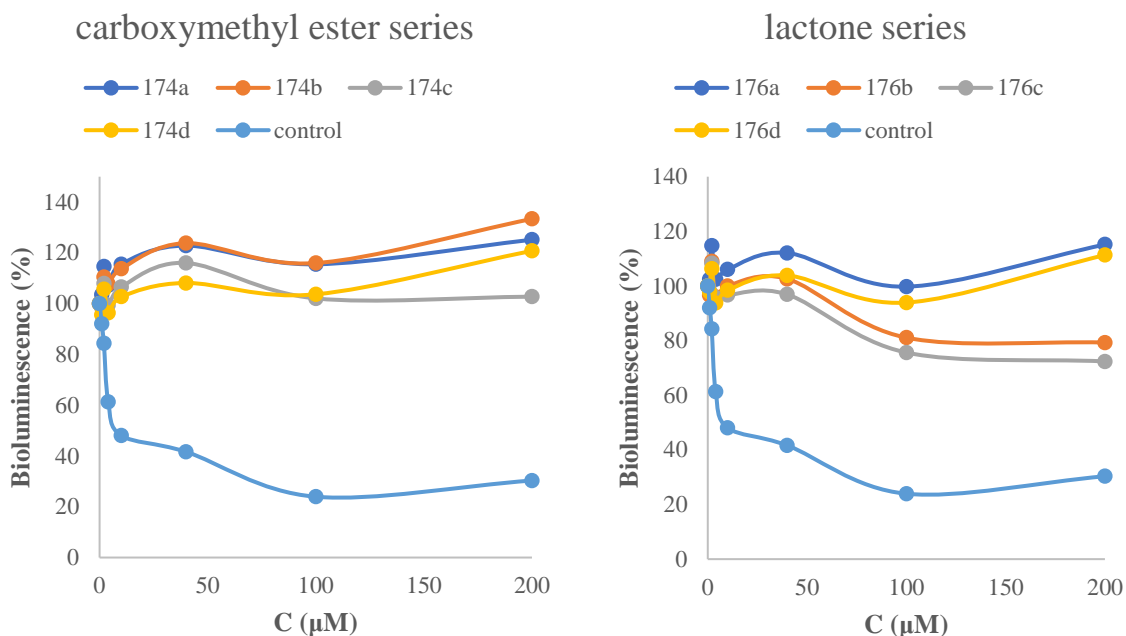


Table 8. Scope of the reaction

Entry	Substrates (174a-174d)	Product (176a-176d)	yields
1 (a)			61%
2 (b)			74%
3 (c)			63%
4 (d)			52%

#### 2.5.4 Biological assays and results

All lactonic compounds and the corresponding counterparts carboxymethyl ester were evaluated for their capability of inducing or inhibiting the bioluminescence, using the same bacterial strain in the previous sections. A known strong antagonist urea L-**137** was used for control. The results indicated that none of these compounds were active in aspects of agonistic activity. Lactones **176b** and **176c** exhibited 19% and 28% inhibitory activity respectively at high concentration (approximately 200 nM) whereas all others were inactive (**Fig 76**). We assume that the slight activity is probably due to the partial match of aromatic rings and natural AHL (3-oxo-C6-HSL).



**Fig 76. Antagonistic activity results of carboxymethyl ester and lactone series of compounds**

### 2.5.5 Conclusion

An alternative cyclization approach towards the core motif lactone of AHL has been developed, and used to prepare a library of four analogues. It has been proved to be an efficient and practical pathway for the synthesis of aromatic and heterocyclic compounds with lactone from their corresponding carboxymethyl esters. More diversified and functionalized substrates need to be developed by this method. The protocol can be used for fast expansion of the library compounds for biological studies in the future.

The compounds as well as their carboxymethyl ester precursors were tested in LuxR-dependent QS systems. Only lactones **176b** and **176c** showed weak antagonistic activity at high concentration, which revealed that this type of compounds with homologous lactone or aromatic rings might be a first step towards more active compounds.

## 2.6 Computer aided design of readily available acylated 2-nitroaniline derivatives as LuxR-regulated QS inhibitors

### 2.6.1 Introduction

In the previous section, we have reported optically pure AHLs analogues act as a LuxR dependent QS modulator, long chain AHLs for purification of enzymes, and six series of new AHLs analogues based on oxadiazole scaffolds serve as potential QS mimics. In this part, we will report acylated 2-nitroaniline derivatives as LuxR-regulated QS inhibitors based on computer aided design.

Over the past few decades, the QS communication system was studied extensively especially on the regulation by small molecules to fight bacterial virulence.<sup>[53][133,164–167]</sup> To our best knowledge, it has been found that there are three QS systems in *pseudomonas*,<sup>[168]</sup> two of them were regulated by homoserine lactones *N*-3-oxo-dodecanoyl-homoserine lactone and *N*-butanoyl-homoserine lactone and interacting respectively with LasR and RhlR. Another system, called PQS (*Pseudomonas* quinolone signal) was regulated via quinolone derivatives. These compounds are biosynthesized from anthranilic acid leading to HHQ.<sup>[169]</sup>

Recently, a secondary metabolite from this biosynthetic pathway, namely 2-aminoacetophenone (2-AA) has been shown by Kviatkovski and co-workers<sup>[170]</sup> to activate LuxR response regulator in *E.coli* based biosensor strain. In their work, they also showed using molecular modeling that this compound is replacing the lactone within the ligand binding site of a LuxR model with hydrogen bonds between the C=O and Trp66 and between the amine and Asp79. The binding mode with hydrogen bond of 2-AA (magenta) is shown in **Fig 77** and is in good agreement with the one obtained by Kviatkovski and co-workers.

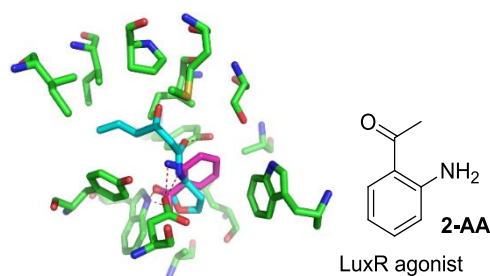


**Fig 77. The binding mode with hydrogen bond of 2-AA**

Inspired by these observations, in the present study, we proposed the biological evaluation of 2-substituted anilines, in particular 2-nitroaniline since the nitro group has been shown to be important in other aromatic systems as LasR modulators.<sup>[171,172]</sup> Indeed, flexible docking experiments investigations<sup>[173,174]</sup> of *N*-3-oxo-hexanoyl-homoserine (OHHL)<sup>[61]</sup> and 2-nitroaniline using a LuxR model described in 2007 by Soulère and co-workers<sup>[175]</sup> showed that this substituted aniline mimicked the lactone ring with hydrogen bonds between the nitro group (replacing the ester function of OHHL) and Trp66 and between the amine (as for the amide of OHHL) and Asp79 (**Fig 78**).

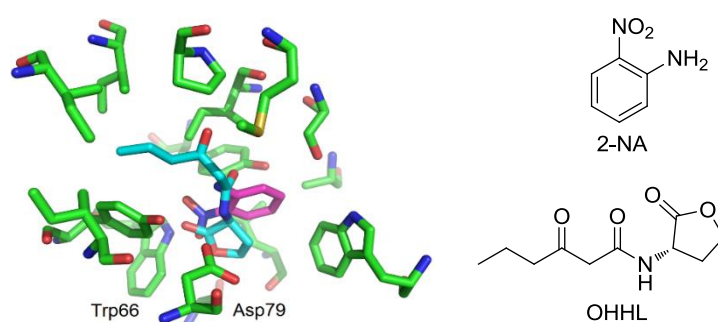


**Fig 78. Proposed binding mode obtained as results of docking experiments of 2-NA (magenta) within the LuxR model binding site. OHHL is also represented in blue.**

In keeping with the same structural analogy, in which the amine function of 2-NA or 2-AA and the NH group of the amide function of OHHL appear in similar positions within the binding site, we studied their *N*-acylated derivatives, on the basis of the imitation of the amide side chain of AHLs. For comparison, we also synthesized and evaluated acyl anilines to examine the effect of the substituent in position 2 (**Fig 79**).

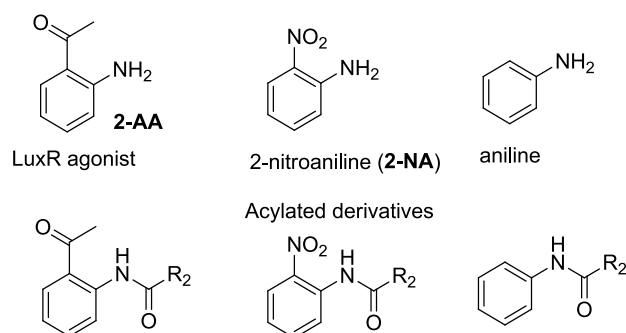
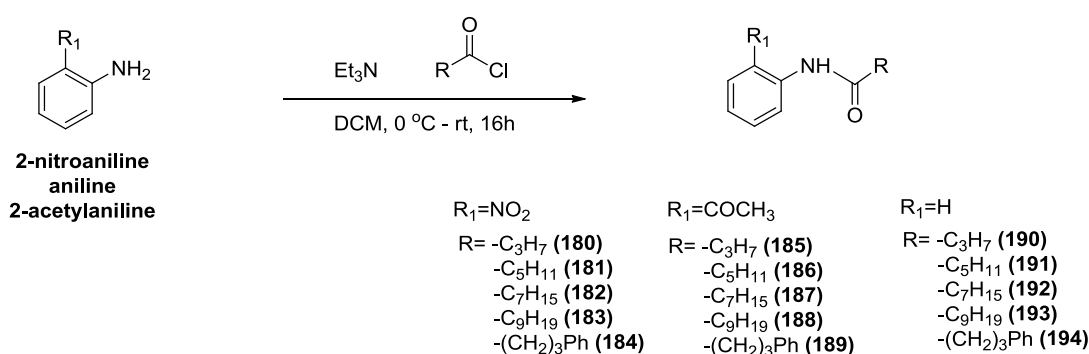


**Fig 79. Structure of substituted anilines and their acylated derivatives.**

## 2.6.2 Synthesis of 2-nitroaniline derivatives

All compounds were easily prepared from 2-NA,<sup>[176]</sup> 2-AA or aniline by direct acylation with the corresponding acyl chloride (**Scheme 50**). In the case of compounds **184** and **189** and **194**, the acyl chloride was synthesized acid using oxalyl chloride from 4-phenylbutyric acid with catalytic dimethylformamide. And for 2-nitroaniline derivatives, 2.5 equivalent of triethylamine and acyl chloride were employed whereas for the 2-acetylaniline and aniline series, only 1.1 equivalents were used for acylation. The yields ranged from 25% to 89%.



**Scheme 50. Synthesis of 2-nitroaniline derivatives**

## 2.6.3 Biological evaluation

Biological evaluation of these derivatives as LuxR agonist or antagonist was achieved following the protocol described in the previous two sections. A known strong antagonist was used for control. This urea AHLs also exhibited weak agonistic activity at high concentration. The agonistic activity results indicated that all compounds were inactive, except 2-aminoacetophenone (2-AA) which was known to be able to activate LuxR (**Fig 80**).

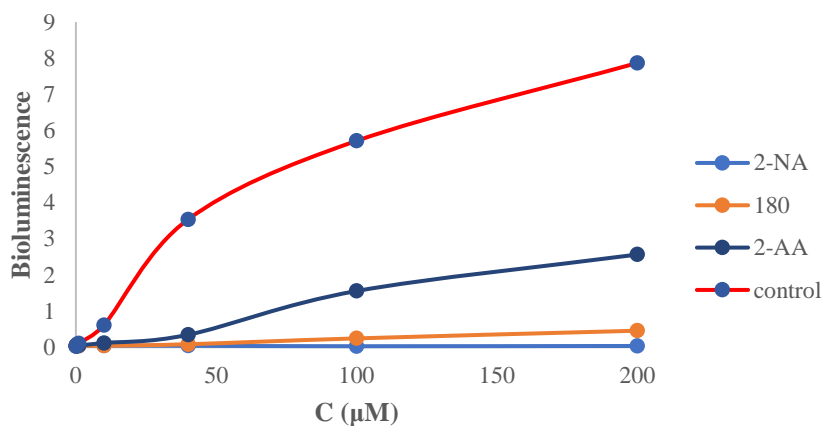


**Fig 80. Agonistic activity of nitroaniline compounds**

Regarding the capability of compounds to reduce the luminescence, some differences were observed among the different series of derivatives. These assays showed that the 2-NA, *N*-(2-Nitrophenyl) butanamide **180** and *N*-(2-Nitrophenyl) hexanamide **181** displayed antagonistic activity whereas other acylated derivatives **182-189** were totally inactive. Surprisingly, *N*-phenylhexanamide compound **191** also exhibited almost the same potency as 2-nitroaniline. But all active compounds were less potent than the control (**Fig 81**).

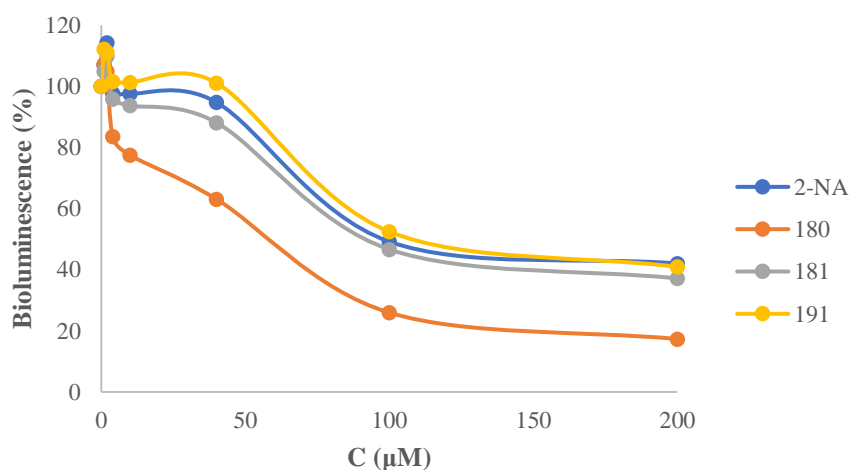


**Fig 81. The bioluminescence was induced by 200 nM of 3-oxo-C6-HSL.**

## 2.6.4 Discussion

For inactive acyl nitroaniline **182-184** with longer acyl chains (C8 and C10) or with a terminal phenyl group, we suggest that these substituents are inappropriate due to the sterical

balance between the nitrophenyl and the side substituents. As shown in **Fig 82**, docking experiments of compounds **180** and **181** (nitro-C4 and nitro-C6) within the LuxR model binding site indeed show a favorable fitting of these compounds, with a binding mode with hydrogen bonds between Trp66 and the nitro function and Asp79 and the NH group. The aromatic part of the compound fits well and replaces the lactone moiety. The difference of activity for compounds **180** and **181** may be due to the change in the orientation of the alkyl chain (**Fig 82**).

Comparison (biological evaluation and docking experiments) for 2-unsubstituted anilines was then performed. As already reported toward LuxR, compound **193** was inactive,<sup>[177]</sup> as well as compounds **192** and **194**. Interestingly, the hexanamide **191** showed significant antagonist activity with IC<sub>50</sub> of 79 μM, in the same range as for *N*-(2-nitrophenyl) hexanamide **181**. However, to our surprise, shortening further the chain to C4 (compound **190**) led to total loss of activity, whereas the corresponding nitrated counterpart was found to be the most active compound of this study. This shows that the two families of compounds behave differently, with a crucial nitro substituent which anchors the molecules within the binding site via hydrogen bond with Trp66, and a less important chain length effect making both the C4 and the C6 derivatives active, whereas for the unsubstituted aniline series, only one very specific derivative, the C6 amide, displays sufficient favorable interaction and sterical balance. This hypothesis is supported by docking experiments showing only one favorable binding mode for hexanoylaniline **191** within the LuxR binding site (**Fig 83**) whereas several binding modes, all unfavorable, were found for compound **190** within the LuxR binding site.

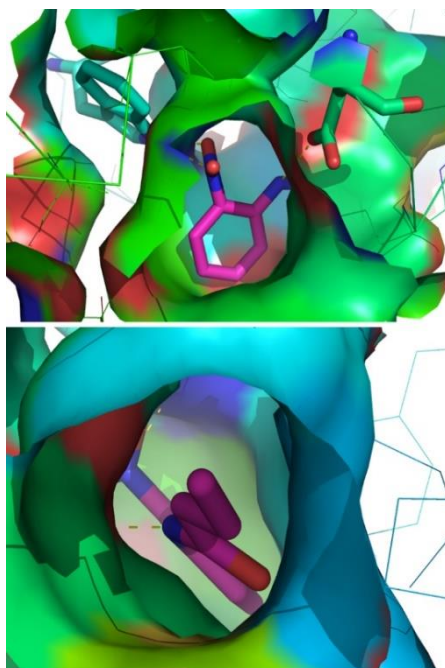


**Fig 82. Proposed binding mode obtained as results of docking experiment of compound 180 (magenta) and 181 (cyan) showing the fitting of the lactone and the alkyl chain within the LuxR model binding site (Trp66 and Asp79 were represented in stick).**

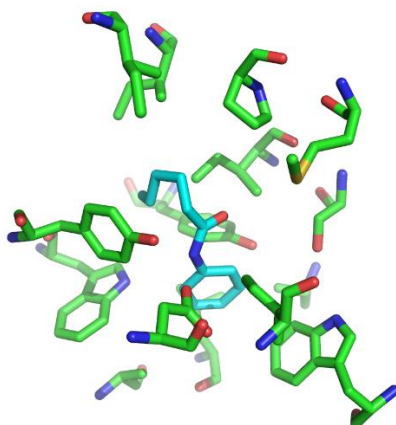


**Fig 83. The binding mode of compound 191 showed a good fitting with hydrogen bond with Asp79 (NH)**

We then examined the H-bonds interactions involving the important and conserved residues of the binding site (Trp66, Asp79 and Tyr62) for 2-AA, 2-NA and compounds **180-181**, **185-186** and **190-191** with appropriated *ortho* substituents (**Table 9**).

**Table 9. Occurrence and distances for hydrogen bonds between Trp66, Asp79 and Tyr 62 and the main chemical functions of studied compounds with distances (Å)<sup>a, b</sup>**

Compounds	Trp66	Asp79	Tyr62
OHHL (natural ligand)	+ 2.34 (C=O lactone) <sup>a</sup>	+ 3.01 (NH amide)	+ 3.01 (C=O amide)
<b>2-AA</b> (agonist)	+ 2.20 (C=O)	+ 3.03 (NH <sub>2</sub> )	No function
<b>2-NA</b> (antagonist)	+ 2.96 and 2.37 (NO <sub>2</sub> )	- NH <sub>2</sub> too far	No function
<b>180</b> (antagonist)	+ 2.47 (NO <sub>2</sub> )	+ 3.00 (NH amide)	- C=O too far
<b>181</b> (antagonist)	+ 2.20 (NO <sub>2</sub> )	+ 3.01 (NH amide)	- C=O too far
185 (No activity)	+ 1.99 (C=OCH <sub>3</sub> )	+ 3.10 (NH amide)	+ 2.97 (C=O amide)
186 (No activity)	+ 2.01 (C=OCH <sub>3</sub> )	+ 2.98 (NH amide)	+ 2.94 (C=O amide)
190 (No activity)	-	-	-
<b>191</b> (antagonist)	No function	+ 3.04 (NH amide)	- C=O too far

(a) + indicates a possible H-bond; (b) The function implicated is indicated in brackets

The autoinducer OHHL displays three hydrogen bonds with Trp66, Asp79 and Tyr62. Agonist **2-AA** displays two hydrogen bonds with the same residues (none with Tyr62 due to the absence of the carboxamide function). In contrast, **2-NA**, which shows antagonist activity, interacts only with Trp66, but in this case through two hydrogen bonds between Trp66 and the nitro group, and does not interact with Asp79. The binding modes for **2-AA** (agonist) and **2-NA** (antagonist) are therefore significantly different with respect to the H-bond interactions. Acylated nitroanilines **180** and **181** display two hydrogen bonds, one with Trp66 and one with Asp79, whereas the simpler hexanoylaniline, **191** shows only one hydrogen bond with Asp79. Thus, antagonists **180**, **181** and **191** display hydrogen bonds with Asp79 and Trp66 (if possible) but not with Tyr62 (**Fig 83**). The combination of a favorable overall binding and the absence

of the interaction with Tyr62 appears as a common feature among compounds showing antagonistic activity.

For the inactive compound **190**, docking experiments show several binding modes due to the size of this compound and the absence of the nitro group. For compounds **185** and **186**, they adopt a binding mode with the same hydrogen bond network as OHHL including the interaction with Tyr62.

In summary, readily available acyl aniline derivatives have been synthesized and evaluated as LuxR mediated QS inhibitors. This study indicated that a rather structurally simple substituted aromatic system such as nitroaniline may serve as non-hydrolysable scaffold for designing LuxR inhibitors, as compared with more elaborated aromatic compounds for other QS systems such as the one regulated by LasR.<sup>[171,172,178]</sup>

## 2.7 Conclusion

The work reported in this chapter aimed at developing of novel QS agonists or antagonists and widening the scope of possible structures being able to inhibit QS and possibly be used as new antibacterial agents.

Firstly, with respect to AHL close analogs, we provided the first systematic investigation of the influence of chirality. Several families of optically pure AHLs analogues were synthesized with high enantiomeric purity, determined by europium complex and chiral HPLC. We concluded that L-isomers of AHLs are likely to be responsible for the QS modulation. However, in some cases, D-isomers also exhibit weak activity. This happens when there is possible regeneration of the H-bonding network in the binding site despite the twist in the lactone ring is necessary to overcome the wrong configuration.

With the aim of designing tools for enzyme purifications, three long chain AHLs analogues were prepared. In particular, HSL-C16 was obtained by the general acylation of HSL with palmitoyl chloride, HSL-C16-NHS was obtained in two steps from hexadecanedioic acid, and HSL-3-oxo-C18-NHS were obtained in five steps from hexadecanedioic acid. The enzyme purification experiments are on their way.

In the field of AHL analogues based on a modified amide linkage, we proposed several new series constructed on an oxadiazole scaffold. Six series of 2,5- and 3,5- di-substituted oxadiazoles varying in substituents and functional group were obtained in different yields based on various synthetic routes. Using the “*Vibrio*” test, all these oxadiazoles were proved to be inactive against LuxR dependent QS. However, they will be tested towards other QS systems related to other strains, together with all compounds belonging to our QSI directed chemical library. Indeed, it is common that inactive compounds on one strain can be active on another one. Anyway, full analysis of the structure properties relationships will be possible only when we also have in hands 1,5-di-substituted systems which are similar to the active systems in the tetrazole series. This part of the work was also the opportunity to establish alternative routes towards homoserine lactone containing systems based on a late lactone formation.

Finally, inspired by some observations that 2-aminoacetophenone could mimic the lactone of AHLs, a set of readily available acyl aniline derivatives have been synthesized and evaluated as LuxR mediated QS inhibitors. It demonstrated that a rather structurally simple substituted aromatic system such as nitroaniline may serve as non-hydrolysable scaffold for designing LuxR inhibitors.

As a perspective to this chapter, collaborations with expectation to other types of biological properties with other biologists will extend evaluation of those compounds, and extend the work to new scaffolds targeting new family of QS inhibitors.



**Part II. Investigation of the role of carbohydrate  
phosphodiester and phosphates in QS Regulation in  
*Agrobacterium tumefaciens***

**Chapter III. Bibliography**



## Bibliography

### QS mediated regulation in *Agrobacterium tumefaciens*

#### 3.1 Introduction

QS has been defined in previous sections as a signaling process through which bacteria are able to sense and monitor their cell density and activate differentiation to diverse community-oriented lifestyles within the bacterial population.

Among many species of bacteria that mediate QS by means of the LuxI/LuxR-type circuit (discussed in Part 1, section 1.2), the *V. fischeri*, *Pseudomonas aeruginosa*, *Agrobacterium tumefaciens*,<sup>[179–181]</sup> and *Erwinia carotovora* systems are the best understood. As for *A. tumefaciens*, the study on the functional characterization of the TraR protein and the LuxR homolog opened a door on understanding the horizontal transfer of virulence Ti plasmids, and also made *A. tumefaciens* species a leading model for the investigation of LuxI/LuxR QS systems.<sup>[182,183]</sup>

In this part, we will sketch out the molecular basis of *A. tumefaciens* in QS with a focus on chemistry of agrocinopine and its derivatives, and the biological relevance of this complex network in terms of dissemination of Ti plasmid genes in the plant tumor environment.

#### 3.2 QS in *Agrobacterium tumefaciens*

##### 3.2.1 *Agrobacterium tumefaciens*

*Agrobacterium* is a genus of Gram-negative bacteria that is responsible for tumors formation using horizontal gene transfer in many plant species including woody ornamental shrubs, vines, shade trees, fruit trees, and herbaceous perennials. It thus plays an important role agricultural production. Pathogenic *Agrobacterium* species includes four types: *A. tumefaciens*, *A. vitis*, *A. rubi*, and *A. rhizogenes*, and all carry mega plasmids that are pathogenic on plants.<sup>[184]</sup> Among them, *A. tumefaciens*, which causes typical crown gall diseases, is the most frequently studied species. The characterization of the disease could be described as a tumor-like growth

or gall usually at the junction of the root and shoot. The species *Agrobacterium vitis* causes cane gall on grapevines while infection of *A. rhizogenes* results in excessive formation of hairy roots or root tumors. *Agrobacterium*–plant interaction is an excellent model for studying both bacterial and plants responses, as well as the role of chemical signaling in these processes, such as the co-inducer 3-oxo-C8-HSL as a QS signaling molecule, and agrocinopine as an opine. Agrocinopine is a low molecular weight compound which was found in plant crown gall tumors or hairy root tumors and produced by *Agrobacterium*. With the significant findings made over the past four decades,<sup>[185–189]</sup> *A. tumefaciens*–plant interaction is now rather well-understood and provides various strategies for controlling plant disease related to bacteria.

### 3.2.2 The infection process of *A. tumefaciens*

The key virulence strain inducing the formation of tumors is the strain C58, whose genome has been sequenced, and is the most studied. It wears a virulence plasmid called plasmid or tumor-inducing Ti which contains the T-DNA and all the genes necessary to transfer it to the plant cell.

*A. tumefaciens* infects the plant through its Ti plasmid by four steps. Initially, the tissues of the wounded plant release phenolic compounds or other plant compounds, which serve as a self-defense mechanism to repair plant wall. However, those compounds attract *A. tumefaciens* and stimulate the expression of virulence genes of the bacteria presenting in the Ti plasmid tumor inducer. In the second step, the Ti plasmid integrates T-DNA into the chromosomal DNA of its host infected plant cells. Then the genes encoded by the T-DNA fragment are expressed in plant cells. On the one hand, the synthesis of plant hormones (**Fig 1**, auxins and cytokinins) induces the formation of a tumor that is colonized by bacteria. On the other hand, these genes induce the synthesis of a metabolite, agrocinopine, which is composed of phosphorylated sugars. The agrocinopine is then used as a nutrient and as a signal for *Agrobacterium* inducing the fourth stage. Indeed, it activates the synthesis of QS signals, which in turn activate the conjugation of the Ti plasmid and thus activate the spread of virulence genes.

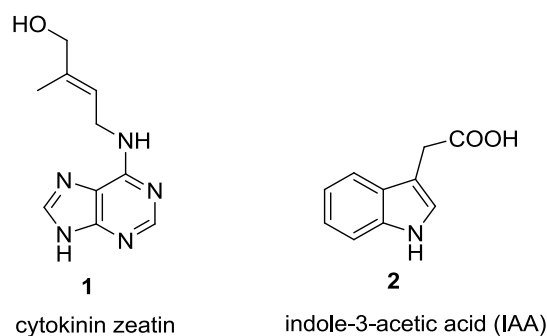


**Fig 1. Adenine-type cytokinins and the most abundant and the basic auxin IAA**

However, the specific mechanisms of the plant-derived chemicals such as the roles of agrocinopine opines are still under discussion.<sup>[190]</sup> This is our research objective in the second main part of this thesis. In the following sections, the different plant-derived signaling molecules in *A. tumefaciens* will be briefly introduced, with a focus on the biological and chemical aspects of specific opines: agrocinopines.

### 3.2.3 A brief overview of *A. tumefaciens* QS

QS system *A. tumefaciens* was firstly discovered with the functional characterization of a traR gene, homologous to *V. fischeri* LuxR, which produce some chemical signals acting as a transcriptional activator in the presence of a co-inducer. The chemical structure of the co-inducer required for TraR activity was determined as 3-oxo-C8-HSL.<sup>[182]</sup> Soon afterward the gene TraI was shown to be responsible for 3-oxo-C8-HSL synthesis.<sup>[191]</sup> There is another component existing in *A. tumefaciens* QS through which the activity of traR and 3-oxo-C8-HSL are negatively modulated and suppressed by Ti plasmid-encoded protein TraM. This component could also be found in other LuxI/LuxR type QS systems.

Therefore, it has been established that QS-regulated genes are involved in feedback control and Ti plasmid dissemination. In this process, the transformed plant cells release a conjugative opine (see section 3.2.5) such as agrocinopine for the initiation of QS signals 3-oxo-C8-HSL and horizontal transfer of the Ti plasmid (**Fig 2**). The QS-regulated genes of *A. tumefaciens* are the 3-oxo-C8-HSL synthesis TraI gene and the Tra genes involved in conjugation of the Ti plasmid.<sup>[183][34][191]</sup> The regulatory gene traM<sup>[192][193]</sup> and the rep genes are required for

vegetative replication of the Ti plasmid and spread of the virulence genes.<sup>[194]</sup> The detailed mechanism will be presented in the next section.

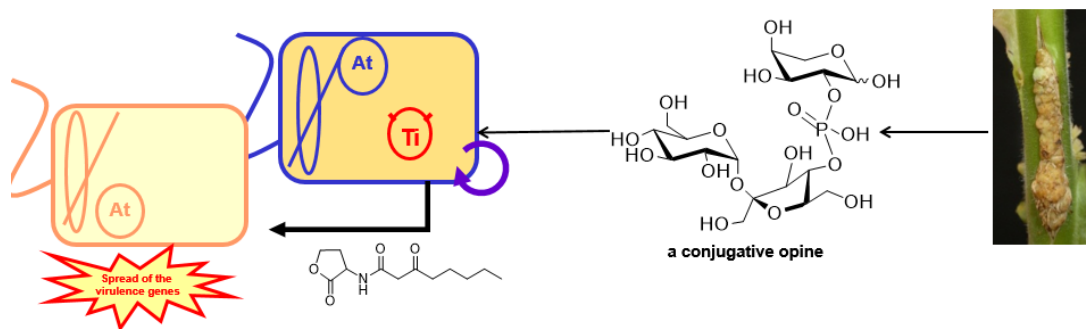


Fig 2. A brief QS process in *Agrobacterium tumefaciens*

### 3.2.4 *Agrobacterium tumefaciens* responses to plant-derived signaling molecules

#### 3.2.4.1 Plant-derived phenolic compounds

Phenolic compounds are secondary metabolites, most of them are derivatives of the pentose phosphate, shikimate, and phenylpropanoid pathways in plants. These compounds play an important role in growth and reproduction, providing protection against pathogens and predators, besides contributing towards the color and sensory characteristics of fruits and vegetables. With respects to *Agrobacterium*, plant-derived phenolic compounds are essential for the induction of *Agrobacterium* virulence<sup>[195]</sup> and serve as chemo-attractants for *Agrobacterium*.<sup>[196,197]</sup>

There are some structural specificities for virulence. For example, most of involved phenolic compounds include a benzene ring bearing a *para*-hydroxyl group and a *meta*-methoxy group (**Fig 3**).<sup>[198]</sup> 3,5-dimethoxyacetophenone and hydroxyacetosyringone were the first identified inducers of *Agrobacterium* virulence.<sup>[195]</sup> These compounds were recognized as a host specific signal and activate vir gene expression by the Ti plasmid.<sup>[199–202]</sup> Moreover, some phenolic acids such as ferulic acid and gallic acid, are also inducers of vir genes, which play important roles in regulation of the pathogenic process of plant. Besides, plant-derived phenolic compounds have been found having potential use in food antioxidants.<sup>[203]</sup>

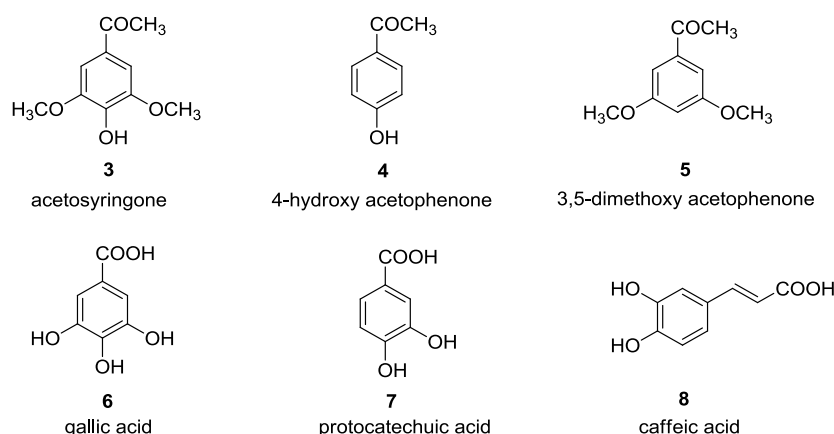


**Fig 3. Phenolic compounds (i.e. derivatives of acetosyringone, hydroxybenzoic and hydroxycinnamic acids)**

### 3.2.4.2 Acidic signals caused by plant-derived chemicals in the rhizosphere

The rhizosphere is the region susceptible to be infected by soil microorganisms since it exists widely in plant-derived and microbe-derived signals.<sup>[204–206]</sup> The acidic conditions found in the rhizosphere are caused by the organic acids such as lactic, citric, oxalic, and malic acids as well as other secondary metabolites, these acids are secreted by the plant (**Fig 4**). As said in the previous section, the wounded plants release phenolic compounds and neutral and acidic sugars for repairing the injured tissue, resulting in the acidification of the rhizosphere.<sup>[206]</sup> In these acidic conditions, *Agrobacterium* primarily infects plant hosts and the plant-derived chemicals acting as signaling pathways and regulatory factors.<sup>[206]</sup> This acidity characteristic of the rhizosphere allows *Agrobacterium* to set up a conserved response to infect plant hosts, which in response endows *Agrobacterium* an adaptability to the rhizosphere by the induction of genes coding for cell envelope synthesis, stress response as well as transporters of sugars and peptides.<sup>[207]</sup>

### 3.2.4.3 Plant released sugars in the rhizosphere

A distinct signaling pathway of inducing the *vir* genes with phenolic inducers of certain sugars that involved *virA* and a chromosomally encoded periplasmic protein was found in two decades ago. ChvE is employed by *Agrobacterium* for detecting and responding to plant-derived sugars.<sup>[208]</sup> ChvE mediates *Agrobacterium* chemotaxis in response to aldose

monosaccharides such as galactose, glucose, arabinose, xylose, and sugar acids. It has been found that the abilities of ChvE to recognize and bind different plant-derived sugars is vital in determining the host range of *Agrobacterium*.<sup>[209]</sup> And the sugar response in *Agrobacterium* has been found to be linked with the acidity responses.<sup>[209]</sup> Moreover, ChvE and associated sugar perception play additive roles in promoting vir gene expression in response to sugars and phenolic compounds, which are essential to vir gene inducing signals.<sup>[208,209]</sup> Detailed mechanism is shown **Fig 4**.

#### **3.2.4.4 Involvement of plant hormones and plant-derived chemicals in modulating *Agrobacterium* virulence**

In *Agrobacterium*, there are several types of plant hormones: indole-3-acetic acid, responsible for plant growth and development; ethylene, a plant stress signal; salicylic acid, a phytohormone activating plant defense responses to incompatible interactions, and some other special chemicals. Plant hormones are necessary for plant growth, defense and stress resistance and presented in a comparative normal level. As mentioned above, the synthesis of cytokinin is controlled by T-DNA, it is involved in the tumor formation. The high concentration of indole-3-acetic acid and cytokinin can facilitate plant cell growth and tumor formation, and that phytohormones significantly influence *Agrobacterium* pathogenicity and tumor formation (**Fig 4**).<sup>[210–212]</sup>

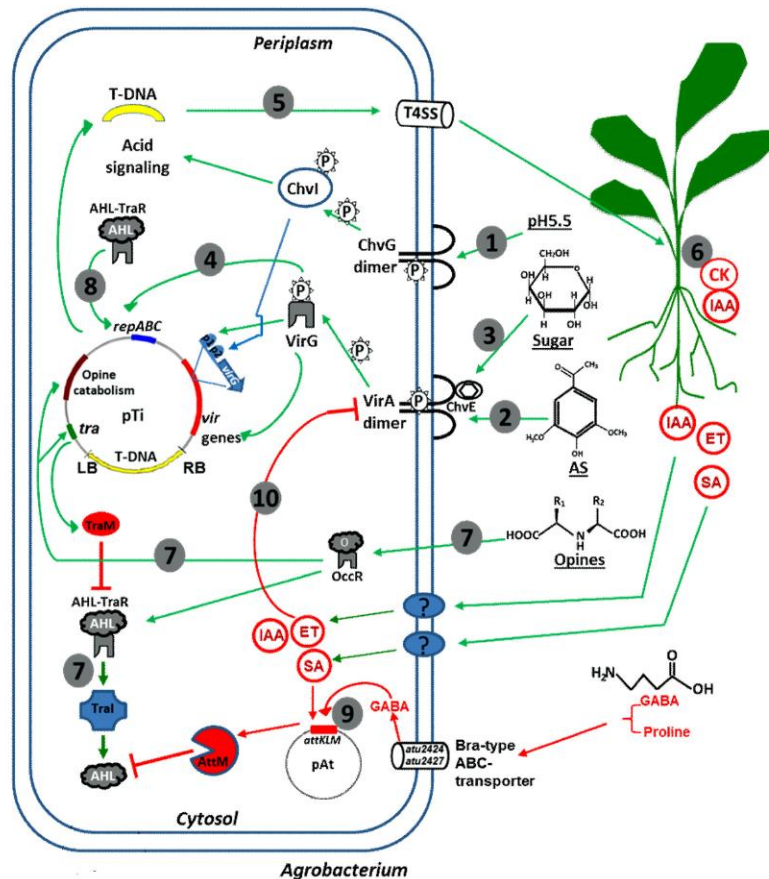


Fig 4. Schematic drawing of *Agrobacterium* responses to plant-derived signals.

(Referred to Sanitha, M., Radha, S., Fatima, A. A., Devi, S. G. & Ramya, M. *Agrobacterium*-mediated transformation of three freshwater microalgal strains.<sup>[213]</sup>)

(1) The acidic conditions in the rhizosphere make the ChvG/I two-component system activate the expression of several virulence genes; (2) The plant-derived phenolics make the VirA/G two-component system activate all vir genes and promote vir gene expression; (3) ChvE binds plant-released sugars and interacts with the VirA to allow maximal vir gene expression; (4) *Agrobacterium* Ti plasmid copy number is up-regulated in response to phenolic compounds; (5) Vir gene products process and deliver T-DNA into plant nuclei; (6) Expression of T-DNA encoded genes in plants leads to the production of indole-3-acetic acid (IAA), cytokinin (CK), and opines; (7) Opine activates *Agrobacterium* genes for opine metabolism, as well as TraR/TraI QS system that subsequently induces Ti plasmid conjugation; (8) QS also up-regulates Ti plasmid copy number for maximal pathogenicity; (9) *Agrobacterium* quorum quenching is activated by plant-derived GABA and SA thereby down-regulates QS; (10) *Agrobacterium* hijacks plant-derived SA (salicylic acid), IAA, and ET (ethylene) to down-regulate vir gene expression.

### 3.2.5 Plant-derived opines as a source of nutriment and activator for *Agrobacterium* QS

Opine biosynthesis is catalyzed by specific enzymes encoded by genes contained in a small segment of DNA, which is part of the Ti plasmid that inserted by the bacterium into the plant genome. The opines are used by the bacterium as an important source of nitrogen and energy. Each strain of *Agrobacterium* induces and catabolizes a specific set of opines.

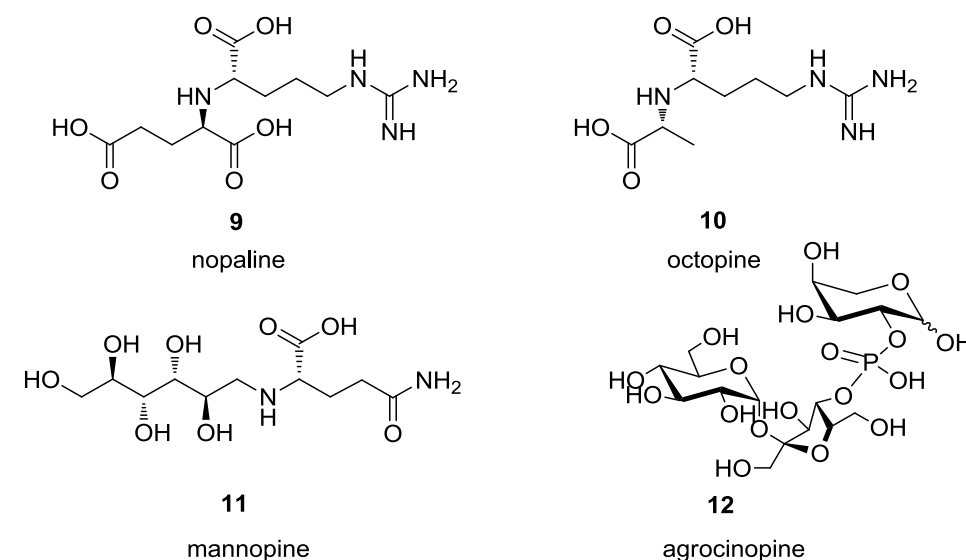
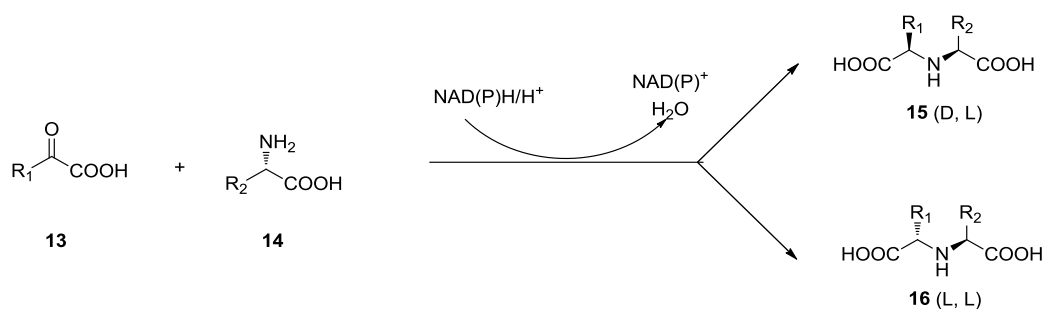


**Fig 5. Four families of opines**

The synthesis of opines is charged by T-DNA. Opines produced by transformed plant cells can be metabolized by *Agrobacterium* as a source of nutrients and signals activating *Agrobacterium* QS. There are over 30 different kinds of opines so far, it could be classified into four families (**Fig 5**): octopine, nopaline, mannopine, and agrocinopine families.<sup>[179][214]</sup> Among them, the octopine and nopaline types are the two mostly studied types whereas mannopine and agrocinopine are less reported. The vast majority are secondary amine derivatives formed by condensation of an amino acid, either with a keto acid or a sugar. The synthesis of octopine is controlled by the T-DNA-encoded enzyme octopine synthase, which condenses pyruvate with different amino acids to produce octopine, lysopine, histopine, or octopinic acid.<sup>[215]</sup> Nopaline is synthesized by nopaline synthase in a parallel method with the aid of  $\alpha$ -ketoglutaric acid and either arginine or ornithine (**Scheme 1**). Opines of the mannopine family is structurally more complicated and originated from various pathways such as condensation of an amino-acid with

mannose, In the agrocinopine family, molecules are constructed by combining sugar and phosphate groups in different manners. The opines are accumulated and released by transformed plant cells into the rhizosphere since the plants are not capable of metabolizing opines. However, opines are present on the plant surface and are part of the soluble plant exudates released into the phylloplane and rhizoplane.<sup>[216]</sup>



**Scheme 1. Synthesis of the octopine and nopaline opines**

In the non-transferrable region of *Agrobacterium* Ti plasmid, there also exists genes for opine uptake and catabolism as well as chemotaxic genes for their corresponding opines (**Fig 6**).<sup>[217][218]</sup> *Agrobacterium* LysR-type transcriptional activator octopine catabolic regulator and nopaline catabolic regulator recognize and bind to opines, subsequently activates the expression of opine catabolic genes.<sup>[218]</sup> In the case of agrocinopine, it is more complicated. When agrocinopines are present, the repressor agrocinopine catabolic regulator (AccR) dissociates from the promoter, allowing for expression of the acc operon which is responsible for agrocinopine metabolism. Some of opine catabolic genes are also under regulation of certain substrates such as succinate.<sup>[219]</sup> Some other species other than *Agrobacterium* are exist in the rhizosphere, and are able to utilize opines, though they comprise of a very small minority of the bacterial population.<sup>[220]</sup> Therefore, the ability to use opines as a carbon, nitrogen, and energy source provides distinct advantages to *Agrobacterium* in the rhizosphere niche.

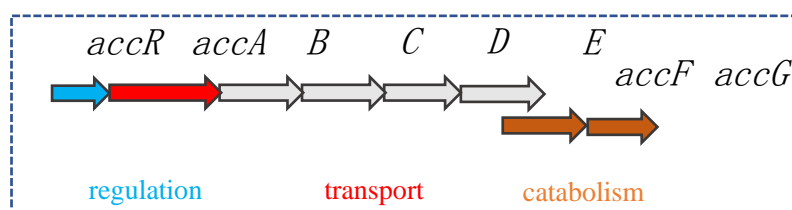


**Fig 6. Key role of the acc operon in *A. tumefaciens* virulence**



regulated by the conjugal opines agrocinopines which are produced by the transformed plant cells (1) and induce production of TraR by releasing AccR repressive action (2). Then, active TraR-3-oxo-C8-HSL dimers activate the production of TraI, thereby triggering a positive feedback in the synthesis of 3-oxo-C8-HSLs (3) which are diffusible molecules (4). The QS activation is delayed by the TraR-antagonist TraM (5), as well as 3-oxo-C8-HSL-cleaving lactonases AiiB and AttM (6) whose expressions are controlled by agrocinopines and GABA, respectively. (SAM, S-adenosylmethionine; ACP, acyl carrier protein).

### 3.3 Agrocinopine

The opines have been discussed in the previous section, and the specific opines, called conjugal opines, are strictly required to enable conjugation of the *A. tumefaciens* Ti plasmid.<sup>[223,224]</sup> In the case of nopaline-type Ti plasmids, agrocinopines A and B which are a mixture of two non-nitrogenous phosphodiester of sugars serve as conjugal opines.<sup>[225]</sup> Like agrocinopine A and B, agrocinopine C and D are also phosphorylated sugars that are able to promote Ti-plasmid transfer from strains harboring agropine Ti-plasmids. The relationship of opines and plasmid types is summarized in **Table 1**.

**Table 1. Ti-plasmid types and the opines whose synthesis in crown gall tumors they control**

Plasmid types	Opines in tumor tissue			
	Pyruvic	$\alpha$ -keto-glutaric	Phosphorylated	Mannose
<b>Octopine</b>	Octopine			Agropine
	Octopinic acid	-	-	
	Lysopine, Histopine			
<b>Nopaline</b>	-	Nopaline Nopalinic acid	Agrocinopine A and B	-
	-	-	Agrocinopine C and D	Agropine

### 3.3.1 Agrocin 84

To have a better understanding of agrocinosines, it is logical to begin with the natural antibiotic agrocin 84. The agrocin 84 which is a highly specific bacteriocin, is produced by the non-pathogenic strain of *Agrobacterium* K84. The plasmid determined function is sensitive to this bacterial strain. It has been found that most bacteria carrying the nopaline type Ti are sensitive to agrocin 84.<sup>[226]</sup>

In 1979, Murphy and Roberts<sup>[227]</sup> found that susceptibility to agrocin 84 was associated with the plasmid-encoded gene set which is responsible for the uptake and catabolism of the agrocinosine type opines. First, only agrobacteria being able to catabolize the agrocinosine opines were susceptible to agrocin 84. Second, mutations abolishing susceptibility to agrocin 84 invariably resulted in the inability to take up and catabolize the opines. Third, mutations resulting in constitutive high-level expression of the opine catabolism locus made the cell super-sensitive to agrocin 84. Fourth, presence of agrocinosines inhibited the uptake of radiolabeled agrocin 84. In this regard, agrocin 84 was taken up via a high-affinity, energy-dependent transport system.<sup>[227]</sup> Moreover, the periplasmic protein contained system specifically bound the antibiotic, and that the presence of this binding protein was dependent upon a Ti plasmid conferring susceptibility to antibiotic and catabolism of the opine.

A detailed analysis of the chemical structure of agrocin 84 indicated that it is a di-substituted adenine nucleotide<sup>[228]</sup> in which the 5' phosphoryl linkage from the fraudulent nucleotide core to the amide group is required for antibiotic activity, while the D-glucofuranosyl or glucopyranosyl-oxyphosphoryl substituent at the N<sup>6</sup> of adenine is responsible of the bacteriocin-like specificity. The precise structure was originally proposed with a connection at C-1 of a glucofuranose moiety,<sup>[229]</sup> then suggested that it could be either pyranose or furanose (**Fig 8**),<sup>[230]</sup> and has been actually fully ascertained in the course of this thesis (chapter 4, and our results published in Plos Pathogen<sup>[231]</sup>). The basis for sensitivity to agrocin 84 resides in the presence of a high affinity uptake system encoded by the Ti plasmid. A nopaline Ti plasmid encoded permease found in the periplasmic space of bacteria harboring the plasmid recognizes

the N<sup>6</sup> substituent of Agrocin 84, and selectively transport it into the cell. This molecule then behaves as an antibiotic, killing the pathogenic bacterium.

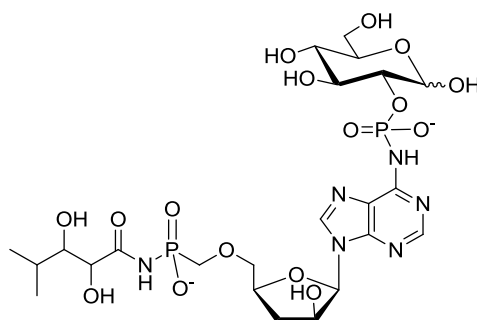


**Fig 8. Proposed structure of agrocin 84 (the glucose part could be either glucopyranose or glucofuranose)**

### 3.3.2 Discovery and chemistry of the agrocinopine opines

The discovery of the agrocinopine opine chart an interesting course in the application of the opine concepts. It had been known that the anti-agrobacterial antibiotic agrocin 84, produced by *A. radiobacter* strain K84 was highly specific. This agent inhibited the growth of only certain isolates of *A. rhizogenes* and *A. tumefaciens*, and its sensitivity was associated with the type of Ti plasmid present in the strain.<sup>[232]</sup> Ellis and Murphy<sup>[233]</sup> found that the specificity of agrocin 84 might be due to its ability of mimicking some unknown opine produced by the neoplasia induced by this susceptible strains. The presence of this unknown opine should be demonstrated by its ability of inducing higher levels of sensitivity to the agrocin antibiotic. After that, an unknown compound was specifically found in tumors induced only by the agrocin 84 sensitive strains of *A. tumefaciens* and that induced super sensitivity of these strains to the antibiotic.<sup>[233]</sup> This compound could be catabolized only by agrobacteria harboring Ti plasmids and conferred susceptibility to agrocin 84. This established the opine nature of the agent, and lined it to agrocin 84 sensitivity. The activity was associated with two closely migrating compounds, because of the relationship with agrocin 84. These new opines were named agrocinopine A and B.

Chemical analysis showed these opines unlikely to be any of the previously characterized tumor metabolites. Indeed, agrocinopine A and B proved to be sugar-phosphodiester. It is not clear whether agrocinopine B comes from agrocinopine A, or whether the two opines are synthesized in parallel. This opine family is associated with classical nopaline-type Ti plasmid

and with certain opine catabolism plasmids present in *A. rhizogenes* and *A. radiobacter* isolates.<sup>[234]</sup> In 1980s, Eillis and Murphy<sup>[233]</sup> identified a second set of two agrocinopine type opines, called agrocinopine C and D which were found in tumors induced by strains harboring the classical agropine type Ti plasmids of the *Lippia* type agrobacteria.<sup>[235]</sup> Moreover, isolates of *agrobacterium* spp. that were innately susceptible to agrocin 84 can catabolized agrocinopine A and B, and surprisingly, agrocinopine D, but not agrocinopine C.<sup>[233]</sup> Interestingly, although it cannot be catabolized, agrocinopine C protects agrocinopine A and B type strains from inhibition by agrocin 84. Strains that can catabolize Agrocinopine C and D are not innately susceptible to agrocin 84. However, if these strains are precultured in the presence of either of these two opines, they express sensitivity to antibiotics.<sup>[236]</sup>

Structurally, the family of agrocinopines belong to carbohydrate phosphodiester or phosphates. All agrocinopines are constructed by one or two monosaccharide bridged through a phosphodiester or phosphate linkage. Agrocinopine A consists in a phosphodiester of L-arabinose linked in position 2 and a sucrose linked in the position 4, and Agrocinopine B consists of  $\beta$ -D-fructose (at position 4) and L-arabinose (at position 2). Agrocinopine C consists of sucrose (at position 4 of fructosyl moiety) and D-glucose whereas Agrocinopine D consists of two D-glucose units joined via a (2 $\leftrightarrow$ 2)-phosphodiester linkage. In all these systems, the presence of free hemiacetals brings additional complexity with mixtures of  $\alpha$  and  $\beta$  anomers and furanose and pyranose forms, leading to their identification and characterization even more difficult (**Fig 9**).

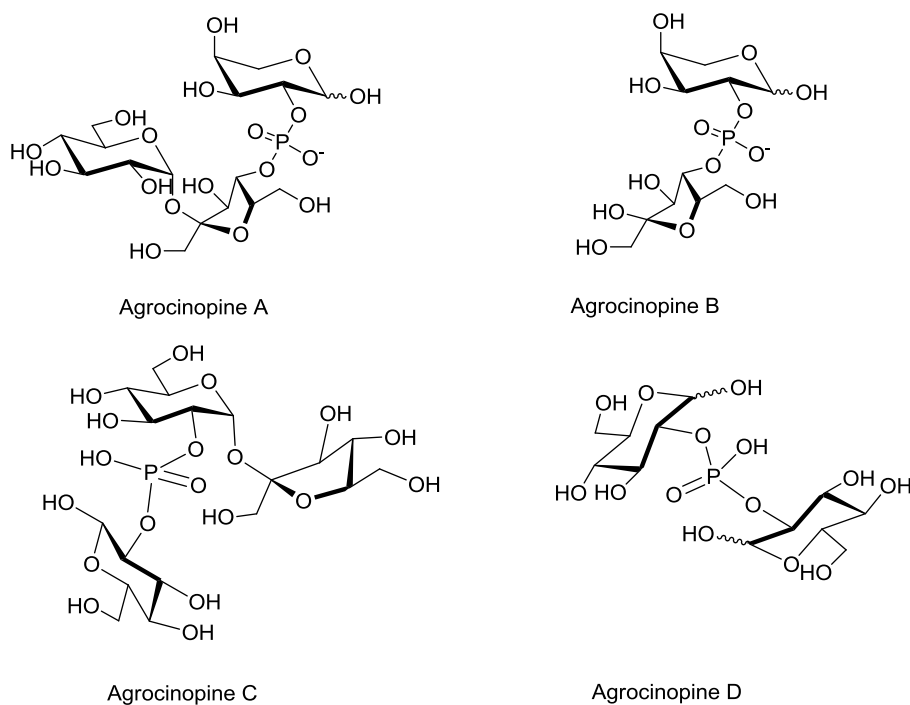
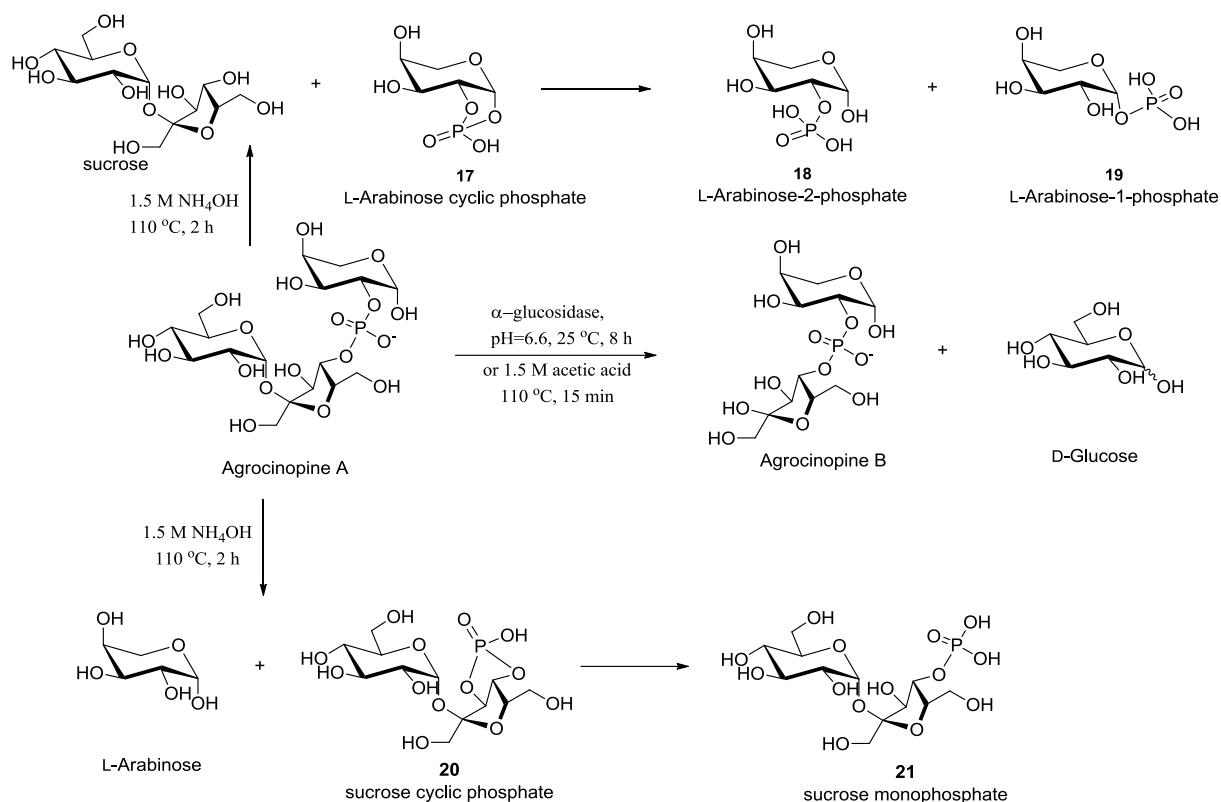


**Fig 9. Structures of agrocinopines**

### 3.3.3 Agrocinopine A and B

#### 3.3.3.1. Structure and identification

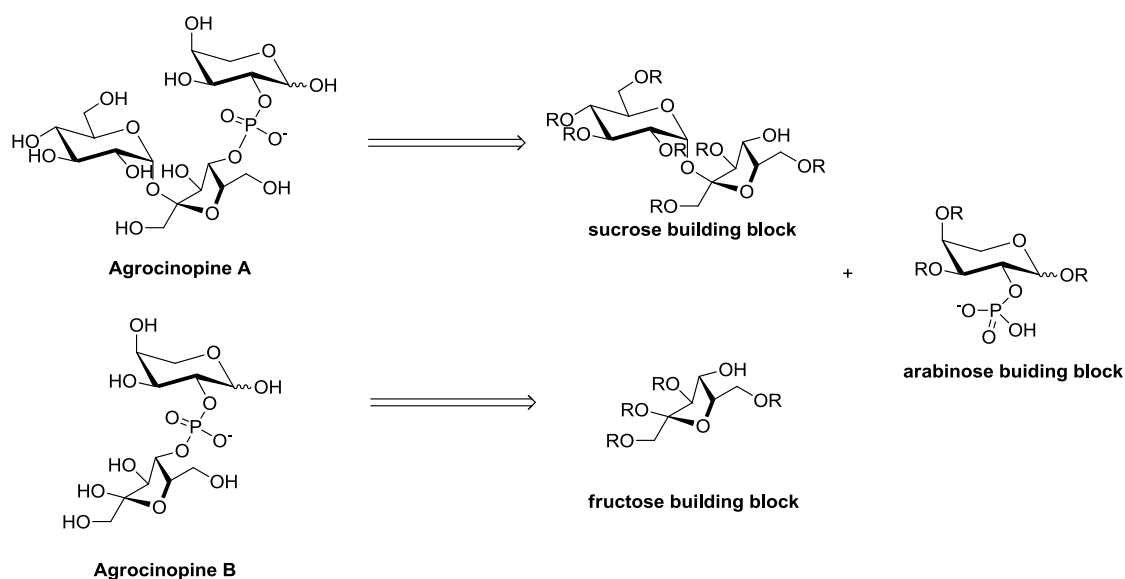
Ryder et al<sup>[237]</sup> firstly investigated the structure of the agrocinopines by degradation experiments (**Scheme 2**) and especially by means of <sup>13</sup>C-NMR spectroscopy. The trisaccharide arrangement was studied by <sup>1</sup>H-NMR and 2D-NMR experiments. They showed the acid and alkaline enzymatic degradative pathways for agrocinopine A, and characterized all degradation products by means of <sup>13</sup>C-NMR. A full comparison of <sup>13</sup>C-NMR spectra of sucrose, agrocinopine A sodium salt, L-arabinose-2-phosphate and L-arabinose was conducted. Evidence was presented to show that agrocinopine A is a phosphodiester linking the 4-hydroxyl of the fructose moiety in sucrose to the 2-hydroxyl of L-arabinose and that agrocinopine B is a related molecule in which the glucose moiety of agrocinopine A has been cleaved to yield a corresponding phosphodiester of D-fructose and L-arabinose as shown in **Scheme 2**.<sup>[237]</sup> Agrocinopine A can be converted into agrocinopine B by acidic hydrolysis or by enzymatic cleavage of the glucose residue with  $\alpha$ -glucosidase.



**Scheme 2. Investigation of the structures of the agrocinopines by degradation experiments**

### 3.3.3.2 Synthesis of agrocinopine A and B

The Thime's group was the first to report some partial synthesis of agrocinopine A and B, but not fully deprotected.<sup>[238]</sup> Then Noberg's group was the first one to report a total synthesis of agrocinopine A and B.<sup>[239]</sup> In both cases, agrocinopine A and B were synthesized through a key condensation step of two saccharide fragments. Thus, for the preparation of the agrocinopines A and B, strategically protected derivatives of sucrose or D-fructose or L-arabinose are the essential saccharide building blocks. For agrocinopine A, the sucrose building block should have an available OH in position 4', and the arabinose building block should have an available OH in position 2. Then the intermediate phosphate precursors can be made either at sucrose or arabinose moiety. Based on the same strategy, agrocinopine B was constructed from the same arabinose building block and fructose building block in which the OH in position-4 is free. In the following sections, a systematic review of the synthesis of these three types of building blocks will be discussed in detail (**Scheme 3**), and several phosphorylation and condensation strategies will also be presented.



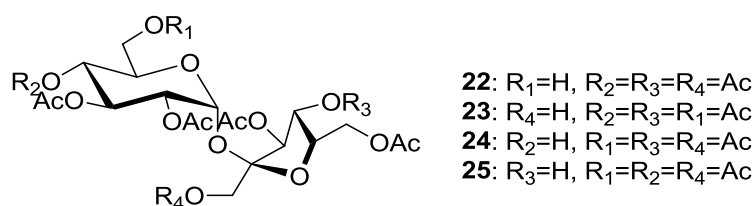
**Scheme 3.** General strategy for synthesis of agrocinopine A and B

### 3.3.3.2.1 Sucrose building block

For the sucrose building block varying only OH-4 unprotected, it was firstly reported by Hough et al<sup>[240][241]</sup> by selective de-*O*-acetylation of sucrose octa-acetate with alumina.<sup>[242]</sup> The desired compound **25** was isolated in only 9% yield with a large amount of starting material and three other isomers **22**, **23** and **24** in which the available OH located in different positions (**Scheme 4**). Surprisingly, the selective de-*O*-deacetylation of the sucrose octa-acetate occurred at secondary positions as well as at the primary 6'-position. However, it is well known<sup>[243]</sup> that facile acetyl migrations from 4- to 6- position occur in hexopyranosides having free primary hydroxyl group. Therefore, it was speculated that the 4- and 4'-hydroxy derivatives **24** and **25** arose from the 6- and 6'-hydroxy derivatives, respectively.<sup>[241]</sup>

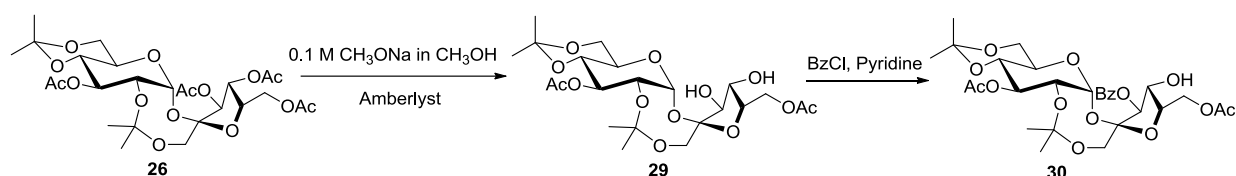
The structures of all isomers **22-25** were characterized by <sup>1</sup>H-NMR. A clear high-field shift of the H-6 and H-6' for compound **22** and the H-1 and H-1' for compound **23** were observed. Compound **23** was formed by the acetyl group migration. The characteristic H-4 resonance at  $\delta$  5.07 of sucrose octa-acetate was absent from the corresponding region for compound **24**, but was observed at higher field  $\delta$  3.52 as a broadened triplet. For other de-acetylation compounds, the chemical shift of H-4 were almost the same with sucrose octa-acetate. The comparison of

the  $^1\text{H-NMR}$  data showed a clear high-field shift of the H-6 and H-6' of **22** compared with the 6-*O*-acetylated derivatives **23-25**.



**Scheme 4. Compounds of selective *O*-deacetylation of the sucrose octa-acetate**

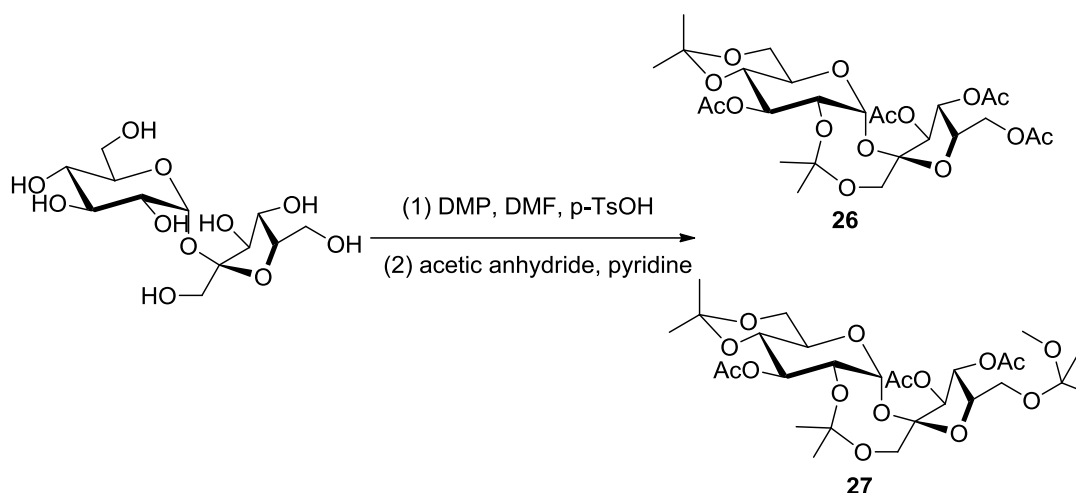
The hept-acetylated sucrose **25** was not the only possible protected sucrose building block bearing a free hydroxyl group in position 4'. In 1987, Lindberg and Norberg<sup>[239]</sup> used 3,6'-di-*O*-acetyl-3'-benzoyl-2,1':4,6-di-*O*-isopropylidene sucrose **30** to synthesize the precursor of agrocinopine A successfully. The synthesis of this sucrose derivative was accomplished from sucrose in three steps.<sup>[244]</sup> The key intermediate was tetra-acetylated 1',2:4,6-di-*O*-isopropylidene-sucrose **26**, which was obtained in two steps. The selective de-acetylation of compound **26** at *O*-3 and *O*-4 of the fructose moiety can be conducted in the presence of a catalytic amount of sodium methoxide in methanol (Zemplen deacetylation)<sup>[244]</sup> or methanolic ammonia<sup>[245]</sup> followed by the treatment with Amberlyst for neutralization. Then selective 3-*O*-benzoylation<sup>[246]</sup> of compound **29** using benzoyl chloride in pyridine gave 3,6'-di-*O*-acetyl-3'-benzoyl-2,1':4,6-di-*O*-isopropylidene sucrose **30** in 37% yield (**Scheme 5**).



**Scheme 5. Synthesis of 3,6'-di-*O*-acetyl-3'-benzoyl-2,1':4,6-di-*O*-isopropylidene sucrose**

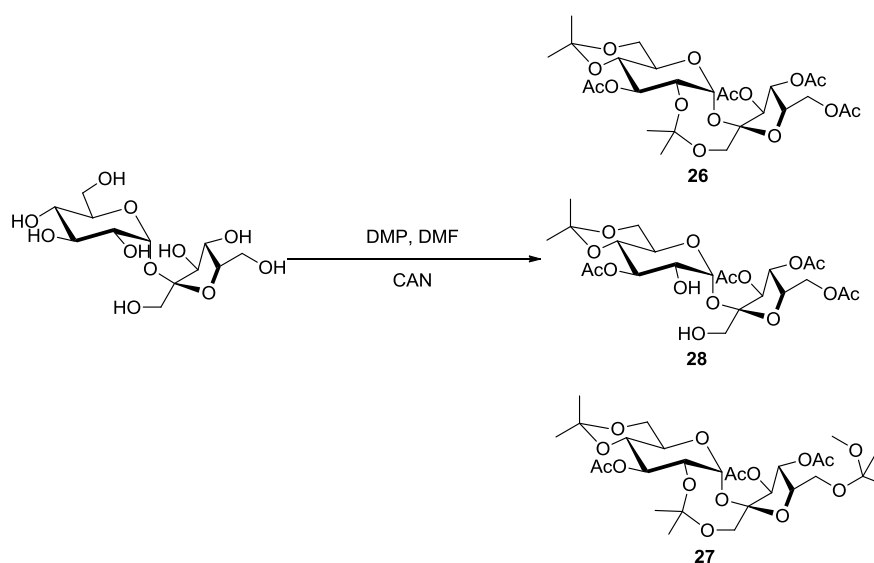
The synthesis of precursor **26** was originally reported by R. Khan et K. S. Mufit<sup>[247]</sup> in 1975, in two separate steps from sucrose in overall 15% yield after purification. The first step was the reaction with 2,2-dimethoxypropane (DMP) in the presence of an acid catalyst *p*-TsOH in DMF to give the 2,1':4,6-di-*O*-isopropylidene sucrose which was then peracetylated to afford compound **26**. This method is the conventional procedure to achieve such a kinetically

controlled transformation.<sup>[248]</sup> However, it was proved to be not an efficient method due to the low yield and the formation of by-product **27** which made purification difficult (**Scheme 6**).



**Scheme 6.** *O*-isopropylideneation of sucrose using DMP and *p*-TsOH

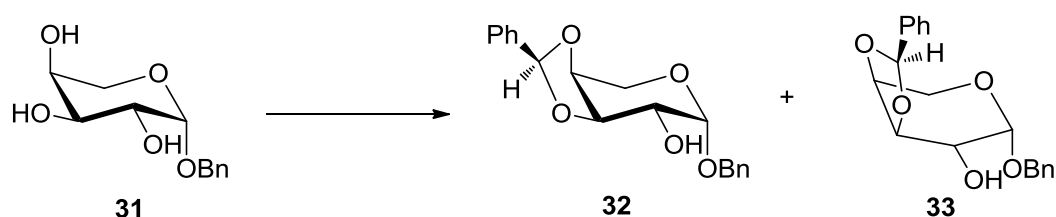
In 2000, Parrilli et al.<sup>[249]</sup> described a procedure using ammonium cerium nitrate (CAN) as a catalyst for the formation of the sucrose diacetal derivative **26**. Selectivity between compounds **26**, **27** and **28** was found to depend on the ratio of sucrose and catalyst, the 1/0.2 sucrose/CAN ratio at room temperature being the best condition for reaching product **26**. Both larger amount of CAN and higher temperature were unfavorable for the formation of product **26**, leading to increasing amounts of compounds **27** and **28** (**Scheme 7**).



**Scheme 7.** *O*-isopropylideneation of sucrose using DMP and CAN

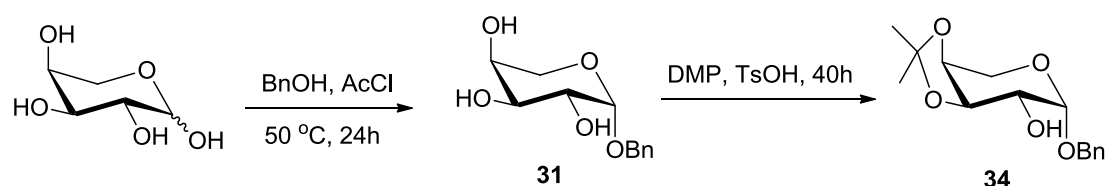
### 3.3.3.2.2 Arabinose building block

A large number of arabinose protection strategies have been reported for achieving a free OH-2. The frequently used method is the protection of OH-3 and OH-4 of benzyl- $\beta$ -L-arabinopyranoside **31** with the aid of benzaldehyde, to give benzyl-3,4-*O*-benzylidene- $\alpha$ -L-arabinopyranoside as a mixture of the exo **32** and endo **33** diastereoisomers. The exo-isomer **32** can be separated by crystallization from acetone, while the endo product **33** can be enriched by crystallization from isopropyl ether (**Scheme 8**).



**Scheme 8.** Synthesis of benzyl 3,4-*O*-benzylidene- $\alpha$ -L-arabinopyranoside

The alternative of this method is the 3,4-*O*-isopropylidene of arabinose. The anomeric hydroxyl can be protected by various substituents such as benzyl, benzoyl, allyl, acetyl and so on. For example, benzyl 3,4-*O*-isopropylidene- $\beta$ -L-arabinoside **34** was prepared from L-arabinose by reaction with benzyl alcohol in acidic conditions, followed *O*-isopropylidene of compound **31** using DMP in the presence of TsOH, in 62% yield over two steps (**Scheme 9**).<sup>[239][250,251]</sup>



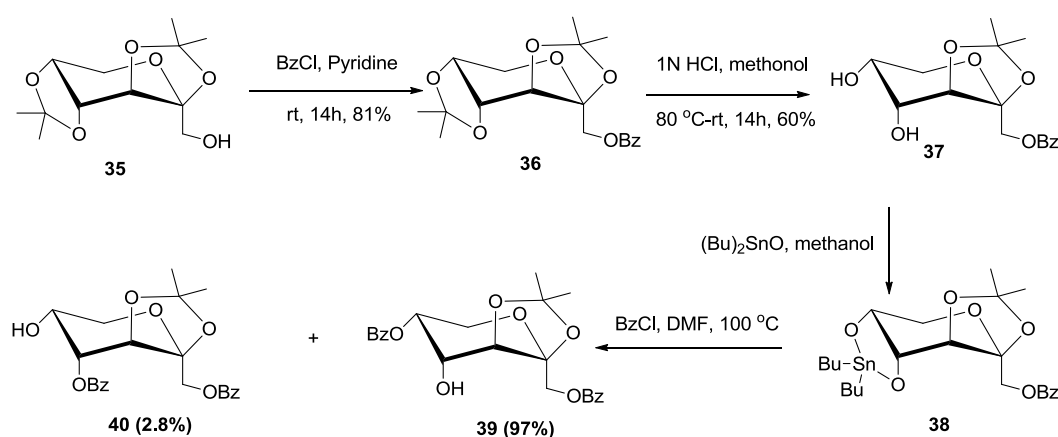
**Scheme 9.** Synthesis of benzyl 3,4-*O*-isopropylidene- $\beta$ -L-arabinoside

### 3.3.3.2.3 Fructose building block

In view of the structure of fructose, there are many possibilities of achieving a specific protected fructose bearing a free OH-3 or OH-4, the latter being the useful one for building agrocinopine B. For example, compound **39** was obtained from the mono-benzoylation of 1-*O*-

benzoyl-2,3-*O*-isopropylidene- $\beta$ -D-fructopyranose **38**, and several methods for this reaction have been reported.<sup>[252][253,254]</sup>

For example, using triethyl orthobenzoate in absolute DMF gave two mono-benzoylation compounds, the ratio of 5-*O*-benzoate **39** and 4-*O*-benzoate **40** being 6/4.<sup>[253]</sup> The acidic hydrolysis in acetonitrile improved the ratio of **39** and **40** to 27/73.<sup>[254]</sup> Obviously, these two conditions were not applicable for obtaining compound **39**. The most efficient method is the use of dibutylstannane in methanol, and the resulted intermediate *O*-dibutylstannylene derivative **38** was then treated by benzoyl chloride in DMF leading to the desired 5-*O*-benzoylated derivative **39** in 97% yield (Scheme 10).<sup>[252]</sup>



**Scheme 10. Synthesis of 5-*O*-benzoate fructose derivative **39****

The high regioselectivity observed in the ring opening of the intermediate *O*-dibutylstannylene derivative **38** is in agreement with that previously reported.<sup>[255]</sup> Probably the most stable conformation of **38** is that shown as **38A**. It is stated that a pyranose *cis*-fused to a 1,3-dioxolane ring must adopt such a skew-boat conformation. The change of an *O*-isopropylidene induced by an *O*-dibutylstannylene group have little conformational significance. It's striking that the oxygen atom at C-5 in conformation **38A** adopts a quasi-equatorial position, and hence the attack of the benzyl bromide occurred at that position<sup>[255]</sup> to yield preferentially compound **39** (Fig 10).

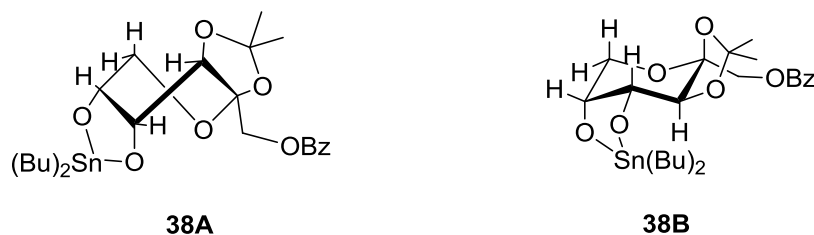
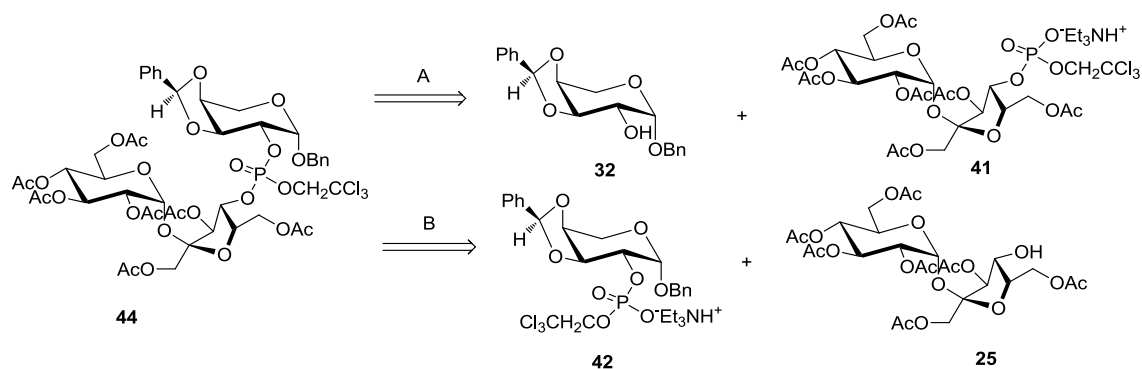


Fig 10. Two conformations of *O*-dibutylstannylene derivative 38

### 3.3.3.2.4 Phosphorylation and condensation towards agrocinopine A and B

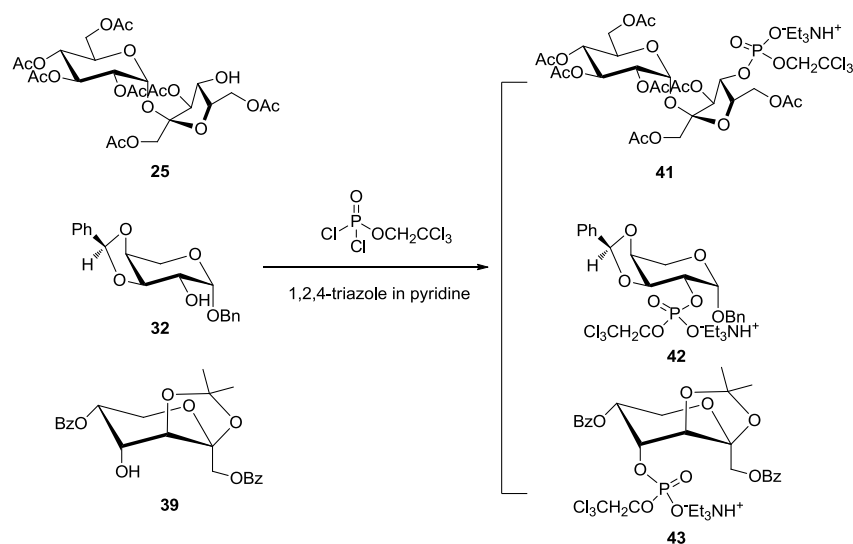
In the previous sections, different approaches for achieving sucrose, arabinose and fructose building blocks via various protection and de-protection strategies, were presented. All building blocks have a specific available hydroxyl group being ready for the phosphorylation and condensation. The precursors of agrocinopine A and B were condensed by J. Thiem et al,<sup>[238]</sup> using (2,2,2-trichloroethyl) phosphorodichloridate as the phosphoric ester linkage.

However, there are two alternatives for the condensation of the two building blocks depending on which of the two sugars is phosphorylated first. The synthesis of the target compound **44** was obtained first by condensation of the peracetylated sucrose phosphate **41** with the arabinose derivative **32** (case A). Alternatively, compound **44** could also be prepared from the phosphorylated arabinose **42** and the sucrose derivative **25** (case B). In the first case, surprisingly, the compound **44** was obtained as a diastereomer mixture (1: 1). The formation of one isomer isomerized in the excess of heptaacetylsuric acid 4-phosphate **41** in the transition state while in the case of B the compound **44** was obtained as a diastereomerically pure product at the phosphorus center (**Scheme 11**).<sup>[238]</sup>



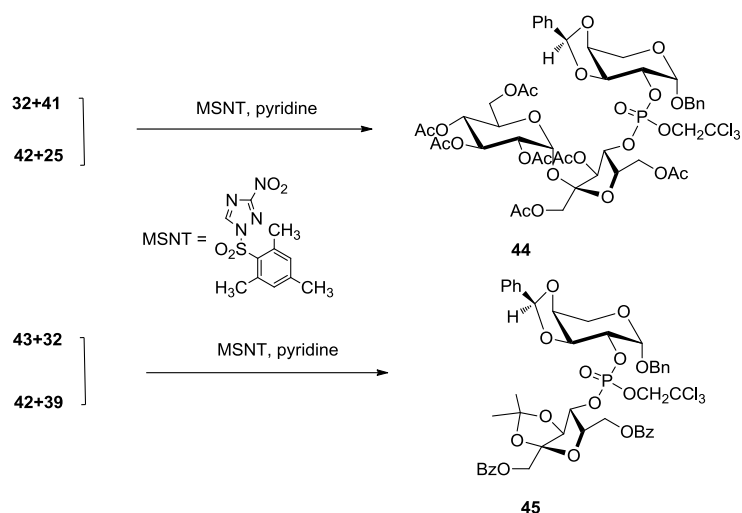
Scheme 11. Two alternative approaches for synthesis of agrocinopine A precursor<sup>[238]</sup>

The phosphorylation was attempted by using substrates **25**, **35** and **39** according to a modified phosphotriester method<sup>[256,257]</sup> using (2,2,2-trichloroethyl) phosphorodichloridate as phosphorylation reagent. The condensation was catalyzed by a reactive bis-triazolide generated from the reaction of (2,2,2-trichloroethyl) phosphorodichloridate with 1,2,4-triazole in pyridine,<sup>[258]</sup> leading to the phosphodiester salts **41**, **42** and **43** in good yields (**Scheme 12**).



**Scheme 12. Phosphorylation of saccharide building blocks**

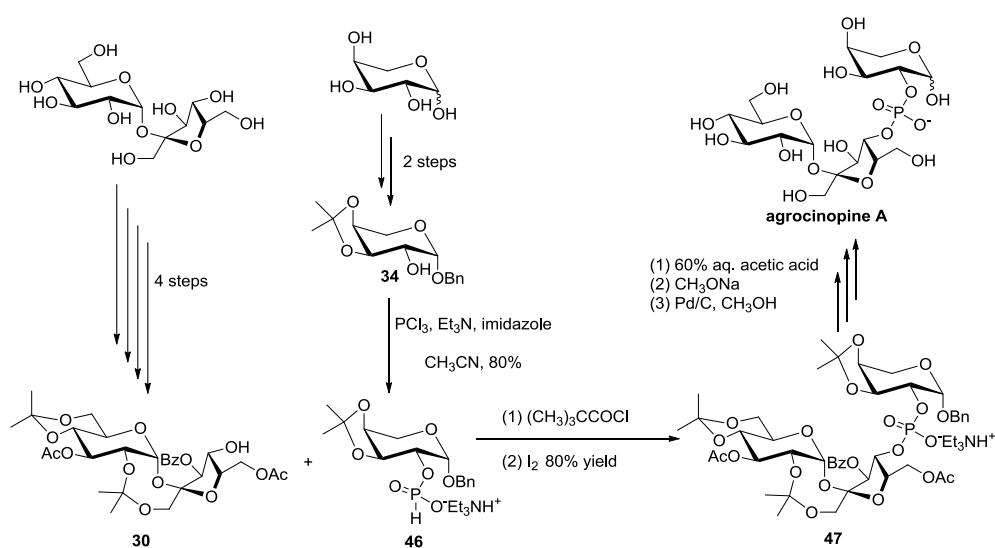
The second condensation step to access precursors **44** and **45** of agrocinopine A and B was accomplished by using 1-methylenesulfonic acid (3-nitro-1,2,4-triazolide) (MSNT). The procedure involved an activation of the diester salts **41**, **42** and **43** with MSNT<sup>[259]</sup> to synthesize phosphodiester-3-nitrotriazolides, which was used subsequently for the condensation with another saccharide component. However, due to the lower reactivity of secondary alcohol functions, an excess amount of MSNT and longer reaction times were required. Tedious purification by means of column chromatography, followed by preparative HPLC, led to protected agrocinopine A derivative **44** in 20% yield (**Scheme 13**).<sup>[238]</sup>



**Scheme 13. Condensation of phosphorylated saccharide building block with various saccharide substrates**

Agrocinopine B precursor **45** was obtained based on the same principle,<sup>[238]</sup> through the condensation of the fructose phosphate **43** with the arabinose derivative **32**, or the reaction of the phosphorylated arabinose unit **42** with the fructose derivative **39**, as a 1:2 mixture of diastereoisomer in 20-50% yields (**Scheme 13**).

In 1988 Lindberg and Norberg<sup>[239]</sup> published the first total synthesis of agrocinopine A in nine steps, based on the same overall principle as previously described by Thiem et al<sup>[238]</sup>. It involved a coupling reaction between the protected L-arabinose phosphate salt and the sucrose building block, which was protected by isopropylidene, acetyl, benzoyl groups (**Scheme 14**).



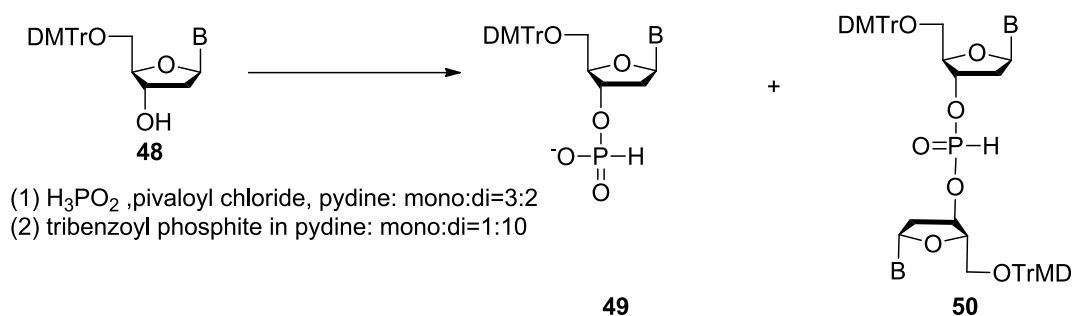
**Scheme 14. An alternative method for synthesis of agrocinopine A reported by Norberg<sup>[239]</sup>**

The H-phosphoric acid monoester **46** was obtained in 80% yield by treatment of compound **34** with phosphorous trichloride, triethylamine, and imidazole in acetonitrile and water. The sucrose building block **30** was not considered due to its complicated synthetic sequence. The condensation reaction<sup>[260]</sup> of **30** with compound **46** was conducted in pyridine using pivaloyl chloride and led to H-phosphoric acid diester (detailed mechanism shown in section 3.3.3.2.5), which was oxidized subsequently with iodine in pyridine-water to give the corresponding phosphodiester **47** in 80% yield. Deprotection of **47** was accomplished by successive treating with 60% aqueous acetic acid, methanolic sodium methoxide, and hydrogen/palladium on charcoal. Agrocinopine A was obtained as a sodium salt after purification by ion exchange chromatography, gel filtration and C-18 Sep-Pak treatment in 70% yield (**Scheme 14**).

### 3.3.3.2.5 Phosphorylation reagents and approaches

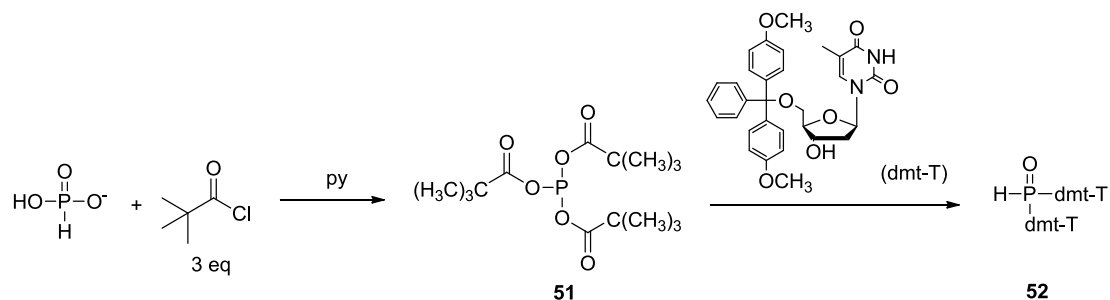
The phosphorylation reaction appears to be a key step in the synthesis of numerous compounds of biological system. There are lots of phosphorylation approaches in oligonucleotide, glycoside and peptide synthesis, and we give a brief overview.

In 1988, T. H. Mitsuo Sekine<sup>[261]</sup> developed a convenient method for the synthesis of nucleoside H-phosphonate monoesters. A mixture of H-phosphonate mono- **49** and di- esters **50** with the ratio of 3:2 was obtained by using three equivalents of phosphonic acid versus the nucleoside substrates **48** in pyridine and pivaloyl chloride. Additionally, treatment of the nucleoside substrates **48** with tribenzoyl phosphite in pyridine furnished the diester as major product. Later on, this method was used for creating the phosphodiester linkage of agrocinopine D precursor by S. Oscarson<sup>[262]</sup> in 1993 (**Scheme 15**).



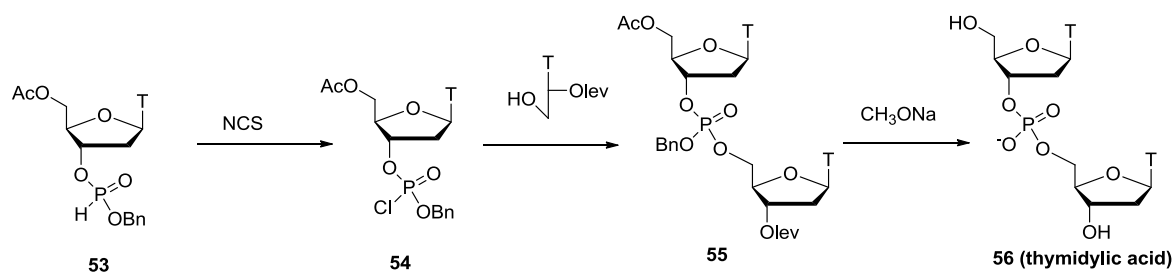
**Scheme 15. Synthesis of nucleoside H-phosphonate monoesters and diesters**

In 1990, Stawinski and Thelin<sup>[263]</sup> investigated the activation of acyl chloride using phosphonic acid. The formation of hydrogenphosphonate diester **52** was drastically improved by adding three equivalents of pivaloyl chloride to an equimolar mixture of phosphonic acid and a partially protected nucleoside (**Scheme 16**).



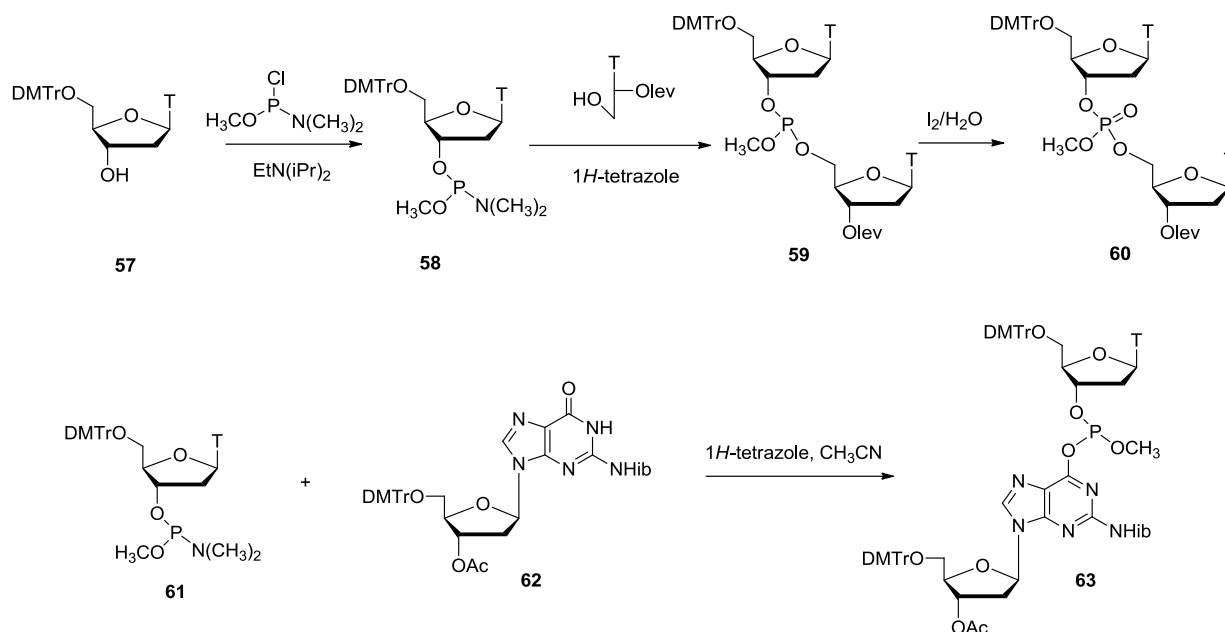
**Scheme 16. Synthesis of nucleoside hydrogenphosphonate diester 99 using pivaloyl chloride and H<sub>3</sub>PO<sub>4</sub>**

In 1955, Michelson and Todd<sup>[264]</sup> published the first phosphoramidite approach to access oligonucleotide. They adopted a substituted phosphochloridate **54** to synthesize the dinucleotide, phosphodiester **56**. However, these chlorophosphates are very reactive, and sensitive to air, which limit their applications (**Scheme 17**).



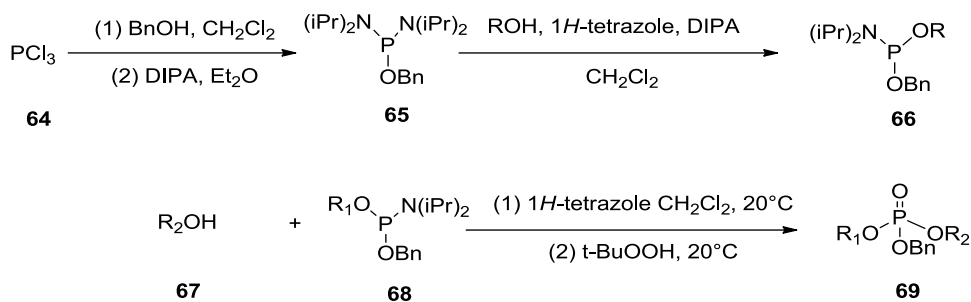
**Scheme 17. The first phosphoramidite approach to access oligonucleotide**

In 1985, Beaucage and Caruthers<sup>[265]</sup> established a method based on a reactive, though more stable phosphoramidite approach for oligonucleotide synthesis. For example, phosphoramidite **58** was used for the synthesis of oligonucleotide **60**. This methodology has been widely used in recent decades, with some modifications such as a preference for diisopropylamine<sup>[266]</sup> instead of dimethylamine (**Scheme 18**).



**Scheme 18. Phosphoramidite approach for synthesis of oligonucleotides**

There are also different methods to obtain the phosphoramidite function from phosphorus trichloride and different alcohols. For example, it was used to synthesize agrocinopine A,<sup>[239]</sup> as described in the previous section. The arabinose H-phosphoric triethylamine ammonium salt was prepared by using phosphorus trichloride in the presence of imidazole and triethylamine. Nowadays, the phosphoramidite approach has been considered as a general method for phosphorylation of various biomolecules such as oligonucleotides, and for *O*-phosphorylation of amino-acids, and etc. For instance, the benzyl diisopropylphosphoramidite **65** can be prepared from phosphorus trichloride and benzyl alcohol in the presence of base, and be used for mono or di-*O* phosphorylation of alcohols. The reaction is catalyzed by 1*H*-tetrazole, and the selectivity towards mono- or di- substituted products depends on the amount of catalyst. When mono-substitution of diisopropylphosphoramidite is targeted, particularly with primary alcohols, a tetrazolide diisopropylammonium salt can give better result.<sup>[251]</sup> Whereas the di-substitution of diisopropylphosphoramidate with any alcohols, at least two equivalent of tetrazole are required (**Scheme 19**).<sup>[267]</sup>



**Scheme 19. Tetrazole catalyzed mono- and di substitution of phosphoramidite**

### 3.3.4 Agrocinopine C and D

Agrocinopine C was originally identified as an anionic trisaccharide compound by P. J. Murphy et al<sup>[233]</sup> from agropine tumors, and induced by the agropine strains Bo542 and its transconjugant strain A281. They also confirmed that the presence of agrocinopine C made the agropine strain A281 sensitive to agrocin 84.<sup>[233]</sup> Agrocinopine D which was on loss of fructose from the sucrose moiety, was obtained during the purification of agrocinopine C.

#### 3.3.4.1 Structure and synthesis

The first structural proposal of agrocinopine C was D-glucos-2-yl sucros-6-yl phosphate. It was prepared via the hydrogen-phosphonate approach of the D-glucose-2-yl phosphodiester and the sucrose-6-yl derivative to phosphodiesters.<sup>[268]</sup> Agrocinopine D is related to agrocinopine C by the lack of the fructofuranosyl part of the sucrose moiety<sup>[262]</sup>. However, it was found that the NMR of this synthetic agrocinopine C **95** was not identical to the one obtained from the native material. Interestingly, the synthetic sucrose-6-yl agrocinopine C **95** exhibited the similar biological activity in its effect of agrocin 84 uptake, but was clearly distinguishable in their degradative behavior. After that, a correction in the agrocinopine C structure was proposed on the basis of the work by A. E. Savage<sup>[269]</sup> at the University of Adelaide, which confirmed that the phosphate diester linkage was actually located in the position C-2 of the sucrose moiety (**Fig 11**).<sup>[268]</sup> Up to now, only S. Oscarson et al<sup>[262]</sup> reported the synthesis of agrocinopine C and D. In this report, two building blocks were used as basic fragments for phosphorylation and condensation. The strategy is shown in **Scheme 20**.

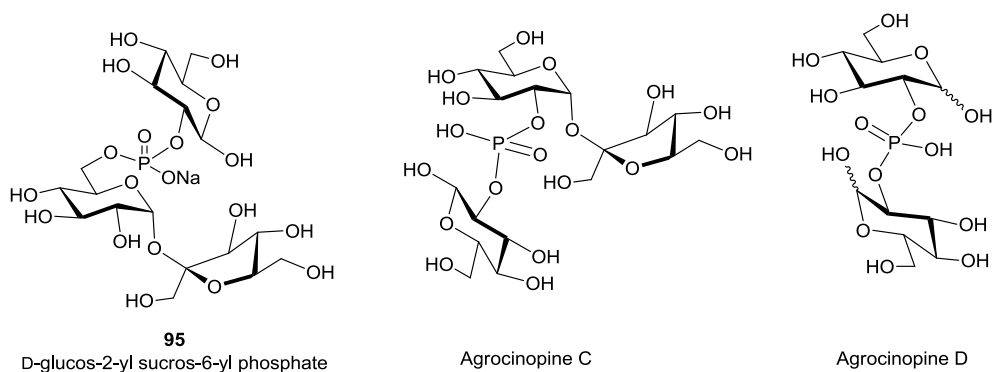
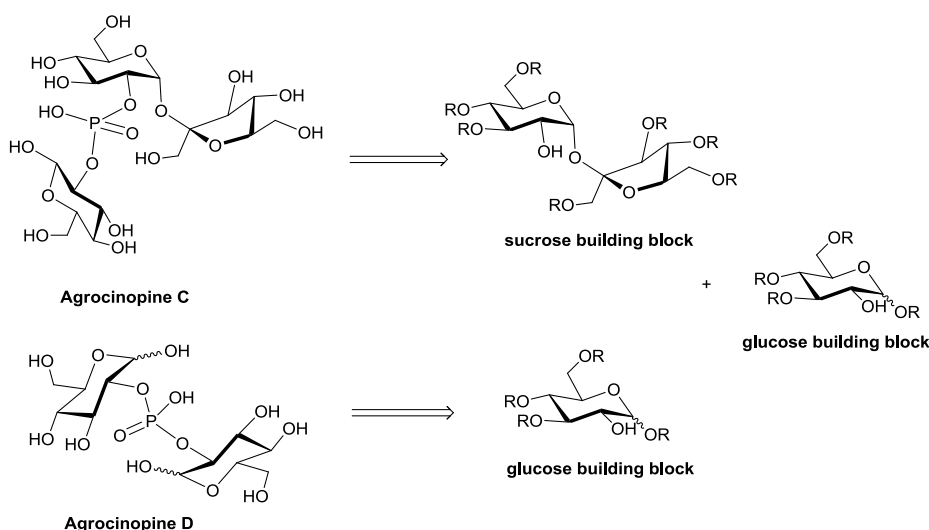


**Fig 11. The first proposed structure of agrocinopine C and the revised structure of agrocinopine C and D**

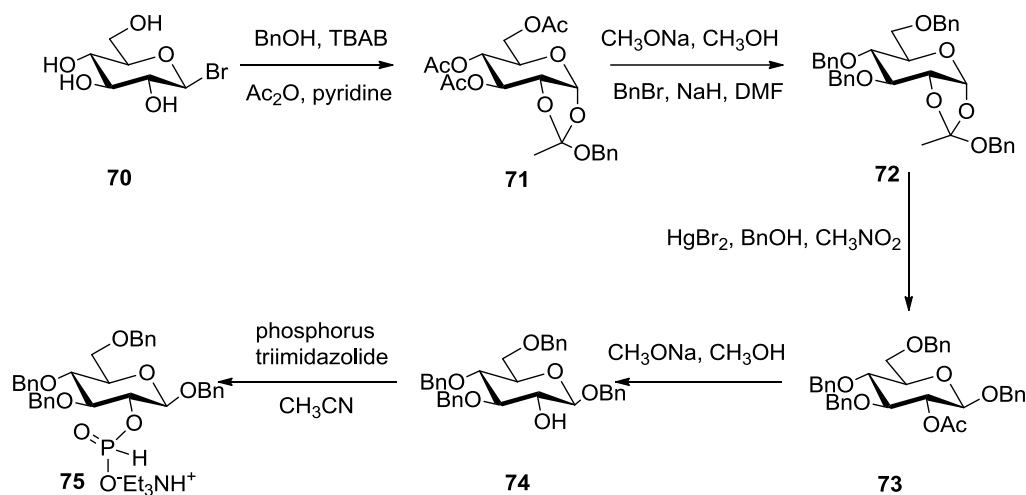


**Scheme 20. General strategy for synthesis of agrocinopine C and D**

### 3.3.4.1.1 Glucose building block

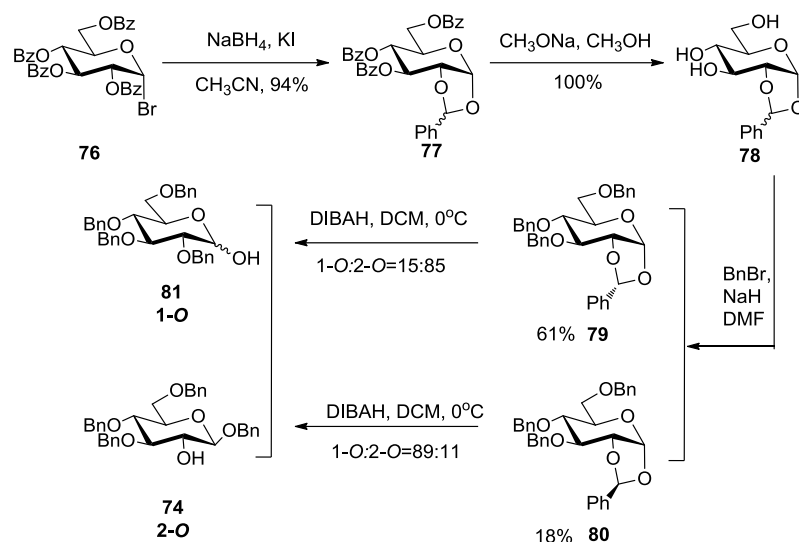
In 1992, S. Oscarson et al<sup>[262]</sup> first synthesized agrocinopine C, and benzyl 3,4,6-tri-*O*-benzyl- $\beta$ -D-glucopyranoside **74** was prepared for the glucose building block. This compound was synthesized in five steps from tetra-*O*-acetyl- $\alpha$ -D-glucopyranosyl bromide.<sup>[270]</sup> The glucosyl bromide **70** was treated with benzyl alcohol and tetra-*n*-butylammonium bromide<sup>[271]</sup> in collidine, followed by the peracetylation to give the exo-isomer of **71** in 66% yield. Deacetylation with methanolic sodium methoxide and subsequent benzylation using benzyl bromide in DMF in the presence of sodium hydride gave compound **72** in 83% yield. Mercury(II) bromide-catalyzed rearrangement<sup>[272]</sup> of compound **72** with benzyl alcohol in refluxing

nitromethane gave compound **73** in 87% yield, which was then deacylated to give compound **74** in 92% yield. Treatment of this alcohol with phosphorus triimidazolide in acetonitrile and water gave benzyl 3,4,6-tri-*O*-benzyl- $\beta$ -D-glucopyranosid-2-yl phosphate **75** in 89% yield (**Scheme 21**).



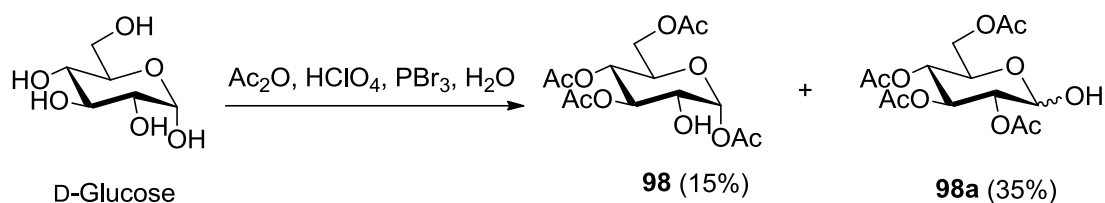
**Scheme 21. Synthesis of benzyl 3,4,6-tri-*O*-benzyl- $\beta$ -D-glucopyranoside phosphate**

There are alternative strategies to obtain protected glucose bearing a free OH-2. A reductive ring opening reaction of 1,2-*O*-benzylidene by using diisobutyl aluminum hydride can be employed.<sup>[273]</sup> For example, compound **81** was prepared from 2-*O*-benzoyl-glucopyranosyl bromide **76** in four steps via 1,2-benzylidenation, debenzoylation, benzylation, and ring opening reaction. The 1-*O*-Bn sugar **81** or 2-*O*-Bn-sugar **74** were obtained in different ratio and yields by treating intermediates exo- or endo- isomers **79**, **80** in the presence of DIBAH (**Scheme 22**).<sup>[273]</sup>



Scheme 22. Synthesis of 1-*O*-Bn sugars or 2-*O*-Bn-sugars

In 1992, S. Oscarson et al<sup>[262]</sup> firstly synthesized agropinopine D, acetyl 3,4,6-tri-*O*-acetyl- $\beta$ -D-glucopyranoside **98** was prepared for the glucose building block. This compound was synthesized in a “one-pot” reaction from D-glucose, reported by J. Zirner<sup>[274]</sup> in 1962, via the peracetylation using acetic anhydride, followed by treatment of the intermediate with HClO<sub>4</sub>, PBr<sub>3</sub> and water, leading to a mixture of 2-*O*- and 1-*O*- deacetylation compounds **98** and **98a**. The desired acetyl 3,4,6-tri-*O*-acetyl- $\beta$ -D-glucopyranoside **98** was obtained in only 15% yield after recrystallization (Scheme 23).

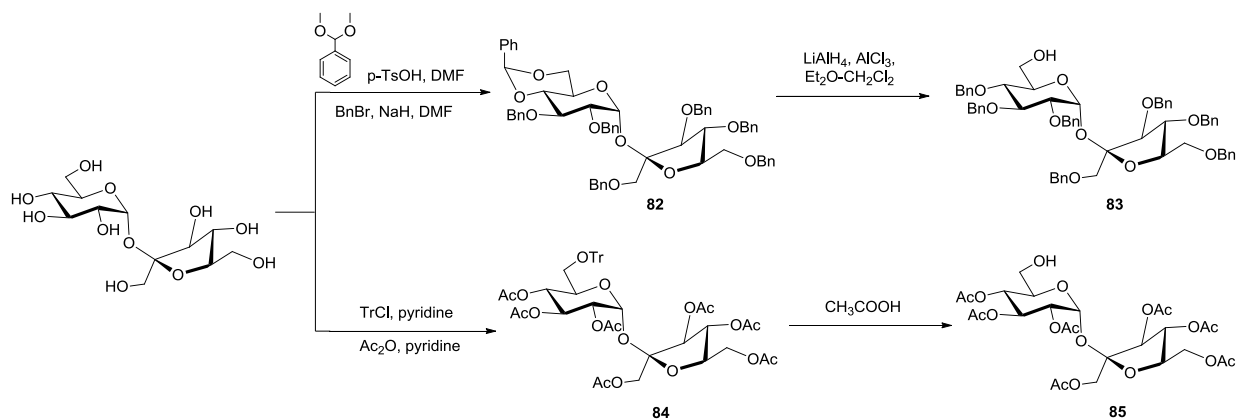


Scheme 23. Synthesis of compound **98**

### 3.3.4.1.2 Sucrose building block

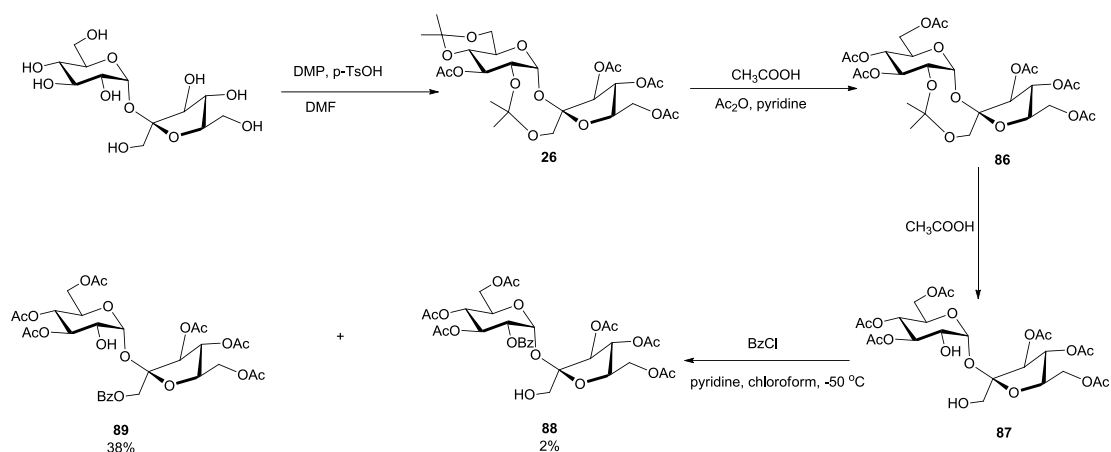
For sucrose part, S. Oscarson et al<sup>[268]</sup> prepared two sucrose derivatives **83** and **85** bearing a free OH-6 because they were bridged a 6-yl sucrose bond phosphodiester. The benzyl protected derivative **83** was prepared from sucrose in three steps via benzylidene 4,6-diol protection and benzylation, followed by reductive opening of the dioxane ring using lithium aluminum

hydride/aluminum chloride in diethyl ether-dichloromethane or borane trimethylamine/aluminum chloride in toluene. The acetyl protected sucrose derivative **85** was obtained through a tritylation-acetylation-detritylation procedure (**Scheme 24**).<sup>[275]</sup>



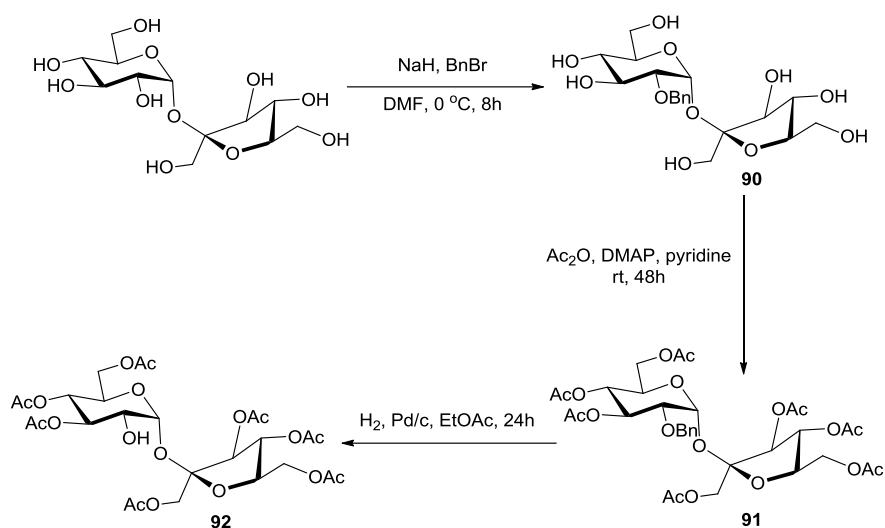
**Scheme 24.** Synthesis of the first proposed sucrose fragment of agrocinopine C

In 1993, S. Oscarson et al.<sup>[262]</sup> synthesized the revised agrocinopine C, namely D-glucos-2-yl sucros-2-yl phosphate, via the hydrogen-phosphonate approach to phosphodiesters. The benzoyl and hepta-acetyl protected sucrose derivative **89** was prepared based on the protocol of R. Khan et al.<sup>[276]</sup> Firstly, 1',2,4,6-di-*O*-isopropylidene-sucrose tetra-acetate **26** was prepared from sucrose by employing 2,2-dimethoxypropane in the presence of *p*-TsOH in DMF followed by acetylation using acetic anhydride in pyridine.<sup>[247]</sup> Cleavage of 4,6-isopropylidene **26** in aqueous acetic acid and then acetylation gave the desired acetal hydrolysis product 3,4,6,3',4',6'-hexa-*O*-acetyl-1',2-*O*-isopropylidene sucrose **86** (23% yield) with together the other possible acetal hydrolysis product (4.7% yield) and a significant amount of peracetylated sucrose (28% yield). After the de-acetylation of compound **86**, the 1',2-*O*-isopropylidene group was removed under the same acidic condition to afford 3,4,6,3',4',6'-hexa-*O*-acetyl sucrose **87**<sup>[277]</sup> which has a primary and secondary hydroxyl group available for the subsequent selective benzylation. Treatment of compound **87** with benzoyl chloride in a mixture of pyridine and chloroform at -50 °C gave a mixture of products that were separated by column chromatography on silica gel.<sup>[276]</sup> The desired benzylation product on the primary alcohol **89** was collected as the major product (**Scheme 25**).



**Scheme 25. Synthesis of 3,4,6,3',4',6'-hexa-*O*-acetyl 1'-*O*-benzoylsucrose 87**

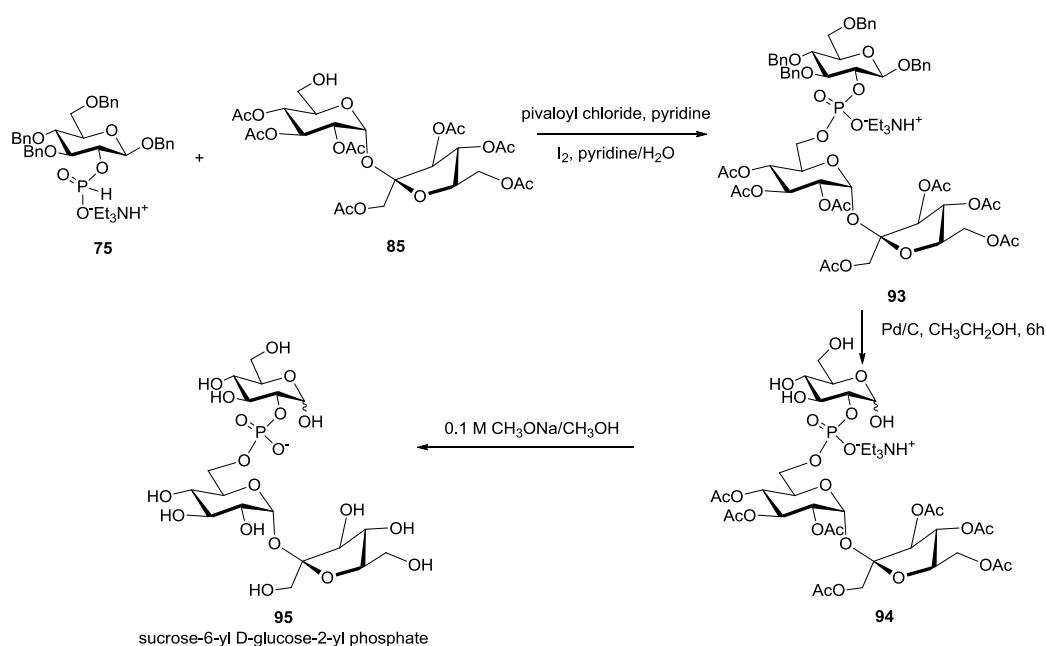
Since then, an alternative access to hepta-acetyl sucrose with free OH-2 has been reported.<sup>[278]</sup> This method was first published by F. W. Lichtenthaler et al<sup>[279]</sup> for the synthesis of 2-deoxy and 2-keto-sucrose derivatives from 2-*O*-benzylated sucrose. 2-*O*-Benzylation compound **90** was obtained by using 0.9 equivalents of NaH in DMF, with benzyl bromide. An 11:2:1 mixture of 2-*O*, 1'-*O* and 3'-*O* benzylated sucrose was obtained, which was then peracetylated. Removal of the benzyl ether of compound **91** by hydrogenolysis led to the desired product 3,4,6,1',3',4',6'-hepta-*O*-acetylsucrose **92**, which was further purified by recrystallization from 2-propanol or hot EtOAc in hexane in 42% yield over the three steps (**Scheme 26**).



**Scheme 26. Synthesis of 3,4,6,1',3',4',6'-hepta-*O*-acetylsucrose 90**

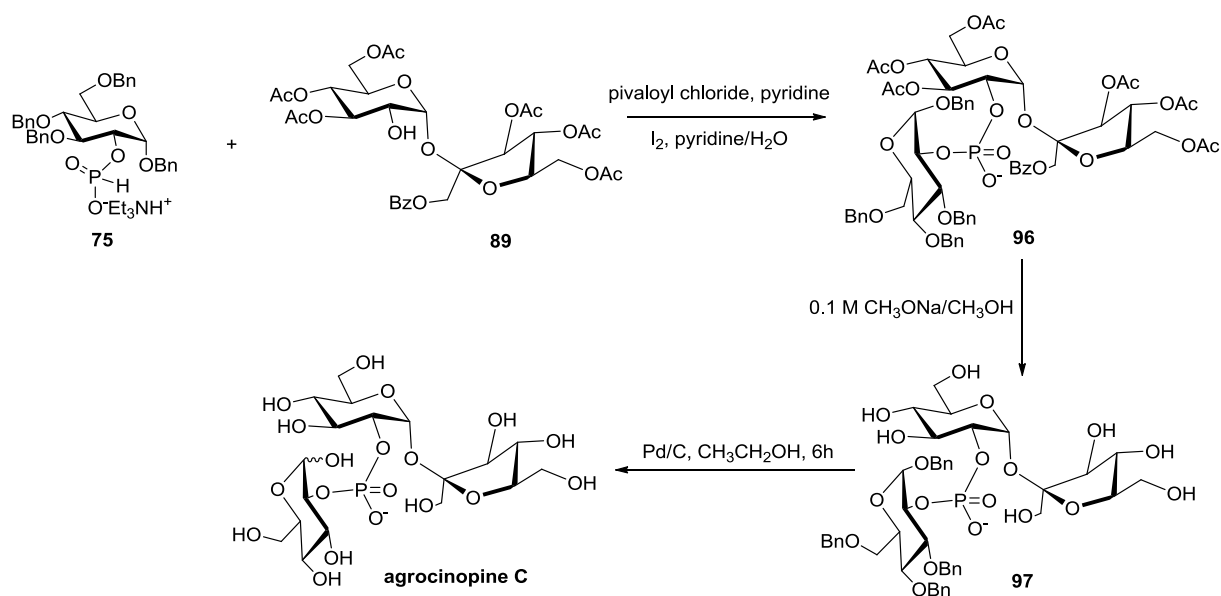
### 3.3.4.1.3 Phosphorylation and condensation towards agrocinopine C and D

Targeting the wrong 6-yl agrocinopine C **95**, S. Oscarson et al<sup>[268]</sup> conducted the condensation of the glucose and sucrose synthons in the presence of pivaloyl chloride in pyridine, followed by treatment with iodine in pyridine-water. Debenzylation of compound **93** was achieved by hydrogenolysis in ethanol using Pd/C to give compound **94**. Subsequent deacetylation with methanolic sodium methoxide gave, after anion exchange chromatography on DEAE-Sephadex and gel filtration, sucrose-6-yl D-glucose-2-yl phosphate **95** in 41% yield as an anomeric mixture (Scheme 27).



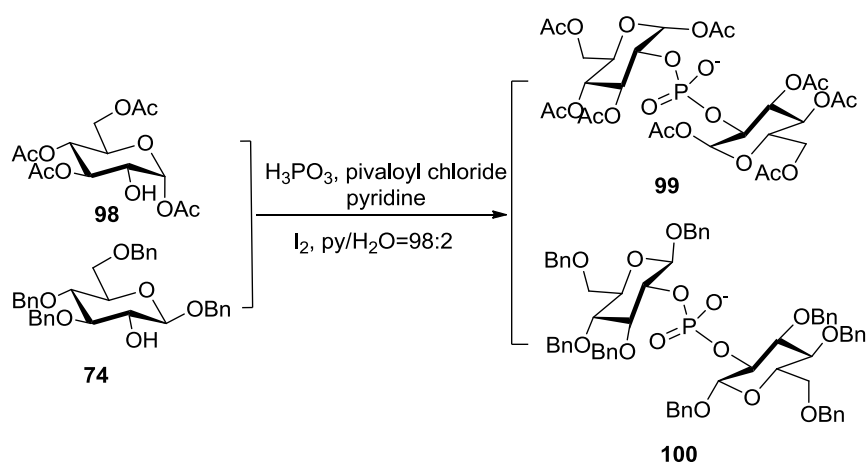
Scheme 27. Synthesis of sucrose-6-yl D-glucose-2-yl phosphate

For their synthesis of the right 2-yl agrocinopine C in 1993, S. Oscarson et al<sup>[262]</sup> condensed the compound **75** and sucrose derivative **89** in pyridine, by using also pivaloyl chloride as activating agent followed by oxidation in situ. Agrocinopine C was then obtained in two steps via Zemplen deacetylation, hydrogenolysis and purified on a Bio-Gel P-2 column in 61% yield over three steps (Scheme 28).



**Scheme 28.** Synthesis of agrocinopine C reported by S. Oscarson

Based on the study on the phosphorylation of nucleoside, S. Oscarson et al.<sup>[262]</sup> synthesized the protected agrocinopine D in two ways. Treatment of compound **74** or **98** with 0.5 molar equivalents of phosphonic acid and 1.5 molar equivalents of pivaloyl chloride in dry pyridine followed by in situ oxidation in the presence of iodine in pyridine-water 98:2 yielded compound **100** and **99** in 82% and 63%, respectively. After hydrogenolysis of compound **100**, agrocinopine D was obtained as a sodium salt in 89% yield, and after deacetylation of compound **99**, agrocinopine D was obtained with some possible bis(glucose-1)-phosphate by-product. Both deprotection methods gave agrocinopine D as an anomeric mixture (**Scheme 29**).



**Scheme 29.** Synthesis precursors of agrocinopine D

### 3.3.5 Biological aspects of agrocinopines

In 1990, the region of pTiC58 encoding catabolism of agrocinopine A+B has been cloned and sequenced by Hayman and Farrand<sup>[218]</sup>. The gene system is composed of eight open reading frames, which are entirely sufficient to confer the ability to take up and utilize the opine as sole carbon source (**Fig 12**).<sup>[218]</sup> The AccR encodes a repressor protein regulating expression of the acc operon. The accABCDE encode an ABC-type, ATP-driven and periplasmic binding protein-dependent transport system. Among of these systems, AccA is related to periplasmic substrate binding proteins of other ABC-type transports, is located in the periplasm, and identical to the agrocin 84 binding protein.<sup>[280]</sup> Overall, the five components of this transport system are most closely related to those of the dipeptide and oligopeptide transport system of *E. coli* and *S. typhimurium*.<sup>[217]</sup> AccF and AccG probably encode the enzymes involved in catabolizing the opines. AccF is a phosphodiesterase that cleaves the opines into their respective sugar subunits, which was confirmed by that the mutations in AccF abolish the ability of the bacteria to grow with agrocinopine A+B as sole source of carbon.<sup>[217]</sup> Moreover, AccF is not required for transport of antibiotic or the opine. AccG could encode a product that is related to myoinositol monophosphatases of eukaryotic origin at the amino acid sequence level.<sup>[217]</sup> The gene is required for the utilization of agrocinopine A+B as sole carbon source, but not necessary for transport of the opine or for susceptibility to agrocin 84.

Presumably, the activity encoded by AccG could be involved in dephosphorylating the sugar phosphate produced from agrocinopine A+B by the action of AccF. But it has been clear recently that the substrate is arabinose-2-phosphate, not sucrose (fructose-4)-phosphate. The observation that cells become super-sensitive to the antibiotic in the presence of agrocinopines suggested that expression of the acc operon is inducible by opines. As described above, primary regulation of the acc gene is mediated by AccR, a transcriptional repressor is related to classic repressors of other sugar catabolism systems including Fucr, DeoR and LacR (**Fig 12**).<sup>[183]</sup>

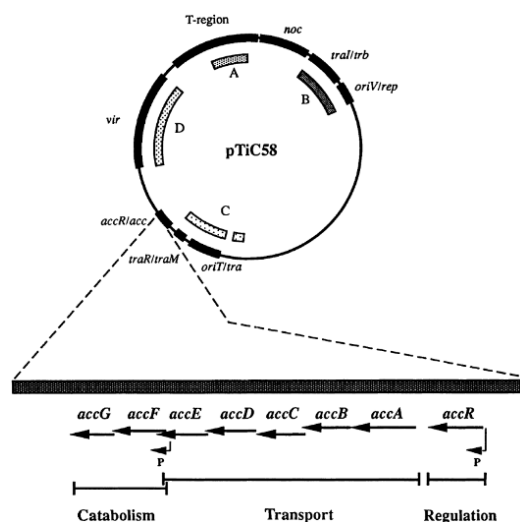


**Fig 12. The agrocinopine catabolic (*acc*) operon.**

The *acc* region has been magnified to show the regulatory gene *accR*, the genes involved in agrocinopine uptake and those involved in degradation of this opine.

Up to now, very limited information is known concerning the gene systems involved in uptake and catabolism of agrocinopine C+D. In 1990, Hayman et al<sup>[234]</sup> found that there are two agrocinopine transport systems, A/B and C/D, distinguished by their ability to selectively transport agrocin 84 when the sugar moiety in N6 substituent is in the appropriate furanosyl or pyranosyl ring form. There was no detectable homology between the agrocinopine A+B catabolism genes of pTiC58 and agrocinopine C+D catabolism genes of pTiBo542, the latter could encode sensitivity to agrocin 84 in the presence of agrocinopines C and D. Given this difference in substrates, it is possible that the *acc* sites of pTiBo542 arose independently from the agrocinopine A and B catabolic genes, which is strengthened by two points: one is that strains harboring pTiBo542 do not take up agrocinopines A and B, and no hybridization was detected between this Ti plasmid and the pTiC58 *acc* probe at the stringency tested; another is that these two agrocinopine-type opine families are different in the gene involved utilization. Moreover, it has been found that the pTiBo542 *acc* transport system does not recognize agrocinopines A and B, it apparently does transport agrocin 84. This might indicate that the agrocinopine A/B and C/D transport systems recognize different portions of the antibiotic molecule.<sup>[234]</sup> Surprisingly, the *Lippia*-type Ti plasmid harboring the agrocinopine C+D

catabolic sites and the pTiC58 harboring the agrocinopine A+B catabolic genes behave similarly. Both are sensitive to agrocin 84 even without the opines, the agrocinopine C+D could induce the sensitivity.<sup>[235]</sup>

In a word, agrocinopine A and B promote the transfer of nopaline plasmids whereas nopaline does not exhibit such ability. And agrocinopine C and D also promote the transfer of agropine plasmids while agropine which is a major opine product of agropine type tumors does not.<sup>[281]</sup> Nor does agropine promote transfer of octopine plasmids.<sup>[225]</sup> The agrocinopine opines and the corresponding opine-mediated conjugal regulatory regions of pTiChry5 and pTiC58 which are two Ti plasmids inducible for transfer by agrocinopine A/B and C/D,<sup>[282]</sup> share a common origin, but that the opine signals for the two Ti plasmids have evolved divergently through changes in the opine synthase enzymes. The alterations in the opines, in turn, necessitated a co-evolutionary change in the opine recognition systems that are responsible for controlling expression of the traR genes on these two types of Ti plasmids.<sup>[282]</sup>

### 3.3.6 Other carbohydrate phosphodiester and phosphates

Carbohydrate products are the most abundant natural compounds existing in the world, especially carbohydrate phosphates and phosphodiester. The carbohydrate phosphates as a new type of opine has been attracted more attention for further investigation. However, to the best of our knowledge, as the major fragments in four agrocinopines, carbohydrate-2-phosphate makes only a smaller parts of carbohydrate phosphates and has not been well studied. The earliest discovered carbohydrate phosphates are carbohydrate-1-phosphates and carbohydrate-6-phosphates which involve pentose phosphate pathway responsible for glycolysis.

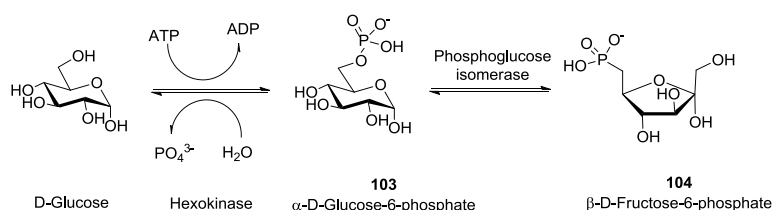
Glucose-1-phosphate is a glucose molecule with a phosphate group on the 1'-carbon. It can exist in either the  $\alpha$ - or  $\beta$ -anomeric form (**Fig 13**).  $\alpha$ -form involves catabolic and anabolic, it's the direct product of the reaction in which glycogen phosphorylase cleaves off a molecule of glucose from a greater glycogen structure. To be utilized in cellular catabolism it must first be converted to glucose 6-phosphate by the enzyme phosphoglucomutase. One reason that cells form glucose 1-phosphate instead of glucose during glycogen breakdown is that the very polar phosphorylated glucose cannot leave the cell membrane and so is marked

for intracellular catabolism. For the anabolic function, in glycogenesis, free glucose 1-phosphate can also react with UTP to form UDP-glucose, by using the enzyme UDP-glucose pyrophosphorylase. It can then return to the greater glycogen structure via glycogen synthase. In terms of  $\beta$ -anomeric form, it is found in some microbes and produced by inverting  $\alpha$ -glucan phosphorylases including maltose phosphorylase, kojibiose phosphorylase and trehalose phosphorylase and is then converted into glucose-6-phosphate by  $\beta$ -phosphoglucomutase.



**Fig 13.  $\alpha$ - and  $\beta$ -anomeric form of glucose-1-phosphate**

Glucose-6-phosphate is a glucose sugar phosphorylated on carbon 6 which exists very common in cells as the vast majority of glucose entering a cell become phosphorylated in this way. It involves two major metabolic pathways including glycolysis and pentose phosphate pathway, as well as the conversion to glycogen or starch for storage in the liver and muscles for most multicellular animals and other organisms. The production of glucose-6-phosphate is accomplished by the phosphorylation of glucose on the sixth carbon via the enzyme hexokinase in cells and animals, the process consumes one molecule ATP. The pentose phosphate pathway was initiated when the ratio of  $\text{NADP}^+/\text{NADPH}$  increase, the body realizes it needs to produce more NADPH, which result in the G6P to be dehydrogenated by G6P dehydrogenase. This irreversible step could generate the useful cofactor NADPH and ribulose-5-phosphate which acts as a carbon source for the synthesis of other molecules. For the glycolysis metabolic pathway, G6P is firstly isomerized to fructose-6-phosphate by phosphor-glucose isomerase when the cells need energy or carbon skeletons for synthesis (**Scheme 30**).



### Scheme 30. The production and transformation of glucose-6-phosphate

Apart from agrocinopines, G1P and G6P, there are also some other carbohydrate phosphate and phosphodiester such as glucose-2-phosphate (G2P), arabinose-2-phosphate (A2P), sucrose-2-phosphate, galactose-1-phosphate, fructose-6-phosphate, sucrose-6-phosphate, adenosine monophosphate, uridine monophosphate, and other nucleoside phosphates. Most of them are responsible for metabolism and nutriment of plant or animals (**Fig 14**). Thus, in the next chapter, some carbohydrate-2-phosphate including G2P, A2P and their derivatives will be discussed in aspects of both synthetic chemistry and biological properties.

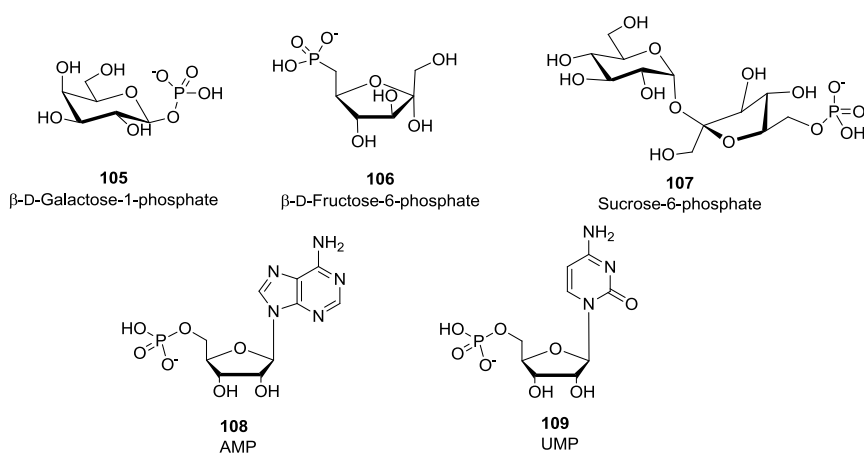


**Fig 14. Other carbohydrate phosphate and phosphodiester**

### 3.4 Conclusion

In this bibliographic chapter, we described the function and regulation of QS in *agrobacterium tumefaciens*, and focused specifically on the important molecules, agrocinopines and the first reported phosphorylated opines.

To date, four agrocinopines have been reported. Agrocinopine A/B which belongs to the nopaline plasmid class induce the transfer of the nopaline-type Ti plasmids, whereas agrocinopine C/D which belongs to agrocine plasmid class induce chrysoptine-type Ti plasmid.<sup>[282]</sup> With respect to their chemical synthesis, only two teams have contributed: J. Thiem,<sup>[238]</sup> T. Norberg and S. Oscarson.<sup>[239,262]</sup> They prepared four agrocinopines by the condensation of arabinose, glucose or fructose building blocks and sucrose building blocks in various manners. Those reported syntheses have inspired us in the work which is reported in

the next section for the synthesis of agrocinopine A, C, D and some other analogues such as glucose-2-phosphate, arabinose-2-phosphate and their derivatives.



## **Chapter IV. Results and Discussion**



# Synthesis of agrocinopine and carbohydrate phosphates and investigation of their binding properties with AccA and their subsequent biological role in *Agrobacterium tumefaciens*

## 4.1 Introduction

In bacteria, periplasmic binding proteins (PBPs) are involved in the import of a wide variety of extracellular compounds and are also potential vehicles that facilitate the penetration of antibiotics.<sup>[283]</sup> In *A. tumefaciens*, the PBP protein AccA is known to bind agrocinopine A, however, the clear role of agrocinopine A in QS regulation is not completely understood. Moreover, AccA also binds the antibiotic agrocin 84, despite of showing a rather different structure. To the best of our knowledge, there are no reports concerning the precise binding mode of agrocinopine A to the PBP AccA, neither of agrocin 84.

In this second part of the thesis, we focus on the investigation of the role of agrocinopine A in the process of QS regulation in *Agrobacterium tumefaciens*. For this aim, our initial study was to characterize the specificity of the interaction of the PBP AccA with agrocinopine, by using agrocinopine itself and some analogues as ligands, and to clarify the mechanism of agrocinopine structural dependent QS. This work was carried out in the frame of a collaboration with biologists at the Institute for Integrative Biology of the Cell (I2BC) in Gif sur Yvette, who established their binding mode to the protein AccA and other biological properties with respect to the acc operon. Our contribution has been to provide the expertise of a carbohydrate chemistry team in the design, synthesis and interpretation of molecular aspects of the carbohydrate-protein binding, which included the synthesis of agrocinopine A as well as the development of a general and facile strategy towards other carbohydrate phosphodiester and phosphates including agrocinopine C, agrocinopine D, arabinose-2-phosphate derivatives and glucose-2-phosphate derivatives. Thus, in the following parts, we will present successively the synthesis of agrocinopine A, arabinose-2-phosphate, glucose-2-phosphate, agrocinopine C, agrocinopine D and their derivatives (**Fig 15**). The biological properties are briefly discussed after each synthesis. The full details of the biological investigations are given in annex 1.

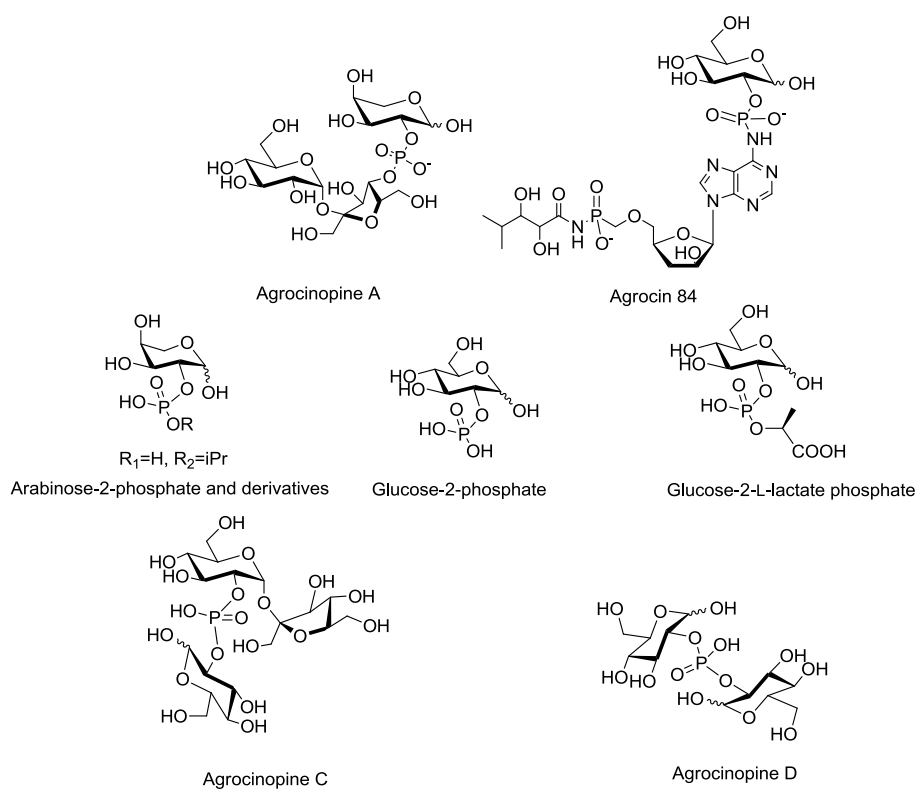
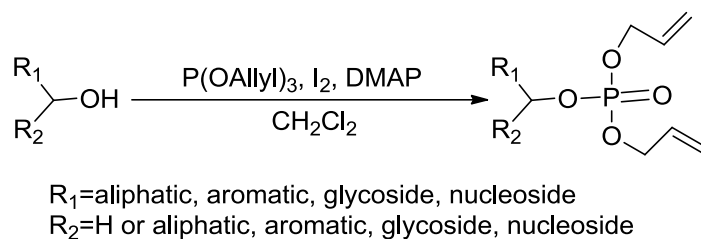


**Fig 15. Agrocinosin 84, agrocinosin A and its analogues synthesized in this part**

In addition, in parallel to the work on agrocinosins and derivatives synthesis, a facile and straightforward method towards phosphorylation of alcohols, phenols, carbohydrates and nucleosides using triallyl phosphite has been established (**Scheme 31**).

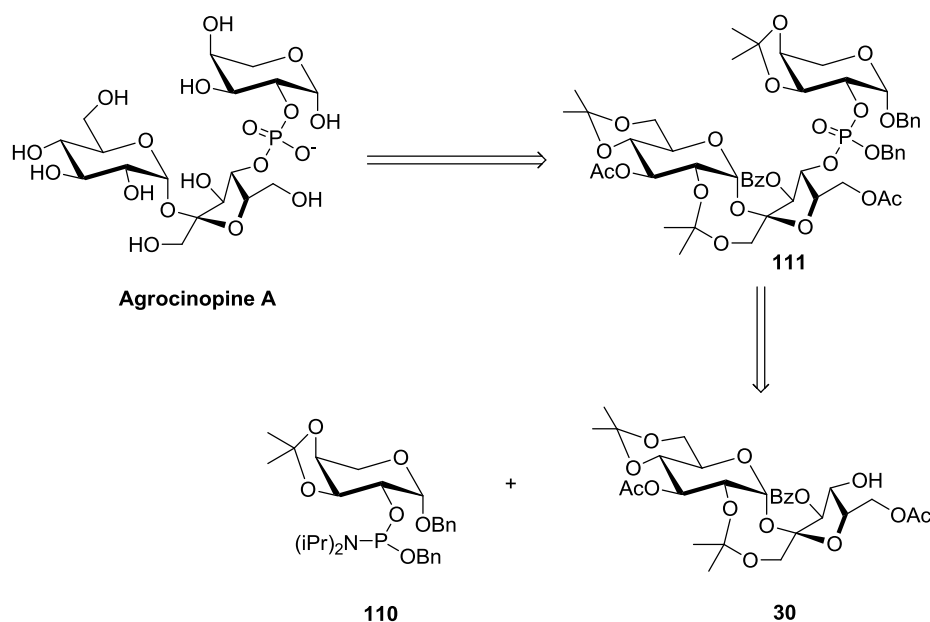


**Scheme 31. A convenient method for phosphorylation towards various alcohols**

## 4.2 Synthesis and binding properties of agrocinopine A

Two strategies for the synthesis of agrocinopine A have been reported in the literature.<sup>[238][284]</sup> (2,2,2-trichloroethyl) phosphorodichloridate and di-substituted phosphoramidite were employed as condensation reagents (bibliographic section). In order to develop an efficient and more general route towards synthesis of agrocinopine A and other phosphodiester derivatives, we proposed a widely used phosphoramidite, namely, benzyloxy-bis-diisopropyl amino phosphine. This phosphorylation reagent allows selective substitution of the diisopropylamide groups by different alkyl groups, making also possible for the synthesis of arabinose-2-phosphate, glucose-2-phosphate for example.

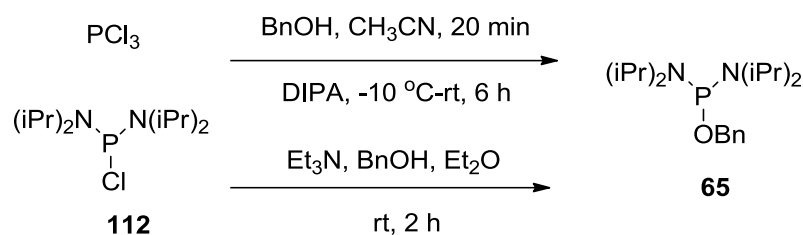
For the synthesis of agrocinopine A, the reported retrosynthetic analysis is shown in **Scheme 32**. Agrocinopine A would be obtained from a multiply protected precursor **111**, which is obtained in two steps by condensation of the sucrose building block **30** and arabinose phosphoramidite **110**. In this section, we describe the whole synthetic route towards agrocinopine A, with details on the preparation of the phosphoramidite, the arabinose fragment, the sucrose fragment, the condensation conditions and order of deprotection.



**Scheme 32. Retrosynthesis of agrocinopine A**

### 4.2.1 Preparation of the phosphoramidite

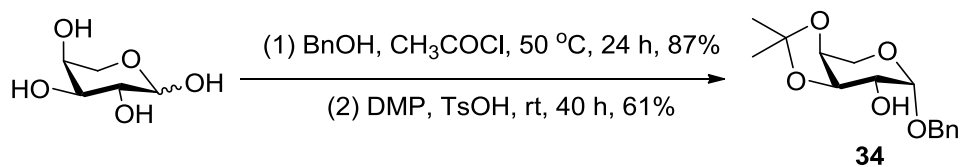
The phosphoramidite **65** was prepared in two steps by treatment of phosphorus trichloride, with benzyl alcohol and di-isopropylamine in anhydrous acetonitrile. Alternatively, compound **65** could also be prepared from the commercially available bis(*N,N*-diisopropylamino) chlorophosphine **112** by reaction with benzyl alcohol in presence of triethylamine and diethyl ether (**Scheme 33**).



**Scheme 33.** Two approaches for the preparation of phosphoramidites **65**

### 4.2.2 Synthesis of the arabinose fragment

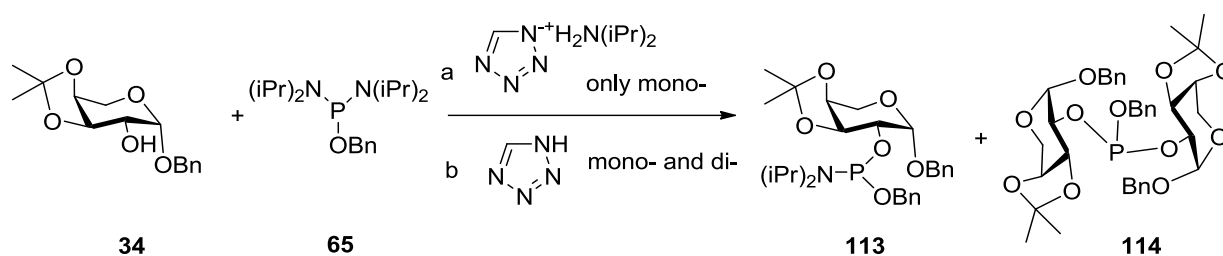
To prepare the arabinose fragment with a free OH-2, the direct and facile method is the protection of anomeric group as a benzyl arabinoside, and afterwards the protection of 3,4-diol with an acetal or benzylacetal. Thus, our target compound, namely 3,4-*O*-isopropylidene benzyl  $\beta$ -L-arabinose **34**, was obtained in two steps. The glycosylation was conducted in benzyl alcohol in the presence of acyl chloride, and then the resulted intermediate was treated with 2,2-dimethoxypropane (DMP) and TsOH in DMF to afford compound **34** in 53% yield over the two steps (**Scheme 34**).



**Scheme 34.** Synthesis of 3,4-*O*-isopropylidene benzyl  $\beta$ -L-arabinose **34**

Then, the arabinose phosphoramidite fragment was prepared by a mono-substitution of phosphoramidite **65** by arabinoside **34**. It involved a dropwise addition of a solution of diisopropylammonium tetrazolide salt in dichloromethane to a mixture of phosphoramidite and

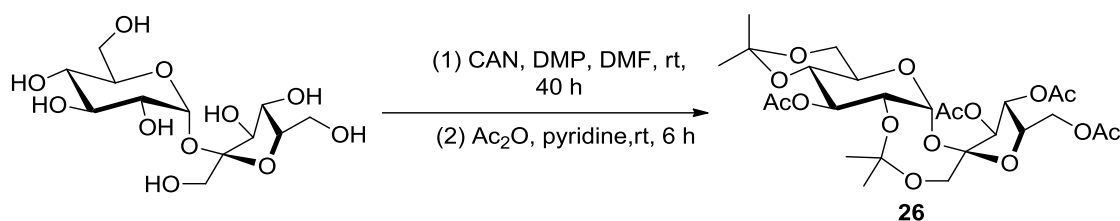
alcohol in dichloromethane or acetonitrile at 0 °C. The mono-substituted product **113** was obtained as a mixture of two diastereoisomers, and <sup>31</sup>P-NMR analysis showed that the ratio of two isomers was about 65/35. This method was proved to be more effective than that using tetrazole alone which led to a mixture of mono and di-substituted products **113** and **114** (Scheme 35).



Scheme 35. Synthesis of compound **113**

#### 4.2.3 Synthesis of the sucrose fragment

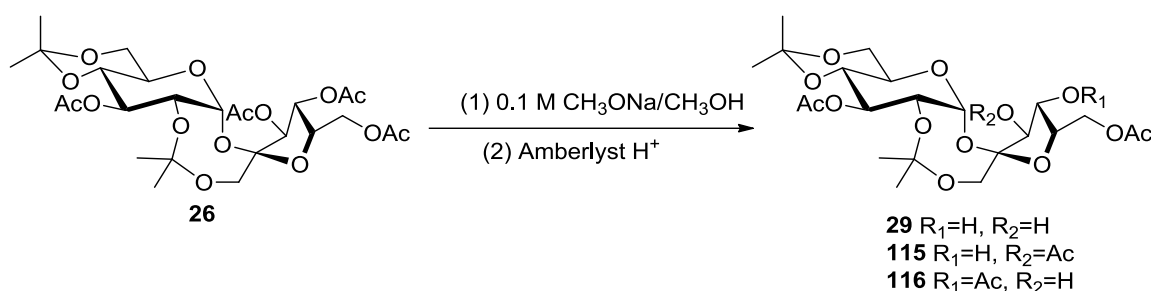
In the bibliographic part, several sucrose building blocks have been shown. Based on previously reported syntheses, we choose the 3,6'-di-*O*-acetyl-3'-benzoyl-2,1':4,6-di-*O*-isopropylidene sucrose **30** which are available from sucrose in three steps. The first step was the synthesis of compound **26**, for which we referred the CAN catalyzed strategy.<sup>[249]</sup> The product **26** was isolated in 42% yield (Scheme 36).



Scheme 36. Synthesis of compound **26** using CAN

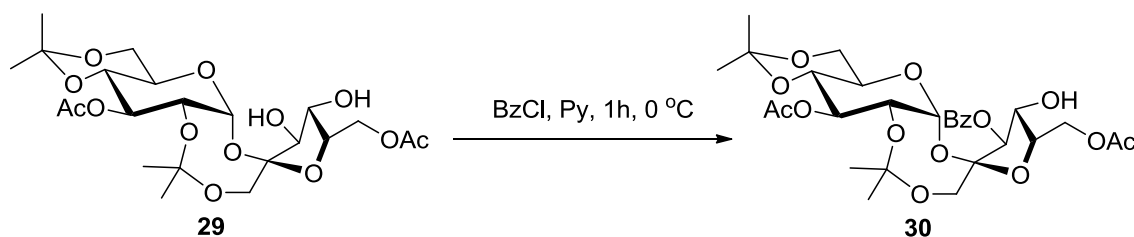
Then, compound **26** was treated with a catalytic amount (0.01 to 0.02 equivalent) of sodium methoxide in methanol. The reaction was carried out at 0 °C in a large scale, and the hydrolysis process took almost 2 h which was followed by TLC until starting material was consumed and appearance of partially deacetylated product. The mixture was then treated with amberlyst H<sup>+</sup>, and the diacetate **29** was obtained in a 50% yield. An early fraction containing **26** and the

triacetates **115** and **116**, was subsequently isolated. The  $^1\text{H-NMR}$  spectra confirmed the structures assigned<sup>[244]</sup> to **115** and **116** in the mixture. Compound **115**, which showed low-field signals at  $\delta$  5.62 (t,  $J_{3,4} = 9.5$  Hz) and 5.45 (dd,  $J_{3',4'} = 7.0$ ,  $J_{4',5'} = 5.5$  Hz), was the 3,4',6'-triacetate, and compound **116**, which showed low-field signals at  $\delta$  5.23 (t,  $J_{3,4} = 9.2$  Hz) and 4.86 (d,  $J_{3',4'} = 6.8$  Hz), was the 3,3',6'-triacetate (**Scheme 37**).



**Scheme 37. Selective deacetylation of compound 26**

The mono-benzoylation of compound **29** was carried out under the same conditions as described in the literature. Treatment of compound **29** with benzoyl chloride in pyridine at  $0^\circ\text{C}$  gave the mono-benzoylation product in 71% yield.  $^1\text{H-NMR}$  was consistent with the previously reported data.<sup>[244]</sup> We hypothesized that there was a fast migration (trans-esterification) of benzoyl from position 4' to 3' since the 4'-benzoyl substituted sucrose derivative was thermodynamic stable product. The structure was confirmed by the following characteristic signals: anomeric proton ( $\delta$  6.16, d), H-3 ( $\delta$  5.41, t,  $J_{3,4} = 9.6$  Hz), and H-3' ( $\delta$  4.89, d,  $J_{3',4'} = 6.2$  Hz) (**Scheme 38**).

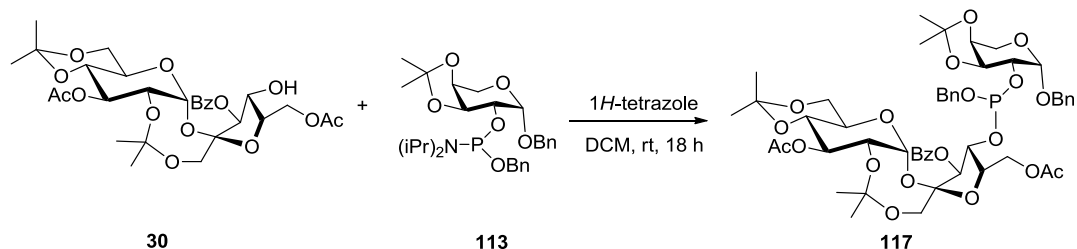


**Scheme 38. Mono-benzoylation of compound 29**

#### 4.2.4 Condensation and deprotection

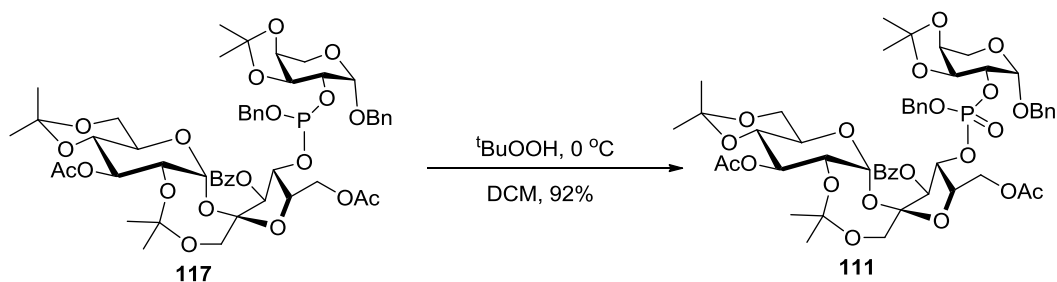
The phosphite **117** was obtained by condensation of sucrose derivative **30** and phosphoramidite **113**. In this step, tetrazole was used as a coupling catalyst, and anhydrous

condition was necessary, which was achieved by co-evaporation of starting material with acetonitrile. The phosphite **117** was obtained as a mixture of diastereoisomers (65/35) in 60% yield (**Scheme 39**).



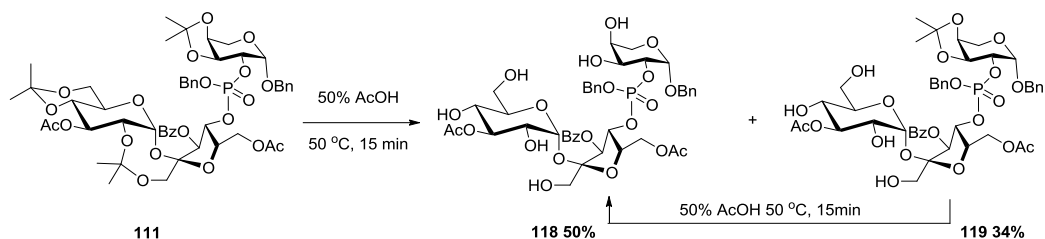
**Scheme 39. Coupling of compound 30 and compound 113**

The oxidation of phosphorus (III) to phosphorus (V) was conducted using tert-butylhydroperoxide instead of *m*-CPBA, as the latter resulted in the cleavage of the sugar moiety in dichloromethane at 0 °C. The oxidation was very effective, and afforded the expected phosphate **111** in 90% yield (**Scheme 40**).



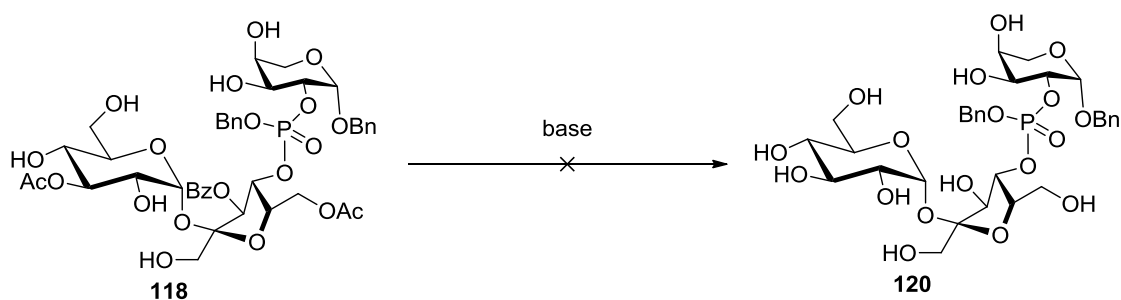
**Scheme 40. Oxidation of compound 117**

An important issue is how to choose the sequence for these deprotection steps, which should remove acetals, esters and benzyl ethers. After having tried various strategies, we confirmed the same better order as reported by Lindberg.<sup>[239]</sup> For isopropylidene removal, treatment of compound **111** with 50% acetic acid in water led to a mixture of compounds **118** and **119**. The structure of the two compounds were confirmed by <sup>1</sup>H-NMR and mass spectrometry. And prolongation of the reaction time was favorable for the transformation of compound **119** to **118** (**Scheme 41**).



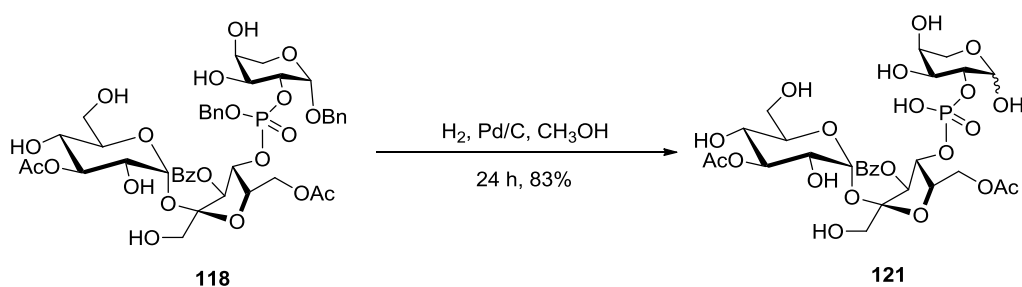
**Scheme 41. Removal of acetals**

Our first attempts of de-acetylation indicated that benzyl-phosphate **120** was not stable in basic medium at this stage. Indeed, treatment of compound **118** in the presence of a base ( $\text{CH}_3\text{ONa}$ , KCN or  $\text{K}_2\text{CO}_3$ ) in methanol mainly led to monosaccharide phosphate or disaccharide phosphate (cleavage of the phosphate sugar esters). Considering these disappointing results, the de-benzylation step had to be performed first (**Scheme 42**).



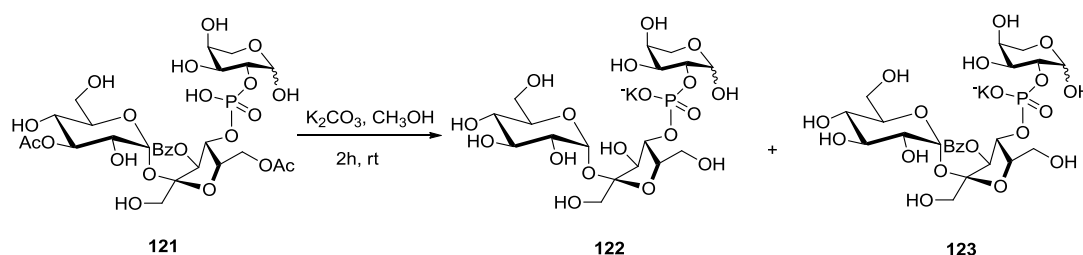
**Scheme 42. Failed ester hydrolysis of compound 118**

The de-benzylation step involved the treatment of compound **118** by hydrogen in the presence of Pd/C in methanol. The hydrogenolysis gave the phosphate **121** in 83% yield without side-products (**Scheme 43**). Identification of this compound was established by  $^1\text{H-NMR}$  and mass spectrometry, which indicated the presence of two isomers (anomeric mixture at C-1 of arabinose).



**Scheme 43. Debenzylation of compound 118**

It was found that compound **121** was significantly more stable than the benzyl phosphate **120** during basic hydrolysis conditions. Reaction of compound **121** with NaOH or K<sub>2</sub>CO<sub>3</sub> in methanol led to the expected sucrose-4'-(β-L-arabinopyranos-2-yl)-phosphate **122**. The structure of compound **122**, established by <sup>1</sup>H, <sup>13</sup>C and <sup>31</sup>P -NMR, was identical to that of the reported natural agrocinopine A.<sup>[238,239][237][285]</sup> In addition, by controlling the hydrolysis condition, agrocinopine A benzoate **123** was also obtained (**Scheme 44**). Both products were used for binding property investigations.



**Scheme 44. Ester hydrolysis of compound 121**

#### 4.2.5 Biological results

Our colleagues in I2BC in Gif-sur-Yvette established their binding mode with AccA (details are given in experimental section Annex 1, **Fig S6**) by using this sample of pure agrocinopine A and a natural extract of agrocin 84. Two main information arose from this investigation. The first one is that the phosphoramidate in agrocin 84 is connected to *O*-2 of a glucopyranose moiety (not at *O*-1 of a glucofuranose moiety).<sup>[229,230,286]</sup> And the second one is that the arabinopyranose moiety of agrocinopine A, when bound to AccA, can perfectly superimpose to the glucopyranose of agrocin 84, suggesting a specific role of this pyranosyl backbone for the recognition. (**Fig 16**)

Extensive protein hydrogen bonding is observed: 8 for L-arabinose and 10 for D-glucose (**Fig 25a** and **25b** in section 4.3.4). Remarkably, the OH-1 group of the pyranose is anchored by 4 hydrogen bonds involving Asn54 and Glu510 from lobe 1, Asn284 from the hinge region and Ser419 from lobe 2. These four side chains form a rigid template which also maintains the lobe closure by interacting together two by two (more details are given in experimental section, Annex 1, **Fig S2**). Moreover, in addition to their pyranose interactions, two of these major

residues Asn54 and Ser419 also tightly interact with the phosphate/phosphoramidate groups. Two more hydrogen bonds involving the side chains of two tyrosines 375 and 376 retain the phosphate/phosphoramidate oxygens. In contrast, the sucrose moiety of agrocinopine A and the TM84 part of agrocin 84 make only 3 and 2 polar interactions with AccA respectively. The sucrose moiety and TM84 do not fully overlap, as shown in **Fig 16**.

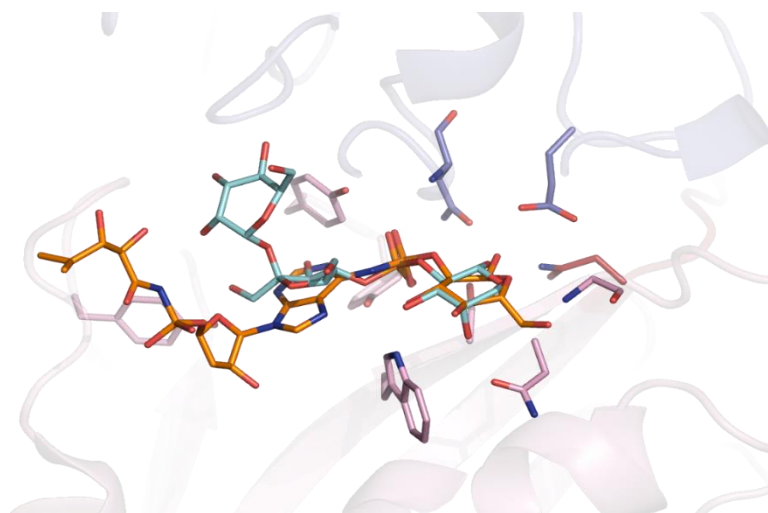


**Fig 16. Superimposition of two bound ligands: agrocinopine A (blue), agrocin 84 (orange) are shown as stick.**

This importance of the 2-pyranose phosphate moiety (either the arabinose in agrocinopine A, or the glucose one in agrocin 84) led us to investigate the binding of other analogues possessing this backbone, including simpler ones, as detailed in next sections.

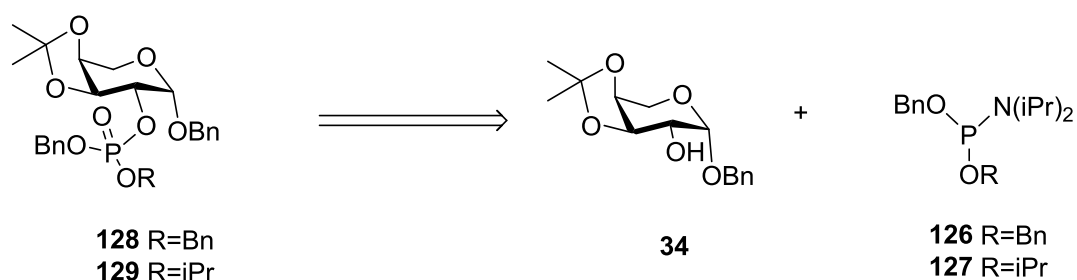
### **4.3 Synthesis and binding properties of L-arabinose-2-phosphate (A2P), D-glucose-phosphate (G2P) and their derivatives**

#### **4.3.1 Synthesis of A2P and its derivatives**

As agrocinopine A is composed of an L-arabinose-2-phosphoramidite linked to sucrose, the question was to establish which components were necessary for the recognition and binding. Thus, we targeted L-arabinose-2-phosphate and its derivatives varying in the substituent in the phosphodiester linkage, namely L-arabinose-2-isopropyl phosphate.

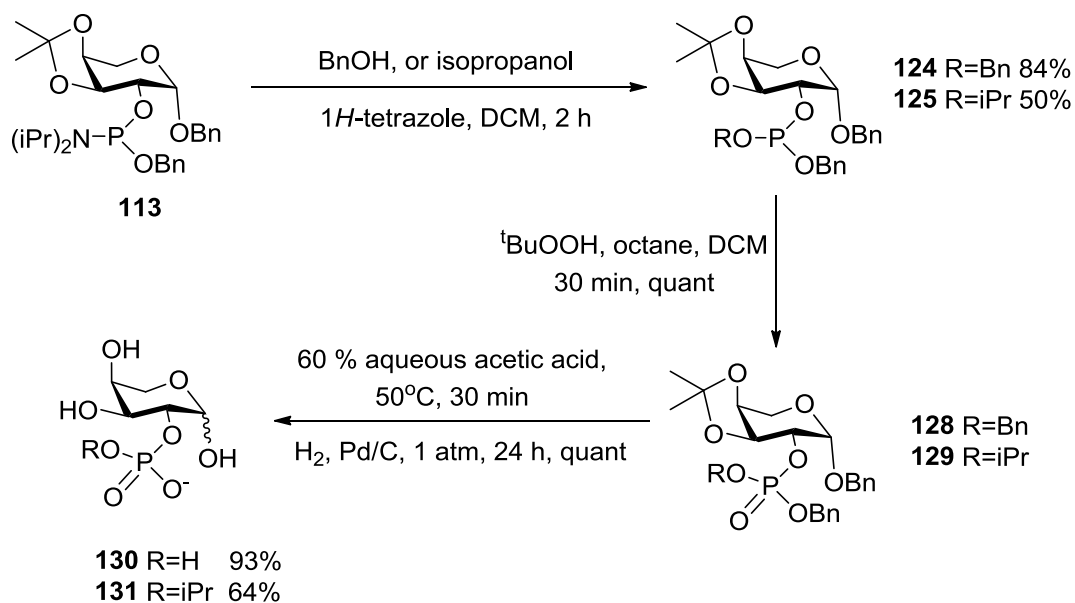
The retrosynthetic analysis is presented in **Scheme 45**. L-arabinose-2-phosphate and L-arabinose-2-isopropyl phosphate could be prepared from the condensation of compound **34**

with two different phosphoramidites **126** and **127**, which was already described in section 4.2 and 4.3.2.



**Scheme 45. Retrosynthesis of A2P and its derivatives**

Treatment of phosphoramidite **113** with benzyl alcohol or isopropanol gave the corresponding phosphotriesters **124** and **125**, and then oxidation by *m*-CPBA or *tert*-butyl hydroperoxide afforded compounds **128** and **129**. The final products **130** and **131** were obtained as an anomeric mixture after removal of isopropylidene and benzyl groups successively. Alternatively, condensation of arabinose derivate **34** with di-substituted phosphoramidite **126** or **127** could also furnish phosphites **124** and **125** (Scheme 46).

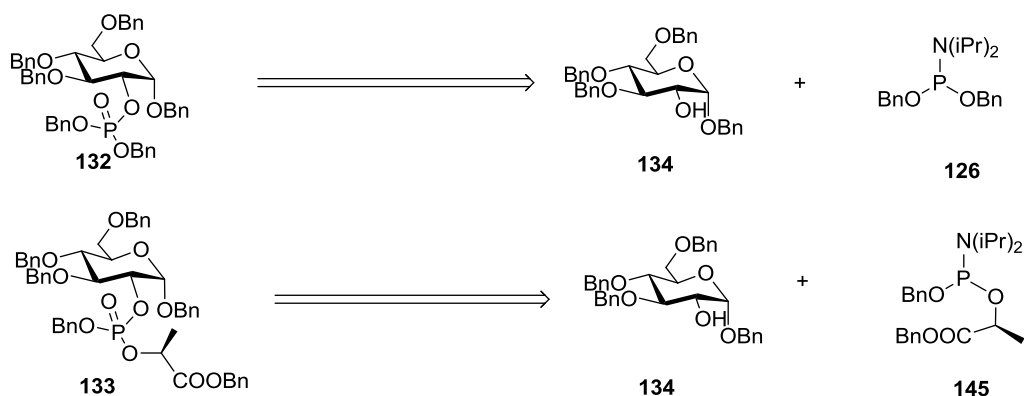


**Scheme 46. Synthesis of A2P and isopropyl A2P**

## 4.3.2 Synthesis of G2P and its derivatives

### 4.3.2.1 Synthesis of benzyl 3,4,6-tri-*O*-benzyl- $\alpha$ -D-glucopyranoside

On the basis of the synthesis scheme towards arabinose-2-phosphate, the retrosynthesis of G2P and G2P lactate is shown in **Scheme 47**. The key step is to obtain the benzyl 3,4,6-tri-*O*-benzyl- $\alpha$ -D-glucopyranoside **134** precursor having only OH-2 free for phosphorylation.

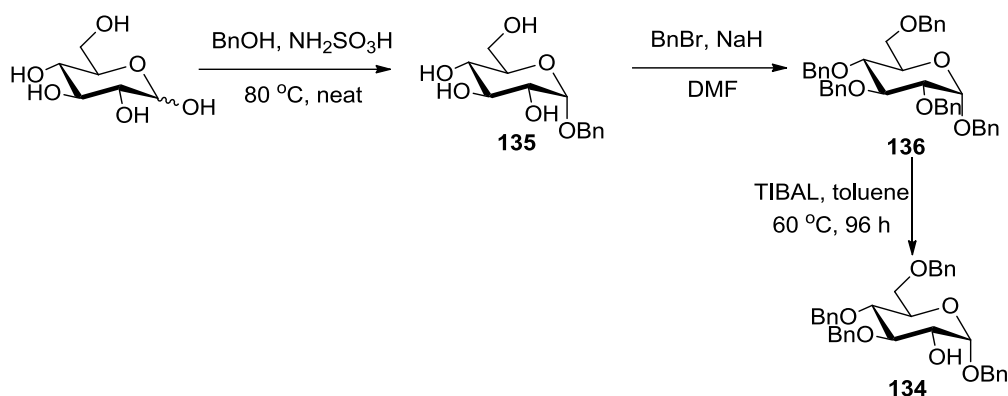


**Scheme 47. Retrosynthesis of G2P and G2P lactate**

There are several protective strategies for making OH-2 available, such as early studies using glucosyl bromide in multiple steps<sup>[270][272]</sup> via a key mercury bromide-catalyzed rearrangement<sup>[271]</sup>, employing a reductive ring opening reaction of 1,2-*O*-benzylidene with diisobutyl aluminum hydride as an efficient catalyst<sup>[287]</sup>, or de-2-*O*-acetylation of penta-acetylated glucose using  $\text{BF}_3\text{Et}_2\text{O}$ ,  $\text{PCl}_5$  and DMF<sup>[288]</sup>. In general, the de-2-*O*-benzyl glucoside is commonly prepared by the ring opening reaction of 1,2-*O*-benzylidene using different catalysts, and the de-2-*O*-acetylation glucoside is prepared by the ring opening reaction of 1,2-cyclic acetate using various acidic or basic conditions.

In this thesis, a straightforward method for achieving de-2-*O*-benzyl glucose in three steps has been proposed (**Scheme 48**). Firstly, treatment of D-glucose in benzyl alcohol in presence of sulfamic acid<sup>[289]</sup> gave benzyl D-glucopyranoside **135** as an anomeric mixture, which was then per-benzylated by benzyl bromide in DMF in the presence of sodium hydride to afford benzyl 2,3,4,6-tetra-*O*-benzyl- $\alpha$ -D-glucopyranoside **136**. Then de-2-*O*-benzylation was

accomplished in toluene with a large amount of TIBAL.<sup>[290]</sup> The overall yield for the three steps was 20% as only the  $\alpha$  anomer can undergo debenzoylation.



**Scheme 48.** Synthesis of benzyl 3,4,6-tri-*O*-benzyl- $\alpha$ -D-glucopyranoside **134**

With respect to the de-2-*O*-benzoylation steps, we tried to optimize the number of equivalent of TIBAL. It was found that shorter reaction time and high temperature were unfavorable for de-benzoylation, and increasing the quantity of TIBAL resulted in the side formation of the 2,6-de-*O*-benzoylation product, which was in agreement with literature.<sup>[290]</sup> In all case, a large amount of starting material was recovered. Overall, 6 equivalent of TIBAL at 50 °C in anhydrous toluene for 60 h was considered as the best set of conditions (**Table 2**).

**Table 2.** Optimization of de-2-*O*-benzoylation

Entry	Temp.	TIBAL	Time	Yields <sup>a</sup>
1	50 °C	6 eq	16 h	14%
2	50 °C	5 eq	60 h	18%
3	60 °C	6 eq	60 h	26%
4	50 °C	6 eq	72 h	22%
5	50 °C	6 eq	60 h	32%
6	50 °C	10 eq	96 h	12% <sup>b</sup>

(a) Isolated yields, in all case, a large amount of starting material was recovered. (b) 15% of by-products 6-de-*O*-benzoylation product was observed.

The structure of benzyl 3,4,6-tri-*O*-benzyl- $\alpha$ -D-glucopyranoside **134** was confirmed by <sup>1</sup>H-NMR which was identical to literature data.<sup>[273]</sup> The chemical shift of the anomeric hydrogen

locates at 5.03 ppm, and  $J_{1,2} = 3.7$  Hz, which indicated the product is the  $\alpha$ -anomer de-2-*O*-benzylation product (**Fig 17**).

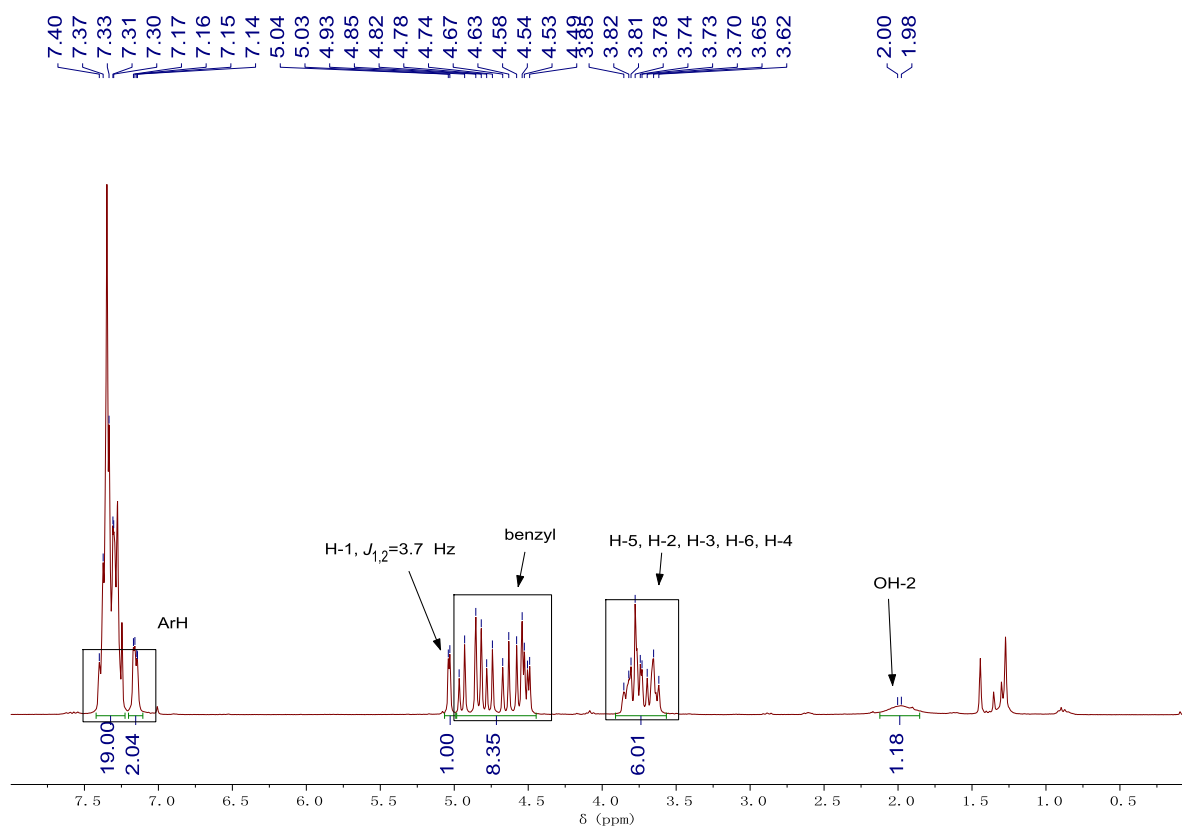
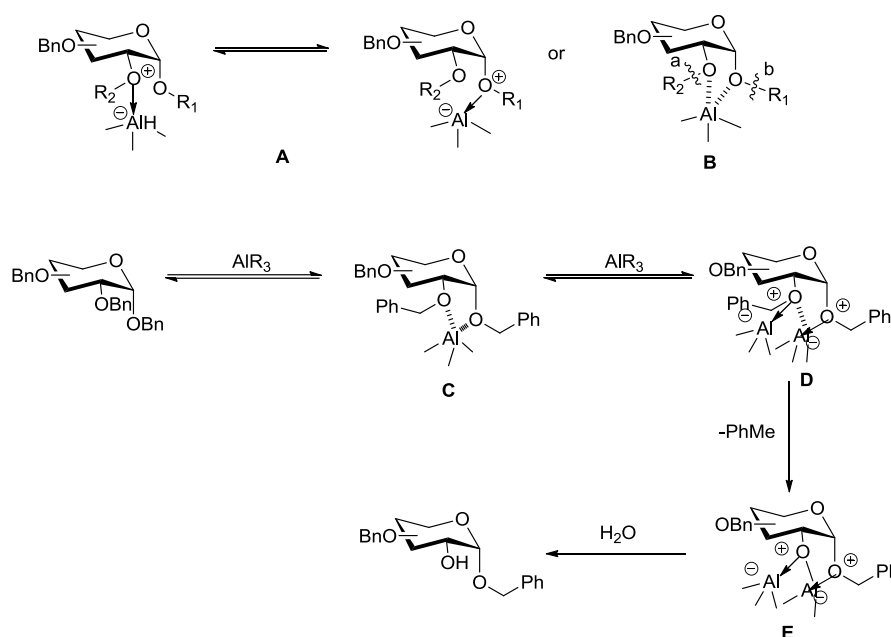


**Fig 17.**  $^1\text{H-NMR}$  of compound 134 ( $\text{CDCl}_3$ , 300 MHz)

For the mechanism of the de-2-*O*-benzylation, it was proposed that the process is initiated by the favorable kinetic formation of a fluxional complex A which could transform to B, but it is unknown whether B is a real pentacoordinate complex or an imaginary formalism, although the intermediacy of pentacoordinate trialkylaluminium complexes as key intermediates in various organic reactions is now well documented and has especially been scrutinized by Maruoka and Ooi.<sup>[291–295]</sup> Actually, two molecules of aluminum reagent are involved in the de-2-*O*-benzylation process. The first aluminum sticks to the most accessible bidentate ligand, or di-oxygenated “tweezers”, forming a fluxional or pentacoordinate complex C (**Scheme 49**) requiring the 1,2-cis-diol pattern. A second aluminum atom then complexes one of the two oxygen atoms of the “tweezers” to orientate the de-*O*-benzylation by activating the C-O bond. According to the model presented by Sollogoub<sup>[290]</sup>, the orbitals of the two oxygen atoms implicated in the process are not equally accessible: the exocyclic anomeric oxygen atom is

axially oriented, and consequently one of its lone pairs is hindered because it is located under the pyranoside ring, whereas both lone pairs of the equatorial 2-oxygen atom are equally available for coordination. Therefore, the second aluminium atom coordinates much more easily to oxygen 2 than to the anomeric oxygen, thereby forming complex **D** and directing the de-*O*-alkylation reaction towards de-2-*O*-benzylation (**Scheme 49**). The lower steric demand of DIBAL-H in relation to TIBAL, allowing some approach on *O*-1, can probably account for the drift in the regioselectivity in the reaction with compound **D**.<sup>[290]</sup>



**Scheme 49.** Formation of a highly fluxional complex **A** or a pentacoordinate complex **B** (proposed mechanism for the TIBAL-mediated de-*O*-benzylation at position 2 of perbenzylated benzyl  $\alpha$ -D-glucopyranoside)

#### 4.3.2.2 Synthesis of phosphorylation reagents

Several phosphorylation intermediates including tribenzyl phosphite **137**, phosphoramidites **65** and **126** have been used (**Fig 18**). Tribenzyl phosphite has been used for direct and efficient phosphorylation towards different alcohol substrates,<sup>[296–298]</sup> and the phosphoramidites were used widely for the phosphorylation of oligonucleotide, glycoside and peptide.<sup>[264,265,299,300]</sup>

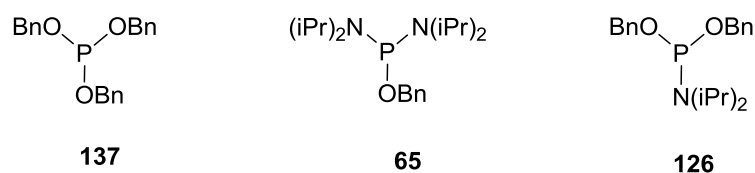
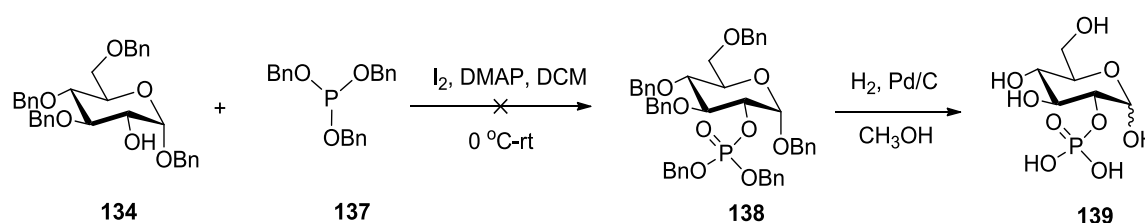


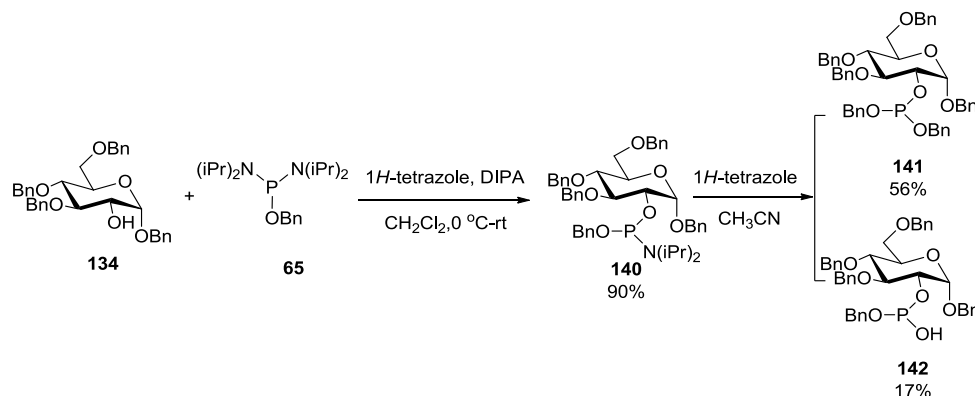
**Fig 18. Three widely used phosphorylation reagents**

Combination of triethyl phosphite or tribenzyl phosphite with iodine and pyridine were frequently used for the diethyl or dibenzyl-phosphorylation of various alcohol substrates.<sup>[296–298]</sup> Based on this, the direct phosphorylation using tribenzyl phosphite for compound **134** was proposed. Unfortunately, due to the low-reactivity of OH-2 and steric hindrance of the anomeric substituent, as well as oxidation susceptibility of the phosphite, no desired product was observed (**Scheme 50**).



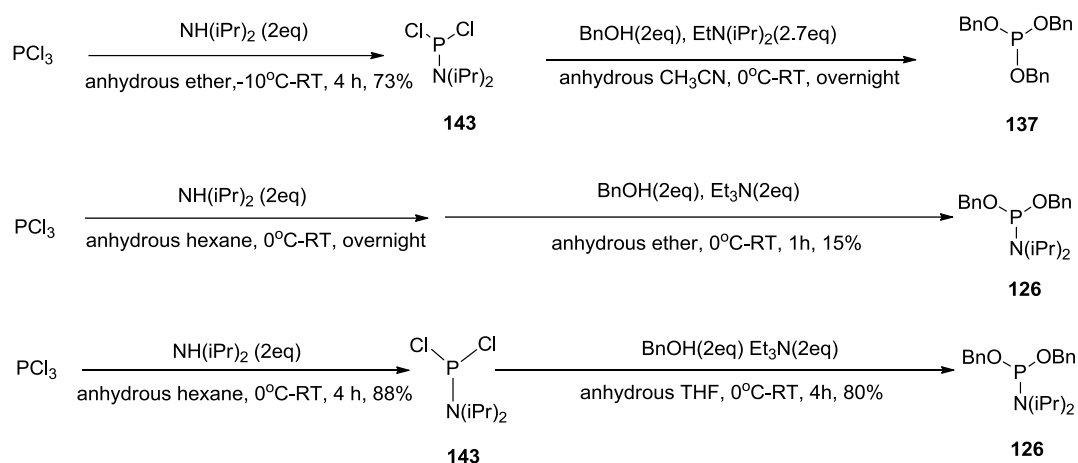
**Scheme 50. Proposed phosphorylation of compound 134 using tribenzyl phosphite**

Thus, our attention was turned to phosphoramidites. Initially, phosphoramidite **65** was used for synthesizing compound **141**, but two substitution steps were necessary. Moreover, the diisopropylamino group was sensitive to weak acidic condition, resulting in the appearance of compound **142** having a hydroxyl substituted in the second substitution step (**Scheme 51**).



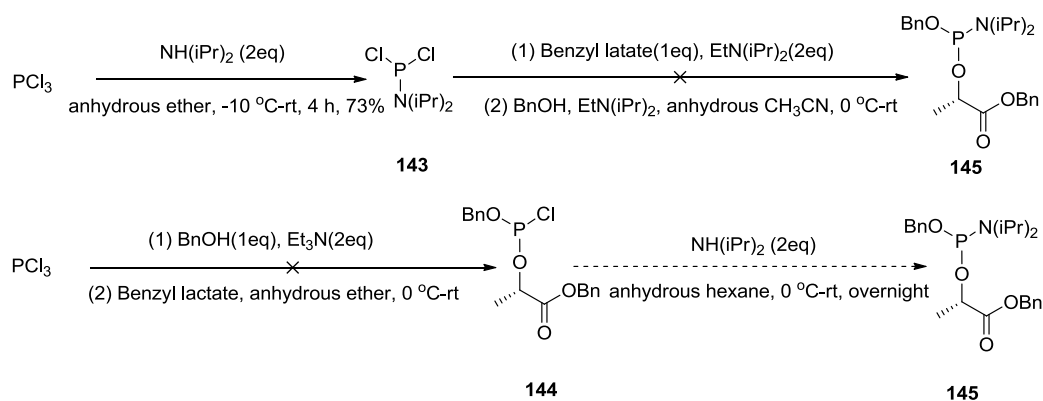
**Scheme 51. Synthesis of compound 141 using phosphoramidite 65**

Then, di-substituted phosphoramidites **126** was employed for the phosphorylation. To prepare dibenzyl diisopropylphosphoramidite **126**, several reported methods<sup>[301–304]</sup> were compared and optimized. In all cases, trichloride phosphorus was used as the starting material. Treatment of phosphorus trichloride with diisopropylamine in ether or hexane gave the intermediate **143**, which was subsequently reacted with benzyl alcohol by using different base. As described in **Scheme 52**, the first case gave tribenzyl phosphite **137** as a major product, and the second one gave the desired compound **126** in 15% yield, only the third set of conditions which afforded compound **126** in good yield, was used for the next step without further purification.



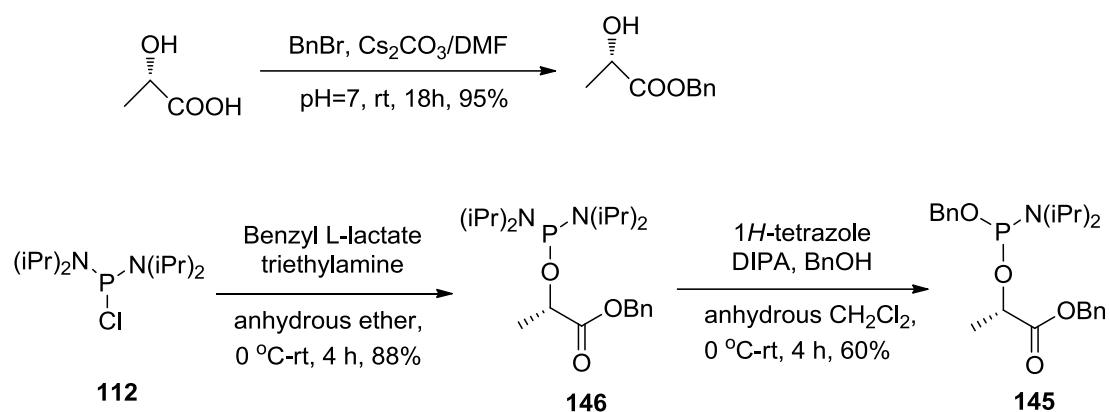
**Scheme 52. Three method for preparation of compound 126**

However, this method revealed unsuccessful preparation of benzyl L-lactate substituted phosphoramidite **145**, even though two sequences of reaction were attempted (**Scheme 53**).



**Scheme 53. Preparation of benzyl L-lactate substituted phosphoramidite 145**

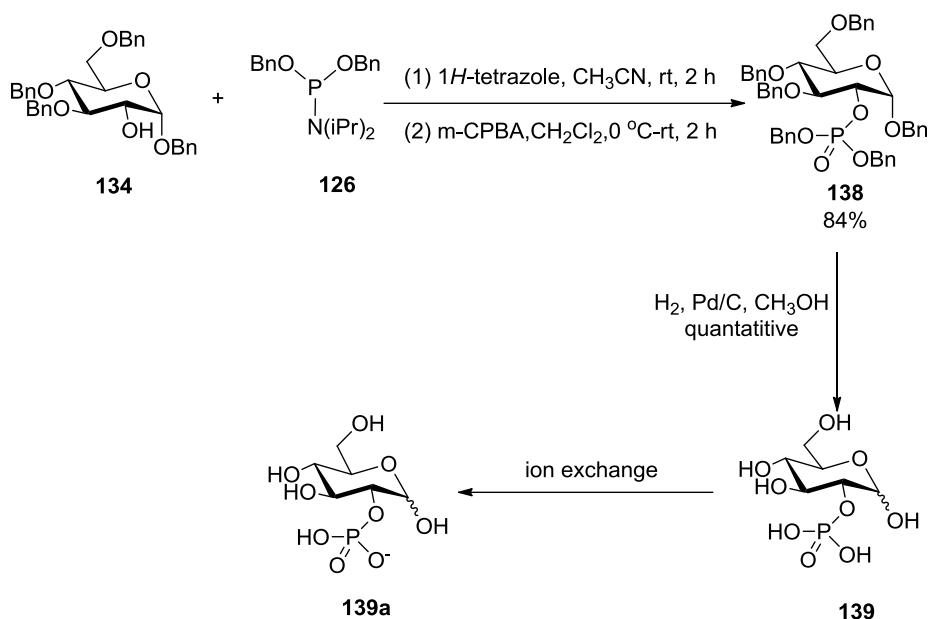
So for this target, we returned to the use of chlorophosphine **112**, which reacted with benzyl L-lactate<sup>[305]</sup> in the presence of triethylamine in ether to furnish intermediate **146** which was subsequently treated with benzyl alcohol, in the presence of tetrazole and diisopropylamine.<sup>[300]</sup> The benzyl L-lactate substituted phosphoramidite **145** was thus obtained in 53% yield (**Scheme 54**).



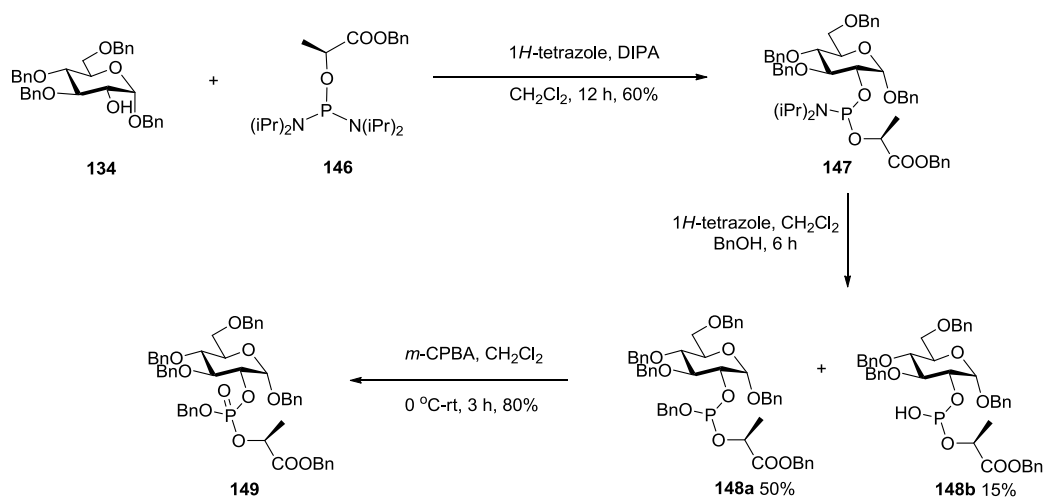
**Scheme 54.** Preparation of benzyl L-lactate phosphoramidite **145** using chlorophosphine **112**

#### 4.3.2.3 Phosphorylation and deprotection in the glucose-2-phosphate series

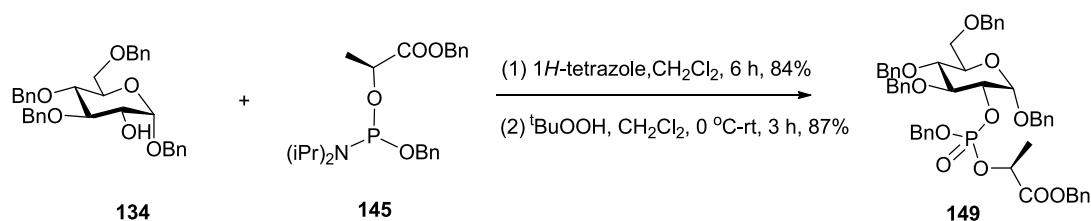
The coupling of compound **134** and phosphoramidite **126** was accomplished by the activation of tetrazole. Among several activating agents such as 1*H*-tetrazole and *p*-nitrophenyl tetrazole, 1*H*-tetrazole is by far the most commonly used. Thus, treatment of compound **134** with compound **126** in the presence of two equivalent of 1*H*-tetrazole in acetonitrile furnished the phosphite intermediate, which was subsequently treated *in situ* by *m*-CPBA or *tert*-butyl hydroperoxide to afford compound **138**. Hydrogenation of compound **138** was accomplished in methanol with 10% Pd/C. Glucose-2-phosphate was obtained as an anomeric mixture ( $\alpha/\beta=13/10$ ) after purification by C18 column. Further salinization by ion exchange chromatography gave the product as a salt which is more stable for storage and more soluble in buffer for bioassay experiments (**Scheme 55**).



The per-benzylated precursor of glucose-2-L-lactate phosphate **149** was obtained in three steps from compound **134** via coupling with compound **146**, reaction with benzyl alcohol, and oxidation. After three steps, desired product **149** was obtained in 24% yield. In the intermediate substitution step, an inevitable hydroxyl substituted side-product **148b** was isolated in 15% yield (**Scheme 56**).

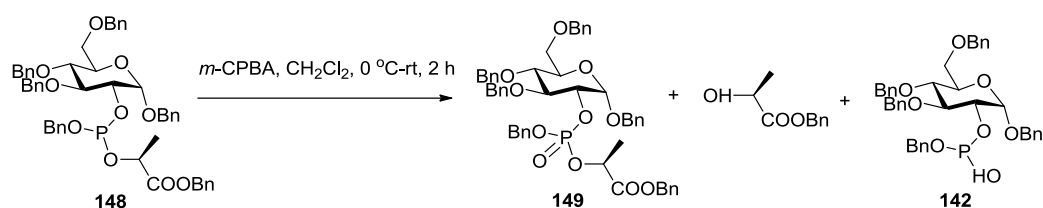


Since the above described scheme consumed a large amount of compound **134**, and produced some side products, we investigated an alternative route using the di-substituted phosphoramidite **145** instead of compound **146** by using this reagent, compound **149** was obtained in a “one-pot” reaction in 73% yield (**Scheme 57**).



**Scheme 57. Synthesis of G2P lactate precursor using phosphoramidite 145**

In the oxidation step, we used *tert*-butyl hydroperoxide instead of *m*-CPBA as the phosphite **148** proved to be unstable even at room temperature, leading to partial cleavage of the phosphate ester (**Scheme 58**).



**Scheme 58. Oxidation of compound 149 using *m*-CPBA**

Then, the hydrogenation of compound **149** as the final step was investigated. Treatment of compound **149** in methanol gave the transesterification product (methyl ester), as confirmed by  $^1\text{H-NMR}$  showing the chemical shift of  $\text{CH}_3$  at 3.77 ppm and mass spectroscopy ( $M=345$ ,  $M\text{-H}$ ). The THF/water solvent system gave complicated results which could not be clarified neither by  $^1\text{H-NMR}$ , nor by mass spectroscopy. The latter gave two different results depending on the ionization mode. In ethanol/water, the  $^1\text{H-NMR}$  and mass showed it that the right product, but it was observed, decomposed after purification by C18 chromatography. We supposed that the final product was unstable due to the lactic acid moiety, and therefore salinization<sup>[251]</sup> might be favorable. Thus, sodium carbonate and potassium carbonate were added to the methanol/water and THF/water solvents. Unfortunately, in both cases, incomplete de-benzylation was observed. Finally, hydrogenation and salinization were performed sequentially: hydrogenation was

conducted in ethanol/water and then *in-situ* salinization was accomplished in the presence of potassium carbonate to afford the target product as an anomeric mixture ( $\alpha/\beta=5/3$ ). Further purification by ammonium exchange chromatography furnished the glucose-2-lactate ammonium phosphate (**Table 3**).

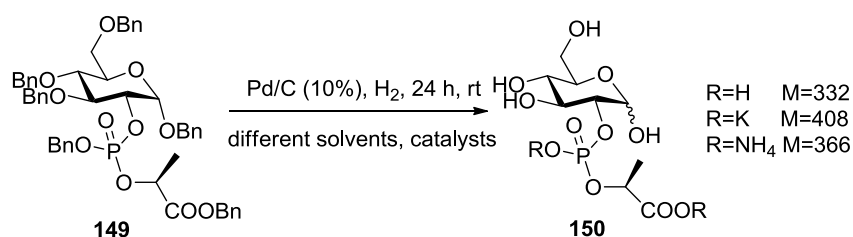


**Table 3. Optimization of hydrogenation conditions**

Entry	Conditions	Results
1	CH <sub>3</sub> OH	R=CH <sub>3</sub> <sup>a</sup>
2	THF/H <sub>2</sub> O (1/1, v/v)	M=390 <sup>b</sup> ; and M=332 <sup>b</sup>
3	Na <sub>2</sub> CO <sub>3</sub> /methanol/H <sub>2</sub> O (1 eq, 1/1, v/v)	incomplete de-benzylation
4	K <sub>2</sub> CO <sub>3</sub> /THF/H <sub>2</sub> O (1 eq, 1/1, v/v)	incomplete de-benzylation
5	ethanol/H <sub>2</sub> O (1/1, v/v)	M=332 <sup>c</sup>
6	Ethanol/H <sub>2</sub> O (1/1, v/v), K <sub>2</sub> CO <sub>3</sub> (1 eq)	R=K, and R=NH <sub>4</sub> <sup>d</sup>

a. transesterification product. b. the mass was measured in both positive and negative ionization mode. c. decomposition after purification. d. purification by IER.

#### 4.3.2.4 Characterization of Glucose-2-phosphate and Glucose-2-lactate phosphate ammonium

Glucose-2-phosphate was characterized by means of 2D-NMR and mass spectroscopy. It confirmed that glucose-2-phosphate is an anomeric mixture ( $\alpha/\beta=13/10$ ), The proton H-1 $\alpha$  appears at 5.39 ppm with  $J_{1,2} = 3.2$  Hz, and the H-1 $\beta$  at 4.74 ppm with  $J_{1,2} = 7.7$  Hz, partially hidden by deuterium oxide. Both of them are split into a doublet. With the help of <sup>1</sup>H-<sup>1</sup>H COSY, we found H-2 $\alpha$  as a multiplet at 3.95 ppm, and H-2 $\beta$  locates at 3.70 ppm, hidden by H-3, H-5 and H-6 (**Fig 19**).

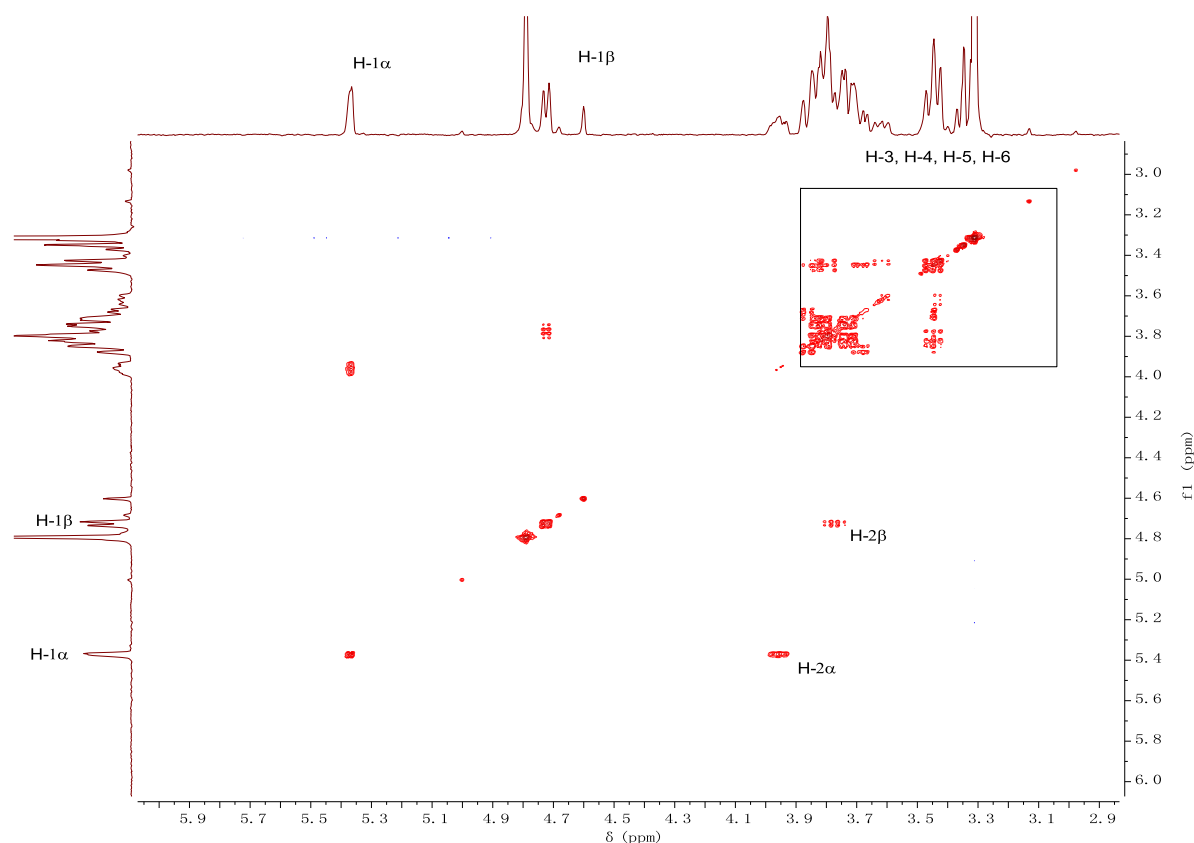


**Fig 19.  $^1\text{H}$ - $^1\text{H}$  COSY of G2P (400 MHz,  $\text{D}_2\text{O}$ )**

Interestingly, due to the coupling with phosphorus carbon,  $^{13}\text{C}$ -NMR of C-1, C-2 and C-3 are split as doublets, with coupling constants varying for different carbons atoms and anomers. The differences are shown in the **Table 4**. The detailed assignment of all protons and carbons NMR, is shown in the experimental part (**Fig 20, Table 4**).

**Table 4. Partial  $^1\text{H}$ -NMR and  $^{13}\text{C}$ -NMR of G2P**

$\alpha$ -anomer				$\beta$ -anomer			
H-1	5.39 ( $J= 3.2$ Hz)	C-1	91.3 ( $J= 2.0$ Hz)	H-1	4.74 ( $J= 7.7$ Hz)	C-1	95.5 ( $J= 4.4$ Hz)
H-2	3.95	C-2	76.2 ( $J= 5.9$ Hz)	H-2	3.70	C-2	79.5 ( $J= 5.9$ Hz)
H-3	3.67 - 3.90	C-3	72.1 ( $J= 5.9$ Hz)	H-3	3.64	C-3	75.6 ( $J= 2.9$ Hz)

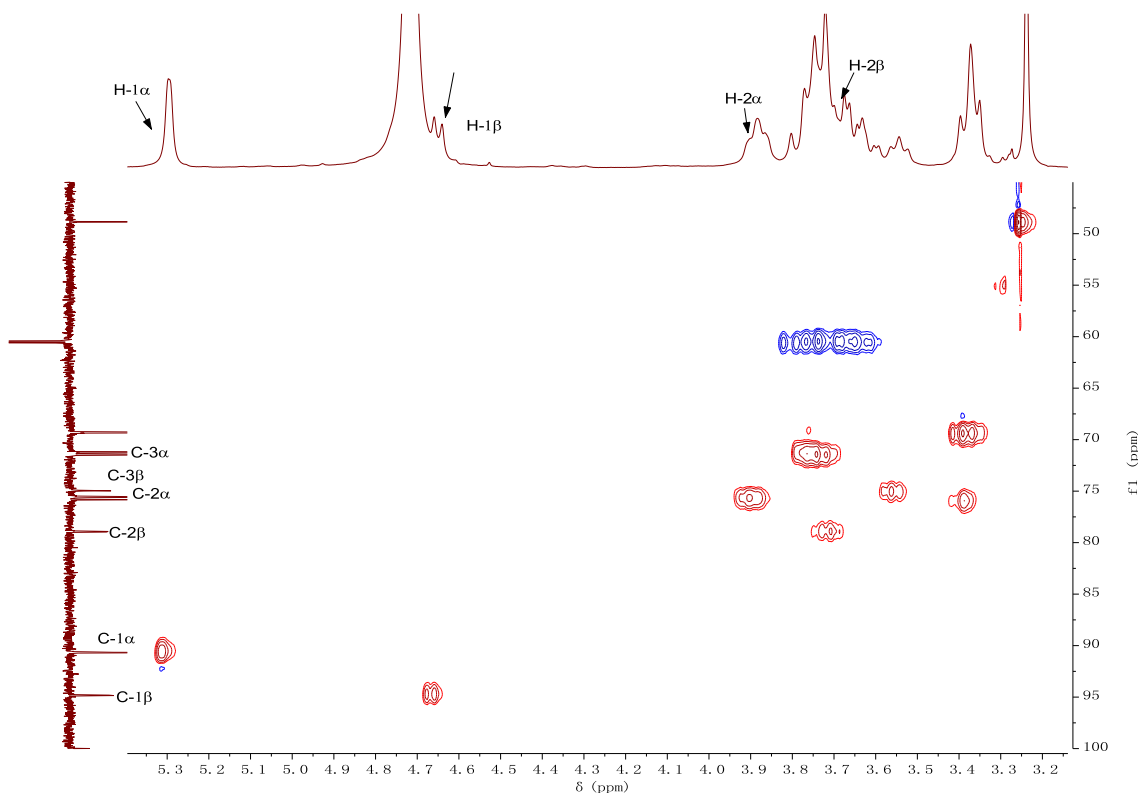


**Fig 20. HSQC of G2P (400 MHz, D<sub>2</sub>O)**

In addition, 2D NMR showing the  $^{31}\text{P}$ - $^1\text{H}$  correlation confirmed the position of the phosphate at *O*-2 for glucose-2-phosphate (iP as inorganic phosphate was used as standard). The phosphorus signals of each anomer appears at -0.26 ppm ( $\beta$ ) and -0.41 ppm ( $\alpha$ ) respectively (**Fig 21**).

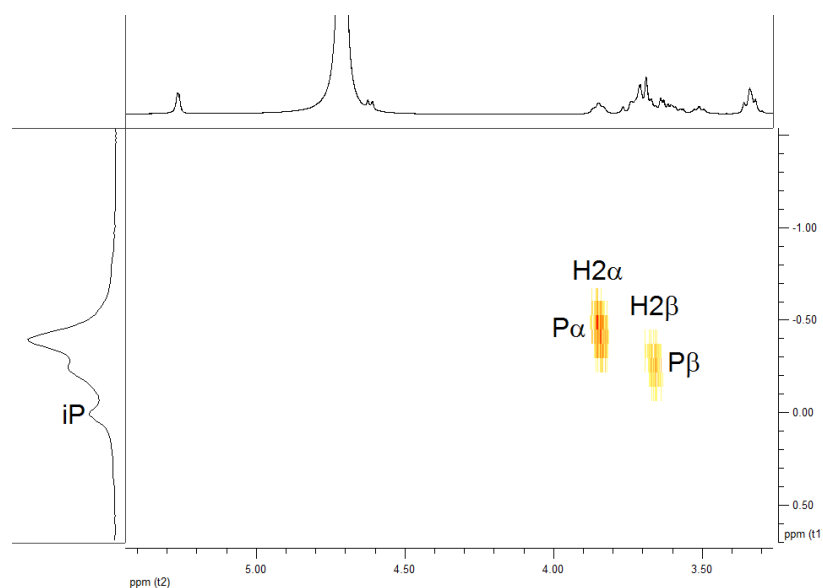


**Fig 21.  $^{31}\text{P}$ - $^1\text{H}$  correlation of G2P (500 MHz, D<sub>2</sub>O)**

Glucose-2-lactate phosphate ammonium salt was also characterized by 2D-NMR. A mixture of  $\alpha/\beta$  with 5/3 ratio was calculated from the integration of H-1 signals. H-1 $\alpha$  at 5.36 ppm with  $J_{1,2} = 3.6$  Hz, and H-1 $\beta$  at 4.68 ppm with  $J_{1,2} = 7.9$  Hz, partially hidden by deuterium oxide. With the help of  $^1\text{H}$ - $^1\text{H}$  COSY, we found H-2 $\alpha$  as a multiplet at 3.95 ppm and H-2 $\beta$  at 3.77 ppm, impaired by H-3 $\alpha$ , H-5 $\alpha$ . In addition, the  $\alpha$  and  $\beta$  CH- group of lactic acid as multiplets were found at 4.5 ppm, and the corresponding  $\alpha$  and  $\beta$  CH<sub>3</sub>- are doublet at 1.40 ppm. Decomposition of G2P lactate can be easily traced signals at 4.5 ppm and 1.4 ppm for free lactic acid (**Fig 22**).

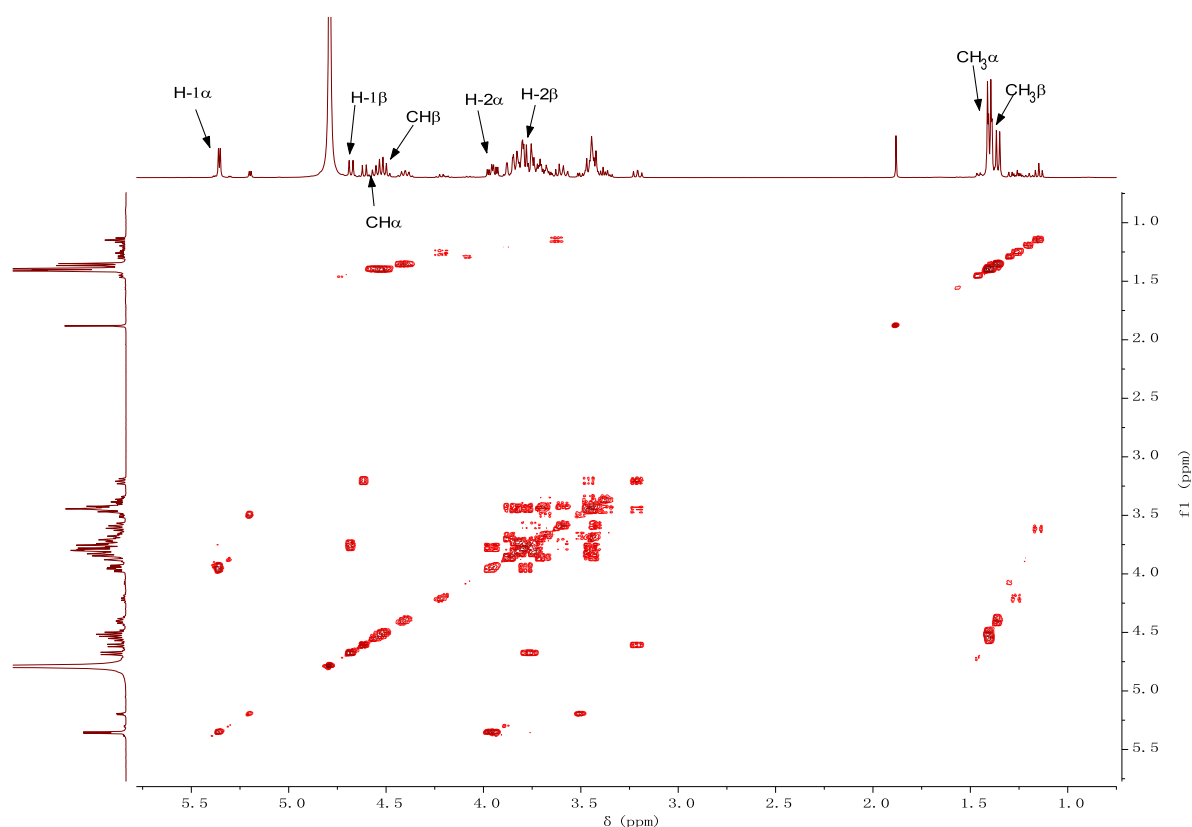


**Fig 22.**  $^1\text{H}$ - $^1\text{H}$  COSY of G2P lactate (400 MHz, D<sub>2</sub>O)

Like G2P, HSQC shows coupling with phosphorus for  $^{13}\text{C}$ -NMR signals. The carbon of  $\alpha$  and  $\beta$  CH- group appears as doublet ( $\delta=73.1$  ppm,  $J_{\text{C-P}} = 5.7$  Hz), and the same splitting is also overserved for C-1, C-2 and C-3 (**Fig 23**). The differences are shown in the **Table 5**.

**Table 5. Partial  $^1\text{H}$ -NMR and  $^{13}\text{C}$ -NMR of G2P lactate**

$\alpha$ -anomer				$\beta$ -anomer			
H-1	5.36 ( $J = 3.6$ Hz)	C-1	90.9 ( $J = 2.0$ Hz)	H-1	4.68 ( $J = 7.9$ Hz)	C-1	95.0 ( $J = 5.1$ Hz)
H-2	3.95	C-2	75.7 ( $J = 6.8$ Hz)	H-2	3.79	C-2	78.9 ( $J = 6.6$ Hz)
H-3	3.75 - 3.81	C-3	71.5 ( $J = 5.6$ Hz)	H-3	3.63 - 3.56	C-3	75.0 ( $J = 2.7$ Hz)
H <sub>CH</sub>	4.56	C <sub>CH</sub>	73.1 ( $J = 5.7$ Hz)	H <sub>CH</sub>	4.49	C <sub>CH</sub>	73.1 ( $J = 5.7$ Hz)

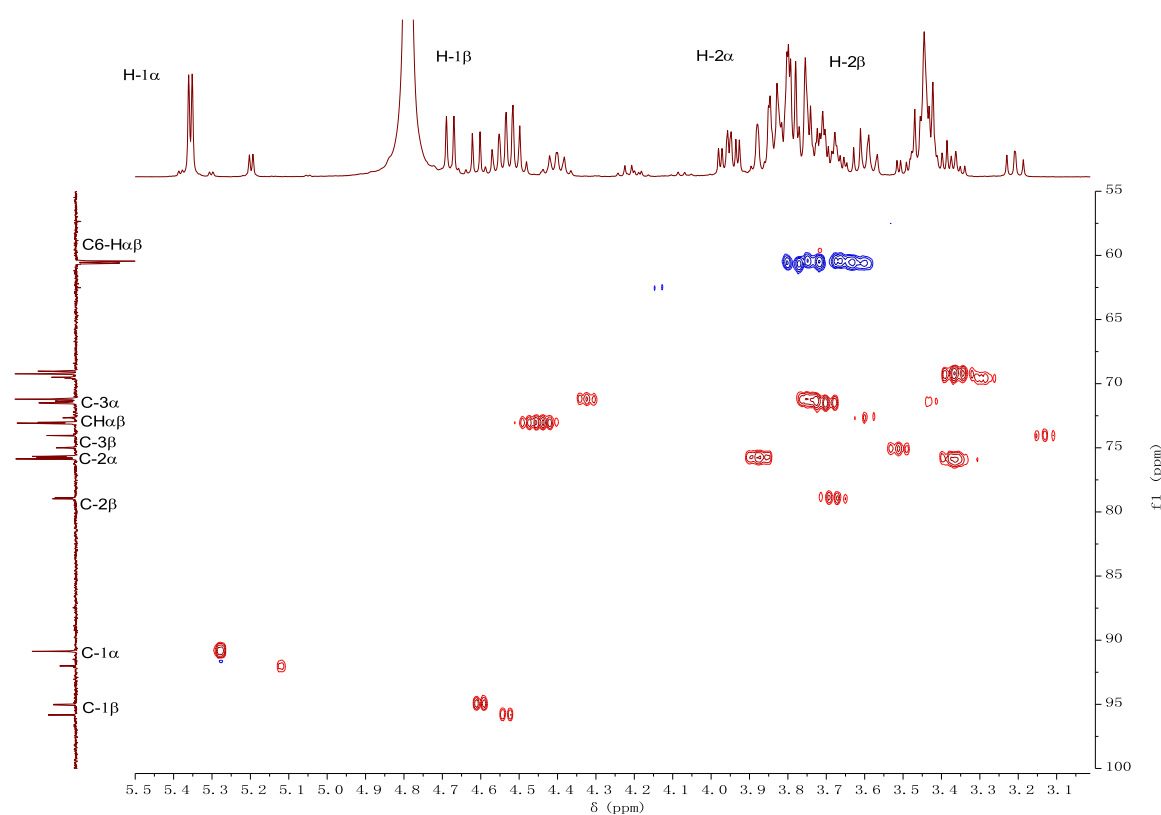


**Fig 23. HSQC of G2P lactate (400 MHz, D<sub>2</sub>O)**

In comparison with glucose-2-phosphate, the carbon shift of C-1, C-2 and C-3 of G2P lactate move to high fields slightly, and the  $\alpha$ -anomer locates in a higher field than  $\beta$ -anomer in both cases. The coupling constant is almost the same except  $J_{\text{C}2\text{-P}}$  of glucose-2-lactate phosphate which is stronger than that of glucose-2-phosphate due to the introduction of lactic acid. This could be explained by the conformation adjustment. Among those three carbons, the  $J$ -coupling of C-2 is the strongest one since the coupling of C-2 and phosphorus is the second-order

coupling whereas others are third-order coupling. More interestingly, for  $\alpha$  and  $\beta$  glucose phosphate, in both case, the  $J$ -coupling of C-1 and C-3 exhibit distinct differences.

2D NMR of the  $^{31}\text{P}$ - $^1\text{H}$  correlation shows the  $^{31}\text{P}$ -NMR of H-2 $\alpha$  and CH $\alpha$  appears at -1.16 ppm, and H-2 $\beta$  and CH $\beta$  at -0.86 ppm. Theoretically, four phosphorus signals should be observed. The proximity of  $^{31}\text{P}$ -NMR chemical signals of CH and H-2 resulted in only two peaks, and the high resolution NMR spectroscopy could give more details (**Fig 24**).

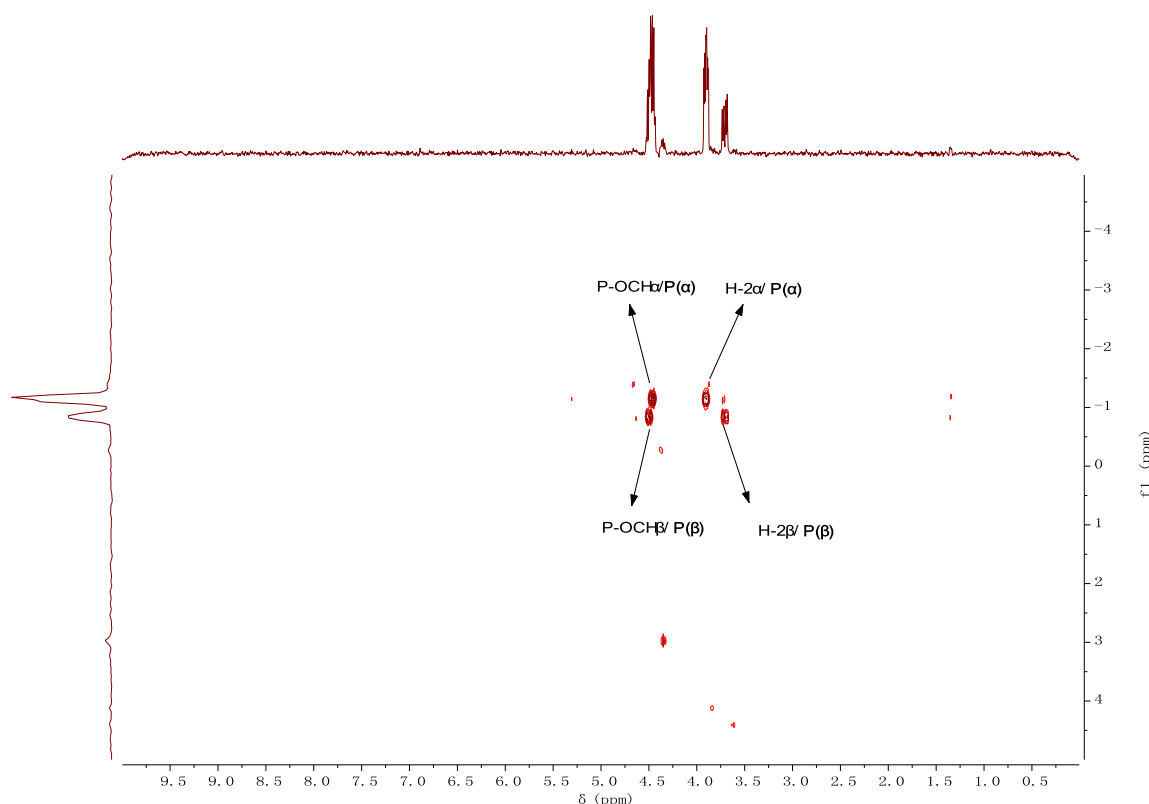


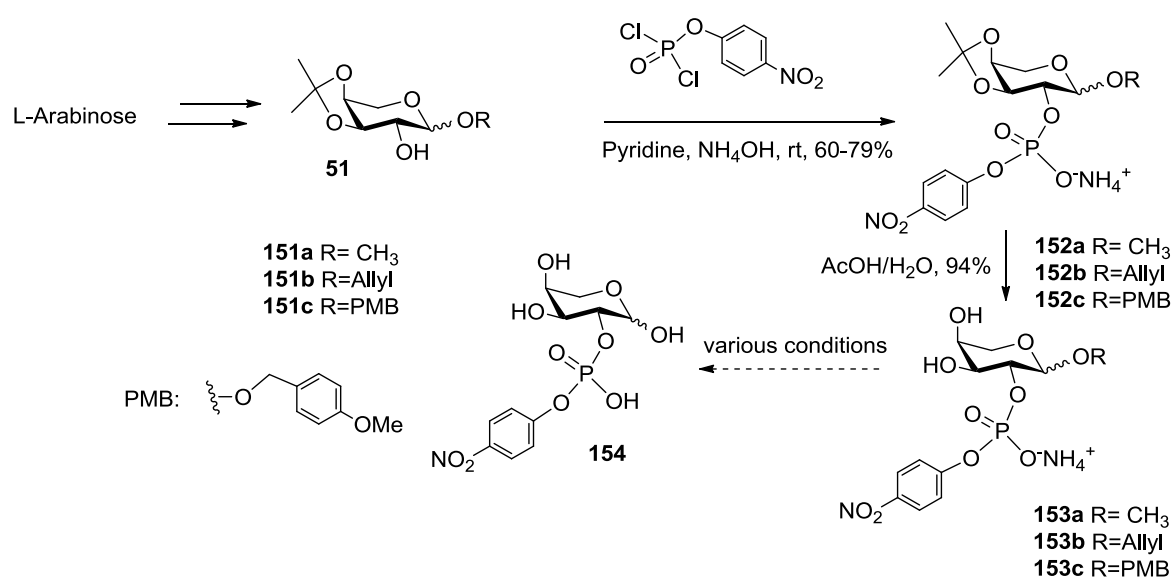
**Fig 24.**  $^{31}\text{P}$ - $^1\text{H}$  correlation of G2P lactate (400 MHz,  $\text{D}_2\text{O}$ )

### 4.3.3 Synthesis of arabinose-2-*p*-nitrophenyl phosphate and glucose-2-*p*-nitrophenyl phosphate

In keeping with our objective to study the structural scope in the A2P and G2P series, we then tried to prepare L-arabinose *p*-nitrophenyl 2-phosphate and glucose *p*-nitrophenyl 2-phosphate. In terms of structures, these two derivatives could not be prepared following the strategies used for A2P and G2P by using benzyl protective groups, and benzyl glycosides, since nitrophenyl group can be hydrogenated. Thus, we switched to other precursors such as

methyl, allyl or *p*-methoxybenzyl glycosides for L-arabinose *p*-nitrophenyl 2-phosphate, and acetyl protected group for glucose *p*-nitrophenyl 2-phosphate. Unfortunately, after several attempts, as briefly shown below, the *p*-nitrophenyl phosphate association proved to be extremely unstable and merely to get these two compounds.

The synthetic scheme of L-arabinose *p*-nitrophenyl 2-phosphate is shown in the **Scheme 59**. The proposed sequence started from L-arabinose in five steps *via* anomeric protection by methyl,<sup>[306][307]</sup> allyl<sup>[308]</sup> or *para*-methoxybenzyl (PMB),<sup>[309]</sup> *O*-isopropylidene<sup>[310,311]</sup> of 3,4-diol, condensation with 4-nitrophenyl phosphorodichloridate,<sup>[312–314]</sup> and deprotection.

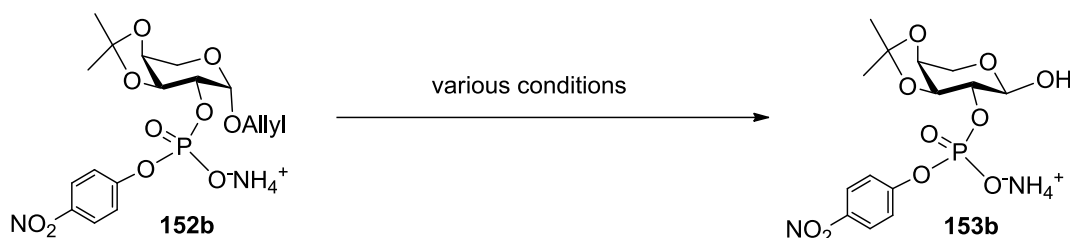


**Scheme 59.** Synthetic scheme of L-arabinose *p*-nitrophenyl 2-phosphate

The preparation of methyl L-arabinoside was conducted by anomeric alkylation.<sup>[307]</sup> Treatment of sugar in the presence of dimethyl sulfate, sodium hydroxide and TBAI in DMF gave the methylation product in a moderate yield. After isopropylideneation, reacting with the dichlorophosphate gave the protected phosphate **152a**. The deprotection was then accomplished under base conditions such as BBr<sub>3</sub> in dichloromethane<sup>[315]</sup> for removal of the methyl and isopropylidene groups, but the *p*-nitrophenyl group because of its leaving group character, was also removed under those conditions. Thus, our attention turned to other glycosides easier to remove, such as allyl and PMB.

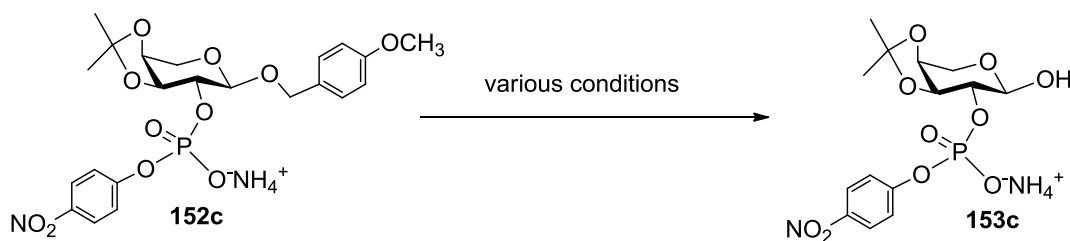
The allyl  $\beta$ -L-arabinopyranoside **152b** was prepared by following a reported method,<sup>[308]</sup> using L-arabinose in the presence of concentrated sulphuric acid and calcium sulphate in allyl alcohol. For 4-methoxybenzyl  $\alpha$ -L-arabinopyranoside **152c**, it was synthesized from L-arabinose in four steps<sup>[309]</sup> *via* acetylation, bromide substitution in the presence of 33% HBr/AcOH, substitution of the bromide using iodine, Ag<sub>2</sub>CO<sub>3</sub> and *p*-methoxybenzyl alcohol, and then deacetylation reaction. Treatment of compounds **151b** and **151c** with 4-nitrophenyl phosphorodichloridate and ammonium hydroxide in pyridine afforded compounds **152b** and **152c** in 60-79% yields.

The Pd(PPh<sub>3</sub>)<sub>4</sub> and PdCl<sub>2</sub><sup>[316,317]</sup> were used for de-allylation. But none of them gave expected results, probably due to the cleavage of the P-O-CH<sub>2</sub>-PhNO<sub>2</sub> phosphate ester (**Scheme 60**).



**Scheme 60. Deprotection of allyl group**

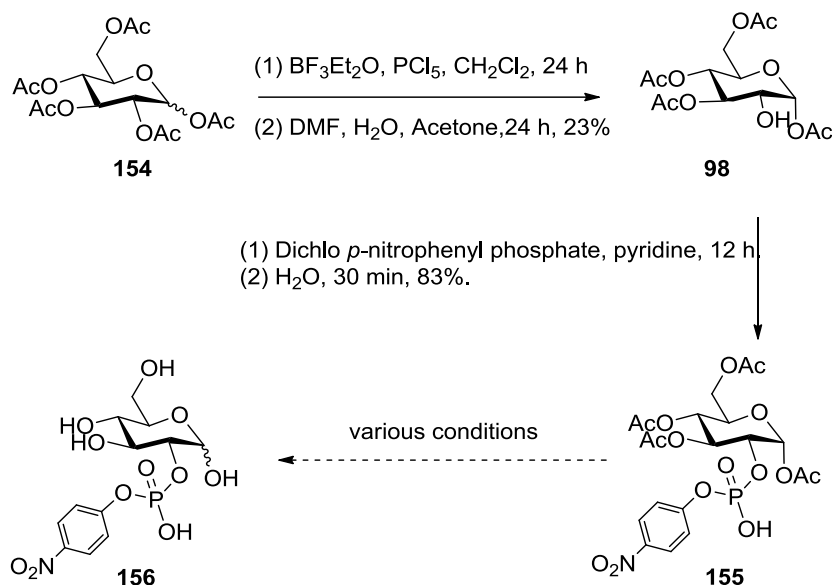
The deprotection of the PMB glycoside was also conducted under several conditions.<sup>[318,319]</sup> Unfortunately, none of these conditions gave the desired products because of the removal of *p*-nitrophenyl group, as confirmed with the absence of phenyl signals in the <sup>1</sup>H-NMR and absence of phosphate signals in the <sup>31</sup>P-NMR (**Scheme 61**).



**Scheme 61. Deprotection of PMB group**

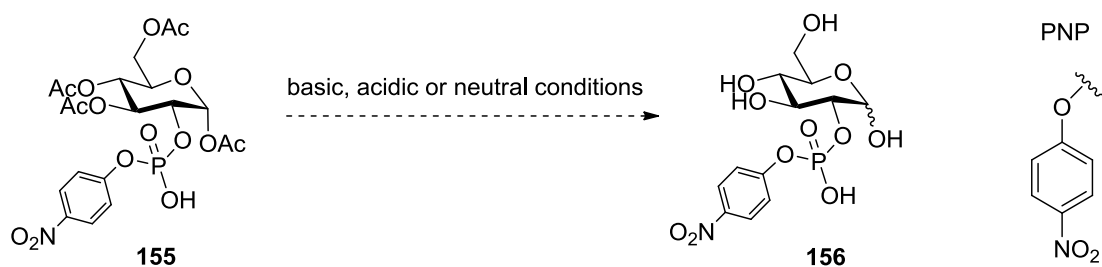
For the synthesis of glucose-2-*p*-nitrophenyl phosphate, we referred to a reported synthesis of acetyl 3,4,6-tri-*O*-acetyl- $\alpha$ -D-glucopyranoside **98** by selective de-acetylation, using BF<sub>3</sub>Et<sub>2</sub>O,

PCl<sub>5</sub> and DMF.<sup>[288]</sup> Then condensation of **98** with 4-nitrophenyl phosphorodichloridate resulted in compound **155** (Scheme 62).



**Scheme 62. Synthetic scheme of glucose-2-*p*-nitrophenyl phosphate**

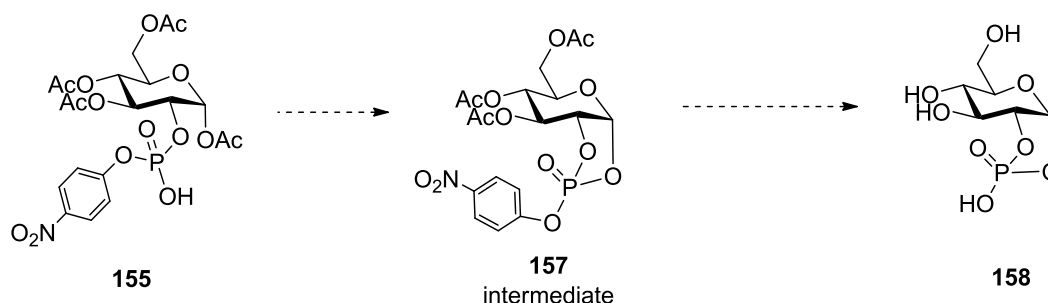
However, deacetylation of compound **155** was unsuccessful, even though we screened twenty sets of conditions including basic, acidic and neutral ones. The different conditions resulted in either removal of PNP group, or complicated non-separable products, or invalid reaction. In a word, as a result of the leaving group character of the PNP group, it was impossible to obtain arabinose-2-*p*-nitrophenyl phosphate and glucose-2-*p*-nitrophenyl phosphate (Scheme 63).



**Scheme 63. Deacetylation of compound 155 using various conditions**

We supposed that a possible 1,2-cyclic-*p*-nitrophenyl glucose phosphate intermediate **157** was formed during this process. As a 5-membered ring, the 1,2-cyclic phosphate intermediate

is a thermodynamic stable product. The PNP group can be substituted by hemiacetalic OH-1 which is released under acidic or basic conditions, to give glucose 1,2-cyclic phosphate **158** (Scheme 64).



**Scheme 64.** The hypothesis explaining the PNP loss during the deacetylation process

#### 4.3.4 Binding mode and biological properties of A2P, G2P and derivatives.

In this section, the biological results obtained by using mainly A2P, G2P, arabinose-2-isopropyl phosphate, glucose-2-phosphate L-lactate, are reported. Together with those focused on agrocinopine A and agrocin 84, they provide a new vision of the role of agrocinopine A in the regulation of *Agrobacterium tumefaciens* virulence. All the biological and structural experiments were achieved by the I2BC team and their colleagues in Gif-sur-Yvette. Most of the experimental work was done by Abbas El Sahili during his biological thesis under the supervision of Dr. Solange Morera. In the following, we present a short overview of these biological and structural investigations.

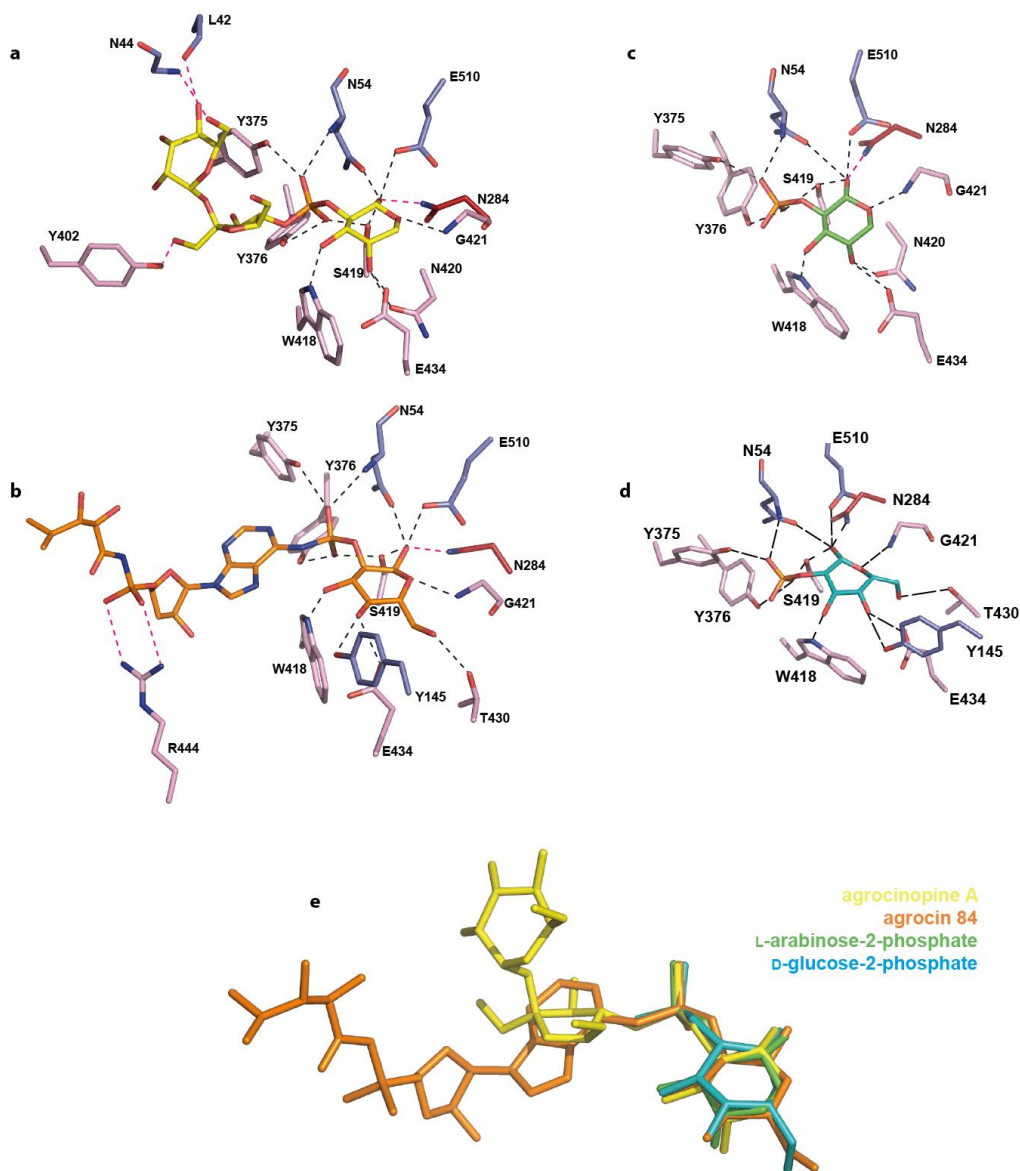


**Fig 25. Ligand-binding site of AccA.**

Ligands and protein residues involved in the ligand binding are shown as stick. Hydrogen bonds are shown as dashed lines in black (for distances below 3.2 Å) and magenta (for distances between 3.2 and 3.4 Å). (a) agrocinopine A. (b) agrocin 84. (c) L-arabinose-2-phosphate. (d) D-glucose-2-phosphate. (e) Superimposition of the four ligands bound in the ligand binding site of AccA, agrocinopine A (yellow), agrocin 84 (orange), L-arabinose-2-phosphate (green) and D-glucose-2-phosphate (cyan) are shown as stick.

### **AccA only recognizes the pyranose-phosphate-like moiety.**

Using synthetic agrocinopine A and agrocin 84 derivatives, the structures of AccA in complex with L-arabinose-2-isopropylphosphate, L-arabinose-2-phosphate and D-glucose-2-phosphate were determined by molecular replacement method. L-arabinose relatives and D-glucose-2-phosphate are well defined in the electron density maps (experimental section, Annex 1, **Fig S1**). The L-arabinose-2-isopropylphosphate and L-arabinose-2-phosphate alone or within agrocinopine A exhibit the same protein interactions and superimpose well (**Figs 25c** and **25e**). A similar observation can be done for the bound D-glucose-2-phosphate (**Figs 25d** and **25e**). To summarize, AccA strongly binds the pyranose-2-phosphate/phosphoramidate key-template through numerous polar interactions and its selectivity for this motif was validated by the structures of AccA in complex with L-arabinopyranose-2-phosphate and D-glucose-2-phosphate.

### **Binding and assimilation of a synthetic bulky ligand containing the minimal pyranose-2-phosphate motif.**

The synthesis process of agrocinopine A allows obtaining bulky agrocinopine A derivatives such as agrocinopine benzoate. AccA was therefore co-crystallized with this compound. The structure at high resolution shows a very well bound defined agrocinopine benzoate (**Fig 26**). Interestingly, while the L-arabinose-2-phosphate between bound agrocinopine benzoate and agrocinopine A superimpose, their sucrose moieties do not occupy the same position. Whereas the benzoate group of the agrocinopine benzoate adopts the position of the sucrose in agrocinopine, its sucrose moiety follows that of the TM84. (**Fig 26**)

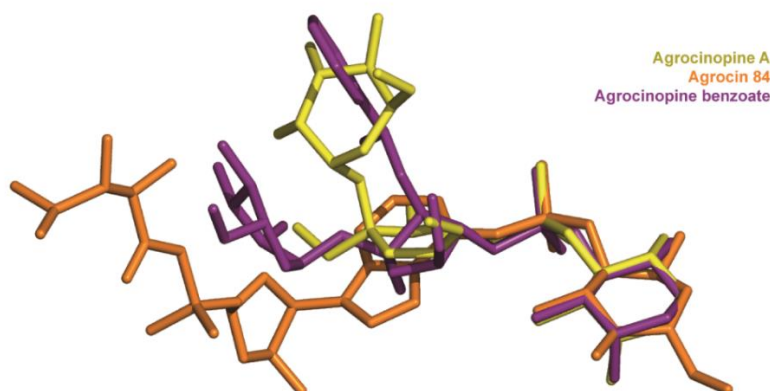


**Fig 26. Superimposition of three bound ligands** (agrociniopine A (yellow), agrocini 84 (orange), agrociniopine benzoate (purple) are shown as stick)

When presented as the sole carbon source for *agrobacterium tumefaciens* C58, agrociniopine benzoate is used as nutrient for bacterial growth (experimental section, Annex 1, **Fig S3**). Notably, agrobacteria behave similarly in presence of L-arabinose-2-phosphate used as unique carbon source, which revealed that agrociniopine benzoate is degraded into bacterial cytoplasm once imported by AccA and its ABC transporter. This experiment highlights that the transporter uptake molecules as bulky as agrociniopine benzoate into the cell.

#### **AccA exhibits a high affinity for the pyranose-phosphate-like motif.**

Ligand binding to the protein AccA was investigated using tryptophan fluorescence spectroscopy, a method that exploits the significant conformational changes that accompanies binding. The autofluorescence intensity enhancement correlates with the ligand concentrations between 0.3 and 20  $\mu\text{M}$  and saturates above 50  $\mu\text{M}$ . Titration experiments yielded apparent  $K_D$  values of  $1.3 \pm 0.17 \mu\text{M}$ ,  $5.88 \pm 1.6 \mu\text{M}$ ,  $2.93 \pm 0.66 \mu\text{M}$ ,  $4.79 \pm 0.6 \mu\text{M}$  and  $2.5 \pm 0.5 \mu\text{M}$  with agrociniopine A, agrociniopine benzoate, L-arabinose-2-phosphate, L-arabinose-2-isopropylphosphate and D-glucose-2-phosphate, respectively (experimental section, Annex 1, **Fig S4, Table S1**). No fluorescence intensity change was detected by incubating AccA with L-arabinose or D-glucose. Unexpectedly, no signal was measured with agrocini 84. This is probably due to the presence of the adenosine in agrocini 84 which provokes a quenching signal. Therefore, isothermal titration microcalorimetry was used to assess binding of agrocini 84 to

AccA which yielded a mean  $K_D$  of  $1.5 \pm 0.41 \mu\text{M}$ . The mean  $K_D$  values were  $0.3 \pm 0.03 \mu\text{M}$ ,  $7.5 \pm 2.2 \mu\text{M}$ ,  $1.33 \pm 0.12 \mu\text{M}$ ,  $2.2 \pm 0.58 \mu\text{M}$  and  $1.16 \pm 0.22 \mu\text{M}$  for agrocinopine A, agrocinopine benzoate, L-arabinose-2-phosphate, L-arabinose-2-isopropylphosphate and D-glucose-2-phosphate respectively, which was consistent with the values obtained from fluorescence spectroscopy. The isothermal titration microcalorimetry data also confirm the 1:1 binding stoichiometry and demonstrate a negative enthalpy change upon each ligand binding (experimental section, Annex 1, **Fig S5**, **Table S2**), suggesting that binding is enthalpy driven. The similar binding isotherm for all ligands means a same binding mechanism involving polar interactions in agreement with what is observed in the complexed structures (**Fig 27**). Nevertheless, the benzoate group of the agrocinopine benzoate molecule appears to be responsible for an entropic effect leading to a 25 fold lower affinity of this ligand with AccA in comparison with agrocinopine A. The binding of L-arabinose, D-glucose and adenosine monophosphate was not detected, which is in line with the results obtained by fluorimetry.

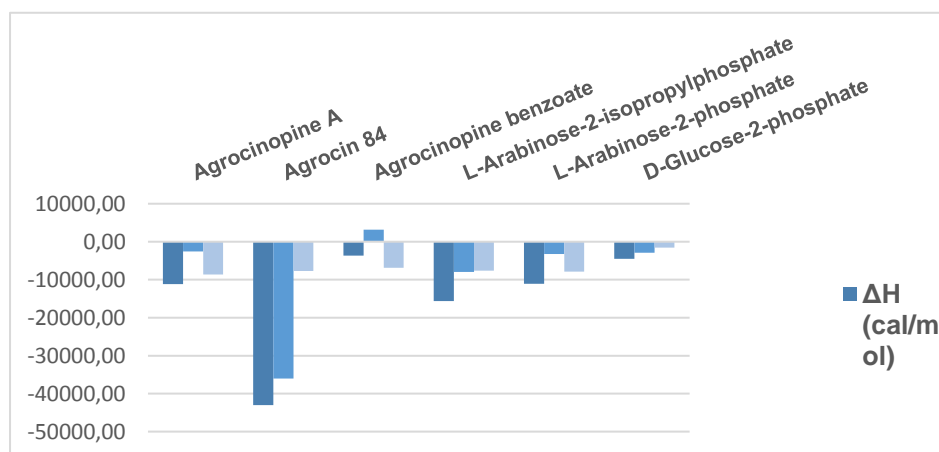


**Fig 27.** Comparison of microcalorimetry derived enthalpy ( $\Delta H$ , deep grey), entropic contribution ( $T\Delta S$ , grey) and free binding enthalpy ( $\Delta G$ , light grey) at 293°K for agrocinopine A, agrocin 84, agrocinopine 3'-*O*-benzoate, L-arabinose-2-isopropylphosphate, L-arabinose-2-phosphate and D-glucose-2-phosphate.

### L-arabinose-2-phosphate and D-glucose-2-phosphate are effectors of AccR

In the *A. tumefaciens* C58 cytoplasm, the enzyme AccF releases the L-arabinose-2-phosphate and D-glucose-2-phosphate from agrocinopine A and agrocin 84. The question arose about their biological role in *A. tumefaciens*, especially in relation to regulation of the AccR/QS

pathway that controls dissemination of the Ti plasmid. Firstly, the affinity of the synthetic agrocinopine A towards purified recombinant AccR was measured by isothermal titration microcalorimetry. An unexpected outcome was that no affinity was detected. In contrast, the isothermal titration microcalorimetry data show that AccR displays affinity to L-arabinose-2-phosphate and D-glucose-2-phosphate in two steps with  $K_D$  values for L-arabinose-2-phosphate of  $K_{D1} = 0.11 \pm 0.06$  ( $n_1 = 0.4$ )  $\mu\text{M}$  for the first step and  $K_{D2} = 1.64 \pm 0.8$  ( $n_2 = 0.9$ )  $\mu\text{M}$  for the second step and for D-glucose-2-phosphate  $K_{D1}^* = 0.43 \pm 0.1$  ( $n_1^* = 0.5$ )  $\mu\text{M}$  and  $K_{D2}^* = 1.64 \pm 0.8$   $\mu\text{M}$  ( $n_2^* = 0.9$ ) (**Fig 28**). The binding stoichiometries of 2:1 (protein: ligand) in the first step and 1:1 in the second step are in line with the fact that AccR forms a dimer in solution as observed by native gel electrophoresis, suggesting that the binding of the effector to AccR may be described as following: first, a ligand binds to one molecule within the dimer before another binds to the second molecule. These results suggest L-arabinose-2-phosphate and D-glucose-2-phosphate are the effector molecules that regulate AccR and thus they should activate QS synthesis in *A. tumefaciens* cells.

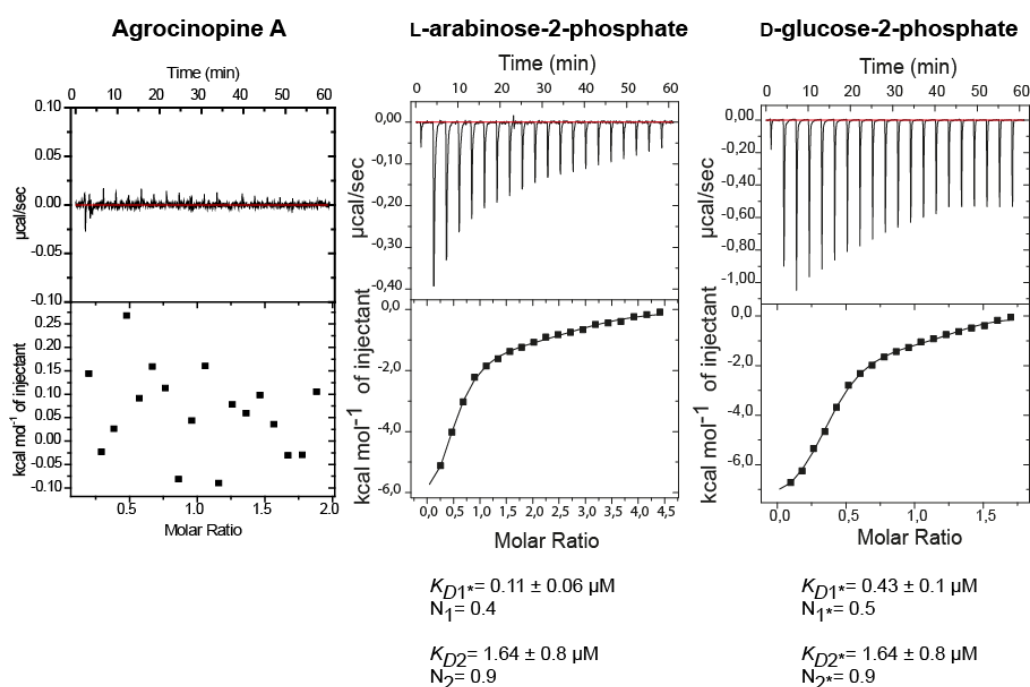


**Fig 28. AccR microcalorimetry measurements.**

The top panels show heat differences upon injection of ligand (L-arabinose-2-phosphate on the left and D- glucose-2-phosphate on the right) and lower panels show integrated heats of injection and the best fit (solid line) using Microcal Origin. Fitting values are indicated below.

### **L-arabinose-2-phosphate and D-glucose-2-phosphate activate the QS and plasmid Ti transfer in *A. tumefaciens* C58**

*In vivo*, the functions of agrocinopine A, L-arabinose-2-phosphate and D-glucose-2-phosphate as QS effectors were examined by measuring the production of QS molecules and efficiency of Ti plasmid transfer in conjugation between *A. tumefaciens* donors and the recipient *A. tumefaciens* C58 which is cured of plasmids (**Fig 29**). Results indicated that all cell cultures supplemented with agrocinopine A, L-arabinose-2-phosphate and D-glucose-2-phosphate accumulate high concentrations of QS molecules (between 50 and 100 nM) compared with mock cultures (less than 1 nM). Consistently, Ti plasmid transconjugants could also be detected in the supplemented cultures, demonstrating that agrocinopine A, L-arabinose-2-phosphate and D-glucose-2-phosphate are activators of the QS pathway of *A. tumefaciens* C58. Finally, because the purified AccR exhibited affinity for L-arabinose-2-phosphate and not for agrocinopine A *in vitro*, and because L-arabinose-2-phosphate activated QS and plasmid Ti conjugation *in vivo*, the hypothesis of the key role of AccF in the maturation of agrocinopine A into L-arabinose-2-phosphate as the efficient activator of QS signal was tested by using an accF defective mutant.<sup>[320]</sup> Remarkably, both accumulation of QS molecules and Ti plasmid conjugation were abolished in the accF mutant supplemented with agrocinopine A, but restored by genetic complementation of accF demonstrating the key role of AccF in QS signaling (**Fig 29**). Moreover, QS signals were still observed in the presence of L-arabinose-2-phosphate in both wild type and accF mutant (**Fig 29**). Altogether, these findings prove that agrocinopine A needs to be degraded into L-arabinose-2-phosphate, whose interaction with the master regulator AccR induces the QS regulation of the conjugative transfer of the Ti plasmid in *A. tumefaciens* C58 cells. The pyranose-2-phosphate motif with L-arabinose-2-phosphate and D-glucose-2-phosphate are the effectors of AccR.

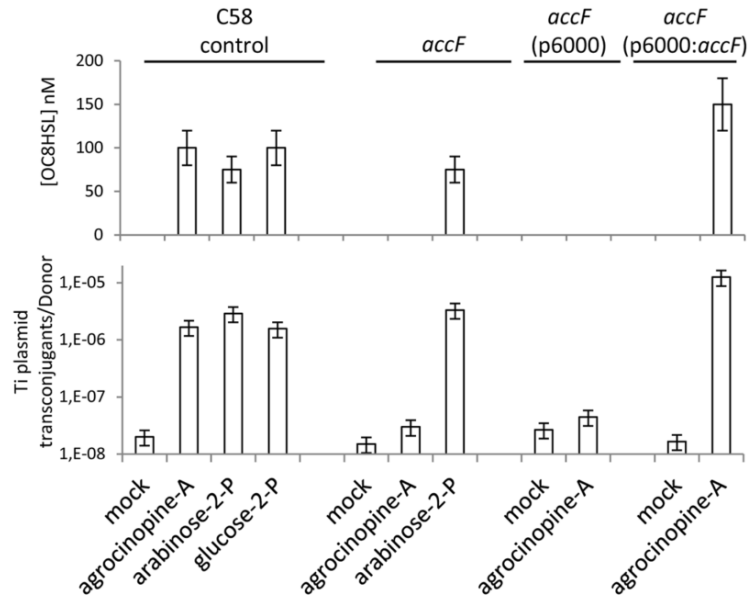


**Fig 29. Quantification of 3-oxo-C8-HSL production and Ti plasmid conjugation induced by agrocinopine A, L-arabinose-2-phosphate and D-glucose- 2-phosphate.**

Different *A. tumefaciens* C58 backgrounds were used as donor cells: C58 control, *accF* mutant, *accF* mutant complemented with p6000: *accF* wild type and *accF* mutant complemented with empty p6000). Results were obtained after 72 h of culture. SDs correspond to physical replicates. Experiments independently repeated between two and four times produce similar results.

For Glucose-2-phosphate L-lactate, it has been observed that its structure is well defined by *AccA* in *A. tumefaciens* C58 cells. The binding mode of G2P-lactate in the active site of *AccA* (with amino-acids (upper) and the surface of the protein (bottom)) as shown in **Fig 30**. The binding mode was obtained from the solved structure of the protein *AccA* bound to G2P lactate. The glucose-2-phosphate appears totally bound to the protein. The binding of the sugar moiety (pyranose) is the same as compared for other structures such as G2P (**Fig 30**). For the experiment of G2PL with *AccF*. The mass of Glucose-2-phosphate L-lactate is 331, verified by us and our colleagues in Gif-sur-Yvette, whereas this mass disappeared after the addition of *AccF* with the buffer containing  $MnCl_2$ . However, *AccF* with the buffer containing  $NaCl$  resulted in 281 mass which could be  $[M+Na^+-H^+]$  of glucose-2-phosphate, and the disappearance of M331 revealed that the G2PL was hydrolyzed by *AccF*, and the appearance

of M281 illustrated that the key motif for AccF binding was glucose-2-phosphate. The kinetics experiments using AccF are on their way.

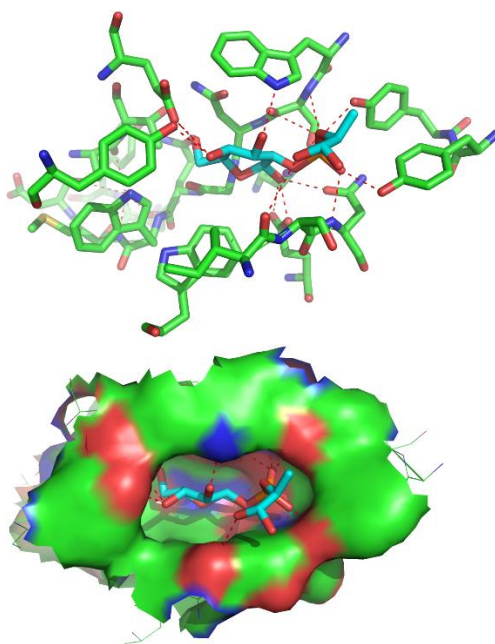


Fig 30. Binding mode of G2P lactate with protein AccA

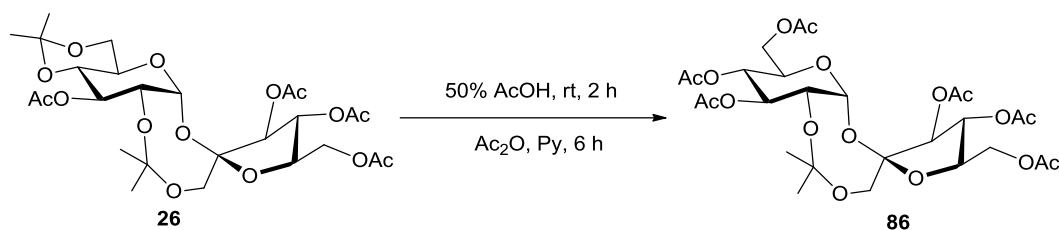
## 4.4 Synthesis and binding properties of agrocinopine C and D

### 4.4.1 Synthesis of agrocinopine C

#### 4.4.1.1 Synthesis of the sucrose fragment

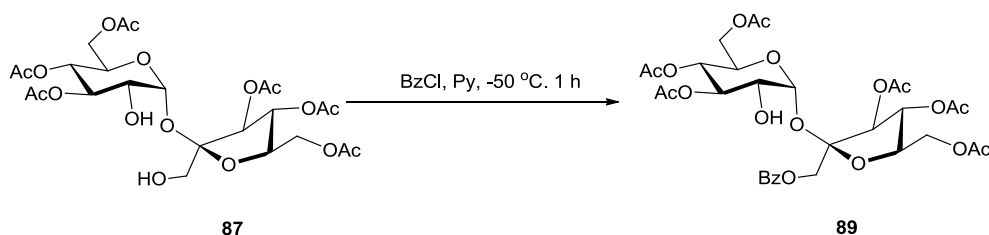
As mentioned in the bibliographic part, the synthesis of agrocinopine C required the preparation of two fragments. The glucose fragment is the same as in the previous section. Below, we focus on two different synthetic strategies for achieving the sucrose fragments, with two possible substituents at 1'-position, a benzoyl group (compound **160**), or an acetyl group (compound **161**) (Scheme 65).





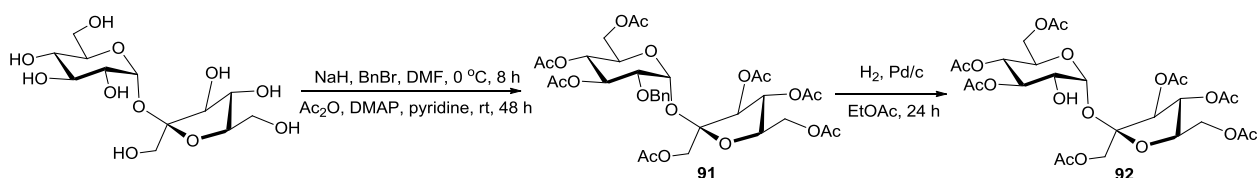
**Scheme 67. Removal of acetal and acetylation of compound 26**

The compound **87** was then obtained by hydrolysis of the remaining acetal in compound **86** under acidic condition, subsequent treatment of compound **87** in the presence of BzCl in pyridine at  $-50\text{ }^{\circ}\text{C}$  afforded the mono-benzoylation<sup>[276]</sup> product **89** in 57% yield. The structure of compound **89** was confirmed by  $^1\text{H-NMR}$ , which revealed a signal at 3.68 ppm due to H-2 de-shielded of a free OH-2, and the overall  $^1\text{H-NMR}$  data was consistent with literature (**Scheme 68**).<sup>[276]</sup>



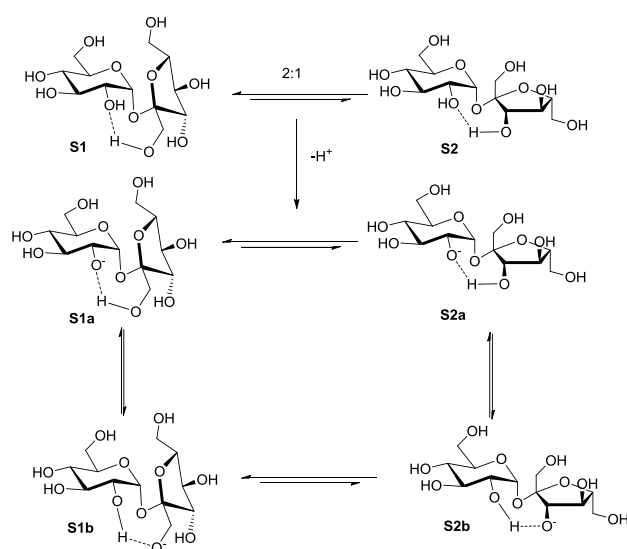
**Scheme 68. Mono-benzoylation of compound 87**

The second strategy is based on a key selective 2-*O*-benzylation of sucrose<sup>[279]</sup>. Treatment of sucrose in the presence of sodium hydride and benzyl bromide in DMF at  $0\text{ }^{\circ}\text{C}$  followed a conventional peracetylation gave compound **91** in 37% yield. Then, debenzoylation was conducted using Pd/C in acetyl acetate under hydrogen atmosphere to afford compound **92** in 90% yield after purification by chromatography and crystallization (**Scheme 69**).



**Scheme 69. Synthesis of compound 92**

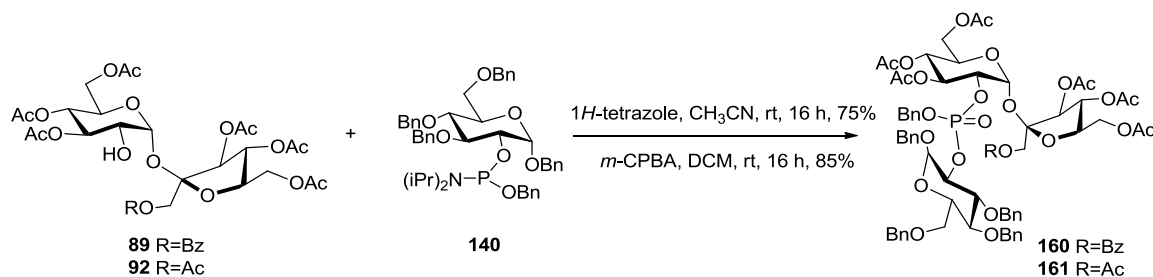
The selective 2-*O*-benzylation at 2-OH is due to the higher acidity of this hydroxyl group compared with the other seven OH, thus, it should be deprotonated firstly under action of base. [279][321–323] In fact, there are three benzylation products (2-*O*-, 1'-*O*-, 3'-*O*-substituted) because of the equilibrium between sucrose conformers. The thermodynamically most stable sucrose mono-alkoxide isomers appear to receive their stabilization by intramolecular hydrogen bonding between the 1'-OH and 2-OH, and, to a lesser extent, between the 3'-OH and the 2-*O*, as indicated in the formulae of **Scheme 70**.



**Scheme 70.** Sucrose in DMF or DMSO, 2:1 equilibrium distribution of conformers S1 and S2<sup>[279]</sup>

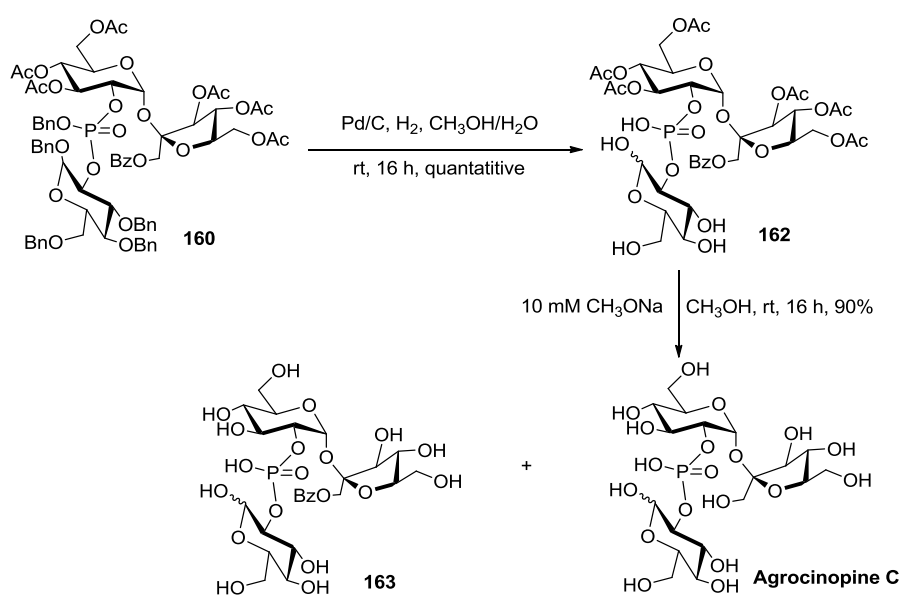
#### 4.4.1.2 Condensation and deprotection

The condensation of compounds **89** and **92** with compound **140** was accomplished in the presence of tetrazole in dichloromethane, followed by oxidation using *m*-CPBA to afford compounds **160** and **161** in 64% and 35% yields respectively (**Scheme 71**).



**Scheme 71.** Condensation of sucrose and glucose fragments

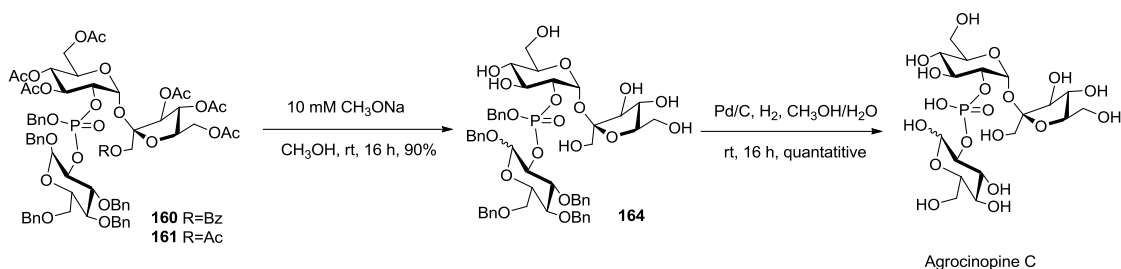
Remembering our experience with respect to deprotection steps for the agrocinopine A synthesis, we first investigated the deprotection order the debenzylation and deacetylation sequence. Firstly, treatment of compound **160** in the presence of Pd/C under hydrogen atmosphere in methanol/water gave the debenzylation product **162** in a quantitative yield, as proved by  $^1\text{H-NMR}$  and mass spectrometry. Then compound **162** was treated with 0.1M sodium methoxide to afford agrocinopine C and another by-product **163** which might be agrocinopine C benzoate. By means of  $^1\text{H-NMR}$ , it was actually suspected that this sequence afforded a mixture of three compounds, in which agrocinopine C was the major product and the benzoyl substituted side-product **163** as well as other unidentified products. Unfortunately, the purification of agrocinopine C from this mixture was proved to be difficult even using C18 and ion exchange chromatography (**Scheme 72**).



**Scheme 72. Debenzylation and deacetylation steps for synthesis of agrocinopine C**

Then, we studied the deprotection sequence in which deacetylation comes first. The deacetylation step gave the pure intermediate **164** (checked by  $^1\text{H-NMR}$ ) which was then used for the next step without further purification. The debenzylation step was accomplished in the presence of Pd/C under hydrogen atmosphere in methanol/water. Agrocinopine C was obtained in 90% yield. TLC (AcOEt/CH<sub>3</sub>OH/CH<sub>3</sub>COOH/H<sub>2</sub>O=9/3/3/2) and  $^1\text{H-NMR}$  proved that this

deprotection order led to much purer agrocinopine C than that of the previous one, although there were still some traces of side products (**Scheme 73**).



**Scheme 73.** Deacetylation and debenylation steps for synthesis of agrocinopine C

Since both methods described above resulted in the presence of side products, the *O*-1(F)-acetylated sucrose precursor **161** was considered for the condensation step instead of the benzoate. After purification and ionization, agrocinopine C was obtained in 90% yield. The structure was characterized by means of  $^1\text{H}$ -NMR and mass spectrometry (**Scheme 73**).

#### 4.4.1.3 Characterization

By means of 2D NMR, agrocinopine C has been fully characterized. It has been found that the anomeric proton of sucrose and of  $\alpha$ -glucose are superimposed and locate at  $\delta$  5.4 ppm with a coupling constant  $J = 3.3$  Hz, but can be differentiated by their carbon shifts which exhibit a minor difference (**Table 6**). The proton and carbon signals of  $\beta$ -anomer were not observed in either  $^1\text{H}$ - or  $^{13}\text{C}$ -NMR, which indicated that the product is likely to be the pure  $\alpha$ -anomer. The partial NMR data is shown in **Table 6**. The coupling of two C-2 with phosphorus is a characteristic of phosphorylation of the C-2 in the two glucose molecules of agrocinopine C. For all other protons and carbons, in general, signals “line up” well with their counterparts in the glucose or sucrose spectrum (**Fig 31**).<sup>[269]</sup>

**Table 6. Partial  $^1\text{H}$ -NMR and  $^{13}\text{C}$ -NMR of agrocinopine C (only  $\alpha$ -anomer in glucosyl)**

Glucose (G')				Glucose moiety in sucrose (G)			
H-1	5.4 ( $J = 3.3$ Hz)	C-1	90.8 ( $J = 4.0$ Hz)	H-1	5.4 ( $J = 3.3$ Hz)	C-1	92.1 ( $J = 4.0$ Hz)
H-2	4.07	C-2	76.4 ( $J = 5.0$ Hz)	H-2	3.70	C-2	71.3 ( $J = 4.5$ Hz)
H-3	3.92 – 3.73	C-3	74.0 ( $J = 6.0$ Hz)	H-3	4.09 – 3.95	C-3	74.4 ( $J = 3.0$ Hz)

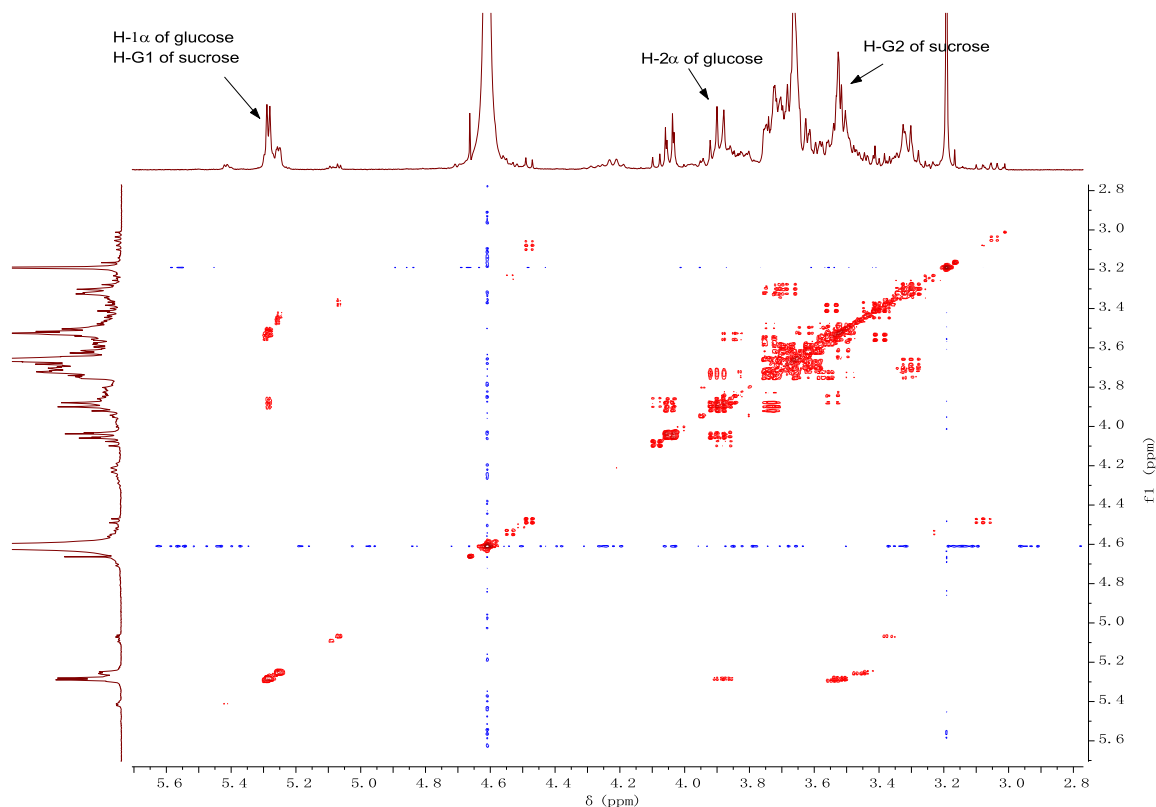


**Fig 31.  $^1\text{H}$ - $^1\text{H}$  correlation of agrocinopine C (400 MHz,  $\text{D}_2\text{O}$ )**

For further verifying the phosphorylation site of sucrose and glucose,  $^1\text{H}$ - $^{31}\text{P}$  correlation NMR was performed. The H-2 $\alpha$  of glucose and H-2G of sucrose correspond to two minor but different phosphorus signals, which indicates that the structure of final compound is D-glucos-2-yl sucros-2-yl phosphate, although there still are some sugar phosphate impurities (**Fig 32**).

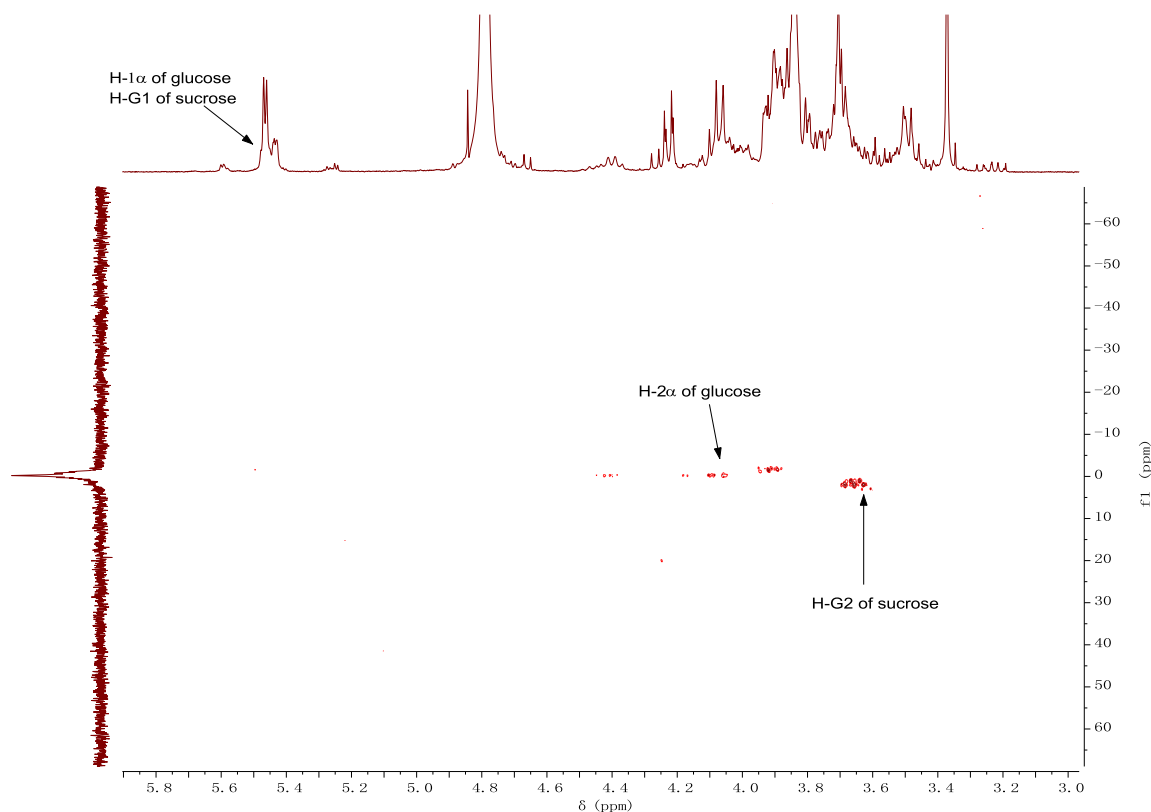
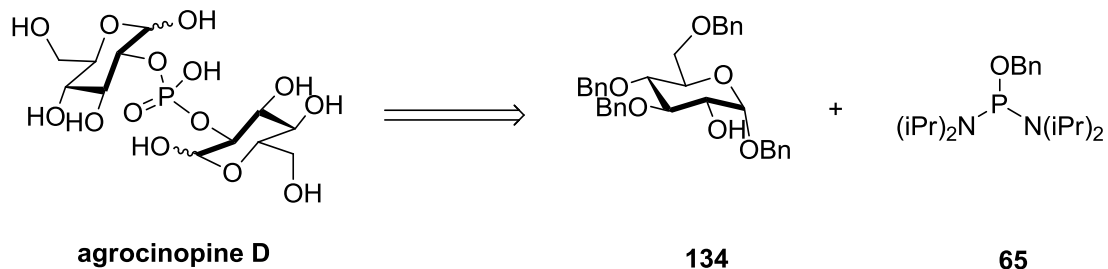


Fig 32.  $^{31}\text{P}$ - $^1\text{H}$  correlation of agrocinopine C (400 MHz,  $\text{D}_2\text{O}$ )

#### 4.4.2 Synthesis of agrocinopine D

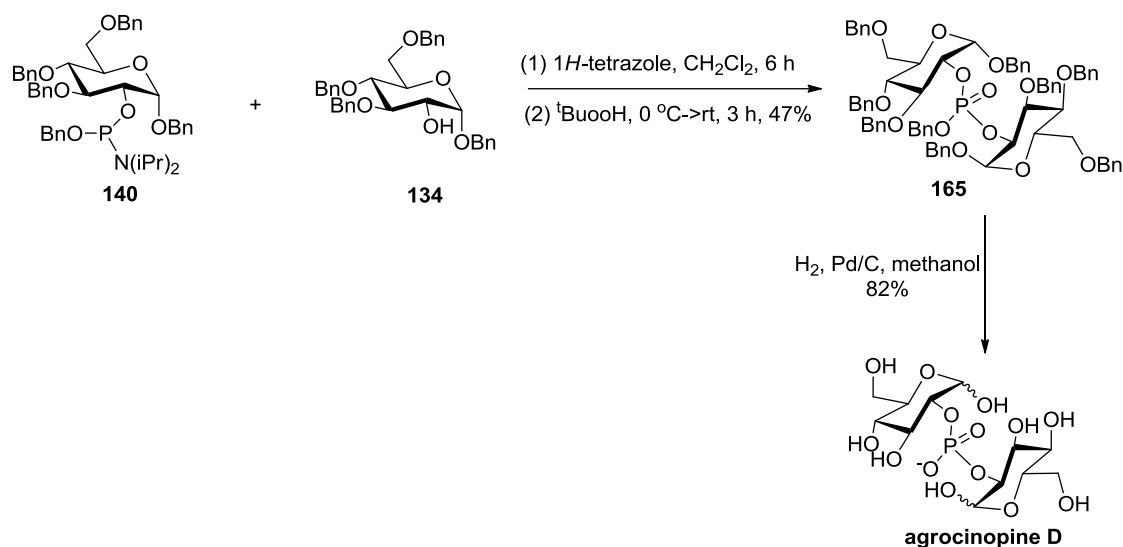
Structurally, agrocinopine D is bis (D-glucos-2-yl) phosphate. Based on the benzyl protective group synthetic strategy used for G2P, it can be obtained from glucose fragment **134** and phosphoramidite **65** (Scheme 74).



Scheme 74. Retrosynthesis of agrocinopine D

#### 4.4.2.1 Condensation and deprotection

The condensation step was accomplished in the same conditions as for G2P and agrocinopine C. Treatment of compound **140** and compound **134** in the presence of tetrazole in dichloromethane afforded the phosphite intermediate, which was oxidized to furnish compound **165** in 47% yield. After hydrogenation and purification, agrocinopine D was obtained as a mixture of anomers ( $\alpha/\beta=2/1$ ), only trace of  $\alpha\beta$  isomer was observed (**Scheme 75**).



**Scheme 75. Synthesis of agrocinopine D**

#### 4.4.2.2 Characterization

With the help of 2D-NMR, agrocinopine D has been fully characterized. <sup>1</sup>H-NMR and <sup>13</sup>C-NMR show almost the same shift and split as G2P, with only minor proton shift to low-field and minor carbon shift to high-field have been observed. The detailed partial NMR data is shown in **Table 7**. The phosphorylation at C-2 was confirmed by the remote coupling of C-1, C-2 and C-3 with phosphorus, shown in the <sup>13</sup>C-NMR spectroscopy (**Fig 33**).

**Table 7. Partial  $^1\text{H}$ -NMR and  $^{13}\text{C}$ -NMR of agrociniopine D**

$\alpha$ -anomer				$\beta$ -anomer			
H-1	5.40 ( $J = 3.0$ Hz)	C-1	90.8 ( $J = 2.0$ Hz)	H-1	4.73 ( $J = 8.0$ Hz)	C-1	95.0 ( $J = 4.0$ Hz)
H-2	4.00	C-2	75.4 ( $J = 6.0$ Hz)	H-2	3.8	C-2	79.0 ( $J = 6.3$ Hz)
H-3	3.67 - 3.90	C-3	71.6 ( $J = 6.0$ Hz)	H-3	3.70-3.61	C-3	75.1 ( $J = 3.0$ Hz)

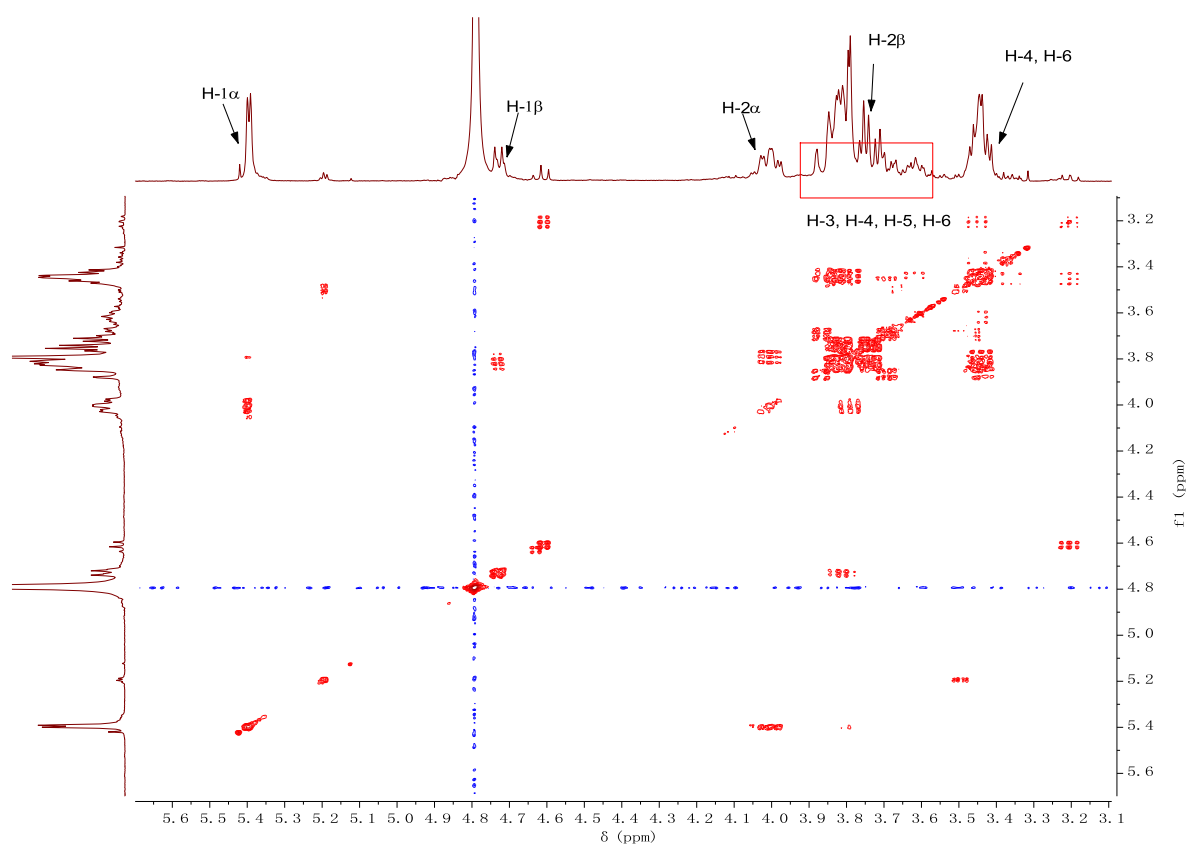


**Fig 33.  $^1\text{H}$ - $^1\text{H}$  correlation of agrociniopine D**

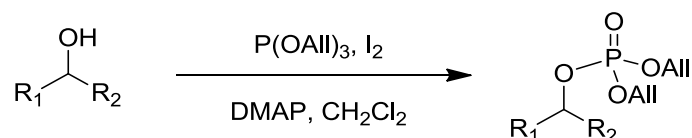
#### 4.4.3 Biological Results for agrocinopine C and D

The biological investigation is still in progress. Preliminary information is that AccA binds agrocinopine D, though the XRD experiment is difficult to analyze. Whereas one glucose seems clearly being fixed in the binding site, therefore showing clear electronic densities, the structure could not be totally resolved, the second glucose not being clearly localized. We are currently elaborating hypothesis regarding these first observations. In agrocinopine A or agocin 84, only pyranose-2-phosphate moiety is precisely bound, and the other part of the molecule is less well localized. This could be the same for agrocinopine D, in which one glucose is bound, like in agrocinopine A and agocin 84, and the other showing a much less fixed scheme, possibly a mixture of pyranose and furanose forms. For agrocinopine C, structural experiments are still to be scheduled.

## 4.5 A convenient phosphorylation method using triallyl phosphite

### 4.5.1 Introduction

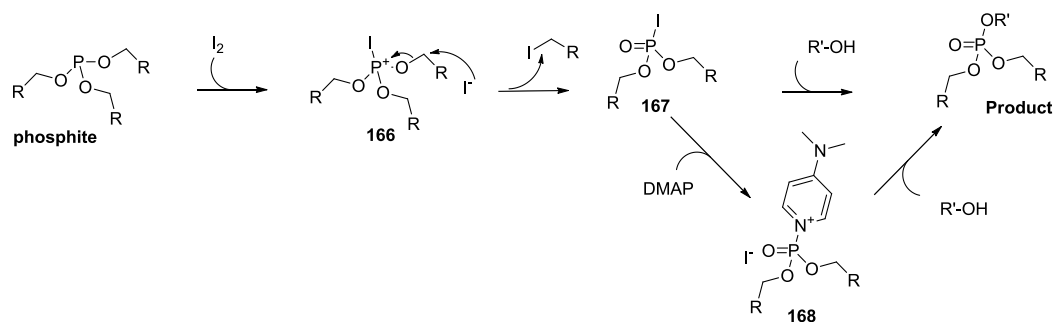
As shown in the section on the synthesis of glucose-2-phosphate, we initially proposed the phosphorylation of compound **134** using tribenzyl phosphite, but it did not work. However, when *p*-cresol was used as substrate, or triethyl phosphite was used as phosphorylation reagents, it gave us some promising results. Inspired by these results, as well as considering the wide use of the allyl protecting group in peptide<sup>[324,325]</sup>, nucleoside<sup>[326][327]</sup>, and total synthesis<sup>[328]</sup>, as well as several advantages such as mild deprotection condition, commercial availability and so on, we developed a convenient, direct method using triallyl phosphite towards allyl phosphorylated alcohols, phenols, nucleosides and glucosides (**Scheme 76**).



**Scheme 76.** General scheme of phosphorylation method using triallyl phosphite

### 4.5.2 Optimization of phosphorylation conditions

The method is a phosphite/iodine phosphorylation, which is based on a proposed mechanism described in the following: first, an Arbuzov reaction of alkyl phosphite with iodine<sup>[329]</sup> leading to the formation of the corresponding dialkyl phosphoriodidate **167**, then reaction with alcohols or phenols directly or via its reaction in pyridine, as initially described<sup>[330,331]</sup>. DMAP can also be used, as shown by Soulère et al.<sup>[332]</sup>, with triethylphosphite leading to the production of 1-(bis(alkyl)phosphoryl)-4-(dimethylamino)pyridin-1-ium **168** (**Scheme 77**).<sup>[331]</sup>



**Scheme 77.** Proposed mechanism of phosphorylation using phosphite:

the dialkyl phosphoriodidate **167** and the 4-(dimethylamino)pyridin-1-ium **168** are the reactants for the phosphorylation process<sup>[329–331]</sup>

To screen several reaction conditions, benzyl alcohol was used as a model primary alcohol and *p*-cresol as a model phenol, respectively. We then examined the influence of temperatures, (0 °C, -10 °C, -30 °C or RT) and of different amounts of iodine (1 or 2 equiv) and triallyl phosphite (1.2 or 2.2 equiv). The phosphite was always used in excess to ensure complete consumption of iodine (**Table 8**). The reaction was efficient, with comparable yields for both alcohols at 0 °C, -10 °C, -30 °C or RT. As expected, the yields of diallyl *p*-tolyl phosphate **183** and diallylbenzylphosphate **184** increased in both cases when 2 equivalents of the phosphorylating agent were used.

**Table 8. Conditions for the phosphorylation of *p*-cresol and benzyl alcohol**

Alcohols	Conditions	Yields %
<i>p</i> -cresol	P(OAll) <sub>3</sub> (1.2 equiv), I <sub>2</sub> (1 equiv), DMAP (1 equiv), RT	52
<i>p</i> -cresol	P(OAll) <sub>3</sub> (1.2 equiv), I <sub>2</sub> (1 equiv), DMAP (1 equiv), 0 °C	52
<i>p</i> -cresol	P(OAll) <sub>3</sub> (1.2 equiv), I <sub>2</sub> (1 equiv), DMAP (1 equiv), -10 °C	49
<i>p</i> -cresol	P(OAll) <sub>3</sub> (1.2 equiv), I <sub>2</sub> (1 equiv), DMAP (1 equiv), -30 °C	47
<i>p</i> -cresol	P(OAll) <sub>3</sub> (1.2 equiv), I <sub>2</sub> (1 equiv), DMAP (1 equiv), 0 °C	75
Benzyl alcohol	P(OAll) <sub>3</sub> (1.2 equiv), I <sub>2</sub> (1 equiv), DMAP (1 equiv), RT	75
Benzyl alcohol	P(OAll) <sub>3</sub> (1.2 equiv), I <sub>2</sub> (1 equiv), DMAP (1 equiv), 0 °C	75
Benzyl alcohol	P(OAll) <sub>3</sub> (1.2 equiv), I <sub>2</sub> (1 equiv), DMAP (1 equiv), -10 °C	75
Benzyl alcohol	P(OAll) <sub>3</sub> (1.2 equiv), I <sub>2</sub> (1 equiv), DMAP (1 equiv), -30 °C	73
Benzyl alcohol	P(OAll) <sub>3</sub> (1.2 equiv), I <sub>2</sub> (1 equiv), DMAP (1 equiv), 0 °C	82

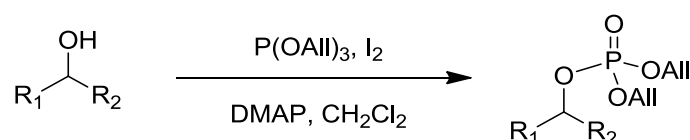
In a typical experiment for the phosphorylation of benzyl alcohol, iodine (2 equiv) was added at 0 °C to a solution of triallyl phosphite (2.2 equiv) in anhydrous DCM (5 mL). After 10 min at 0 °C, the solution was warmed up to room temperature and added, drop-wise, to a solution of benzyl alcohol (0.5 mmol) and DMAP (2 equiv) in anhydrous DCM (5 mL) at RT.

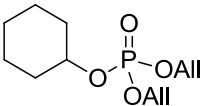
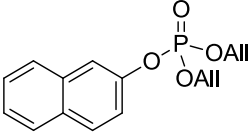
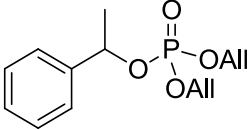
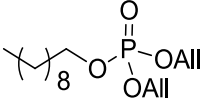
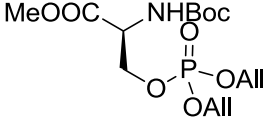
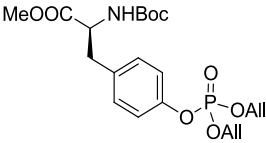
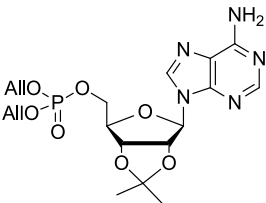
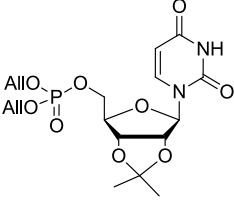
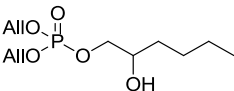
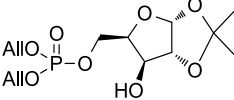
After 4 h, the solution was diluted with DCM and washed with saturated NaHSO<sub>4</sub>, saturated NaHCO<sub>3</sub> and brine. The organic layer was dried over Na<sub>2</sub>SO<sub>4</sub> and evaporated under reduced pressure. The diallylbenzylphosphate was purified by flash chromatography and characterized by standard analytical procedures.

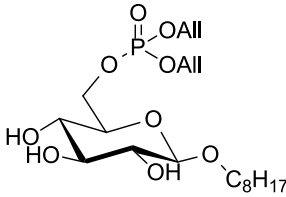
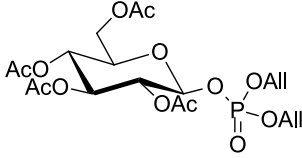
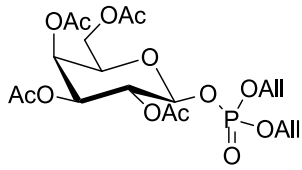
### 4.5.3 Scope of the reaction

The scope of the reaction was investigated using various alcohols, including secondary and functionalized alcohols such as BocSerOMe, BocTyrOMe, 2',3'-isopropylideneadenosine and 2',3'-isopropylideneuridine. We also used 1,2-hexanediol, 1,2-*O*-isopropylidene- $\alpha$ -D-xylofuranose and octyl  $\beta$ -D-glucopyranoside as polyols to examine the selectivity towards primary alcohols (**Table 9**). The phosphorylation reaction was less effective on secondary alcohols, such as cyclohexanol or  $\alpha$ -methylbenzyl alcohol, with 39 and 42% yields respectively (entry 1 and 3). For all other alcohols, the reaction was found to be efficient with yields ranging from 62 to 98%. As shown for the reaction with tribenzyl phosphite,<sup>[331]</sup> the reaction proved to be selective for primary alcohols with good to excellent yields when conducted on 1,2-hexanediol, 1,2-*O*-isopropylidene- $\alpha$ -D-xylofuranose and octyl  $\beta$ -D-glucopyranoside. Most reactions were performed using the conditions optimized for benzyl alcohol (2.2 equiv of phosphite, 2 equiv of iodine, 2 equiv of DMAP, DCM). However, some substrates required alternative conditions, such as the nucleosides (entries 7 and 8) which were dissolved in THF instead of DCM and for which a larger excess of DMAP was required to obtain an acceptable yield. The reaction was finally applied to 2,3,4,6-tetra-*O*-acetyl-D-glucopyranose and galactopyranose (entry 12 and 13, **Table 9**) leading, selectively, to the corresponding  $\beta$ -phosphates with similar selectivity, yields and conditions (7.8 equiv of phosphite, 10 equiv of DMAP) to those recently reported by Vincent and co-workers, who used diallyl chlorophosphate as the phosphorylation agent.<sup>[333]</sup>

**Table 9. Phosphorylation of various alcohols using triallyl phosphite**

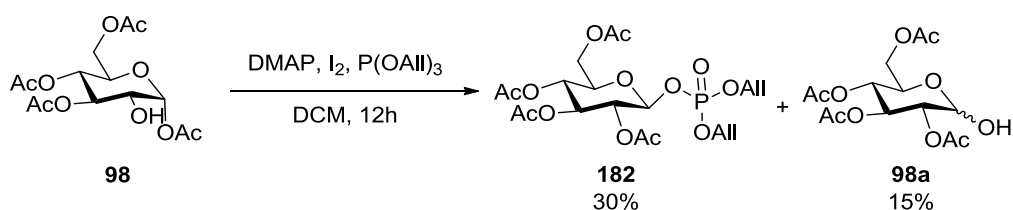


Entry	Alcohols	Products <sup>a</sup>	Yields (%)
1 (169)	cyclohexanol		39
2 (170)	2-naphtol		98
3 (171)	$\alpha$ -Methylbenzyl alcohol		42
4 (172)	Decan-1-ol		94
5 (173)	BocSerOMe		64
6 (174)	BocTyrOMe		77
7 <sup>b</sup> (175)	2',3'-isopropylidene adenosine		62
8 <sup>b</sup> (176)	2',3'-isopropylidene uridine		68
9 (177)	1,2-Hexanediol		72
10 (178)	1,2-O-isopropylidene- $\alpha$ -D-xylofuranose		67

11 ( <b>179</b> )	Octyl β-D-glucopyranoside		67
12 <sup>c</sup> ( <b>180</b> )	2,3,4,6-tetra-O-acetyl-D-glucopyranose		73
13 <sup>c</sup> ( <b>181</b> )	2,3,4,6-tetra-O-acetyl-D-galactopyranose		55

- a. All reactions were conducted using the standard procedure except for nucleosides and the synthesis of β-glycosyl-1-phosphates: triallyl phosphite (2.2 equiv), I<sub>2</sub> (2 equiv) and DMAP (2 equiv), DCM as solvent.
- b. Nucleosides were dissolved with DMAP (4 equiv) in THF and the phosphorylating agent prepared in DCM was added at -30 °C. The reaction was stirred overnight at RT.
- c. For the synthesis of β-glycosyl-1-phosphates, triallyl phosphite (7.8 equiv), I<sub>2</sub> (7.5 equiv) and DMAP (10 equiv) were used according to the standard procedure. The reaction was stirred overnight at RT.

Interestingly, when compound **98** bearing a vacant OH-2 was used for phosphorylation by this method, no 2-substituted diallyl phosphate was observed, instead, the 1-substituted diallyl phosphate **182** was obtained as a major product and compound **98a** was a side product with a small quantity of starting material. We speculated that the acetyl group migration process appeared during the activation of hydroxyl under basic conditions such as DMAP (**Scheme 78**).



**Scheme 78. Phosphorylation of compound 98 using triallyl phosphite**

To further investigate the solvent scope of the reaction, the phosphorylation was performed on solutions of benzyl alcohol in THF, pyridine, acetonitrile, DMF and DMSO, in the presence

of DMAP (except for pyridine). The phosphorylating agent was prepared in anhydrous DCM, as described above. These reactions showed that DCM, pyridine and acetonitrile were all appropriate solvents, with yields of approximately 80%, thus widening the choice when substrates are not soluble enough in DCM (Table 10).

**Table 10: Phosphorylation of benzyl alcohol in various solvents.<sup>a</sup>**

<b>R</b>	<b>Solvents</b>	<b>Yield %</b>
Bn-OH	DCM	<b>82</b>
	THF	56
	Pyridine <sup>b</sup>	<b>84</b>
	Acetonitrile	<b>85</b>
	DMF	41
	DMSO	24

a. All reactions were conducted with triallyl phosphite (2.2 equiv), I<sub>2</sub> (2equiv) and DMAP (2 equiv) at RT. The solution of the phosphorylation reagent was prepared in DCM. b. Without DMAP.

In summary, a convenient direct phosphorylation method towards allyl-protected phosphorylated compounds from triallylphosphite was established. The method was applied to simple primary and secondary alcohols, as well as to more complex substrates, such as nucleosides or carbohydrate derivatives. Diols or polyols possessing both primary and secondary alcohol functions can be selectively phosphorylated at their primary position.

#### 4.6 Conclusion

On the basis of various synthetic strategies towards glucose, arabinose and sucrose building blocks, we succeeded in developing a general method for synthesizing agrocinopine A and several analogues. Most importantly, with the aids of these agrocinopine derivatives and analogues, we contributed to elaborating the mechanism by which the periplasmic protein AccA from the pathogen *A. tumefaciens* can bind both the pyranose-2-phosphate-like moiety shared by plant compound agrocinopine and the antibiotic agrocin 84. Namely, as a key recognition template for AccA, the importation of any compound possessing a pyranose-2-phosphate motif is charged by AccA. Furthermore, arabinose-2-phosphate and glucose-2-phosphate, resulting

from the cleavage of agrocinopine and agrocin 84 respectively by AccF, is proved to be the effector of the transcriptional repressor AccR, that controls QS and virulence plasmid dissemination. Therefore, we identified that the key role of the pyranose-2-phosphate moiety of agrocinopine is responsible for both its recognition by transport proteins and the QS regulation, it opens a new insight for developing new approaches fighting against bacterial infections.

In addition, a direct method for the phosphorylation of alcohols, phenols, saccharides and nucleosides using triallyl phosphite is described. The method was found to be selective for primary alcohols and to be applicable to diverse simple and functionalized alcohols, containing amino acids, carbohydrates and nucleosides moieties.



## General conclusion

This thesis has elaborated two different aspects of the chemistry of QS. The first part contributed to the design, synthesis and evaluation of novel QS inhibitors, with various structure-properties relationships investigations for Acyl Homoserine Lactones (AHLs) close analogues (focusing notably on the influence of the chirality of homoserine lactone or the replacement of the central amide group by heterocyclic scaffolds), and some AHL structurally unrelated compounds. With respect to AHL chirality, we confirmed that the L-isomer is always the only or at least the most active enantiomer. However, through this first systematic study of the influence of chirality, we also demonstrated that in several cases, (mostly for very close AHL analogues) the D- isomer should not be considered as totally inactive on QS. Moreover, this activity was found to be either activation or inhibition. Modelling showed that when possible, the lactone moiety of the D-isomer could twist in the way the lactone carbonyl group would still interact with the key residues in the binding site. With respect to the imitation of the amide function by heterocyclic scaffolds, the work revealed that 2,5- and 3,5-disubstituted oxadiazoles and triazoles could not serve as potential platform for designing QS inhibitors. This work still must be completed with 1,5-disubstituted systems which could be better candidates if analogy is made with tetrazolic series previously studied. For reaching some of these compounds, we elaborated a new “late-lactone-construction” strategy which will be of general usefulness for future series. Finally, a series of nitroaniline compounds was investigated indicating that a rather structurally simple substituted aromatic system may serve as non-hydrolysable scaffold for designing LuxR inhibitors.

The second part investigated the role of carbohydrate phosphodiester and phosphates in QS regulation in *Agrobacterium tumefaciens*. Specifically, a series of analogues of agrocinopine A have been synthesized based on several strategies, and their binding properties with AccA, as well as their biological role in *Agrobacterium tumefaciens* have been established. This part identified the pyranose-2-phosphate-like moiety as the key recognition template for AccA.

Arabinose-2-phosphate, resulting from the cleavage of agrocinopine by AccF, glucose-2-phosphate, resulting from the cleavage of agrocin 84, were proved to be effectors of the transcriptional repressor AccR, which controls QS and virulence plasmid propagation. Overall, through an interdisciplinary approach, we could identify an original and specific key pyranose-2-phosphate motif that not only allows selective passage of active compounds into the pathogen cells, but also, once these compounds are cleaved, keeps to the matured products their ability to act as signals. This work opens up new opportunities to rationally design novel strategies for entering into pathogens and delivering various chemical species

Overall, this thesis is the combination of two synthetic organic chemistry studies, both relating to QS, both aimed at improving basic knowledge on biological processes in bacteria. ultimately contributing to innovative strategies useful in plant and human health, notably through the design of new antibacterial agents.

# **Experimental section**



## General

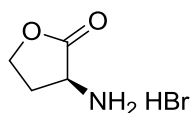
Reagents and solvents were supplied by Aldrich, Acros, Lancaster, Alfa Aesar, Fluka or TCI and purchased to be used without further purification. NMR spectra were recorded on a Bruker 300 MHz ( $^1\text{H}$ : 300 MHz;  $^{13}\text{C}$ : 75 MHz), Bruker 400 MHz ( $^1\text{H}$ : 400 MHz;  $^{13}\text{C}$ : 100 MHz), or Bruker 500 MHz ( $^1\text{H}$ : 500 MHz;  $^{13}\text{C}$ : 125 MHz) spectrometers, at 215-298K, using  $\text{CDCl}_3$ ,  $\text{CD}_3\text{OD}$  and  $\text{DMSO-d}_6$  or  $\text{D}_2\text{O}$  as solvents. The chemical shifts (ppm) are referenced to the solvent residual peak and coupling constants are reported in Hz. The following abbreviations are used to explain the multiplicities: s = singlet, d = doublet, t = triplet, q = quartet, quint. = quintuplet, sext. = sextuplet, hept. = heptuplet, m = multiplet, br = broad. Electrospray ionization (ESI) mass spectrometry (MS) experiments were performed on a Thermo Finnigan LCQ Advantage mass. High-resolution mass spectra (HRMS) were recorded on a Finnigan Mat 151xL mass spectrometer using electrospray. Analytical thin-layer chromatography was carried out on silica gel Merck 60 D254 (0.25 mm). Flash chromatography was performed on Merck Si 60 silica gel (40–63  $\mu\text{m}$ ). Optical rotations were measured on a Perkin Elmer 241 or Jasco P1010 polarimeter with a 10 cm cell (concentration  $c$  expressed as g/100 mL). Chiral HPLC was performed on DAICEL ADH Chiralpak column, and UV (220 nm) for detector.

## Binding mode studies

Docking experiments were performed with the docking module of ArgusLab. The protein model of LuxR<sup>[175]</sup> was created using SWISS-MODEL<sup>[334]</sup> with ClustalW.<sup>[335]</sup> The binding mode of OHHL was obtained according to the method described by Estephane and co-workers.<sup>[61]</sup> Docking experiments were performed with the following parameters: Docking box:  $X = Y = Z = 15 \text{ \AA}$ , ligand option: flexible; calculation type: Dock; Docking engine: GADock (Genetic Algorithm);<sup>[173]</sup> Genetic algorithm dock settings: default advanced parameters; hydrogen bonds were assigned within a distance of 3  $\text{Å}$ .

## Part I. Supplementary information

### L-Homoserine lactone hydrobromide (L-133)

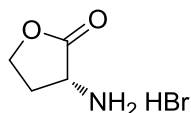


L-133

A mixture of bromoacetic acid (3 g, 21.6 mmol) and L-methionine (2.92 g, 19.6 mmol) in 40 mL of a 2-propanol-H<sub>2</sub>O-AcOH mixture (5:5:2, v/v) was refluxed for 9 h with TLC monitoring (DCM/methanol = 4/1, R<sub>f</sub> = 0.55). The solvent was then removed under reduced pressure to afford a sticky oil, further drying using a vacuum pump to give a beige semi-solid. It was dissolved in 30 mL of a 4/1 (v/v) mixture of 2-propanol/HBr (33% in AcOH). The product was collected as a pink solid by filtration and the purification procedure repeated starting from evaporation of the orange filtrate to dryness. Compound was collected as a pink powder after drying of both portions in vacuo (m=2.77 g, 78%),

<sup>1</sup>H NMR (300 MHz, Deuterium Oxide) δ 4.61 (t, *J* = 9.2 Hz, 1H, CH-NH<sub>2</sub>), 4.54 – 4.34 (m, 2H, CH-O), 2.85 – 2.75 (m, 1H, CH), 2.51 – 2.36 (m, 1H, CH). [ $\alpha$ ]<sub>D</sub><sup>22</sup> = -15.8(c=1, H<sub>2</sub>O).

### D-Homoserine lactone hydrobromide (D-133)



D-133

A mixture of bromoacetic acid (8.15 g, 59.1 mmol) and D-methionine (8.0 g, 53.7 mmol) in 75 mL of a 2-propanol-H<sub>2</sub>O-AcOH mixture (5:5:2, v/v) was refluxed for 9h with TLC monitoring (DCM/methanol = 4/1, R<sub>f</sub> = 0.55). The solvent was then removed under reduced pressure to afford a sticky oil, further drying using a vacuum pump to give a beige semi-solid. It was dissolved in 40 mL of a 4/1 (v/v) mixture of 2-propanol/HBr (33% in AcOH). The product was collected as a pink solid by filtration and the purification procedure repeated starting from evaporation of the orange filtrate to dryness. Compound was collected as a pink powder after drying of both portions in vacuo (m = 8.62 g, 89%),

<sup>1</sup>H NMR (300 MHz, Deuterium Oxide) δ 4.63 (t, *J* = 9.3 Hz, 1H, CH-NH<sub>2</sub>), 4.54 – 4.39 (m, 2H, CH-O), 2.86 – 2.77 (m, 1H, CH), 2.53 – 2.42 (m, 1H, CH). [ $\alpha$ ]<sub>D</sub><sup>22</sup> = +16.2(c=1, H<sub>2</sub>O).

## General procedure for the synthesis of acyl homoserine lactone analogues

### Procedure A<sup>[145]</sup>:

To a solution of L/D-Homoserine lactone hydrobromide in 10.0 mL of dichloromethane was added 1.2 equivalent of acyl chloride and 2.2 equivalent of triethylamine at 0 °C. The reaction mixture was stirred under ice-bath for 30 min, and then was warmed up to room temperature and stirred for additional 3h until the starting material was consumed. Then 20 mL of 2 M HCl solution was poured into the reaction medium and the mixture was stirred for 10 min. The organic layer was separated and the aqueous layer was washed with dichloromethane (10 mLx2), the organic layers was combined together and dried over MgSO<sub>4</sub>, evaporated and further purified by chromatography column (pentane/AcOEt) to afford final product as a solid.

### Procedure B:

The acyl chloride was dissolved in 5.0 mL of anhydrous dichloromethane and added dropwise at room temperature to a rigorously stirred mixture of L/D-Homoserine lactone hydrobromide and Na<sub>2</sub>CO<sub>3</sub> in 5.0 mL H<sub>2</sub>O. The reaction mixture was stirred rigorously at room temperature for 2h with TLC monitoring (pentane/AcOEt). Then 10 mL CH<sub>2</sub>Cl<sub>2</sub> was poured into the reaction and the organic layer was separated, the aqueous layer was washed with dichloromethane (20 mLx2), the organic layer was combined together and washed with sat. NaHCO<sub>3</sub> solution (2x40 mL), dried over MgSO<sub>4</sub>, evaporated and further purified by chromatography column (pentane/AcOEt) to afford final product as a solid.

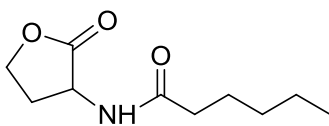
### Procedure C:

To a solution of 4-phenylbutanoic acid (1 g, 6.1 mmol) in 30 mL of anhydrous dichloromethane was added oxalyl dichloride (1.55 g, 12.2 mmol) dropwise at room temperature under argon, the reaction mixture was stirred for 2h, the solvent and excess oxalyl dichloride were removed under reduced pressure and the crude 4-phenylbutanoyl chloride was used for next step without further purification.

### Procedure D:

To a solution of L/D-Homoserine lactone hydrobromide and diisopropylamine in 15 mL dichloromethane was added acyl chloride dropwise at 0 °C. The reaction was stirred at 0 °C for 30 min and then warmed up to room temperature for 6h. Then the reaction mixture was diluted in 20 mL dichloromethane and 40 mL water, the organic layer was separated and the aqueous layer was washed with dichloromethane (20 mLx2), the organic layers was combined together and dried over MgSO<sub>4</sub>, evaporated and further purified by chromatography column (pentane/AcOEt) to afford final product as a solid.

(S)/(R)-*N*-(2-oxotetrahydrofuran-3-yl)hexanamide (L-134, D-134)



L-134, D-134

Following the procedure A, L- and D- enantiomers were obtained by using hexanoyl chloride (0.267 g, 2 mmol), L/D-Homoserine lactone hydrobromide (0.3 g, 1.66 mmol) and triethylamine (0.37 g, 3.65 mmol), as a white solid in 74% (L: 0.244 g) and 73% (D: 0.240 g) yield after purification by flash chromatography column (pentane/AcOEt = 2/3).

Following the procedure B, L- and D- enantiomers were obtained by using hexanoyl chloride (0.173 g, 1.3 mmol), L/D-Homoserine lactone hydrobromide (0.3 g, 1.66 mmol) and Na<sub>2</sub>CO<sub>3</sub> (0.35 g, 3.32 mmol), as a white solid in 84% (L: 0.213 g) and 94% (D: 0.240 g) yields after purification by flash chromatography column (pentane/AcOEt = 2/3).

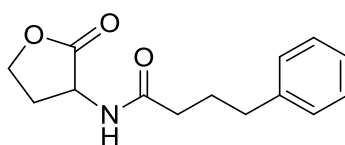
**<sup>1</sup>H NMR (300 MHz, Chloroform-*d*)** δ: 6.03 (s, 1H, NH), 4.60 – 4.51 (m, 1H, CH-O-lactone), 4.51 – 4.43 (m, 1H, CHNH), 4.34 – 4.22 (m, 1H, CH-O-lactone), 2.94 – 2.78 (m, 1H, CH<sub>2</sub>-lactone), 2.29 – 2.21 (m, 2H, CH<sub>2</sub>-CO), 2.21 – 2.03 (m, 1H, CH<sub>2</sub>-lactone), 1.71 – 1.57 (m, 2H, CH<sub>2</sub>), 1.31 (dt, *J* = 7.4, 3.7 Hz, 4H, 2CH<sub>2</sub>), 0.97 – 0.78 (m, 3H, CH<sub>3</sub>).

Procedure A: L-enantiomer  $[\alpha]_D^{22} = +15.0$  (c=1, CHCl<sub>3</sub>), D-enantiomer  $[\alpha]_D^{22} = -15.0$  (c=1, CHCl<sub>3</sub>).

Procedure B: L-enantiomer  $[\alpha]_D^{22} = +14.6$  (c=1, CHCl<sub>3</sub>), D-enantiomer  $[\alpha]_D^{22} = -14.7$  (c=1, CHCl<sub>3</sub>).

Chiral HPLC: 93:7 heptane/isopropanol, flow 1 mL/min; retention times: racemic 26.85 min and 29.28 min, L-enantiomer 27.3 min, D-enantiomer, 29.59 min.

(S)/(R)-*N*-(2-oxotetrahydrofuran-3-yl)-4-phenylbutanamide (L-135, D-135)



L-135, D-135

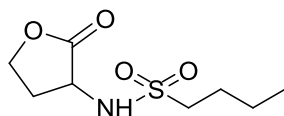
Following the procedure A, L- and D- enantiomers were obtained by using 4-phenylbutanoyl chloride which was prepared according to general procedure C, L/D-Homoserine lactone hydrobromide (0.23 g, 1.27 mmol) and trimethylamine (0.28 g, 2.8 mmol) as a white solid in 83% (L: 0.260 g) and 78% (D: 0.243 g) yields after purification by flash chromatography column (pentane/AcOEt = 1/4).

**<sup>1</sup>H NMR (300 MHz, Chloroform-*d*)** δ: 7.30 – 7.16 (m, 6H, Phenyl-H), 6.19 (s, 1H, NH), 4.62 – 4.49 (m, 1H, CH-O-lactone), 4.44 (t, *J* = 8.9 Hz, 1H, CH-NH), 4.33 – 4.20 (m, 1H, CH-O-lactone), 2.80 (dd, *J* = 11.4, 6.6 Hz, 1H, CH<sub>2</sub>-lactone), 2.65 (t, *J* = 7.4 Hz, 2H, CH<sub>2</sub>-CO), 2.25 (t, *J* = 7.4 Hz, 2H, CH<sub>2</sub>-Ph), 2.18 – 2.06 (m, 1H, CH<sub>2</sub>-lactone), 2.03 – 1.92 (m, 2H, CH<sub>2</sub>).

L-enantiomer  $[\alpha]_D^{22} = +8.5$  (c=0.67, CHCl<sub>3</sub>), D-enantiomer  $[\alpha]_D^{22} = -8.5$  (c=0.67, CHCl<sub>3</sub>).

Chiral HPLC: 85:15 heptane/isopropanol, flow 1 mL/min; retention times: racemic 17.07 min and 20.08 min, L-enantiomer 19.32 min, D-enantiomer, 16.93 min.

**(S)/(R)-N-(2-oxotetrahydrofuran-3-yl)butane-1-sulfonamide (L-136, D-136)**



**L-136, D-136**

Following the procedure A, L- and D- enantiomers were obtained by using 1-butanefulfonyl chloride (0.31 g, 2 mmol), L/D-Homoserine lactone hydrobromide (0.3 g, 1.66 mmol) and trimethylamine (0.37 g, 3.65 mmol), as a white solid in 64% (L: 0.234 g) and 76% (D:0.278 g) yield after purification by flash chromatography column (pentane/AcOEt = 2/1).

Following the procedure B, L- and D- enantiomers were obtained by using 1-butanefulfonyl chloride (0.2 g, 1.28 mmol), L/D-Homoserine lactone hydrobromide (0.3 g, 1.66 mmol) and Na<sub>2</sub>CO<sub>3</sub> (0.35 g, 3.32 mmol), as a white solid in 53% (L: 0.15 g) and 64% (D:0.18 g) yield after purification by flash chromatography column (pentane/AcOEt=2/1).

Following the procedure D, L- and D- enantiomers were obtained by using 1-butanefulfonyl chloride (0.312 g, 2 mmol), L/D-Homoserine lactone hydrobromide (0.3 g, 1.66 mmol) and diisopropylamine (0.472 g, 3.65 mmol) as a white solid in 33% (L: 0.121 g) and 27% (D: 0.10 g) yield after purification by flash chromatography column (pentane/AcOEt=2/1).

**<sup>1</sup>H NMR (300 MHz, Chloroform-*d*)** δ: 5.04 (s, 1H, NH), 4.45 (t, *J* = 8.9 Hz, 1H, CH-NH), 4.39 – 4.18 (m, 2H, CH<sub>2</sub>-O-lactone), 3.29 – 3.07 (m, 2H, CH<sub>2</sub>), 2.76 (m, 1H, CH<sub>2</sub>-lactone), 2.39 – 2.15 (m, 1H, CH<sub>2</sub>-lactone), 1.96 – 1.74 (m, 2H, CH<sub>2</sub>), 1.47 (q, *J* = 7.4 Hz, 2H, CH<sub>2</sub>), 0.96 (t, *J* = 7.3 Hz, 3H, CH<sub>3</sub>).

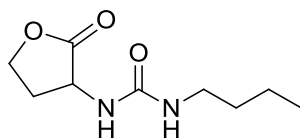
Procedure A: L-isomer  $[\alpha]_D^{22} = -9.3$  (c=0.33, CHCl<sub>3</sub>), D-isomer  $[\alpha]_D^{22} = +9.5$  (c=0.33, CHCl<sub>3</sub>).

Procedure B: L-isomer  $[\alpha]_D^{22} = -10.6$  (c=0.33, CHCl<sub>3</sub>), D-isomer  $[\alpha]_D^{22} = +9.5$  (c=0.33, CHCl<sub>3</sub>).

Procedure D: L-isomer  $[\alpha]_D^{22} = -8.5$  (c=0.33, CHCl<sub>3</sub>), D-isomer  $[\alpha]_D^{22} = +8.7$  (c=0.33, CHCl<sub>3</sub>).

Chiral HPLC: 85:15 heptane/isopropanol, flow 1 mL/min; retention times: racemic 24.1 min and 30.68 min, L-enantiomer 24.0 min, D-enantiomer, 29.67 min.

**(S)/(R)-1-butyl-3-(2-oxotetrahydrofuran-3-yl)urea (L-137, D-137)**



**L-137, D-137**

Following the procedure A, L- and D- enantiomers were obtained by using 1-isocyanatobutane (0.164 g, 1.66 mmol), L/D-Homoserine lactone hydrobromide (0.3 g, 1.66 mmol) and trimethylamine (0.168 g, 1.66 mmol), as a white solid in 51% (L: 0.17 g) and 50% (D: 0.16 g) yield after purification by flash chromatography column (pentane/AcOEt = 1/11).

**<sup>1</sup>H NMR (300 MHz, Chloroform-*d*)**  $\delta$ : 5.69 (s, 1H, NH), 5.34 (s, 1H, NH), 4.55 (s, 1H, CH<sub>2</sub>-O-lactone), 4.43 (t, *J* = 8.2 Hz, 1H, CH-NH), 4.27 (s, 1H, CH<sub>2</sub>-O-lactone), 3.15 (s, 2H, CH<sub>2</sub>), 2.71 (s, 1H, CH<sub>2</sub>-lactone), 2.33 – 2.04 (m, 1H, CH<sub>2</sub>-lactone), 1.54 – 1.22 (m, 4H, CH<sub>2</sub>), 0.90 (t, *J* = 6.9 Hz, 3H, CH<sub>3</sub>).

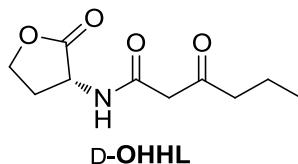
L-isomer  $[\alpha]_D^{22} = -9.0$  (c=1, CHCl<sub>3</sub>), D-isomer  $[\alpha]_D^{22} = +6.0$  (c=1, CHCl<sub>3</sub>).

Chiral HPLC: 85:15 heptane/isopropanol, flow 1 mL/min; retention times: racemic 8.78 min and 11.87 min, L-enantiomer 8.83 min, D-enantiomer, 11.87 min.

### General procedure for synthesis of $\beta$ -ketoamide AHLs:

To a solution of Meldrum's acid in 50 mL dichloromethane was added butyric acid or isovaleric acid, DMAP and DCC. The reaction mixture was allowed to stir at room temperature for 14h, the precipitate was filtered and the yellow solution was washed with 3M HCl (100 mL x2), the organic layer was dried over anhydrous Na<sub>2</sub>SO<sub>4</sub> and evaporated to give a yellow oil as crude product which was used for the next step without further purification. Then the Meldrum's acid was dissolved in 20 mL of anhydrous 1,2-dichloromethane or acetonitrile followed with the addition of L- or D- Homoserine lactone hydrobromide and triethylamine. The mixture was stirred at room temperature for 1h and was allowed to stir for refluxing for 14h until L- or D- HSL hydro-bromide was consumed. Then the solvent was removed under reduced pressure, the residue was dissolved in 20 mL dichloromethane and washed with 1M HCl (20 mL), saturated NaHCO<sub>3</sub> (20 mL) and water (20 mL), the organic layer was separated and dried over anhydrous Na<sub>2</sub>SO<sub>4</sub>, evaporated and purified by flash chromatography column to afford final product.

#### (*R*)-3-oxo-*N*-(2-oxotetrahydrofuran-3-yl)hexanamide (D-OHHL)



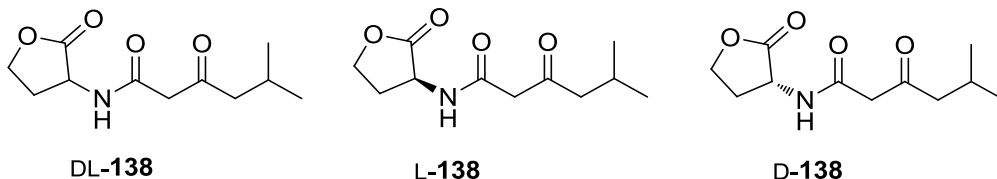
Following the general procedure, the product was obtained in 74% yield (180 mg) as a white solid after purification by flash chromatography (pentane/acetone=2/1). Meldrum's acid (1.64 g, 11.53 mmol), butyric acid (1 g, 11.35 mmol), DMAP (1.46 g, 11.92 mmol), DCC (2.58 g, 12.49 mmol) was used for synthesis of Meldrum's acid intermediate. The intermediate (247 mg, 1.15 mmol), D-HSL hydrobromide (200 mg, 1.1 mmol), triethylamine (134 mg, 1.32 mmol) was used for amidation step.

**<sup>1</sup>H NMR (300 MHz, Chloroform-*d*)**:  $\delta$  7.68 (d, *J* = 6.2 Hz, 1H, NH), 4.66 – 4.53 (m, 1H, CH<sub>2</sub>-O-lactone), 4.49 – 4.40 (m, 1H, CHCO lactone), 4.33 – 4.17 (m, 1H, CH<sub>2</sub>-O-lactone), 3.45 (s, 2H, COCH<sub>2</sub>CO), 2.79 – 2.62 (m, 1H, CH<sub>2</sub> of lactone), 2.50 (t, *J* = 7.3 Hz, 2H, COCH<sub>2</sub>), 2.34 – 2.17 (m, 1H, CH<sub>2</sub> of lactone), 1.59 (h, *J* = 7.4 Hz, 2H, CH<sub>2</sub>), 0.90 (t, *J* = 7.4 Hz, 3H, CH<sub>3</sub>).

$[\alpha]_D^{22} = -5.7$  (c=1, CHCl<sub>3</sub>).

Chiral HPLC: 85:15 heptane/isopropanol, flow 1 mL/min; retention times: racemic 17.63 min, L-enantiomer 17.08 min, D-enantiomer, 17.83 min.

**(RS)/(R)/(S)-5-methyl-3-oxo-N-(2-oxotetrahydrofuran-3-yl)hexanamide (DL-138, L-138, D-138)**



Following the general procedure, the product was obtained in 55% (racemic, 207 mg), 57% (L-enantiomer, 215 mg), 65% (D-enantiomer, 244 mg) yields as a white solid after purification by flash chromatography (pentane/AcOEt=1/1). Meldrum's acid (2.83 g, 19.58 mmol), isovaleric acid (2 g, 19.58 mmol), DMAP (2.50 g, 20.56 mmol), DCC (4.45 g, 21.54 mmol) was used for synthesis of Meldrum's acid intermediate. The intermediate (395 mg, 1.73 mmol), D-HSL hydro-bromide (300 mg, 1.65 mmol), triethylamine (200 mg, 1.98 mmol) was used for amidation step.

**<sup>1</sup>H NMR (300 MHz, Chloroform-*d*):**  $\delta$  7.67 (d,  $J$  = 5.6 Hz, 1H, NH), 4.59 (ddd,  $J$  = 11.5, 8.7, 6.7 Hz, 1H, CH<sub>2</sub>-O-lactone), 4.47 (td,  $J$  = 9.1, 1.3 Hz, 1H, CHCO lactone), 4.27 (ddd,  $J$  = 11.0, 9.3, 6.1 Hz, 1H, CH<sub>2</sub>-O-lactone), 3.45 (s, 2H, COCH<sub>2</sub>CO), 2.85 – 2.67 (m, 1H, CH<sub>2</sub> of lactone), 2.41 (d,  $J$  = 6.9 Hz, 2H, CH<sub>2</sub>), 2.33 – 2.07 (m, 2H, CH<sub>2</sub> of lactone, CH), 0.93 (d,  $J$  = 6.6 Hz, 6H, 2CH<sub>3</sub>).

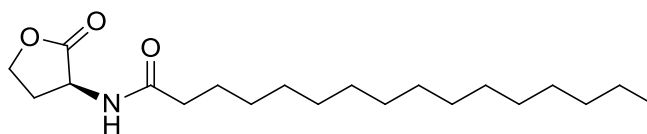
L-enantiomer:  $[\alpha]_D^{22} = +6.5$  (c=1, CHCl<sub>3</sub>); D-enantiomer:  $[\alpha]_D^{22} = -6.7$  (c=1, CHCl<sub>3</sub>).

Chiral HPLC: 85:15 heptane/isopropanol, flow 1 mL/min; retention times: racemic, L-enantiomer 18.23 min, D-enantiomer, 17.2 min.

**General procedure for determination of optical purity of AHLs enantiomers**

- (1) 5 mg racemic AHLs + different concentration of Eu(hfc)<sub>3</sub> (0%, 10%, 20%, 30% 40% and 50% molar) to compare the differences of chemical shifts and integration.
- (2) Choose a most obvious spectrum and confirm the concentration of Eu(hfc)<sub>3</sub>.
- (3) 5mg AHLs enantiomer (*R* and *S*) + specified concentration of Eu(hfc)<sub>3</sub>.
- (4) Comparison of chemical shifts or calculation of integration of each complex.

**(S)-N-(2-oxotetrahydrofuran-3-yl)palmitamide (146)**

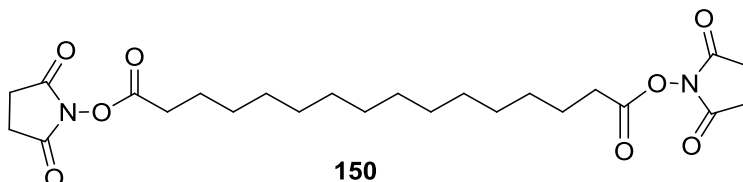


**146**

To a solution of L-Homoserine lactone hydrobromide (0.2 g, 1.11 mmol) and triethylamine (0.246 g, 2.431 mmol) in 10 mL dichloromethane was added palmitoyl chloride (0.365 g, 1.326 mmol) dropwise at 0 °C, after the addition of palmitoyl chloride, the ice-bath was removed and the reaction was allowed to stir rigorously at rt for 12h with TLC monitoring (pentane/AcOEt =10/1). Lots of white solid emerging, then the mixture was dissolved in 100 mL DCM and washed with 100 mL 1 M HCl solution, the aqueous layer was extracted with DCM (30 mLx2), and the organic layers were combined and dried over anhydrous Na<sub>2</sub>SO<sub>4</sub>. filtration and concentration afford a crude product, and further purification by recrystallization in 50 mL AcOEt gave pure product as a white solid (260 mg, 69%).

**<sup>1</sup>H NMR (300 MHz, Chloroform-*d*):** δ 6.04 (s, 1H, NH), 4.60 – 4.51 (m, 1H, CH<sub>2</sub>-O-lactone), 4.48 (d, *J* = 9.7 Hz, 1H, CH-NH), 4.37 – 4.18 (m, 1H, CH<sub>2</sub>-O-lactone), 2.94 – 2.77 (m, 1H, CH<sub>2</sub> of lactone), 2.24 (t, *J* = 7.6 Hz, 2H, α-CH<sub>2</sub>), 2.19 – 2.01 (m, 1H, CH<sub>2</sub> of lactone), 1.64 (s, 4H, β-CH<sub>2</sub> and γ-CH<sub>2</sub>), 1.28 (s, 22H, aliphatic), 0.85 (s, 3H, CH<sub>3</sub>).

**Di-NHS activated tether (hexadecanedioic acid bis-(2,5-dioxo-pyrrolidin-1yl)ester) (150)**

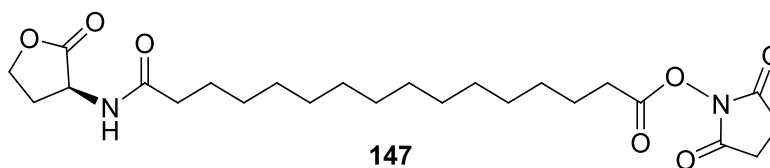


**150**

To a solution of hexadecanedioic acid (500 mg, 1.75 mmol) in 40 mL of DCM was added EDCI (830 mg, 4.64 mmol), NHS (480 mg, 4.19 mmol), DMAP (110 mg, 0.837 mmol), and DIPEA (451 mg, 3.49 mmol). The mixture was stirred at rt for 3h, after stirring for 3h at rt, the mixture was washed with brine (2x30 mL), 5% citric acid (2x30 mL), and sat. Na<sub>2</sub>CO<sub>3</sub> (2x30 mL) and brine (2x30 mL). The organic solution was dried with MgSO<sub>4</sub>, filtered, and the solvent was removed in vacuo to yield the desired product as a pure, white solid (630 mg, 74%).

**<sup>1</sup>H NMR (300 MHz, Chloroform-*d*):** δ 2.83 (s, 8H, α-in NHS), 2.59 (t, *J* = 7.5 Hz, 4H, α-CH<sub>2</sub>), 1.78 – 1.67 (m, 4H, β-CH<sub>2</sub>), 1.25 (s, 16H, aliphatic).

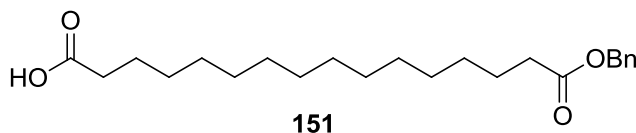
### 2,5-dioxopyrrolidin-1-yl (S)-16-oxo-16-((2-oxotetrahydrofuran-3-yl)amino)hexadecanoate (147)



To a solution of L-Homoserine lactone hydrobromide (60 mg, 0.31 mmol) in 5 mL of anhydrous DCM was added di-NHS activated tether (hexadecanedioic acid bis-(2,5-dioxo-pyrrolidin-1-yl)ester) (300 mg, 0.61 mmol), and Et<sub>3</sub>N (38 mg, 0.372 mmol). The reaction mixture was allowed to stir at room temperature for 12h with TLC monitoring (DCM/methanol = 30/1, R<sub>f</sub> = 0.3). After the reaction is complete, the reaction mixture was washed by 60 mL water, and the aqueous layer was washed by DCM (20 mLx2), the organic layer was combined and dried over MgSO<sub>4</sub>, filtered, evaporated and further purified by column chromatography (DCM/methanol=30/1) to afford desired product as a white solid (80 mg, 58%).

**<sup>1</sup>H NMR (300 MHz, Chloroform-*d*)** δ 6.04 (d, *J* = 5.1 Hz, 1H, NH), 4.60 – 4.51 (m, 1H, CH<sub>2</sub>-O-lactone), 4.46 (t, *J* = 9.7 Hz, 1H, CH-NH), 4.34 – 4.23 (m, 1H, CH<sub>2</sub>-O-lactone), 2.83 (s, 4H, α-in NHS), 2.60 (t, *J* = 7.5 Hz, 2H, α-CH<sub>2</sub> close to NHS), 2.28 – 2.20 (m, 2H, α-CH<sub>2</sub> close to AHL), 2.20 – 2.03 (m, 1H, CH<sub>2</sub> of lactone), 1.69 (dp, *J* = 29.6, 7.2 Hz, 5H, 2β-CH<sub>2</sub>, CH<sub>2</sub> of lactone), 1.25 (s, 20H, aliphatic).

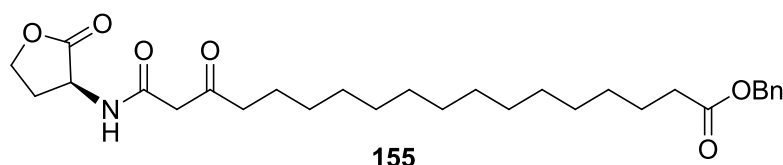
### 16-(benzyloxy)-16-oxohexadecanoic acid (151)



To a solution of hexadecanedioic acid (500 mg, 1.75 mmol) in 12 mL of methanol was added dropwise with stirring a solution of 10% KOH (115 mg, 1.75 mmol) in 2 mL methanol. The reaction was stirred at room temperature for an additional 30 min. The solvent was evaporated and dried under high vacuum, and the residue was suspended in 20 mL of toluene and TBAB (57 mg, 0.175 mmol) and benzyl bromide (329 mg, 1.92 mmol) were added. The solution was heated under reflux for 15h. after cooling, the solvent was removed and the residue was purified by flash chromatography column (pentane/AcOEt=4/1) to afford 285 mg pure product as a white solid (43% yield).

**<sup>1</sup>H NMR (300 MHz, Chloroform-*d*)** δ 7.35 (m, 5H, ArH), 5.11 (s, 2H, PhCH<sub>2</sub>), 2.35 (td, *J* = 7.5, 0.9 Hz, 4H, COCH<sub>2</sub>), 1.72 – 1.51 (m, 4H, CH<sub>2</sub>), 1.25 (m, 20H, 10CH<sub>2</sub>).

**(S)-benzyl 16,18-dioxo-18-((2-oxotetrahydrofuran-3-yl)amino)octadecenoate (155)**

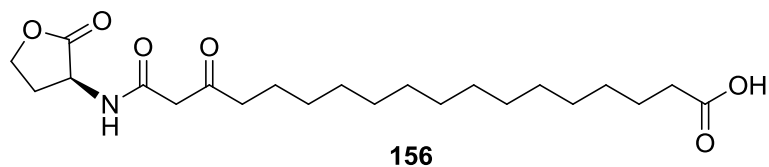


To a solution of mono-benzyl ester in 15 mL of anhydrous dichloromethane was added Meldrum's acid (147 mg, 1.02 mmol), DMAP (130 mg, 1.1 mmol) and DCC (240 mg, 1.164 mmol) at room temperature. The reaction was stirred at the same temperature for 36h. After the starting material was consumed, the precipitate was filtered and the filtrate was concentrated, and the residue was dissolved in 60 mL AcOEt, washed with 2M HCl (50 mL x3), dried over anhydrous Na<sub>2</sub>SO<sub>4</sub>, evaporated and used for the next step without further purification. The precedent product (694 mg, 1.382 mmol) was dissolved in 30 mL CH<sub>3</sub>CN, followed by the addition of L-HSL hydro-bromide (302 mg, 1.66 mmol), and triethylamine (224 mg, 2.22 mmol) was added at room temperature, the reaction was stirred for additional 2h, then was warmed up to reflux and stirred for 20h. Then the solvent was removed under reduced pressure, the residue was dissolved in 100 mL AcOEt and washed with 1M HCl (100 mL) and saturated NaHCO<sub>3</sub> (100 mL), the aqueous layer was extracted with AcOEt (50 mL x2), and the combine organic layers were dried over anhydrous Na<sub>2</sub>SO<sub>4</sub>, evaporated and purified by flash chromatography column (dichloromethane/methanol=15/1) to afford 530 mg (77% yield) of the product as a white solid.

**<sup>1</sup>H NMR (300 MHz, Chloroform-*d*)** δ: 7.64 (d, *J* = 18.8 Hz, 1H, NH), 7.40 – 7.28 (m, 4H, ArH), 5.11 (s, 2H, PhCH<sub>2</sub>), 4.58 (ddd, *J* = 11.5, 8.7, 6.6 Hz, 1H, OCH<sub>2</sub> of lactone), 4.48 (td, *J* = 9.1, 1.4 Hz, 1H, COCH of lactone), 4.27 (ddd, *J* = 11.0, 9.3, 6.0 Hz, 1H, OCH<sub>2</sub> of lactone), 3.46 (s, 2H, COCH<sub>2</sub>CO), 2.76 (dddd, *J* = 12.5, 8.7, 6.0, 1.4 Hz, 1H, CH<sub>2</sub> of lactone), 2.52 (t, *J* = 7.4 Hz, 2H, BnOOCCH<sub>2</sub>), 2.35 (t, *J* = 7.5 Hz, 2H, COCH<sub>2</sub>COCH<sub>2</sub>-long chain), 2.22 (dd, *J* = 12.5, 9.0 Hz, 1H, CH<sub>2</sub> of lactone), 1.62 (m, 4H, 2β-CH<sub>2</sub>), 1.26 (m, 20H, 10CH<sub>2</sub>).

**HRMS (ESI)** [M + Na]<sup>+</sup> calculated for C<sub>29</sub>H<sub>43</sub>NNaO<sub>6</sub> 524.2988, found 524.2980.

**(S)-16,18-dioxo-18-((2-oxotetrahydrofuran-3-yl)amino)octadecanoic acid (156)**



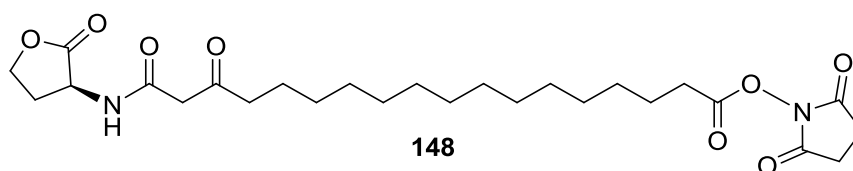
To a solution of (S)-benzyl 16,18-dioxo-18-((2-oxotetrahydrofuran-3-yl)amino)octadecenoate (70 mg, 0.14 mmol) in 10 mL of THF was added Pd/C. The reaction was stirred under H<sub>2</sub> atmosphere for 6h until the starting material was consumed. Then Pd/C was filtered through a celite plug, the filtrate was concentrated to afford the crude product as a white solid, further purification by flash chromatography column (DCM/methanol=25/1) to give 55 mg (96% yield) of product as a white solid.

**<sup>1</sup>H NMR (300 MHz, DMSO-*d*<sub>6</sub>)** δ: 12.01 (s, 1H, COOH), 8.63 (d, *J* = 7.7 Hz, 1H, NH), 4.59 (dt, *J* = 10.7, 8.5 Hz, 1H, OCH<sub>2</sub> of lactone), 4.48 – 4.30 (m, 1H, COCH of lactone), 4.27 – 4.12 (m, 1H, OCH<sub>2</sub> of lactone), 3.37 (s, 2H, COCH<sub>2</sub>CO), 2.53 (t, *J* = 6.9 Hz, 2H, COCH<sub>2</sub>COCH<sub>2</sub>-long chain), 2.46 – 2.37 (m, 1H, CH<sub>2</sub> of lactone), 2.26 – 2.12 (m, 3H, CH<sub>2</sub> of lactone and CH<sub>2</sub>COOH), 1.58 – 1.40 (m, 4H, 2β-CH<sub>2</sub>), 1.27 (m, 20H, 10CH<sub>2</sub>).

**<sup>13</sup>C NMR (75 MHz, DMSO-*d*<sub>6</sub>)** δ: 204.9 (COCH<sub>2</sub>CO-long chain), 175.5 (COOH), 175 (CO of lactone), 166.7 (COCH<sub>2</sub>CO-long chain), 65.8 (OCH<sub>2</sub> of lactone), 50.7 (COCH of lactone), 48.6 (COCH<sub>2</sub>CO), 42.4 (COCH<sub>2</sub>COCH<sub>2</sub>), 34.1 (CH<sub>2</sub>COOH), 29.5 (4CH<sub>2</sub>), 29.4 (2CH<sub>2</sub>), 29.3 (CH<sub>2</sub>), 29.2 (CH<sub>2</sub>), 29.0 (CH<sub>2</sub>), 28.9 (CH<sub>2</sub>), 28.7 (CH<sub>2</sub>), 25 (CH<sub>2</sub>CH<sub>2</sub>COOH), 23.3 (COCH<sub>2</sub>COCH<sub>2</sub>CH<sub>2</sub>).

**HRMS (ESI)** [M + Na]<sup>+</sup> calculated for C<sub>22</sub>H<sub>37</sub>NNaO<sub>6</sub> 434.2519, found 434.2508.

**(S)-2,5-dioxopyrrolidin-1-yl 16,18-dioxo-18-((2-oxotetrahydrofuran-3-yl)amino)octadecenoate  
(148)**



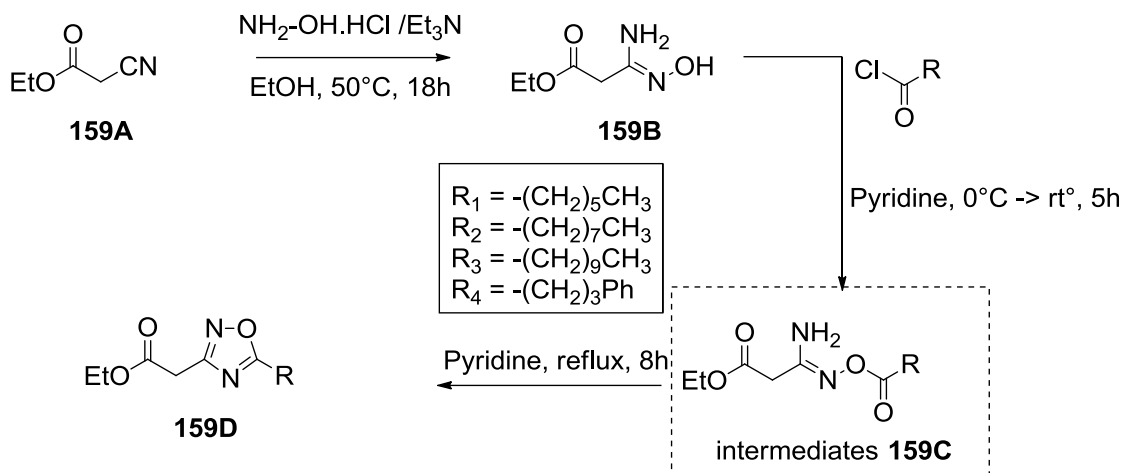
To a solution of (S)-16,18-dioxo-18-((2-oxotetrahydrofuran-3-yl)amino)octadecanoic acid (35 mg, 0.085 mmol) in 5 mL of dichloromethane was added *N*-hydroxysuccinimide (11 mg, 0.094 mmol), DCC (19 mg, 0.094 mmol). The reaction was stirred at room temperature for 48h. Then the precipitate was filtered, and the filtrate was concentrated and purified by flash chromatography column (pentane/AcOEt=3/2 for first purification, and DCM/methanol=45/1 for second purification) to afford 30 mg of the product as a white solid (70% yield).

**<sup>1</sup>H NMR (300 MHz, Chloroform-*d*)** δ: 7.66 (d, *J* = 5.8 Hz, 1H, NH), 4.58 (ddd, *J* = 11.5, 8.7, 6.6 Hz, 1H, OCH<sub>2</sub> of lactone), 4.47 (td, *J* = 9.1, 1.3 Hz, 1H, COCH of lactone), 4.27 (ddd, *J* = 11.0, 9.3, 6.1 Hz, 1H, OCH<sub>2</sub> of lactone), 3.46 (s, 2H, COCH<sub>2</sub>CO), 2.83 (s, 4H, 2CH<sub>2</sub> of NHS), 2.75 (dddd, *J* = 12.5, 8.7, 6.1, 1.4 Hz, 1H, CH<sub>2</sub> of lactone), 2.55 (dt, *J* = 23.0, 7.4 Hz, 4H, 2α-CH<sub>2</sub>), 2.22 (ddd, *J* = 23.7, 11.3, 8.9 Hz, 1H, CH<sub>2</sub> of lactone), 1.73 (p, *J* = 7.4 Hz, 2H, β-CH<sub>2</sub>), 1.63 – 1.52 (m, 2H, β-CH<sub>2</sub>), 1.42 – 1.25 (m, 20H, 10CH<sub>2</sub>).

**<sup>13</sup>C NMR (75 MHz, Chloroform-*d*)** δ 206.6 (COCH<sub>2</sub>CO-long chain), 174.7 (CO of lactone), 169.2 (2CO of NHS), 168.7 (COONHS), 166.3 (COCH<sub>2</sub>CO-long chain), 65.9 (OCH<sub>2</sub> of lactone), 49.0 (COCH of lactone), 48.0 (COCH<sub>2</sub>CO), 44.0 (COCH<sub>2</sub>COCH<sub>2</sub>), 30.9 (CH<sub>2</sub>COONHS), 29.9 (CH<sub>2</sub>), 29.5 (4CH<sub>2</sub>), 29.4 (CH<sub>2</sub>), 29.30 (2CH<sub>2</sub>), 29.1 (CH<sub>2</sub>), 29.0 (CH<sub>2</sub>), 28.8 (CH<sub>2</sub>), 25.6 (2CH<sub>2</sub>), 24.6 (CH<sub>2</sub>CH<sub>2</sub>COONHS), 23.3 (COCH<sub>2</sub>COCH<sub>2</sub>CH<sub>2</sub>).

**HRMS (ESI)** [M + Na]<sup>+</sup> calculated for C<sub>26</sub>H<sub>40</sub>N<sub>2</sub>NaO<sub>8</sub> 531.2682, found 531.2677.

## Synthesis of 3,5 disubstituted 1,2,4-oxadiazole with carboxymethyl ester in position 3



### Ethyl (Z)-3-amino-3-(hydroxyimino)propanoate (159B)



To a solution of cyanoacetate ethyl (2.45 g, 21.6 mmol) in 50 mL of ethanol was added  $\text{Et}_3\text{N}$  (1.46 g, 14.4 mmol) and  $\text{NH}_2\text{-OH HCl}$  (1 g, 14.4 mmol), the reaction mixture was allowed to stir at  $50^\circ\text{C}$  overnight under argon. TLC monitoring (pentane/ $\text{AcOEt}$ =1/1,  $R_f$ =0.15), 18h later, showed that the reaction was complete, and the solvents was removed under reduced pressure to give a red residue, which was subjected into column chromatography for further purification (pentane/ $\text{AcOEt}$ =1/1 to pure  $\text{AcOEt}$ ) to afford 0.9g (40%) of the desired product as an orange oil.

$^1\text{H NMR}$  (300 MHz,  $\text{Chloroform-}d$ )  $\delta$ : 5.01 (s, 2H,  $\text{NH}_2$ ), 4.17 (p,  $J = 6.9$  Hz, 2H,  $\text{CH}_2$ ), 3.17 (s, 2H,  $\text{CH}_2$ ), 2.04 (s, 1H, OH), 1.26 (q,  $J = 7.3$  Hz, 3H,  $\text{CH}_3$ ).

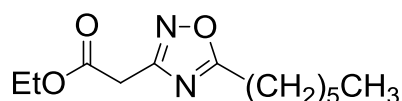
### General procedure for acylation and cyclization steps:

To a solution of ethyl (Z)-3-amino-3-(hydroxyimino)propanoate in 10 mL of anhydrous Pyridine was added acyl chloride at  $0^\circ\text{C}$ , the mixture was allowed to stir at room temperature for 3h until TLC (pentane/ $\text{AcOEt}$ ) showed the starting material was consumed. Then the temperature was raised to  $120^\circ\text{C}$  and the reaction was stirred under refluxing overnight. 12h later, TLC (pentane/ $\text{DCM}$ =1/4) showed all intermediate had been consumed, and pyridine was removed under reduced pressure to give a dark liquid residue as crude product, which was then dissolved in 30 mL of  $\text{AcOEt}$  and washed with 30 mL of sat.  $\text{NaHCO}_3$  solution, the aqueous layer was extracted with  $\text{AcOEt}$  (20 mLx2), the combined organic layer was dried over anhydrous  $\text{Na}_2\text{SO}_4$ , filtered, concentrated for further purification by column chromatography (pentane/ $\text{DCM}$ ) to afford final products.

### General procedure for preparation of acyl chloride:

To a solution of undecanoic acid (308 mg, 1.65 mmol) or 4-phenylbutyric (271 mg, 1.65 mmol) in 5 mL of anhydrous DCM was added oxalyl dichloride (314 mg, 2.48 mmol) and one drop of DMF at 0 °C, the reaction was allowed to stir at room temperature 12h, then solvent and the redundant oxalyl dichloride were removed under reduced pressure to afford a colourless oil as crude product, which was used for the next step without further purification.

### Ethyl 2-(5-hexyl-1,2,4-oxadiazol-3-yl)acetate (159D1)



**159D1**

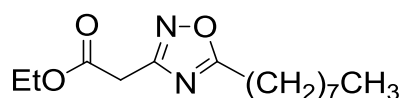
The product was obtained as a brown oil in 31% yield (100 mg) according to the general procedure by using ethyl (Z)-3-amino-3-(hydroxyimino)propanoate (200 mg, 1.37 mmol), heptanoyl chloride (246 mg, 1.65 mmol) after purification by flash chromatography (Petane/AcOEt=1/1, intermediate product  $R_f=0.36$ ; and for final product, pentane/DCM=1/5).

**$^1\text{H}$  NMR (300 MHz, Chloroform-*d*)**  $\delta$ : 4.21 (q,  $J = 7.2$  Hz, 2H,  $\text{OCH}_2\text{CH}_3$ ), 3.79 (s, 2H,  $\text{CH}_2$ ), 2.88 (t,  $J = 7.7$  Hz, 2H,  $\alpha\text{-CH}_2$ ), 1.81 (p,  $J = 7.3$  Hz, 2H,  $\beta\text{-CH}_2$ ), 1.47 – 1.19 (m, 9H, 3 $\text{CH}_2$  and  $\text{OCH}_2\text{CH}_3$ ), 0.97 – 0.80 (m, 3H,  $\text{CH}_3$ ).

**$^{13}\text{C}$  NMR (101 MHz, Chloroform-*d*)**  $\delta$  180.6 (C=O), 167.8 (OC=N), 164.5 (NC=N), 61.8 ( $\text{OCH}_2$ ), 32.4 ( $\text{CH}_2$ ), 31.3 ( $\text{CH}_2$ ), 28.7 ( $\text{CH}_2$ ), 26.7 ( $\text{CH}_2$ ), 26.5 ( $\text{CH}_2$ ), 22.5 ( $\text{CH}_2$ ), 14.2 ( $\text{CH}_3$ ), 14.1 ( $\text{CH}_3$ ).

**HRMS (ESI)**  $[\text{M} + \text{Na}]^+$  calculated for  $\text{C}_{12}\text{H}_{20}\text{N}_2\text{NaO}_3$  263.1372, found 263.1361.

### Ethyl 2-(5-octyl-1,2,4-oxadiazol-3-yl)acetate (159D2)



**159D2**

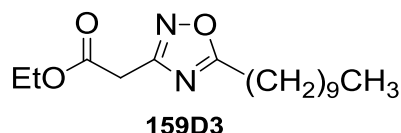
The product was obtained as a yellow oil in 68% yield (250 mg) according to the general procedure by using ethyl (Z)-3-amino-3-(hydroxyimino)propanoate (200 mg, 1.37 mmol), nonanoyl chloride (290 mg, 1.65 mmol) after purification by flash chromatography (Petane/AcOEt=2/3, intermediate product  $R_f=0.43$ ; and for final product, pentane/DCM=1/4).

**$^1\text{H}$  NMR (300 MHz, Chloroform-*d*)**  $\delta$  4.21 (q,  $J = 7.1$  Hz, 2H,  $\text{OCH}_2\text{CH}_3$ ), 3.78 (s, 2H,  $\text{CH}_2$ ), 2.88 (t,  $J = 7.7$  Hz, 2H,  $\alpha\text{-CH}_2$ ), 1.81 (p,  $J = 7.4$  Hz, 2H,  $\beta\text{-CH}_2$ ), 1.42 – 1.16 (m, 13H, 5 $\text{CH}_2$  and  $\text{OCH}_2\text{CH}_3$ ), 0.93 – 0.79 (m, 3H,  $\text{CH}_3$ ).

**<sup>13</sup>C NMR (101 MHz, Chloroform-*d*)** δ 180.6 (C=O), 167.8 (OC=N), 164.6 (NC=N), 61.8 (OCH<sub>2</sub>), 32.4 (CH<sub>2</sub>), 31.9 (CH<sub>2</sub>), 29.1 (3CH<sub>2</sub>), 26.7 (CH<sub>2</sub>), 26.6 (CH<sub>2</sub>), 22.7 (CH<sub>2</sub>), 14.2 (2CH<sub>3</sub>).

**HRMS (ESI)** [M + Na]<sup>+</sup> calculated for C<sub>14</sub>H<sub>24</sub>N<sub>2</sub>NaO<sub>3</sub> 291.1685, found 291.1691.

**Ethyl 2-(5-decyl-1,2,4-oxadiazol-3-yl)acetate (159D3)**

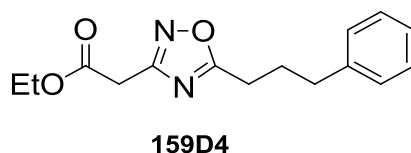


The product was obtained as a yellow oil in 33% yield (80 mg) according to the general procedure by using ethyl (*Z*)-3-amino-3-(hydroxyimino)propanoate (200 mg, 1.37 mmol), undecanoyl chloride (338 mg, 1.65 mmol) after purification by flash chromatography (Petane/AcOEt=1/1, intermediate product R<sub>f</sub>=0.56; and for final product, pentane/DCM=1/5).

**<sup>1</sup>H NMR (300 MHz, Chloroform-*d*)** δ 4.21 (q, *J* = 7.1 Hz, 2H, OCH<sub>2</sub>CH<sub>3</sub>), 3.78 (s, 2H, CH<sub>2</sub>), 2.88 (t, *J* = 7.7 Hz, 2H, α-CH<sub>2</sub>), 1.81 (p, *J* = 7.5 Hz, 2H, β-CH<sub>2</sub>), 1.36 – 1.20 (m, 17H, 7CH<sub>2</sub> and OCH<sub>2</sub>CH<sub>3</sub>), 0.87 (t, *J* = 6.4 Hz, 3H, CH<sub>3</sub>).

**HRMS (ESI)** [M + Na]<sup>+</sup> calculated for C<sub>16</sub>H<sub>28</sub>N<sub>2</sub>NaO<sub>3</sub> 319.1998, found 319.2003.

**Ethyl 2-(5-(3-phenylpropyl)-1,2,4-oxadiazol-3-yl)acetate (159D4)**

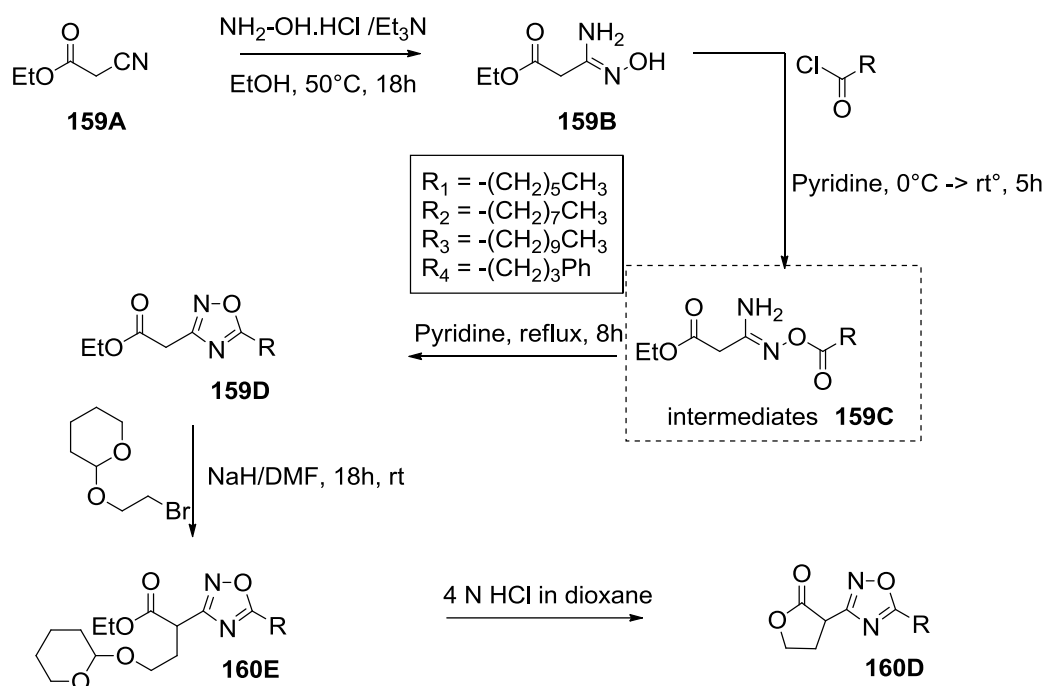


The product was obtained as a yellow oil in 22% yield (30 mg) according to the general procedure by using ethyl (*Z*)-3-amino-3-(hydroxyimino)propanoate (200 mg, 1.37 mmol), 4-phenylbutanoyl chloride (301 mg, 1.65 mmol) after purification by flash chromatography (Petane/AcOEt=1/1, intermediate product R<sub>f</sub>=0.5; and for final product, pentane/DCM=1/5).

**<sup>1</sup>H NMR (300 MHz, Chloroform-*d*)** δ 7.39 – 7.13 (m, 5H, ArH), 4.24 (q, *J* = 7.2 Hz, 2H, OCH<sub>2</sub>CH<sub>3</sub>), 3.81 (s, 2H, CH<sub>2</sub>), 2.91 (t, *J* = 7.6 Hz, 2H, α-CH<sub>2</sub>), 2.74 (t, *J* = 7.5 Hz, 2H, Ph-CH<sub>2</sub>), 2.18 (p, *J* = 7.6 Hz, 2H, β-CH<sub>2</sub>), 1.29 (t, *J* = 7.1 Hz, 3H, CH<sub>3</sub>).

**HRMS (ESI)** [M + Na]<sup>+</sup> calculated for C<sub>15</sub>H<sub>18</sub>N<sub>2</sub>NaO<sub>3</sub> 297.1215, found 297.1219.

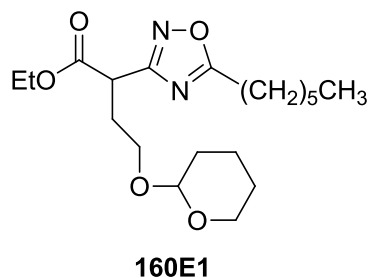
### Synthesis of 3,5 disubstituted 1,2,4-oxadiazole with the $\gamma$ -lactone in position 3



### General procedure for the synthesis of compounds 160E

To a solution of **159D** (**159D1**: 0.32 mmol, **159D2**: 0.746 mmol, **159D3**: 0.676 mmol, **159D4**: 0.73 mmol,) in 5 mL of anhydrous DCM was added NaH (**159D1**: 0.64 mmol, **159D2**: 1.5 mmol, **159D3**: 1.352 mmol, **159D4**: 1.46 mmol) at 0 °C, the reaction mixture was allowed to stir at room temperature for 20 min, followed the 2-(2-bromoethoxy)tetrahydro-2H-pyran (**159D1**: 0.51 mmol, **159D2**: 1.194 mmol, **159D3**: 1.08 mmol, **159D4**: 1.17 mmol) was added into the mixture and the reaction was stirred vigorously for 18h at room temperature with TLC monitoring, then DMF was removed under reduced pressure to afford a yellow residue as crude product which was dissolved in 20 mL of DCM and washed with 20 mL of water, the aqueous phase was extracted with DCM (10 mL x2), and the organic phases were combined, dried over Na<sub>2</sub>SO<sub>4</sub>, filtered and evaporated for further purification by chromatography column.

**Ethyl 2-(5-hexyl-1,2,4-oxadiazol-3-yl)-4-((tetrahydro-2H-pyran-2-yl)oxy)butanoate (160E1)**

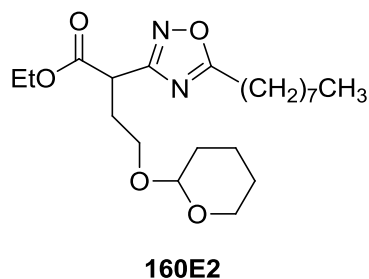


Purification by column chromatography (eluent: pentane/Diethyl ether=2/1) afford 30 mg of product as a colorless oil (25% yield).

**<sup>1</sup>H NMR (300 MHz, Chloroform-*d*)**  $\delta$ : 4.55 (dt,  $J = 13.3, 3.3$  Hz, 1H, Pyran-CH<sub>2</sub>CH(O)-O), 4.18 (q,  $J = 7.1$  Hz, 2H, OCH<sub>2</sub>CH<sub>3</sub>), 4.10 (t,  $J = 7.4$  Hz, 1H, COCH-Oxadiazole), 3.88 – 3.66 (m, 2H, Pyran-CH<sub>2</sub>-O), 3.55 – 3.23 (m, 2H, -CH<sub>2</sub>CH<sub>2</sub>O-Pyran), 2.86 (t,  $J = 7.6$  Hz, 2H, Oxadiazole-CH<sub>2</sub>), 2.52 – 2.18 (m, 2H, CH<sub>2</sub>CH<sub>2</sub>O-Pyran), 1.77 (td,  $J = 13.3, 11.9, 5.9$  Hz, 4H, Oxadiazole-CH<sub>2</sub>CH<sub>2</sub>, Pyran-CH<sub>2</sub>CH<sub>2</sub>), 1.61 – 1.42 (m, 4H, Pyran-CH<sub>2</sub>CH<sub>2</sub>), 1.36 – 1.19 (m, 9H, OCH<sub>2</sub>CH<sub>3</sub>, Oxadiazole-CH<sub>2</sub>CH<sub>2</sub>CH<sub>2</sub>CH<sub>2</sub>CH<sub>2</sub>CH<sub>3</sub>), 0.95 – 0.81 (m, 3H, Oxadiazole-CH<sub>2</sub>CH<sub>2</sub>CH<sub>2</sub>CH<sub>2</sub>CH<sub>2</sub>CH<sub>3</sub>).

**HRMS (ESI)** [M + Na]<sup>+</sup> calculated for C<sub>19</sub>H<sub>32</sub>N<sub>2</sub>NaO<sub>5</sub> 391.2209, found 391.2213.

**Ethyl 2-(5-octyl-1,2,4-oxadiazol-3-yl)-4-((tetrahydro-2H-pyran-2-yl)oxy)butanoate (160E2)**

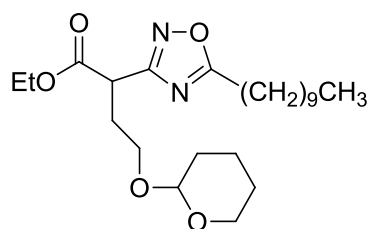


Purification by column chromatography (eluent: pentane/Diethyl ether=3/1) afford 90 mg product as a colorless oil (31% yield).

**<sup>1</sup>H NMR (300 MHz, Chloroform-*d*)**  $\delta$ : 4.55 (dd,  $J = 13.2, 3.4$  Hz, 1H, Pyran-CH<sub>2</sub>CH(O)-O), 4.26 – 4.06 (m, 3H, OCH<sub>2</sub>CH<sub>3</sub>, COCH-Oxadiazole), 3.92 – 3.66 (m, 2H, Pyran-CH<sub>2</sub>-O), 3.56 – 3.26 (m, 2H, -CH<sub>2</sub>CH<sub>2</sub>O-Pyran), 2.87 (t,  $J = 7.6$  Hz, 2H, Oxadiazole-CH<sub>2</sub>), 2.35 (ddt,  $J = 48.7, 14.0, 7.8$  Hz, 2H, CH<sub>2</sub>CH<sub>2</sub>O-Pyran), 1.89 – 1.64 (m, 4H, Oxadiazole-CH<sub>2</sub>CH<sub>2</sub>, Pyran-CH<sub>2</sub>CH<sub>2</sub>), 1.61 – 1.45 (m, 4H, Pyran-CH<sub>2</sub>CH<sub>2</sub>), 1.40 – 1.17 (m, 13H, OCH<sub>2</sub>CH<sub>3</sub>, Oxadiazole-CH<sub>2</sub>CH<sub>2</sub>CH<sub>2</sub>CH<sub>2</sub>CH<sub>2</sub>CH<sub>2</sub>CH<sub>2</sub>CH<sub>3</sub>), 0.87 (t,  $J = 6.7$  Hz, 3H, Oxadiazole-CH<sub>2</sub>CH<sub>2</sub>CH<sub>2</sub>CH<sub>2</sub>CH<sub>2</sub>CH<sub>2</sub>CH<sub>3</sub>).

**HRMS (ESI)** [M + Na]<sup>+</sup> calculated for C<sub>21</sub>H<sub>36</sub>N<sub>2</sub>NaO<sub>5</sub> 419.2522, found 419.2507.

**Ethyl 2-(5-decyl-1,2,4-oxadiazol-3-yl)-4-((tetrahydro-2H-pyran-2-yl)oxy)butanoate (160E3)**



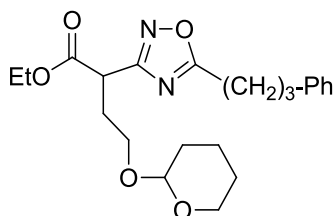
**160E3**

Purification by column chromatography (eluent: pentane/Diethyl ether=4/1) afford 50 mg product as a colorless oil (17% yield).

**<sup>1</sup>H NMR (300 MHz, Chloroform-*d*)**  $\delta$ : 4.55 (dt,  $J = 13.2, 3.3$  Hz, 1H, Pyran-CH<sub>2</sub>CH(O)-O), 4.26 – 4.07 (m, 3H, OCH<sub>2</sub>CH<sub>3</sub>, COCH-Oxadiazole), 3.90 – 3.67 (m, 2H, Pyran-CH<sub>2</sub>-O), 3.54 – 3.26 (m, 2H, -CH<sub>2</sub>CH<sub>2</sub>O-Pyran), 2.86 (t,  $J = 7.6$  Hz, 2H, Oxadiazole-CH<sub>2</sub>), 2.52 – 2.19 (m, 2H, CH<sub>2</sub>CH<sub>2</sub>O-Pyran), 1.76 (dt,  $J = 17.7, 8.6$  Hz, 4H, Oxadiazole-CH<sub>2</sub>CH<sub>2</sub>, Pyran-CH<sub>2</sub>CH<sub>2</sub>), 1.61 – 1.46 (m, 4H, Pyran-CH<sub>2</sub>CH<sub>2</sub>), 1.40 – 1.18 (m, 17H, OCH<sub>2</sub>CH<sub>3</sub>, Oxadiazole-CH<sub>2</sub>CH<sub>2</sub>CH<sub>2</sub>CH<sub>2</sub>CH<sub>2</sub>CH<sub>2</sub>CH<sub>2</sub>CH<sub>2</sub>CH<sub>2</sub>CH<sub>2</sub>CH<sub>3</sub>), 0.94 – 0.80 (t, 3H, Oxadiazole-CH<sub>2</sub>CH<sub>2</sub>CH<sub>2</sub>CH<sub>2</sub>CH<sub>2</sub>CH<sub>2</sub>CH<sub>2</sub>CH<sub>2</sub>CH<sub>2</sub>CH<sub>3</sub>).

**HRMS (ESI)** [M + Na]<sup>+</sup> calculated for C<sub>23</sub>H<sub>40</sub>N<sub>2</sub>NaO<sub>5</sub> 447.2835, found 447.2830.

**Ethyl 2-(5-(3-phenylpropyl)-1,2,4-oxadiazol-3-yl)-4-((tetrahydro-2H-pyran-2-yl)oxy)butanoate (160E4)**



**160E4**

Purification by column chromatography (eluent: pentane/Diethyl ether=3/1) afford 95 mg product as a colorless oil (32% yield).

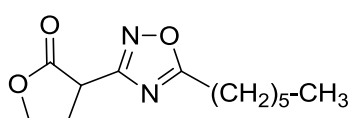
**<sup>1</sup>H NMR (300 MHz, Chloroform-*d*)**  $\delta$ : 7.31 – 7.16 (m, 5H, Ph-H), 4.55 (d,  $J = 14.1$  Hz, 1H, Pyran-CH<sub>2</sub>CH(O)-O), 4.30 – 4.02 (m, 3H, OCH<sub>2</sub>CH<sub>3</sub>, COCH-Oxadiazole), 3.92 – 3.64 (m, 2H, Pyran-CH<sub>2</sub>-O), 3.37 (dd,  $J = 42.5, 7.6$  Hz, 2H, -CH<sub>2</sub>CH<sub>2</sub>O-Pyran), 2.88 (t,  $J = 7.5$  Hz, 2H, Oxadiazole-CH<sub>2</sub>CH<sub>2</sub>CH<sub>2</sub>-Ph), 2.70 (t,  $J = 7.5$  Hz, 2H, Oxadiazole-CH<sub>2</sub>CH<sub>2</sub>CH<sub>2</sub>-Ph), 2.53 – 2.35 (m, 1H, CH<sub>2</sub>CH<sub>2</sub>O-Pyran), 2.36 – 2.20 (m, 1H, CH<sub>2</sub>CH<sub>2</sub>O-Pyran), 2.20 – 2.05 (m, 2H, Oxadiazole-CH<sub>2</sub>CH<sub>2</sub>CH<sub>2</sub>-Ph), 1.55 (m,  $J = 23.8$  Hz, 6H, Pyran-CH<sub>2</sub>CH<sub>2</sub>CH<sub>2</sub>), 1.23 (t,  $J = 7.1$  Hz, 3H, OCH<sub>2</sub>CH<sub>3</sub>).

**HRMS (ESI)** [M + Na]<sup>+</sup> calculated for C<sub>22</sub>H<sub>30</sub>N<sub>2</sub>NaO<sub>5</sub> 425.2052, found 425.2045.

### General procedure for the synthesis of 1,2,4-oxadiazole with lactone function in position 3 (160D)

**160E1** (0.082 mmol), **160E2** (0.227 mmol), **160E3** (0.106 mmol), **160E4** (0.236 mmol) was dissolved in 4 N HCl in dioxane (**160E1**: 0.5 mL, **160E2**: 1 mL, **160E3**: 0.8 mL, **160E4**: 1 mL) and the reaction was allowed to stir at room temperature for 16h until TLC showed no starting material in the reaction medium, then solvent was removed under reduced pressure and the residue was purified by chromatography column.

#### 3-(5-hexyl-1,2,4-oxadiazol-3-yl)dihydrofuran-2(3H)-one (160D1)



**160D1**

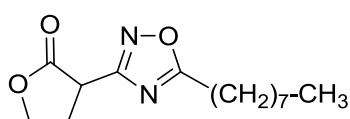
Purification by column chromatography (eluent: pentane/Diethyl ether=3/2) afford 17 mg product as a colorless oil (87% yield).

**<sup>1</sup>H NMR (300 MHz, Chloroform-*d*)**  $\delta$ : 4.58 (q,  $J = 7.4$  Hz, 1H, OCH<sub>2</sub> of lactone), 4.41 (q,  $J = 8.2$  Hz, 1H, OCH<sub>2</sub> of lactone), 4.06 (t,  $J = 9.2$  Hz, 1H, COCH of lactone), 2.87 (t,  $J = 7.6$  Hz, 2H, Oxadiazole-CH<sub>2</sub>CH<sub>2</sub>(CH<sub>2</sub>)<sub>3</sub>CH<sub>3</sub>), 2.71 (d,  $J = 8.3$  Hz, 2H, CH<sub>2</sub> of lactone), 1.89 – 1.73 (m, 2H, CH<sub>2</sub>CH<sub>2</sub>(CH<sub>2</sub>)<sub>3</sub>CH<sub>3</sub>), 1.31 (s, 6H, CH<sub>2</sub>CH<sub>2</sub>(CH<sub>2</sub>)<sub>3</sub>CH<sub>3</sub>), 0.88 (s, 3H, CH<sub>2</sub>CH<sub>2</sub>(CH<sub>2</sub>)<sub>3</sub>CH<sub>3</sub>).

**<sup>13</sup>C NMR (75 MHz, Chloroform-*d*)**  $\delta$  181.1 (C=O), 173.3 (OC=N), 166.5 (N=CN), 67.2 (OCH<sub>2</sub>), 38.0 (CH), 31.2 (CH<sub>2</sub>), 28.7 (CH<sub>2</sub>), 27.9 (CH<sub>2</sub>), 26.6 (CH<sub>2</sub>), 26.4 (CH<sub>2</sub>), 22.4 (CH<sub>2</sub>), 14.0 (CH<sub>3</sub>).

**HRMS (ESI)** [M + Na]<sup>+</sup> calculated for C<sub>12</sub>H<sub>18</sub>N<sub>2</sub>NaO<sub>3</sub> 297.1215, found 297.1207.

#### 3-(5-octyl-1,2,4-oxadiazol-3-yl)dihydrofuran-2(3H)-one (160D2)



**160D2**

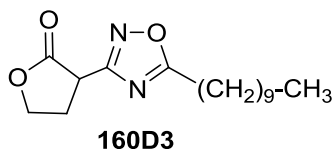
Purification by column chromatography (eluent: pentane/Diethyl ether=2/1) afford 50 mg product as a colorless oil (83% yield).

**<sup>1</sup>H NMR (300 MHz, Chloroform-*d*)**  $\delta$  4.57 (td,  $J = 8.3, 7.5, 4.9$  Hz, 1H, OCH<sub>2</sub> of lactone), 4.48 – 4.33 (m, 1H, OCH<sub>2</sub> of lactone), 4.05 (t,  $J = 9.3$  Hz, 1H, COCH of lactone), 2.93 – 2.79 (m, 2H, Oxadiazole-CH<sub>2</sub>CH<sub>2</sub>(CH<sub>2</sub>)<sub>5</sub>CH<sub>3</sub>), 2.78 – 2.62 (m, 2H, CH<sub>2</sub> of lactone), 1.79 (p,  $J = 7.8$  Hz, 2H, CH<sub>2</sub>CH<sub>2</sub>(CH<sub>2</sub>)<sub>5</sub>CH<sub>3</sub>), 1.29 (dt,  $J = 20.6, 6.5$  Hz, 10H, CH<sub>2</sub>CH<sub>2</sub>(CH<sub>2</sub>)<sub>5</sub>CH<sub>3</sub>), 0.93 – 0.76 (m, 3H, CH<sub>2</sub>CH<sub>2</sub>(CH<sub>2</sub>)<sub>5</sub>CH<sub>3</sub>).

**<sup>13</sup>C NMR (75 MHz, Chloroform-*d*)** δ 181.1 (C=O), 173.4 (OC=N), 166.5 (N=CN), 67.2 (OCH<sub>2</sub>), 38.0 (CH), 31.7 (CH<sub>2</sub>), 29.0 (3CH<sub>2</sub>), 27.9 (CH<sub>2</sub>), 26.6 (CH<sub>2</sub>), 26.4 (CH<sub>2</sub>), 22.6 (CH<sub>2</sub>), 14.1 (CH<sub>3</sub>).

**HRMS (ESI)** [M + Na]<sup>+</sup> calculated for C<sub>14</sub>H<sub>22</sub>N<sub>2</sub>NaO<sub>3</sub> 289.1528, found 289.1518.

### 3-(5-decyl-1,2,4-oxadiazol-3-yl)dihydrofuran-2(3H)-one (160D3)



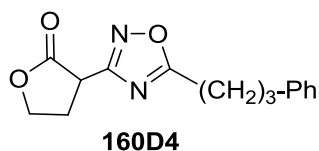
Purification by column chromatography (eluent: pentane/Diethyl ether=1/1) afford 38 mg product as a white solid (98% yield).

**<sup>1</sup>H NMR (300 MHz, Chloroform-*d*)** δ: 4.58 (q, *J* = 7.6 Hz, 1H, OCH<sub>2</sub> of lactone), 4.41 (q, *J* = 8.2 Hz, 1H, OCH<sub>2</sub> of lactone), 4.06 (t, *J* = 9.2 Hz, 1H, COCH of lactone), 2.87 (t, *J* = 7.6 Hz, 2H, Oxadiazole-CH<sub>2</sub>CH<sub>2</sub>(CH<sub>2</sub>)<sub>7</sub>CH<sub>3</sub>), 2.70 (q, *J* = 7.1 Hz, 2H, CH<sub>2</sub> of lactone), 1.87 – 1.71 (m, 2H, CH<sub>2</sub>CH<sub>2</sub>(CH<sub>2</sub>)<sub>7</sub>CH<sub>3</sub>), 1.25 (s, 14H, CH<sub>2</sub>CH<sub>2</sub>(CH<sub>2</sub>)<sub>7</sub>CH<sub>3</sub>), 0.86 (d, *J* = 6.6 Hz, 3H, CH<sub>2</sub>CH<sub>2</sub>(CH<sub>2</sub>)<sub>7</sub>CH<sub>3</sub>).

**<sup>13</sup>C NMR (75 MHz, Chloroform-*d*)** δ: 181.1 (C=O), 173.3 (OC=N), 166.5 (N=CN), 67.2 (OCH<sub>2</sub>), 38.0 (CH), 31.9 (CH<sub>2</sub>), 29.5 (CH<sub>2</sub>), 29.3 (CH<sub>2</sub>), 29.3 (CH<sub>2</sub>), 29.0 (CH<sub>2</sub>), 29.0 (CH<sub>2</sub>), 27.9 (CH<sub>2</sub>), 26.6 (CH<sub>2</sub>), 26.4 (CH<sub>2</sub>), 22.7 (CH<sub>2</sub>), 14.1 (CH<sub>3</sub>).

**HRMS (ESI)** [M + Na]<sup>+</sup> calculated for C<sub>16</sub>H<sub>26</sub>N<sub>2</sub>NaO<sub>3</sub> 317.1841, found 317.1832.

### 3-(5-(3-phenylpropyl)-1,2,4-oxadiazol-3-yl)dihydrofuran-2(3H)-one (160D4)



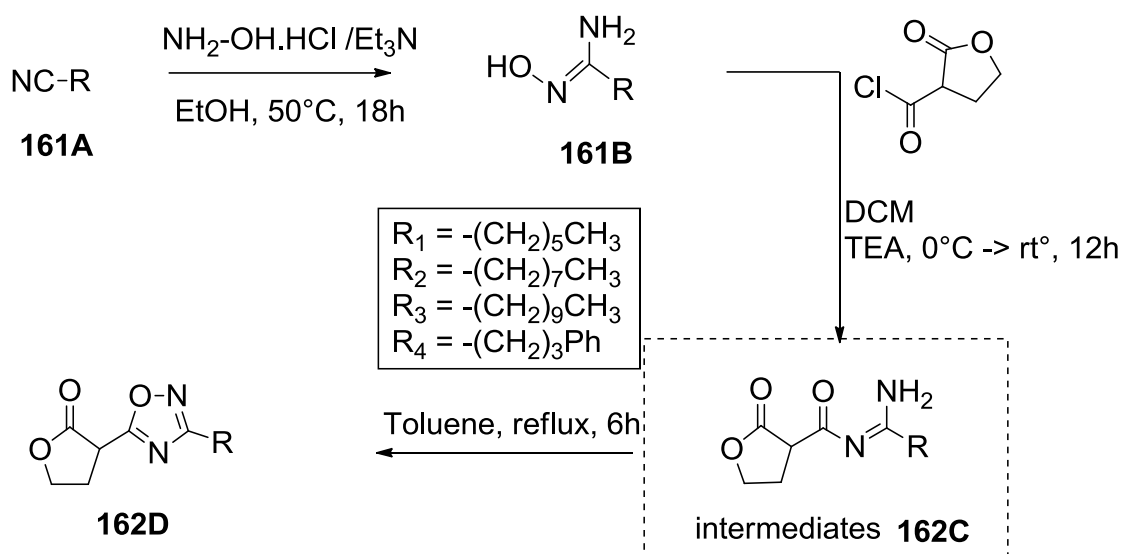
Purification by column chromatography (eluent: pentane/Diethyl ether=1/1) afford 55 mg product as a yellow oil (86% yield).

**<sup>1</sup>H NMR (300 MHz, Chloroform-*d*)** δ: 7.34 – 7.08 (m, 5H, ArH), 4.54 (td, *J* = 8.2, 7.5, 5.0 Hz, 1H, OCH<sub>2</sub> of lactone), 4.37 (q, *J* = 8.2 Hz, 1H, OCH<sub>2</sub> of lactone), 4.03 (t, *J* = 9.3 Hz, 1H, COCH of lactone), 2.86 (t, *J* = 7.6 Hz, 2H, PhCH<sub>2</sub>), 2.66 (dt, *J* = 14.6, 7.7 Hz, 4H, CH<sub>2</sub> of lactone and oxadiazole-CH<sub>2</sub>), 2.12 (p, *J* = 7.6 Hz, 2H, CH<sub>2</sub>).

**<sup>13</sup>C NMR (75 MHz, Chloroform-*d*)** δ: 180.7 (C=O), 173.4 (OC=N), 166.6 (N=CN), 140.5 (ArC), 128.5 (d, 4ArC), 126.3 (ArC), 67.3 (OCH<sub>2</sub>), 38.0 (CH), 34.9 (PhCH<sub>2</sub>), 27.9 (d, oxadiazole-CH<sub>2</sub>CH<sub>2</sub>), 25.9 (CH<sub>2</sub> of lactone).

**HRMS (ESI)** [M + Na]<sup>+</sup> calculated for C<sub>15</sub>H<sub>16</sub>N<sub>2</sub>NaO<sub>3</sub> 295.1059, found 295.1052.

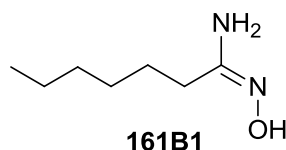
## Synthesis of 3,5 disubstituted 1,2,4-oxadiazole with the $\gamma$ -lactone in position 5



### General procedure for synthesis of nimidamide (161B):

To a solution of heptanenitrile **161A1** (0.018 mol) or nonanenitrile **161A2** or 4-phenylbutyronitrile **161A4** (0.0138 mol) and hydroxylamine hydrochloride (**161A1**: 0.036 mol, **161A4**: 0.0276 mol) in 20 mL ethanol was added the trimethylamine (**161A1**: 0.036 mol, **161A4**: 0.0276 mol). The mixture was refluxed and stirred for 18h. After termination of the reaction (TLC), ethanol was evaporated and the residue was suspended between 60 mL ethyl acetate and 60 mL of water. The aqueous layer was washed with ethyl acetate (30 mL x7). The organic layer was dried over Na<sub>2</sub>SO<sub>4</sub> and concentrated. The crude amidoxime was purified by column chromatography.

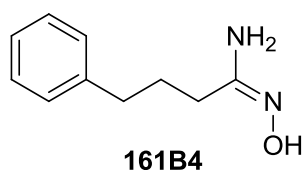
### (E)-N'-hydroxyheptanimidamide (161B1)



Purification by column chromatography (eluent: pentane/AcOEt=1/3) afford 1.5 g of product as a grey solid (yield 58%).

<sup>1</sup>H NMR (300 MHz, Chloroform-*d*)  $\delta$  4.54 (s, 2H, NH<sub>2</sub>), 2.18 – 2.06 (m, 2H, CH<sub>2</sub>), 1.55 (p, *J* = 7.3 Hz, 2H, CH<sub>2</sub>), 1.31 (q, *J* = 9.8, 9.2 Hz, 6H, 3CH<sub>2</sub>), 0.93 – 0.81 (m, 3H, CH<sub>3</sub>).

### (E)-N'-hydroxy-4-phenylbutanimidamide (**161B4**)



Purification by column chromatography (eluent: pentane/AcOEt=1/3) afford 0.94 g product as a yellow oil (yield 38%).

**<sup>1</sup>H NMR (300 MHz, Chloroform-*d*)**  $\delta$ : 7.32 – 7.14 (m, 5H, ArH), 4.53 (s, 2H, NH<sub>2</sub>), 2.71 – 2.61 (m, 2H, CH<sub>2</sub>), 2.22 – 2.12 (m, 2H, CH<sub>2</sub>), 1.89 (p, *J* = 7.6 Hz, 2H, CH<sub>2</sub>).

### Synthesis of 2-oxotetrahydrofuran-3-carboxylic acid

TBAB (2.31 mmol) was added to a solution of 1,1-cyclopropanedicarboxylic acid (23 mmol) in 50 mL of anhydrous CH<sub>3</sub>CN and the reaction was stirred and refluxed for 18h. After 18h, acetonitrile was evaporated and the residue was dissolved with 50 mL of AcOEt, following the organic layer was washed with 0.1 M HCl (5x10 mL), and the aqueous layer was extracted with AcOEt (5x 20 mL), the combined organic layers were dried over Na<sub>2</sub>SO<sub>4</sub> and concentrated. 2.4g of the desired product was obtained as a yellow oil and used for the next step without further purification (yield 80%).

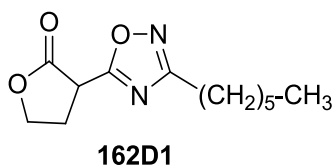
### Synthesis of 2-oxotetrahydrofuran-3-carbonyl chloride

The oxalyl chloride (**161B1**: 2.5 mmol; **161B2**: 2.25 mmol; **161B3**: 2 mmol; **161B4**: 2.01 mmol) was added dropwise to a solution of 2-oxotetrahydrofuran-3-carboxylic acid (**161B1**: 1.7 mmol; **161B2**: 1.5 mmol; **161B3**: 1.34 mmol; **161B4**: 1.37 mmol) in 5 mL of anhydrous DCM at 0 °C and one drop of DMF was added to the reaction medium. The mixture was allowed to stir at room temperature for 6h. The DCM was evaporated and a yellowed oil was obtained which was used for the next step without further purification.

### General procedure for the synthesis of 1,2,4-oxadiazole with $\gamma$ -lactone in position 5 (**162D**)

To a stirred solution of amidoxime (**161B1**: 1.39 mmol; **161B2**: 1.13 mmol; **161B3**: 1 mmol; **161B4**: 1.12 mmol) in anhydrous DCM (10 mL) was added the trimethylamine (**161B1**: 2.78 mmol; **161B2**: 2.25 mmol; **161B3**: 2 mmol; **161B4**: 2.25 mmol). Then the mixture was cooled to 0 °C and following the 2-oxotetrahydrofuran-3-carbonyl chloride was added dropwise to the mixture, the reaction was performed under an argon atmosphere. After 10 min, the mixture was stirred at room temperature for 12h and the reaction was monitored by TLC until the amidoxime was consumed. Then DCM was evaporated under reduced pressure, toluene (10 mL) was added and the reaction mixture was refluxed for 5h with monitoring with TLC. After completion of the reaction, toluene was removed and the dark residue was diluted in 50 mL of DCM and washed by water (50 mL), the aqueous phase was extracted by DCM (20 mL x2), the combined organic layers were dried over Na<sub>2</sub>SO<sub>4</sub>, evaporated and purified by column chromatography.

### 3-(3-hexyl-1,2,4-oxadiazol-5-yl)dihydrofuran-2(3H)-one (162D1)



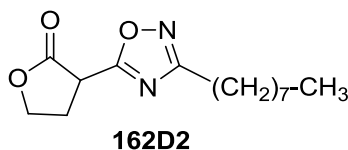
Purification by column chromatography (eluent: pentane/Diethyl ether=3/2) afford 120 mg product as a colorless oil (yield 36%).

**<sup>1</sup>H NMR (300 MHz, Chloroform-*d*)**  $\delta$ : 4.57 (td,  $J = 8.4, 7.6, 4.9$  Hz, 1H, OCH<sub>2</sub> of lactone), 4.41 (q,  $J = 9.0, 8.3$  Hz, 1H, OCH<sub>2</sub> of lactone), 4.17 (t,  $J = 9.3$  Hz, 1H, COCH- of lactone), 2.90 – 2.65 (m, 4H, CH<sub>2</sub> of lactone and Oxadiazole-CH<sub>2</sub>-CH<sub>2</sub>-(CH<sub>2</sub>)<sub>3</sub>-CH<sub>3</sub>), 1.70 (p,  $J = 7.5$  Hz, 2H, -CH<sub>2</sub>-CH<sub>2</sub>-(CH<sub>2</sub>)<sub>3</sub>-CH<sub>3</sub>), 1.49 – 1.17 (m, 6H, -CH<sub>2</sub>-CH<sub>2</sub>-(CH<sub>2</sub>)<sub>3</sub>-CH<sub>3</sub>), 0.93 – 0.75 (m, 3H, -CH<sub>2</sub>-CH<sub>2</sub>-(CH<sub>2</sub>)<sub>3</sub>-CH<sub>3</sub>).

**<sup>13</sup>C NMR (75 MHz, Chloroform-*d*)**  $\delta$ : 173.9 (C=O), 171.4 (OC=N), 171.1 (N=CN), 67.3 (OCH<sub>2</sub>), 38.8 (CH), 31.3 (CH<sub>2</sub>), 28.7 (CH<sub>2</sub>), 28.0 (CH<sub>2</sub>), 26.8 (CH<sub>2</sub>), 25.9 (CH<sub>2</sub>), 22.4 (CH<sub>2</sub>), 14.0 (CH<sub>3</sub>).

**HRMS (ESI)** [M + Na]<sup>+</sup> calculated for C<sub>12</sub>H<sub>18</sub>N<sub>2</sub>NaO<sub>3</sub> 261.1215, found 261.1215.

### 3-(3-octyl-1,2,4-oxadiazol-5-yl)dihydrofuran-2(3H)-one (162D2)



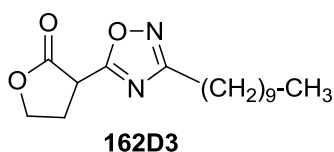
Purification by column chromatography (eluent: pentane/Diethyl ether=3/2) afford 99 mg product as a yellow oil (yield 33%).

**<sup>1</sup>H NMR (300 MHz, Chloroform-*d*)**  $\delta$  4.67 – 4.51 (m, 1H, OCH<sub>2</sub> of lactone), 4.51 – 4.35 (m, 1H, OCH<sub>2</sub> of lactone), 4.18 (t,  $J = 9.3$  Hz, 1H, COCH- of lactone), 2.88 – 2.66 (m, 4H, CH<sub>2</sub> of lactone and Oxadiazole-CH<sub>2</sub>-CH<sub>2</sub>-(CH<sub>2</sub>)<sub>5</sub>-CH<sub>3</sub>), 1.82 – 1.62 (m, 2H, -CH<sub>2</sub>-CH<sub>2</sub>-(CH<sub>2</sub>)<sub>5</sub>-CH<sub>3</sub>), 1.28 (d,  $J = 16.7$  Hz, 10H, -CH<sub>2</sub>-CH<sub>2</sub>-(CH<sub>2</sub>)<sub>5</sub>-CH<sub>3</sub>), 0.95 – 0.78 (m, 3H, -CH<sub>2</sub>-CH<sub>2</sub>-(CH<sub>2</sub>)<sub>5</sub>-CH<sub>3</sub>).

**<sup>13</sup>C NMR (75 MHz, Chloroform-*d*)**  $\delta$  173.8 (C=O), 171.3 (OC=N), 171.1 (N=CN), 67.3 (OCH<sub>2</sub>), 38.8 (CH), 31.8 (CH<sub>2</sub>), 29.1 (d, 3CH<sub>2</sub>), 28.0 (CH<sub>2</sub>), 26.8 (CH<sub>2</sub>), 26.0 (CH<sub>2</sub>), 22.6 (CH<sub>2</sub>), 14.1 (CH<sub>3</sub>).

**HRMS (ESI)** [M + H]<sup>+</sup> calculated for C<sub>14</sub>H<sub>23</sub>N<sub>2</sub>O<sub>3</sub> 267.1709, found 267.1701.

### 3-(3-decyl-1,2,4-oxadiazol-5-yl)dihydrofuran-2(3H)-one (162D3)



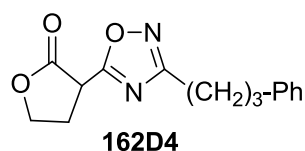
Purification by column chromatography (eluent: pentane/Diethyl ether=1/1) afford 118 mg of product as a white solid (yield 33%).

**<sup>1</sup>H NMR (300 MHz, Chloroform-*d*)**  $\delta$ : 4.70 – 4.55 (m, 1H, OCH<sub>2</sub> of lactone), 4.53 – 4.35 (m, 1H, OCH<sub>2</sub> of lactone), 4.18 (t, *J* = 9.2 Hz, 1H, COCH- of lactone), 2.94 – 2.62 (m, 4H, CH<sub>2</sub> of lactone and Oxadiazole-CH<sub>2</sub>-CH<sub>2</sub>-(CH<sub>2</sub>)<sub>7</sub>-CH<sub>3</sub>), 1.86 – 1.64 (m, 2H, CH<sub>2</sub>-CH<sub>2</sub>-(CH<sub>2</sub>)<sub>7</sub>-CH<sub>3</sub>), 1.29 (d, *J* = 20.2 Hz, 14H, -CH<sub>2</sub>-CH<sub>2</sub>-(CH<sub>2</sub>)<sub>7</sub>-CH<sub>3</sub>), 0.88 (t, *J* = 6.6 Hz, 3H, -CH<sub>2</sub>-CH<sub>2</sub>-(CH<sub>2</sub>)<sub>7</sub>-CH<sub>3</sub>).

**<sup>13</sup>C NMR (75 MHz, Chloroform-*d*)**  $\delta$ : 173.9 (C=O), 171.4 (OC=N), 171.1 (N=CN), 67.3 (OCH<sub>2</sub>), 38.8 (CH), 31.8 (CH<sub>2</sub>), 29.5 (CH<sub>2</sub>), 29.4 (CH<sub>2</sub>), 29.3 (CH<sub>2</sub>), 29.1 (CH<sub>2</sub>), 29.1 (CH<sub>2</sub>), 28.0 (CH<sub>2</sub>), 26.8 (CH<sub>2</sub>), 25.9 (CH<sub>2</sub>), 22.6 (CH<sub>2</sub>), 14.1 (CH<sub>3</sub>).

**HRMS (ESI)** [M + Na]<sup>+</sup> calculated for C<sub>16</sub>H<sub>26</sub>N<sub>2</sub>NaO<sub>3</sub> 317.1841, found 317.1840.

### 3-(3-(3-phenylpropyl)-1,2,4-oxadiazol-5-yl)dihydrofuran-2(3H)-one (162D4)



Purification by column chromatography (eluent: pentane/Diethyl ether=1/1) afford 169 mg product as a colorless oil (yield 56%).

**<sup>1</sup>H NMR (300 MHz, Chloroform-*d*)**  $\delta$ : 7.34 – 7.14 (m, 5H, ArH), 4.60 (td, *J* = 8.9, 4.7 Hz, 1H, OCH<sub>2</sub> of lactone), 4.43 (q, *J* = 8.9, 8.2 Hz, 1H, OCH<sub>2</sub> of lactone), 4.17 (t, *J* = 9.3 Hz, 1H, COCH- of lactone), 2.87 – 2.65 (m, 6H, CH<sub>2</sub> of lactone and Oxadiazole-CH<sub>2</sub>-CH<sub>2</sub>-CH<sub>2</sub>-Ph), 2.09 (p, *J* = 7.6 Hz, 2H, Oxadiazole-CH<sub>2</sub>-CH<sub>2</sub>-CH<sub>2</sub>-Ph).

**<sup>13</sup>C NMR (75 MHz, Chloroform-*d*)**  $\delta$  173.9 (C=O), 171.3 (OC=N), 170.8 (N=CN), 141.2 (ArC), 128.5 (2ArC), 128.4 (2ArC), 126.0 (ArC), 67.3 (OCH<sub>2</sub>), 38.8 (CH), 35.1 (CH<sub>2</sub>), 28.3 (CH<sub>2</sub>), 28.0 (CH<sub>2</sub>), 25.4 (CH<sub>2</sub>).

**HRMS (ESI)** [M + Na]<sup>+</sup> calculated for C<sub>15</sub>H<sub>16</sub>N<sub>2</sub>NaO<sub>3</sub> 295.1059, found 295.1059.

### General procedure of the synthesis of *N*-(2-nitrophenyl) amide

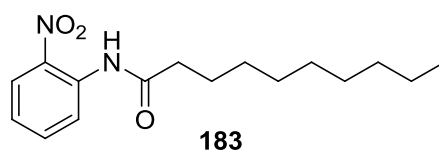
To a solution of 2-Nitroaniline (1.0 eq) in 10 mL of anhydrous dichloromethane was added trimethylamine (2.5 eq) and acyl chloride (2.5 eq: butyryl chloride, hexanoyl chloride, octanoyl chloride, decanoyl chloride, 4-phenylbutanoyl chloride was prepared from 4-phenylbutanoic acid and oxalyl chloride with catalytic DMF) at 0°C, the reaction mixture was allowed to warm up to room temperature and stirred for 16h. The mixture was diluted in 30 mL dichloromethane and washed with 40 mL 2M HCl, 40 mL 1M NaOH and 40 mL of brine, the organic layer was dried over anhydrous Na<sub>2</sub>SO<sub>4</sub>, evaporated. The residue was purified by flash chromatography column to give the desired products (29 % to 85 % yield).

### General procedure of the synthesis of *N*-phenyl amide compounds and *N*-(2-acetylphenyl) amide compounds

To a solution of aniline or 2-Aminoacetophenone (1.0 eq) in 10 mL of anhydrous dichloromethane was added trimethylamine (1.1 eq) and acyl chloride (1.1 eq: butyryl chloride, hexanoyl chloride, octanoyl chloride, decanoyl chloride, 4-phenylbutanoyl chloride was prepared from 4-phenylbutanoic acid and oxalyl chloride with catalytic DMF) at 0°C, the reaction mixture was allowed to warm up to room temperature and stirred for 16h. The mixture was diluted in 30 mL dichloromethane and washed with 40 mL 1M HCl, 40 mL sat. NaHCO<sub>3</sub> and 40 mL brine, the organic layer was dried over anhydrous Na<sub>2</sub>SO<sub>4</sub> and evaporated. The residue was purified by flash chromatography column to afford the desired products (36 % to 94 % yields).

*N*-(2-nitrophenyl)butyramide (180), *N*-(2-nitrophenyl)hexanamide (181), *N*-(2-nitrophenyl)octanamide (182), see reference<sup>[176]</sup>; *N*-phenylbutyramide (190) see reference<sup>[336]</sup>, *N*-phenylhexanamide (191) see reference<sup>[337]</sup>, *N*-phenyloctanamide (192) see reference<sup>[338]</sup>; *N*,4-diphenylbutanamide (194) see reference<sup>[339]</sup>.

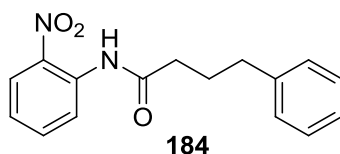
### *N*-(2-nitrophenyl)decanamide (183)



Purification: pentane/diethyl ether=10/1; yellow solid (43%);

<sup>1</sup>H NMR (300 MHz, Chloroform-*d*) δ 10.30 (s, 1H, NH), 8.74 (dd, *J* = 8.6, 1.4 Hz, 1H, Ph-H), 8.15 (dd, *J* = 8.5, 1.6 Hz, 1H, Ph-H), 7.58 (ddd, *J* = 8.8, 7.2, 1.6 Hz, 1H, Ph-H), 7.10 (ddd, *J* = 8.5, 7.2, 1.4 Hz, 1H, Ph-H), 2.42 (t, *J* = 7.5 Hz, 2H, COCH<sub>2</sub>), 1.69 (p, *J* = 7.5 Hz, 2H, CH<sub>2</sub>), 1.35 – 1.11 (m, 12H, 6CH<sub>2</sub>), 0.81 (t, *J* = 7.4 Hz, 3H, CH<sub>3</sub>).

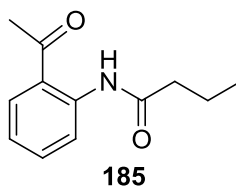
***N*-(2-nitrophenyl)-4-phenylbutanamide (184)**



Purification: pentane/AcOEt=15/1; yellow liquid (29%);

**<sup>1</sup>H NMR (300 MHz, Chloroform-*d*)**  $\delta$  10.38 (d,  $J = 5.5$  Hz, 1H, NH), 8.83 (d,  $J = 8.3$  Hz, 1H, Ph-H), 8.46 – 8.15 (m, 1H, Ph-H), 7.85 – 7.49 (m, 1H, Ph-H), 7.44 – 7.02 (m, 6H, Ph-H), 2.77 (t,  $J = 7.3$  Hz, 2H, PhCH<sub>2</sub>), 2.55 (t,  $J = 7.3$  Hz, 2H, COCH<sub>2</sub>), 2.16 (q,  $J = 7.4$  Hz, 2H, CH<sub>2</sub>).

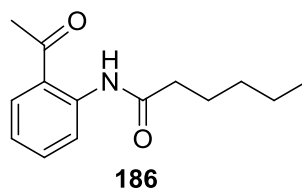
***N*-(2-acetylphenyl)butyramide (185)**



Purification: pentane/AcOEt=15/1; white solid (36%);

**<sup>1</sup>H NMR (300 MHz, Chloroform-*d*)**  $\delta$ : 11.71 (s, 1H, NH), 8.95 – 8.61 (m, 1H, Ph-H), 7.97 – 7.79 (m, 1H, Ph-H), 7.55 (dddd,  $J = 8.5, 7.3, 1.6, 0.5$  Hz, 1H, Ph-H), 7.10 (ddd,  $J = 8.0, 7.3, 1.2$  Hz, 1H, Ph-H), 2.67 (s, 3H, COCH<sub>3</sub>), 2.41 (t,  $J = 7.5$  Hz, 2H, COCH<sub>2</sub>), 1.92 – 1.66 (m, 2H, CH<sub>2</sub>), 1.01 (t,  $J = 7.4$  Hz, 3H, CH<sub>3</sub>).

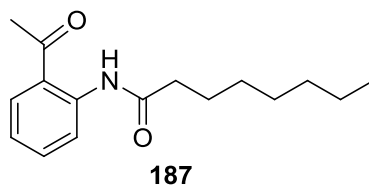
***N*-(2-acetylphenyl)hexanamide (186)**



Purification: pentane/AcOEt=13/1; colorless oil (92%);

**<sup>1</sup>H NMR (300 MHz, Chloroform-*d*)**  $\delta$  11.71 (s, 1H, NH), 8.85 – 8.68 (m, 1H, Ph-H), 7.98 – 7.82 (m, 1H, Ph-H), 7.63 – 7.46 (m, 1H, Ph-H), 7.10 (ddd,  $J = 8.0, 7.3, 1.2$  Hz, 1H, Ph-H), 2.67 (s, 3H, COCH<sub>3</sub>), 2.43 (t,  $J = 7.5$  Hz, 2H, COCH<sub>2</sub>), 1.85 – 1.66 (m, 2H, CH<sub>2</sub>), 1.41 – 1.24 (m, 4H, 2CH<sub>2</sub>), 1.00 – 0.79 (t,  $J = 7.4$  Hz, 3H, CH<sub>3</sub>).

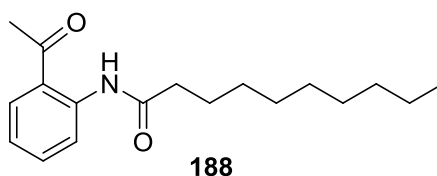
***N*-(2-acetylphenyl)octanamide (187)**



Purification: pentane/AcOEt=15/1; colorless oil (85%);

**<sup>1</sup>H NMR (300 MHz, Chloroform-*d*)**  $\delta$ : 11.70 (s, 1H, NH), 8.77 (dd,  $J$  = 8.5, 1.2 Hz, 1H, Ph-H), 7.89 (dd,  $J$  = 8.0, 1.6 Hz, 1H, Ph-H), 7.54 (ddd,  $J$  = 8.5, 7.2, 1.6 Hz, 1H, Ph-H), 7.10 (ddd,  $J$  = 8.0, 7.3, 1.2 Hz, 1H, Ph-H), 2.66 (s, 3H, COCH<sub>3</sub>), 2.43 (t,  $J$  = 7.5 Hz, 2H, COCH<sub>2</sub>), 1.83 – 1.62 (m, 2H, CH<sub>2</sub>), 1.44 – 1.16 (m, 8H, 4CH<sub>2</sub>), 0.96 – 0.72 (t,  $J$  = 7.4 Hz, 3H, CH<sub>3</sub>).

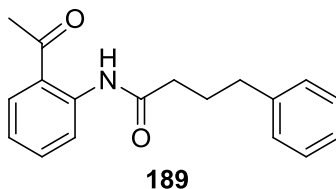
***N*-(2-acetylphenyl)decanamide (188)**



Purification: pentane/AcOEt=15/1; white solid (37%);

**<sup>1</sup>H NMR (300 MHz, Chloroform-*d*)**  $\delta$ : 11.64 (s, 1H, NH), 8.71 (dd,  $J$  = 8.6, 1.2 Hz, 1H, Ph-H), 7.83 (dd,  $J$  = 8.0, 1.5 Hz, 1H, Ph-H), 7.59 – 7.35 (m, 1H, Ph-H), 7.04 (ddd,  $J$  = 8.0, 7.3, 1.2 Hz, 1H, Ph-H), 2.60 (s, 3H, COCH<sub>3</sub>), 2.36 (t,  $J$  = 7.5 Hz, 2H, COCH<sub>2</sub>), 1.68 (p,  $J$  = 7.6 Hz, 2H, CH<sub>2</sub>), 1.27 – 1.19 (m, 12H, 6CH<sub>2</sub>), 0.92 – 0.67 (t,  $J$  = 7.4 Hz, 3H, CH<sub>3</sub>).

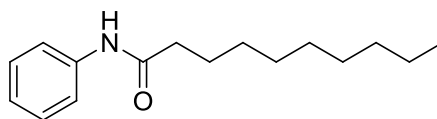
***N*-(2-acetylphenyl)-4-phenylbutanamide (189)**



Purification: pentane/AcOEt=13/1; colorless oil (44%);

**<sup>1</sup>H NMR (300 MHz, Chloroform-*d*)**  $\delta$ : 11.75 (s, 1H, NH), 8.80 (dd,  $J$  = 8.5, 1.2 Hz, 1H, Ph-H), 7.92 (dd,  $J$  = 8.0, 1.6 Hz, 1H, Ph-H), 7.70 – 7.50 (m, 1H, Ph-H), 7.41 – 7.06 (m, 6H, Ph-H), 2.75 (t,  $J$  = 7.4 Hz, 2H, PhCH<sub>2</sub>), 2.69 (s, 3H, COCH<sub>3</sub>), 2.50 (t,  $J$  = 7.5 Hz, 2H, COCH<sub>2</sub>), 2.20 – 2.05 (m, 2H, CH<sub>2</sub>).

**N-phenyldecanamide (193)**



**193**

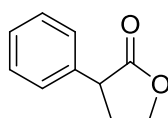
Purification: pentane/AcOEt=10/1; white solid (94%);

**<sup>1</sup>H NMR (300 MHz, Chloroform-*d*)**  $\delta$ : 7.58 – 7.44 (m, 2H, Ph-H), 7.31 (t,  $J = 7.9$  Hz, 2H, Ph-H), 7.09 (t,  $J = 7.5$  Hz, 1H, Ph-H), 2.35 (t,  $J = 7.6$  Hz, 2H, COCH<sub>2</sub>), 1.72 (p,  $J = 7.5$  Hz, 2H, CH<sub>2</sub>), 1.33 – 1.24 (m, 12H, 6CH<sub>2</sub>), 0.88 (t,  $J = 7.4$  Hz, 3H, CH<sub>3</sub>).

### General procedure for straightforward cyclization from carboxymethyl ester:

To a solution of LiHMDS (1.2 eq) in 2 mL anhydrous THF was added dropwise various ethyl ester substrates (1 eq) which were dissolved in 2 mL anhydrous THF at -15 °C. The reaction mixture was stirred at -15 °C for 40 min, a solution of cyclic sulfate (1.2 eq) in 2 mL anhydrous THF was added to the mixture -15 °C. The reaction was allowed to stir for 6h while the temperature was warmed up to rt. Then THF was evaporated under reduced pressure to give a yellow solid, which was subsequently treated with 2 mL 4M HCl in dioxane, additional 4 mL dioxane were added, and the reaction was stirred at 80 °C for 14h. After the termination of reaction, dioxane was evaporated in vacuo to give a brown syrup, which was dissolved in 20 mL dichloromethane and washed with water (2x20 mL), the aqueous layer was extracted with dichloromethane (20 mL x2), the organic layers were combined, dried over Na<sub>2</sub>SO<sub>4</sub>, concentrated, and purified by flash chromatography.

### 3-phenyldihydrofuran-2(3H)-one (176b)



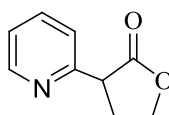
176b

Following the general procedure, ethyl 2-phenylacetate (200 mg, 1.22 mmol), cyclic sulfate (182 mg, 1.46 mmol), LiHMDS (244 mg, 1.46 mmol, 1.5 mL THF solution), and 6 mL of THF were used. Purification by flash chromatography (pentane/AcOEt=4/1) afforded 147 mg product as a colorless oil (75% yield).

<sup>1</sup>H NMR (300 MHz, Chloroform-*d*) δ: 7.40 – 7.19 (m, 5H, ArH), 4.42 (td, *J* = 8.7, 3.3 Hz, 1H, OCH<sub>2</sub>), 4.28 (td, *J* = 9.2, 6.7 Hz, 1H, OCH<sub>2</sub>), 3.76 (dd, *J* = 10.2, 9.1 Hz, 1H, COCH), 2.74 – 2.58 (m, 1H, CH<sub>2</sub>), 2.38 (dddd, *J* = 12.8, 10.3, 9.3, 8.2 Hz, 1H, CH<sub>2</sub>).

<sup>13</sup>C-DEPT135 NMR (75 MHz, Chloroform-*d*) δ: 128.9 (2ArC), 127.9 (2ArC), 127.6 (ArC), 66.6 (OCH<sub>2</sub>), 45.5 (COCH), 31.6 (CH<sub>2</sub>).

### 3-(pyridin-2-yl)dihydrofuran-2(3H)-one (176a)



176a

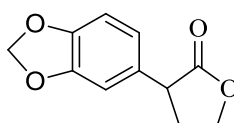
Following the general procedure, ethyl 2-(pyridin-2-yl)acetate (200 mg, 1.21 mmol), cyclic sulfate (180 mg, 1.45 mmol), LiHMDS (242 mg, 1.45 mmol, 1.5 mL in THF solution), and 6 mL of THF were used. Purification by flash chromatography (pentane/AcOEt=1/1) afforded 120 mg product as a colorless oil (61%).

**<sup>1</sup>H NMR (300 MHz, Chloroform-*d*)**  $\delta$  8.54 (ddd,  $J = 5.0, 1.8, 0.9$  Hz, 1H, ArH), 7.66 (td,  $J = 7.7, 1.8$  Hz, 1H, ArH), 7.35 (dt,  $J = 7.8, 1.1$  Hz, 1H, ArH), 7.19 (ddd,  $J = 7.6, 4.9, 1.2$  Hz, 1H, ArH), 4.55 (ddd,  $J = 8.7, 8.1, 4.9$  Hz, 1H, OCH<sub>2</sub>), 4.37 (dt,  $J = 8.8, 7.5$  Hz, 1H, OCH<sub>2</sub>), 4.01 – 3.84 (m, 1H, COCH), 2.93 – 2.47 (m, 2H, CH<sub>2</sub>).

**<sup>13</sup>C NMR (75 MHz, Chloroform-*d*)**  $\delta$ : 177.0 (CO), 156.4 (ArC), 149.8 (ArC), 137.0 (ArC), 123.6 (ArC), 122.8 (ArC), 67.5 (OCH<sub>2</sub>), 47.6 (COCH), 29.2 (CH<sub>2</sub>).

**HRMS m/z (ESI):** Calcd. for C<sub>9</sub>H<sub>9</sub>NNaO<sub>2</sub> (M+Na)<sup>+</sup>: 186.0531. Found: 186.0525.

### 3-(benzo[d][1,3]dioxol-5-yl)dihydrofuran-2(3H)-one (176c)



**176c**

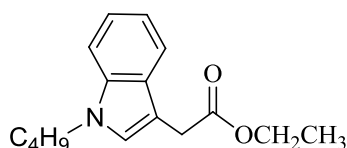
Following the general procedure, ethyl 2-(benzo[d][1,3]dioxol-5-yl)acetate (200 mg, 0.962 mmol), cyclic sulfate (143 mg, 1.154 mmol), LiHMDS (189 mg, 1.154 mmol, 1.2 mL of THF solution), and 6 mL of THF were used. Purification by flash chromatography (pentane/AcOEt=3/1) afforded 125 mg product as a yellow oil (63%).

**<sup>1</sup>H NMR (300 MHz, Chloroform-*d*)**  $\delta$ : 6.73 (q,  $J = 8.0$  Hz, 3H, ArH), 5.91 (s, 2H, OCH<sub>2</sub>O), 4.40 (td,  $J = 8.7, 2.9$  Hz, 1H, OCH<sub>2</sub>), 4.27 (td,  $J = 9.3, 6.7$  Hz, 1H, OCH<sub>2</sub>), 3.78 – 3.60 (m, 1H, COCH), 2.63 (ddd,  $J = 12.0, 9.4, 6.5$  Hz, 1H, CH<sub>2</sub>), 2.34 (dt,  $J = 21.1, 9.7$  Hz, 1H, CH<sub>2</sub>).

**<sup>13</sup>C NMR (75 MHz, Chloroform-*d*)**  $\delta$ : 177.5 (CO), 148.1 (ArC), 147.1 (ArC), 130.3 (ArC), 121.3 (ArC), 108.5 (ArC), 108.3 (ArC), 101.2 (OCH<sub>2</sub>O), 66.5 (OCH<sub>2</sub>), 45.2 (COCH), 31.6 (CH<sub>2</sub>).

**HRMS m/z (ESI):** Calcd. for C<sub>11</sub>H<sub>10</sub>NaO<sub>4</sub> (M+Na)<sup>+</sup>: 229.0477. Found: 229.0471.

### Ethyl 2-(1-butyl-1H-indol-3-yl)acetate (176d')

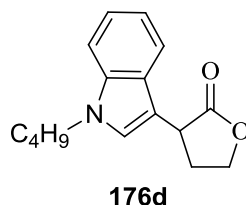


**176d'**

To a solution of ethyl 2-(1H-indol-3-yl)acetate (200 mg, 1.14 mmol) in 10 mL of DMF was added NaH (60% in oil, 30 mg, 1.26 mmol) at 0 °C, the mixture was stirred at 0 °C for 30 min. And BnBr (188 mg, 150  $\mu$ L, 1.37 mmol) was added, the reaction was stirred at room temperature for 6h until the starting material was consumed. Then DMF was removed under reduced pressure, the residue was dissolved in 40 mL AcOEt and extracted with 40 mL 1M HCl and 40 mL saturated NaHCO<sub>3</sub>, the aqueous layer was washed with AcOEt (30 mL x2), the combined organic layer was dried over Na<sub>2</sub>SO<sub>4</sub>, concentrated and purified by column chromatography (pentane/AcOEt = 15/1) to afford 160 mg desired product as a colorless oil. (54% yield)

**<sup>1</sup>H NMR (300 MHz, Chloroform-*d*)**  $\delta$  7.54 (ddd,  $J = 7.9, 1.2, 0.7$  Hz, 1H, ArH), 7.25 – 7.22 (m, 1H, ArH), 7.16 – 7.09 (m, 1H, ArH), 7.07 – 6.99 (m, 2H, ArH), 4.12 – 3.98 (m, 4H, NCH<sub>2</sub>, OCH<sub>2</sub>), 3.68 (s, 2H, COCH<sub>2</sub>), 1.78 – 1.68 (m, 2H, CH<sub>2</sub>), 1.27 (t,  $J = 7.1$  Hz, 3H, CH<sub>2</sub>), 1.18 (t,  $J = 7.1$  Hz, 3H, CH<sub>3</sub>), 0.86 (t,  $J = 7.4$  Hz, 3H, CH<sub>3</sub>).

**3-(1-butyl-1H-indol-3-yl)dihydrofuran-2(3H)-one (176d)**



Following the general procedure, ethyl 2-(1-butyl-1H-indol-3-yl)acetate (195 mg, 0.753 mmol), cyclic sulfate (113 mg, 0.904 mmol), LiHMDS (148 mg, 0.904 mmol, 0.91 mL of THF solution), and 6 mL of THF were used. Purification by flash chromatography (pentane/AcOEt=9/1 to 7/1) afforded 100 mg product as a colorless oil (52%).

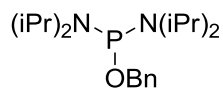
**<sup>1</sup>H NMR (300 MHz, Chloroform-*d*)**  $\delta$ : 7.57 (dt,  $J = 7.9, 1.0$  Hz, 1H, ArH), 7.36 (dt,  $J = 8.3, 0.9$  Hz, 1H, ArH), 7.29 – 7.20 (m, 1H, ArH), 7.18 – 7.09 (m, 2H, ArH), 4.48 (ddd,  $J = 9.0, 8.1, 3.8$  Hz, 1H, OCH<sub>2</sub>), 4.39 (td,  $J = 9.0, 6.7$  Hz, 1H, OCH<sub>2</sub>), 4.14 – 4.05 (m, 3H, COCH, NCH<sub>2</sub>), 2.80 (dddd,  $J = 12.6, 8.8, 6.7, 3.8$  Hz, 1H, CH<sub>2</sub> of lactone), 2.47 (dddd,  $J = 12.7, 9.7, 8.9, 8.1$  Hz, 1H, CH<sub>2</sub> of lactone), 1.89 – 1.76 (m, 2H, CH<sub>2</sub>), 1.44 – 1.29 (m, 2H, CH<sub>2</sub>), 0.95 (t,  $J = 7.3$  Hz, 3H, CH<sub>3</sub>).

**<sup>13</sup>C NMR (75 MHz, Chloroform-*d*)**  $\delta$ : 177.9 (CO), 136.6 (ArC), 126.8 (ArC), 125.8 (ArC), 121.9 (ArC), 119.3 (ArC), 119.0 (ArC), 109.8 (ArC), 109.5 (ArC), 66.8 (OCH<sub>2</sub>), 46.2 (COCH), 37.4 (NCH<sub>2</sub>), 32.4 (CH<sub>2</sub>), 31.1 (CH<sub>2</sub>), 20.3 (CH<sub>2</sub>), 13.8 (CH<sub>3</sub>).

**HRMS *m/z* (ESI)**: Calcd. for C<sub>16</sub>H<sub>19</sub>NNaO<sub>2</sub> (M+Na)<sup>+</sup>: 280.1313. Found: 280.1308.

## Part II. Supplementary information

### Benzyloxy-bis(diisopropylamino)phosphine (65)

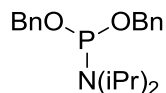


65

To a solution of distilled phosphorus trichloride ( $\text{PCl}_3$ ) (10.5 mL, 7 eq) in 20 mL of  $\text{CH}_3\text{CN}$ , a  $\text{BnOH}$  solution (1.7 mL, 1 eq) in 45 mL of  $\text{CH}_3\text{CN}$  was added dropwise for 5 min under nitrogen. The mixture was stirred for 10 minutes at room temperature, and then the solvent and the excess  $\text{PCl}_3$  was evaporated. The residue was then diluted in  $\text{Et}_2\text{O}$  (50 mL) anhydrous and then cooled to  $-10^\circ\text{C}$ . The diisopropylamine (15 mL, 6 eq) was then added dropwise under nitrogen and the mixture was stirred at room temperature for 18 h. The mixture was then washed with saturated  $\text{NaHCO}_3$  solution (50 mL), dried over  $\text{Na}_2\text{SO}_4$  and evaporated in vacuo. The product was obtained in 69% yield (3.95g) as a colorless oil after purification on silica gel with a pentane /  $\text{Et}_3\text{N}$  / (97/3) mixture as eluent.

$^1\text{H-NMR}$  (300 MHz,  $\text{CDCl}_3$ ): 7,2-7,5 (m, 5H, Ph), 4,65 (d, 2H,  $^2J = 6\text{Hz}$ ,  $\text{CH}_2\text{-Ph}$ ), 3,58(m, 2H,  $\text{CH-CH}_3$ ), 1,18 (d, 12H,  $^3J = 3\text{Hz}$ ,  $\text{CH-CH}_3$ ).  $^{13}\text{C-NMR}$  (75 MHz,  $\text{CDCl}_3$ ): 24, 24.1, 24.7, 24.8 ( $\text{CH-CH}_3$ ), 44.5, 44.7 ( $\text{CH-CH}_3$ ), 66.2 ( $\text{CH}_2\text{-Ph}$ ), 126.9, 128.2, 140.6 (Ph).  $^{31}\text{P-NMR}$  (300 MHz,  $\text{CDCl}_3$ ): 123.63.

### Dibenzyl diisopropylphosphoramidite (126)

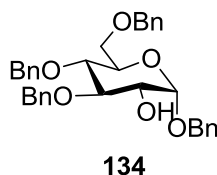


126

To a solution of phosphorus trichloride (7.87 g, 57.3 mmol) in 50 mL of anhydrous hexane was added diisopropylamine (11.6 g, 16 mL, 114.6 mmol) at  $0^\circ\text{C}$ , the reaction was allowed to stir from  $0^\circ\text{C}$  to room temperature for 4h, the organic salt was filtered off and washed with 50 mL hexane, then the solvent was evaporated to give a colorless oil which was used for next step without further purification. To a cooled solution of *N,N*-diisopropyl dichlorophosphoramidite (7.3 g, 36.13 mmol) in 100 mL of anhydrous THF was added dropwise triethylamine (7.68 g, 75.87 mmol) and benzyl alcohol (7.7 g, 72 mmol) at  $0^\circ\text{C}$ . The reaction was allowed to stir at room temperature for 14 h. Then the inorganic salt was filtered off and the organic phase was washed with 1M  $\text{NaHCO}_3$  and saturated  $\text{NaCl}$  solution, dried over anhydrous  $\text{Na}_2\text{SO}_4$ , concentrated in vacuo to afford 11 g of product as a colorless oil (56% yield).

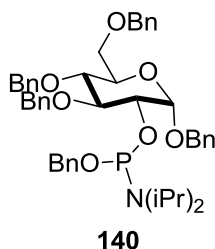
$^1\text{H NMR}$  (300 MHz, Chloroform-*d*)  $\delta$ : 7.44 – 7.22 (m, 10H, ArH), 4.77 (qd,  $J = 12.6, 8.4\text{ Hz}$ , 4H,  $\text{ArCH}_2$ ), 3.83 – 3.64 (m, 2H, CH), 1.24 (d,  $J = 6.8\text{ Hz}$ , 12H,  $\text{CH}_3$ ).  $^{31}\text{P NMR}$  (122 MHz, Chloroform-*d*)  $\delta$  147.70 .

### Benzyl 3,4,6-tri-*O*-benzyl- $\alpha$ -D-glucopyranoside (**134**):



For the synthesis of compound **134**, D-glucose was glycosylated and benzylated leading to known compound **Benzyl 2,3,4,6-tetra-*O*-benzyl- $\alpha$ -D-glucopyranoside** which gave analytical data identical to those reported in literature.<sup>[289][340]</sup> TIBAL (2.4 mL, 9.5 mmol) was added to a solution of compound **Benzyl 2,3,4,6-tetra-*O*-benzyl- $\alpha$ -D-glucopyranoside** (1 g, 1.59 mmol) in toluene (10 mL) and the mixture was stirred for 60 h at 50°C. The reaction mixture was then cooled to 0°C and HCl 1 M was added drop wise. Ethyl acetate was added, the organic phase was collected and the aqueous phase was extracted twice with ethyl acetate. The organic phases were combined, dried over MgSO<sub>4</sub>, filtered and evaporated. After purification by silica gel chromatography (petroleum ether/AcOEt 4:1), compound **134** (220 mg, 26%) was obtained as a colorless oil and gave analytical data identical to those reported in literature.<sup>[290][287]</sup>

### Benzyl ((2*S*,3*R*,4*S*,5*R*,6*R*)-2,4,5-tris(benzyloxy)-6-((benzyloxy)methyl)tetrahydro-2*H*-pyran-3-yl) diisopropylphosphoramidite (**140**)



To a solution of **benzyl 3,4,6-tri-*O*-benzyl- $\alpha$ -D-glucopyranoside (**134**)** (210 mg, 0.389 mmol) in 5 mL of dichloromethane was added tetrazole salt and benzyloxy-bis(diisopropylamino)phosphine (**65**) (200 mg, 0.583 mmol). The mixture was co-evaporated with toluene for three times before dichloromethane was added. The reaction was stirred from 0 °C to rt for 18h until the starting material was consumed. Then the mixture was diluted in 15 mL of dichloromethane and washed with saturated NaHCO<sub>3</sub> and brine (20 mL respectively), the organic layer was separated, dried over anhydrous Na<sub>2</sub>SO<sub>4</sub>, concentrated and purified by flash chromatography column (pentane/AcOEt=13/1 with 1% triethylamine) to afford 230 mg product as a colorless oil (73% yield).

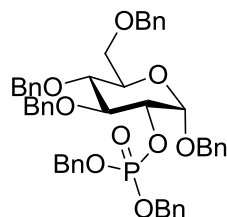
The tetrazole salt was prepared by using 519  $\mu$ L tetrazole (0.6 eq, 0.2334 mmol, 0.45 M in CH<sub>3</sub>CN), 40  $\mu$ L diisopropylamine (0.7 eq, 0.2723 mmol) in 1 mL anhydrous dichloromethane. The mixture was stirred at room temperature for 10 min, then dichloromethane was evaporated to give white solid which was used as a catalyst directly for the condensation reaction.

**<sup>1</sup>H NMR (300 MHz, Chloroform-*d*)**  $\delta$ : 7.40 – 7.20 (m, 23H, ArH), 7.08 (dd,  $J = 6.8, 2.9$  Hz, 2H, ArH), 5.14 (d,  $J = 3.6$  Hz, 1H, H-1), 4.83 – 4.40 (m, 10H, PhCH<sub>2</sub>), 4.13 (q,  $J = 7.1$  Hz, 1H, H-5), 4.04 – 3.96 (m, 1H, H-2), 3.92 – 3.83 (m, 2H, H-6, H-3), 3.67 (ddd,  $J = 28.7, 9.8, 3.6$  Hz, 4H, H-6, H-4, 2CH), 1.14 (t,  $J = 6.7$  Hz, 12H, 4CH<sub>3</sub>).

**<sup>31</sup>P NMR (122 MHz, Chloroform-*d*)**  $\delta$  149.94, 148.80.

**HRMS m/z (ESI)**: Calcd. for C<sub>47</sub>H<sub>56</sub>NO<sub>7</sub>P (M+H)<sup>+</sup>: 778.3873. Found: 778.3.

### Benzyl 2-*O*-dibenzyl phosphate 3,4,6-tri-*O*-benzyl- $\alpha$ -D-glucopyranoside (**138**)



**138**

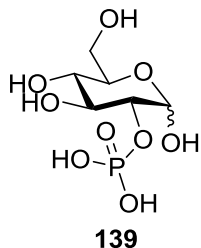
*N,N*-diisopropyl dibenzyl phosphoramidite (**126**) (1.6 g, 4.63 mmol) was stirred with 1*H*-tetrazole (0.45 mol/L in acetonitrile, 10.3 mL, 4.63 mmol) in dry CH<sub>2</sub>Cl<sub>2</sub> (20 mL) under argon for 30 min at room temperature. Compound **134** (1 g, 1.85 mmol) dissolved in dry CH<sub>2</sub>Cl<sub>2</sub> (30 mL) was added and the resulting mixture was stirred for 2h. TLC (petroleum ether/ethyl acetate 5:1) showed that the reaction was completed. The mixture was cooled to 0°C, and 3-chloroperoxybenzoic acid (800 mg, 4.63 mmol) was added. The resulting mixture was allowed to warm up to room temperature and stirred for 2h, the reaction was checked by TLC (petroleum ether/ethyl acetate 1:1). Then 10% aqueous solution of NaHSO<sub>4</sub> (2x100 mL) was added to quench *m*-CPBA, the layers were separated, and the aqueous layer was extracted with CH<sub>2</sub>Cl<sub>2</sub> (2x100 mL). The combined organic layers were washed with HCl 1 M (2x100 mL), a saturated solution of NaHCO<sub>3</sub> (2x100 mL) and brine (2x100 mL) respectively. The organic phase was dried over MgSO<sub>4</sub>, filtered, and concentrated under reduced pressure. Purification by silica gel column chromatography (petroleum ether/ethyl acetate 4:1) yield **138** (1.25 g, 84%) as a colorless oil.

**<sup>1</sup>H-NMR** (400 MHz, CDCl<sub>3</sub>)  $\delta$ : 3.52 (dd,  $J = 2$  and 10.8, 1H, H6), 3.59-3.66 (m, 2H, H6 and H4), 3.75-3.79 (m, 1H, H5), 3.97 (t,  $J = 9.3$ , 1H, H3), 4.30-4.35 (m, 1H, H2), 4.39-4.43 (m, 3H, CH<sub>2</sub>Ph), 4.52-4.62 (m, 2H, CH<sub>2</sub>Ph), 4.68-4.72 (m, 2H, CH<sub>2</sub>Ph), 4.75-4.91 (m, 5H, CH<sub>2</sub>Ph), 5.17 (d,  $J = 3.7$ , 1H, H $\alpha$ ), 7.02-7.05 (m, 2H, Ar), 7.07-7.10 (m, 2H, Ar), 7.12-7.26 (m, 26H, Ar); **<sup>13</sup>C-NMR** (100 MHz, CDCl<sub>3</sub>): 68.3 (C6), 69.2 (d,  $J_{C-P} = 5.1$ , CH<sub>2</sub>Ph), 69.4 (d,  $J_{C-P} = 5.1$ , CH<sub>2</sub>Ph), 70.0 (CH<sub>2</sub>Ph), 70.6 (C5), 73.5 (CH<sub>2</sub>Ph), 75.2 (CH<sub>2</sub>Ph), 75.5 (CH<sub>2</sub>Ph), 77.4 (d,  $J_{C-P} = 5.9$ , C2), 77.8 (C4), 80.8 (d,  $J_{C-P} = 7.3$ , C3), 96.6 (C1), 127.6, 127.8, 127.8, 127.8, 127.9, 127.9, 128.0, 128.1, 128.4, 128.4, 128.4, 128.5, 128.5, 128.6, 135.9 (t,  $J_{C-P} = 7.3$ , P-OCH<sub>2</sub>-CAr), 137.3, 138.0, 138.1, 138.5;

**<sup>31</sup>P-NMR**: (120 MHz, CDCl<sub>3</sub>): -1.53.  $[\alpha]_D^{20} = +48.7$  (c1.0, CHCl<sub>3</sub>).

**HRMS m/z (ESI)**: Calcd. for C<sub>48</sub>H<sub>49</sub>NaO<sub>9</sub>P (M+Na)<sup>+</sup>: 823.3006. Found: 823.2988.

### **D-Glucose-2-phosphate (139)**



Pd/C (40 mg) was added to a solution of compound **138** (0.1 g, 0.125 mmol) in methanol (10 mL) and the mixture was stirred under an H<sub>2</sub> atmosphere for 18 h at room temperature. The solution was then filtered through celite and concentrated to give **139** as white solid. Further purification by C18 column to afford product as a phosphate form (25 mg, 87%).

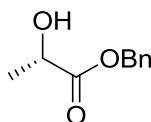
**<sup>1</sup>H-NMR** (400 MHz, D<sub>2</sub>O)  $\delta$ : 3.44-3.49 (m, 1.3H, H4 $\alpha$  and  $\beta$ , H5 $\beta$ ), 3.64 (t,  $J$  = 8.9, 0.4H, H3 $\beta$ ), 3.67-3.90 (m, 3.85H, H2 $\beta$ , H3 $\alpha$ , H5 $\alpha$ , H6 $\alpha$  and  $\beta$ ), 3.94-4.0 (m, 0.7H, H2 $\alpha$ ), 4.74 (d,  $J$  = 7.7, 0.47H, H $\beta$ ), 5.39 (d,  $J$  = 3.2, 0.65H, H $\alpha$ );

**<sup>13</sup>C-NMR** (100 MHz, D<sub>2</sub>O): 61.1 (C6 $\alpha$ ), 61.3 (C6 $\beta$ ), 69.9 (C4 $\beta$ ), 70.0 (C4 $\alpha$ ), 71.9 (C5 $\alpha$ ), 72.1 ( $J_{C-P}$  = 5.9, C3 $\alpha$ ), 75.6 ( $J_{C-P}$  = 2.9, C3 $\beta$ ), 76.2 ( $J_{C-P}$  = 5.9, C2 $\alpha$ ), 76.5 (C5 $\beta$ ), 79.5 ( $J_{C-P}$  = 5.9, C2 $\beta$ ), 91.3 (C1 $\alpha$ ), 95.5 ( $J_{C-P}$  = 4.4, C1 $\beta$ )

**<sup>31</sup>P-NMR**: (200 MHz, D<sub>2</sub>O): -0.01( $\beta$ ) and -0.30( $\alpha$ ); [ $\alpha$ ]<sub>D</sub> = +40 ( $c$ 1.0, MeOH).

**HRMS m/z (ESI)**: Calcd. for C<sub>6</sub>H<sub>12</sub>O<sub>9</sub>P (M-H)<sup>-</sup>: 259.0224. Found: 259.0215.

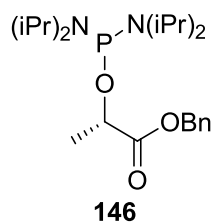
### **L-Benzyl lactate**



The product was prepared from a modified procedure to that described in the literature<sup>[341]</sup>. A 50 mL round bottom flask was equipped with a stir bar and a septum. L-lactic acid (313 mg, 3.45 mmol) was added followed by 7 mL of a MeOH: H<sub>2</sub>O (9:1) solution. The solution was then treated with a 20% CsCO<sub>3</sub> solution drop wise until a pH of 7 was achieved. The solvent was then removed under reduced pressure. DMF (4 mL) was added to the flask and removed under reduced pressure revealing the cesium salt of lactic acid. The salt was suspended in DMF (4.0 mL) and cooled to 0 °C and benzyl bromide (560 mg, 3.11 mmol) was added drop wise. The mixture was then allowed to warm to ambient temperature and stirred for 18 h. The crude was extracted with ether (50 mL) and partitioned with 50 mL of water. The aqueous layer was then extracted with ether (3x 50 mL) and the organic layers combined and washed with sat. NaHCO<sub>3</sub>, brine, and dried over sodium sulfate. Filtration followed by solvent removal under reduced pressure gave a product as a colorless oil, further purification by chromatography column (pentane/AcOEt=4/1) to afford 523 mg (93% yield) of the desired lactate.

$^1\text{H NMR}$  (300 MHz,  $\text{CDCl}_3$ )  $\delta$  ppm 7.40-7.33 (m, 5H, ArH), 5.21 (s, 2H,  $\text{PhCH}_2$ ), 4.32 (q,  $J = 6.8$  Hz, 1H, -CH), 2.87 (br, 1H, -OH), 1.43 (d,  $J = 6.8$  Hz, 3H,  $-\text{CH}_3$ ).  $[\alpha]_{\text{D}} = -17.8$  (c1.0, acetone).

**Benzyl (S)-2-((bis(diisopropylamino)phosphanyl)oxy)propanoate (146)**



To a suspension of bis(diisopropylaminochlorophosphine) (1.0 g, 3.76 mmol) in dry  $\text{Et}_2\text{O}$  (40 mL), a solution of benzyl L-lactate (812 mg, 4.512 mmol) and  $\text{Et}_3\text{N}$  (1.05 mL, 7.52 mmol) in dry  $\text{Et}_2\text{O}$  (10 mL) was added dropwise at  $0^\circ\text{C}$  and then the white solid were removed by filtration, the solvent of the filtrate was evaporated, and the residue was further purified by chromatography column (pentane/ $\text{Et}_3\text{N}$ =30:1) to yield Benzyl (S)-2-((bis(diisopropylamino)phosphanyl)oxy)propanoate **146** (1.21 g, yield 79%) as a colorless oil.

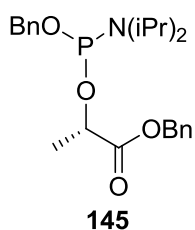
$^1\text{H NMR}$  (300 MHz, Chloroform-*d*)  $\delta$  7.39 – 7.03 (m, 5H, ArH), 5.07 (s, 2H,  $\text{PhCH}_2$ ), 4.40 – 4.04 (m, 1H, CH-O), 3.63 – 3.16 (m, 4H, 4CH), 1.36 (d,  $J = 6.8$  Hz, 3H,  $\text{CH}_3$ ), 1.19 – 0.80 (m, 24H, 8 $\text{CH}_3$ ).

$^{31}\text{P NMR}$  (122 MHz, Chloroform-*d*)  $\delta$  118.79.

$^{13}\text{C NMR}$  (75 MHz, Chloroform-*d*)  $\delta$ : 173.6 (d,  $J = 3.9$  Hz, C=O), 136.0 (ArC), 128.4 (2ArC), 128.1 (2ArC), 69.0 (d,  $J = 20.0$  Hz, PO-CH- $\text{CH}_3$ ), 66.2 ( $\text{PhCH}_2$ ), 44.7 (CH-N-CH), 44.5 (CH-N-CH) 24.4 ( $\text{CH}_3$ ), 24.3 ( $\text{CH}_3$ ), 24.24 ( $\text{CH}_3$ ), 24.19 ( $\text{CH}_3$ ), 24.1 (2 $\text{CH}_3$ ), 24.0 (2 $\text{CH}_3$ ), 20.23 (d,  $J = 4.5$  Hz,  $\text{CH}_3$ ).

**HRMS m/z (ESI):** Calcd. for  $\text{C}_{22}\text{H}_{39}\text{NaN}_2\text{O}_3\text{P}$  ( $\text{M}+\text{Na}$ ) $^+$ : 433.2698. Found: 433.2616.

**Benzyl (2S)-2-(((benzyloxy)(diisopropylamino)phosphanyl)oxy)propanoate (145)**



The product was synthesized from a similar procedure described in the literature<sup>[342]</sup>. To a solution of 1H-tetrazole (3.88 mL 0.45 M  $\text{CH}_3\text{CN}$  solution, 1.746 mmol) in 5 mL of anhydrous  $\text{CH}_2\text{Cl}_2$  was added diisopropylamine (0.286 mL, 2.037 mmol) under argon at room temperature, the mixture was allowed to stir at the same temperature for 30 min, and the solvent was removed under reduced procedure to afford diisopropylammonium tetrazolide as a white solid. Then a solution of Benzyl (S)-2-((bis(diisopropylamino)phosphanyl)oxy)propanoate **146** (1.21 g, 2.91 mmol) in dry  $\text{CH}_2\text{Cl}_2$  (10.0 mL) was added dropwise to a stirred solution of diisopropylammonium tetrazolide (0.380 g, 2.22 mmol), which was dried by repeated co-evaporation with dry MeCN prior to use, and benzyl alcohol (0.318 mL, 3.054 mmol) in dry  $\text{CH}_2\text{Cl}_2$  (20.0 mL) at  $0^\circ\text{C}$  under argon. After being stirred for 4 h at  $0^\circ\text{C}$ , the mixture was diluted with  $\text{CH}_2\text{Cl}_2$  (30 mL) and washed with a saturated  $\text{NaHCO}_3$  aqueous solution (30 mL). The

aqueous layer was separated and extracted with CH<sub>2</sub>Cl<sub>2</sub> (10 mL). The organic layers were combined, dried over Na<sub>2</sub>SO<sub>4</sub>, filtered and concentrated under reduced pressure. The residue was purified by silica gel column chromatography (hexane/AcOEt=30/1, v/v with 2% TEA) to afford Benzyl (2S)-2-(((benzyloxy)(diisopropylamino)phosphanyl)oxy)propanoate **145** (0.8 g, 66%) as a colorless oil. The spectrum showed that the product is a pair of enantiomers (ratio 1/1).

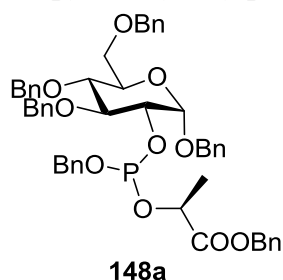
<sup>1</sup>H NMR (300 MHz, Chloroform-*d*) δ: 7.40 – 7.25 (m, 10H, ArH), 5.24 – 5.11 (m, 2H, ArCH<sub>2</sub>), 4.79 – 4.64 (m, 2H, PhCH<sub>2</sub>OOC-), 4.54 – 4.37 (m, 1H, -CH), 3.68 (tt, *J* = 10.3, 5.2 Hz, 2H, N-CH), 1.49 (d, *J* = 6.9 Hz, 3H, CH<sub>3</sub>), 1.25 – 1.10 (m, 12H, 4CH<sub>3</sub>).

<sup>13</sup>C NMR (75 MHz, Chloroform-*d*) δ: 173.1 (d, *J* = 2.8 Hz, C=O), 172.7 (d, *J* = 2.8 Hz, C=O), 139.5 (d, *J* = 7.8 Hz, ArC), 139.4 (d, *J* = 7.7 Hz, ArC), 135.7 (ArC), 128.5 (ArC), 128.2 (ArC), 128.1 (ArC), 127.3 (ArC), 127.1 (ArC), 127.0 (ArC), 126.9 (ArC), 68.9 (d, *J* = 17.8 Hz, CH-O), 68.2 (d, *J* = 18.5 Hz, CH-O), 66.6 (d, *J* = 7.0 Hz, COOCH<sub>2</sub>Ph), 65.7 (d, *J* = 17.6 Hz, PhCH<sub>2</sub>), 65.4 (d, *J* = 18.1 Hz, PhCH<sub>2</sub>), 43.4 (CH), 43.2 (2CH), 43.0 (CH), 24.7 (CH<sub>3</sub>), 24.6 (CH<sub>3</sub>), 24.5 (CH<sub>3</sub>), 24.4 (CH<sub>3</sub>), 20.1 (d, *J* = 3.6 Hz, CH<sub>3</sub>), 20.0 (d, *J* = 4.8 Hz, CH<sub>3</sub>).

<sup>31</sup>P NMR (122 MHz, Chloroform-*d*) δ 148.63, 148.47.

HRMS *m/z* (ESI): Calcd. for C<sub>23</sub>H<sub>32</sub>NaNO<sub>4</sub>P (M+Na)<sup>+</sup>: 440.2069. Found: 433.2026.

**Benzyl (2S)-2-(((benzyloxy)((2S,3R,4S,5R,6R)-2,4,5-tris(benzyloxy)-6-  
(benzyloxy)methyl)tetrahydro-2H-pyran-3-yl)oxy)phosphanyl)oxy)propanoate (148a)**



Benzyl (2S)-2-(((benzyloxy)(diisopropylamino)phosphanyl)oxy)propanoate **145** (520 mg, 1.247 mmol) was stirred with 1*H*-tetrazole (0.45 mol/L in acetonitrile, 2.8 mL, 1.25 mmol) in dry CH<sub>2</sub>Cl<sub>2</sub> (20 mL) under argon for 30 min at room temperature. Compound **134** (225 mg, 0.416 mmol) dissolved in dry CH<sub>2</sub>Cl<sub>2</sub> (5 mL) was added and the resulting mixture was stirred for 2h. TLC (petroleum ether/ethyl acetate 10:1) showed that the reaction was completed. The reaction was diluted in 50 mL DCM and washed with 50 mL of saturated NaHCO<sub>3</sub> solution, the aqueous layer was washed with DCM (2x 20 mL), the combined organic layer was washed with brine (50 mL) and dried over Na<sub>2</sub>SO<sub>4</sub>, filtered, and concentrated under reduced pressure. Purification by silica gel column chromatography (petroleum ether/ethyl acetate 13:1) yield **12** (300 mg, 84%) as a colorless oil. The spectrum showed that the product is a pair of diastereomers with 1/1 ratio.

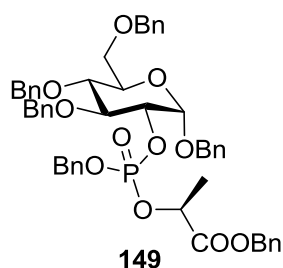
<sup>1</sup>H NMR (400 MHz, Chloroform-*d*) δ: 7.45 – 7.28 (m, 27H, ArH), 7.24 (dd, *J* = 2.0, 1.6 Hz, 1H, ArH), 7.18 (m, 2H, ArH), 5.19 (d, *J* = 4.0 Hz, 0.5H, H-1), 5.19 – 5.16 (d, 1H, ArCH<sub>2</sub>), 5.12 – 5.07 (m, 1H, ArCH<sub>2</sub>), 5.09 (d, *J* = 4 Hz, 0.5H, H-1), 4.98 (d, *J* = 8.0 Hz, 0.5H, ArCH<sub>2</sub>), 4.92 – 4.82 (m, 3.5H, ArCH<sub>2</sub>), 4.81 – 4.67 (m, 3H, ArCH<sub>2</sub>), 4.78 (dd, 0.5H, *J* = 2 Hz, CH<sub>3</sub>CH-O), 4.75 (dd, 0.5H, *J* = 2 Hz, CH<sub>3</sub>CH-O), 4.61 – 4.51 (m, 3H, ArCH<sub>2</sub>), 4.35 – 4.28 (m, 1H, H-2), 4.08 (td, *J* = 8.0, 12.0, 4.0 Hz, 1H, H-3), 3.92 (t, *J* = 12.0 Hz, 1H, H-5), 3.79 (dt, *J* = 9.2, 4.6 Hz, 1H, H-6), 3.76 – 3.71 (m, 1H, H-4), 3.70 – 3.64 (m, 1H, H-6), 1.39 (dd, *J* = 15.6, 6.9 Hz, 3H, CH<sub>3</sub>).

**<sup>13</sup>C NMR (101 MHz, Chloroform-*d*)**  $\delta$ : 172.0 (d,  $J = 4.0$  Hz, C=O), 171.9 (d,  $J = 2.0$  Hz, C=O), 138.8 (2Glu-OCH<sub>2</sub>-CPh), 138.7 (2Glu-OCH<sub>2</sub>-CPh), 138.2 (P-OCH<sub>2</sub>-CPh), 138.0 (d,  $J = 6.7$  Hz, P-OCH<sub>2</sub>-CPh), 137.5 (2Glu-OCH<sub>2</sub>-CPh), 137.4 (2Glu-OCH<sub>2</sub>-CPh), 135.5 (d,  $J = 2.0$  Hz, COOCH<sub>2</sub>CPh), 128.7 (ArC), 128.6 (2ArC), 128.5 (ArC), 128.4 (6ArC), 128.3 (2ArC), 128.2 (2ArC), 128.1 (ArC), 128.0 (3ArC), 127.9 (2ArC), 127.8 (4ArC), 127.7 (ArC), 127.6 (2ArC), 127.5 (2ArC), 127.16 (ArC), 97.8 (d,  $J = 2.0$  Hz, C-1), 97.6 (d,  $J = 2.0$  Hz, C-1), 81.4 (t,  $J = 4.0$  Hz, 2C-3), 78.0 (C-4), 77.9 (C-4), 75.5 (2OBn), 75.1 (2OBn), 73.9 (d,  $J = 10.0$  Hz, C-2), 73.6 (d,  $J = 9.0$  Hz, C-2), 73.5 (2OBn), 70.6 (d,  $J = 6.5$  Hz, 2C-5), 69.6 (OBn), 69.5 (OBn), 68.5 (C-6), 68.4 (C-6), 67.9 (d,  $J = 11.6$  Hz, CH-O-P), 67.3 (d,  $J = 11.6$  Hz, CH-O-P), 66.8 (d,  $J = 4.0$  Hz, 2OBn), 64.1 (d,  $J = 10.0$  Hz, P-OBn), 64.0 (d,  $J = 13.0$  Hz, P-OBn), 20.0 (t,  $J = 3.8$  Hz, 2CH<sub>3</sub>).

**<sup>31</sup>P NMR (122 MHz, Chloroform-*d*)**  $\delta$ : 139.12, 138.88.

**HRMS *m/z* (ESI)**: Calcd. for C<sub>51</sub>H<sub>54</sub>O<sub>10</sub>P (M+H)<sup>+</sup>: 857.3376. Found: 857.3449. [ $\alpha$ ]<sub>D</sub> = +22.5 (*c* 3.0, CHCl<sub>3</sub>).

**Benzyl (2*S*)-2-(((benzyloxy)((2*S*,3*R*,4*S*,5*R*,6*R*)-2,4,5-tris(benzyloxy)-6-((benzyloxy)methyl)tetrahydro-2*H*-pyran-3-yl)oxy)phosphoryl)oxy)propanoate (**149**)**



To a solution of compound **149a** (220 mg, 0.257 mmol) in 10 mL anhydrous DCM was added *t*-BuOOH (47  $\mu$ L, 6 mol/L in decane, 0.283 mmol) at 0 °C, the reaction was allowed to stir at 0 °C for 2h, then room for 1h until the TLC (pentane/AcOEt=3:1) showed the starting material was consumed completely, then the reaction solvent was evaporated and the residue was purified by chromatography column (pentane/ether=1:1) to afford **149** (180 mg, yield=80%) as colorless syrup. The spectrum showed that the product is a pair of diastereomers with ratio 3/2.

**<sup>1</sup>H NMR (400 MHz, Chloroform-*d*)**  $\delta$ : 7.34 – 7.14 (m, 28H, ArH), 7.11 – 7.04 (m, 2H, ArH), 5.36 (d,  $J = 3.7$  Hz, 0.6H, H-1), 5.22 (d,  $J = 3.7$  Hz, 0.4H, H-1), 5.11 (dd,  $J = 12.3, 7.9$  Hz, 1H, ArCH<sub>2</sub>), 5.06 – 4.88 (m, 3H, ArCH<sub>2</sub>), 4.83 (d,  $J = 11.3$  Hz, 1H, CHO-P), 4.87-4.81 (m, 0.5H, ArCH<sub>2</sub>), 4.77 – 4.70 (m, 2H, ArCH<sub>2</sub>), 4.70 – 4.59 (m, 2H, ArCH<sub>2</sub>), 4.58 – 4.44 (m, 3.5H, ArCH<sub>2</sub>), 4.43 (m, 0.6H, H-2), 4.35 (ddd,  $J = 2.0, 8.0, 3.0$  Hz, 0.4H, H-2), 4.03 – 3.93 (m, 1H, H-3), 3.84 - 3.79 (m, 1H, H-5), 3.68 (dd,  $J = 4.0, 4.0$  Hz, 1H, H-6), 3.65 - 3.60 (m, 1H, H-4), 3.59 - 3.55 (m, 1H, H-6), 1.38 (d,  $J = 6.9$  Hz, 2H, CH<sub>3</sub>), 1.34 (d,  $J = 6.8$  Hz, 1H, CH<sub>3</sub>).

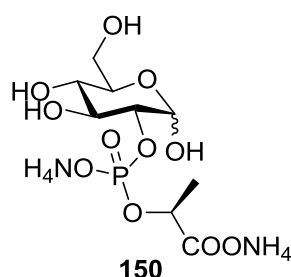
**<sup>13</sup>C NMR (101 MHz, Chloroform-*d*)**  $\delta$ : 170.3 (d,  $J = 4.6$  Hz, C=O), 170.1 (d,  $J = 5.8$  Hz, C=O), 138.5 (d,  $J = 2.0$  Hz, 2Glu-OCH<sub>2</sub>-CPh), 138.1 (2Glu-OCH<sub>2</sub>-CPh), 138.0 (d,  $J = 5.0$  Hz, 2Glu-OCH<sub>2</sub>-CPh), 137.4 (Glu-OCH<sub>2</sub>-CPh), 137.2 (Glu-OCH<sub>2</sub>-CPh), 135.8 (d,  $J = 8.0$  Hz, P-OCH<sub>2</sub>-CPh), 135.7 (d,  $J = 7.6$  Hz, P-OCH<sub>2</sub>-CPh), 135.3 (COOCH<sub>2</sub>-CPh), 135.2 (COOCH<sub>2</sub>-CPh), 128.7 (2ArC), 128.50 (2ArC), 128.4 (d,  $J = 2.3$  Hz, 6ArC), 128.3 (d,  $J = 2.1$  Hz, 6ArC), 128.2 (ArC), 128.1 (ArC), 128.0 (d,  $J = 2.1$  Hz,

4ArC), 127.9 (ArC), 127.8 (d,  $J = 2.4$  Hz, 4ArC), 127.7 (ArC), 127.6 (d,  $J = 5.1$  Hz, 2ArC), 96.6 (C-1), 96.5 (C-1), 80.7 (C-3), 80.6 (C-3), 77.73 (C-4), 77.67 (C-4), 77.5 (d,  $J = 6.2$  Hz, C-2), 77.30 (d,  $J = 6.2$  Hz, C-2), 75.5 (OCH<sub>2</sub>Ph), 75.4 (OCH<sub>2</sub>Ph), 75.21 (d,  $J = 2.0$  Hz, 2OCH<sub>2</sub>Ph), 73.52 (d,  $J = 2.9$  Hz, 2OCH<sub>2</sub>Ph), 72.26 (d,  $J = 5.1$  Hz, P-OCH), 72.04 (d,  $J = 5.2$  Hz, P-OCH), 70.6 (C-5), 70.5 (C-5), 70.1 (OCH<sub>2</sub>Ph), 70.0 (OCH<sub>2</sub>Ph), 69.6 (d,  $J = 5.8$  Hz, P-OCH<sub>2</sub>Ph), 69.4 (d,  $J = 5.5$  Hz, P-OCH<sub>2</sub>Ph), 68.4 (C-6), 68.3 (C-6), 67.2 (d,  $J = 5.3$  Hz, 2OCH<sub>2</sub>Ph), 19.1 (d,  $J = 5.2$  Hz, CH<sub>3</sub>).

**<sup>31</sup>P NMR (122 MHz, Chloroform-*d*)**  $\delta$ : -2.38, -2.61.

**HRMS m/z (ESI):** Calcd. for C<sub>51</sub>H<sub>53</sub>ClO<sub>11</sub>P (M+Cl)<sup>-</sup>: 907.3020. Found: 907.3020. [ $\alpha$ ]<sub>D</sub> = +40.4 (*c* 5.5, CHCl<sub>3</sub>).

### **D-Glucose-2-L-lactic acid phosphate ammonium (150)**



Pd/C (70 mg) was added to a solution of compound **149** (70 mg, 0.082 mmol) in ethanol and water (10 mL, v/v) and the mixture is stirred under H<sub>2</sub> atmosphere for 24 h at room temperature. The solution was then filtered through celite and K<sub>2</sub>CO<sub>3</sub> was added to the filtrate, the mixture was stirred for 30 min, then the solvent was evaporated to give a residue as white solid, which was further purified by Chromabond C18 column to afford 21mg desired compound as a potassium salt. The solid was dissolved in water and further purified by ion exchange chromatography on a DEAE-Sephadex column eluted with NH<sub>4</sub>CO<sub>3</sub>, to give 19 mg compound in 63% yield ( $\alpha/\beta=5/3$ ).

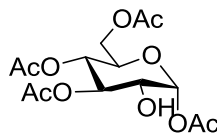
**<sup>1</sup>H NMR (400 MHz, Deuterium Oxide)**  $\delta$ : 5.36 (d,  $J = 3.6$  Hz, 1H, H-1 $\alpha$ ), 4.68 (d,  $J = 7.9$  Hz, 0.6H, H-1 $\beta$ ), 4.60 – 4.46 (m, 1.6H, P-OCH $\alpha\beta$ ), 3.95 (td,  $J = 4.0, 8.0, 4.0$ Hz, 1H, H-2 $\alpha$ ), 3.89 – 3.82 (m, 1.6H, H-6 $\alpha\beta$ ), 3.81 – 3.75 (m, 2.6H, H-5 $\alpha$ , H-3 $\alpha$ , H-2 $\beta$ ), 3.73 – 3.65 (m, 1.6H, H-6 $\alpha\beta$ ), 3.63 – 3.56 (m, 0.6H, H-3 $\beta$ ), 3.47 – 3.42 (m, 2.2H, H-4 $\alpha\beta$ , H-5 $\beta$ ), 1.40 (dd,  $J = 6.9, 2.8$  Hz, 5H, CH<sub>3</sub> $\alpha\beta$ ).

**<sup>13</sup>C NMR (101 MHz, Deuterium Oxide)**  $\delta$ : 180.4 (d,  $J = 4.7$  Hz, C=O), 180.1 (d,  $J = 5.8$  Hz, C=O), 95.0 (d,  $J = 5.1$  Hz, C-1 $\beta$ ), 90.9 (d,  $J = 2.0$  Hz, C-1 $\alpha$ ), 78.9 (d,  $J = 6.6$  Hz, C-2 $\beta$ ), 75.9 (C-5 $\beta$ ), 75.7 (d,  $J = 6.8$  Hz, C-2 $\alpha$ ), 75.0 (d,  $J = 2.7$  Hz, C-3 $\beta$ ), 73.1 (t,  $J = 5.7$  Hz, P-OCH), 71.5 (d,  $J = 5.6$  Hz, C-3 $\alpha$ ), 71.2 (C-5 $\alpha$ ), 69.2 (C-4 $\alpha$ ), 69.0 (C-4 $\beta$ ), 60.6 (d,  $J = 5.0$  Hz, C-6 $\beta$ ), 60.5 (C-6 $\alpha$ ), 20.2 (d,  $J = 2.3$  Hz, CH<sub>3</sub> $\beta$ ), 19.8 (d,  $J = 3.2$  Hz, CH<sub>3</sub> $\alpha$ ).

**<sup>31</sup>P NMR (122 MHz, Deuterium Oxide)**  $\delta$ : -0.86( $\beta$ ), -1.16 ( $\alpha$ ).

**HRMS m/z (ESI):** Calcd. for C<sub>9</sub>H<sub>16</sub>K<sub>2</sub>O<sub>11</sub>P (M+H)<sup>+</sup>: 408.9699. Found: 409.0126. [ $\square$ ]<sub>D</sub> = +45.0 (*c* 1.0, H<sub>2</sub>O).

### Acetyl 3,4,6-tri-*O*-acetyl- $\alpha$ -D-glucopyranoside (**98**)

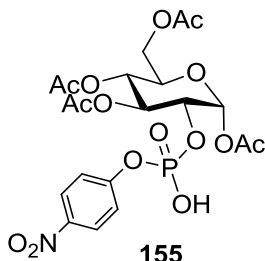


**98**

To a solution of penta-*O*-acetyl- $\beta$ -D-glucopyranose (8.0 g, 21 mmol) and phosphorus pentachloride (PCl<sub>5</sub>) (5.0 g, 23.8 mmol) in 40 mL CH<sub>2</sub>Cl<sub>2</sub> was added BF<sub>3</sub>·OEt<sub>2</sub> (45  $\mu$ L, 0.35 mmol). The mixture was stirred at room temperature overnight and then washed with water, saturated NaHCO<sub>3</sub>, and brine, respectively. The organic layer was dried over anhydrous Na<sub>2</sub>SO<sub>4</sub> and concentrated. The resulting pale yellow solid was dissolved in a mixed solvent of acetone (40 mL), DMF (16.0 mL), and water (37 mL). After being stirred at room temperature for 24h, the solvents were removed under vacuum. The residue was dissolved with CH<sub>2</sub>Cl<sub>2</sub> and washed with water and brine. The organic layer was dried over anhydrous Na<sub>2</sub>SO<sub>4</sub> and then concentrated. The residue was purified by flash chromatography column (pentane/AcOEt=1/1 and pentane/diethyl ether=1/4) and crystallized from diethyl ether to give product (1.7 g, 23%) as a white solid.

**<sup>1</sup>H NMR (300 MHz, Chloroform-*d*)**  $\delta$ : 6.21 (d, *J* = 3.8 Hz, 1H, H-1), 5.24 (t, *J* = 9.7 Hz, 1H, H-3), 5.06 (t, *J* = 9.8 Hz, 1H, H-4), 4.29 – 4.20 (m, 1H, H-6), 4.06 – 3.97 (m, 2H, H-5, H-6), 3.87 (dd, *J* = 9.9, 3.7 Hz, 1H, H-2), 2.17 (s, 3H, Ac), 2.07 (s, 3H, Ac), 2.05 (s, 3H, Ac), 2.02 (s, 3H, Ac).

### (2R,3R,4S,5R,6R)-6-(acetoxymethyl)-3-((hydroxy(4-nitrophenoxy)phosphoryl)oxy)tetrahydro-2H-pyran-2,4,5-triyl triacetate (**155**)



**155**

To a solution of acetyl 3,4,6-tri-*O*-acetyl- $\alpha$ -D-glucopyranoside **98** (1 g, 2.874 mmol) in 35 mL anhydrous pyridine was added 4-nitrophenyl dichlorophosphate (0.88 g, 3.45 mmol) at 0 °C. The reaction was stirred at 0 °C for addition 2h and rt for 14h, then 10 mL water was added to the reaction and the mixture was allowed to stir for 3h until the starting material was consumed. The solvent was removed in vacuo to give a yellow residue, which was purified by flash chromatography column (DCM/methanol=20/1) to afford 1.23 g product as a white solid (78% yield).

**<sup>1</sup>H NMR (400 MHz, DMSO-*d*<sub>6</sub>)**  $\delta$ : 8.16 (d, *J* = 8.8 Hz, 2H, ArH), 7.31 (d, *J* = 8.6 Hz, 2H, ArH), 6.20 (d, *J* = 8.0 Hz, 1H, H-1), 5.26 (t, *J* = 9.8 Hz, 1H, H-3), 4.94 (t, *J* = 9.9 Hz, 1H, H-4), 4.40 – 4.28 (m, 1H, H-2), 4.18 – 3.89 (m, 3H, H-5, H-6), 2.03 (s, 3H, Ac), 1.99 (s, 3H, Ac), 1.95 (s, 3H, Ac), 1.67 (s, 3H, Ac).

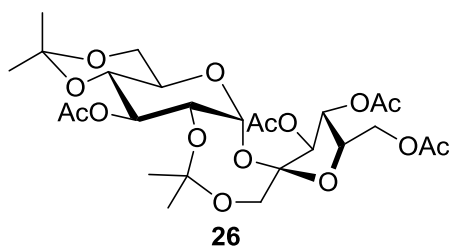
**<sup>13</sup>C NMR (101 MHz, DMSO-*d*<sub>6</sub>)**  $\delta$  170.5 (CO), 170.0 (CO), 169.6 (CO), 169.3 (CO), 146.1 (ArC), 142.1 (ArC), 126.2 (ArC), 125.7 (2ArC), 120.2 (d, *J* = 5.5 Hz, ArC), 90.1 (C-1), 71.5 (d, *J* = 5.6 Hz, C-

2), 70.9 (d,  $J = 7.0$  Hz, C-3), 69.0 (C-5), 68.1 (C-4), 61.7 (C-6), 21.1 (Ac), 21.0 (Ac), 20.8 (Ac), 20.7 (Ac).

$^{31}\text{P}$  NMR (122 MHz, DMSO- $d_6$ )  $\delta$ : -8.45.

HRMS  $m/z$  (ESI): Calcd. for  $\text{C}_{20}\text{H}_{24}\text{NNaO}_{15}\text{P}$  ( $\text{M}+\text{Na}$ ) $^+$ : 572.0781. Found: 572.0790.  $[\alpha]_{\text{D}}^{20} = +30.6$  (c 1.0,  $\text{CHCl}_3$ ).

### 3,3',4', 6'-tetra-*O*-acetyl-2,1':4,6-di-*O*-isopropylidene sucrose (26)

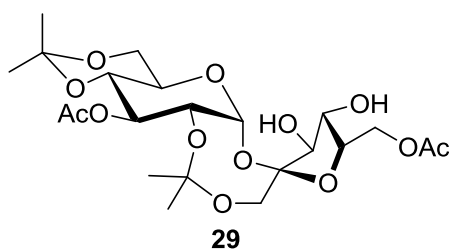


The sucrose (6 g, 17.5 mmol), 2,2-dimethoxypropane (21.6 mL, 10 eq) and Ceric ammonium nitrate (CAN) (1.92 g, 0.2 eq) are added to a flask containing 15 mL of anhydrous DMF in a flask. The mixture is stirred for 40 h at room temperature. Pyridine (28 mL, 20 eq) followed by acetic anhydride (24.76 mL, 15 eq) were added at 0 ° C. The reaction is allowed to return to room temperature and then stirred overnight. The mixture is then concentrated in vacuo and the product is chromatographed on silica gel (220 g) with a pentane / ether (2/3) mixture in the presence of triethylamine (1 mL / 100 mL) as eluent, 2.26 g (30% yield) of product **26** are obtained.

$^1\text{H}$ -NMR (300MHz,  $\text{CDCl}_3$ )  $\delta$ : 6.1 (d, 1H,  $^3J = 6$  Hz, G1), 5.31 (dd, 1H,  $^3J = 6$  Hz, F4), 5.25 (t, 1H,  $^3J = 12$  Hz, G3), 5.15 (d, 1H,  $^3J = 6$  Hz, F3), 4.4 (d, 1H,  $^3J = 6$  Hz, F6<sub>b</sub>), 4.25 (m, 2H, F5 and F6<sub>a</sub>), 4.03 (d, 1H,  $^2J = 12$  Hz, F1<sub>b</sub>), 3.96 (dd, 1H,  $^2J = 12$  Hz and  $^3J = 6$  Hz, G6<sub>b</sub>), 3.88 (dd, 1H,  $^3J = 6$  Hz,  $^2J = 18$  Hz, G5), 3.81 (dd, 1H,  $^3J = 3$  Hz,  $^2J = 9$ Hz, G2), 3.66 (dd, 2H,  $^3J = 9$  Hz,  $^2J = 21$  Hz, G4, G6<sub>a</sub>), 3.52 (d, 1H,  $^2J = 12$  Hz, F1<sub>a</sub>), 2-2.3 (4s, 12H, OAc), 1.4-1.6 (4s, 12H,  $\text{CH}_3$ ).

$^{13}\text{C}$ -NMR (75MHz,  $\text{CDCl}_3$ )  $\delta$ : 104.7 (F2), 99.7 and 101.5 (CH- $\text{CH}_3$ ), 91.6 (G1), 79.8 (F5), 77.3 (F3), 77.1 (F4), 71.9 (G4), 71.5 (G2), 70.6 (G3), 64.5 (G5), 66.0 (F1), 65.1 (F6), 62.1 (G6), 19.1, 23.8, 25.4, 29.1 (CO- $\text{CH}_3$ ).

### 3,6'-di-*O*-acetyl-2,1' : 4,6-di-*O*-isopropylidene sucrose (29)

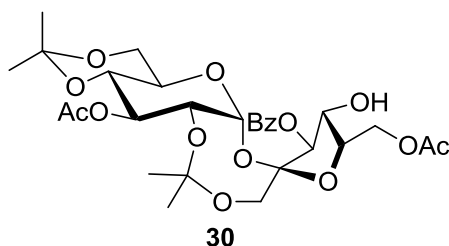


The product **26** (2.47 g, 4.186 mmol) is dissolved in 55 mL of anhydrous methanol and the mixture obtained is treated at 0 °C with a freshly prepared solution of MeONa (615 μL, 0.1 M in MeOH). The evolution of the reaction is followed by TLC (ether) until the total consumption of the starting material (approximately 1 h). A spatula of Amberlist H + is immediately added to the mixture and after about three minutes of stirring the whole is filtered on filter paper and the solvent is evaporated. The product is obtained as a white solid (1.1 g, 52% yield) after purification on a silica gel column with ether or ethyl acetate as eluent, in the presence of approximately 1% of Et<sub>3</sub>N.

**<sup>1</sup>H-NMR** (300Mhz, CDCl<sub>3</sub>) δ: 6.105 (d, 1H, <sup>3</sup>J = 3 Hz, G1), 5.22 (t, 1H, <sup>3</sup>J = 9 Hz, G3), 4.315 (dd, 1H, <sup>3</sup>J = 3 and 12 Hz, F4), 4.205 (d, 1H, <sup>3</sup>J = 9 Hz, F3), 4.14 (d, 1H, <sup>2</sup>J = 6 Hz, F6<sub>b</sub>), 4.1 (m, 2H, F5<sub>a</sub>, F6<sub>a</sub>), 3.90 (dd, 1H, <sup>3</sup>J = 3 Hz, <sup>2</sup>J = 9 Hz, G6<sub>b</sub>), 3.84 (dd, 1H, <sup>3</sup>J = 3 and 9 Hz, G5 and G4), 3.76 (dd, 1H, <sup>3</sup>J = 3 and 9 Hz, G2), 3.70 (d, 1H, <sup>2</sup>J = 12 Hz, F1<sub>b</sub>), 3.635 (d, 1H, <sup>2</sup>J = 9 Hz, G6<sub>a</sub>), 3.48 (d, 1H, <sup>2</sup>J = 12 Hz, F1<sub>a</sub>), 2.71 (s, 2H, OH), 2.04-2.07 (2s, 6H, OAc), 1.2-1.5 (4s, 12H, CH<sub>3</sub>).

**<sup>13</sup>C-NMR** (75MHz, CDCl<sub>3</sub>) δ: 104.1 (F2), 99.9 and 101.5 (C-CH<sub>3</sub>), 91.3 (G1), 79.9 (F5), 77.7 (F3), 78.1 (F4), 71.9 (G4), 71.7 (G2), 71.1 (G3), 64.0 (G5), 65.9 (F1), 65.9 (F6), 62.3 (G6), 19.1, 24.1, 25.4, 29.1 (CO-CH<sub>3</sub>).

### 3,6'-di-*O*-acetyl-3'-benzoyl-2,1':4,6-di-*O*-isopropylidene sucrose (**30**)

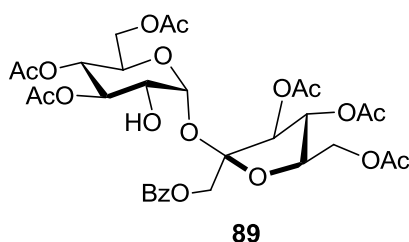


A solution of compound **29** (1.1 g, 2.17 mmol) in 8 mL of pyridine was treated with benzoyl chloride (277 μL, 2.39 mmol) under nitrogen at 0 °C. After stirring for 1 h at room temperature, the pyridine is evaporated in vacuo, and the product was obtained as a white solid in a 74% (0.98g) after purification by chromatography on silica gel (eluent pentane / ether: 1/1) in the presence of approximately 1% Et<sub>3</sub>N.

**<sup>1</sup>H-NMR** (300Mhz, CDCl<sub>3</sub>) δ: 7.55-8.22 (m, 5H, Ph), 6.16 (d, 1H, <sup>3</sup>J = 3 Hz, G1), 5.44 (t, 1H, <sup>3</sup>J = 9 Hz, G3), 4.85 (d, 1H, <sup>3</sup>J = 6 Hz, F3), 4.33 (dd, 1H, <sup>3</sup>J = 3 and 6 Hz, F4), 4.27-4.36 (m, 3H, F5<sub>a</sub>, F6<sub>a</sub>, F6<sub>b</sub>), 4.13 (d, 1H, <sup>2</sup>J = 12 Hz, F1<sub>b</sub>), 3.92 (dd, 1H, <sup>3</sup>J = 3 Hz, G6<sub>b</sub>), 3.92 (dd, 1H, <sup>3</sup>J = 3 and 6 Hz, G5), 3.82 (dd, 1H, <sup>3</sup>J = 3 and 9 Hz, G2), 3.67 (dd, 2H, <sup>3</sup>J = 9 Hz, <sup>2</sup>J = 18 Hz, G6<sub>a</sub>, G4), 3.48 (d, 1H, <sup>2</sup>J = 12 Hz, F1<sub>a</sub>), 2.52 (s, 1H, OH), 2.07-2.09 (2s, 6H, OAc), 1.29-1.48 (4s, 12H, CH<sub>3</sub>).

**<sup>13</sup>C-NMR** (75MHz, CDCl<sub>3</sub>) δ: 104.9 (F2), 99.6 and 101.5 (C-CH<sub>3</sub>), 91.3 (G1), 81.7 (F5), 82.5 (F3), 76.8 (F4), 72.1 (G4), 71.5 (G2), 70.6 (G3), 64.4 (G5), 65.7 (F1), 65.7 (F6), 62.2 (G6), 19.0, 23.9, 25.5, 29.0 (CO-CH<sub>3</sub>).

### 3,4,6,3',4',6'-hexa-*O*-acetyl-1'-*O*-benzoylsucrose (**89**)



#### Step 1: Selective hydrolysis of acetal groups

**3,3',4',6'-tetra-*O*-acetyl-2,1'-*O*-isopropylidene sucrose **159**:** A solution of 3,3',4',6'-tetra-*O*-acetyl-2,1':4,6-di-*O*-isopropylidene sucrose **26** (5.0 g, 8.5 mmol) in 10 mL of acetone was treated with a solution of 40% acetic acid at room temperature for 4 h. The reaction mixture was then diluted with dichloromethane and washed with saturated NaHCO<sub>3</sub>, and the organic layer was dried over Na<sub>2</sub>SO<sub>4</sub> and concentrated to give a syrup, which was purified by flash chromatography column (pentane/AcOEt=1/1) to afford 3,3',4',6'-tetra-*O*-acetyl-2,1'-*O*-isopropylidene sucrose **159** (1.17 g, 25% yield) as a white solid. The NMR data is consistent with the previously reported one in the literature<sup>[277]</sup>.

#### Step 2: Acylation and hydrolysis of acetal groups

**3,4,6,3',4',6'-hexa-*O*-acetyl-sucrose **87**:** To a solution of the previous synthesized 3,3',4',6'-tetra-*O*-acetyl-2,1'-*O*-isopropylidene sucrose **159** (1.17 g, 2.1 mmol) in 30 mL of anhydrous pyridine was added acetic anhydride (0.87 g, 8.5 mmol) and catalytic amount of DMAP at 0 °C. The reaction was stirred at room temperature for 8h, then pyridine was evaporated and the residue was dissolved in 50 mL of AcOEt, and washed with 2 M HCl (50 mL x2), saturated NaHCO<sub>3</sub> (50 mL) and brine (50 mL), dried over Na<sub>2</sub>SO<sub>4</sub>, and concentrated. Then the crude intermediate was dissolved in 20 mL of acetone and treated with 40% acetic acid at room temperature for 4 h, following the same workup procedure as described above to afford 3,4,6,3',4',6'-hexa-*O*-acetyl-sucrose **87** in quantitative yield (1.1 g). The NMR data are consistent with the previously reported<sup>[277][343]</sup>.

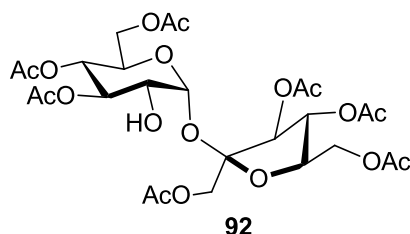
#### Step 3: Mono-benzoylation

**3,4,6,3',4',6'-hexa-*O*-acetyl-1'-*O*-benzoylsucrose **89**:** A solution of 3,4,6,3',4',6'-hexa-*O*-acetyl-sucrose **87** (1.10 g, 1.85 mmol) in 30 mL pyridine and 15 mL chloroform was cooled to -50 °C, and benzoyl chloride (312 mg, 2.22 mmol, 260 μL) was added dropwise. The mixture was stirred at -50 °C for 2 h, and then poured into ice water. The product was extracted into dichloromethane (2 x 500 ml), which was washed successively with water (50 ml x2), saturated NaHCO<sub>3</sub> (50 ml), and brine (50 ml). Concentration of the organic layer afforded a syrup which was purified by flash chromatography column (pentane/diethyl ether=1/4) to give 0.74 g of 3,4,6,3',4',6'-hexa-*O*-acetyl-1'-*O*-benzoylsucrose **89** as a white solid (54% yield).

**<sup>1</sup>H NMR (300 MHz, Chloroform-*d*)** δ: 8.09 – 8.03 (m, 2H, Bz), 7.62 – 7.54 (m, 1H, Bz), 7.45 (td, *J* = 7.5, 4.9 Hz, 2H, Bz), 5.61 (d, *J* = 3.5 Hz, 1H, H-1), 5.47 – 5.39 (m, 2H, H-3' and H-4'), 5.18 (t, *J* = 9.7 Hz, 1H, H-3), 5.04 (t, *J* = 9.8 Hz, 1H, H-4), 4.36 – 4.13 (m, 8H, H-5, H-6, H-1', H-5', H-6'), 3.77 – 3.56 (m, 1H, H-2), 2.13 (s, 3H, OAc), 2.11 (s, 3H, OAc), 2.10 (s, 9H, 2OAc), 2.07 (s, 3H, OAc), 2.03 (s, 3H, OAc). **<sup>13</sup>C NMR (75 MHz, Chloroform-*d*)** δ 171.0 (CO), 170.7 (CO), 170.5 (CO), 170.1 (2CO), 169.9 (CO), 169.5 (CO), 140.9 (ArC), 133.6 (ArC), 129.9 (2ArC), 129.1 (ArC), 128.6 (ArC), 128.4 (ArC), 104.2 (C-2'), 92.7 (C-1), 79.5 (C-5'), 76.8 (C-3'), 75.0 (C-4'), 73.1 (C-3), 70.5 (C-2), 68.9 (C-5), 67.7

(C-4), 63.7 (C-1'), 63.2 (C-6'), 61.7 (C-6), 20.9 (Ac), 20.7 (3Ac), 20.6 (2Ac). **HRMS m/z (ESI):** Calcd. for C<sub>31</sub>H<sub>38</sub>O<sub>18</sub>Na [M+Na]<sup>+</sup>: 721.1956. Found: 721.1960. [ $\alpha$ ]<sub>D</sub> = +65.0 (c 1.0, CHCl<sub>3</sub>)

**3,4,6,3',4',6'-hexa-O-acetyl-1'-O-acetylsucrose (92)**



**Step 1: Selective 2-O-benylation of sucrose (2-O-Benzylsucrose 90):** To a 250 mL round-bottom flask equipped with a magnetic stir bar was added sucrose (6.8 g, 20 mmol, 1.25 equiv.) and anhydrous DMF (130 mL, 0.10 M wt sucrose). The suspension was stirred at RT until a homogeneous solution was obtained. The solution was then cooled to 0 °C. Sodium hydride (NaH) 60% dispersion in mineral oil (692 mg, 17.3 mmol, 1.1 equiv) was added portion wise, and the suspension was stirred for 1 h at 0 °C. Benzyl bromide (2.7 g, 1.9 mL, 16 mmol, 1.0 equiv) was then added dropwise at 0 °C and the reaction was stirred for 8 h at 0 °C. Then DMF was evaporated to give a clear, thick oil which was purified by flash chromatography using (DCM/methanol=3/2). After purification, a white solid was obtained which is a mixture of 2, 1', and 3'-monobenzylated products, the mixture were carried to the next step without further purification (3.51 g).

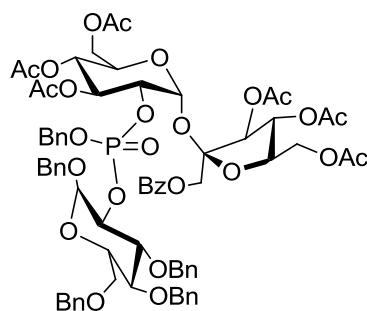
**Step 2: Peracetylation of mono-benzyl sucrose (Hepta-O-acetyl-2-O-benzylsucrose 91):** To a 250 mL round-bottom flask containing the previously synthesized mono-benzyl sucroses was added a magnetic stir bar and DMAP (64 mg, 0.5 mmol, 0.03 equiv.). The reactants were dissolved in pyridine (80 mL, 0.20 M wrt 16 mmol of sucrose) and the solution was cooled to 0 °C. Then acetic anhydride (11.4 g, 10.7 mL, 112 mmol, 7.0 equiv.) was added slowly, and the reaction was stirred from 0 °C to RT over 24 h. The reaction was then evaporated resulting in a reddish oil. The oil was then dissolved in AcOEt (150 mL), and washed with 10 w/w% aqueous citric acid solution (150 mLx2), saturated NaHCO<sub>3</sub> (150 mL) and water (100 mL). The organic layer was separated, dried over Na<sub>2</sub>SO<sub>4</sub>, filtered, and evaporated to dryness, resulting in a yellow oil that was purified by flash chromatography column (pentane/AcOEt=1/1), a white foam was isolated (5.3 g, 37%) and used for the next step directly.

**Step 3: Hydrogenolysis of benzyl group (3,4,6,1',3',4',6'-Hepta-O-acetylsucrose 92):** To a 100 mL flask containing the previously synthesized peracetylated mono-benzyl sucroses (2.6 g) was added Pd/C (760 mg, 0.1 equiv). The reactant was dissolved in AcOEt (40 mL). The reaction was stirred at room temperature under an H<sub>2</sub> atmosphere for 6h until the starting material was consumed. Then Pd/C was filtered through a celite, and the filtrate was evaporated and purified by flash chromatography (pentane/AcOEt=2/3) to afford 1.7 g product as a white solid, which was further recrystallized from AcOEt in hexanes (1:2 v/v), resulting in a crystalline white solid (1.5 g, 66%).

**<sup>1</sup>H NMR** (400 MHz, CDCl<sub>3</sub>)  $\delta$ : 5.54 (d, *J* = 3.5 Hz, 1H, H-1), 5.42–5.38 (m, 2H, H-3' and H-4'), 5.15 (t, *J* = 10.0 Hz, 1H, H-3), 5.03 (t, *J* = 10.0 Hz, 1H, H-4), 4.36–4.12 (m, 8H, H-5, H-6, H-1', H-5', H-6'), 3.71 (dt, *J* = 3.5 Hz, 10.0 Hz, 1H, H-2), 2.31 (d, *J* = 10.5 Hz, 1H, OH), 2.19 (s, 3H, Ac), 2.11 (s, 3H, Ac), 2.10 (s, 6H, 2Ac), 2.07 (s, 6H, 2Ac), 2.03 (s, 3H, Ac); **<sup>13</sup>C NMR** (101 MHz, CDCl<sub>3</sub>)  $\delta$  171.2 (CO), 170.8 (CO), 170.6 (CO), 170.3 (CO), 170.1 (CO), 170.0 (CO), 169.6 (CO), 104.1(C-2'), 92.6 (C-

1), 79.3 (C-5'), 76.6 (C-3'), 75.0 (C-4'), 73.3 (C-3), 70.7 (C-2), 69.1 (C-5), 67.8 (C-4), 63.5 (C-1'), 63.3 (C-6'), 61.9 (C-6), 21.0 (Ac), 20.9 (Ac), 20.8 (5Ac); **HRMS m/z (ESI)**: Calcd. for C<sub>26</sub>H<sub>36</sub>O<sub>18</sub>Na [M+Na]<sup>+</sup>: 659.1799. Found: 659.1794. [ $\alpha$ ]<sub>D</sub> = +66.0 (c 1.0, CHCl<sub>3</sub>)

**(Benzyl 3,4,6-Tri-*O*-benzyl- $\alpha$ -D-glucopyranoside-2-yl)-(3,4,6,3',4',6'-Hexa-*O*-acetyl-1'-*O*-benzoilsucrose-2-yl) benzylphosphate (160)**



**160**

To a solution of **3,4,6,3',4',6'-hexa-*O*-acetyl-1'-*O*-benzoilsucrose 89** (100 mg, 0.143 mmol) in 5 mL of anhydrous CH<sub>3</sub>CN was added **benzyl 3,4,6-tri-*O*-benzyl- $\alpha$ -D-glucopyranoside diisopropylphosphoramidite 140** (134 mg, 0.172 mmol) and 1*H*-tetrazole (0.157 mmol, 350  $\mu$ L, 0.45 M in CH<sub>3</sub>CN) at room temperature. The reaction was stirred at the same temperature for 6h until the sucrose derivatives was consumed. Then the *m*-CPBA (27 mg, 0.157 mmol) was added to the reaction at 0 °C, the mixture was allowed to stir under ice-bath for an addition 30 min, and rt for 2h, after the totally consumption of the intermediate phosphite, the solvent was removed in vacuo to give a syrup as crude product, which was then dissolved in 20 mL dichloromethane and washed with saturated NaHCO<sub>3</sub> (20 mL), brine (20 mL), dried over Na<sub>2</sub>SO<sub>4</sub>, purified by flash chromatography column (pentane/AcOEt=1/1) to afford 130 mg product as a white solid (54% yield).

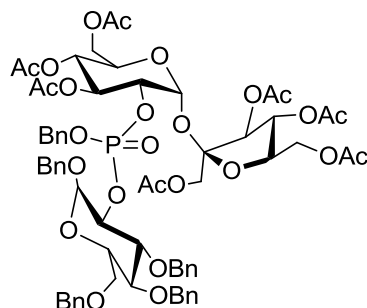
**<sup>1</sup>H NMR (400 MHz, Chloroform-*d*)**  $\delta$ : 8.04 – 7.96 (m, 2H, Bz), 7.50 (dt, *J* = 13.7, 7.5 Hz, 1H, Bz), 7.43 – 7.16 (m, 25H, Bn, Bz), 7.06 (dd, *J* = 6.5, 2.8 Hz, 2H, Bn), 5.78 (d, *J* = 3.6 Hz, 1H, G1), 5.59 – 5.38 (m, 2H, F3 and F4), 5.26 (t, *J* = 3.9 Hz, 1H, G3), 5.07 – 4.84 (m, 2H, G4, G'1), 4.80 – 4.61 (m, 4H, 2Bn), 4.58 – 4.43 (m, 7H, G2, 3Bn), 4.35 (t, *J* = 3.9 Hz, 1H, G'2), 4.30 – 4.17 (m, 4H, G5, G6, F1), 4.18 – 4.04 (m, 3H, F5, F6), 3.94 (t, *J* = 9.2 Hz, 1H, G'3), 3.80 – 3.51 (m, 4H, G'6, G'4, G'5), 2.04 (s, 3H, OAc), 2.03 (s, 3H, OAc), 2.03 (s, 3H, OAc), 2.02 – 2.01 (m, 6H, 2OAc), 1.90 (s, 3H, OAc).

**<sup>13</sup>C NMR (101 MHz, Chloroform-*d*)**  $\delta$ : 170.7 (CO), 170.6 (CO), 170.4 (CO), 170.0 (CO), 169.8 (CO), 169.39 (CO), 165.3 (Bz), 138.2 (BnC), 138.0 (d, *J* = 7.3 Hz, BzC), 137.9 (BnC), 137.9 (BnC), 137.3 (BnC), 137.0 (BnC), 129.8 (ArC), 129.7 (ArC), 128.5 (5ArC), 128.4 (13ArC), 128.1 (ArC), 128.0 (5ArC), 127.9 (ArC), 127.8 (3ArC), 127.6 (ArC), 103.5 (F-C2), 96.6 (G'-C1), 90.2 (G-C1), 80.6 (d, *J* = 7.3 Hz, G'-C3), 78.6 (F-C5), 77.6 (G'-C4), 77.3 (G'-C2), 76.8 (F-C3), 75.5 (d, *J* = 2.8 Hz, F-C4, OBn), 75.3 (OBn), 74.4, 74.1 (G-C3), 73.5 (OBn), 71.8, 70.5 (G'-C5), 70.4 (G-C2), 70.3 (OBn), 70.1 (G-C5), 68.5 (G-C4), 68.2 (G'-C6), 63.8 (F-C1), 63.2 (F-C6), 61.9 (G-C6), 61.6 (OBn), 20.8 (2Ac), 20.7 (2Ac), 20.6 (Ac), 20.5 (Ac). (G=glucose part of sucrose, G'=glucose).

**<sup>31</sup>P NMR (162 MHz, Chloroform-*d*)**  $\delta$ : -0.64 – -0.92 (m), -1.32 – -1.63 (m).

**HRMS m/z (ESI):** Calcd. for C<sub>72</sub>H<sub>79</sub>O<sub>26</sub>NaP [M+Na]<sup>+</sup>: 1413.4495. Found: 1413.4489. [α]<sub>D</sub> = +26.0 (c 1.0, CHCl<sub>3</sub>).

**(Benzyl 3,4,6-Tri-*O*-benzyl- $\alpha$ -D-glucopyranoside-2-yl)-(3,4,6,3',4',6'-Hexa-*O*-acetyl-1'-*O*-acetylsucrose-2-yl) benzylphosphate (161)**



**161**

Following the same procedure for synthesis of compound **160**, **3,4,6,3',4',6'-hexa-*O*-acetyl-1'-*O*-acetylsucrose **92** (232 mg, 0.364 mmol), **benzyl 3,4,6-tri-*O*-benzyl- $\alpha$ -D-glucopyranoside diisopropylphosphoramidite **140** (340 mg, 0.437 mmol), 1*H*-tetrazole (0.40 mmol, 890  $\mu$ l, 0.45 M in CH<sub>3</sub>CN) and *m*-CPBA (0.168 mmol, 30 mg) were used. After purification by flash chromatography (pentane/AcOEt=1/1), 168 mg (35% yield) of the desired product) was obtained as a white solid.****

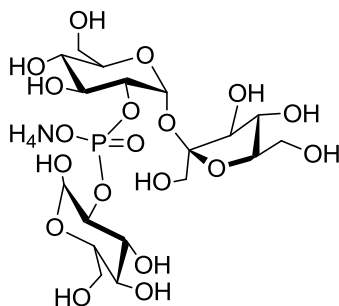
**<sup>1</sup>H NMR (400 MHz, Chloroform-*d*)**  $\delta$ : 7.40 – 7.21 (m, 23H, Bn), 7.10 (dd, *J* = 6.7, 2.9 Hz, 2H, Bn), 5.75 (d, *J* = 3.7 Hz, 1H, G1), 5.53 – 5.37 (m, 2H, F3 and F4), 5.27 (dd, *J* = 8.8, 3.6 Hz, 1H, G3), 5.12 – 4.91 (m, 2H, G4, G'1), 4.83 – 4.66 (m, 4H, 2Bn), 4.63 – 4.42 (m, 7H, G2, 3Bn), 4.37 – 4.07 (m, 10H, G'2, G5, G6, F1, F5, F6, G'3), 3.81 (d, *J* = 6.9 Hz, 1H, G'6), 3.76 – 3.54 (m, 3H, G'6, G'4, G'5), 2.10 (s, 3H, Ac), 2.08 (s, 3H, Ac), 2.07 (s, 3H, Ac), 2.06 (s, 3H, Ac), 2.04 (s, 3H, Ac), 2.03 (s, 3H, Ac), 1.92 (s, 3H, Ac).

**<sup>13</sup>C NMR (101 MHz, Chloroform-*d*)**  $\delta$ : 170.7 (CO), 170.5 (CO), 170.3 (CO), 169.9 (CO), 169.8 (CO), 169.8 (CO), 169.4 (CO), 138.2 (ArC), 138.1 (d, *J* = 3.3 Hz, ArC), 137.9 (ArC), 137.9 (ArC), 137.0 (ArC), 128.5 (ArC), 128.5 (ArC), 128.4 (ArC), 128.4 (ArC), 128.3 (ArC), 128.2 (ArC), 128.1 (ArC), 128.00 (ArC), 127.9 (ArC), 127.8 (ArC), 127.7 (ArC), 103.4 (F-C2), 96.6 (G'-C1), 90.2 (d, *J* = 2.1 Hz, G-C1), 80.6 (d, *J* = 6.8 Hz, G'-C3), 78.4 (F-C5), 77.7 (G'-C4), 77.3 (G'-C2), 75.5 (OBn), 75.3 (OBn), 75.1 (F-C4), 74.1 (F-C3), 73.9 (G-C3), 73.5 (OBn), 70.5 (G'-C5), 70.3 (OBn), 69.9 (d, *J* = 5.6 Hz, G-C2), 68.4 (G-C4), 68.2 (G'-C6, G-C5), 63.4 (F-C6), 63.2 (F-C1), 61.9 (G-C6), 61.5 (d, *J* = 5.4 Hz, OBn), 20.8 (Ac), 20.7 (2Ac), 20.6 (Ac), 20.5 (2Ac), 20.4 (Ac). (G=glucose part of sucrose, G'=glucose).

**<sup>31</sup>P NMR (162 MHz, Chloroform-*d*)**  $\delta$ : -0.65 – -0.92 (m), -1.54 (p, *J* = 7.2 Hz).

**HRMS m/z (ESI):** Calcd. for C<sub>67</sub>H<sub>77</sub>O<sub>26</sub>NaP [M+Na]<sup>+</sup>: 1351.4338. Found: 1351.4333. [α]<sub>D</sub> = +33.0 (c 1.0, CHCl<sub>3</sub>)

### Agrocinopine C ammonium salt



Agrocinopine C ammonium salt

Compound **160** (45 mg, 0.0324 mmol) or compound **161** (40 mg, 0.0301 mmol) were treated with fresh 0.1 M CH<sub>3</sub>ONa solution in methanol (5 mL, 5 mL respectively) at room temperature, a large amount of salt was emerged, and the reaction was monitored by TLC (AcOEt/CH<sub>3</sub>COOH/CH<sub>3</sub>OH/H<sub>2</sub>O=9/3/3/2) until the sucrose derivatives were consumed (5h). Then a spatula of Dowex 50 (H<sup>+</sup>) was added, and the mixture was allowed to stir at room temperature for 5 min, and filtered. The filtrate was evaporated in vacuo to give a white solid as crude product, the structure of intermediate was confirmed by <sup>1</sup>H-NMR and mass spectroscopy (ESI: Calcd. for C<sub>53</sub>H<sub>63</sub>O<sub>19</sub>NaP [M+Na]<sup>+</sup>: 1057.36. Found: 1057.40), it was used for the next step directly. The obtained products previous were dissolved in 5 mL methanol and water (v/v, 1/1), and treated with Pd/C (20 mg, 20 mg respectively) under hydrogen atmosphere for 14h. The Pd/C was filtered through a celite layer and the filtrate was concentrated and purified by C18 column and ion exchange chromatography on a DEAE-Sephadex column eluted with NH<sub>4</sub>CO<sub>3</sub> to afford agrocinopine C ammonium salt as a white solid (10 mg, 53%; 15 mg, 79%).

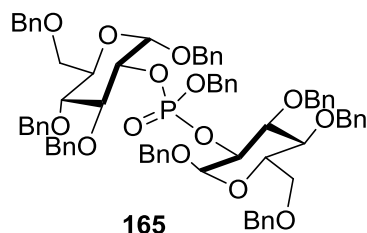
<sup>1</sup>H NMR (500 MHz, Deuterium Oxide) δ: 5.45 (d, *J* = 3.7 Hz, 2H, G1, G'1), 4.39 (q, *J* = 8.4, 7.9 Hz, 1H, F4), 4.21 (dd, *J* = 8.8, 2.4 Hz, 1H, F3), 4.09 – 3.95 (m, 4H, G'2, F6, G3), 3.92 – 3.73 (m, 6H, G'3, G6, F5, G5, G'5), 3.70 – 3.69 (dt, *J* = 9.5, 5.3 Hz, 5H, G2, F1, G'6), 3.51 – 3.44 (m, 2H, G'4, G4).

<sup>13</sup>C NMR (101 MHz, Deuterium Oxide) δ: 103.7 (F-C2), 92.1 (G'-C1), 90.8 (G-C1), 81.3 (F-C4), 78.5 (F-C5), 76.5 (d, *J* = 5.0 Hz, G-C2), 75.9 (F-C3), 74.4 (G-C3), 74.1 (G-C5), 74.0 (G'-C3), 72.1 (G'-C4), 71.6 (G'-C5), 71.3 (d, *J* = 4.5 Hz, G'-C2), 69.4 (G-C4), 62.3 (F-C6), 61.3 (F-C1), 60.5 (G-C6), 60.0 (G'-C6).

<sup>31</sup>P NMR (202 MHz, Deuterium Oxide) δ: 0.06 – -0.49 (m), -0.62 – -0.97 (m).

HRMS *m/z* (ESI): Calcd. for C<sub>18</sub>H<sub>32</sub>O<sub>19</sub>P [M-H]<sup>-</sup>: 583.1281. Found: 583.1273. [α]<sub>D</sub> = +49.6 (*c* 1.0, H<sub>2</sub>O).

**Bis(benzyl 3,4,6-Tri-*O*-benzyl- $\alpha$ -D-glucopyranosid-2-yl) benzylphosphate (165)**



To a solution of **benzyl 3,4,6-tri-*O*-benzyl- $\alpha$ -D-glucopyranoside 134** (139 mg, 0.257 mmol) in 10 mL of dichloromethane was added **benzyl 3,4,6-tri-*O*-benzyl- $\alpha$ -D-glucopyranoside benzyl diisopropylamine phosphoramidite 140** (240 mg, 0.308 mmol), 1*H*-tetrazole (1.14 mL, 0.514 mmol, 0.45 M in CH<sub>3</sub>CN) at room temperature. The reaction was stirred at rt for 2h with monitoring by TLC (pentane/AcOEt=4/1). After the completion of reaction, *t*-BuOOH (28 mg, 50  $\mu$ l, 0.308 mmol) was added at 0 °C, and the reaction was allowed to stir at room temperature for 4h until the intermediate was consumed, then the solvent was evaporated in vacuo to give a syrup, which was subsequently dissolved in 20 mL AcOEt, and washed with saturated NaHCO<sub>3</sub> (20 mL), brine (20 mL). The organic layer was separated and dried over Na<sub>2</sub>SO<sub>4</sub>, concentrated, purified by flash chromatography column (pentane/diethyl ether=1/1) to afford 182 mg product as a white solid (48% yield).

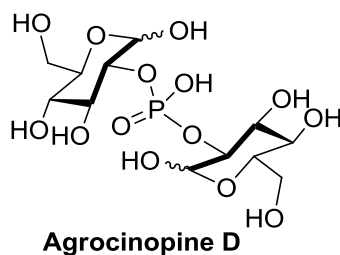
**<sup>1</sup>H NMR (400 MHz, Chloroform-*d*)**  $\delta$ : 7.32 – 7.07 (m, 40H, ArH), 7.07 – 6.97 (m, 5H, ArH), 5.29 (*J* = 3.7 Hz, 2H, H-1), 5.27 (dd, *J* = 3.7 Hz, 2H, H-1), 4.92 – 4.73 (m, 2H, Bn), 4.67 – 4.33 (m, 16H, Bn), 4.34 – 4.28 (m, 2H, H-2), 3.94 (td, *J* = 9.3, 3.9 Hz, 2H, H-3), 3.78 (ddt, *J* = 10.3, 6.0, 3.0 Hz, 2H, H-5), 3.61 (dd, *J* = 10.8, 4.1 Hz, 2H, H-6), 3.56 – 3.39 (m, 4H, H-4, H-6).

**<sup>13</sup>C NMR (101 MHz, Chloroform-*d*)**  $\delta$ : 138.6 (ArC), 138.5 (ArC), 138.1 (d, *J* = 2.7 Hz, ArC), 137.3 (d, *J* = 3.1 Hz, ArC), 135.8 (ArC), 135.7 (ArC), 128.5 (ArC), 128.4 (ArC), 128.3 (ArC), 128.1 (ArC), 128.0 (ArC), 127.9 (ArC), 127.8 (ArC), 127.7 (ArC), 127.4 (ArC), 96.7 (d, *J* = 2.6 Hz, G1), 80.7 (dd, *J* = 7.3, 7.6 Hz, G3), 77.7 (C-4), 77.5 (d, *J* = 7.3 Hz, C-2), 75.4 (Bn), 75.2 (d, *J* = 4.6 Hz, Bn), 75.1 (Bn), 73.5 (2Bn), 70.5 (d, *J* = 3.7 Hz, G5), 70.2 (Bn), 70.0 (Bn), 69.4 (Bn), 69.3 (Bn), 68.4 (G6), 68.3 (G6).

**<sup>31</sup>P NMR (122 MHz, Chloroform-*d*)**  $\delta$  -1.64 .

**HRMS *m/z* (ESI):** Calcd. for C<sub>75</sub>H<sub>77</sub>O<sub>14</sub>NaP [M+Na]<sup>+</sup>: 1255.4949. Found: 1255.4943. [ $\alpha$ ]<sub>D</sub> = -32.6 (*c* 1.0, CHCl<sub>3</sub>).

### Bis(Glucose-2)-phosphate (agrocinopine D)



Pd/C (80 mg) was added to a solution of compound **165** (50 mg, 0.082 mmol) in methanol (5 mL) and the mixture was allowed to stir under H<sub>2</sub> atmosphere for 24 h at room temperature. Pd/C was filtered with a celite layer, and the filtrate was concentrated to give a residue as white solid, which was further purified by C18 to afford 14 mg compound **14** as a white solid (yield=82%). The ratio of  $\alpha/\beta = 2/1$ .

**<sup>1</sup>H NMR (400 MHz, Deuterium Oxide)**  $\delta$ : 5.40 (d,  $J = 3.3$  Hz, 2H, H-1 $\alpha$ ), 4.73 (d,  $J = 7.6$  Hz, 1H, H-1 $\beta$ ), 4.06 – 3.95 (m, 2H, H-2 $\alpha$ ), 3.89 – 3.68 (m, 12H, H-2 $\beta$ , H-3 $\alpha$ , H-3 $\beta$ , H-5 $\alpha$ , H-6 $\alpha$ , H-6 $\beta$ ), 3.50 – 3.39 (m, 5H, H-4 $\alpha$ , H-4 $\beta$ , H-5 $\beta$ ).

**<sup>13</sup>C NMR (101 MHz, Deuterium Oxide)**  $\delta$  95.8 (C-1 $\beta$ ), 95.0 (d,  $J = 4.5$  Hz, C-1 $\beta$ ), 90.8 (C-1 $\alpha$ ), 79.0 (d,  $J = 6.4$  Hz, C-2 $\beta$ ), 75.9 (C-5 $\beta$ ), 75.4 (d,  $J = 6.4$  Hz, C-2 $\alpha$ ), 75.1 (d,  $J = 3.0$  Hz, C-3 $\beta$ ), 71.6 (d,  $J = 6.0$  Hz, C-3 $\alpha$ ), 71.2 (d,  $J = 3.2$  Hz, C-5 $\alpha$ ), 69.4 (C-4 $\alpha$ ), 69.3 (d,  $J = 7.0$  Hz, C-4 $\beta$ ), 60.5 (d,  $J = 18.2$  Hz, C-6 $\alpha\beta$ ).

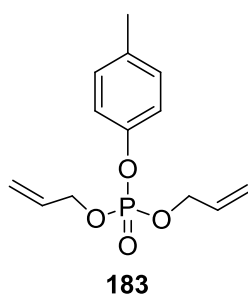
**<sup>31</sup>P NMR (122 MHz, Deuterium Oxide)**  $\delta$ : -0.8 ( $\beta$ ), -1.5 ( $\alpha$ ). **HRMS m/z (ESI)**: Calcd. for C<sub>12</sub>H<sub>22</sub>O<sub>14</sub>P (M-H)<sup>-</sup>: 421.0753. Found: 421.8.  $[\alpha]_D = +49.6$  (c 1.0, H<sub>2</sub>O).

## Phosphorylation Procedures

Procedure for nucleosides: To a solution of nucleoside (50 mg) with DMAP (4 equiv.) in anhydrous THF (5 mL) was added the prepared phosphorylation reagent via cannula at -30 °C, the preparation of phosphorylation reagent was conducted according to the typical experiment with triallyl phosphite (2.2 equiv), iodine (2 equiv) in anhydrous dichloromethane (5 mL). The reaction mixture was stirred at room temperature overnight. The solvent was removed under reduced pressure to afford a crude residue which was dissolved in DCM. The solution was washed with aqueous saturated NaHSO<sub>4</sub>, saturated NaHCO<sub>3</sub> and brine solution respectively. The organic layer was dried over anhydrous Na<sub>2</sub>SO<sub>4</sub>, evaporated and further purified by column chromatography affording pure products in different yields.

Procedure for β-Stereoselective Phosphorylation: To a solution of 2,3,4,6-tetra-*O*-acetyl-D-gluco or -galactopyranose (50 mg) with DMAP (10 equiv) in anhydrous dichloromethane (5 mL) was added the prepared phosphorylation reagent via cannula at rt, the preparation of phosphorylation reagent was conducted according to the typical experiment with triallyl phosphite (7.8 equiv), iodine (7.5 equiv) in anhydrous dichloromethane (5 mL). The reaction mixture was stirred at room temperature overnight. The solution was then diluted with DCM and washed with saturated NaHSO<sub>4</sub>, saturated NaHCO<sub>3</sub> and brine solution respectively. The organic layer was dried over anhydrous Na<sub>2</sub>SO<sub>4</sub>, evaporated and further purified by column chromatography affording pure products in different yields.

### Diallyl *p*-tolyl Phosphate (183)



Purification by flash chromatography using petroleum ether/AcOEt=4/1 or pentane/diethyl ether=1/1 as eluent afforded Diallyl *p*-tolyl Phosphate (100 mg, 75%) as a colourless oil.

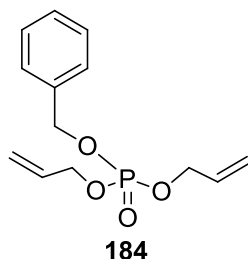
**<sup>1</sup>H NMR (300 MHz, Chloroform-*d*)** δ: 7.11 (s, 4H, ArH), 5.93 (m, 2H, OCH<sub>2</sub>-CH=CH<sub>2</sub>), 5.31 (dd, 4H, OCH<sub>2</sub>-CH=CH<sub>2</sub>), 4.76 – 4.52 (m, 4H, OCH<sub>2</sub>-CH=CH<sub>2</sub>), 2.31 (s, 3H, CH<sub>3</sub>).

**<sup>13</sup>C NMR (75 MHz, Chloroform-*d*)** δ 148.4 (d, *J* = 7 Hz, ArC), 134.7 (d, *J* = 1.3 Hz, ArC), 132.1 (d, *J* = 7.0 Hz, OCH<sub>2</sub>-CH=CH<sub>2</sub>), 130.1(ArC), 119.7 (d, *J* = 4.7 Hz, ArC), 118.5 (OCH<sub>2</sub>-CH=CH<sub>2</sub>), 68.7 (d, *J* = 5.7 Hz, OCH<sub>2</sub>-CH=CH<sub>2</sub>), 20.7 (CH<sub>3</sub>).

**<sup>31</sup>P NMR (121.5 MHz, Chloroform-*d*)** δ -5.96

**HRMS (ESI)** [M + Na]<sup>+</sup> calculated for C<sub>13</sub>H<sub>17</sub>O<sub>4</sub>NaP 291.0900, found 291.0762.

### Diallyl Benzyl Phosphate (184)



Purification by flash chromatography using pentane/diethyl ether=1/1 as eluent afforded Diallyl Benzyl Phosphate (112 mg, 82%) as a colourless oil.

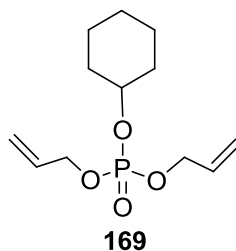
**<sup>1</sup>H NMR (300 MHz, Chloroform-*d*)**  $\delta$  7.45 – 7.31 (m, 5H, ArH), 6.07 – 5.76 (m, 2H, OCH<sub>2</sub>-CH=CH<sub>2</sub>), 5.44 – 5.16 (m, 4H, OCH<sub>2</sub>-CH=CH<sub>2</sub>), 5.08 (d, *J* = 8.1 Hz, 2H, PhCH<sub>2</sub>), 4.49 (m, 4H, OCH<sub>2</sub>-CH=CH<sub>2</sub>).

**<sup>13</sup>C NMR (75 MHz, Chloroform-*d*)**  $\delta$  135.8 (d, *J* = 6.8 Hz, ArC), 132.4 (d, *J* = 7.0 Hz, OCH<sub>2</sub>-CH=CH<sub>2</sub>), 128.6 (ArC), 128.5 (ArC), 127.9 (ArC), 118.3 (OCH<sub>2</sub>-CH=CH<sub>2</sub>), 69.3 (d, *J* = 5.5 Hz, PhCH<sub>2</sub>O-), 68.2 (d, *J* = 5.5 Hz, OCH<sub>2</sub>-CH=CH<sub>2</sub>).

**<sup>31</sup>P NMR (121.5 MHz, Chloroform-*d*)**  $\delta$  -0.76

**HRMS (ESI)** [M + Na]<sup>+</sup> calculated for C<sub>13</sub>H<sub>17</sub>O<sub>4</sub>NaP 291.0900, found 291.0756.

### Diallyl Cyclohexyl Phosphate (169)



Purification by flash chromatography using pentane/diethyl ether=3/2 as eluent afforded Diallyl Cyclohexyl Phosphate (50 mg, 39%) as a colourless oil.

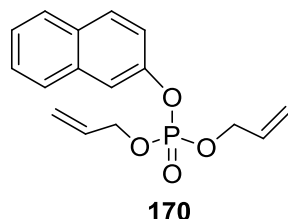
**<sup>1</sup>H NMR (300 MHz, Chloroform-*d*)**  $\delta$ : 6.08 – 5.83 (m, 2H, OCH<sub>2</sub>-CH=CH<sub>2</sub>), 5.30 (dd, 4H, OCH<sub>2</sub>-CH=CH<sub>2</sub>), 4.62 – 4.46 (m, 4H, OCH<sub>2</sub>-CH=CH<sub>2</sub>), 4.40 (s, 1H, cyclohexyl), 2.05 – 1.10 (m, 10H, cyclohexyl).

**<sup>13</sup>C NMR (75 MHz, Chloroform-*d*)**  $\delta$ : 132.6 (d, *J* = 7.2 Hz, OCH<sub>2</sub>-CH=CH<sub>2</sub>), 117.9 (OCH<sub>2</sub>-CH=CH<sub>2</sub>), 77.5 (d, *J* = 9.6 Hz, cyclohexyl-CH-OP), 67.9 (d, *J* = 5.5 Hz, OCH<sub>2</sub>-CH=CH<sub>2</sub>), 33.3 (d, *J* = 4.4 Hz, cyclohexyl-C), 25.1 (cyclohexyl-C), 23.5 (cyclohexyl-C).

**<sup>31</sup>P NMR (121.5 MHz, Chloroform-*d*)**  $\delta$  -1.59

**HRMS (ESI)** [M + Na]<sup>+</sup> calculated for C<sub>12</sub>H<sub>21</sub>O<sub>4</sub>NaP 283.1200, found 283.1073.

### Diallyl Naphthalen-2-yl Phosphate (170)



Purification by flash chromatography using pentane/diethyl ether=1/1 as eluent afforded Diallyl Naphthalen-2-yl phosphate (150 mg, 98%) as a colourless oil.

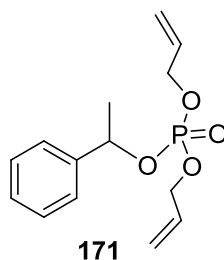
**<sup>1</sup>H NMR (300 MHz, Chloroform-*d*)**  $\delta$ : 7.85 – 7.24 (m, 7H, naphH), 6.04 – 5.74 (m, 2H, OCH<sub>2</sub>-CH=CH<sub>2</sub>), 5.26 (dd,  $J$  = 13.7 Hz, 4H, OCH<sub>2</sub>-CH=CH<sub>2</sub>), 4.73 – 4.49 (m, 4H, OCH<sub>2</sub>-CH=CH<sub>2</sub>).

**<sup>13</sup>C NMR (75 MHz, Chloroform-*d*)**  $\delta$ : 148.2 (d,  $J$  = 7.1 Hz, ArC), 133.9 (ArC), 132.1 (d,  $J$  = 6.8 Hz, OCH<sub>2</sub>-CH=CH<sub>2</sub>), 131.0 (ArC), 129.9 (ArC), 127.7 (ArC), 127.5 (ArC), 126.8 (ArC), 125.6 (ArC), 120.0 (d,  $J$  = 5.2 Hz, ArC), 118.7 (OCH<sub>2</sub>-CH=CH<sub>2</sub>), 116.5 (d,  $J$  = 4.8 Hz, ArC), 68.9 (d,  $J$  = 5.7 Hz, OCH<sub>2</sub>-CH=CH<sub>2</sub>).

**<sup>31</sup>P NMR (121.5 MHz, Chloroform-*d*)**  $\delta$  -6.08

**HRMS (ESI)** [M + Na]<sup>+</sup> calculated for C<sub>16</sub>H<sub>17</sub>O<sub>4</sub>NaP 327.0900, found 327.0760.

### Diallyl (1-phenylethyl) Phosphate (171)



Purification by flash chromatography using pentane/diethyl ether=1/1 as eluent afforded Diallyl (1-phenylethyl) Phosphate (64 mg, 42%) as a colourless oil.

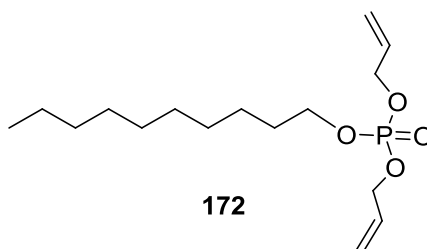
**<sup>1</sup>H NMR (300 MHz, Chloroform-*d*)**  $\delta$ : 7.35 (d,  $J$  = 13.7 Hz, 5H, PhH), 6.07 – 5.68 (m, 2H, OCH<sub>2</sub>-CH=CH<sub>2</sub>), 5.50 (d,  $J$  = 13.8 Hz, 1H, CH), 5.39 – 5.06 (m, 4H, OCH<sub>2</sub>-CH=CH<sub>2</sub>), 4.65 – 4.40 (m, 2H, OCH<sub>2</sub>-CH=CH<sub>2</sub>), 4.42 – 4.25 (m, 2H, OCH<sub>2</sub>-CH=CH<sub>2</sub>), 1.64 (d,  $J$  = 6.5 Hz, 3H, CH<sub>3</sub>).

**<sup>13</sup>C NMR (75 MHz, Chloroform-*d*)**  $\delta$ : 141.5 (d,  $J$  = 4.7 Hz, ArC), 132.4 (d,  $J$  = 6.9 Hz, OCH<sub>2</sub>-CH=CH<sub>2</sub>), 128.5 (ArC), 128.2 (ArC), 125.9 (ArC), 118.2 (s, d,  $J$  = 10.5 Hz, OCH<sub>2</sub>-CH=CH<sub>2</sub>), 77.1 (d,  $J$  = 5.6 Hz, PhCH-OP), 68.0 (dt,  $J$  = 5.5 Hz, OCH<sub>2</sub>-CH=CH<sub>2</sub>), 24.1 (d,  $J$  = 5.3 Hz, CH<sub>3</sub>).

**<sup>31</sup>P NMR (121.5 MHz, Chloroform-*d*)**  $\delta$ : -1.66

**HRMS (ESI)** [M + Na]<sup>+</sup> calculated for C<sub>14</sub>H<sub>19</sub>O<sub>4</sub>NaP: 305.1000, found: 305.0919.

### Diallyl Decyl Phosphate (172)



Purification by flash chromatography using pentane/diethyl ether=1/1 as eluent afforded Diallyl Decyl Phosphate (150 mg, 94%) as a colourless oil.

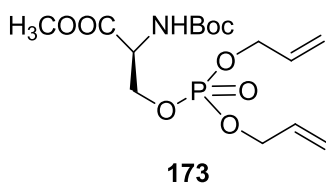
**<sup>1</sup>H NMR (300 MHz, Chloroform-*d*)**  $\delta$  5.94 (m, 2H, OCH<sub>2</sub>-CH=CH<sub>2</sub>), 5.45 – 5.16 (m, 4H, OCH<sub>2</sub>-CH=CH<sub>2</sub>), 4.61 – 4.44 (m, 4H, OCH<sub>2</sub>-CH=CH<sub>2</sub>), 4.04 (q, *J* = 6.7 Hz, 2H, OCH<sub>2</sub>), 1.67 (p, *J* = 6.6 Hz, 2H, OCH<sub>2</sub>CH<sub>2</sub>), 1.25 (s, 14H, decyl-H), 0.87 (t, *J* = 6.6 Hz, 3H, CH<sub>3</sub>).

**<sup>13</sup>C NMR (75 MHz, Chloroform-*d*)**  $\delta$  132.5 (d, *J* = 6.9 Hz, OCH<sub>2</sub>-CH=CH<sub>2</sub>), 117.9 (OCH<sub>2</sub>-CH=CH<sub>2</sub>), 67.89 (d, *J* = 6.0 Hz, OCH<sub>2</sub>-CH=CH<sub>2</sub>), 67.89 (d, *J* = 5.3 Hz, P-OCH<sub>2</sub>), 31.8 (CH<sub>2</sub>), 30.2 (CH<sub>2</sub>), 30.1 (CH<sub>2</sub>), 29.4 (CH<sub>2</sub>), 29.2 (CH<sub>2</sub>), 29.0 (CH<sub>2</sub>), 25.3 (CH<sub>2</sub>), 22.6 (CH<sub>2</sub>), 14.0 (CH<sub>3</sub>).

**<sup>31</sup>P NMR (121.5 MHz, Chloroform-*d*)**  $\delta$ : -0.70

**HRMS (ESI)** [M + Na]<sup>+</sup> calculated for C<sub>16</sub>H<sub>31</sub>O<sub>4</sub>NaP 341.2000, found 341.1854.

### Diallyl BocSerOMe Phosphate (173)



Purification by flash chromatography using pentane/diethyl ether=1/2 as eluent afforded Diallyl-BocSerOMe-Phosphate (120 mg, 64%) as a colourless oil.

**<sup>1</sup>H NMR (300 MHz, Chloroform-*d*)**  $\delta$ : 5.99 – 5.77 (m, 2H, OCH<sub>2</sub>-CH=CH<sub>2</sub>), 5.39 – 5.16 (m, 4H, OCH<sub>2</sub>-CH=CH<sub>2</sub>), 4.55 – 4.42 (m, 5H, OCH<sub>2</sub>-CH=CH<sub>2</sub>, CH<sub>2</sub>O-diallylphosphate), 4.37 (dd, *J* = 7.3, 2.8 Hz, 1H, CH<sub>2</sub>O-diallylphosphate), 4.25 (m, 1H, CH), 3.73 (s, 3H, OCH<sub>3</sub>), 1.40 (s, 9H, Boc).

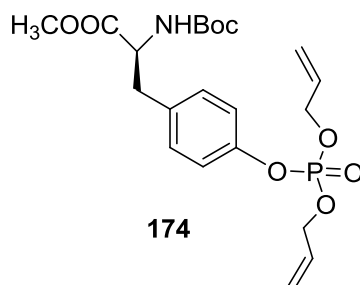
**<sup>13</sup>C NMR (75 MHz, Chloroform-*d*)**  $\delta$ : 169.7 (C=O), 155.1 (C=O), 132.14 (d, *J* = 6.0 Hz, OCH<sub>2</sub>-CH=CH<sub>2</sub>), 132.06 (d, *J* = 6.75 Hz, OCH<sub>2</sub>-CH=CH<sub>2</sub>), 118.5 (OCH<sub>2</sub>-CH=CH<sub>2</sub>), 80.2 ( (CH<sub>3</sub>)<sub>3</sub>CO ), 68.41 (d, *J* = 6.0 Hz, OCH<sub>2</sub>-CH=CH<sub>2</sub>), 68.39 (d, *J* = 5.3 Hz, OCH<sub>2</sub>-CH=CH<sub>2</sub>), 67.5 (d, *J* = 5.3 Hz, P-OCH<sub>2</sub>), 53.9 (d, *J* = 7.4 Hz, CH), 52.7 (OCH<sub>3</sub>), 28.2 ( C(CH<sub>3</sub>)<sub>3</sub> ).

**<sup>31</sup>P NMR (121.5 MHz, Chloroform-*d*)**  $\delta$ : -0.76

**HRMS (ESI)** [M + Na]<sup>+</sup> calculated for C<sub>15</sub>H<sub>26</sub>NO<sub>8</sub>NaP 402.1400, found 402.1289.

$[\alpha]_D^{22} = +14.8$  (c 2.54, CHCl<sub>3</sub>)

### Diallyl BocTyrOMe Phosphate (174)



Purification by flash chromatography using pentane/AcOEt=2/1 as eluent afforded Diallyl-BocTyrOMe-Phosphate (175 mg, 77%) as a colourless oil.

**<sup>1</sup>H NMR (300 MHz, Chloroform-*d*)**  $\delta$ : 7.10 (q,  $J = 8.4$  Hz, 4H, PhH), 5.92 (m, 2H, OCH<sub>2</sub>-CH=CH<sub>2</sub>), 5.41 – 5.16 (m, 4H, OCH<sub>2</sub>-CH=CH<sub>2</sub>), 4.97 (d,  $J = 8.2$  Hz, 1H, NH), 4.68 – 4.44 (m, 5H, OCH<sub>2</sub>-CH=CH<sub>2</sub>, CH), 3.69 (s, 3H, OCH<sub>3</sub>), 3.04 (qd,  $J = 13.9, 5.9$  Hz, 2H, PhCH<sub>2</sub>), 1.40 (s, 9H, Boc).

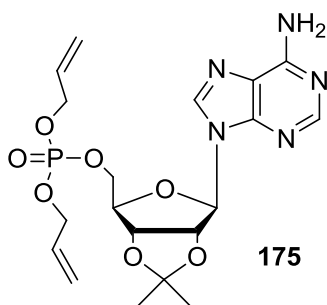
**<sup>13</sup>C NMR (75 MHz, Chloroform-*d*)**  $\delta$ : 172.1 (C=O), 155.0 (C=O), 149.6 (d,  $J = 6.9$  Hz, ArC), 133.0 (d,  $J = 1.1$  Hz, ArC), 132.1 (d,  $J = 6.8$  Hz, OCH<sub>2</sub>-CH=CH<sub>2</sub>), 130.5 (ArC), 120.0 (d,  $J = 4.9$  Hz, ArC), 118.6 (OCH<sub>2</sub>-CH=CH<sub>2</sub>), 79.9 ( (CH<sub>3</sub>)<sub>3</sub>CO ), 68.8 (d,  $J = 5.7$  Hz, OCH<sub>2</sub>-CH=CH<sub>2</sub>), 54.4 (CH), 52.2 (OCH<sub>3</sub>), 37.5 (PhCH<sub>2</sub>), 28.3 ( C(CH<sub>3</sub>)<sub>3</sub> ).

**<sup>31</sup>P NMR (121.5 MHz, Chloroform-*d*)**  $\delta$  -6.25

**HRMS (ESI)** [M + Na]<sup>+</sup> calculated for C<sub>21</sub>H<sub>30</sub>NO<sub>8</sub>NaP 478.1700, found 478.1601.

$[\alpha]_D^{22} = +27.8$  (c 2.06, CHCl<sub>3</sub>)

### Diallyl 2',3'-isopropylideneadenosine Phosphate (175)



Purification by flash chromatography using DCM/Methanol=30/1 as eluent afforded Diallyl 2',3'-isopropylideneadenosine-Phosphate (45 mg, 62%) as a colourless oil.

**<sup>1</sup>H NMR (300 MHz, Chloroform-*d*)**  $\delta$ : 8.32 (s, 1H, H-2), 7.95 (s, 1H, H-8), 6.17 (s, 2H, NH<sub>2</sub>), 6.13 (d,  $J = 2.3$  Hz, 1H, H-1'), 5.85 (m, 2H, OCH<sub>2</sub>-CH=CH<sub>2</sub>), 5.39 (dd,  $J = 6.3$  Hz, 1H, H-2'), 5.32 (dq,  $J = 7.1$  Hz, 1H, OCH<sub>2</sub>-CH=CH<sub>2</sub>), 5.26 (d,  $J = 7.2$  Hz, 1H, OCH<sub>2</sub>-CH=CH<sub>2</sub>), 5.23 – 5.14 (m, 2H, OCH<sub>2</sub>-

CH=CH<sub>2</sub>), 5.12 – 5.03 (m, 1H, H-3'), 4.47 (q, *J* = 7.0 Hz, 5H, H-4', OCH<sub>2</sub>-CH=CH<sub>2</sub>), 4.35 – 4.13 (m, 2H, H-5'), 1.60 (s, 3H, CH<sub>3</sub>), 1.37 (s, 3H, CH<sub>3</sub>).

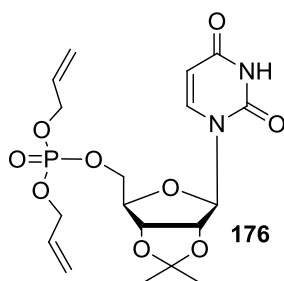
<sup>13</sup>C NMR (101 MHz, Chloroform-*d*) δ: 154.8 (C-6), 152.2 (C-2), 148.2 (C-4), 138.5 (C-8), 131.14 (d, *J* = 7.0 Hz, OCH<sub>2</sub>-CH=CH<sub>2</sub>), 131.11 (d, *J* = 7.0 Hz, OCH<sub>2</sub>-CH=CH<sub>2</sub>), 119.1 (C-5), 117.5 (d, *J* = 2.0 Hz, OC(CH<sub>3</sub>)<sub>3</sub>), 113.5 (OCH<sub>2</sub>-CH=CH<sub>2</sub>), 89.9 (C-1'), 84.3 (d, *J* = 8.0 Hz, C-2'), 83.2 (C-4'), 80.4 (C-3'), 67.36 (d, *J* = 6.0 Hz, OCH<sub>2</sub>-CH=CH<sub>2</sub>), 67.35 (d, *J* = 5.0 Hz, OCH<sub>2</sub>-CH=CH<sub>2</sub>), 65.9 (d, *J* = 5.7 Hz, C-5'), 26.1 (CH<sub>3</sub>), 24.3 (CH<sub>3</sub>).

<sup>31</sup>P NMR (121.5 MHz, Chloroform-*d*) δ: -1.03

HRMS (ESI) [M + H]<sup>+</sup> calculated for C<sub>19</sub>H<sub>27</sub>N<sub>5</sub>O<sub>7</sub>P 468.1600, found 468.1631.

[α]<sub>D</sub><sup>22</sup> = -17.2 (c 1.5, CHCl<sub>3</sub>)

### Diallyl 2',3'-isopropylideneuridine Phosphate (176)



Purification by flash chromatography using DCM/Methanol=35/1 as eluent and then pentane/AcOEt=1/4 allowed to the desired product and by-products Diallyl 2',3'-isopropylideneuridine Phosphate (53 mg, 68%) as a colourless oil.

Note: 2',3'-isopropylideneuridine was prepared with Uridine (0.5 g, 2.05 mmol) in Acetone (25 mL) and H<sub>2</sub>SO<sub>4</sub> (0.25 mL, 4.7 mmol) at room temperature for 1 h in 89% yield.

<sup>1</sup>H NMR (300 MHz, Chloroform-*d*) δ: 9.75 (s, 1H, NH), 7.36 (d, *J* = 8.1 Hz, 1H, H-6), 6.00 – 5.82 (m, 2H, OCH<sub>2</sub>-CH=CH<sub>2</sub>), 5.77 (d, *J* = 2.4 Hz, 1H, H-5), 5.71 (d, *J* = 8.0 Hz, 1H, H-1'), 5.42 – 5.16 (m, 4H, OCH<sub>2</sub>-CH=CH<sub>2</sub>), 4.96 – 4.77 (m, 2H, H-2', H-3'), 4.61 – 4.45 (m, 4H, OCH<sub>2</sub>-CH=CH<sub>2</sub>), 4.36 – 4.30 (m, 1H, H-4'), 4.26 (dt, *J* = 7.9 Hz, 2H, H-5'), 1.55 (s, 3H, CH<sub>3</sub>), 1.32 (s, 3H, CH<sub>3</sub>).

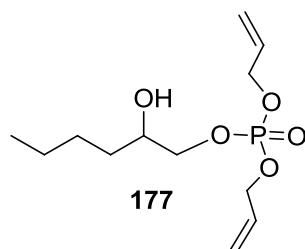
<sup>13</sup>C NMR (101 MHz, Chloroform-*d*) δ: 163.5 (C=O), 150.1 (C=O), 141.8 (C-6), 132.2 (d, *J* = 6.8 Hz, OCH<sub>2</sub>-CH=CH<sub>2</sub>), 118.6 (OCH<sub>2</sub>-CH=CH<sub>2</sub>), 114.6 (OC(CH<sub>3</sub>)<sub>2</sub>), 102.7 (C-5), 93.7 (C-1'), 85.2 (d, *J* = 7.6 Hz, C-4'), 84.4 (C-2'), 80.6 (C-3'), 68.5 (d, *J* = 5.4 Hz, OCH<sub>2</sub>-CH=CH<sub>2</sub>), 67.0 (d, *J* = 5.6 Hz, C-5'), 27.1 (CH<sub>3</sub>), 25.3 (CH<sub>3</sub>).

<sup>31</sup>P NMR (121.5 MHz, Chloroform-*d*) δ -3.08

HRMS (ESI) [M + H]<sup>+</sup> calculated for C<sub>18</sub>H<sub>26</sub>N<sub>2</sub>O<sub>9</sub>P 445.1600, found 445.1370.

[α]<sub>D</sub><sup>22</sup> = +1.0 (c 1.0, CHCl<sub>3</sub>)

### Diallyl (2-hydroxyhexyl) phosphate (177)



Purification by flash chromatography using pentane/diethyl ether=1/2 - 1/3 as eluent afforded Diallyl (2-hydroxyhexyl) Phosphate (100 mg, 72%) as a colourless oil.

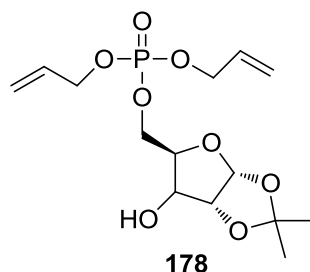
**<sup>1</sup>H NMR (300 MHz, Chloroform-*d*)**  $\delta$ : 5.93 (m, 2H, OCH<sub>2</sub>-CH=CH<sub>2</sub>), 5.44 – 5.15 (m, 4H, OCH<sub>2</sub>-CH=CH<sub>2</sub>), 4.65 – 4.41 (m, 4H, OCH<sub>2</sub>-CH=CH<sub>2</sub>), 4.06 (m, 1H, POCH<sub>2a</sub>), 3.97 – 3.86 (m, 1H, POCH<sub>2b</sub>), 3.80 (m, 1H, CH-), 2.86 (m, 1H, -OH), 1.54 – 1.18 (m, 6H, CH<sub>2</sub>CH<sub>2</sub>CH<sub>2</sub>), 0.89 (t, *J* = 7.0 Hz, 3H, CH<sub>3</sub>).

**<sup>13</sup>C NMR (75 MHz, Chloroform-*d*)**  $\delta$ : 132.3 (d, *J* = 6.7 Hz, OCH<sub>2</sub>-CH=CH<sub>2</sub>), 118.5 (OCH<sub>2</sub>-CH=CH<sub>2</sub>), 72.2 (d, *J* = 6.2 Hz, CH<sub>2</sub>OP), 70.4 (d, *J* = 5.7 Hz, CHOH), 68.4 (d, *J* = 5.4 Hz, OCH<sub>2</sub>-CH=CH<sub>2</sub>), 32.3 (CH<sub>2</sub>), 27.5 (CH<sub>2</sub>), 22.6 (CH<sub>2</sub>), 13.9 (CH<sub>3</sub>).

**<sup>31</sup>P NMR (121.5 MHz, Chloroform-*d*)**  $\delta$ : -0.01

**HRMS (ESI) [M + H]<sup>+</sup>** calculated for C<sub>12</sub>H<sub>24</sub>O<sub>5</sub>P 279.1300, found 279.1354.

### Diallyl 1,2-*O*-isopropylidene- $\alpha$ -D-xylofuranose Phosphate (178)



Purification by flash chromatography using DCM/methanol=35/1 as eluent afforded Diallyl 1,2-*O*-isopropylidene- $\alpha$ -D-xylofuranose phosphate (118 mg, 67%) as a colourless oil.

**<sup>1</sup>H NMR (300 MHz, Chloroform-*d*)**  $\delta$  6.04 – 5.80 (m, 3H, H-1, OCH<sub>2</sub>-CH=CH<sub>2</sub>), 5.42 – 5.23 (m, 4H, OCH<sub>2</sub>-CH=CH<sub>2</sub>), 4.60 – 4.49 (m, 5H, H-2, OCH<sub>2</sub>-CH=CH<sub>2</sub>), 4.40 (d, *J* = 4.1 Hz, 1H, OH), 4.36 – 4.29 (m, 2H, H-5a, H-4), 4.27 (d, *J* = 4.1 Hz, 1H, H-3), 4.16 (m, 1H, H-5b), 1.49 (s, 3H, CH<sub>3</sub>), 1.30 (s, 3H, CH<sub>3</sub>).

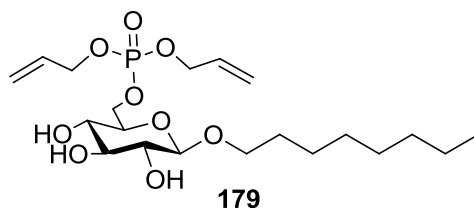
**<sup>13</sup>C NMR (101 MHz, Chloroform-*d*)**  $\delta$ : 132.0 (d, *J* = 7.0 Hz, OCH<sub>2</sub>-CH=CH<sub>2</sub>), 131.9 (d, *J* = 7.0 Hz, OCH<sub>2</sub>-CH=CH<sub>2</sub>), 118.9 (d, *J* = 7.5 Hz, OCH<sub>2</sub>-CH=CH<sub>2</sub>), 111.8 (OC(CH<sub>3</sub>)<sub>2</sub>), 105.1 (C-1), 85.1 (C-2), 78.9 (d, *J* = 5.2 Hz, C-4), 73.7 (C-3), 68.8 (d, *J* = 4.0 Hz, OCH<sub>2</sub>-CH=CH<sub>2</sub>), 68.7 (d, *J* = 5.0 Hz, OCH<sub>2</sub>-CH=CH<sub>2</sub>), 63.5 (d, *J* = 5.1 Hz, C-5), 26.9 (CH<sub>3</sub>), 26.2 (CH<sub>3</sub>).

**<sup>31</sup>P NMR (121.5 MHz, Chloroform-*d*)**  $\delta$ : -0.63

**HRMS (ESI) [M + Na]<sup>+</sup>** calculated for C<sub>14</sub>H<sub>23</sub>O<sub>8</sub>NaP 373.1600, found 373.1015.

**$[\alpha]_D^{22}$**  = +6.9 (c 2.0, CHCl<sub>3</sub>)

### Diallyl Octyl $\beta$ -D-glucopyranoside phosphate (179)



Purification by flash chromatography using DCM/methanol=15/1 as eluent afforded Diallyl Octyl  $\beta$ -D-glucopyranoside phosphate (152 mg, 67%) as a colourless oil.

**$^1\text{H}$  NMR (300 MHz, Chloroform-*d*+D<sub>2</sub>O)**  $\delta$ : 5.99-5.88 (m, 2H, OCH<sub>2</sub>-CH=CH<sub>2</sub>), 5.39 – 5.33 (m, 2H, OCH<sub>2</sub>-CH=CH<sub>2</sub>), 5.23 (d,  $J$  = 10.4 Hz, 2H, OCH<sub>2</sub>-CH=CH<sub>2</sub>), 4.57 – 4.51 (m, 4H, OCH<sub>2</sub>-CH=CH<sub>2</sub>), 4.34 – 4.19 (m, 3H,  $J$  = 7.5 Hz, H-1, H-6), 3.81 (q,  $J$  = 6.9 Hz, 1H, OCH<sub>2a</sub>), 3.53 – 3.48 (m, 2H, H-3, OCH<sub>2b</sub>), 3.44 – 3.42 (m, 2H, H-4, H-5) 3.32 (t,  $J$  = 9 Hz, 1H, H-2), 1.58 (q, 2H, OCH<sub>2</sub>CH<sub>2</sub>C<sub>6</sub>H<sub>13</sub>), 1.25 (s, 10H, C<sub>5</sub>H<sub>10</sub>-CH<sub>3</sub>), 0.86 (t,  $J$  = 6.4 Hz, 3H, CH<sub>3</sub>).

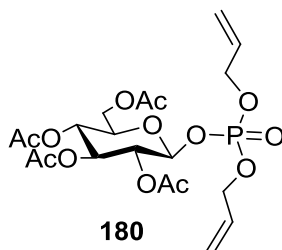
**$^{13}\text{C}$  NMR (101 MHz, Chloroform-*d*)**  $\delta$ : 132.28 (d,  $J$  = 6.0 Hz, OCH<sub>2</sub>-CH=CH<sub>2</sub>), 132.27 (d,  $J$  = 6.0 Hz, OCH<sub>2</sub>-CH=CH<sub>2</sub>), 118.5 (d,  $J$  = 1.2 Hz, OCH<sub>2</sub>-CH=CH<sub>2</sub>), 102.7 (C-1), 76.0 (C-3), 74.4 (d,  $J$  = 6.4 Hz, C-5), 73.3 (C-2), 70.2 (OCH<sub>2</sub>CH<sub>2</sub>C<sub>6</sub>H<sub>13</sub>), 69.3 (C-4), 68.6 (d,  $J$  = 5.0 Hz, OCH<sub>2</sub>-CH=CH<sub>2</sub>), 68.5 (d,  $J$  = 6.0 Hz, OCH<sub>2</sub>-CH=CH<sub>2</sub>), 66.9 (d,  $J$  = 5.4 Hz, C-6), 31.8 (CH<sub>2</sub>), 29.6 (CH<sub>2</sub>), 29.4 (CH<sub>2</sub>), 29.3 (CH<sub>2</sub>), 25.9 (CH<sub>2</sub>), 22.6 (CH<sub>2</sub>), 14.1 (CH<sub>3</sub>).

**$^{31}\text{P}$  NMR (121.5 MHz, Chloroform-*d*)**  $\delta$ : -0.58.

**HRMS (ESI)** [M + Na]<sup>+</sup> calculated for C<sub>20</sub>H<sub>37</sub>O<sub>9</sub>NaP 475.1600, found 475.2063.

$[\alpha]_D^{22}$  = -36 (c 1.35, CHCl<sub>3</sub>).

### Diallyl 2,3,4,6-tetra-*O*-acetyl-D-glucopyranose phosphate (180)



Purification by flash chromatography using pentane/AcOEt=1/2 as eluent afforded diallyl 2,3,4,6-tetra-*O*-acetyl-D-glucopyranose Phosphate (53 mg, 73%) as a colourless oil.

**$^1\text{H}$  NMR (300 MHz, Chloroform-*d*)**  $\delta$ : 5.90 (m, 2H, OCH<sub>2</sub>-CH=CH<sub>2</sub>), 5.46 – 4.98 (m, 8H, OCH<sub>2</sub>-CH=CH<sub>2</sub>, H-1, H-2, H-3, H-4), 4.53 (dt,  $J$  = 13.7, 6.6 Hz, 4H, OCH<sub>2</sub>-CH=CH<sub>2</sub>), 4.35 – 4.02 (m, 2H, H-6), 3.82 (d,  $J$  = 14.2 Hz, 1H, H-5), 2.03 (4s, 12H, CH<sub>3</sub>CO).

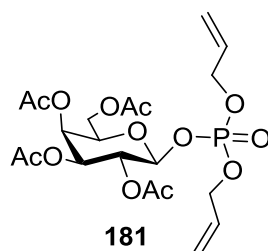
**$^{13}\text{C}$  NMR (101 MHz, Chloroform-*d*)**  $\delta$ : 169.4 (C=O), 169.0 (C=O), 168.4 (C=O), 168.2 (C=O), 131.0 (d,  $J$  = 7.6 Hz, OCH<sub>2</sub>-CH=CH<sub>2</sub>), 130.8 (d,  $J$  = 7.3 Hz, OCH<sub>2</sub>-CH=CH<sub>2</sub>), 117.6 (d,  $J$  = 9.3, OCH<sub>2</sub>-CH=CH<sub>2</sub>), 95.2 (d,  $J$  = 4.6 Hz, C-1), 71.6 (C-5), 71.3 (d,  $J$  = 1.6 Hz, C-3), 70.2 (d,  $J$  = 9.2 Hz, C-2), 67.7 (d,  $J$  = 5.8 Hz, OCH<sub>2</sub>-CH=CH<sub>2</sub>), 67.6 (d,  $J$  = 5.6 Hz, OCH<sub>2</sub>-CH=CH<sub>2</sub>), 66.9 (C-4), 60.5 (C-6), 19.7 (CH<sub>3</sub>), 19.6(CH<sub>3</sub>), 19.5 (2CH<sub>3</sub>).

**$^{31}\text{P}$  NMR (121.5 MHz, Chloroform-*d*)**  $\delta$ : -3.06

**HRMS (ESI):**  $[M + Na]^+$  calculated for  $C_{20}H_{29}NaO_{13}P$ : 531.1254; found: 531.1226.

$[\alpha]_D^{22} = +2.6$  (c 1.75,  $CHCl_3$ ).

**Diallyl 2,3,4,6-tetra-*O*-acetyl-D-galactopyranose phosphate (181)**



Purification by flash chromatography using pentane/ $AcOEt=1/2$  as eluent afforded Diallyl 2,3,4,6-tetra-*O*-acetyl-D-galactopyranose Phosphate (40 mg, 55%) as a colourless oil.

**$^1H$  NMR (300 MHz, Chloroform-*d*)**  $\delta$ : 5.88 (m, 2H,  $OCH_2-\underline{CH}=\underline{CH}_2$ ), 5.45 – 5.33 (m, 2H, H-4,  $OCH_2-\underline{CH}=\underline{CH}_2$ ), 5.33 – 5.14 (m, 5H,  $OCH_2-\underline{CH}=\underline{CH}_2$ , H-1, H-2), 5.01 (dd,  $J = 7.6, 2.7$  Hz, 1H, H-3), 4.63 – 4.39 (m, 4H,  $\underline{OCH}_2-\underline{CH}=\underline{CH}_2$ ), 4.19 – 3.97 (m, 3H, H-6, H-5), 2.13 (s, 3H,  $CH_3CO$ ), 2.03 (s, 3H,  $CH_3CO$ ), 1.99 (s, 3H,  $CH_3CO$ ), 1.95 (s, 3H,  $CH_3CO$ ).

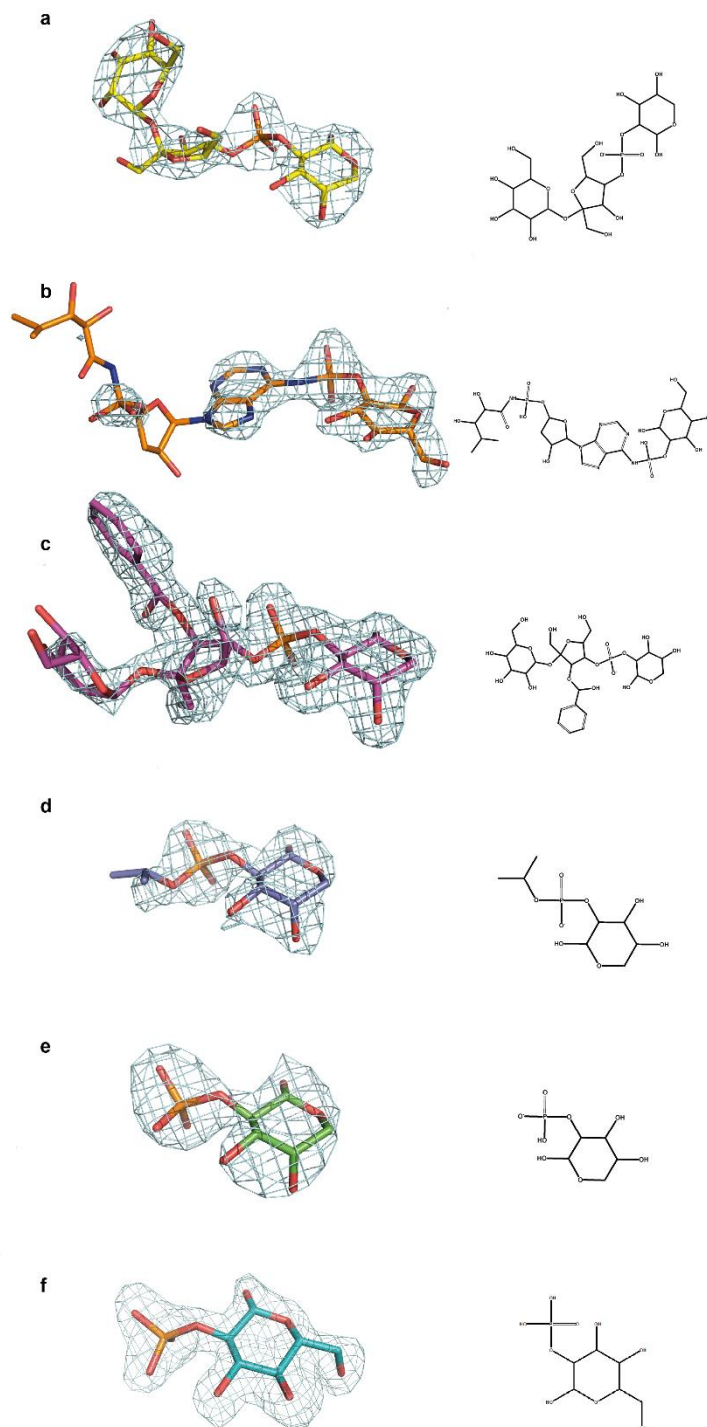
**$^{13}C$  NMR (101 MHz, Chloroform-*d*)**  $\delta$ : 170.2 (C=O), 170.0 (C=O), 169.9 (C=O), 169.4 (C=O), 132.1 (d,  $J = 7.7$  Hz,  $OCH_2-\underline{CH}=\underline{CH}_2$ ), 131.9 (d,  $J = 7.4$  Hz,  $OCH_2-\underline{CH}=\underline{CH}_2$ ), 118.6 (d,  $J = 7.5$  Hz,  $OCH_2-\underline{CH}=\underline{CH}_2$ ), 96.7 (d,  $J = 4.6$  Hz, C-1), 71.7 (C-5), 70.5 (d,  $J = 1.7$  Hz, C-3), 68.7 (d,  $J = 9.1$  Hz, C-2), 68.7 (d,  $J = 5.0$  Hz,  $\underline{OCH}_2-\underline{CH}=\underline{CH}_2$ ), 68.6 (d,  $J = 6.0$  Hz,  $\underline{OCH}_2-\underline{CH}=\underline{CH}_2$ ), 66.7 (C-4), 61.1 (C-6), 20.7 ( $CH_3$ ), 20.5 (2 $CH_3$ ), 20.5 ( $CH_3$ ).

**$^{31}P$  NMR (121.5 MHz, Chloroform-*d*)**  $\delta$ : -3.03

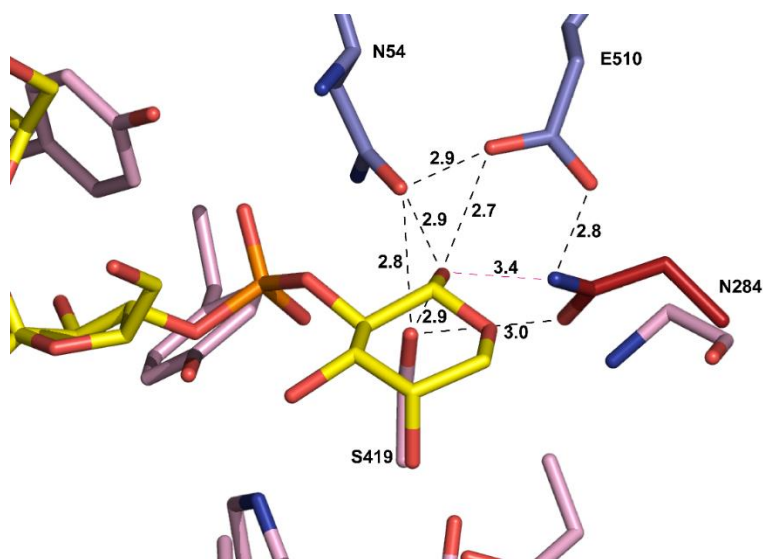
**HRMS (ESI):**  $[M + Na]^+$  calculated for  $C_{20}H_{29}NaO_{13}P$ : 531.1254; found: 531.1245.

$[\alpha]_D^{22} = +12.6$  (c 1.65,  $CHCl_3$ ).

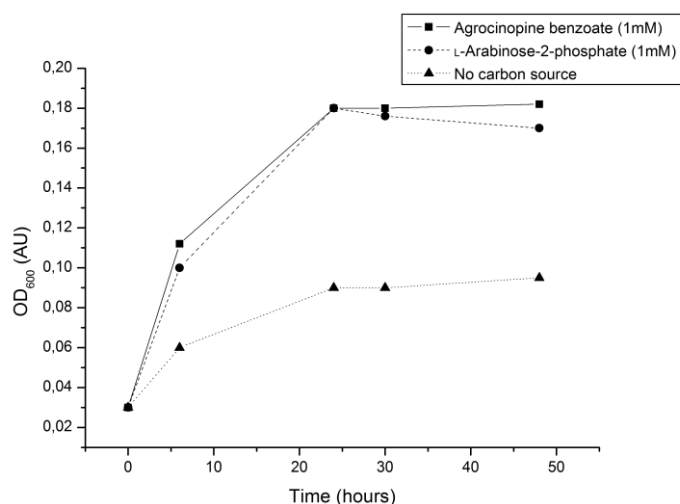
## Annex 1



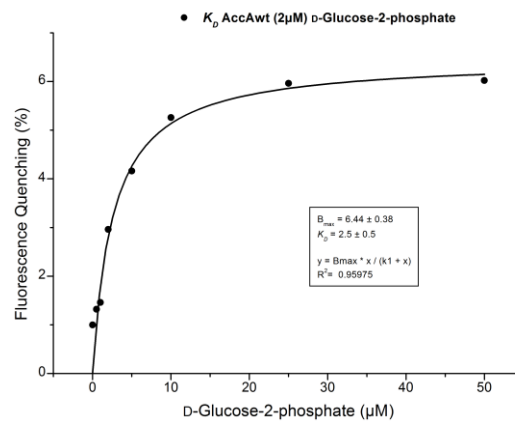
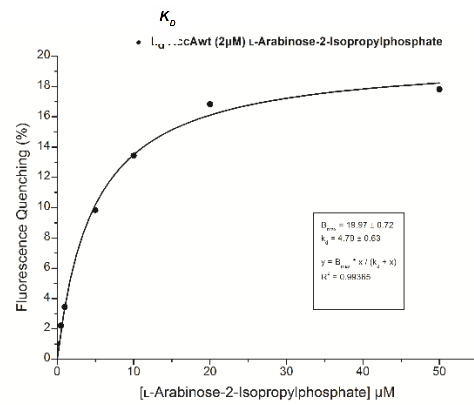
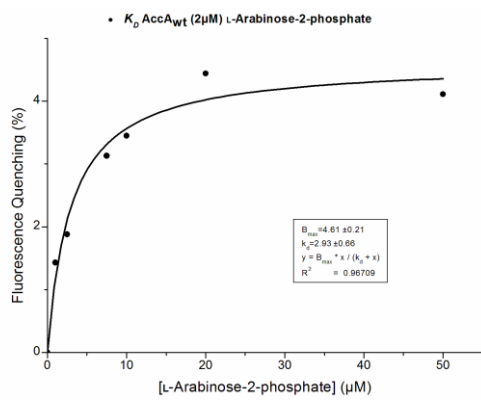
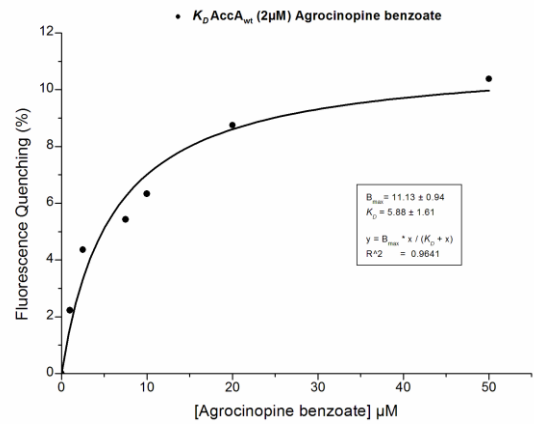
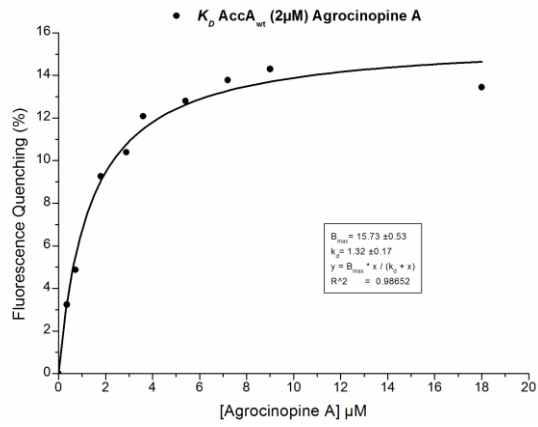
**Supplementary Figure S1.** Ligand bound to the ligand binding site of AccA in their annealing Fo-Fc omit map contoured at  $4\sigma$  (a) agrocinopine A, (b) agrocin 84, (c) agrocinopine benzoate, (d) L-arabinose-2-isopropylphosphate, (e) L-arabinose-2-phosphate, (f) D-glucose-2-phosphate.



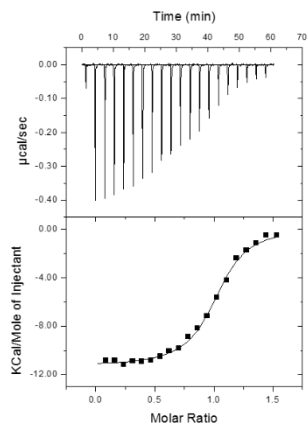
**Supplementary Figure S2.** Stick representation of AccA residues interacting with arabinose O1H group in agrocinopine A (in yellow). Residues from the lobe 1, lobe 2 and hinge region are shown in slate, pink and red respectively.



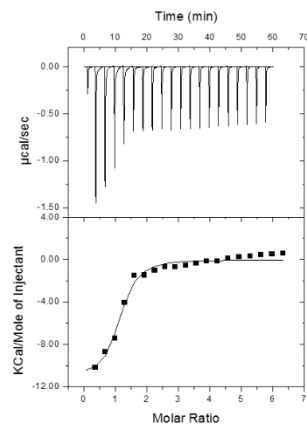
**Supplementary Figure S3.** Agrocinopine benzoate is used as a carbon source. OD monitoring (600 nm) of cultures in presence of agrocinopine benzoate (■) L-arabinose-2-phosphate (●) as a carbon source and in absence of any carbon source (▲) in AB minimum media.



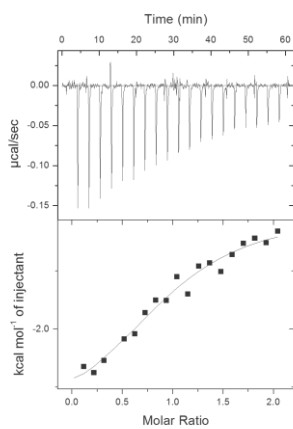
**Supplementary Figure S4.** AccA fluorescence monitoring upon titration with each ligand and fit (solid line) to a single binding model using Origin®. Measures were done in triplicates.



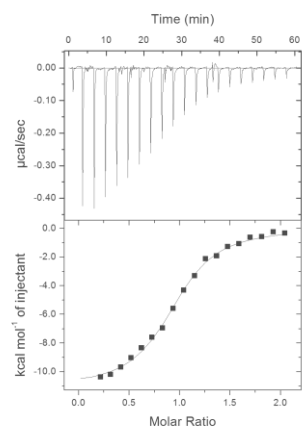
Agrociniopine A



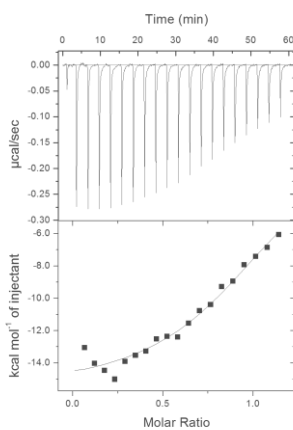
Agrocini 84



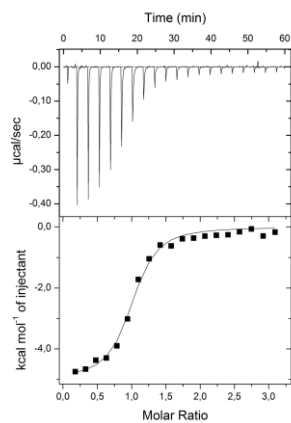
Agrociniopine benzoate



L-Arabinose-2-phosphate



L-Arabinose-2-isopropylphosphate



D-Glucose-2-phosphate

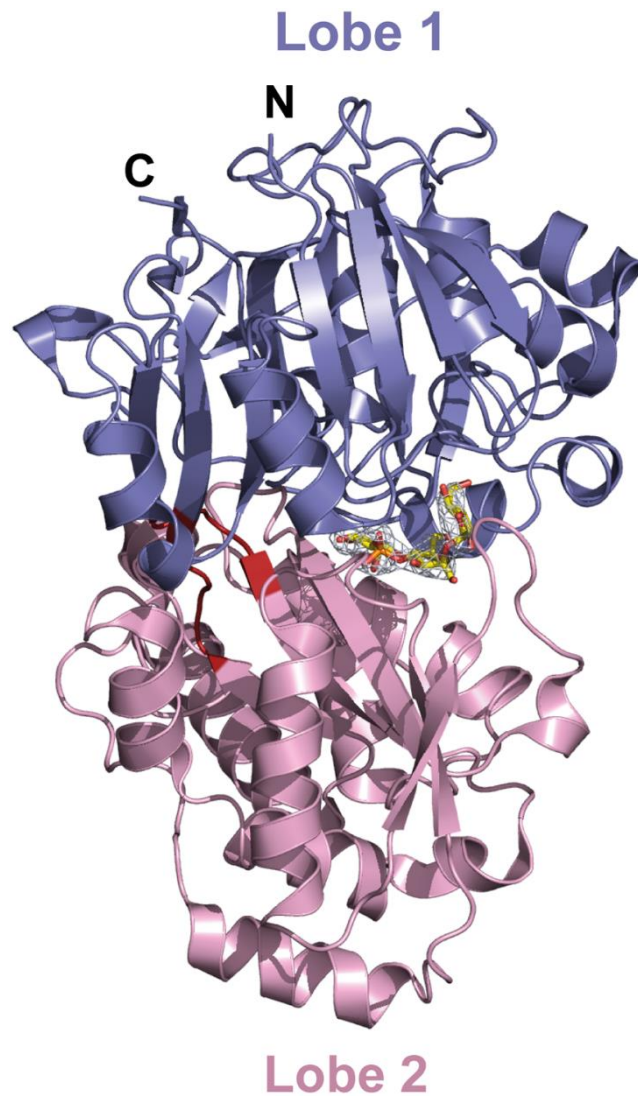
**Supplementary Figure S5.** AccA ITC measurements. The top panel show heat differences upon injection of ligand and lower panel show integrated heats of injection and the best fit (solid line) to a single binding model using Microcal Origin®.

	Agrocinopine A	Agrocin 84	Agrocinopine benzoate	L-Arabinose-2- isopropylphosphate	L- Arabinose-2- phosphate	D- Glucose- 2- phosphate
$K_D$ ( $\mu\text{M}$ )	$1.32 \pm 0.17$	ND	$5.88 \pm 1.6$	$4.79 \pm 0.63$	$2.93 \pm 0.66$	$2.50 \pm 0.5$

**Table S1.** Autofluorescence affinity results. The  $K_D$  values were obtained using Microcal Origin®, and fitting to a one binding site model using the following equation:  $f = \Delta\text{Fluorescence}_{\text{max}} * \text{abs}(x) / (K_D + \text{abs}(x))$ . ND: no signal detected.

	Agrocinopine A	Agrocin 84	Agrocinopine benzoate	L-Arabinose-2- isopropylphosphate	L- Arabinose-2- phosphate	D- glucose- 2- phosphate
$K_D$ ( $\mu\text{M}$ )	$0.3 \pm 0.03$	$1.5 \pm 0.41$	$7.5 \pm 2.2$	$2.2 \pm 0.58$	$1.33 \pm 0.12$	$1.16 \pm 0.22$
N	$1 \pm 0.006$	$0.8 \pm 0.043$	$0.99 \pm 0.06$	$1.08 \pm 0.03$	$0.95 \pm 0.01$	$0.970 \pm 0.01$
K	$2.99\text{E}6 \pm 2.9\text{E}5$	$6.83\text{E}5 \pm 1.8\text{E}5$	$1.33\text{E}5 \pm 3.61\text{E}4$	$4.72\text{E}5 \pm 1.2\text{E}5$	$7.54\text{E}5 \pm 6.5\text{E}4$	$8.61\text{E}5 \pm 1.6$
$\Delta\text{H}$ (cal/mol)	$-1.12\text{E}4 \pm 98$	$-4.37\text{E}4 \pm 3.8\text{E}3$	$-3.7\text{E}3 \pm 374$	$-1.56\text{E}4 \pm 493$	$-1.11\text{E}4 \pm 168$	$-4.5\text{E}3 \pm 123$
T $\Delta\text{S}$ (cal/mol/K)	$-2.6\text{E}3 \pm$	$-3.6\text{E}4$	$3.2\text{E}3$	$-8\text{E}3$	$-3.2\text{E}3$	$-2.9\text{E}3$
$\Delta\text{G}$ (cal/mol)	$-8.6\text{E}3$	$-7.7\text{E}3$	$-6.9\text{E}3$	$-7.6\text{E}3$	$-7.9\text{E}3$	$-7.4\text{E}3$

**Table S2.** Microcalorimetry results. The values were obtained using Microcal Origin®, and fitting to a one binding site model. No signal detected for L-arabinose and D-glucose.



**Supplementary Figure S6. Ribbon representation of AccA in complex with agrocinopine A shown in its annealing Fo-Fc omit map contoured at  $4\delta$ .**

Agrocinopine A is located in the cleft between the lobe 1 (residues 29–280 and 494–521) in slate and the lobe 2 (residues 285–489) in pink and is represented as yellow stick. The short hinge region is shown in red.



## References

- [1] K. H. Nealson, T. Platt, J. W. Hastings, *J. Bacteriol.* **1970**, *104*, 313–322.
- [2] N. A. Whitehead, A. M. L. Barnard, H. Slater, N. J. L. Simpson, G. P. C. Salmond, *FEMS Microbiol Rev* **2001**, *25*, 365–404.
- [3] J. E. González, N. D. Keshavan, *Microbiol. Mol. Biol. Rev.* **2006**, *70*, 859–875.
- [4] M. B. Miller, B. L. Bassler, *Annu. Rev. Microbiol.* **2001**, *55*, 165–199.
- [5] K. Papenfort, B. L. Bassler, *Nat. Rev. Microbiol.* **2016**, *14*, 576–588.
- [6] E. P. Greenberg, *ASM News* **1997**, *63*, 371–377.
- [7] E. S. Kempner, F. E. Hanson, *J. Bacteriol.* **1968**, *95*, 975–979.
- [8] A. Eberhard, *J. Bacteriol.* **1972**, *109*, 1101–1105.
- [9] A. Eberhard, A. L. Burlingame, C. Eberhard, G. L. Kenyon, K. H. Nealson, N. J. Oppenheimer, *Biochem.* **1981**, *20*, 2444–2449.
- [10] J. Engebrecht, K. Nealson, M. Silverman, *Cell.* **1983**, *32*, 773–781.
- [11] G. J. Lyon, T. W. Muir, *Chem. Biol.* **2003**, *10*, 1007–1021.
- [12] K. Winzer, K. R. Hardie, N. Burgess, N. Doherty, D. Kirke, M. T. G. Holden, R. Linforth, K. A. Cornell, A. J. Taylor, P. J. Hill, et al., *Microbiology* **2002**, *148*, 909–922.
- [13] B. L. Bassler, *Cell* **2002**, *109*, 421–424.
- [14] B. L. Bassler, E. P. Greenberg, A. M. Stevens, *J. Bacteriol.* **1997**, *179*, 4043–4045.
- [15] L. A. Gallagher, S. L. McKnight, M. S. Kuznetsova, E. C. Pesci, C. Manoil, *J. Bacteriol.* **2002**, *184*, 6472–6480.
- [16] R. P. Garg, W. Yindeeyoungyeon, A. Gilis, T. P. Denny, D. van der Lelie, M. A. Schell, *Mol. Microbiol.* **2000**, *38*, 359–367.
- [17] J. Loh, R. W. Carlson, W. S. York, G. Stacey, *Proc. Natl. Acad. Sci. U. S. A.* **2002**, *99*, 14446–14451.
- [18] V. Sperandio, A. G. Torres, B. Jarvis, J. P. Nataro, J. B. Kaper, *Proc. Natl. Acad. Sci. U. S. A.* **2003**, *100*, 8951–8956.
- [19] B. M. M. Ahmer, *Mol. Microbiol.* **2004**, *52*, 933–945.
- [20] S. R. Chhabra, P. Stead, N. J. Bainton, G. P. Salmond, G. S. Stewart, P. Williams, B. W. Bycroft, *J. Antibiot. (Tokyo)*. **1993**, *46*, 441–454.
- [21] N. J. Bainton, P. Stead, S. R. Chhabra, B. W. Bycroft, G. P. Salmond, G. S. Stewart, P. Williams, *Biochem. J.* **1992**, *288*, 997–1004.
- [22] N. J. Bainton, B. W. Bycroft, S. R. Chhabra, P. Stead, L. Gledhill, P. J. Hill, C. E. D. Rees, M. K. Winson, G. P. C. Salmond, G. S. A. B. Stewart, et al., *Gene* **1992**, *116*, 87–91.
- [23] M. J. Gambello, B. H. Iglewski, *J. Bacteriol.* **1991**, *173*, 3000–3009.
- [24] J. P. Pearson, K. M. Gray, L. Passador, K. D. Tucker, A. Eberhard, B. H. Iglewski, E. P. Greenberg, *Proc. Natl. Acad. Sci. U. S. A.* **1994**, *91*, 197–201.
- [25] A. Latifi, M. K. Winson, M. Foglino, B. W. Bycroft, G. S. A. B. Stewart, A. Lazdunski, P. Williams, *Mol. Microbiol.* **1995**, *17*, 333–343.
- [26] M. K. Winson, M. Camara, A. Latifi, M. Foglino, S. R. A. M. Chhabra, M. Daykin, M. Bally, V. Chapon, G. P. C. Salmond, B. W. Bycroft, et al., *Proc. Natl. Acad. Sci. U. S. A.* **1995**, *92*, 9427–9431.
- [27] M. K. Winson, S. Swift, L. Fish, J. P. Throup, F. J. Jørgensen, S. R. Chhabra, B. W. Bycroft, P. Williams, G. S. A. . Stewart, *FEMS Microbiol. Lett.* **1998**, *163*, 185–192.
- [28] B. L. Bassler, M. Wright, R. E. Showalter, M. R. Silverman, *Mol. Microbiol.* **1993**, *9*, 773–786.
- [29] J. G. Cao, E. A. Meighen, *J. Biol. Chem.* **1989**, *264*, 21670–21676.

- [30] B. L. Bassler, M. Wright, M. R. Silverman, *Mol. Microbiol.* **1994**, *13*, 273–286.
- [31] E. Swartzman, E. A. Meighen, *J. Biol. Chem.* **1993**, *268*, 16706–16716.
- [32] J. A. Freeman, B. L. Bassler, *J. Bacteriol.* **1999**, *181*, 899–906.
- [33] J. A. Freeman, B. L. Bassler, *Mol. Microbiol.* **1999**, *31*, 665–677.
- [34] W. C. Fuqua, S. C. Winans, E. P. Greenberg, *J. Bacteriol.* **1994**, *176*, 269–275.
- [35] C. Fuqua, E. P. Greenberg, *Nat. Rev. Mol. cell Biol.* **2002**, *3*, 685–695.
- [36] X. Chen, S. Schauder, N. Potier, A. Van Dorsselaer, I. Pelczer, B. L. Bassler, F. M. Hughson, *Nature* **2002**, *415*, 545–549.
- [37] V. Thiel, R. Vilchez, H. Sztajer, I. Wagner-Döbler, S. Schulz, *ChemBioChem* **2009**, *10*, 479–485.
- [38] B. L. Bassler, M. Wright, M. R. Silverman, *Mol. Microbiol.* **1994**, *13*, 273–286.
- [39] C. A. Lowery, T. J. Dickerson, K. D. Janda, *Chem. Soc. Rev.* **2008**, *37*, 1337–1346.
- [40] M. G. Surette, M. B. Miller, B. L. Bassler, *Proc. Natl. Acad. Sci. U. S. A.* **1999**, *96*, 1639–1644.
- [41] K. B. Xavier, B. L. Bassler, *Curr. Opin. Microbiol.* **2003**, *6*, 191–197.
- [42] A. Vendeville, K. Winzer, K. Heurlier, C. M. Tang, K. R. Hardie, *Nat. Rev. Microbiol.* **2005**, *3*, 383–396.
- [43] T. Zang, B. W. K. Lee, L. M. Cannon, K. A. Ritter, S. Dai, D. Ren, T. K. Wood, Z. S. Zhou, *Bioorg. Med. Chem. Lett.* **2009**, *19*, 6200–6204.
- [44] M. Li, N. Ni, H. T. Chou, C. D. Lu, P. C. Tai, B. Wang, *ChemMedChem* **2008**, *3*, 1242–1249.
- [45] T. Sams, Y. Baker, J. Hodgkinson, J. Gross, D. Spring, M. Welch, *Isr. J. Chem.* **2016**, *56*, 282–294.
- [46] E. C. Pesci, J. B. J. Milbank, J. P. Pearson, S. McKnight, A. S. Kende, E. P. Greenberg, B. H. Iglewski, *Proc. Natl. Acad. Sci. U. S. A.* **1999**, *96*, 11229–11234.
- [47] E. Déziel, F. Lépine, S. Milot, J. He, M. N. Mindrinos, R. G. Tompkins, L. G. Rahme, *Proc. Natl. Acad. Sci. U. S. A.* **2004**, *101*, 1339–1344.
- [48] F. Lépine, S. Milot, E. Déziel, J. He, L. G. Rahme, *J. Am. Soc. Mass Spectrom.* **2004**, *15*, 862–869.
- [49] Z. A. Machan, G. W. Taylor, T. L. Pitt, P. J. Cole, R. Wilson, *J. Antimicrob. Chemother.* **1992**, *30*, 615–623.
- [50] P. Ball, *J. Antimicrob. Chemother.* **2000**, *46*, 17–24.
- [51] R. Ruimy, A. Brisabois, C. Bernede, D. Skurnik, S. Barnat, G. Arlet, S. Momcilovic, S. Elbaz, F. Moury, M. A. Vibet, et al., *Environ. Microbiol.* **2010**, *12*, 608–615.
- [52] T. Defoirdt, N. Boon, P. Bossier, W. Verstraete, *Aquaculture* **2004**, *240*, 69–88.
- [53] A. M. Stevens, Y. Queneau, L. Soulère, S. Von Bodman, A. Doutheau, *Chem. Rev.* **2011**, *111*, 4–27.
- [54] A. Eberhard, C. A. Widrig, P. McBath, J. B. Schineller, *Arch. Microbiol.* **1986**, *146*, 35–40.
- [55] M. Manefield, T. B. Rasmussen, M. Henzter, J. B. Andersen, P. Steinberg, S. Kjelleberg, M. Givskov, *Microbiology* **2002**, *148*, 1119–1127.
- [56] M. Givskov, R. de Nys, M. Manefield, L. Gram, R. Maximilien, L. Eberl, S. Molin, P. D. Steinberg, S. Kjelleberg, *J. Bact.* **1996**, *178*, 6618–6622.
- [57] K. M. Smith, Y. Bu, H. Suga, *Chem. Biol.* **2003**, *10*, 81–89.
- [58] K. M. Smith, Y. Bu, H. Suga, *Chem. Biol.* **2003**, *10*, 563–571.
- [59] G. J. Jog, J. Igarashi, H. Suga, *Chem. Biol.* **2006**, *13*, 123–128.
- [60] T. Ishida, T. Ikeda, N. Takiguchi, A. Kuroda, H. Ohtake, J. Kato, *Appl. Environ. Microbiol.* **2007**, *73*, 3183–3188.
- [61] J. Estephane, J. Dauvergne, L. Soulère, S. Reverchon, Y. Queneau, A. Doutheau, *Bioorg. Med. Chem. Lett.* **2008**, *18*, 4321–4324.
- [62] M. Sabbah, F. Fontaine, L. Grand, M. Boukraa, M. L. Efrit, A. Doutheau, L. Soulère, Y. Queneau, *Bioorg. Med. Chem.* **2012**, *20*, 4727–4736.
- [63] S. Reverchon, B. Chantegrel, C. Deshayes, A. Doutheau, N. Cotte-Pattat, *Bioorg. Med. Chem. Lett.* **2002**, *12*, 1153–1157.

- [64] G. D. Geske, J. C. O'Neill, D. M. Miller, M. E. Mattmann, H. E. Blackwell, *J. Am. Chem. Soc.* **2007**, *129*, 13613–13625.
- [65] S. Castang, B. Chantegrel, C. Deshayes, R. Dolmazon, P. Gouet, R. Haser, S. Reverchon, W. Nasser, N. Hugouvieux-Cotte-Pattat, A. Doutheau, *Bioorg. Med. Chem. Lett.* **2004**, *14*, 5145–5149.
- [66] M. Frezza, S. Castang, J. Estephane, L. Soullère, C. Deshayes, B. Chantegrel, W. Nasser, Y. Queneau, S. Reverchon, A. Doutheau, *Bioorg. Med. Chem.* **2006**, *14*, 4781–4791.
- [67] M. Frezza, L. Soullère, S. Reverchon, N. Guiliani, C. Jerez, Y. Queneau, A. Doutheau, *Bioorg. Med. Chem.* **2008**, *16*, 3550–3556.
- [68] S. P. Diggle, P. Lumjiaktase, F. Dipilato, K. Winzer, M. Kunakorn, D. A. Barrett, S. R. Chhabra, M. Cámara, P. Williams, *Chem. Biol.* **2006**, *13*, 701–710.
- [69] Y. Deng, J. Wu, F. Tao, L. H. Zhang, *Chem. Rev.* **2011**, *111*, 160–179.
- [70] A. B. Flavier, S. J. Clough, M. A. Schell, T. P. Denny, *Mol. Microbiol.* **1997**, *26*, 251–259.
- [71] J. Loh, D. P. Lohar, B. Andersen, G. Stacey, *J. Bacteriol.* **2002**, *184*, 1759–1766.
- [72] V. Sperandio, A. G. Torres, B. Jarvis, J. P. Nataro, J. B. Kaper, *Proc. Natl. Acad. Sci. U. S. A.* **2003**, *100*, 8951–8956.
- [73] U. Müh, M. Schuster, R. Heim, A. Singh, E. R. Olson, E. P. Greenberg, *Antimicrob. Agents Chemother.* **2006**, *50*, 3674–3679.
- [74] M. Sabbah, L. Soullère, S. Reverchon, Y. Queneau, A. Doutheau, *Bioorg. Med. Chem.* **2011**, *19*, 4868–4875.
- [75] W. K. Goh, G. Iskander, D. S. Black, N. Kumar, *Tetrahedron Lett.* **2007**, *48*, 2287–2290.
- [76] E. A. Meyer, R. K. Castellano, F. Diederich, *Angew. Chem. Int. Ed.* **2003**, *42*, 1210–1250.
- [77] G. Brackman, M. Risseuw, S. Celen, P. Cos, L. Maes, H. J. Nelis, S. Van Calenbergh, T. Coenye, *Bioorg. Med. Chem.* **2012**, *20*, 4737–4743.
- [78] D. M. Stacy, S. T. Le Quement, C. L. Hansen, J. W. Clausen, T. Tolker-Nielsen, J. W. Brummond, M. Givskov, T. E. Nielsen, H. E. Blackwell, *Org. Biomol. Chem.* **2013**, *11*, 938–954.
- [79] M. R. Hansen, T. H. Jakobsen, C. G. Bang, A. E. Cohrt, C. L. Hansen, J. W. Clausen, S. T. Le Quement, T. Tolker-Nielsen, M. Givskov, T. E. Nielsen, *Bioorg. Med. Chem.* **2015**, *23*, 1638–1650.
- [80] R. Shchepin, D. H. M. L. P. Navarathna, R. Dumitru, S. Lippold, K. W. Nickerson, P. H. Dussault, *Bioorg. Med. Chem.* **2008**, *16*, 1842–1848.
- [81] R. Shchepin, J. M. Hornby, E. Burger, T. Niessen, P. Dussault, K. W. Nickerson, *Chem. Biol.* **2003**, *10*, 743–750.
- [82] R. J. Herr, *Bioorg. Med. Chem.* **2002**, *10*, 3379–3393.
- [83] A. Eberhard, C. A. Widrig, P. McBath, J. B. Schineller, *Arch. Microbiol.* **1986**, *146*, 35–40.
- [84] L. Passador, K. D. Tucker, K. R. Guertin, M. P. Journet, A. S. Kende, B. H. Iglewski, *J. Bacteriol.* **1996**, *178*, 5995–6000.
- [85] T. Ikeda, *J. Incl. Phenom. Macrocycl. Chem.* **2002**, *44*, 381–382.
- [86] J. C. A. Janssens, K. Metzger, R. Daniels, D. Ptacek, T. Verhoeven, L. W. Habel, J. Vanderleyden, D. E. De Vos, S. C. J. De Keersmaecker, *Appl. Environ. Microbiol.* **2007**, *73*, 535–544.
- [87] K. Riedel, M. Köthe, B. Kramer, W. Saeb, A. Gotschlich, A. Ammendola, L. Eberl, M. Ko, *Antimicrob. Agents Chemother.* **2006**, *50*, 318–323.
- [88] A. Steidle, K. Sigl, R. Schuegger, A. Ihring, M. Schmid, S. Gantner, M. Stoffels, K. Riedel, M. Givskov, A. Hartmann, et al., *Appl. Environ. Microbiol.* **2001**, *67*, 5761–5770.
- [89] J. A. Olsen, R. Severinsen, T. B. Rasmussen, M. Hentzer, M. Givskov, J. Nielsen, *Bioorg. Med. Chem. Lett.* **2002**, *12*, 325–328.
- [90] M. O. Taha, A. G. Al-Bakri, W. A. Zalloum, *Bioorg. Med. Chem. Lett.* **2006**, *16*, 5902–5906.
- [91] T. Persson, T. H. Hansen, T. B. Rasmussen, M. E. Skinderso, M. Givskov, J. Nielsen, *Org. Biomol. Chem.* **2005**, *3*, 253–262.

- [92] H. B. Liu, J. H. Lee, J. S. Kim, S. Park, *Biotechnol. Bioeng.* **2010**, *106*, 119–126.
- [93] T. Benneche, G. Herstad, M. Rosenberg, S. Assev, A. A. Scheie, *RSC Adv.* **2011**, *1*, 323–332.
- [94] T. Benneche, E. J. Chamgordani, I. Reimer, *Tetrahedron Lett.* **2012**, *53*, 6982–6983.
- [95] A. Vermote, G. Brackman, M. D. P. Risseeuw, B. Vanhoutte, P. Cos, K. Van Hecke, K. Breyne, E. Meyer, T. Coenye, S. Van Calenbergh, *Angew. Chem. Int. Ed.* **2016**, *55*, 6551–6555.
- [96] M. F. Semmelhack, S. R. Campagna, C. Hwa, M. J. Federle, B. L. Bassler, *Org. Lett.* **2004**, *6*, 2635–2637.
- [97] K. M. McKenzie, M. M. Meijler, C. Lowery, G. E. Boldt, K. D. Janda, *Chem. Commun.* **2005**, *0*, 4863–4865.
- [98] C. A. Lowery, K. M. McKenzie, L. Qi, M. M. Meijler, K. D. Janda, *Bioorg. Med. Chem. Lett.* **2005**, *15*, 2395–2398.
- [99] J. Boström, A. Hogner, A. Llinàs, E. Wellner, A. T. Plowright, *J. Med. Chem.* **2012**, *55*, 1817–1830.
- [100] A. Pace, P. Pierro, *Org. Biomol. Chem.* **2009**, *7*, 4337–4348.
- [101] R. Aharoni, M. Bronstheyn, A. Jabbour, B. Zaks, M. Srebnik, D. Steinberg, *Bioorg. Med. Chem.* **2008**, *16*, 1596–1604.
- [102] L. Yang, M. T. Rybtke, T. H. Jakobsen, M. Hentzer, T. Bjarnsholt, M. Givskov, T. Tolker-Nielsen, *Antimicrob. Agents Chemother.* **2009**, *53*, 2432–2443.
- [103] M. Dunkel, M. Fullbeck, S. Neumann, R. Preissner, *Nucleic Acids Res.* **2006**, *34*, D678–D683.
- [104] A. Goede, M. Dunkel, N. Mester, C. Frommel, R. Preissner, *Bioinformatics* **2005**, *21*, 1751–1753.
- [105] R. Thomsen, M. H. Christensen, *J. Med. Chem.* **2006**, *49*, 3315–3321.
- [106] T. B. Rasmussen, T. Bjarnsholt, M. E. Skindersoe, M. Hentzer, P. Kristoffersen, M. Kôte, J. Nielsen, L. Eberl, M. Givskov, *J. Bacteriol.* **2005**, *187*, 1799–814.
- [107] G. Brackman, A. A. A. Al Quntar, C. D. Enk, I. Karalic, H. J. Nelis, S. Van Calenbergh, M. Srebnik, T. Coenye, *Bioorg. Med. Chem.* **2013**, *21*, 660–667.
- [108] G. Brackman, K. Forier, A. A. A. Al Quntar, E. De Canck, C. D. Enk, M. Srebnik, K. Braeckmans, T. Coenye, *J. Appl. Microbiol.* **2014**, *116*, 492–501.
- [109] D. K. Park, K. E. Lee, C. H. Baek, I. H. Kim, J. H. Kwon, W. K. Lee, K. H. Lee, B. S. Kim, S. H. Choi, K. S. Kim, *J. Bacteriol.* **2006**, *188*, 2214–2221.
- [110] G. Degrassi, C. Aguilar, M. Bosco, S. Zahariev, S. Pongor, V. Venturi, *Curr. Microbiol.* **2002**, *45*, 250–254.
- [111] M. T. G. Holden, S. R. Chhabra, R. De Nys, P. Stead, N. J. Bainton, P. J. Hill, M. Manefield, N. Kumar, M. Labatte, D. England, et al., *Mol. Microbiol.* **1999**, *33*, 1254–1266.
- [112] J. Campbell, Q. Lin, G. D. Geske, H. E. Blackwell, *ACS Chem. Biol.* **2009**, *4*, 1051–1059.
- [113] J. Campbell, H. E. Blackwell, *J. Comb. Chem.* **2009**, *11*, 1094–1099.
- [114] V. C. Scoffone, L. R. Chiarelli, V. Makarov, G. Brackman, A. Israyilova, A. Azzalin, F. Forneris, O. Riabova, S. Savina, T. Coenye, et al., *Sci. Rep.* **2016**, *6*, 32487.
- [115] K. Tateda, R. Comte, J. Pechere, K. Yamaguchi, C. Van Delden, *Antimicrob. Agents Chemother.* **2001**, *45*, 1930–1933.
- [116] K. Tateda, T. J. Standiford, K. Yamaguchi, *Antibiotics as Anti-Inflammatory Immunomodulatory Agents*, **2005**, pp. 5–21.
- [117] M. Hentzer, M. Givskov, *J. Clin. Invest.* **2003**, *112*, 1300–1307.
- [118] M. E. Skindersoe, M. Alhede, R. Phipps, L. Yang, P. O. Jensen, T. B. Rasmussen, T. Bjarnsholt, T. Tolker-Nielsen, N. Høiby, M. Givskov, *Antimicrob. Agents Chemother.* **2008**, *52*, 3648–3663.
- [119] C. Lu, B. Kirsch, C. Zimmer, J. C. de Jong, C. Henn, C. K. Maurer, M. Müsken, S. Häussler, A. Steinbach, R. W. Hartmann, *Chem. Biol.* **2012**, *19*, 381–390.
- [120] C. Cugini, M. W. Calfee, J. M. Farrow, D. K. Morales, E. C. Pesci, D. A. Hogan, *Mol. Microbiol.* **2007**, *65*, 896–906.
- [121] W. R. J. D. Galloway, J. T. Hodgkinson, S. D. Bowden, M. Welch, D. R. Spring, *Chem. Rev.* **2011**, *111*, 28–67.
- [122] S. P. Diggle, S. Matthijs, V. J. Wright, M. P. Fletcher, S. R. Chhabra, I. L. Lamont, X. Kong, R. C. Hider, P. Cornelis, M. Cámara, et al., *Chem. Biol.* **2007**, *14*, 87–96.

- [123] J. W. Schertzer, S. A. Brown, M. Whiteley, *Mol. Microbiol.* **2010**, *77*, 1527–1538.
- [124] C. Lu, C. K. Maurer, B. Kirsch, A. Steinbach, R. W. Hartmann, *Angew. Chem. Int. Ed.* **2014**, *53*, 1109–1112.
- [125] M. Hentzer, H. Wu, J. B. Andersen, K. Riedel, T. B. Rasmussen, N. Bagge, N. Kumar, M. A. Schembri, Z. Song, P. Kristoffersen, et al., *EMBO J.* **2003**, *22*, 3803–3815.
- [126] H. P. Steenackers, J. Levin, J. C. Janssens, A. De Weerd, J. Balzarini, J. Vanderleyden, D. E. De Vos, S. C. De Keersmaecker, *Bioorg. Med. Chem.* **2010**, *18*, 5224–5233.
- [127] Y. Han, S. Hou, K. A. Simon, D. Ren, Y. Y. Luk, *Bioorg. Med. Chem. Lett.* **2008**, *18*, 1006–1010.
- [128] M. Hentzer, K. Riedel, T. B. Rasmussen, A. Heydorn, J. B. Andersen, M. R. Parsek, S. A. Rice, L. Eberl, S. Molin, N. Høiby, et al., *Microbiology* **2002**, *148*, 87–102.
- [129] M. Manefield, T. B. Rasmussen, M. Hentzer, J. B. Andersen, P. Steinberg, S. Kjelleberg, M. Givskov, *Microbiology* **2002**, *148*, 1119–1127.
- [130] N. N. Biswas, S. K. Kutty, G. M. Iskander, M. Mielczarek, M. M. Bhadbhade, C. R. Gardner, D. S. Black, N. Kumar, *Tetrahedron* **2016**, *72*, 539–546.
- [131] T. T. Tung, T. H. Jakobsen, T. T. Dao, A. T. Fuglsang, M. Givskov, S. B. Christensen, J. Nielsen, *Eur. J. Med. Chem.* **2017**, *126*, 1011–1020.
- [132] E. C. Meng, D. A. Gschwend, J. M. Blaney, I. D. Kuntz, *Proteins Struct. Funct. Genet.* **1993**, *17*, 266–278.
- [133] G. Brackman, T. Coenye, *Curr. Pharm. Des.* **2015**, *21*, 5–11.
- [134] N. R. Emmadi, K. Atmakur, C. Bingi, N. R. Godumagadda, G. K. Chityal, J. B. Nanubolu, *Bioorg. Med. Chem. Lett.* **2014**, *24*, 485–489.
- [135] G. D. Geske, J. C. O'Neill, H. E. Blackwell, *Chem. Soc. Rev.* **2008**, *37*, 1432–1447.
- [136] N. Ni, M. Li, J. Wang, B. Wang, *Med. Res. Rev.* **2009**, *29*, 65–124.
- [137] F. G. Glansdorp, G. L. Thomas, J. K. Lee, J. M. Dutton, G. P. C. Salmond, M. Welch, D. R. Spring, *Org. Biomol. Chem.* **2004**, *2*, 3329–3336.
- [138] S. R. Chhabra, C. Harty, D. S. W. Hooi, M. Daykin, P. Williams, G. Telford, D. I. Pritchard, B. W. Bycroft, *J. Med. Chem.* **2003**, *46*, 97–104.
- [139] A. L. Schaefer, D. L. Val, B. L. Hanzelka, J. E. Cronan, E. P. Greenberg, *Proc. Natl. Acad. Sci. U. S. A.* **1996**, *93*, 9505–9509.
- [140] K. M. Pappas, C. L. Weingart, S. C. Winans, *Mol. Microbiol.* **2004**, *53*, 755–769.
- [141] T. Persson, T. H. Hansen, T. B. Rasmussen, M. E. Skindersø, M. Givskov, J. Nielsen, *Org. Biomol. Chem.* **2005**, *38*, 253–262.
- [142] J. T. Hodgkinson, W. R. J. D. Galloway, M. Casoli, H. Keane, X. Su, G. P. C. Salmond, M. Welch, D. R. Spring, *Tetrahedron Lett.* **2011**, *52*, 3291–3294.
- [143] F. Xu, J. D. Armstrong, G. X. Zhou, B. Simmons, D. Hughes, Z. Ge, E. J. J. Grabowski, *J. Am. Chem. Soc.* **2004**, *126*, 13002–13009.
- [144] M. K. Winson, S. Swift, L. Fish, J. P. Throup, F. Jørgensen, S. R. Chhabra, B. W. Bycroft, P. Williams, G. S. A. B. Stewart, *FEMS Microbiol. Lett.* **1998**, *163*, 185–192.
- [145] S. Castang, B. Chantegrel, C. Deshayes, R. Dolmazon, P. Gouet, R. Haser, S. Reverchon, W. Nasser, N. Hugouvieux-Cotte-Pattat, A. Doutheau, *Bioorg. Med. Chem. Lett.* **2004**, *14*, 5145–5149.
- [146] M. Frezza, S. Castang, J. Estephane, L. Soulère, C. Deshayes, B. Chantegrel, W. Nasser, Y. Queneau, S. Reverchon, A. Doutheau, *Bioorg. Med. Chem.* **2006**, *14*, 4781–4791.
- [147] R. J. Spandl, R. L. Nicholson, D. M. Marsden, J. T. Hodgkinson, X. Su, G. L. Thomas, G. P. C. Salmond, M. Welch, D. R. Spring, *Synlett* **2008**, 2122–2126.
- [148] (a) C. Fuqua, E. P. Greenberg, *Curr. Opin. Microbiol.* **1998**, *1*, 183–189. (b) J. D. Moore, F. M. Rossi, M. A. Welsh, K. E. Nyffeler, H. E. Blackwell, *J. Am. Chem. Soc.* **2015**, *137*, 14626–14639.

- [149] Y. S. Hwang, J. Chmielewski, *J. Med. Chem.* **2005**, *48*, 2239–2242.
- [150] T. Birnkammer, A. Spickenreither, I. Brunskole, M. Lopuch, N. Kagermeier, G. Bernhardt, S. Dove, R. Seifert, S. Elz, A. Buschauer, *J. Med. Chem.* **2012**, *55*, 1147–1160.
- [151] N. S. Curvey, S. E. Luderer, J. K. Walker, G. W. Gokel, *Synth.* **2014**, *46*, 2771–2779.
- [152] X. X. Zhang, C. A. H. Prata, J. A. Berlin, T. J. McIntosh, P. Barthelemy, M. W. Grinstaff, *Bioconjug. Chem.* **2011**, *22*, 690–699.
- [153] M. Jackson, Q. Au, *US 2011/0081297 A1*, **2009**.
- [154] C. J. Chen, B. A. Song, S. Yang, G. F. Xu, P. S. Bhadury, L. H. Jin, D. Y. Hu, Q. Z. Li, F. Liu, W. Xue, et al., *Bioorg. Med. Chem.* **2007**, *15*, 3981–3989.
- [155] M. Di Braccio, G. Grossi, G. Roma, D. Piras, F. Mattioli, M. Gosmar, *Eur. J. Med. Chem.* **2008**, *43*, 584–594.
- [156] K. J. Hale, L. Lazarides, J. Cai, *Org. Lett.* **2001**, *3*, 2927–2930.
- [157] Z. Jakopin, M. Dolenc, *Curr. Org. Chem.* **2008**, *12*, 850–898.
- [158] G. Nagendra, R. S. Lamani, N. Narendra, V. V. Sureshbabu, *Tetrahedron Lett.* **2010**, *51*, 6338–6341.
- [159] A. R. Gangloff, J. Litvak, E. J. Shelton, D. Sperandio, V. R. Wang, K. D. Rice, *Tetrahedron* **2001**, *42*, 1441–1443.
- [160] R. M. Srivastava, I. M. Brinn, J. O. MacHuca-Herrera, H. B. Faria, G. B. Carpenter, D. Andrade, C. G. Venkatesh, L. P. Lécia, *J. Mol. Struct.* **1997**, *406*, 159–167.
- [161] L. Soulère, M. Sabbah, F. Fontaine, Y. Queneau, A. Doutheau, *Bioorg. Med. Chem. Lett.* **2010**, *20*, 4355–4358.
- [162] D. Katayev, V. Matousek, R. Koller, A. Togni, *Org. Lett.* **2015**, *17*, 5898–5901.
- [163] A. K. Strunz, A. J. M. Zweemer, C. Weiss, D. Schepmann, A. Junker, L. H. Heitman, M. Koch, B. Wunsch, *Bioorg. Med. Chem.* **2015**, *23*, 4034–4049.
- [164] B. LaSarre, M. J. Federle, *Microbiol. Mol. Biol. Rev.* **2013**, *77*, 73–111.
- [165] K. Reuter, A. Steinbach, V. Helms, *Perspect. Medicin. Chem.* **2016**, *8*, 1–15.
- [166] S. B. Tay, W. S. Yew, *Int. J. Mol. Sci.* **2013**, *14*, 16570–16599.
- [167] Y. Wang, S. Ma, *Curr. Med. Chem.* **2013**, *21*, 296–311.
- [168] V. Dekimpe, E. Déziel, *Microbiology* **2009**, *155*, 712–723.
- [169] S. L. Drees, S. Fetzner, *Chem Biol.* **2015**, *22*, 611–618.
- [170] I. Kviatkovski, L. Chernin, T. Yarnitzky, I. Frumin, N. Sobel, Y. Helman, *Chem. Commun.* **2015**, *51*, 3258–3261.
- [171] M. C. O'Reilly, H. E. Blackwell, *ACS Infect. Dis.* **2016**, *2*, 32–38.
- [172] U. Müh, B. J. Hare, B. a Duerkop, M. Schuster, B. L. Hanzelka, R. Heim, E. R. Olson, E. P. Greenberg, *Proc. Natl. Acad. Sci. U. S. A.* **2006**, *103*, 16948–16952.
- [173] G. M. Morris, D. S. Goodsell, R. S. Halliday, R. Huey, W. E. Hart, R. K. Belew, A. J. Olson, *J. Comput. Chem.* **1998**, *19*, 1639–1662.
- [174] S. Thompson, M.A.ArgusLaB 4.0.1, *WA planetaria Softw. LLC* **2004**.
- [175] L. Soulère, M. Frezza, Y. Queneau, A. Doutheau, *J. Mol. Graph. Model.* **2007**, *26*, 581–590.
- [176] S. Darvesh, R. S. McDonald, K. V. Darvesh, D. Mataija, S. Mothana, H. Cook, K. M. Carneiro, N. Richard, R. Walsh, E. Martin, *Bioorg. Med. Chem.* **2006**, *14*, 4586–4599.
- [177] C. E. McInnis, H. E. Blackwell, *Bioorg. Med. Chem.* **2011**, *19*, 4812–4819.
- [178] J. T. Hodgkinson, W. R. J. D. Galloway, M. Wright, I. K. Mati, R. L. Nicholson, M. Welch, D. R. Spring, *Org. Biomol. Chem.* **2012**, *10*, 6032–6044.
- [179] C. Fuqua, S. C. Winans, E. P. Greenberg, *Annu. Rev. Microbiol.* **1996**, *50*, 727–751.
- [180] W. C. Fuqua, S. C. Winans, *J. Bacteriol.* **1994**, *176*, 2796–2806.
- [181] E. K. Shiner, D. Terentyev, A. Bryan, S. Sennoune, R. Martinez-zaguilan, G. Li, S. Gyorke, S. C. Williams, K. P. Rumbaugh, *Cell. Microbiol.* **2006**, *8*, 1601–1610.
- [182] L. Zhang, P. J. Murphy, A. Kerr, M. E. Tate, *Nature* **1993**, *362*, 446–448.

- [183] K. R. Piper, S. Beck von Bodman, S. K. Farrand, *Nature* **1993**, 362, 448–450.
- [184] J. E. Peter J. ChristieGordon, *Microbiol Spectr.* **2015**, 2, 1–29.
- [185] S. B. Gelvin, *Microbiol. Mol. Biol. Rev.* **2003**, 67, 16–37.
- [186] A. Brenic, S. C. Winans, *Microbiol. Mol. Biol. Rev.* **2005**, 69, 155–194.
- [187] C. A. McCullen, A. N. Binns, *Annu. Rev. Cell Dev. Biol.* **2006**, 22, 101–127.
- [188] Z. C. Yuan, M. Williams, *Plant Cell* **2012**, 12, 1–12.
- [189] A. Pitzschke, *Front. Plant Sci.* **2013**, 4, 1–12.
- [190] J. Nam, *Plant Cell* **1997**, 9, 317–333.
- [191] I. Hwang, P. L. Li, L. Zhang, K. R. Piper, D. M. Cook, M. E. Tate, S. K. Farrand, *Proc. Natl. Acad. Sci. U. S. A.* **1994**, 91, 4639–4643.
- [192] I. Hwang, D. M. Cook, S. K. Farrand, *J. Bacteriol.* **1995**, 177, 449–458.
- [193] C. Fuqua, M. Burbea, S. C. Winans, *J. Bacteriol.* **1995**, 177, 1367–1373.
- [194] P. L. Li, S. K. Farrand, *J. Bacteriol.* **2000**, 182, 179–188.
- [195] S. E. Stachel, E. Messens, M. Van Montagu, P. Zambryski, *Nature* **1985**, 318, 624–629.
- [196] D. Parke, L. N. Ornston, E. W. Nester, *J. Bacteriol.* **1987**, 169, 5336–5338.
- [197] L. S. Melchers, A. J. Regensburg-Tuink, R. A. Schilperoort, P. J. Hooykaas, *Mol Microbiol* **1989**, 3, 969–977.
- [198] R. A. Dixon, N. L. Paiva, *Plant Cell* **1995**, 7, 1085–1097.
- [199] S. C. Winans, P. R. Ebert, S. E. Stachel, M. P. Gordon, E. W. Nester, *Proc. Natl. Acad. Sci. U. S. A.* **1986**, 83, 8278–8282.
- [200] S. C. Winans, *J. Bacteriol.* **1990**, 172, 2433–2438.
- [201] C. H. Shaw, A. M. Ashby, A. Brown, C. Royal, G. J. Loake, *Mol Microbiol* **1988**, 2, 413–417.
- [202] B. Leroux, M. F. Yanofsky, S. C. Winans, J. E. Ward, S. F. Ziegler, E. W. Nester, *EMBO J.* **1987**, 6, 849–856.
- [203] N. Balasundram, K. Sundram, S. Samman, *Food Chem.* **2006**, 99, 191–203.
- [204] H. P. Bais, B. Prithiviraj, A. K. Jha, F. M. Ausubel, J. M. Vivanco, *Nature* **2005**, 434, 217–221.
- [205] D. A. Phillips, T. C. Fox, M. D. King, T. V. Bhuvanewari, L. R. Teuber, *Plant Physiology* **2004**, 136, 2887–2894.
- [206] S. C. Winans, *Microbiol. Rev.* **1992**, 56, 12–31.
- [207] Z. C. Yuan, P. Liu, P. Saenkham, K. Kerr, E. W. Nester, *J. Bacteriol.* **2008**, 190, 494–507.
- [208] G. A. Cangelosi, R. G. Ankenbauer, E. W. Nester, *Proc. Natl. Acad. Sci. U. S. A.* **1990**, 87, 6708–6712.
- [209] X. Hu, J. Zhao, W. F. DeGrado, A. N. Binns, *Proc. Natl. Acad. Sci. U. S. A.* **2013**, 110, 678–683.
- [210] D. Veselov, M. Langhans, W. Hartung, R. Aloni, I. Feussner, C. Götz, S. Veselova, S. Schlomski, C. Dickler, K. Bächmann, et al., *Planta* **2003**, 216, 512–522.
- [211] Z.-C. Yuan, M. P. Edlind, P. Liu, P. Saenkham, L. M. Banta, A. A. Wise, E. Ronzone, A. N. Binns, K. Kerr, E. W. Nester, *Proc. Natl. Acad. Sci. U. S. A.* **2007**, 104, 11790–11795.
- [212] M. Zottini, A. Costa, R. De Michele, M. Ruzzene, F. Carimi, F. Lo Schiavo, *J. Exp. Bot.* **2007**, 58, 1397–1405.
- [213] M. Sanitha, S. Radha, A. A. Fatima, S. G. Devi, M. Ramya, *Polish J. Microbiol.* **2014**, 63, 387–392.
- [214] K. R. Piper, S. Beck Von Bodman, I. Hwang, S. K. Farrand, *Mol. Microbiol.* **1999**, 32, 1077–1089.
- [215] N. C. L. Hess, D. J. Carlson, J. D. Inder, E. Jesulola, J. R. Mcfarlane, N. A. Smart, *Physiol. Res.* **2016**, 65, 461–468.
- [216] M. A. Savka, S. K. Farrand, *Plant Physiol.* **1992**, 98, 784–789.
- [217] H. Kim, S. K. Farrand, *J. Bacteriol.* **1997**, 179, 7559–7572.
- [218] S. Beck von Bodman, G. T. Hayman, S. K. Farrand, *Proc. Natl. Acad. Sci. U. S. A.* **1992**, 89, 643–647.
- [219] S. B. Hong, Y. Dessaux, W. S. Chilton, S. K. Farrand, *J. Bacteriol.* **1993**, 175, 401–410.
- [220] C. S. Nautiyal, P. Dion, *Appl. Environ. Microbiol.* **1990**, 56, 2576–2579.
- [221] I. Hwang, A. J. Smyth, Z. Q. Luo, S. K. Farrand, *Mol. Microbiol.* **1999**, 34, 282–294.
- [222] J. Lang, D. Faure, *Front. Plant Sci.* **2014**, 5, 1–13.

- [223] A. Kerr, P. Manigault, J. Tempé, *Nature* **1977**, *265*, 560–561.
- [224] A. Petit, T. Tempé, A. Kerr, M. Holsters, M. van Montagu, J. Schell, *Nature* **1978**, *271*, 570–572.
- [225] J. G. Ellis, A. Kerr, A. Petit, J. Tempe, *MGG Mol. Gen. Genet.* **1982**, *186*, 269–274.
- [226] A. Kerr, *Plant Dis.* **1980**, *64*, 24–30.
- [227] P. J. Murphy, W. P. Roberts, *J. Gen. Microbiol.* **1979**, *114*, 207–213.
- [228] A. TATE, M.E. Murphy, P. J. Kerr, *Nature* **1979**, *280*, 697–699.
- [229] W. P. Roberts, M. E. Tate, A. Kerr, *Nature* **1977**, *265*, 379–81.
- [230] R. J. Thompson, R. H. Hamilton, C. F. Pootjes, *Antimicrob. Agents Chemother.* **1979**, *16*, 293–296.
- [231] A. El Sahili, S. Z. Li, J. Lang, C. Virus, S. Planamente, M. Ahmar, B. G. Guimaraes, M. Aumont-Nicaise, A. Vigouroux, L. Soullère, et al., *PLoS Pathog.* **2015**, *11*, 1–24.
- [232] H. Bouzar, N. Daouzli, Z. Krimi, A. Alim, E. Khemici, *Agronomie* **1991**, *11*, 901–908.
- [233] J. G. Ellis, P. J. Murphy, *MGG Mol. Gen. Genet.* **1981**, *181*, 36–43.
- [234] G. T. Hayman, S. K. Farrand, *Mol. Genet. Genomics* **1990**, *223*, 465–473.
- [235] L. Unger, S. F. Ziegler, G. A. Huffman, V. C. Knauf, R. Peet, L. W. Moore, M. P. Gordon, E. W. Nester, *J. Bacteriol.* **1985**, *164*, 723–730.
- [236] P. H. Herman P. Spaink, Adam Kondorosi, *The Rhizobiaceae Molecular Biology of Model Plant-Associated Bacteria*, **1998**, *27*, 183-186.
- [237] M. H. Ryders, M. E. Tateq, P. Jonesn, *J. Biol. Chem.* **1984**, *259*, 9704–9710.
- [238] M. Franzkowiak, J. Thiem, *Liebigs Ann. der Chemie* **1987**, *1987*, 1065–1071.
- [239] M. Lindberg, T. Norberg, *J. Carbohydr. Chem.* **1988**, *7*, 749–755.
- [240] R. Khan, *Carbohydr. Res.* **1972**, *22*, 441–445.
- [241] A. C. Ballard, John M, Hough Leslie, Richardson, *Carbohydr. Res.* **1974**, *34*, 184–188.
- [242] A. C. Ballard, J M, Hough L, Richardson, *Carbohydr. Res.* **1972**, *22*, 152–153.
- [243] J. P. Barrette, *J. Am. Chem. Soc* **1958**, *17*, 1953–1956.
- [244] D. M. Clode, W. A. Laurie, D. McHale, J. B. Sheridan, *Carbohydr. Res.* **1985**, *139*, 161–183.
- [245] H. L. Riaz Khan, Michael R. Jenner, *Carbohydr. Res.* **1978**, *65*, 99–108.
- [246] J. B. S. David M. Clode, William A. Laurie, David Mchale, *Carbohydr. Res.* **1985**, *39*, 147–160.
- [247] K. S. M. Riaz Khan, *Carbohydr. Res.* **1975**, *43*, 247–253.
- [248] A. Poschalko, T. Rohr, H. Gruber, A. Bianco, G. Guichard, J. P. Briand, V. Weber, D. Falkenhagen, *J. Am. Chem. Soc.* **2003**, *125*, 13415–13426.
- [249] E. Manzo, G. Barone, M. Parrilli, *Synlett.* **2000**, *2000*, 887–889.
- [250] T. Rolle, R. W. Hoffmann, *Helv. Chim. Acta* **2004**, *87*, 1214–1227.
- [251] L. Y. Wu, M. O. Anderson, Y. Toriyabe, J. Maung, T. Y. Campbell, C. Tajon, M. Kazak, J. Moser, C. E. Berkman, *Bioorg. Med. Chem.* **2007**, *15*, 7434–7443.
- [252] M. T. P. L.-E. Isidore Izquierdo Cubero, *J. Carbohydr. Chem.* **1986**, *5*, 299–311.
- [253] H. H. Per J. Gregg, *Carbohydr. Res.* **1979**, *28*, 367–376.
- [254] D. R. B. Hans-Peter Wessel, *Carbohydr. Res.* **1983**, *124*, 301–311.
- [255] L. A. Mina A. Nashed, *Carbohydr. Res.* **1977**, *56*, 325–336.
- [256] C. P. B. and R. W. J. Stawinski, T. Hozumi, S. A. Narang, *Nucleic Acids Res.* **1977**, *4*, 353–372.
- [257] J. C. Catlin, F. Cramer, *J. Org. Chem.* **1973**, *38*, 245–250.
- [258] N. Katagiri, K. Itakura, S. A. Narang, *J. Am. Chem. Soc.* **1975**, *97*, 7332–7337.
- [259] M. U. S.S. Jones, B. Rayner, C.B. Reese, A. Ubasawa, *Tetrahedron* **1980**, *36*, 3075–3085.
- [260] P. J. Garegg, T. Regberg, J. Stawinski, *Nucleosides Nucleotides* **1987**, *6*, 655–662.
- [261] T. H. Mitsuo Sekine, Sin-ichiro Narui, *Tetrahedron Lett.* **1988**, *29*, 1037–1040.

- [262] M. Lindberg, S. Oscarson, *J. Carbohydr. Chem.* **1993**, *12*, 1139–1147.
- [263] J. Stawinski, M. Thelin, *J. Chem. Soc., Perkin Trans. 2.* **1990**, 849–853.
- [264] A. T. AM Michelson, *J. Chem. Soc.* **1955**, 2632–2638.
- [265] S. L. Beaucage, M. H. Caruthers, *Tetrahedron Lett.* **1981**, *22*, 1859–1862.
- [266] S. P. Adams, K. S. Kavka, E. J. Wykes, et al., *J. Am. Chem. Soc.* **1983**, *105*, 661–663.
- [267] J. H. van B. C. M. Dreef-Tromp, A. W. M. Lefeber, G. A. van der Marel, *Synthesis* **1992**, 1269–1272.
- [268] M. Lindberg, T. Norberg, S. Oscarson, *J. Carbohydr. Chem.* **1992**, *11*, 243–253.
- [269] A. E. Savage, *The Isolation and Structural Elucidation of Agrociniopine C*, The university of Adelaide, **1983**.
- [270] H. J. Lemieux R U, *Methods Carbohydr. Chem.* **1963**, *2*, 221.
- [271] R. U. L. A. A. R. MORGAN, *Can. J. Chem.* **1965**, *43*, 2199–2204.
- [272] P. J. Garegg, I. Kvarnstrom, *Acta Chem. Scand. Ser. B* **1977**, *B31*, 509–513.
- [273] K. Suzuki, H. Nonaka, M. Yamaura, *J. Carbohydr. Chem.* **2004**, *23*, 253–259.
- [274] B. Helferich, J. Zirner, *Chem. Ber.* **1962**, *95*, 2604–2611.
- [275] T. and N. E. V. Otake, *Bull. Chem. Soc. Jpn.* **1970**, *43*, 3199–3205.
- [276] H. L. Riaz Khan, Michael R. Jenner, *Carbohydr. Res.* **1980**, *78*, 173–183.
- [277] R. Khan, H. Lindseth, *Carbohydr. Res.* **1979**, *71*, 327–330.
- [278] G. Pelletier, A. Zwicker, C. L. Allen, A. Schepartz, S. J. Miller, *J. Am. Chem. Soc.* **2016**, *138*, 3175–3182.
- [279] F. W. Lichtenthaler, S. Immel, P. Pokinskyj, *Liebigs Ann.* **1995**, *1995*, 1939–1947.
- [280] G. T. Hayman, S. B. Von Bodman, H. Kim, P. Jiang, S. K. Farrand, *J. Bacteriol.* **1993**, *175*, 5575–5584.
- [281] P. Guyon, M. D. Chilton, A. Petit, J. Tempé, *Proc. Natl. Acad. Sci. U. S. A.* **1980**, *77*, 2693–2697.
- [282] P. Oger, S. K. Farrand, *Microbiology* **2002**, *184*, 1121–1131.
- [283] R. P. A. Berntsson, S. H. J. Smits, L. Schmitt, D. J. Slotboom, B. Poolman, *FEBS Lett.* **2010**, *584*, 2606–2617.
- [284] W. Bannwarth, A. Trzeciak, *Helv. Chim. Acta.* **1987**, *70*, 175–186.
- [285] E. Messens, A. Lenaerts, R. W. Hedges, M. Van Montagu, *EMBO J.* **1985**, *4*, 571–577.
- [286] M. E. Tate, P. J. Murphy, W. P. Roberts, A. Kerr, *Nature* **1979**, *280*, 697–699.
- [287] K. Suzuki, H. Nonaka, M. Yamaura, *J. Carbohydr. Chem.* **2004**, *23*, 253–259.
- [288] Y. Ma, G. Lian, Y. Li, B. Yu, *Chem. Commun.* **2011**, *47*, 7515–7517.
- [289] G. Guchhait, A. K. Misra, *Catal. Commun.* **2011**, *14*, 52–57.
- [290] T. Lecourt, A. Herault, A. J. Pearce, M. Sollogoub, P. Sinay, *Chem. Eur. J.* **2004**, *10*, 2960–2971.
- [291] T. Ooi, D. Uraguchi, N. Kagoshima, K. Maruoka, *J. Am. Chem. Soc.* **1998**, *120*, 5327–5328.
- [292] K. Maruoka, T. Ooi, *Chem. Eur. J.* **1999**, *5*, 829–833.
- [293] T. Ooi, J. Morikawa, D. Uraguchi, K. Maruoka, *Tetrahedron Lett.* **1999**, *40*, 2993–2996.
- [294] T. Ooi, N. Kagoshima, K. Maruoka, *J. Am. Chem. Soc.* **1997**, *119*, 5754–5755.
- [295] T. Ooi, N. Kagoshima, H. Ichikawa, K. Maruoka, *J. Am. Chem. Soc.* **1999**, *121*, 3328–3333.
- [296] D. T. Fox, C. D. Poulter, *J. Org. Chem.* **2005**, *70*, 1978–1985.
- [297] A. T. Koppisch, C. D. Poulter, A. C. D. Mep, C. D., *J. Org. Chem.* **2002**, 5416–5418.
- [298] A. Fontana, *J. Org. Chem.* **2001**, *66*, 2506–2508.
- [299] V. Wittmann, C. H. Wong, *J. Org. Chem.* **1997**, *62*, 2144–2147.
- [300] N. Oka, Y. Morita, Y. Itakura, K. Ando, *Chem. Commun.* **2013**, *49*, 11503–11505.
- [301] E. Drent, R. van Dijk, R. van Ginkel, B. van Oort, R. I. Pugh, *Chem. Commun.* **2002**, *31*, 964–965.
- [302] M. Dvorakova, R. Nencka, M. Dejmek, E. Zbornikova, A. Brezinova, M. Pribylova, R. Pohl, M. E. Migaud, T. Vanek, *Org. Biomol. Chem.* **2013**, *11*, 5702–5713.
- [303] F. Song, J. Zhang, Y. Zhao, W. Chen, L. Li, Z. Xi, *Org. Biomol. Chem.* **2012**, *10*, 3642–3654.

- [304] M. V. De Almeida, D. Dubreuil, J. Cleophax, C. Verre-sebri, M. Pipelier, G. Prestat, G. Vass, D. Gero, *Tetrahedron* **1999**, *55*, 7251–7270.
- [305] R. W. Clark, T. M. Deaton, Y. Zhang, M. I. Moore, S. L. Wiskur, *Org. Lett.* **2013**, *15*, 6132–6135.
- [306] S. Prabhakar, L. Lemiègre, T. Benvegna, S. Hotha, V. Ferrières, L. Legentil, *Carbohydr. Res.* **2016**, *433*, 63–66.
- [307] A. Merz, *Angew. Chem. Int. Ed.* **1973**, *12*, 846–847.
- [308] P. Finch, G. M. Iskander, A. H. Siriwardena, *Carbohydr. Res.* **1991**, *210*, 319–325.
- [309] K. Plé, M. Chwalek, L. Voutquenne-Nazabadioko, *European J. Org. Chem.* **2004**, 1588–1603.
- [310] J. -L. Imbach, C. Phigaud, G. Gosselin, *J. Chem. Soc., Perkin Trans. I.* **1992**, 1943–1952.
- [311] J. J. Forsman, R. Leino, *Carbohydr. Res.* **2010**, *345*, 1548–1554.
- [312] A. Zarrelli, A. Sgambato, V. Petit, L. De Napoli, L. Previtiera, G. Di Fabio, *Bioorg. Med. Chem. Lett.* **2011**, *21*, 4389–4392.
- [313] S. F. Martin, A. S. Wagman, *J. Org. Chem.* **1996**, *61*, 8016–8023.
- [314] A. V. Rukavishnikov, T. O. Zaikova, O. H. Griffith, J. F. W. Keana, *Chem. Phys. Lipids* **1997**, *89*, 153–157.
- [315] P. A. Grieco, M. Nishizawa, T. Oguri, S. D. Burke, N. Marinovic, *J. Am. Chem. Soc.* **1977**, *99*, 5773–5780.
- [316] K. Nishiyama, Y. Takakusagi, T. Kusayanagi, Y. Matsumoto, S. Habu, K. Kuramochi, F. Sugawara, K. Sakaguchi, H. Takahashi, H. Natsugari, et al., *Bioorg. Med. Chem.* **2009**, *17*, 195–202.
- [317] A. B. Smith, R. A. Rivero, K. J. Hale, H. A. Vaccaro, *J. Am. Chem. Soc.* **1991**, *113*, 2092–2112.
- [318] W. A. S. Andrew R. Vaino, *Synlett.* **1995**, *11*, 1157–1158.
- [319] J. A. Wright, J. Yu, J. B. Spencer, *Tetrahedron Lett.* **2001**, *42*, 4033–4036.
- [320] H. S. Kim, H. Yi, J. Myung, K. R. Piper, S. K. Farrand, *J. Bacteriol.* **2008**, *190*, 3700–3711.
- [321] P. Carl Heinz Hamann, Susanne Fischer, Herbert Polligkeit, Wolf, *J. Carbohydr. Chem.* **1993**, *12*, 173–190.
- [322] K.-D. H. Erich Reinefeld, *Chem. Ber.* **1971**, *104*, 265–269.
- [323] C. Chauvin, K. Baczko, D. Plusquellec, *J. Org. Chem.* **1993**, 2291–2295.
- [324] F. Guibe, *Tetrahedron* **1998**, *54*, 2967–3042.
- [325] D. Sebastian, H. Waldmann, *Tetrahedron Lett.* **1997**, *38*, 2927–2930.
- [326] Y. Hayakawa, S. Wakabayashi, T. Nobori, R. Noyori, *Tetrahedron Lett.* **1987**, *28*, 2259–2262.
- [327] S. Iii, N. Institutes, M. J. Heeg, **1985**, *8*, 2400–2402.
- [328] H. Matsushashi, K. Shimada, *Tetrahedron* **2002**, *58*, 5619–5626.
- [329] D. C. and S. T. A. Skowrońska, M. Pakulski, J. Michalski, *Tetrahedron Lett.* **1980**, *21*, 321–322.
- [330] J. K. Stowell, T. S. Widlanski, *Tetrahedron Lett.* **1995**, *36*, 1825–1826.
- [331] S. Ladame, S. Claustre, M. Willson, *Phosphorus Sulfur Silicon Relat. Elem.* **2001**, *174*, 37–47.
- [332] L. Soullère, C. Aldrich, O. Daumke, R. Gail, L. Kissau, A. Wittinghofer, H. Waldmann, *ChemBioChem* **2004**, *5*, 1448–1453.
- [333] T. Li, A. Tikad, W. Pan, S. P. Vincent, *Org. Lett.* **2014**, *16*, 5628–5631.
- [334] T. Schwede, J. Kopp, N. Guex, M. C. Peitsch, *Nucleic Acids Res.* **2003**, *31*, 3381–3385.
- [335] J. D. Thompson, D. G. Higgins, T. J. Gibson, *Nucleic Acids Res.* **1994**, *22*, 4673–4680.
- [336] A. Correa, S. Elmore, C. Bolm, *Chem. Eur. J.* **2008**, *14*, 3527–3529.
- [337] S. Jammi, S. Sakthivel, L. Rout, *J. Org. Chem.* **2009**, *74*, 1971–1976.
- [338] M. Hosseini-Sarvari, E. Sodagar, M. M. Doroodmand, *J. Org. Chem.* **2011**, *76*, 2853–2859.
- [339] S. Kim, K. C. Lim, S. Kim, *Chem. Asian J.* **2008**, *3*, 1692–1701.
- [340] S. Hotha, S. Kashyap, *J. Am. Chem. Soc.* **2006**, *128*, 9620–9621.
- [341] S. J. Gharpure, M. K. Shukla, U. Vijayasree, *Org. Lett.* **2009**, *11*, 5466–5469.
- [342] R. W. Clark, T. M. Deaton, Y. Zhang, M. I. Moore, S. L. Wiskur, *Org. Lett.* **2013**, *15*, 6132–6135.
- [343] R. Jeanloz, D. Jeanloz, *J. Am. Chem. Soc.* **1957**, *79*, 2579–2583.

## Abstract

Over the past decades, it has been recognized that the social communication of bacteria either play a beneficial role or can worsen pathogenicity in plant and human health. The language of bacteria used for communication are signal molecules called auto-inducers (AIs), which are regulated by themselves. This specific bacterial regulation process is termed as “quorum sensing (QS)”, by which bacteria coordinate various phenotypes such as biofilm formation or virulence factors in many microorganisms. To artificially alter the QS response of bacteria through design of QS chemical signal molecules for improving the pathogenicity have attracted the attention with innovative antibacterial strategies. Two chemical approaches towards bacteria QS have been studied in this thesis. One contributed to the design, synthesis and biological evaluation of novel QS inhibitors, another focused on the investigation of the role of agrocinopine and analogues in QS regulation in a specific bacteria *Agrobacterium tumefaciens* (*AT*). Both aimed at improving basic knowledge on QS biological processes in bacteria.

The first part figured out the chirality-activity relationship of Acyl Homoserine Lactones (AHLs), studied the replacement of the central amide group of AHLs by heterocyclic scaffolds, and designed a family of nitroaniline derivatives as LuxR-regulated QS inhibitors. The L-one of enantiomeric AHLs was found to be predominant in QS modulation, and some AHLs unrelated nitroaniline compounds were capable of inhibiting LuxR type of QS, whereas the bioactivity of heterocyclic scaffolds depends on its substitution sites.

The second part elaborated the mechanism by which agrocinopine A and its analogues were able to involve QS process, and activate virulence spread in *AT*. A series of analogues of agrocinopine A have been synthesized for investigating their binding properties with AccA. A specific key pyranose-2-phosphate motif has been identified to be responsible for both antibiotic import and QS regulation in *AT*.

**Key words:** Quorum sensing, autoinducer, AHLs analogues, chirality, heterocycle, nitroaniline, *Agrobacterium tumefaciens*, Agrocinopine, AccA, virulence, phosphodiester, phosphate.



## Résumé

Les bactéries ont longtemps été considérées comme des organismes unicellulaires. Cependant, elles se comportent comme des systèmes multicellulaires dans lesquels des cellules séparées communiquent ensemble en utilisant des systèmes moléculaires appelés autoinducteurs. Ce processus, appelé Quorum Sensing (QS), est capable de détecter la densité de population bactérienne et régule ainsi l'expression de certaines fonctions biologiques importantes, telles que la virulence bactérienne ou la formation de biofilm, liées à la pathogénicité humaine ou à la croissance végétale. Comme le QS implique plusieurs types de molécules, il s'agit donc d'une thématique intéressante pour les études à l'interface chimie biologie visant à synthétiser des molécules capables de moduler le QS.

Deux aspects du QS sont étudiés dans cette thèse: Le premier est la conception, la synthèse et l'évaluation biologique d'analogues d'autoinducteurs en tant que modulateur QS bactérien. Dans cette section, différentes relations structure-propriété d'un type d'auto-inducteur chez les bactéries Gram-négatives : les Acyl Homoserine Lactones (AHL) ont été étudiées. Ces études montrent que la chiralité de l'homosérine lactone est importante, que le remplacement du groupe amide central par des hétérocycliques ou des composés AHL structurellement non apparentés jouent un rôle important dans la modulation QS. Dans une deuxième partie, une étude structurale a permis de comprendre comment l'agrocinopine A a été en mesure d'intervenir dans le processus du QS c'est à dire la production de signaux AHL et d'activer la virulence bactérienne chez la bactérie *Agrobacterium tumefaciens*. Le rôle clé du groupement pyranose-2-phosphate de l'agrocinopine est démontré comme étant responsable de sa reconnaissance par les protéines de transport AccA et de la régulation du QS. Dans l'ensemble, cette thèse est la combinaison de deux composés organiques synthétiques liés au QS, tous deux destinés à améliorer les connaissances de base de ce processus biologique, contribuant potentiellement à l'avenir à de nouvelles stratégies capables d'influencer la pathogénicité bactérienne.

**Mot clés:** Quorum sensing, autoinducteur, analogues AHL, chiralité, hétérocycle, nitroaniline, *Agrobacterium tumefaciens*, Agrocinopine, AccA, virulence, phosphodiester, phosphate.

